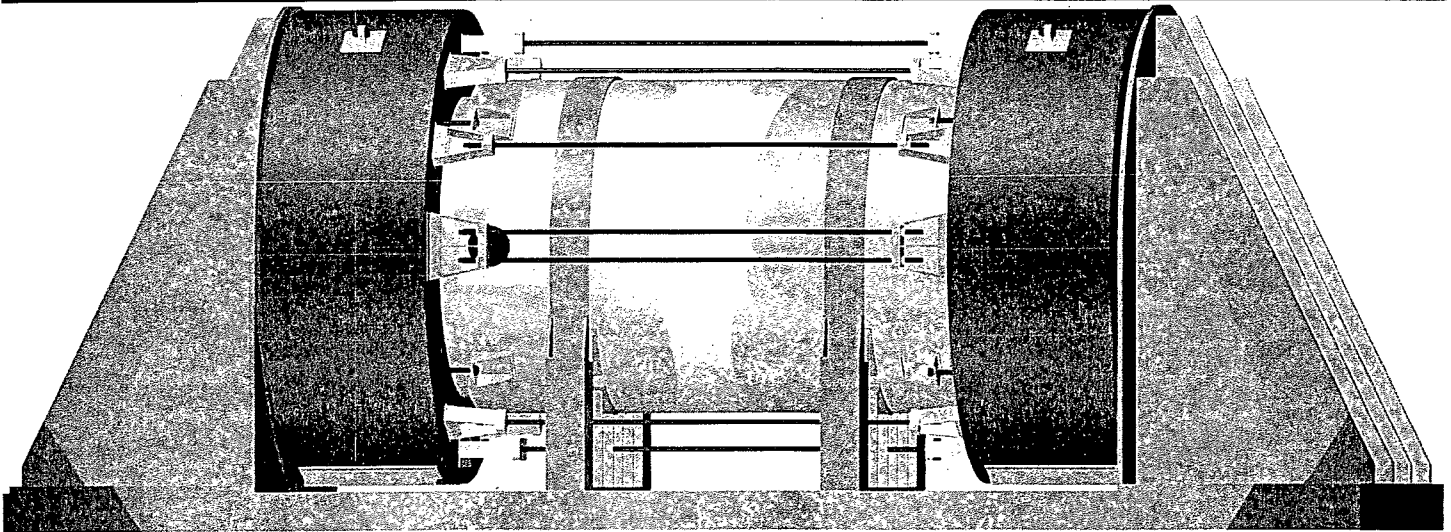


NON-PROPRIETARY

TN-40 TRANSPORTATION PACKAGING



SAFETY ANALYSIS REPORT



AREVA
TRANSNUCLEAR, INC.

E-23861

Rev. 0 / August 2006

NON-PROPRIETARY



AREVA
Transnuclear, Inc.

TN-40
TRANSPORTATION PACKAGING
SAFETY ANALYSIS REPORT

TABLE OF CONTENTS

	<u>PAGE</u>
1.0 GENERAL INFORMATION.....	1-1
1.1 Introduction	1-1
1.2 Package Description	1-1
1.2.1 Packaging.....	1-1
1.2.2 Operational Features.....	1-6
1.2.3 Contents of Packaging	1-7
1.3 References	1-8
1.4 Appendices	1-9
1.4.1 TN-40 Packaging Drawings.....	1-9

LIST OF TABLES

Table 1-1	Nominal Dimensions And Weights Of The TN-40 Packaging	1-10
Table 1-2	Fuel Qualification Table	1-11

LIST OF FIGURES

Figure 1-1	General Arrangement	1-12
------------	---------------------------	------

2.0 STRUCTURAL EVALUATION.....	2-1
2.1 Structural Design	2-1
2.1.1 Discussion	2-1
2.1.2 Design Criteria.....	2-3
2.2 Weights and Center-Of-Gravity.....	2-6
2.3 Mechanical Properties of Materials	2-6
2.3.1 Cask Material Properties	2-6
2.3.2 Basket Material Properties	2-6
2.3.3 Impact Limiter Material Properties	2-6
2.3.4 Fracture Toughness Requirements	2-7
2.4 General Standards For All Packages.....	2-7
2.4.1 Minimum Package Size	2-7
2.4.2 Tamper-proof Feature	2-7
2.4.3 Positive Closure	2-7
2.4.4 Chemical and Galvanic Reactions.....	2-7

2.5	Lifting And Tie-Down Standards	2-10
2.5.1	Lifting Devices	2-10
2.5.2	Tie-Down Devices	2-11
2.6	Normal Conditions Of Transport	2-11
2.6.1	Heat.....	2-13
2.6.2	Cold Environment.....	2-14
2.6.3	Increased External Pressure (N4)	2-14
2.6.4	Reduced External Pressure (N5).....	2-14
2.6.5	Transport Shock Loading (N14 & N15).....	2-15
2.6.6	Transport Vibration Loading (N12 & N13)	2-15
2.6.7	Water Spray	2-16
2.6.8	Free Drop (N6 through N11).....	2-16
2.6.9	Corner Drop.....	2-16
2.6.10	Compression	2-16
2.6.11	Penetration	2-16
2.6.12	Lid Bolt Analysis	2-16
2.6.13	Fatigue Analysis of the Containment Boundary.....	2-17
2.6.14	Structural Evaluation of the Basket under Normal Condition Loads	2-20
2.6.15	Summary of NCT Cask Body Structural Analysis.....	2-21
2.7	Hypothetical Accident Conditions	2-21
2.7.1	30 Foot Free Drop	2-22
2.7.2	Puncture	2-24
2.7.3	Thermal	2-27
2.7.4	Water Immersion	2-27
2.7.5	Structural Evaluation of the Basket under Accident Loads	2-29
2.7.6	Summary of HAC Cask Body Structural Analysis.....	2-30
2.8	Special Forms / Fuel Rods.....	2-30
2.8.1	Special Form	2-30
2.8.2	Fuel Rods	2-30
2.9	References	2-31
2.10	Appendices	2-33
2.11	ASME Code and NUREG-0612 Alternatives	2-34

LIST OF TABLES

Table 2-1	Evaluation Method Employed to Demonstrate Compliance with Specific Regulatory Requirements.....	2-39
Table 2-2	Containment Vessel Stress Limits	2-40
Table 2-3	Cover Bolt Stress Limits.....	2-41
Table 2-4	Non Containment Structure Stress Limits	2-42
Table 2-5	Basket Stress Limits	2-43
Table 2-6	Cask Weight and Center of Gravity	2-44
Table 2-7	Trunnion Section Properties and Applied Loads	2-45
Table 2-8	Trunnion Stresses when Loaded by 6 and 10 Times Cask Weight (Lifting).....	2-46
Table 2-9	TN-40 Performance Evaluation Overview (Normal Conditions of Transport)	2-47
Table 2-10	Individual Load Cases for Normal Conditions of Transport TN-40 Cask Body Analysis	2-48
Table 2-11	Summary of Load Combinations for Normal Condition of Transport.....	2-49
Table 2-12	Reference Temperatures for Stress Analysis Acceptance Criteria	2-51
Table 2-13	Summary of Load Combination Stresses for Normal Conditions of Transport	2-52
Table 2-14	Linearized Stress Evaluation of Normal Condition of Transport Load Combinations	2-54
Table 2-15	TN-40 Performance Evaluation Overview (Hypothetical Accident Conditions of Transport)	2-58
Table 2-16	Summary of Individual Load Factors for Hypothetical Accident Condition of Transport	2-59
Table 2-17	Summary of Load Combinations for Hypothetical Accident Condition of Transport	2-60
Table 2-18	Summary of Load Combination Stresses for Hypothetical Accident Condition of Transport	2-61
Table 2-19	Linearized Stress Evaluation for Hypothetical Accident Condition Load Combinations	2-62

LIST OF FIGURES

Figure 2-1	Geometry of Upper (front) and Lower (rear) Trunnions.....	2-64
Figure 2-2	290 psig Immersion Analysis Finite Element Model Loads and Boundary Conditions	2-65

Chapter 2 - Appendices

2.10.1	STRUCTURAL ANALYSIS OF CASK BODY	2.10.1-1
2.10.2	LID BOLT ANALYSIS	2.10.2-1
2.10.3	STRUCTURAL ANALYSIS OF THE OUTER SHELL	2.10.3-1
2.10.4	FRACTURE TOUGHNESS EVALUATION OF THE TN-40 CASK	2.10.4-1
2.10.5	STRUCTURAL ANALYSIS OF THE TN-40 BASKET	2.10.5-1
2.10.6	DYNAMIC LOAD FACTOR FOR BASKET DROP ANALYSIS	2.10.6-1
2.10.7	STRUCTURAL EVALUATION OF THE FUEL ROD CLADDING UNDER ACCIDENT IMPACT	2.10.7-1
2.10.8	STRUCTURAL EVALUATION OF THE IMPACT LIMITERS	2.10.8-1
2.10.9	IMPACT LIMITER TEST SPECIFICATION	2.10.9-1
3.0	THERMAL EVALUATION	3-1
3.1	Discussion	3-1
3.2	Summary of Thermal Properties of Materials	3-3
3.3	Technical Specifications for Components	3-8
3.4	Thermal Evaluation for Normal Conditions of Transport	3-8
3.4.1	Thermal Models	3-8
3.4.2	Maximum Temperatures	3-13
3.4.3	Maximum Accessible Surface Temperature in the Shade	3-13
3.4.4	Minimum Temperatures	3-14
3.4.5	Maximum Internal Pressure	3-14
3.4.6	Maximum Thermal Stresses	3-14
3.4.7	Evaluation of Cask Performance for Normal Conditions of Transport	3-14
3.5	Thermal Evaluation for Hypothetical Accident Conditions	3-14
3.5.1	Fire Accident Evaluation	3-15
3.5.2	Boundary conditions for the HAC	3-15
3.5.3	Crushed Impact Limiter Models	3-15
3.5.4	Summary of Results	3-17
3.5.5	Evaluation of Package Performance During and after the HAC Fire	3-17
3.6	References	3-18
3.7	Appendices	3-20

LIST OF TABLES

Table 3-1	NCT Component Temperatures In The TN-40 Package.....	3-21
Table 3-2	Temperature Distribution In The TN-40 Package (Low Ambient Temperature, Max Decay Heat).....	3-22
Table 3-3	Maximum HAC Transient Temperatures During Fire Accident	3-23

LIST OF FIGURES

Figure 3-1	Schematic Of The Cask Body	3-24
Figure 3-2	Thermal Model 90 Degree Radial Cross Section	3-25
Figure 3-3	Finite Element Model Of TN-40 Transport Cask	3-26
Figure 3-4	Finite Element Model Of The TN-40 Transport Cask, Details	3-27
Figure 3-5	Finite Element Model Of The TN-40 Basket Cross Section	3-28
Figure 3-6	Finite Element Model Of The TN-40 Basket, Details	3-29
Figure 3-7	Finite Element Model Of The TN-40 Basket Compartment Weld Joint Details	3-30
Figure 3-8	Details of Impact Limiters.....	3-31
Figure 3-9	Mesh Of Finite Element Model.....	3-32
Figure 3-10	Temperature Distribution In The TN-40 Cask, NCT, 100° F	3-33
Figure 3-11	Temperature Distributions In The TN-40 Cask, Fuel & Resin NCT, 100° F	3-34
Figure 3-12	Temperature Distributions In The TN-40 Cask, Impact Limiters & Rail Normal Conditions Of Transport NCT, 100° F	3-35
Figure 3-13	Temperature Distributions In The TN-40 Cask Low Ambient Temperatures	3-36
Figure 3-14	Maximum Temperature Distribution in the TN-40 Cask HAC, End of Fire / Smoldering	3-37
Figure 3-15	Maximum Temperature Distribution in the TN-40 Cask HAC, Cool-Down Period.....	3-38

Chapter 3 - Appendices

3.7.1	EFFECTIVE THERMAL PROPERTIES FOR THE FUEL ASSEMBLY.....	3.7.1-1
-------	---	---------

4.0	CONTAINMENT	4-1
4.1	Containment Boundary	4-1
4.1.1	Containment Vessel	4-1
4.1.2	Containment Penetrations	4-1
4.1.3	Seals and Welds	4-2
4.1.4	Closure	4-2
4.2	Requirements For Normal Conditions Of Transport.....	4-3
4.2.1	Containment of Radioactive Material.....	4-3
4.2.2	Pressurization of Containment Vessel.....	4-8
4.2.3	Containment Criterion.....	4-10
4.3	Containment Requirements for Hypothetical Accident Conditions	4-10
4.3.1	Source Terms.....	4-11
4.3.2	Containment of Radioactive Material.....	4-11
4.3.3	Containment Criterion.....	4-11
4.4	Special Requirements.....	4-13
4.5	References	4-14

LIST OF TABLES

Table 4-1	Radionuclide Inventory And A2 Values.....	4-15
Table 4-2	Activity Concentration By Source.....	4-16
Table 4-3	Normal Conditions of Transport And Hypothetical Accident Conditions Effective A ₂ Values	4-17
Table 4-4	Normal Condition of Transport And Hypothetical Accident Conditions Permissible Leakage Rates From the TN-40	4-18
Table 4-5	Total Moles Of Fission Gas For a WE 14x14 Std. Assembly	4-19
Table 4-6	Cask Gas Mixtures Under Normal Conditions of Transport and Hypothetical Accident Conditions	4-20

LIST OF FIGURES

Figure 4-1	TN-40 Containment Boundary Components.....	4-21
Figure 4-2	Lid, Vent Port And Drain Port Metal Seals	4-22

5.0	SHIELDING EVALUATION.....	5-1
5.1	Discussion And Results	5-1
5.2	Source Specification	5-2
5.2.1	Axial Source Distribution	5-3
5.2.2	Gamma Source	5-3
5.2.3	Neutron Source	5-4
5.2.4	Source Conversion Factors	5-4
5.2.5	Fuel Qualification.....	5-5
5.3	Model Specification.....	5-6
5.3.1	Description of Radial and Axial Shielding Configuration.....	5-6
5.3.2	Shield Regional Densities.....	5-7
5.4	Shielding Evaluation	5-7
5.5	References	5-10
5.6	Appendix.....	5-11
5.6.1	SAS2H/ORIGEN-S Input File	5-11
5.6.2	MCNP Neutron Model Input File.....	5-13
5.6.3	MCNP Primary Gamma Input File	5-30

LIST OF TABLES

Table 5-1	TN-40 Cask Shield Materials	5-50
Table 5-2	Summary Of TN-40 Dose Rates	5-51
Table 5-3	PWR Fuel Assembly Design Characteristics	5-52
Table 5-4	Westinghouse 14 X 14 STD Fuel Assembly Hardware Characteristics	5-53
Table 5-5	Material Compositions For Fuel Assembly Hardware Materials.....	5-54
Table 5-6	Source Distribution	5-55
Table 5-7	TPA Gamma Source.....	5-55
Table 5-8	Fuel Qualification Table	5-56
Table 5-9	Minimum Cooling (Years) Required To Meet Radiation and Decay Heat Limits.....	5-57
Table 5-10	Estimated 2 Meter Side Dose Rates (MREM/HR)	5-58
Table 5-11	Decay Heat Output (kW PER CASK).....	5-59
Table 5-12	Axial Source Term Peaking Summary	5-60
Table 5-13	Fuel Assembly Materials Input For MCNP	5-61
Table 5-14	Package Materials Input for MCNP.....	5-63

Table 5-15	Flux-to-Dose Rate Conversion Factors For Gamma.....	5-64
Table 5-16	Flux-Dose-Rate Conversion Factors For Neutron.....	5-65
Table 5-17	Average End Dose Rates As A Function Of Railcar Length	5-66

LIST OF FIGURES

Figure 5-1	Cask Shielding Configuration.....	5-67
Figure 5-2	Axial Burnup Profile For Design Basis Fuel	5-68
Figure 5-3	Side View Of TN-40 Transport MCNP Model.....	5-69
Figure 5-4	Detail Views Of TN-40 Transport MCNP Model.....	5-70
Figure 5-5	Plan View Of TN-40 Transport MCNP Model Basket Structure	5-71
Figure 5-6	Details Of Lattice Unit Cell And Rails/Outer SST	5-72
Figure 5-7	Summary of TN-40 Side NCT Dose Rates	5-73
Figure 5-8	Dose Rates Above the Neutron Shield	5-74

6.0	Criticality Evaluation	6-1
6.1	Discussion and Results.....	6-1
6.2	Package Fuel Loading	6-2
6.3	Model Specification.....	6-3
6.4	Criticality Calculations.....	6-3
6.4.1	Calculational Method	6-3
6.4.2	Fuel Loading Optimization.....	6-3
6.4.3	Criticality Results.....	6-3
6.5	Critical Benchmark Experiments.....	6-4
6.5.1	Benchmark Experiments and Applicability.....	6-4
6.5.2	Results of the Benchmark Calculations	6-5
6.6	References	6-6
6.7	Input File Listing.....	6-8
6.7.1	SAS2H Input Deck for Design Basis Fuel Assembly – Zone 8	6-8
6.7.2	CSAS25 Input Deck for Design Basis Criticality Case.....	6-8

LIST OF TABLES

Table 6-1	Minimum Burnup as a Function of Enrichment	6-9
Table 6-2	Parameters For PWR Assemblies For Shipment.....	6-10
Table 6-3	Required Assembly and Reactor Parameters for SAS2H Models	6-10
Table 6-4	Axial Burnup Profiles from Reference [10].....	6-10
Table 6-5	Modified Axial Burnup Profiles Used for SAS2H Depletion Analysis	6-11
Table 6-6	BPRA Design Parameters for SAS2H Models	6-11
Table 6-7	Burnup Dependent Horizontal Burnup Gradients.....	6-11
Table 6-8	Basket and Cask Design Dimensions for the CSAS25 Models.....	6-11
Table 6-9	Description of the KENO Model	6-12
Table 6-10	Best-Estimate Correction Factors for SAS2H Isotopic Content	6-12
Table 6-11	Burned Fuel Isotopic Composition	6-12
Table 6-12	Material Property Data	6-12
Table 6-13	Material ID IN KENO	6-13
Table 6-14	Most Reactive Configuration – Fresh Fuel Assumption	6-13
Table 6-15	Most Reactive Configuration – Burned Fuel	6-13
Table 6-16	Results of Burnup Credit Calculations	6-13
Table 6-17	Moderator Density Variations.....	6-14
Table 6-18	Results of the Additional Reactivity Margin Calculations	6-15
Table 6-19	Dancoff Factor Calculation for Density Variations.....	6-15
Table 6-20	CSAS25 Results	6-16
Table 6-21	USL-1 Results.....	6-20
Table 6-22	USL Determination for Criticality Analysis.....	6-21

LIST OF FIGURES

Figure 6-1	TN-40 Loading Curve.....	6-22
Figure 6-2	Example SAS2H Model.....	6-23
Figure 6-3	Fuel Assembly Positions within the Basket.....	6-23
Figure 6-4	Radial Cross Section of the Basket with Centered Fuel Assemblies	6-23
Figure 6-5	Radial Cross Section of the Basket with Stainless Steel.....	6-23
Figure 6-6	Axial Cross Section of the Basket with Cuboid Plugs	6-24
Figure 6-7	Radial Cross Section of the Basket with Inward Fuel Assemblies	6-24
Figure 6-8	TN-40 KENO Model for Horizontal Burnup Gradient.....	6-24
Figure 6-9	TN-40 KENO Model with Internal Moderator between Poison Plates ...	6-24
Figure 6-10	TN-40 KENO Model for Cask A Loading Configuration.....	6-25
Figure 6-11	TN-40 KENO Model for Cask B Loading Configuration.....	6-25
Figure 6-12	TN-40 KENO Model for Cask C Loading Configuration	6-25

7.0	OPERATING PROCEDURES	7-1
7.1	Package Loading	7-1
7.1.1	Preparation for Loading	7-1
7.1.2	Loading.....	7-2
7.1.3	Preparation for Transport	7-3
7.2	Package Unloading.....	7-5
7.2.1	Receipt of Package from Carrier	7-5
7.2.2	Preparation for Unloading.....	7-6
7.2.3	Contents Removal.....	7-7
7.3	Preparation Of Empty Package For Transport.....	7-8
7.4	Other Procedures	7-10
7.4.1	Preparation of Cask Used in Storage for Transport.....	7-10
7.5	References	7-13

LIST OF FIGURES

Figure 7-1	Torquing Patterns	7-14
Figure 7-2	Typical Setup for Filling Cask with Water.....	7-15

8.0	ACCEPTANCE TESTS AND MAINTENANCE PROGRAM	8-1
8.1	Acceptance Tests	8-1
8.1.1	Visual Inspection	8-1
8.1.2	Structural and Pressure Tests	8-1
8.1.3	Containment Boundary Leak Tests	8-2
8.1.4	Component Tests	8-3
8.1.5	Shielding Tests	8-4
8.1.6	Neutron Absorber Tests	8-5
8.1.7	Thermal Acceptance Tests	8-5
8.2	Maintenance Program.....	8-5
8.2.1	Structural and Pressure Tests	8-5
8.2.2	Leak Tests	8-5
8.2.3	Subsystem Maintenance	8-6
8.2.4	Shielding	8-7
8.2.5	Thermal.....	8-7
8.3	References	8-8

CHAPTER 1

GENERAL INFORMATION

TABLE OF CONTENTS

	<u>PAGE</u>
1.0 GENERAL INFORMATION.....	1-1
1.1 Introduction	1-1
1.2 Package Description	1-1
1.2.1 Packaging	1-1
1.2.2 Operational Features	1-6
1.2.3 Contents of Packaging.....	1-7
1.3 References	1-8
1.4 Appendices	1-9
1.4.1 TN-40 Packaging Drawings	1-9

LIST OF TABLES

Table 1-1	Nominal Dimensions And Weights Of The TN-40 Packaging	1-10
Table 1-2	Fuel Qualification Table	1-11

LIST OF FIGURES

Figure 1-1	General Arrangement	1-12
------------	---------------------------	------

1.0 GENERAL INFORMATION

1.1 Introduction

This Safety Analysis Report (SAR) presents the evaluation of a Type B(U) spent fuel transport packaging developed by Transnuclear, Inc. and designated the TN-40. This SAR describes the design features and presents the safety analyses which demonstrate that the TN-40 complies with applicable requirements of 10 CFR 71 [1]. The format and content of this SAR follow the guidelines of Regulatory Guide 7.9 [2].

The TN-40 is a dual purpose cask intended for both storage and transport. The TN-40 is currently licensed for storage at the Prairie Island Nuclear Generating Plant (Docket No. 72-0010). A separate storage SAR was submitted by Prairie Island in support of the storage license application. It addresses the safety related aspects of storing spent fuel in TN-40 casks in accordance with 10 CFR 72 [3].

The packaging is intended to be shipped as exclusive use. The Transport Index for nuclear criticality control for the TN-40 cask is determined to be zero (0) in accordance with 10 CFR 71.59 [1]. See Chapter 6 for details of this determination.

Transnuclear, Inc. has an NRC approved quality assurance program (Docket Number 71-0250) which satisfies the requirements of 10 CFR 71 Subpart H [1].

1.2 Package Description

1.2.1 Packaging

The TN-40 packaging will be used to transport 40 intact PWR fuel assemblies with or without fuel inserts. Only intact fuel will be transported in the cask. Known or suspected failed fuel assemblies (rods) and fuel with cladding defects greater than pin holes or hairline cracks are not to be transported in the TN-40 packaging. In its transport configuration, the TN-40 packaging consists of the following components:

- A basket assembly which locates and supports the fuel assemblies, transfers heat to the cask inner shell, and provides sufficient neutron absorption to satisfy nuclear criticality requirements.
- A containment vessel including a closure lid and metallic seals which provides radioactive materials containment and maintains an inert gas atmosphere.
- A thick-walled, forged steel gamma shield shell, bottom shield and lid shield plate provide shielding that surrounds the containment vessel.
- A radial neutron shield surrounding the gamma shield shell which provides additional radiation shielding. The neutron shielding is enclosed in a steel outer shell.

- A set of impact limiters consisting of balsa and redwood, encased in stainless steel shells, which are attached to either end of the cask body during the shipment. An aluminum spacer is also present to provide a smooth contact surface between the top impact limiter and the cask lid. The impact limiters are held in place with tie rods and attachment bolts.
- Sets of upper and lower trunnions that provide support, lifting, and rotation capability for the cask.

A personnel barrier is mounted to the transport frame to prevent unauthorized access to the cask body. The overall dimensions of the TN-40 packaging are 260.87 in. long and 144 in. in diameter with the impact limiters installed. The cask body is 183.75 in. long (with the lid installed) and 91 in. in diameter. The lid is 82.75 in. in diameter. The cask outside diameter including the radial neutron shield is 101.0 in. The cask cavity is 163 in. long and 72.0 in. in diameter. The general arrangement of the TN-40 packaging is depicted in Figure 1-1. Detailed design drawings for the TN-40 packaging are provided in Appendix 1.4. The materials used to fabricate the cask are shown in the Parts List on drawing 10421-71-1 and the materials used to fabricate the impact limiters are shown in the Parts List on drawing 10421-71-41. Where more than one material has been specified for a component, the most limiting properties are used in the analyses in the subsequent chapters of this SAR.

The gross weight of the loaded package is 271.5 kips including a payload of 52.0 kips. Table 1-1 summarizes the dimensions and weights of the TN-40 packaging. Trunnions attached to the cask body are provided for lifting and handling operations, including rotation of the packaging between the horizontal and vertical orientations. The TN-40 packaging is loaded in the vertical configuration and transported in the horizontal orientation on a specially designed shipping frame.

The maximum normal operating pressure of the TN-40 is 15.7 psig. A cask cavity pressure of 100 psig is conservatively used for the purposes of structural analyses. The spent fuel payload is shipped dry in a helium atmosphere. The heat generated by the spent fuel assemblies is rejected to the surrounding air by convection and radiation. No forced cooling or cooling fins are required.

The following sections provide a physical and functional description of each major component. Engineering drawings showing dimensions of significance to the safety analyses, welding and NDE information, and a complete materials list are provided in Appendix 1.4. Reference to these drawings is made in the following physical description sections and in general, throughout this SAR. Fabrication of the TN-40 packaging is performed in accordance with these drawings.

1.2.1.1 Containment Vessel

The containment boundary components consist of the inner shell and bottom inner plate, shell flange, lid outer plate, lid bolts, penetration cover plates and bolts (vent and drain) and the inner metallic seals of the lid seal and the vent and drain seals (Figure 4-

1). The containment vessel prevents leakage of radioactive material from the cask cavity. It also maintains an inert atmosphere (helium) in the cask cavity. Helium assists in removal of decay heat and provides a non-reactive environment to protect fuel assemblies against fuel cladding degradation which might otherwise lead to gross cladding rupture.

The overall containment vessel length is approximately 170.5 in. with a wall thickness of 1.5 in. The cylindrical cask cavity has a nominal diameter of 72.0 in. and a length of 163 in. The lid outer plate is 4.5 in. thick and is fastened to the body by 48 lid closure bolts. Double metallic seals are provided for the lid closure. To preclude air in-leakage, the cask cavity is pressurized with helium above atmospheric pressure.

The cask cavity can be accessed using two penetrations through the lid. These penetrations are for draining and venting. Double metallic seals are utilized to seal these two lid penetrations.

The over-pressure (OP) port provides access to the volumes between the double seals in the lid and cover plates for leak testing purposes. The OP port cover is not part of the containment boundary.

The inner shell and bottom inner plate materials are SA-203, Grade E or Grade D. The lid outer plate material is SA-350, Grade LF3 or SA-203 Grade E. The TN-40 containment vessel is designed, fabricated, examined and tested in accordance with the requirements of Subsection NB [4] of the ASME Code to the maximum practical extent. In addition, the design meets the requirements and Regulatory Guides 7.6 [5] and 7.8 [6]. Alternatives to the ASME Code are discussed in Section 2.11. The construction of the containment boundary is shown on drawings 10421-71-3, 4 and 5 provided in Appendix 1.4. The design of the containment boundary is discussed in Chapter 2 and the fabrication requirements (including examination and testing) of the containment boundary are discussed in Chapter 4.

1.2.1.2 Gamma and Radial Neutron Shielding

A gamma shield is provided around the inner shell and the bottom inner plate of the containment vessel, by an independent shell and bottom plate of carbon steel (Drawing 10421-71-3). The gamma shield shell completely surrounds the containment vessel inner shell and bottom inner plate. The 8.0 in. thick gamma shield shell and the 8.75 in. thick bottom shell are SA-105, SA-516, Grade 70, or SA-266 Class 4 material.

In order to obtain a close fit between the inner shell and the gamma shield shell for heat transfer, the gamma shield shell is heated prior to assembly with the inner shell. As the gamma shield shell cools, an axial gap may form between the shell flange and the top of the gamma shield shell. This gap is filled with shims. The shims are machined to fill the gap and act as a backing plate for the weld between the shell flange and the gamma shield shell.

A 6.0 in. thick shield plate (SA-105 or SA-516, Grade 70) is also welded to the inside of the lid outer plate (drawing 10421-71-4).

Radial neutron shielding is provided by a borated polyester resin compound surrounding the gamma shield shell. The resin compound is cast into long, slender aluminum alloy containers. The total radial thickness of the resin and aluminum is 4.50 in. The array of resin-filled containers is enclosed within a 0.50 in. thick outer steel shell (SA-516, Grade 55 or equivalent) constructed of two half cylinders. In addition to serving as resin containers, the aluminum containers provide a conduction path for heat transfer from the gamma shield shell to the outer shell. A pressure relief valve is mounted on top of the resin enclosure to limit the internal pressure increase that may be caused by heating of the resin enclosure for hypothetical accident conditions.

The resin material is an unsaturated polyester cross-linked with styrene, with approximately 50 weight % mineral and fiberglass reinforcement. The components are polyester resin, styrene monomer, alpha methyl styrene, aluminum oxide, zinc borate, and chopped fiberglass which produce the elemental resin composition shown below.

Element	wt%
H	5.05
B	1.05
C	35.13
Al	14.93
O + Zn (balance)	43.84

The structural analysis of the TN-40 cask shielding is presented in Chapter 2

Noncontainment welds are inspected in accordance with the NDE acceptance criteria of ASME B&PV Code Subsection NF [8].

1.2.1.3 Impact Limiters

Top (front) and bottom (rear) impact limiters, shown on drawings 10421-71-2 and -40 through -44, form a part of the TN-40 packaging. The impact limiters are attached to each other using 13 tie rods and to the cask by bolt attachment brackets welded to the outer shell in eight locations (four bolting locations per impact limiter). The impact limiters consist of balsa wood and redwood blocks, encased in sealed stainless steel shells (A-240, Grade 304) that maintain a dry atmosphere for the wood and confine the wood when crushed during a free drop. The impact limiters have internal radial gussets for added strength and confinement.

The impact limiters have an outside diameter of 144 in., and an inside diameter of 92 in. to accommodate the cask ends. The bottom limiter is notched to fit over the lower trunnions. The impact limiters extend axially 37.75 in. from either end of the cask, and overlap the sides of the cask by 12.25 in.

Thirteen 1.5 in. diameter tie-rods are used to hold the impact limiters in place. The tie-rods span the length of the cask and connect to both impact limiters via mounting brackets (See drawings 10421-71-40, and 10421-71-44). The impact limiters are also attached to the outer shell of the cask with eight 1.5 in. diameter bolts. The bolts are inserted through brackets (welded to the cask outer shell) and thread into each impact limiter. There are a total of eight bracket sets, four per impact limiter.

Each impact limiter is provided with nine fusible plugs that are designed to melt during a fire accident, thereby relieving excessive internal pressure. Each impact limiter has two lifting lugs for handling, and two support angles for holding the impact limiter in a vertical position during storage. The lifting lugs and the support angles are welded to the stainless steel shells.

An aluminum spacer is placed on the cask lid prior to mounting the top impact limiter. The purpose of the aluminum spacer is to provide a smooth contact surface between the lid and the top impact limiter. The top plate of the spacer has 48 holes to allow clearance for the lid bolt heads. The lip of the spacer is designed to make up the difference between the lid and cask outer diameters so that the top impact limiter cavity mates with a surface of constant diameter (drawing 10421-71-7).

The functional description as well as the performance analysis of the impact limiters is provided in Appendix 2.10.8.

1.2.1.4 Tiedown and Lifting Devices

Threaded holes are provided in the lid for attachment of component lifting devices. These are used as attachment points for sling systems or other lifting tools. These threaded holes are equally spaced 90° apart as shown on drawing 10421-71-4. Prior to transport, any attachments will be removed. Access to these threaded holes is prevented by the presence of the top impact limiter.

Four trunnions, which form part of the cask body, are attached for lifting and rotating of the cask. Two of the trunnions are located near the top of the body, and two near the bottom.

The upper trunnions are welded to the gamma shield shell and are designed to meet the requirements of NUREG-0612 [9] for non-redundant lifting fixture. This is accomplished by evaluating the trunnions to the stress design factors required by ANSI N14.6 [7]. See Section 2.11 for testing alternatives to ANSI N14.6[7] requirements that were imposed. The lower trunnions are welded to the gamma shield shell and bottom shield, and are used for rotating the cask between the vertical and the horizontal positions.

The tiedown devices are described in Section 2.5.2 of Chapter 2.

1.2.1.5 Fuel Basket

The basket structure is designed, fabricated and inspected in accordance with ASME B&PV Code Subsection NB [4]. Section 2.1.2.2 of Chapter 2 discusses use of NB instead of NG. Alternatives to the NB code are provided in Section 2.11. The basket structure consists of an assembly of stainless steel cells joined by a fusion welding process and separated by aluminum and poison plates which form a sandwich panel. The panel consists of two aluminum plates which sandwich a poison plate. The aluminum plates provide the heat conduction paths from the fuel assemblies to the cask inner plate. The poison material provides the necessary criticality control. This method of construction forms a very strong honeycomb-like structure of cell liners which provide compartments for 40 fuel assemblies. The open dimension of each cell is 8.05 in. x 8.05 in. which provides a minimum of 1/8 in. clearance around the fuel assemblies. The overall basket length (160.0 in.) is less than the cask cavity length to allow for thermal expansion and fuel assembly handling.

1.2.2 Operational Features

There are no complex operational features associated with the TN-40 packaging. The TN-40 cask and basket are designed to be compatible with spent fuel pool loading/unloading methods. The sequential steps to be followed for cask loading, testing, and unloading operations are provided in Chapter 7. Chapter 7 also provides criteria and limits for operational tests. The loading operations are summarized below.

Upon arrival, the empty cask is inspected. Preparation of the packaging for loading/unloading requires that the top (front) and bottom (rear) impact limiters including the tie-rods and attachment bolts are first removed from the cask. The cask is lifted from the transport frame to an upending/downending frame. The cask is then rotated from the horizontal transport orientation to the vertical orientation using a crane and lift beam attached to the upper trunnions. The lower trunnions pivot in the upending/downending frame as the cask is rotated.

The cask is brought into the spent fuel building. Access to the cask cavity and fuel basket is obtained by untorquing and removing the 48 closure lid bolts, and removing the lid using hoist rings threaded into the lid. The cask is then lowered into the cask pit/spent fuel pool. Fuel assemblies are loaded into the 40 basket compartments.

The lid is installed and the cavity is vented. The cask is lifted so that the lid is above the surface of water and some of the lid bolts are installed hand tight. The cask may be drained at this time, or after removal from the pool. The cask is moved from the cask pit/spent fuel pool to the decontamination area. The remaining lid bolts are installed and tightened to the specified torque. The cask cavity is then dried by means of a vacuum system and then back-filled with helium. The lid seals and penetration cover seals are leak tested. The external surface radiation levels are checked to assure that they are within limits.

1.2.3 Contents of Packaging

The contents of the TN-40 packaging are limited to 40 unconsolidated intact 14x14 PWR fuel assemblies with zircaloy cladding. The fuel may be transported with or without fuel inserts (burnable poison rod assemblies (BPRA) and thimble plug assemblies (TPA). Permissible fuel assembly types are listed below:

Fuel Designations	Exxon Std (14x14)	Exxon Toprod (14x14)	Exxon High Burnup (14 x 14)	Westinghouse Standard (14x14)	Westinghouse OFA (14x14)
Max Length (in.)	161.3	161.3	161.3	161.3	161.3
Max Width (in.)	7.763	7.763	7.763	7.763	7.763
No of Fueled Rods	179	179	179	179	179
Clad Material	Zr-4	Zr-4	Zr-4	Zr-4	Zr-4
Guide Tube #	16	16	16	16	16
Instrument Tube #	1	1	1	1	1
Maximum MTU/assembly	370	370	370	410	360

Provided all the requirements listed in this section are met, the bounding fuel characteristics are:

<u>Characteristic</u>	<u>Parameter</u>
Maximum initial bundle average enrichment	3.85 wt. % U235
Maximum assembly average burnup	45,000 MWD/MTU
Minimum cooling time	15 to 25 years
Maximum heat load	0.525 kW/assy

Given the fuel requirements listed above, the package payload must meet the following requirements:

- The total weight of the PWR fuel assemblies (with inserts) shall not exceed 52.0 kips.
- The total decay heat of the cavity contents shall not exceed 21 kW.
- Measured external radiation levels shall not exceed the requirements of 10 CFR 71.47. Measured surface contamination levels shall not exceed the requirements of 10 CFR 71.87(i).
- Table 1-2 provides the minimum cooling time required for various combinations of assembly average initial enrichment and maximum burnup.

1.3 References

1. 10 CFR 71, Packaging and Transportation of Radioactive Material.
2. USNRC Regulatory Guide 7.9, "Standard Format and Content of Part 71 Applications for Approval of Packages for Radioactive Material," Rev. 2, March 2005.
3. 10 CFR 72, Licensing Requirements for the Independent Storage of Spent Nuclear Fuel and High-Level Radioactive Waste.
4. American Society of Mechanical Engineers, ASME Boiler and Pressure Vessel Code, Section III, 1989 without addenda.
5. USNRC Regulatory Guide 7.6, "Design Criteria for the Structural Analysis of Shipping Cask Containment Vessel," Rev. 1, March 1978.
6. USNRC Regulatory Guide 7.8, "Load Combinations for the Structural Analysis of Shipping Cask," Rev. 1, March 1989.
7. ANSI N14.6-1986, "American National Standard For Radioactive Materials-Special Lifting Devices for Shipping Containers Weighing 10,000 Pounds (4500 Kg) or More," American National Standards Institute, Inc., New York, New York.
8. American Society of Mechanical Engineers, ASME Boiler and Pressure Vessel Code, Subsection NF, 1989 without addenda.
9. NUREG-0612 "Control of Heavy Loads at Nuclear Power Plants", July 1980.

1.4 Appendices

1.4.1 TN-40 Packaging Drawings

The following Transnuclear drawings are enclosed:

<u>Drawing No</u>	<u>Title</u>
10421-71-1	TN-40 Transport Packaging Parts List and Notes
10421-71-2	TN-40 Transport Packaging Transport Configuration
10421-71-3	TN-40 Transport Packaging General Arrangement
10421-71-4	TN-40 Transport Packaging Lid Assembly and Details
10421-71-5	TN-40 Transport Packaging Lid Details
10421-71-6	TN-40 Transport Packaging Trunnion, Basket Rail and Neutron Shield Details
10421-71-7	TN-40 Transport Packaging Impact Limiter Spacer Detail
10421-71-8	TN-40 Transport Packaging Basket Assembly
10421-71-9	TN-40 Transport Packaging Basket Details
10421-71-10	TN-40 Transport Packaging Regulatory Plate
10421-71-40	TN-40 Transport Packaging Impact Limiters General Arrangement
10421-71-41	TN-40 Transport Packaging Impact Limiters Parts List and Notes
10421-71-42	TN-40 Transport Packaging Impact Limiters Assembly
10421-71-43	TN-40 Transport Packaging Impact Limiters Details
10421-71-44	TN-40 Transport Packaging Impact Limiters Parts

Table 1-1
Nominal Dimensions And Weights Of The TN-40 Packaging

Overall length (with impact limiters, in.)	261
Overall length (without impact limiters, in.)	184
Impact Limiter Outside diameter (in.)	144
Outside diameter (without impact limiters, in.)	101
Cavity diameter (in.)	72.0
Cavity length (in.)	163
Containment shell thickness (in.)	1.5
Containment vessel length (in.)	170.5
Body wall thickness (in.)	9.5
Containment Lid thickness (in.)	4.5
Overall Lid thickness (in.)	10.5
Bottom thickness (in.)	10.3
Resin and aluminum box thickness (in.)	4.5
Outer shell thickness (in.)	0.5
Overall basket length (in.)	160
Weight of Fuel Assemblies (with inserts) (kips)	52.0
Loaded Weight of TN-40 Cask (without impact limiters) (kips)	236.5
Weight of Impact Limiters, Aluminum Spacer, and Tie-Rods (kips)	35.0
Total Loaded Weight of TN-40 Packaging (w/o shipping frame) (kips)	271.5

Table 1-2
Fuel Qualification Table

MINIMUM COOLING TIMES (YEARS)

Maximum Assembly Average Burnup (GWD/MTU)	Assembly Average Enrichment (wt. % U235)								
	2	2.25	2.35	2.75	3	3.25	3.4	3.6	3.85
17	15	15	15	15	15	15	15	15	15
18	15	15	15	15	15	15	15	15	15
19	15	15	15	15	15	15	15	15	15
20	15	15	15	15	15	15	15	15	15
21	15	15	15	15	15	15	15	15	15
22	15	15	15	15	15	15	15	15	15
23	15	15	15	15	15	15	15	15	15
24	15	15	15	15	15	15	15	15	15
25	15	15	15	15	15	15	15	15	15
26	15	15	15	15	15	15	15	15	15
27	15	15	15	15	15	15	15	15	15
28	15	15	15	15	15	15	15	15	15
29			15	15	15	15	15	15	15
30			15	15	15	15	15	15	15
31			15	15	15	15	15	15	15
32			15	15	15	15	15	15	15
33			16	15	15	15	15	15	15
34			17	15	15	15	15	15	15
35			17	16	15	15	15	15	15
36			18	16	15	15	15	15	15
37			19	17	16	15	15	15	15
38			20	18	17	16	16	15	15
39			21	19	18	17	16	16	15
40			23	20	19	18	17	16	16
41			24	21	20	19	18	17	17
42			25	22	21	19	19	18	18
43					22	20	20	20	19
44						21	21	21	21
45						23	22	22	22

Note:

1. For fuel characteristics that fall between the assembly average enrichment values in the table, use the next lower enrichment, and next higher burnup to determine minimal cooling time.
2. Enrichment and burnup are also required to meet criticality requirements as defined in Figure 6-1.

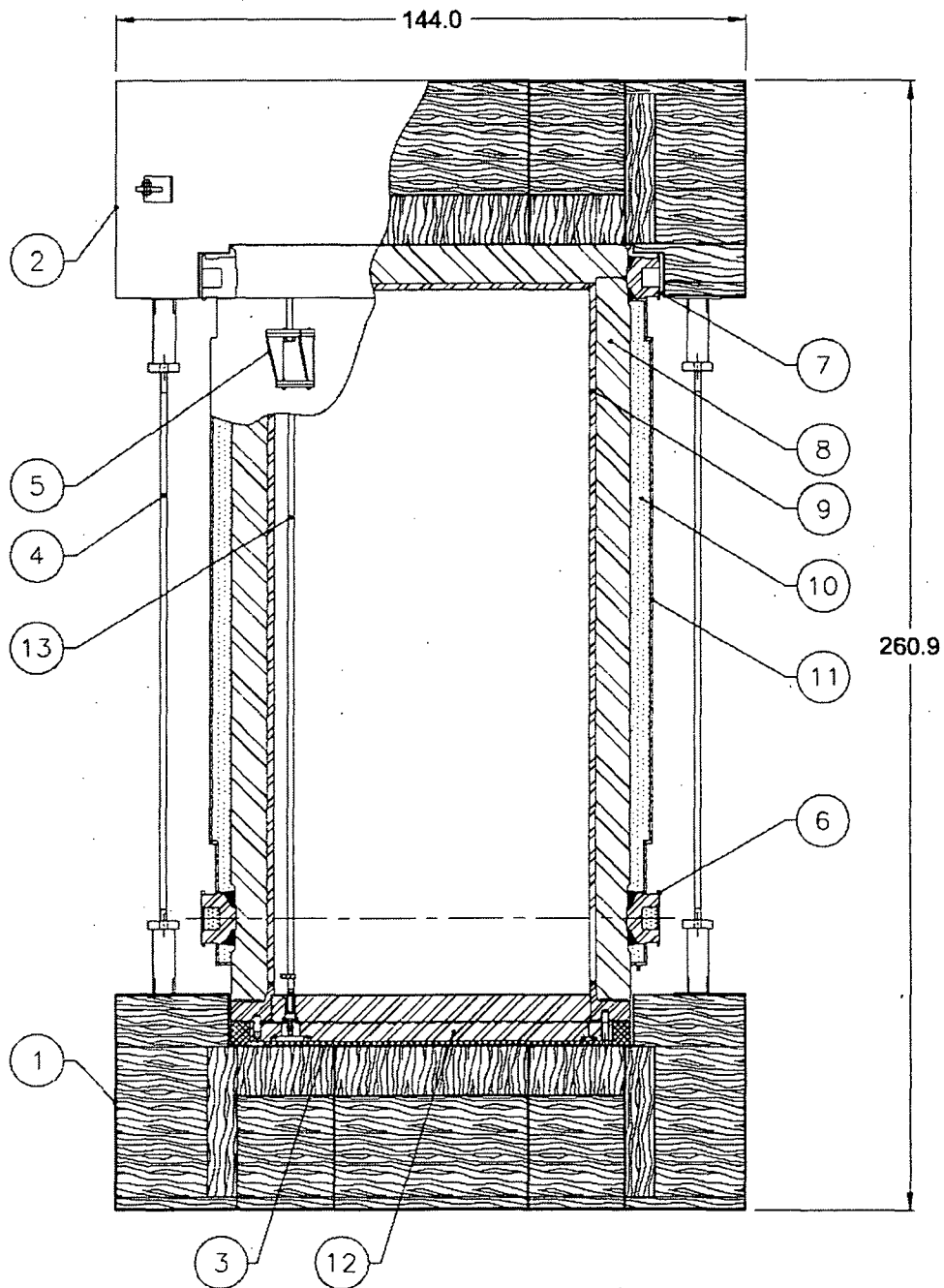


Figure 1-1
General Arrangement
TN-40 PACKAGING

Figure 1-1
General Arrangement Cont'd
TN-40 PACKAGING

Notes to Figure 1-1

- A. Some details exaggerated for clarity.
- B. Components are listed below:
- 1 Top (front) Impact Limiter
 - 2 Bottom (rear) Impact Limiter
 - 3 Top Impact Limiter Spacer
 - 4 Tie Rod
 - 5 Impact Limiter Bolting & Bracket
 - 6 Upper Trunnions
 - 7 Lower Trunnions
 - 8 Cask Body (Gamma Shield Shell & Bottom Shield)
 - 9 Containment Shell (Inner Shell & Bottom Inner Plate)
 - 10 Radial Neutron Shielding
 - 11 Outer Shell
 - 12 Lid Assembly
 - 13 Drain Tube

SECURITY RELATED INFORMATION
WITHHELD UNDER 10 CFR 2.390



TN-40 TRANSPORT PACKAGING
PARTS LIST AND NOTES

NONE	B	10421-71-1	0
SCALE	SIZE	DRAWING NUMBER	REV.

DO NOT SCALE DRAWING

SECURITY RELATED INFORMATION
WITHHELD UNDER 10 CFR 2.390



TN-40 TRANSPORT PACKAGING
TRANSPORT CONFIGURATION

NONE	B	10421-71-2	0
SCALE	SIZE	DRAWING NUMBER	REV.
DO NOT SCALE DRAWING		1 OF 2	

10421-71-2
1 OF 2
DRAWING NO.

SECURITY RELATED INFORMATION
WITHHELD UNDER 10 CFR 2.390



TN-40 TRANSPORT PACKAGING
TRANSPORT CONFIGURATION

NONE	B	10421-71-2	0
SCALE	SIZE	DRAWING NUMBER	REV.
DO NOT SCALE DRAWING		2 OF 2	

DRAWING NO. 10421-71-2
SHEET 2 OF 2

SECURITY RELATED INFORMATION
WITHHELD UNDER 10 CFR 2.390



TN-40 TRANSPORT PACKAGING
GENERAL ARRANGEMENT

NONE	B	10421-71-3	0
SCALE	SIZE	DRAWING NUMBER	REV.

DO NOT SCALE DRAWING

13345 10421-71-3

SECURITY RELATED INFORMATION
WITHHELD UNDER 10 CFR 2.390



TN-40 TRANSPORT PACKAGING
LID ASSEMBLY AND DETAILS

NONE	B	10421-71-4	0
SCALE	SIZE	DRAWING NUMBER	REV.

DO NOT SCALE DRAWING

SECURITY RELATED INFORMATION
WITHHELD UNDER 10 CFR 2.390



TN-40 TRANSPORT PACKAGING
LID DETAILS

NONE	B	10421-71-5	0
SCALE	SIZE	DRAWING NUMBER	REV.
DO NOT SCALE DRAWING			

DRAWING NO. 10421-71-5
SHEET

SECURITY RELATED INFORMATION
WITHHELD UNDER 10 CFR 2.390



TN-40 TRANSPORT PACKAGING
TRUNNION, BASKET RAIL AND
NEUTRON SHIELD DETAILS

NONE	B	10421-71-6	0
SCALE	SIZE	DRAWING NUMBER	REV.

DO NOT SCALE DRAWING

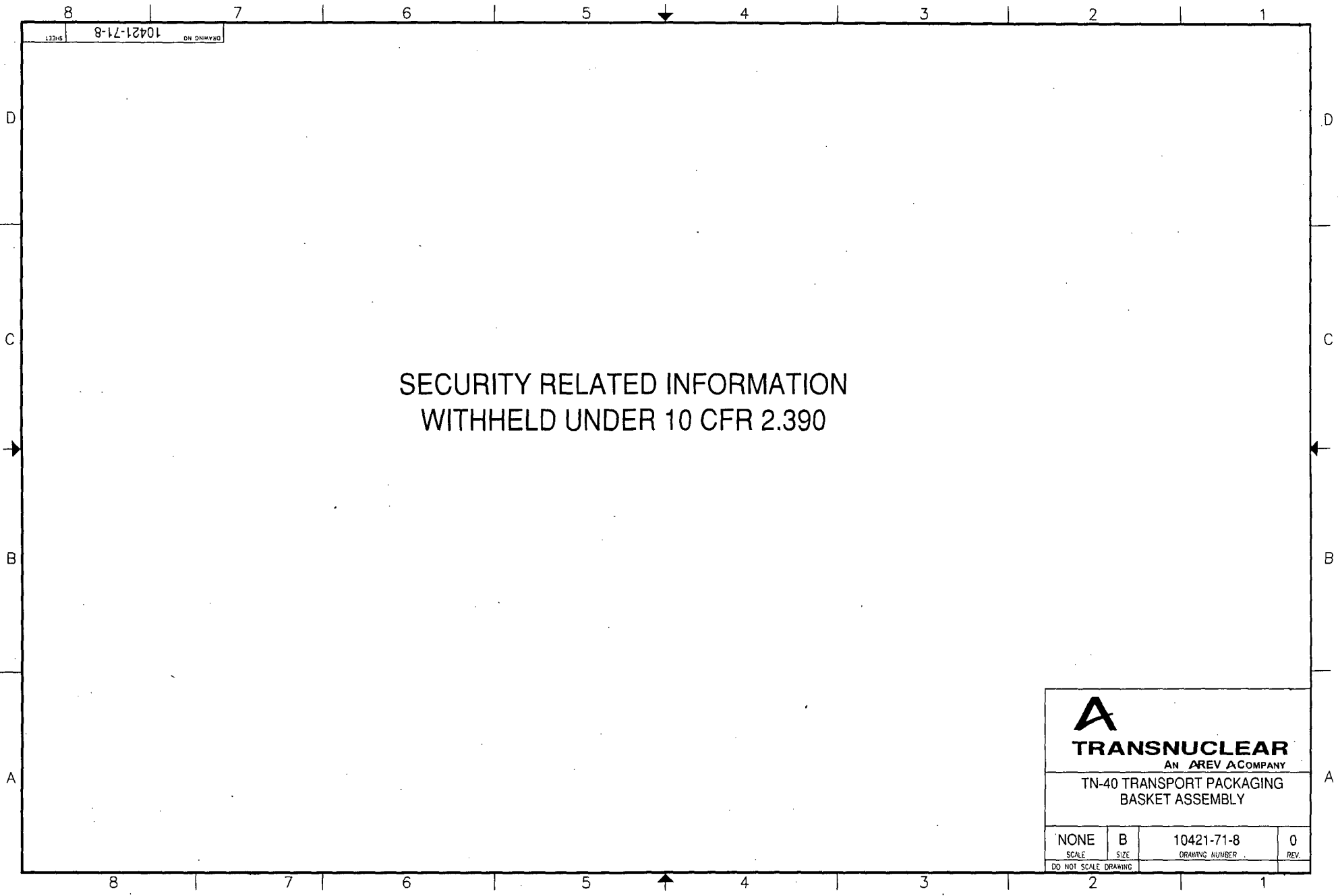
SECURITY RELATED INFORMATION
WITHHELD UNDER 10 CFR 2.390



TN-40 TRANSPORT PACKAGING
IMPACT LIMITER SPACER DETAIL

NONE	B	10421-71-7	0
SCALE	SIZE	DRAWING NUMBER	REV.

DO NOT SCALE DRAWING




SECURITY RELATED INFORMATION
WITHHELD UNDER 10 CFR 2.390

A
TRANSNUCLEAR
AN AREV COMPANY

TN-40 TRANSPORT PACKAGING
BASKET DETAILS

NONE	B	10421-71-9	0
SCALE	SIZE	DRAWING NUMBER	REV.
DO NOT SCALE DRAWING			

SECURITY RELATED INFORMATION
WITHHELD UNDER 10 CFR 2.390

 TRANSNUCLEAR AN AREV COMPANY			
TN-40 TRANSPORT PACKAGING REGULATORY PLATE			
NONE SCALE	B SIZE	10421-71-10 DRAWING NUMBER	0 REV.
DO NOT SCALE DRAWING			

SECURITY RELATED INFORMATION
WITHHELD UNDER 10 CFR 2.390



TN-40 TRANSPORT PACKAGING
IMPACT LIMITERS
GENERAL ARRANGEMENT

NONE	B	10421-71-40	0
SCALE	SIZE	DRAWING NUMBER	REV.

DO NOT SCALE DRAWING

10421-71-40

DRAWING NO.

SHEET

SECURITY RELATED INFORMATION
WITHHELD UNDER 10 CFR 2.390




TN-40 TRANSPORT PACKAGING
IMPACT LIMITERS
PARTS LIST & NOTES


NONE	B	10421-71-41	0
SCALE	SIZE	DRAWING NUMBER	REV.

DO NOT SCALE DRAWING

SECURITY RELATED INFORMATION
WITHHELD UNDER 10 CFR 2.390

 TRANSNUCLEAR AN AREVA COMPANY			
TN-40 TRANSPORT PACKAGING IMPACT LIMITERS ASSEMBLY			
NONE	B	10421-71-42	0
SCALE	SIZE	DRAWING NUMBER	REV.
DO NOT SCALE DRAWING			

SECURITY RELATED INFORMATION
WITHHELD UNDER 10 CFR 2.390

 TRANSNUCLEAR AN AREVA COMPANY			
TN-40 TRANSPORT PACKAGING IMPACT LIMITERS DETAILS			
NONE	B	10421-71-43	0
SCALE	SIZE	DRAWING NUMBER	REV.
DO NOT SCALE DRAWING			

DRAWING NO. 10421-71-43
SHEET

SECURITY RELATED INFORMATION
WITHHELD UNDER 10 CFR 2.390



TN-40 TRANSPORT PACKAGING
IMPACT LIMITERS
PARTS

NONE	B	10421-71-44	0
SCALE	SIZE	DRAWING NUMBER	REV.
DO NOT SCALE DRAWING			

CHAPTER 2

STRUCTURAL EVALUATION

TABLE OF CONTENTS

	<u>Page</u>
2.0 STRUCTURAL EVALUATION.....	2-1
2.1 Structural Design	2-1
2.1.1 Discussion	2-1
2.1.2 Design Criteria.....	2-3
2.2 Weights and Center-Of-Gravity.....	2-6
2.3 Mechanical Properties of Materials.....	2-6
2.3.1 Cask Material Properties	2-6
2.3.2 Basket Material Properties	2-6
2.3.3 Impact Limiter Material Properties	2-6
2.3.4 Fracture Toughness Requirements	2-7
2.4 General Standards For All Packages.....	2-7
2.4.1 Minimum Package Size	2-7
2.4.2 Tamper-proof Feature	2-7
2.4.3 Positive Closure	2-7
2.4.4 Chemical and Galvanic Reactions.....	2-7
2.5 Lifting And Tie-Down Standards	2-10
2.5.1 Lifting Devices	2-10
2.5.2 Tie-Down Devices	2-11
2.6 Normal Conditions Of Transport	2-11
2.6.1 Heat.....	2-13
2.6.2 Cold Environment.....	2-14
2.6.3 Increased External Pressure (N4)	2-14
2.6.4 Reduced External Pressure (N5).....	2-14

2.6.5	Transport Shock Loading (N14 & N15).....	2-15
2.6.6	Transport Vibration Loading (N12 & N13)	2-15
2.6.7	Water Spray	2-16
2.6.8	Free Drop (N6 through N11):.....	2-16
2.6.9	Corner Drop.....	2-16
2.6.10	Compression	2-16
2.6.11	Penetration	2-16
2.6.12	Lid Bolt Analysis	2-16
2.6.13	Fatigue Analysis of the Containment Boundary.....	2-17
2.6.14	Structural Evaluation of the Basket under Normal Condition Loads	2-20
2.6.15	Summary of NCT Cask Body Structural Analysis	2-21
2.7	Hypothetical Accident Conditions	2-21
2.7.1	30 Foot Free Drop	2-22
2.7.2	Puncture	2-24
2.7.3	Thermal	2-27
2.7.4	Water Immersion	2-27
2.7.5	Structural Evaluation of the Basket under Accident Loads	2-29
2.7.6	Summary of HAC Cask Body Structural Analysis.....	2-30
2.8	Special Forms / Fuel Rods.....	2-30
2.8.1	Special Form	2-30
2.8.2	Fuel Rods	2-30
2.9	References	2-31
2.10	Appendices	2-33
2.11	ASME Code and NUREG-0612 Alternatives	2-34

LIST OF TABLES

Table 2-1	Evaluation Method Employed to Demonstrate Compliance with Specific Regulatory Requirements.....	2-39
Table 2-2	Containment Vessel Stress Limits	2-40
Table 2-3	Cover Bolt Stress Limits.....	2-41
Table 2-4	Non Containment Structure Stress Limits	2-42
Table 2-5	Basket Stress Limits	2-43
Table 2-6	Cask Weight and Center of Gravity	2-44
Table 2-7	Trunnion Section Properties and Applied Loads.....	2-45
Table 2-8	Trunnion Stresses when Loaded by 6 and 10 Times Cask Weight (Lifting).....	2-46
Table 2-9	TN-40 Performance Evaluation Overview (Normal Conditions of Transport)	2-47
Table 2-10	Individual Load Cases for Normal Conditions of Transport TN-40 Cask Body Analysis	2-48
Table 2-11	Summary of Load Combinations for Normal Condition of Transport.....	2-49
Table 2-12	Reference Temperatures for Stress Analysis Acceptance Criteria	2-51
Table 2-13	Summary of Load Combination Stresses for Normal Conditions of Transport	2-52
Table 2-14	Linearized Stress Evaluation of Normal Condition of Transport Load Combinations.....	2-54
Table 2-15	TN-40 Performance Evaluation Overview (Hypothetical Accident Conditions of Transport)	2-58
Table 2-16	Summary of Individual Load Factors for Hypothetical Accident Condition of Transport	2-59
Table 2-17	Summary of Load Combinations for Hypothetical Accident Condition of Transport	2-60
Table 2-18	Summary of Load Combination Stresses for Hypothetical Accident Condition of Transport	2-61
Table 2-19	Linearized Stress Evaluation for Hypothetical Accident Condition Load Combinations.....	2-62

LIST OF FIGURES

Figure 2-1 Geometry of Upper (front) and Lower (rear) Trunnions.....2-64

Figure 2-2 290 psig Immersion Analysis Finite Element Model Loads and
Boundary Conditions2-65

2.0 STRUCTURAL EVALUATION

2.1 Structural Design

This chapter, including its appendices, presents the structural evaluation of the TN-40 transport packaging. This evaluation consists of numerical analyses and impact limiter testing which demonstrate that the TN-40 packaging satisfies applicable requirements for a Type B(U) packaging.

2.1.1 Discussion

The structural integrity of the packaging under normal conditions of transport (NCT) and hypothetical accident conditions (HAC) specified in 10CFR71 [1] is shown to meet the design criteria described in Section 2.1.2. The TN-40 transport package consists of three major structural components: the cask body, the fuel basket, and the impact limiters (top and bottom). These components are described in Chapter 1 and are shown on drawings provided in Appendix 1.4.1.

The cask body is described in Section 1.2. Drawing 10421-71-1 shows the parts list. Drawing 10421-71-2 shows the overall transport configuration of the TN-40 transport package. Drawing 10421-71-3 shows the general arrangement of the TN-40 packaging. Drawings 10421-71-4 and 10421-71-5 present the lid assembly and details. Drawing 10421-71-6 shows the trunnion/basket rail/neutron shield details and 10421-71-7 shows the impact limiter top spacer. Drawings 10421-71-8 and 10421-71-9 show the basket assembly. The regulatory plate is provided on Drawing 10421-71-10. Drawings 10421-71-40 through 10421-71-44 provide details of the impact limiter design.

The inner shell and the bottom inner plate are made of SA-203, Grade D or E. The shell flange is SA-350 Grade LF3 and the lid outer plate is constructed with SA-350 Grade LF3 or SA-203 Grade E. The gamma shield shell and bottom shield are SA-266, CL 4, SA-516, Grade 70, or SA-105. The lid shield plate is constructed from SA-105 or SA-516 Grade 70.

In order to obtain a close fit between the inner shell and the gamma shield shell, for better heat transfer, the gamma shield shell is heated prior to assembling it with the inner shell. As the gamma shield shell cools, an axial gap may form between the shell flange and the gamma shield. Shims may be machined to fill the gap and act as a backing plate for the 0.50 inch weld, between the shell flange and the gamma shield shell.

The four upper and lower trunnions are cylindrical, SA-105 or SA-266 Class 4 forgings that are welded to the gamma shield shell of the cask body. The two upper trunnions are designed to lift the loaded TN-40 cask vertically. The lower trunnions provide the capability to rotate the cask on the upending/downending frame. The upper trunnions are designed to meet the requirements of NUREG-0612[29] for a non-redundant lifting fixture, see Section 2.11 for a detailed description. The trunnions are shown in Drawing 10421-71-6.

The outer shell around the neutron shield consists of a cylindrical shell section, with closure plates at each end of the neutron shield. The closure plates are welded to the outer surface of the gamma shield shell. The outer shell provides an enclosure for the resin-filled aluminum containers, and maintains the resin in the proper location with respect to the active length of the fuel assemblies in the cask cavity. The shell is made of SA516 Grade 55 or equivalent carbon steel.

The basket is a welded assembly of stainless steel fuel compartment boxes, and is designed to accommodate 40 fuel assemblies. The fuel compartment stainless steel box sections are attached together locally by cylindrical stainless steel plugs (that pass through the aluminum and Boral[®] plates) that are fusion welded to the adjacent box sections. The basket contains 40 compartments for proper spacing and support of the fuel assemblies. Neutron poison plates, constructed from Boral[®], are sandwiched between the sections of the stainless steel walls of the adjacent box and the adjacent stainless steel plates. Drawings 10421-71-8 and 10421-71-9 show details of the basket.

Structural rails oriented parallel to the axis of the cask are attached to the inner surface of the inner shell to establish and maintain basket orientation, to prevent twisting of the basket assembly, and to support the edges of those plates adjacent to the rails, which would otherwise be free to slide tangentially around the cask cavity wall under lateral inertial loadings.

The cask body and the fuel basket together with the two impact limiters, form the packaging which is designed to meet all of the applicable 10CFR71 [1] requirements for a Type B(U) packaging. The maximum normal operating pressure (MNOP) is 15.7 psig.

The wall thickness of the cask body (excluding the outer shell and outer shell closure plates) enables the packaging to withstand the hypothetical puncture accident. The gamma shield shell is designed to be both strong and ductile. The top and bottom impact limiters absorb the kinetic energy for the 1 foot NCT and 30 foot HAC free drops.

Table 2-1 summarizes the specific evaluation methods that are used to demonstrate compliance with the regulations. Numerical analyses have been performed for the NCT and HAC event, as well as for the lifting and tie-down loads. In general, numerical analyses have been performed for all of the regulatory events. These analyses are summarized in the main body of this section, and are described in detail in Appendices 2.10.1 through 2.10.8. Testing of the impact limiters is planned to confirm the analytical results from the Transnuclear in-house computer program (ADOC) [28]. The test specification is included in Appendix 2.10.9.

The detailed structural analyses of the TN-40 packaging are included in the following appendices:

- Appendix 2.10.1 Structural Analysis of the Cask Body
- Appendix 2.10.2 Lid Bolt Analysis
- Appendix 2.10.3 Structural Analysis of the Outer Shell

- Appendix 2.10.4 Fracture Toughness Evaluation of the TN-40 Cask
- Appendix 2.10.5 Structural Analysis of the TN-40 Basket
- Appendix 2.10.6 Dynamic Load Factor for Basket Drop Analysis
- Appendix 2.10.7 Structural Evaluation of the Fuel Rod Cladding Under Accident Impact
- Appendix 2.10.8 Structural Evaluation of the Impact Limiters
- Appendix 2.10.9 Impact Limiter Test Specification

2.1.2 Design Criteria

The packaging consists of three major components:

- Cask Body
- Fuel Basket
- Impact Limiters

The structural design criteria for these components are described below.

2.1.2.1 Cask Body

2.1.2.1.1 Containment Vessel

The containment vessel consists of the inner shell with the shell flange out to the seal seating surface, the bottom inner plate, and the lid. The lid bolts and seals are also part of the containment vessel as are the drain and vent port cover plates, bolts and seals. The containment vessel is designed to the maximum practical extent as an ASME Class I component in accordance with the rules of the ASME Boiler and Pressure Vessel Code, Section III, Subsection NB [3]. The Subsection NB rules for materials, design, fabrication and examination are applied to all of the above components to the maximum practical extent. In addition, the design meets the requirements of Regulatory Guides 7.6 [5] and 7.8 [6]. Alternatives to the ASME Code are discussed in Section 2.11 of this Chapter.

The acceptability of the containment vessel under the applied loads is based on the following criteria:

- Title 10, Chapter 1, Code of Federal Regulations, Part 71
- Regulatory Guide 7.6 Design Criteria
- ASME Code Design Stress Intensity Limits
- Preclusion of Fatigue Failure
- Preclusion of Brittle Fracture

The stresses due to each load are categorized as to the type of stress induced (e.g., membrane, bending) and the classification of stress (e.g., primary, secondary). Stress limits for containment vessel components, other than bolts, for NCT and HAC loads are given in Table 2-2. The stress limits used for HAC conditions, determined on an elastic

basis, are based on the entire structure (containment vessel and gamma shielding material) resisting the accident load. Local yielding is permitted at the point of contact where the load is applied.

The primary membrane stresses and primary membrane plus bending stresses in the cask are limited under NCT to S_m (S_m is the code allowable stress intensity) and $1.5 S_m$, respectively.

The HAC impact events are evaluated as short duration, Level D conditions. The stress criteria are taken from Section III, Appendix F of the ASME Code [7]. For elastic quasi-static analysis, the primary membrane stress intensity P_m is limited to $0.7 S_u$, and membrane plus bending stress intensities ($P_m + P_b$) are limited to S_u .

The allowable stress limits for the cover bolts are listed in Table 2-3. The allowable stress limits for the lid closure bolts are listed separately in Appendix 2.10.2, Tables 2.10.2-3 and 2.10.2-4.

The allowable stress intensity values S_m or S_u as defined by the Code, are taken at the maximum component temperature calculated for each service load condition.

2.1.2.1.2 Non-Containment Structure

Certain components of the cask body such as the gamma shield shell, the neutron shield outer shell and the trunnions do not provide containment but do have structural functions. These components (referred to as non-containment structures) are required to withstand the environmental loads, and in some cases share the loads with the containment vessel. The stress limits for these non-containment structures are given in Table 2-4. The gamma shield shell and neutron shield outer shell are designed, fabricated and inspected in accordance with the ASME Code Subsection NF [3], to the maximum practical extent. Structural and structural attachment welds are examined by the liquid penetrant or the magnetic particle method, in accordance with Section V, Article 6 of the ASME Code [8]. The magnetic particle and liquid penetrant examination acceptance standards are in accordance with Section III, Subsection NF, Paragraphs NF-5340 and NF-5350 [3].

The welding procedures, welders and weld operators are qualified in accordance with Section IX of the ASME Code [10].

The radial neutron shield, including the carbon steel outer shell, has not been designed to withstand all of the HAC loads.

2.1.2.2 Basket

The basket is designed in accordance with the ASME Code Subsection NB [3], to the maximum practical extent. The TN-40 was developed as a storage cask and as such the basket and containment were designed using the stress limits from ASME Code Subsection NB. NCT stress limits specified in NB are the same as NG which is

currently used for transportation packages. For HAC, both NB and NG require use of Appendix F for the stress limits. Therefore, the basket design meets the NG stress limits as specified in the current Standard Review Plan [12]. The alternatives to ASME codes are listed in Section 2-11.

The neutron poison sheets are not included in the structural analysis. Therefore, the materials are not required to be ASME Code materials. The aluminum plates between the fuel compartments and aluminum basket rail are not Class 1 material. Aluminum was selected for its excellent thermal conductivity and a high strength to weight ratio. NUREG-3854 [11] and NUREG-1617 [12] allow materials other than ASME Code materials to be used in the cask fabrication. The ASME Code does provide the material properties for the aluminum alloy and also allows the material to be used for Section III applications (Class 2 or 3).

The stress limits for the basket are summarized in Table 2-5. The wall thickness of the basket fuel compartment is designed to meet the heat transfer, nuclear criticality, and the structural requirements. The basket structure provides sufficient rigidity to maintain a subcritical configuration under the applied loads.

The basis for the allowable stresses for the compartment box and the fusion welds is Section III, Division I, Subsection NB of the ASME Code [3]. The primary membrane stresses and primary membrane plus bending stresses in the basket are limited to S_m (S_m is the code allowable stress intensity) and $1.5 S_m$, respectively, for NCT loads.

The HAC events are evaluated as short duration, Level D conditions. The stress criteria are taken from Section III, Appendix F of the ASME Code [7]. The membrane and membrane plus bending stresses were compared against $0.7 S_u$ and $0.9 S_u$ elastic-plastic analysis stress criteria values for the HAC drop events.

The fuel compartment walls under compressive loads are also evaluated to ensure that buckling will not occur. ANSYS nonlinear buckling analysis is used to calculate the buckling load. See Appendix 2.10.5 for complete details of criteria for these conditions.

2.1.2.3 Impact Limiters (Top and Bottom)

The TN-40 packaging includes impact limiters at each end of the cask body. The limiters are nearly identical. The inside diameter of the limiter is determined by the diameter of the gamma shield shell. The length and outside diameter of the limiter are sized to limit the cask inertial loads during the 1 foot NCT and 30 foot HAC drop events so that the containment vessel (and the non-containment structures) meets the design criteria.

The impact limiter stainless steel cylinders, gussets, and end plates are designed to position and confine the balsa and redwood blocks so that the impact energy is properly absorbed. The stainless steel shell is also designed to support and protect the wood blocks under NCT environmental conditions (moisture, pressure, temperature, etc.).

The impact limiters and attachments are designed to withstand the applied loads and to prevent separation of the limiters from the cask during any NCT or HAC impact. The design criteria for the impact limiters and attachments are specified in Appendix 2.10.8.

2.1.2.4 Trunnions

The evaluation and design criteria for the lifting trunnions are based on the requirements of 10CFR71.45 [1]. The details of the evaluation are presented in Section 2.5. The evaluation demonstrates that the upper trunnions, used for lifting, have a minimum factor of safety of six against yield or ten against ultimate, whichever is most restrictive. The top trunnions are designed to meet the requirements of NUREG-0612[29] for a non-redundant lifting fixture. This is accomplished by evaluating the trunnions to the stress design factors required by ANSI N14.6[2].

2.2 Weights and Center-Of-Gravity

The weight of the TN-40 packaging is 271.46 kips. The weights of the major individual subassemblies are listed in Table 2-6. The center of gravity of the cask is located on the axial centerline approximately 91.4 inches from the base of the cask.

The calculations that follow typically use conservative weights that are slightly higher than those listed in Table 2-6. These are:

1. Lifting (w/o impact limiters), 250 kips
2. Tiedown analyses, 271.7 kips
3. Cask Body analysis 271.7 kips

2.3 Mechanical Properties of Materials

2.3.1 Cask Material Properties

This section provides the mechanical properties of materials used in the structural evaluation of the TN-40 cask. Drawing 10421-71-1 (see Appendix 1.4.1) lists the materials selected for each component of the transport cask. The minimum yield, ultimate, and design stress values are taken from ASME Code, Section III, Appendices [7].

2.3.2 Basket Material Properties

The material properties of the 304 stainless steel plates are taken from the ASME Code, Section III, Appendices. The material properties of the aluminum alloy (6061-T6) are also taken from the ASME Code [7] and aluminum standards and data [23].

2.3.3 Impact Limiter Material Properties

Mechanical properties of the energy absorbing wood and wood adhesive used in the impact limiters are specified in Appendix 2.10.8 (Table 2.10.8-1).

2.3.4 Fracture Toughness Requirements

The cask body and closure lid material is a ferritic steel and is therefore subject to fracture toughness requirements in order to assure ductile behavior at the lowest service temperature (LST) of -20°F . See Appendix 2.10.4 for fracture toughness evaluation. The fracture toughness evaluations in Appendix 2.10.4 show that the TN 40 cask materials meet the fracture toughness criteria of NUREG/CR-3826 [21] and NUREG/CR-1815 [22].

2.4 General Standards For All Packages

The TN-40 is designed to comply with the general standards for all packages specified by 10CFR71.43 [1].

2.4.1 Minimum Package Size

The overall package dimensions of 260.87 inches long and 144 inches in diameter exceed the minimum dimension requirement of 10 cm (4 inches).

2.4.2 Tamper-proof Feature

The only access path into the package is through the closure lid and associated lid closure bolts. During transport the top (front) impact limiter entirely covers and prevents access to the cask closure lid and the vent and access port penetrations in the lid. A wire security seal is installed in the top (front) impact limiter attachment tierod prior to each shipment. The presence of this seal demonstrates that unauthorized opening of the package has not occurred.

2.4.3 Positive Closure

Positive fastening of all access openings through the containment vessel is accomplished by bolted closures which preclude unintentional opening. In addition, the presence of the impact limiters and security seal described in Section 2.4.2 provide further protection against unintentional opening.

2.4.4 Chemical and Galvanic Reactions

The materials of the TN-40 cask have been reviewed to determine whether chemical, galvanic or other reactions between the materials, contents and environment might occur during any phase of loading, unloading, handling or transport.

The TN-40 cask components are exposed to the following environments:

- During loading and unloading, the casks are submerged in pool water. For PWR plants the pool water is borated. The casks are only kept in the spent fuel pool for a short period of time, typically about 24 hours to load or unload fuel. After removing the cask from the pool, water or water vapor is present during the draining and drying process. This takes approximately 1 - 2 hours to drain, and another 20-24 hours to completely dry, evacuate and backfill the cask with helium.

- During handling and transportation, the exterior of the cask is exposed to normal environmental conditions of temperature, rain, snow, etc.
- During transportation, the interior of the cask is exposed to an inert helium environment. The helium environment does not support chemical or galvanic reactions because both moisture and oxygen must be present for a reaction to occur. The cask is thoroughly dried by a vacuum drying process before transport. It is then sealed and backfilled with helium.
- The radial neutron shielding materials and the aluminum resin boxes are sealed inside the outer shell during normal operations. The resin material is inert after it has cured and does not affect the aluminum boxes or the carbon steel housing.

2.4.4.1 Cask Interior

The TN-40 cask materials are shown in the Parts List on Drawing 10421-71-1 (see Appendix 1.4.1).

The containment vessel is made from SA-203 Grade D or E and SA-350 Grade LF3. The vessel interior surfaces are grit blasted and then metal-sprayed with aluminum/zinc alloy.

The metal-spray coating is subject to the following service environments:

- After fabrication, the cask is closed and shipped with air in the cask cavity.
- At fuel loading, borated spent fuel pool water is present in the cavity for a short duration.
- The cask is vacuum-dried and helium backfilled for storage lifetime of 20 years and/or off-site transport.
- At fuel removal, the coating may again be exposed to borated spent fuel pool water for a short duration.

The coating is not subject to abrasion except for the one-time insertion of the basket into the containment vessel.

All sealing surfaces are stainless steel clad by weld overlay. The metallic seals have a stainless steel liner and an aluminum jacket.

Within the cask cavity, there are 6 basket rails made from 6061-T6 or -T651 aluminum. The rails are shown on the drawings provided in Appendix 1.4. These rails are not coated.

The cask basket is assembled from SA-240, Type 304 stainless steel boxes which are joined together by a fusion welding process and are separated by aluminum and poison plates which form a sandwich panel. The aluminum plates are 6061 -T651 aluminum.

The aluminum plates are held in place by the stainless steel plugs to which the boxes are welded. The aluminum is not welded or bolted to the stainless steel.

The Boral[®] sheets are also held in place by the stainless steel plugs and are captured between the stainless steel boxes. The Boral[®] is not welded or bolted to the stainless steel.

2.4.4.2 Cask Exterior

The exterior of the cask is carbon steel. The exterior of the cask, with the exception of the trunnion bearing surfaces is thermal sprayed and then painted using an epoxy, acrylic urethane, or equivalent enamel coating. The paint is selected to be compatible with the pool water and easy to decontaminate.

The paint is visually inspected prior to immersion of the cask in the spent fuel pool and prior to transport. Touch up painting is performed if the paint deteriorates.

2.4.4.3 Lubricants and Cleaning Agents

Neolube, Loctite N-5000 or equivalent may be used to coat the threads and bolt shoulders of the TN-40 closure bolts. Never-seez or equivalent is used to coat the contact areas of the top and bottom trunnions prior to lifting operations to prevent impregnation of contamination into the trunnion surface. The lubricant should be selected for compatibility with the spent fuel pool water and the cask materials.

The cask body is cleaned in accordance with approved procedures to remove cleaning residues prior to shipment to the loading site. The basket is also cleaned prior to installation in the cask. The cleaning agents and lubricants have no significant effect on the cask materials and their safety related functions.

2.4.4.4 Hydrogen Generation

Prairie Island's report to the NRC [13] [14] in response to NRC Bulletin 96-04 demonstrates that galvanic reactions in hydrogen generation are insignificant for the TN-40 cask. Unlike welded canisters, the TN-40 cask has a bolted closure. There is no source of ignition to result in an explosion or fire.

2.4.4.5 Effect of Galvanic Reactions on the Performance of the Cask

There are no significant reactions that could reduce the overall integrity of the cask or its contents during storage. The cask and fuel cladding thermal properties are provided in Chapter 3. The emissivity of the basket fuel compartment is 0.3, which is typical for non-polished stainless steel surfaces. If the stainless steel is oxidized, this value would increase, improving heat transfer. The fuel rod emissivity value used is 0.8, which is a typical value for oxidized Zircaloy. Therefore, the passivation reactions would not reduce the thermal properties of the component cask materials or the fuel cladding.

There are no reactions that would cause binding of the mechanical surfaces or the fuel to basket compartment boxes due to galvanic or chemical reactions.

The stainless steel, aluminum, Boral[®] and thermal spray are negligibly affected by the short term exposure to borated water during loading. While formation of blisters in Boral[®] during vacuum drying and heating has been reported, this has not been associated with displacement of the Boral[®] core material containing the boron carbide and therefore has no effect on the Boral[®] criticality safety design function. Furthermore, in the TN-40, the Boral[®] is captured between the structural basket components to provide it with added mechanical support and durability. The outer aluminum lid seals may experience some combination of crevice and galvanic corrosion if they are exposed to water for an extended period of storage prior to transport. However, this would affect only the outer (non-containment) seal, and the seals are tested prior to transport.

There is no significant degradation of any safety components caused directly by the effects of the reactions or by the effects of the reactions combined with the effects of long term exposure of the materials to neutron or gamma radiation, high temperatures, or other possible ambient or operating conditions.

2.5 Lifting And Tie-Down Standards

2.5.1 Lifting Devices

10CFR 71.45(a) [1] requires that a minimum factor of safety of three against yield is required for all lifting attachments which are structural parts of the package. In addition, the package must be designed such that failure of any lifting device under excessive load would not impair the ability of the package to meet the requirements of 10CFR71 [1]. The stress analyses of the trunnions are provided in the following section.

2.5.1.1 Trunnion Analysis

The trunnion geometry is shown in Figure 2-1. The front (upper) and rear (lower) trunnions are constructed from SA-105 or SA-266 Class 4 forgings and are groove welded to the cask body. A flat surface is machined on the cask body outer surface at each trunnion location for this purpose.

The two front trunnions are used for lifting the cask and are evaluated to the requirements of ANSI N14.6 [2] with alternatives listed in Section 2.11. They can support a loading equal to 6 times the weight of the cask without generating stresses in excess of the minimum yield strength of the material. They can also lift 10 times the weight of the cask without exceeding the ultimate tensile strength of the material.

The rear trunnions are used to rotate the cask from a horizontal orientation to the vertical orientation. The lower trunnions will not be used to lift a loaded cask. The lower trunnions are conservatively designed to support 50% of the load carried by the front trunnions.

A cask weight of 250,000 lb is used in this analysis. Table 2-7 shows the cross sectional area and moment of inertia at shoulder and weld cross sections of both front and rear trunnions. In addition, the loads applied to these sections (for 6g and 10g loadings) to evaluate the yield and ultimate limits are also listed.

Table 2-8 presents a summary of the stresses at the same locations to compare against the trunnion yield and ultimate strengths. Also listed are the allowable stresses (yield and ultimate strengths).

The reported data show that all of the calculated stresses in both the front and rear trunnions are acceptable, and that the minimum margin of safety is 0.06 for the yield condition and 0.28 for the ultimate condition. Both minimums occur in the front trunnions. Therefore the requirements of 10CFR 71.45(a) are met.

2.5.2 Tie-Down Devices

There are no tiedown devices that are a structural part of the package.

The longitudinal forces experienced by the transport package, per 10 CFR 71.45(b), are resisted by steel end restraints which flush up against the impact limiters. The vertical and lateral forces that act on the transport package, according to 10 CFR 71.45(b) and NUREG 766510 [17], are restrained by a dual saddle/strap tie-down system. Specifically, the tie-down straps resist uplifting and lateral overturning forces whereas the saddles react downward and strap reaction forces. This restraint system is also designed to preclude yielding in the load bearing material of the transport package during normal transport conditions. The premise for both of these tie-down systems is to add extra safety margin by utilizing the large load-bearing surface areas available to distribute transport loads, instead of creating the relatively large localized stresses associated with using the trunnions as transport tie-down points. This loading condition is analyzed in Appendix 2.10.1 (Load Step IL-9). The stress results from the tie-down load are presented in Table 2.10.1-2. All the calculated stresses are less than the lowest yield strength of 31.8 ksi (gamma shield shell).

2.6 Normal Conditions Of Transport

Overview

This section describes the response of the TN-40 package to the loading conditions specified by 10CFR71.71 [1]. The design criteria established for the TN-40 for the NCT are described in Section 2.1.2. These criteria are selected to ensure that the package performance standards specified by 10CFR71.43 and 71.51 [1] are satisfied. Under NCT, there will be no loss or dispersal of radioactive contents, no significant increase in external radiation levels, and no substantial reduction in the effectiveness of the packaging.

Detailed structural analyses of various TN-40 package components subjected to individual loads are provided in the Appendices to this chapter. The limiting results from

these analyses are used in this section to quantify package performance in response to the NCT load combinations, specified in 10CFR71.71 [1] and Regulatory Guide 7.8 [6]. Table 2-9 provides an overview of the performance evaluations reported in each load combination subsection. Each subsection provides the limiting structural analysis result for the affected cask component(s) in comparison to the established design criteria. This comparison permits the minimum margin of safety for a given component subjected to a given loading condition to be readily identified. In all cases, the acceptability of the TN-40 packaging design with respect to established criteria, and consequently with respect to 10CFR71 [1] performance standards is demonstrated.

The structural analysis of the cask body is presented in Appendix 2.10.1 and covers a wide range of individual loading conditions. The stress results from the various individual loads must be combined in order to represent the stress condition in the cask body under the specified condition evaluated in this section. An explanation of the reporting format used for the results, and the stress combination technique used in applying the results from Appendix 2.10.1 is provided here.

Reporting Method for Cask Body Stresses

Appendix 2.10.1 provides the detailed description of the structural analyses of the TN-40 cask body. The appendix describes the detailed ANSYS [15] model used to analyze various applied loads. Table 2-10 identifies the individual loads (IL) analyzed which are applicable to NCT.

Detailed stresses are available at as many locations as there are nodes in the finite element model. However, for practical considerations, only the maximum stresses in the lid, flange, inner shell, gamma shield shell, and bottom shield are reported for each load case. These components were selected to be representative of the stress distribution in the cask body. The maximum stress may occur in different components for each individual load.

The stress results for the individual load case (tables reported in Appendix 2.10.1) are for one individual load only. Two or more individual load cases must be combined to determine the total stresses at the standard stress reporting locations for the various load combinations. This is accomplished using the ANSYS post-processor.

For those load combinations that include trunnion reactions, the local stresses at the trunnion locations found by the Bijlaard [16] method are superimposed on the ANSYS combined stresses.

Table 2-11 provides a matrix of the individual loads, and the various combinations, to determine the cask body stresses for the specified NCT. An "x" in Table 2-11 indicates that the stress results for the individual load case are used in the load combinations.

For the increased external pressure load combination, it is assumed that the TN-40 cask cavity is at 0 psia. For conservatism, a 25 psig external pressure is used for load combinations.

2.6.1 Heat

Chapter 3 describes the thermal analyses of the TN-40 package, subjected to high and low temperature environmental conditions. The analyses results are used to support various aspects of the structural evaluations as described in the following subsections.

2.6.1.1 Maximum Temperatures

Allowable stresses for the packaging components are a function of the component temperatures, which are based on actual maximum calculated temperatures or conservatively selected higher temperatures. Chapter 3 summarizes the significant temperatures calculated for the TN-40 package subjected to high temperature environmental conditions. These temperatures are used in establishing the allowable stress values for every NCT load combination, evaluated in this Safety Analysis Report.

Table 2-12 summarizes the thermal analysis results from Chapter 3. The table also lists the selection of cask and basket component design temperatures for structural analysis purposes.

2.6.1.2 Maximum Internal Pressure

The thermal analysis, presented in Chapter 3, also provides the average cavity gas temperature under high temperature environmental conditions. This value is used in Chapter 4 to determine the Maximum Normal Operating Pressure (MNOP). For purposes of the structural analysis of containment, a value of 100 psig (much higher than the Chapter 4 value, 15.7 psig) is conservatively assumed for the cask body stress calculation. This pressure loading is analyzed using the ANSYS model of the cask body described in Appendix 2.10.1, and the results are reported in Table 2.10.1-2. This load case and corresponding results are designated as individual load IL-3. IL-3 is used to support evaluations of the load combinations listed in Table 2-11.

2.6.1.3 Thermal Stresses (Hot)

The thermal analysis of the TN-40 is performed as described in Chapter 3. The temperature distribution from that analysis is used to perform an ANSYS thermal stress analysis of the cask body. The stress results for this load case are reported on Table 2.10.1-2. This load case is designated as IL-5 (thermal stresses at 100°F ambient) and is used to support various load combinations.

2.6.1.4 Hot Environment Load Combinations (N1)

Cask body stresses for the high temperature environment for NCT, are obtained by a combination of individual loads as summarized in Table 2-11. For this condition, it is assumed that the cask is in its transport configuration, mounted horizontally on the transport cradle, and supported by the front and rear saddles. Pre-load effects on the lid bolts, fabrication stress, 100 psig internal pressure, thermal stresses, and the local stresses at the tiedown straps are combined to give the maximum nodal stress intensity in each component for this load combination. The results are given in Tables 2-13 and 2-14.

2.6.2 Cold Environment

2.6.2.1 Thermal Stresses for Cold Environment at -20°F Ambient Temperature (N2)

The Regulatory Guide 7.8 [6] requires that the stresses due to the normal load condition to be combined with the thermal stresses for cold environment conditions at -20° F ambient temperature. The thermal stresses are determined in load case IL-6 with results tabulated in Table 2.10.1-2. Again, lid bolt preload, fabrication stress, external pressure, and gravity loads are also included in this combination. The maximum nodal stress intensity in each component for this load combination is listed in Tables 2-13 and 2-14.

2.6.2.2 Cold Environment Load Combinations at -40°F Ambient Temperature (N3)

The Regulatory Guide 7.8 [6] cold environment load combination results in all cask components in thermal equilibrium at -40° F. Containment vessel thermal stresses do occur in this case due to the differential thermal expansion between the steels. The thermal stresses are determined in load case IL-7 with results tabulated in Table 2.10.1-2. The cask cavity pressure at the cold environment condition is conservatively assumed to be 0 psia. This results in a net external pressure loading of 14.7 psig (25 psig is conservatively used). The stresses due to 25 psig external pressure are determined in load case IL-4 with results also given in Table 2.10.1-2. Again, lid bolt preload, fabrication stress, and gravity loads are included. The maximum nodal stress intensity in each component for this load combination is listed in Tables 2-13 and 2-14.

2.6.3 Increased External Pressure (N4)

Cask body stresses for the NCT increased external pressure, 20 psia, are obtained by a combination of individual loads as summarized in Table 2-11. The conservatively assumed minimum cask cavity pressure of 0 psia results in a net external pressure loading of 20 psig (25 psig is conservatively used). For this condition, the cask is assumed to be in the horizontal orientation, supported on the transport cradle front and rear saddles. Lid bolt pre-load, fabrication stress, gravity and the local tiedown strap effects are included. In addition, the thermal stresses for the -20°F minimum temperature are also included in the combination. The maximum nodal stress intensity in each component for this load combination is listed in Tables 2-13 and 2-14.

2.6.4 Reduced External Pressure (N5)

Cask body stresses for the 3.5 psia ambient NCT external pressure decrease are obtained by a combination of individual loads as summarized in Table 2-11. The net internal pressure is calculated as $(15.7 + 14.7 - 3.5) = 26.9$ psig (cask stresses are conservatively calculated based on 100 psig pressure). For this condition, the cask is in the horizontal orientation supported on the transport cradle by front and rear saddles. Lid bolt pre-load, fabrication stress, gravity, and the local tiedown strap effects are included. The thermal stresses for the hot thermal condition are included in the load

combination. The maximum nodal stress intensity in each component for this load combination is listed in Tables 2-13 and 2-14.

2.6.5 Transport Shock Loading (N14 & N15)

The transport rail shock loadings used to evaluate the TN-40 transport cask are based on NUREG 766510 [17] which specifies a maximum inertia loading of 4.7g in each of the three x-y-z coordinate directions:

- Vertical 4.7g
- Longitudinal 4.7g
- Lateral 4.7g

The resultant transverse load is $(4.7^2 + 4.7^2)^{1/2} = 6.65$ g

The stresses due to the transport rail shock individual load case are presented in Table 2.10.1-2. Tables 2-13 and 2-14 list the combined stresses (N14) under hot thermal conditions where the load combination is performed for the maximum temperature thermal stresses. Lid bolt pre-load, fabrication stress, internal pressure, and the local tiedown strap effects are included.

In addition, Tables 2-13 and 2-14 list the combined stresses (N15) under -20°F thermal conditions where the load combination is performed for the -20°F thermal stresses. Lid bolt pre-load, fabrication stress, external pressure, and the local tiedown strap effects are included.

2.6.6 Transport Vibration Loading (N12 & N13)

The input loading conditions used to evaluate the TN-40 cask for transport rail vibration are obtained from NUREG 766510 [17]. The peak inertia values used are:

- Vertical 0.37g
- Longitudinal 0.19g
- Lateral 0.19g

The resultant transverse load is $(0.37^2 + 0.19^2)^{1/2} = 0.42$ g

The stresses due to the transport rail car vibration individual load case are presented in Table 2.10.1-2. Tables 2-13 and 2-14 list the combined stresses (N12) under hot thermal conditions where the load combination is performed for the maximum temperature thermal stresses. Lid bolt pre-load, fabrication stress, internal pressure, and the local tiedown strap effects are included.

In addition, Tables 2-13 and 2-14 also list the combined stresses (N13) under -20°F thermal conditions where the load combination is performed for the -20°F thermal stresses. Lid bolt pre-load, fabrication stress, external pressure, and the local tiedown strap effects are included.

2.6.7 Water Spray

All exterior surfaces of the TN-40 cask body are metal and therefore not subject to soaking or structural degradation from water absorption. The water spray condition is therefore of no consequence to the TN-40.

2.6.8 Free Drop (N6 through N11)

Two drop orientations are considered credible for the one-foot NCT free drop (see Section 2.10.8.7 of Appendix 2.10.8 for detail descriptions). The structural response of the TN-40 cask body is evaluated for a one-foot end drop of the package on the bottom end, one foot end drop of the package on the lid end, and a one-foot side drop. The assessment of cask body stresses follows the same logic as that established in the previous sections. For the three drop cases, the evaluations are performed for both the hot temperature environment and at the -20°F minimum transport temperature.

The load combinations performed to evaluate these drop events are indicated in Table 2-11. In all cases, bolt pre-load effects and fabrication stress are included. For the hot environment condition, thermal stress load, 100 psig internal pressure, and impact load cases are combined. For the cold environment evaluation, -20°F thermal stress, 25 psig external pressure, and impact load cases are combined.

Tables 2-13 and 2-14 list the combined stress intensities for the bottom end, lid end and side drop under hot and cold environment conditions.

2.6.9 Corner Drop

This test does not apply to the TN-40 Package since the package weight is in excess of 100 kg (220 lbs.).

2.6.10 Compression

This test does not apply to the TN-40 Package since the package weight is in excess of 5,000 kg (11,000 lbs.).

2.6.11 Penetration

Due to lack of external protuberances, the one meter (40 inch) drop of a 13 pound steel cylinder of 1-1/4 inch diameter, with a hemispherical head, is of negligible consequence to the TN-40 Package.

2.6.12 Lid Bolt Analysis

The lid bolts are analyzed for both NCT and HAC loadings in Appendix 2.10.2. The analysis is based on NUREG/CR-6007 [18]. The bolts are analyzed for the following NCT loadings: operating pre-load, gasket seating load, internal pressure, temperature changes, and impact loads.

The bolt preload is calculated to withstand the worst case load combination and to maintain a clamping (compressive) force on the closure joint, during NCT and HAC events.

A summary of the calculated stresses is listed Section 2.10.2.6. The calculations result in a maximum NCT average tensile stress of 50.1 ksi, which is below the allowable tensile stress of 63.8 ksi. The average NCT shear stress in the bolts is due to torsion during pre-loading. This stress is 13.5 ksi, which is well below the allowable shear stress of 38.3 ksi. The maximum combined stress intensity due to NCT tension plus shear plus bending is 59.3 ksi which is also less than the allowable maximum stress intensity of 86.1 ksi.

The bolt fatigue analysis is also presented in Appendix 2.10.2. This analysis shows that the bolts should be replaced after approximately 50 shipments. This is primarily due to the pre-load stresses.

2.6.13 Fatigue Analysis of the Containment Boundary

The purpose of the fatigue analysis is to show that the containment vessel stresses are within acceptable NCT fatigue limits. This is done by determining the fatigue damage factor for each NCT event at locations on the containment vessel with the highest stresses. The cumulative fatigue damage or usage factor for all of the events is conservatively determined by adding the fatigue usage factors for the individual events, assuming these maximum stress intensities occur at the same location.

The fatigue analysis is based on the procedure described in Regulatory Guide 7.6 [5] and ASME Section III Appendices [7]. When determining the stress cycles, consideration is given to the superposition of individual loads which can occur together and produce a total stress intensity range greater than the stress intensity range of individual loads. Also, the maximum stress intensities for all individual loads are conservatively combined simultaneously. The sequence of events assumed for the fatigue evaluation is given below. The fatigue evaluation is based on 450 shipments.

1. Bolt Preload
2. Lifting
3. Test pressure
4. Road shock/vibration
5. Pressure and temperature fluctuations
6. 1 foot normal condition drop

Preload

The bolt preload specified to ensure a leak tight seal produces significant stresses in the lid. Therefore, this loading is conservatively included in the fatigue evaluation. The maximum stress calculated in Table 2.10.1-2 is 8,060 psi. It is assumed that the lid is installed twice per round trip resulting in 900 cycles.

Lifting

The stresses due to the 6g lifting load are listed in Table 2-10.1-2. The maximum stress intensity, which occurs in the lid, is 2,810 psi. However, when local stress due to the trunnion loading, 15,848 psi calculated in Table 2.10.1-3 is added to the maximum inner shell stress intensity of 1,840 psi (Table 2.10.1-2), the resulting total is 17,688 psi. This value is conservatively used in the fatigue evaluation. This loading is assumed to occur twice per round trip, so the total number of cycles is 900.

Test Pressure

The proof test is $1.25 \times (\text{maximum design pressure}) = 125 \text{ psi}$, and will only be performed once. The test pressure stresses are obtained by ratioing the 100 psig internal pressure stresses given in Table 2.10.1-2.

The maximum stress in the flange portion of the containment vessel due to a 100 psi internal pressure is 2,210 psi. Therefore, the stress due to the test pressure is $1.25 \times 2,210 = 2,763 \text{ psi}$. This pressure test only occurs once.

Shock

Since the TN-40 Cask may be shipped by rail car, the shock and vibration loadings are taken from reference [17].

Rail Car Shock

Rail car shock values were obtained from reference [17]. This reference states that the rail car can be expected to experience a 4.7g load in each direction 9 times every 100 miles. Again, assume 450 round trip shipments, averaging 2000 miles each way. Therefore the total number of cycles is $2000 (\text{miles}) \times 2 (\text{round trip}) \times 450 (\text{shipments}) \times 0.09 (\text{Shocks per mile}) = 162,000 \text{ cycles}$.

The stress intensities due to the rail shock load are listed in Tables 2-10.1-2. The maximum stress intensity in the lid is 1,750 psi.

Vibration

According to reference [17], the peak vibration loads at the bed of a railcar are 0.19g longitudinal, 0.19g lateral and 0.37g vertical. The maximum stress intensity resulting from these loads in any of the containment components is 110 psi, which is negligible.

Pressure and Temperature Fluctuations

There are four environmental conditions identified for normal condition of transport. These are hot environment, cold environment, reduced external pressure, and increase external pressure. The containment vessel stresses in response to these environmental load combinations were reported in Table 2-13. The highest total stress intensity from

these four cases, 18,090 psi, was calculated to occur in the inner shell during the hot environment condition.

The temperature and pressure fluctuations are assumed to occur once per round trip, since there is no cargo during the return trip, and therefore no pressurization or heat generation. So the total number of cycles of pressure and temperature fluctuation is 450.

1 Foot NCT Drop

The stress intensities due to the 1 foot end drop on bottom are listed in Table 2.10.1-2. The maximum stress intensity is in the lid portion of the containment vessel and is 120 psi (1g). Therefore, for a 12 g normal condition end drop, the maximum stress intensity is $120 \times 12 = 1,440$ psi.

The stress intensities due to the 1 foot end drop on lid end are listed in Table 2.10.1-2. The maximum stress intensity is in the flange portion of the containment vessel and is 170 psi (1g). Therefore, for 12 g normal condition end drop, the maximum stress intensity is $170 \times 12 = 2,040$ psi.

The stress intensities due to the 1 foot side drop are listed in Table 2.10.1-2. The maximum stress intensity at the containment vessel (flange) is 710 psi (1g). Therefore, for 16 g normal condition side drop, the maximum stress intensity is $710 \times 16 = 11,360$ psi.

This fatigue evaluation conservatively assumes that the cask is dropped once per shipment, resulting in 450 normal condition drops and using the maximum side stress intensity of 11,360 psi for the damage factor calculation.

Damage Factor Calculation

The following table is a summary of the fatigue evaluation. Although the maximum stress intensities for the different loading conditions do not occur at the same location, it is conservatively assumed that they do for the purpose of the fatigue evaluation. The value of the alternating stress, S_a , is determined as follows:

If one cycle goes from 0 to S.I (stress intensity):

$$S_a = S.I. \times K_F \times K_E / 2$$

If one cycle goes from -S.I. to S.I:

$$S_a = S.I. \times K_F \times K_E$$

where:

K_F = fatigue strength reduction factor, 4

K_E = correction factor for modulus of elasticity, $30 \times 10^6 / 27.8 \times 10^6 = 1.08$

The fatigue curve shown in Table I-9.1 of ASME Section III Appendices [7] is used for this evaluation.

Summary of Fatigue Evaluation

Event	Stress Intensity (psi)	S.I. $\times K_F \times K_E$ (psi)	S_a (psi)	Cycles		Damage Factor n / N
				n	N	
Lid Stress due to Bolt Preload	8,060	34,819	17,410	900	165,200	0.01
Lifting	17,608	76,412	38,206	900	9,807	0.09
Test Pressure	2,763	11,963	5,968	1	1×10^6	0.00
Rail Car Shock	1,750	7,560	7,560	162,000	1×10^6	0.16
Pressure and Temperature	18,090	78,150	39,075	450	9205	0.049
1 Foot Normal Condition Drop	11,360	49,075	24,538	450	41,000	0.01
Σ						0.319

The above table shows that the total damage factor is less than one. Therefore the fatigue effects on the TN-40 containment vessel are acceptable.

A separate fatigue analysis of the lid bolts is presented in Appendix 2.10.2.

2.6.14 Structural Evaluation of the Basket under Normal Condition Loads

The loading conditions considered in the evaluation of the fuel basket consist of inertial loads resulting from NCT drop loading (1 foot drop), HAC drop loading (30 foot drop) and thermal loads. The inertial loads of significance for the basket analysis are those transverse to the cask and basket structural longitudinal axes, so that the loading from the fuel assemblies is applied normal to the basket plates and transferred to the cask wall by the basket.

To determine the structural adequacy of the basket plate in the TN-40 fuel assembly basket under a NCT free drop, the basket is evaluated for 20 g end drop and 20 g side drop. The g-loads and drop orientations used for structural analysis of the basket are described in Appendix 2.10.8. The stress analysis of the basket due to inertial loading analysis is described in detail in Appendix 2.10.5. The results of the analyses are summarized in Appendix 2.10.5, Tables 2.10.5-4 through 2.10.5-6. Based on the results of these analyses, the basket is structurally adequate and it will properly support and position the fuel assemblies under normal loading conditions.

2.6.15 Summary of NCT Cask Body Structural Analysis

Table 2-13 lists the highest NCT stress intensities in each of the TN-40 transport package components based on the Section 2.1.2 structural design criteria. From the analysis results presented in Tables 2-13 and 2-14, it can be seen that the NCT loads will not result in any structural damage to the cask and that the containment function of the cask will be maintained.

2.7 Hypothetical Accident Conditions

Overview

This section describes the response of the TN-40 package to the HAC loading conditions specified by 10CFR71.73 [1]. The design criteria established for the TN-40 packaging for these conditions are described in Section 2.1.2. These criteria are selected to ensure that the packaging performance standards specified by 10CFR71.51 are satisfied.

The presentation of the HAC analyses and results is accomplished in the same manner as that used above for the NCT. The detailed analyses of the various packaging components under different loading conditions are presented in the Appendices to this chapter. The limiting results for the specified HAC loadings are taken from the Appendices and summarized here and compared to the design criteria. In all cases, the acceptability of the TN-40 packaging design with respect to HAC loads is demonstrated. Table 2-15 provides an overview of the performance evaluations presented in this section. The stress results for the cask body are obtained by combining the stresses from appropriate individual load cases reported in Appendix 2.10.1, to represent the stress condition under the specified HAC. This combination method is essentially the same as that presented in Section 2.6. Stress analysis results for the lid bolts are taken directly from Appendix 2.10.2. The impact limiter attachment evaluations are described in Appendix 2.10.8.

Reporting Method for Cask body Stresses

The structural analysis of the cask body was performed using an ANSYS finite element model. Stress results are reported at selected representative locations as described in Section 2.6.

Appendix 2.10.1 provides the detailed description of the structural analyses of the TN-40 cask body. That Appendix describes the detailed ANSYS model used to analyze the cask under various applied loads. Table 2-16 identifies the individual HAC loads (IL) analyzed using the ANSYS model.

Detailed stresses are available at each node in the finite element model. However, for practical considerations, only the maximum stresses in the lid, shell flange, inner shell, shield shell cylinder, and bottom plates are reported for each load case. These components were selected to be representative of the stress distribution in the cask body. The maximum stress may occur in different components for each individual load.

The stress results for the individual load case (tables reported in Appendix 2.10.1) are for one individual load only. Two or more individual load cases must be combined to determine the total stresses at the standard stress reporting locations for the various load combinations. This is accomplished using the ANSYS post-processor.

An "x" in Table 2-17 indicates that the stress results for the individual load case are used in the load combinations.

2.7.1 30 Foot Free Drop

The response of the TN-40 Packaging to free drops from a height of 30 feet onto an unyielding surface is evaluated at various orientations. The inertial loading applied to the TN-40 components is determined in the dynamic analysis presented in Appendix 2.10.8. The 30 foot drop is measured from the impact surface to the bottom of the impact limiter.

The stresses in the cask body are reported for the following drop orientations:

- End drop onto bottom (rear) end
- End drop onto lid (front) end
- Side drop
- C. G. over corner drop on bottom (rear) end
- C. G. over corner drop on lid (front) end
- 20° slap down impact on lid (front) end.

2.7.1.1 End Drop

The dynamic impact analysis of the TN-40 Packaging shows that the maximum expected inertia loading from the 30-foot end drop is 49 g. Because of the symmetry of the cask and impact limiters, these values are applicable for both the bottom end drop and lid end drop.

The load combinations performed to evaluate these drop events are indicated in Table 2-17. In all cases, bolt pre-load effects and fabrication stresses are included. For the hot environment condition, 100 psig internal pressure, and impact load cases are combined. For the cold environment evaluation, 25 psig external pressure, and impact load cases are combined.

Table 2-18 lists the maximum combined stress intensities ($P_L + P_b$) for the bottom and lid end drop under hot environment conditions and cold environment conditions. The stress results indicate that the cask structure can withstand much higher impact loadings than used in the analysis.

2.7.1.2 Side Drop

The impact analysis of the 30-foot side drop provided a maximum expected inertial loading of 51g (Appendix 2.10.8). The structural analysis of the cask body for this

loading condition is performed using this inertial loading. The load combinations performed to evaluate these drop events are indicated in Table 2-17. In all cases, bolt pre-load effects and fabrication stress are included. For the hot environment condition, 100 psig internal pressure, and impact load cases are combined. For the cold environment evaluation, the 25 psig external pressure, and impact load cases are combined.

Table 2-19 lists the combined stress intensities for the side drop under hot and -20°F cold environment conditions. The minimum factor of safety of 2.66 indicates that the cask can withstand higher impact loads than used in this analysis.

2.7.1.3 C.G. Over Corner Drop

The response of the TN-40 Package to the 30-foot corner drops are analyzed for impact on the bottom end and lid end. The analyses are performed using the ANSYS model as described in Appendix 2.10.1. The C.G. over corner drop occurs at a drop angle of 63.8°. That is, the longitudinal axis of the containment vessel is at an angle of 63.8° from the impact surface. The dynamic analysis (Appendix 2.10.8) of the 63.8° drop orientation calculated maximum inertia loadings of 32 g (axial) along the cask longitudinal axis and 14 g transverse to the longitudinal axis.

The load combinations performed to evaluate these two drop events are given in Table 2-17. In all cases, bolt pre-load effects and fabrication stresses are included. For the hot environment condition, 100 psig internal pressure, and impact load cases are combined. For the cold environment evaluation, 25 psig external pressure, and impact load cases are combined.

Table 2-19 lists the combined stress intensities for the C.G. over corner bottom end drop and lid end drop under both hot and cold (-20°F) environment conditions. The minimum factor of safety of 2.35 indicates that the cask structure can withstand higher impact loading than used in the analysis.

2.7.1.4 20° Slap Down Impact at Lid End

The 20° slap down impact at lid end (second impact) has a maximum transverse inertia load of 39 g at the lid end. The simultaneous inertial axial load is 22 g. The stress analysis is performed using the ANSYS model as described in Appendix 2.10.1.

The load combinations performed to evaluate this drop event are indicated in Table 2-17. In all cases, bolt pre-load effects and fabrication stresses are included. For the hot environment condition, 100 psig internal pressure, and impact load cases are combined. For the cold environment evaluation, the 25 psig external pressure, and impact load cases are combined.

Table 2-19 lists the combined stress intensities for the 20° slap down impact under both hot and cold (-20°F) environment conditions. The maximum factor of safety of 1.96 indicates that the cask structure can withstand higher impact loads than used in this analysis.

2.7.1.5 Lid Bolts

The lid bolts are analyzed for normal and accident condition loadings in Appendix 2.10.2. The analysis is based on NUREG/CR-6007 [18]. The bolts are analyzed for the following normal and accident conditions: operating pre-load, gasket seating load, internal pressure, temperature changes, impact loads, and puncture loads.

A summary of the calculated stresses is listed in Section 2.10.2.6. The calculations result in a maximum HAC average tensile stress of 64.2 ksi, which is below the allowable tensile stress of 87.5 ksi. The average HAC shear stress in the bolts is due to torsion during pre-loading. This stress is 13.5 ksi, which is well below the allowable shear stress of 52.5 ksi.

2.7.1.6 Impact Limiter Attachments

The impact limiters must remain attached to the cask body before, during, and after each HAC drop condition.

The limiting loading condition for the impact limiter attachments is the secondary impact (slap-down) associated with the 20° slap down under a 30 foot drop. This loading condition applies the greatest overturning moment to the impact limiter at the cask body interface. Although this loading condition is not limiting with respect to any other cask components, an evaluation of the attachments is performed to demonstrate that the affected impact limiter remains in place to insulate the cask during the subsequent HAC thermal event.

The analysis and results are provided in detail in Section 2.10.8.6.

The analysis concludes that the impact limiter attachment design is sufficiently strong to ensure that the impact limiters remain attached to the cask body during and following all HAC drop events.

2.7.2 Puncture

The impact limiters will protect the ends of the cask body from a 40-inch drop onto a 6-inch diameter bar. The most severe damage to the body resulting from the puncture drop will occur on the side walls of the gamma shield shell, between the impact limiters. This portion of the package is not the containment vessel, so that a release of the contents cannot occur unless both the gamma shield shell and the inner vessel are punctured.

An evaluation of the puncture drop event includes the local effects on the gamma shield shell at the impact point as well as the overall inertia loading on the packaging components.

For this load condition it is assumed that the gamma shield shell surface impacts the puncture bar directly. No credit is taken for the outer shell or the radial neutron shield.

The puncture bar as specified in 10CFR71 [1], is a vertical, cylindrical, mild steel bar 6 inches in diameter.

The impact force exerted by the bar on the gamma shield surface is calculated assuming the bar behaves as an elastic, perfectly plastic material with yield strength of 50 ksi which is a typical yield strength of mild steel. The gamma shield shell is assumed to be SA-266 Cl.4 steel which bounds the three possible fabrication options described in Section 2.1.1 above.

The weight of the TN-40 Transport Package is 271.46 kips. A conservatively higher weight of 275,000 lb is used in this analysis.

Two independent methods are used to compute the stresses in the TN-40 cask shell due to a puncture event.

Puncture Analysis Method 1

The maximum force, F_p , acting on the cask body due to impact on the puncture bar is:

$$F_p = \sigma_y A_b$$

Where σ_y is the yield strength of the bar, 50 ksi, and A_b is cross sectional area of the 6 inch diameter bar, 28.27 in.²

Therefore,

$$F_p = 1.414 \times 10^6 \text{ lb}$$

This force produces a cask deceleration and induces a bending moment at the midsection of the cask. If the cask is considered a beam uniformly loaded (downward) by its inertial load only (conservatively ignoring the 1g gravity force) and supported by the puncture bar at the center, the deceleration g caused by the puncture bar force, F_p , is then the following.

$$g = \frac{F_p}{W_{\text{package}}} = \frac{1.414 \times 10^6}{275,000} = 5.14 g$$

If the cask body is considered to be uniformly loaded and supported as described above, then the maximum moment M in the cask shell is:

$$M = \frac{F_p L}{8} = \frac{(1.414 \times 10^6)(183.75)}{8} = 3.248 \times 10^7 \text{ in. lb.}$$

Here, L is the length of the TN-40 cask. Conservatively neglecting the inner shell, outer shell and neutron shield, the moment of inertia of the cask shell is:

$$I = \frac{\pi}{4} (r_o^4 - r_i^4) = \frac{\pi}{4} (45.50^4 - 37.5^4) = 1.813 \times 10^6 \text{ in.}^4$$

The gamma shield shell bending stress is then:

$$\sigma_b = \frac{Mr_0}{I} = \frac{(3.248 \times 10^7)(45.50)}{1.813 \times 10^6} = 815 \text{ psi.}$$

Since the stress is nearly constant through the wall thickness, it should be treated as a membrane stress, P_m . The allowable stress for this accident condition is taken at 300° F as the smaller of $0.7S_u$ ($0.7(70,000) = 49,000$ psi) or $2.4S_m$ ($2.4(21,300) = 51,120$ psi) per Appendix F-1331.1 [7] where SA-105 is the bounding material. The allowable stress of 49,000 psi is well above σ_b .

The thickness of the containment vessel is 8.00 inches which provides the following shear area.

$$A = \pi(6)(8.00) = 151 \text{ in.}^2$$

The resulting maximum shear stress is the following.

$$\tau = F_p/A = 1.414 \times 10^6 / 151 = 9,364 \text{ psi.}$$

The corresponding stress intensity is 2τ or 18,750 psi. The allowable stress intensity for the gamma shield (ASME SA-105) is $0.7S_u$ or $0.7(70,000) = 49,000$ psi, which is well above the calculated stress intensity.

The deceleration of 5.14 g is small compared to the g-loads that will occur during the 30 foot free drop. Therefore, the global stresses that result from the inertial forces will be neglected during the load combination analysis. The bending stress of 815 psi at the center of the cask is also negligible compared to stresses due to other loads considered.

Puncture Analysis Method 2

An additional cask wall puncture analysis is performed using the equations presented in ORNL NSIC-22 [25]. This method provides a conservative estimate for the puncture threshold thickness of a steel element subjected to nondeformable missile perforation. The following equation is a problem specific reproduction of the analysis carried out in Reference [25].

$$T_p = \frac{(E_K)^{2/3}}{672D}$$

Where T_p is the cask wall thickness required to prevent puncture, D is the puncture rod outer diameter (in.), and E_K is the kinetic energy (ft-lbs) absorbed by the puncture event. E_K is taken to be the potential energy of the TN-40 Transport Package, 40 inches above the puncture rod. Therefore, $E_K = 275,000 \times 40 = 1.100 \times 10^7$ in. lb. = 9.167×10^5 ft. lb. Substituting E_K and $D = 6$ in. back into the above equation gives a threshold steel thickness of

$$T_p = \frac{(9.167 \times 10^5)^{2/3}}{(672)(6)} = 2.34 \text{ in.}$$

For the purpose of design, the total required thickness is $1.15 (T_p) = 2.69 \text{ in.}$ [25]. Since the cask wall is 8.00 inches thick ($> 2.69 \text{ inches}$), the cask wall will not fail due to a puncture event.

2.7.3 Thermal

2.7.3.1 Summary of Pressures and Temperatures

The analysis of the thermal accident is presented in Chapter 3. The maximum internal pressure during the HAC thermal accident is calculated in Section 4.3. The calculated pressure is 4.8 atm, or 55.9 psig. The structural analysis is, however, performed conservatively, assuming 100 psig internal pressure for the pressure stress calculations. An ANSYS transient thermal analysis of the cask for the 30 minute thermal fire accident is reported in Chapter 3. The initial condition is steady state, at an ambient temperature of 100°F and maximum decay heat. The initial steady state condition is followed by a 0.5 hour fire at 1475°F which is then followed by a cool-down period. The temperatures from the thermal analysis are reported in Chapter 3.

The temperature through the cross section of the cask, at the time of the maximum thermal gradient, is used as input to the cask model for thermal stress analysis.

2.7.3.2 Fire Accident Stresses

Stress analysis of the cask body due to fire accident is performed as part of the HAC load combination A15 (Table 2-17). The stress component results of this analysis using the same ANSYS structural model are presented in Table 2-18.

2.7.3.3 Combined Stresses

The stress components are combined with those due to the lid bolt pre-load, the internal pressure and fabrication stress, using the same procedure described above for the 30 foot drop events. Tables 2-18 and 2-19 presents the combined stress intensities in the lid, flange, inner shell, gamma shield shell, bottom, and trunnion region.

2.7.4 Water Immersion

2.7.4.1 Immersion - Fissile Material (Water Head of 3 feet, 1.3 psi External Pressure)

The criticality evaluation presented in Chapter 6 considers the effect of water in-leakage. Thus, the requirements of 10CFR71.73(c)(5) [1] are met. The cask body stresses for this immersion condition (1.3 psi external pressure) is enveloped by the immersion condition for all packages (water pressure of 290 psi) described in Section 2.7.4.3 below.

2.7.4.2 Immersion - All Packages (Water Head of 50 feet, 21.7 psig External Pressure)

The immersion loading condition results in an external pressure applied to the cask body corresponding to a 50 foot head of water. Assuming a 0 psia cask cavity pressure, this results in a maximum external pressure loading of 36.4 psig (21.7 + 14.7). The cask body stresses resulting from this immersion pressure are enveloped by the immersion condition for all packages (water pressure of 290 psig) described in Section 2.7.4.3 below.

2.7.4.3 Immersion - All Packages (Water Pressure of 290 psig)

10CFR 71.61 [1] requires that the containment vessel be subjected to an external water pressure of 290 psig for a period of not less than one hour without collapse, buckling, or in leakage of water. The containment boundary consists of the inner shell, bottom inner plate shell flange out to the seating surface, and lid assembly outer plate (Figure 4-1). This analysis evaluates the containment vessel stresses when the 290 psig external pressure is directly applied to the outer surface of the containment vessel. A helpful feature of the packaging design is that the inner shell and bottom inner plate of the containment vessel are completely enclosed by the gamma shield shell and bottom shield. Therefore, they will never be exposed to an external pressure due to immersion.

The finite element model of the cask described in detail in Appendix 2.10.1, is modified to analyze the immersion accident event. The gamma shield structure elements are deleted from the original model. Bilinear material properties were defined for the existing material models to account for plasticity and simulate correct material behavior. The material properties are obtained from the ASME Code [7]. All properties are taken at 300°F.

All existing loads are removed and replaced by 350 psig pressure loads over the outer surface of the model. The finite element model loads and boundary conditions are shown in Figure 2-2.

A large displacement static analysis is conducted using ANSYS [15]. The 350 psig external pressure is applied in a number of sub-steps. The containment vessel is assumed to buckle at the load sub-step where the solution begins to diverge.

Additionally, results for membrane and bending stresses at the load step of 290 psig external pressure were compared to ASME code allowables.

The critical membrane and membrane plus bending stress intensities for each of the cask components are summarized in the table below. The ultimate strengths of the component materials are obtained from Reference [7].

Containment Vessel Component	Stress Category	Computed Stress Intensity (psi)	Allowable Stress Intensity (psi)
Bottom Inner Plate (section at center)	P_m	21,520	45,500
	$P_m + P_b$	47,060	58,500
Inner Plate (bottom plate intersection)	P_m	8,157	45,500
	$P_m + P_b$	56,610	58,500
Flange	P_m	1,572	49,000
	$P_m + P_b$	4,400	63,000
Lid Outer Plate (section near outer edge)	P_m	4,228	49,000
	$P_m + P_b$	6,275	63,000
Lid Shield Plate (section at center)	P_m	836	49,000
	$P_m + P_b$	5,856	63,000

A converged solution was obtained for the last sub-step of the analysis corresponding to a 350 psig external pressure, and thus there is no potential of buckling of the containment vessel structure.

The maximum membrane and membrane plus bending stress intensities in each cask component are less than the ASME code HAC allowable stresses. Therefore, it is concluded that cask is adequate for 290 psig external pressure.

2.7.5 Structural Evaluation of the Basket under Accident Loads

To determine the structural adequacy of the basket plates in the TN-40 fuel assembly basket under HAC free drops, the basket is conservatively evaluated for a 75 g end drop and a 75 g side drop. The g-loads and drop orientations used for structural analysis of the basket are described in Appendix 2.10.8. The stress analysis of the basket due to inertial loading is described in detail in Appendix 2.10.5. The results of the analyses are summarized in Tables 2.10.5-7 through 2.10.5-9. Based on the results of these analyses, the basket and rails are structurally adequate for loads up to 75 g. A buckling analysis of the TN-40 basket is also performed in Appendix 2.10.5 for the HAC side drop loads. The details of the buckling analysis is provided in Section 2.10.5.3. The following table summarizes the maximum buckling load and factor of safety computed for five different azimuth orientations.

Basket Side Drop Orientation	Maximum Load used in analyses			Last Converged Load (g)	Actual Max. Load (g)	Factor of Safety
	Maximum Acceleration (g)	Vertical Pressure (psi)	Horizontal Pressure (psi)			
0°	200	222	0	145	75	1.93
30°	200	192	111	88	75	1.17
45°	200	157	157	92	75	1.23
60°	200	111	192	92	75	1.23
90°	200	0	222	115	75	1.53

Based on the results of this analysis, the basket and rails are structurally adequate up to 88 g. This g-load is higher than the calculated g-load of 75 g from 30 foot side drop.

The analyses summarized above demonstrate that the basket is structurally adequate and will properly support and position the fuel assemblies during HAC loading conditions.

2.7.6 Summary of HAC Cask Body Structural Analysis

Table 2-18 lists the highest stress intensities in each of the TN-40 transport package components for all HAC load combinations described above. Also listed in the tables are the stress limits for the service condition based on the Section 2.1.2 structural design criteria.

From the analysis results presented in Tables 2-18 and 2-19, it can be seen that the HAC loads will not result in any structural damage to the cask and that the containment functions of the cask and the support functions of the basket will be maintained.

As described above, the integrity of the TN-40 Packaging is not compromised by the accident test sequence set forth in 10 CFR71.73 [1], since it meets the design criteria of Regulatory Guide 7.6 [5] for the Load Combinations identified in Regulatory Guide 7.8 [6].

2.8 Special Forms / Fuel Rods

2.8.1 Special Form

This section does not apply to the TN-40 Packaging.

2.8.2 Fuel Rods

As discussed in Chapter 4, containment of the radioactive material is provided by the cask containment boundary. Analyses of the cask boundary for NCT and HAC defined by the 10CFR71 [1] demonstrate that the cask remains leak tight.

In addition, Appendix 2.10.7 of the SAR assesses the response of a typical PWR fuel assembly to a 30 foot HAC end drop and a 30 foot HAC side drop. Results from these analyses indicate that the buckling of the fuel rod does not occur during the 75g top and bottom end drops and the maximum stress due to the side drop load is much less than the yield stress of the irradiated Zircaloy cladding. Therefore, the integrity of the fuel rods will not be breached during the NCT and HAC.

2.9 References

1. 10 CFR PART 71, Packaging and Transportation of Radioactive Material.
2. American National Standards Institute, ANSI N14.6, American National Standard for Special Lifting Devices for Shipping Containers Weighing 10,000 Pounds or More for Nuclear Materials, 1986.
3. American Society of Mechanical Engineers, ASME Boiler and Pressure Vessel Code, Section III, 1989.
4. Not used.
5. USNRC Regulatory Guide 7.6, "Design Criteria for the Structural Analysis of Shipping Cask Containment Vessel", Rev. 1, March 1978.
6. USNRC Regulatory Guide 7.8, "Load Combinations for the Structural Analysis of Shipping Cask", Rev. 1, March 1989.
7. American Society of Mechanical Engineers, ASME Boiler and Pressure Vessel Code, Section III, Appendices, 1989.
8. American Society of Mechanical Engineers, ASME Boiler and Pressure Vessel Code, Section V, 1989.
9. Not used.
10. American Society of Mechanical Engineers, ASME Boiler and Pressure Vessel Code, Section IX, 1989.
11. NUREG/CR-3854, "Fabrication Criteria for Shipping Container".
12. NUREG-1617, "Standard Review Plan for Transportation Packages for Spent Nuclear Fuel", March 1998.
13. Northern States Power Company, Response to Bulletin 96-04, August 19, 1996, Docket No. 72-10, Materials License No. SNM-2506.
14. Hydrogen Generation Analysis Report for TN-40 Cask Materials, Test Report No. 61123-99N, Rev 0, Oct 23, 1998, National Technical Systems.
15. ANSYS Computer Code and Users Manuals, Release. 8.0.
16. WRC Bulletin 107, March 1979 Revision "Local Stresses in Spherical and Cylindrical Shells Due to External Loadings."

17. NUREG 766510, "Shock and Vibration Environments for Large Shipping Containers on Rail Cars and Trucks", June, 1977.
18. NUREG/CR-6007, "Stress Analysis of Closure Bolts for Shipping Casks", Lawrence Livermore National Laboratory, 1992.
19. Not used.
20. Not used.
21. NUREG/CR-3826, "Recommendations for Protecting against Failure by Brittle Fracture in Ferritic Steel Shipping Containers Greater than Four Inches Thick", April 1984.
22. NUREG/CR-1815, "Recommendations for Protecting Against Failure by Brittle Fracture in Ferritic Steel Shipping Containers up to Four Inches Thick."
23. Aluminum Standards and Data-1, 1976, published by the aluminum association.
24. American Society of Mechanical Engineers, ASME Boiler and Pressure Vessel Code, Section VIII, Divisions 1 and 2, 1989.
25. Gwaltney, R.C., "Missile Generation and Protection in Light-Water-Cooled Power Reactor Plants," ORNL NSIC-22, Oak Ridge National Laboratory, Oak Ridge, TN, For the UXAEC, September 1968.
26. Letter, R.O. Anderson (NSP) to US Nuclear Regulatory Commission, dated March 27, 1995, "Response to Request for Additional Information Regarding NUREG-0612, 'Control of Heavy Loads'."
27. Letter, B.A., Wetzel (NRC) to R.O. Anderson (NSP), transmittal date June 12, 1995, "Safety Evaluation and Safety Assessment Related to Dry Cask Storage At Prairie Island."
28. Transnuclear ADOC computer program, Rev. 1.
29. NUREG-0612 "Control of Heavy Loads at Nuclear Power Plants", July 1980.

2.10 Appendices

The detailed structural analyses of the TN-40 packaging are included in the following appendices:

- Appendix 2.10.1 Structural Analysis of the Cask Body
- Appendix 2.10.2 Lid Bolt Analysis
- Appendix 2.10.3 Structural Analysis of the Outer Shell
- Appendix 2.10.4 Fracture Toughness Evaluation of the TN-40 Cask
- Appendix 2.10.5 Structural Analysis of the TN-40 Basket
- Appendix 2.10.6 Dynamic Load Factor for Basket Drop Analysis
- Appendix 2.10.7 Structural Evaluation of the Fuel Rod Cladding Under Accident Impact
- Appendix 2.10.8 Structural Evaluation of the Impact Limiters
- Appendix 2.10.9 Impact Limiter Test Specification

2.11 ASME Code and NUREG-0612 Alternatives

Both the cask containment boundary and basket are designed, fabricated and inspected in accordance with the ASME Code Subsection NB to the maximum practical extent. The gamma shielding, which is primarily for shielding, but also provides structural support to the containment boundary during NCT and HAC events, was designed in accordance with Subsection NF of the code. Inspections of the gamma shielding are performed in accordance with ASME code Subsection NF as detailed in the SAR. Other cask components, such as the protective cover, outer shell and neutron shielding are not governed by the ASME Code.

Component	Reference ASME Code/Section	Code Requirement	Alternatives, Justification & Compensatory Measures
TN-40 Cask	NB-1100/ Subsection NCA NB-2000	Stamping and preparation of reports by the Certificate Holder, Surveillances, Use of ASME Certificate Holders	The TN-40 cask is not N/TP stamped; nor is there a code design specification or stress report generated. A design criteria document is generated in accordance with Transnuclear's QA Program and the design and analysis is performed under TN's QA Program and presented in the SAR. The cask may also be fabricated by other than N-stamp holders and materials may be supplied by other than ASME Certificate holders. Surveillances are performed by TN and utility personnel rather than by an Authorized Nuclear Inspector (ANI)
TN-40 Cask	NCA-3800	QA Requirements	The quality assurance requirements of NQA-1 or 10 CFR 71 are imposed in lieu of NCA-3800 requirements.
Pressure Test of the Containment Boundary	NB-6200	Hydrostatic Testing	The containment vessel is hydrostatically tested in accordance with the requirements of the ASME B&PV Code, Section III, Articles NB-6200 with the exception that some of the containment vessel is installed in the gamma shield shell during testing. The containment vessel is supported by the gamma shield during all design and accident events.
Weld of bottom inner plate to the containment shell	NB-5231	Full penetration corner welded joints require the fusion zone and the parent metal beneath the attachment surface to be UT after welding.	The required UT inspection will be performed on a best efforts basis. The joint will be examined by RT and either PT or MT methods in accordance with ASME Subsection NB requirements. The joint may be welded after the containment shell is shrink fitted into the gamma shield shell. The geometry of the joint does not allow for UT inspection.

Component	Reference ASME Code/Section	Code Requirement	Alternatives, Justification & Compensatory Measures
Containment Shell Rolling Qualification	NB-4213	The rolling process used to form the inner vessel should be qualified to determine that the required impact properties of NB-2300 are met after straining by taking test specimens from three different heats.	If the plates are made from less than three heats, each heat will be tested to verify the impact properties.
Containment Vessel	NB-7000	Vessels are required to have overpressure protection	No overpressure protection is provided. Function of containment vessel is to contain radioactive contents under normal and accident conditions of transport. Containment vessel is designed to withstand maximum internal pressure considering 100% fuel rod failure and maximum accident temperatures.
Containment Vessel	NB-8000	Requirements for nameplates, stamping and reports per NCA-8000	TN-40 cask is to be marked and identified in accordance with 10 CFR71 requirements. Code stamping is not required. QA data package to be in accordance with TN approved QA program.
Containment Vessel	NB-1131	The design specification shall define the boundary of a component to which other component is attached.	A code design specification was not prepared for the TN-40 cask. A TN design criteria specification was prepared in accordance with TN's QA program.

Component	Reference ASME Code/Section	Code Requirement	Alternatives, Justification & Compensatory Measures
Containment Vessel Material	NB-2120	Materials to be ASME Class 1 material	<p>Standard Review Plan, NUREG-1536 has accepted the use of either Subsection NB (Class 1) or NC (Class 2 or 3) of the Code for the containment. SA-203 Grade D is similar to SA-203 Grade E which is a Class 1 material. The chemical content of the two grades are identical, except that Grade E restricts the carbon to 0.20 max., while Grade D further restricts the carbon content to 0.17 max. Grade D is acceptable as a class 2 material up to 500°F.</p> <p>Grade D was selected because of its ductility, since the higher strength is not required. SA-203 Grade D has better elongation than Grade E and due to its lower strength is more likely to have the good fracture toughness at low temperatures.</p> <p>In selecting materials for storage and transport casks, one of the major selection criteria is fracture toughness at low temperatures. Grade D was selected on this basis. There is no similar requirement for pressure vessels, as they are used at much higher temperatures.</p>
Weld of Shield Plate to Lid Outer Plate	NB-4335	Impact testing of weld and heat affected zone of lid to shield plate	<p>If two different materials are joined, the fracture toughness requirements of either may be used for the weld metal. There are no fracture toughness requirements on the shield plate, and therefore none are performed on the base metal or the heat affected zones. This weld is not subject to low temperatures, as it is inside the cask cavity. An evaluation of this weld at low temperatures is presented in Appendix 2.10.4 of the SAR.</p>
Containment Vessel and Lid Penetration Cover Materials	NB-2000	Requires materials to be supplied by ASME approved material supplier; Quality assurance to meet NCA requirements.	<p>Material will be supplied by TN approved suppliers with Certified Material Test reports (CMTR) in accordance with NB-2000 requirements. The cask is not code stamped. The quality assurance requirements of NQA-1 or 10CFR71 are imposed in lieu of the requirements of NCA-3800.</p>

Component	Reference ASME Code/Section	Code Requirement	Alternatives, Justification & Compensatory Measures
Gamma Shielding	NB-1132.2	Non-pressure retaining structural attachments shall conform to Subsection NF.	The primary function of the gamma shield is shielding, although credit is taken for the gamma shielding in the structural analysis. The welds are examined in accordance with NF acceptance criteria. A fracture toughness evaluation is presented in Appendix 2.10.4 of the SAR.
Gamma Shielding	NB-2190	Material in the component support load path and not performing a pressure retaining function welded to pressure retaining material shall meet the requirements of NF-2000.	The gamma shielding materials were procured to ASTM or ASME material specifications. Materials testing is performed in accordance with the applicable specification. Impact testing is not performed on the gamma shielding materials (including welding materials). An evaluation of the gamma shielding due to impact at low temperatures is provided in Appendix 2.10.4 of the SAR.
Lid & Flange	NB-4121.3	Repetition of surface examination after machining.	Critical Flaw size determination is performed in Appendix 2.10.4
Basket	NB-4000/5000	Fabrication/Welding / NDE inspection	Basket fabrication and welding procedures are qualified in accordance with ASME Section IX. Due to the unique nature of these basket and welds, special inspections and tests were developed for these welds.
Basket neutron poison material	NB-2000	Use of ASME Materials	The basket neutron poison material is not used for structural analysis, but to provide criticality control and heat transfer. They are not code materials.
Aluminum used for basket rails, aluminum plates between the compartments, and aluminum plates at the basket periphery	NB-2000	Use of ASME Materials	The aluminum plate is not a Class 1 material. It was selected for its properties. Aluminum has excellent thermal conductivity and a high strength to weight ratio. NUREG-3854 and 1617 allow materials other than ASME Code materials to be used in the cask and basket fabrication. ASME Code does provide the material properties for the aluminum and also allows the material to be used for Section III applications (Class 2 and 3). Stress values for temperatures above 400°F are taken from "Aluminum Standards and Data", 1976.

Component	Reference NUREG-0612 Section	NUREG Requirement	Alternatives, Justification & Compensatory Measures
Upper Trunnion	NUREG-0612 (Section 5.1.6(3)(b))	A non-redundant or non-dual lift point system should have a design safety factor of ten (10) times the maximum combined concurrent static and dynamic load.	This design requirement is accomplished by applying design criteria 7.2.1 of ANSI N14.6 [2]. Hence the trunnions are designed to support 6g when compared to yield strength and 10g when compared to tensile strength. The upper trunnions are load tested to 1.5g, see NRC Safety Evaluation dated May 11, 1995 [27] for acceptability of this load tests for Part 72 storage.

Table 2-1
Evaluation Method Employed to Demonstrate Compliance With
Specific Regulatory Requirements

10CFR71		Numerical Analysis	Material Test**	Model Tests
Normal Condition of Transport	Heat	X		
	Cold	X		
	Reduced External Pressure	X		
	Increased External Pressure	X		
	Shock and Vibration	X		
	One Foot Free drop	X		
Hypothetical Accident Condition	30 foot Free Drop - Cask and Basket	X	X	
	30 foot Free Drop- Impact Limiters	X	X	X
	Puncture	X		
	Thermal Event	X		
	Water Immersion	X		
others	Lifting	X		
	Tie-Down	X		

** Material tests include crush and shear tests of the wood, and charpy and tensile tests of the containment materials.

Table 2-2
Containment Vessel Stress Limits

Classification	Stress Intensity Limit
Normal (Level A) Conditions⁽¹⁾	
P_m	S_m
P_l	$1.5 S_m$
$(P_m \text{ or } P_l) + P_b$	$1.5 S_m$
Shear Stress	$0.6 S_m$
Bearing Stress	S_y
$(P_m \text{ or } P_l) + P_b + Q$	$3 S_m$
$(P_m \text{ or } P_l) + P_b + Q + F$	S_a
Hypothetical Accident (Level D)⁽²⁾	
P_m	$0.7 S_u$
P_l	$S_u^{(3)}$
$(P_m \text{ or } P_l) + P_b$	$S_u^{(3)}$
Shear Stress	$0.42 S_u$

Notes:

1. Classifications and Stress Intensity Limits are as defined in ASME B&PV Code, Section III, Subsection NB [3].
2. Stress intensity limits are in accordance with ASME B&PV Code, Section III, Appendix F [7].
3. When evaluating the results from the nonlinear elastic plastic analysis for the accident conditions, the general primary membrane stress intensity, P_m , shall not exceed $0.7S_u$ and maximum primary stress intensity at any location (P_l or $P_l + P_b$) shall not exceed $0.9S_u$ [7].

Table 2-3
Cover Bolt Stress Limits

Classification	Stress Intensity Limit ⁽¹⁾⁽⁵⁾
Normal (Level A) Conditions ⁽²⁾	
Average Tensile Stress	$2 S_m$
Maximum Combined Stress	$3 S_m$
Bearing Stress	S_y
Hypothetical Accident (Level D)⁽³⁾	
Average Tensile Stress	Smaller of S_y or $0.7 S_u$
Average Shear Stress	Smaller of $0.42 S_u$ or $0.6 S_y$
Maximum Combined Stress	S_u
Combined Shear & Tension ⁽⁴⁾	$R_t^2 + R_s^2 \leq 1$

Notes:

1. The stress analysis of the lid bolts is performed in accordance with NUREG/CR-6007 [18] described in Appendix 2.10.2. The stress limits for the lid bolts are listed separately in Appendix 2.10.2, Tables 2.10.2-3 and 2.10.2-4.

The stress limits for the impact limiter tie rod and attachment bolt are described in Appendix 2.10.8 "Structural Analysis of Impact Limiter."

2. Classification and stress limits are as defined in ASME B&PV Code, Section III, Subsection NB [3].
3. Stress limits are in accordance with ASME B&PV Code, Section III, Appendix F [7].
4. R_t : Ratio of average tensile stress to allowable average tensile stress
 R_s : Ratio of average shear stress to allowable average shear stress
5. All stresses include the effect of tensile and torsional loads due to bolt preloading.

Table 2-4
Non Containment Structure Stress Limits

Classification	Stress Intensity Limit
Normal (Level A) Conditions ⁽¹⁾	
P_m	S_m
P_l	$1.5 S_m$
$(P_m \text{ or } P_l) + P_b$	$1.5 S_m$
$(P_m \text{ or } P_l) + P_b + Q$	$3 S_m$
Shear Stress	$0.60 S_m$
Bearing Stress	S_y
Hypothetical Accident (Level D) ⁽²⁾	
P_m	$0.7 S_u$
P_l	S_u
$(P_m \text{ or } P_l) + P_b$	S_u
Shear Stress	$0.42 S_u$

Weld Allowable ⁽¹⁾		
Normal Load Condition	Full Penetration	Same as base metal
	Partial Grove/Fillet	Tension - $0.3 \times S_u$ Shear - $0.4 \times S_y$
Accident Load Condition	Full Penetration	Same as base metal
	Partial Grove/Fillet	Normal Condition allowables are increased by a factor: Smaller of 2 or $1.67 S_u / S_y$ if $S_u > 1.2 S_y$

Notes:

1. Classifications and stress intensity limits are as defined in ASME B&PV Code, Section III, Subsection NF [3].
2. Stress intensity limits are in accordance with ASME B&PV Code, Section III, Appendix F [7].

Table 2-5
Basket Stress Limits

Classification	Stress Intensity Limit
Normal (Level A) Conditions ⁽¹⁾	
P_m	S_m
P_l	$1.5 S_m$
$(P_m \text{ or } P_l) + P_b$	$1.5 S_m$
$(P_m \text{ or } P_l) + P_b + Q$	$3 S_m$
$(P_m \text{ or } P_l) + P_b + Q + F$	S_a
Shear Stress	$0.8 S_m$
Hypothetical Accident (Level D) ⁽²⁾	
P_m	Smaller of $2.4 S_m$ or $0.7 S_u$
P_l	Smaller of $3.6 S_m$ or $S_u^{(3)}$
$(P_m \text{ or } P_l) + P_b$	Smaller of $3.6 S_m$ or $S_u^{(3)}$
Shear Stress	$0.42 S_u$

Notes:

1. Classifications and stress intensity limits are as defined in ASME B&PV Code, Section III, Subsection NB [3].
2. Limits are in accordance with ASME B&PV Code, Section III, Appendix F [7].
3. When evaluating the results from the nonlinear elastic plastic analysis for the accident conditions, the general primary membrane stress intensity, P_m , shall not exceed $0.7 S_u$ and maximum primary stress intensity at any location (P_l or $P_l + P_b$) shall not exceed $0.9 S_u$ [7].

Table 2-6
Cask Weight and Center of Gravity

Component	Weight (kips)
Cask	
Body	116.33
Lid	13.91
Bottom	18.87
Aluminum Boxes	1.99
Resin	10.58
Outer Shell	7.45
Trunnions	0.67
Fuel Assemblies	52.00
Basket	
Steel Boxes	5.44
Aluminum Plates of the Basket	5.40
Boral [®] Plates	0.58
Steel Plates at Periphery	1.17
Aluminum Rails at Periphery	1.29
Aluminum Plates at Periphery	0.81
Top Impact Limiter	16.34
Bottom Impact Limiter	16.33
Tie Rods (13)	0.91
Impact Limiter Bolting Brackets (8)	0.24
Top Impact Limiter Spacer	1.15
Total with Fuel, Impact Limiters and Tie Rods	271.46

* Center of Gravity of the package is approximately 91.4 inches and is measured along the axial centerline from the rear (bottom) of the cask.

Summary of weights used for Analysis:

1. Front (Top) Trunnion Lifting (w/o impact limiters) 250,000 lbs.
2. Cask Body Analysis 271,700 lbs.

Table 2-7
Trunnion Section Properties and Applied Loads

Item	Front Trunnions		Rear Trunnions	
	Section A-A (Weld)	Section B-B (Shoulder)	Section A-A (Weld)	Section B-B (Shoulder)
Cross Section Area (in ²)	93.415	79.73	54.95	46.0
Area Moment Of Inertia (in ⁴)	987.20	755.60	379.69	285.10
Yield Condition Shear Force (lb)	750,000		375,000	
Yield Condition Bending Moment, (in lb)	4,185,000	1,312,500	2,092,500	656,250
Ultimate Condition Shear Force (lb)	1,250,000		625,000	
Ultimate Condition Bending Moment (in lb)	6,975,000	2,187,500	3,487,500	1,093,750

Notes:

- Trunnion geometry (Sections A-A and B-B) is in Figure 2-1.
- * Trunnion Loads to Support 6 times Cask Weight
- ** Trunnion Loads to Support 10 times Cask Weight

Table 2-8
Trunnion Stresses when Loaded by 6 and 10 Times Cask Weight (Lifting)

Location / Stress	Yield Limit		Ultimate Limit	
	Section A-A (Weld)	Section B-B (Shoulder)	Section A-A (Weld)	Section B-B (Shoulder)
Front Trunnions				
Shear Stress (psi)	8,025	9,402	13,381	15,678
Bending Stress (psi)	25,436	9,771	42,393	16,285
Stress Intensity (psi)	30,076	21,192	50,134	35,333
Rear Trunnions				
Shear Stress (psi)	6,821	8,147	11,374	13,589
Bending Stress (psi)	26,178	10,220	43,629	17,033
Stress Intensity (psi)	29,519	19,234	49,203	32,074
Allowable Stress (psi)	$S_y = 31,900$		$S_u = 70,000$	

Notes:

1. Trunnion geometry (Sections A-A and B-B) is shown in Figure 2-1.
2. Minimum margin of safety is 0.06 for yield limit and 0.28 for ultimate limit (front trunnion).

Table 2-9
TN-40 Performance Evaluation Overview
(Normal Conditions of Transport)

Loading Condition	SAR Section	Scope of Evaluation
Heat 71.71(c)(1)	2.6.1.1	Maximum component temperatures for material allowables
	2.6.1.2	Cask cavity maximum pressure, 100 psig
	2.6.1.3	Cask body thermal gradients
	2.6.1.4	Cask body stresses due to hot environment load combinations
Cold 71.71(c)(2)	2.6.2	Cask body stresses due to cold environment load combinations
Increase External Pressure 71.71(c)(4)	2.6.3	Cask body stresses due to 25 psig external pressure load combinations
Reduced External pressure 71.71(c)(3)	2.6.4	Cask body stresses due to 100 psig internal pressure load combinations
Shock Loads 71.71(c)(5)	2.6.5	Cask body stresses due to rail shock loads
Vibration Loads 71.71(c)(5)	2.6.6	Cask body stresses due to rail vibration loads
Water Spray 71.71(c)(6)	2.6.7	Negligible for TN-40 cask
Free Drop 71.71(c)(7)	2.6.8	Cask body stresses due to 1 foot bottom end drop
		Cask body stresses due to 1 foot lid end drop
		Cask body stresses due to 1 foot side drop
Corner Drop 71.71(c)(8)	2.6.9	Not applicable
Compression 71.71(c)(9)	2.6.10	Not applicable
Penetration 71.71(c)(10)	2.6.11	Not applicable
Lid Bolt Analysis	2.6.12	Bolt stresses due to preload, pressure loads, temperature, impact and puncture loads
Fatigue Analysis of Containment Boundary	2.6.13	Fatigue evaluation of containment vessel due to lifting, pressure, temperature, shock/vibration, and 1 foot drop loads
Basket Evaluation	2.6.14	Structural analysis of the basket due to 1 foot end drop and 1 foot side drop loads
Summary of Normal Condition Structural Analysis	2.6.15	Lists the highest stress intensities in the containment vessel and gamma shield and compares results with the allowables

Table 2-10
Individual Load Cases for Normal Conditions of Transport
TN-40 Cask Body Analysis

Run No.	Individual Load Type	Load used in Analysis	Factor Used for Normal Conditions Load Combinations
IL-1	Bolt preload and lid seating pressure	-	1.0
IL-2	Fabrication Stresses	-	1.0
IL-3	Internal pressure	100 psig	1.0
IL-4	External pressure	25 psig	1.0
IL-5	Thermal stresses at 100°F hot environment	-	1.0
IL-6	Thermal stresses at -20°F cold environment	-	1.0
IL-7	Thermal stresses at -40°F cold environment	-	1.0
IL-8	Cask Horizontal – 1g Down Gravity	1g	1.0
IL-10	Horizontal cask, Rail Vibrations Rail car shock	0.19g, 0.19g, 0.37g	1.0
IL-11	Horizontal cask, Rail Shock tie-down	4.7g all direction	1.0
IL-12	End drop on bottom	1g	12.0
IL-13	End drop on lid	1g	12.0
IL-15	Side drop	1g	16.0

Table 2-11
Summary of Load Combinations for Normal Condition of Transport

Load Combination	Applicable Individual Loads											Comb. Abbr.
	IL-1	IL-2	IL-8	IL-3	IL-4	IL-5	IL-6	IL-7	IL-12	IL-13	IL-15	
	Bolt Pre-load	Fabrication	Gravity 1g	Internal Pressure	External Pressure	Thermal 100°F	Thermal -20°F	Thermal -40°F	Bottom Drop	Top Drop	Side Drop	
Hot Environment (100° F amb.)	X	X	X	X		X						N1
Cold Environment (-20° F amb.)	X	X	X		X		X					N2
Cold Environment (-40° F amb.)	X	X	X		X			X				N3
Increased External Pressure	X	X	X		X		X					N4
Reduced External Pressure	X	X	X	X		X						N5
1 Ft End Bottom Drop	X	X			X		X		X			N6
	X	X		X		X			X			N7
1 Ft End Top Drop	X	X			X		X			X		N8
	X	X		X		X				X		N9
1 Ft Side Drop	X	X			X		X				X	N10
	X	X		X		X					X	N11

Table 2 –11
Summary of Load Combinations for Normal Condition of Transport
 (Concluded)

Load Combination	Applicable Individual Loads								Combination Abbreviation
	IL-1	IL-2	IL-3	IL-4	IL-5	IL-6	IL-10	IL-11	
	Bolt Pre-load	Fabrication	Internal Pressure	External Pressure	Thermal (100°F)	Thermal (-20°F)	Rail Vibration	Rail Shock	
Rail Vibration	X	X	X		X		X		N12
	X	X		X		X	X		N13
Rail Shock	X	X	X		X			X	N14
	X	X		X		X		X	N15

Table 2-12
Reference Temperatures for Stress Analysis Acceptance Criteria

Component	Normal Transport*	
	Maximum from Chapter 3 (°F)	Selected Design** Temperature (°F)
Outer Shell	214	250
Inner Shell	251	300
Basket Rail	257	...
Basket Plate	444	...
Gamma Shell	248	300
Fuel Cladding	495	500
Lid Bolt	<250	300

* For normal loading condition.

** Temperatures specified are used to determine allowable stresses. They are not a maximum use temperature for material.

*** Allowable stresses for the basket are taken at the temperatures.

Table 2-13
Summary of Load Combination Stresses for Normal Conditions of Transport

Load Comb.	Stress Type	Cask Component Nodal Stress Intensity (ksi)						Allowable (ksi)
		Lid	Flange	Inner Shell	Gamma Shield Shell	Bottom Shield	Trunnion	
N1 Hot (100° F)	Primary	8.70	12.65	13.74*	7.32	7.13	3.70	19.6
	Primary + Secondary	9.17	14.93	18.09	7.29	15.50	3.84	58.8
N2 Cold (-20° F)	Primary	8.19	13.38*	14.63*	5.72	3.32	3.10	19.6
	Primary + Secondary	8.27	14.52	17.46	5.30	7.19	3.19	58.8
N3 Cold (-40° F)	Primary	8.19	13.38*	14.63*	5.72	3.32	3.10	19.6
	Primary + Secondary	8.22	14.29	17.15	5.27	6.50	3.16	58.8
N4 External Pressure	Primary	8.19	13.38*	14.63*	5.72	3.32	3.10	19.6
	Primary + Secondary	8.27	14.52	17.46	5.30	7.19	3.19	58.8
N5 Internal Pressure	Primary	8.70	12.65	13.74*	7.32	7.13	3.70	19.6
	Primary + Secondary	9.17	14.93	18.09	7.29	15.50	3.84	58.8
N6 Drop Bottom (C)	Primary	8.10	13.88*	15.72*	4.65	3.50	3.11	19.6
	Primary + Secondary	8.19	15.03	18.56	4.31	7.26	3.29	58.8
N7 Drop Bottom (H)	Primary	8.59	13.13*	14.84*	6.23	7.15	3.70	19.6
	Primary + Secondary	9.06	15.43	19.19	6.27	15.62	3.83	58.8
N8 Drop Top (C)	Primary	8.93	14.35*	15.03*	4.86	3.36	3.18	19.6
	Primary + Secondary	9.00	15.52	17.88	4.41	5.21	3.72	58.8
N9 Drop Top (H)	Primary	9.41	13.60*	14.13*	6.41	5.00	3.67	19.6
	Primary + Secondary	9.88	15.91	18.50	6.36	13.26	4.11	58.8
N10 Drop Side (C)	Primary	9.55	13.40*	14.74*	13.49*	7.93	4.26	19.6
	Primary + Secondary	9.67	14.66	17.56	13.39	10.97	4.20	58.8
N11 Drop Side (H)	Primary	9.86	12.67	13.85*	13.44*	12.78	4.82	19.6
	Primary + Secondary	10.19	15.07	18.17	13.38	19.31	4.89	58.8

Table 2-13
Summary of Load Combination Stresses for Normal Condition of Transport
(Concluded)

Load Comb.	Stress Type	Cask Component Nodal Stress Intensity (ksi)						Allowable Stress
		Lid	Flange	Inner Shell	Gamma Shield Shell	Bottom Shield	Trunnion	(ksi)
N12 Vib. (H)	Primary	8.70	12.66	13.75*	7.24	7.02	3.69	19.6
	Primary + Secondary	9.17	14.94	18.11	7.23	15.43	3.83	58.8
N13 Vib. (C)	Primary	8.20	13.39*	14.64*	5.64	3.30	3.09	19.6
	Primary + Secondary	8.27	14.53	17.48	5.25	7.12	3.18	58.8
N14 Shock (H)	Primary	8.64	12.83	14.19*	7.52	8.24	3.81	19.6
	Primary + Secondary	9.05	15.15	18.53	7.30	16.27	4.21	58.8
N15 Shock (C)	Primary	8.23	13.56*	15.08*	5.91	3.84	3.29	19.6
	Primary + Secondary	8.31	14.74	17.91	5.28	7.91	3.58	58.8

*The stresses which result in factor of safety less than 1.5, are linearized in Table 2-14.

Table 2-14
Linearized Stress Evaluation of Normal Condition of
Transport Load Combinations

Load Comb.	Component	Nodal Stress Intensity (ksi)	Linearized Stress Intensity			Allowable (ksi)	Factor of Safety
			Node Nos.	Type	Magnitude (ksi)		
N1 (Hot)	Inner Shell	13.74	224-254	P _M	13.01	19.6	1.51
				P _L + P _B	13.47	29.4	2.18
N2 (Cold)	Flange	13.38	4482-4485	P _M	4.90	19.6	4.00
				P _L + P _B	11.88	29.4	2.47
	Inner Shell	14.63	373-15591	P _M	13.63	19.6	1.44
				P _L + P _B	14.06	29.4	2.09
N3(Cold)	Flange	13.38	4482-4485	P _M	4.90	19.6	4.00
				P _L + P _B	11.88	29.4	2.47
	Inner Shell	14.63	373-15591	P _M	13.63	19.6	1.44
				P _L + P _B	14.06	29.4	2.09
N4(Cold)	Flange	13.38	4482-4485	P _M	4.90	19.6	4.00
				P _L + P _B	11.88	29.4	2.47
	Inner Shell	14.63	373-15591	P _M	13.63	19.6	1.44
				P _L + P _B	14.06	29.4	2.09
N5 (Hot)	Inner Shell	13.74	224-254	P _M	13.01	19.6	1.51
				P _L + P _B	13.47	29.4	2.18

Table 2-14
Linearized Stress Evaluation of Normal Condition of
Transport Load Combinations
 (Continued)

Load Comb.	Component	Nodal Stress Intensity (ksi)	Linearized Stress Intensity			Allowable (ksi)	Factor of Safety
			Node Nos.	Type	Magnitude (ksi)		
N6 (Cold) Bottom Drop	Flange	13.88	4482-4485	P _M	5.07	19.6	3.87
				P _L + P _B	12.25	29.4	2.40
	Inner Shell	15.72	224-254	P _M	13.52	19.6	1.45
				P _L + P _B	13.98	29.4	2.10
N7(Hot) Bottom Drop	Flange	13.13	375-374	P _M	4.77	19.6	4.11
				P _L + P _B	11.71	29.4	2.51
	Inner Shell	14.84	224-254	P _M	13.00	19.6	1.51
				P _L + P _B	13.46	29.4	2.18
N8(Cold) Top Drop	Flange	14.35	375-374	P _M	5.54	19.6	3.54
				P _L + P _B	12.66	29.4	2.32
	Inner Shell	15.03	373-15591	P _M	13.6	19.6	1.44
				P _L + P _B	14.02	29.4	2.10
N9(Hot) Top Drop	Flange	13.60	375-374	P _M	5.23	19.6	3.75
				P _L + P _B	12.12	29.4	2.43
	Inner Shell	14.13	373-15591	P _M	13.03	19.6	1.50
				P _L + P _B	13.44	29.4	2.19

Table 2-14
Linearized Stress Evaluation of Normal Condition of Transport Load
Combinations
 (Continued)

Load Comb.	Component	Nodal Stress Intensity (ksi)	Linearized Stress Intensity			Allowable (ksi)	Factor of Safety
			Node Nos.	Type	Magnitude (ksi)		
N10 (Cold) Side Drop	Flange	13.40	4655-4654	P _M	5.22	19.6	3.75
				P _L + P _B	11.92	29.4	2.47
	Inner Shell	14.74	8153-7883	P _M	14.04	19.6	1.40
				P _L + P _B	14.31	29.4	2.05
	Gamma Shield Shell	13.49	4886-5589	P _M	1.75	19.6	11.2
				P _L + P _B	5.65	29.4	5.20
N11 (Hot) Side Drop	Inner Shell	13.85	8153-7883	P _M	13.39	19.6	1.46
				P _L + P _B	13.68	29.4	2.15
	Gamma Cylinder	13.44	4886-5589	P _M	1.73	19.6	11.33
				P _L + P _B	5.70	29.4	5.16
N12 (Hot) Vibration	Inner Shell	13.75	224-254	P _M	13.01	19.6	1.51
				P _L + P _B	13.47	29.4	2.18
N13 (Cold) Vibration	Flange	13.39	4482-4485	P _M	4.89	19.6	4.01
				P _L + P _B	11.89	29.4	2.47
	Inner Shell	14.64	373-15591	P _M	13.60	19.6	1.44
				P _L + P _B	14.02	29.4	2.10

Table 2-14
Linearized Stress Evaluation of Normal Condition of
Transport Load Combinations
 (Concluded)

Load Comb.	Component	Nodal Stress Intensity (ksi)	Linearized Stress Intensity			Allowable (ksi)	Factor of Safety
			Node Nos.	Type	Magnitude (ksi)		
N14 (Hot) Shock	Inner Shell	14.19	372-15590	P _M	13.42	19.6	1.46
				P _L + P _B	13.96	29.4	2.11
N15 (Cold) Shock	Flange	13.56	4482-4485	P _M	5.08	19.6	3.86
				P _L + P _B	12.04	29.4	2.44
	Inner Shell	15.08	372-15590	P _M	14.02	19.6	1.40
				P _L + P _B	14.57	29.4	2.02

Table 2-15
TN-40 Performance Evaluation Overview
(Hypothetical Accident Conditions of Transport)

Loading Conditions	SAR Section	Scope of Evaluation
30 foot Free Drop 71.73-(c)(1)	2.7.1.1	Cask body stresses due to bottom end drop
		Cask body stresses due to lid end drop
	2.7.1.2	Cask body stresses due to side drop
	2.7.1.3	Cask body stresses due to CG over corner drop
	2.7.1.4	Cask body stresses due to 20° slap down impact at lid end
	2.7.1.5	Lid bolt analysis
	2.7.1.6	Impact limiter attachment analysis
Puncture 71.73-(c)(2)	2.7.2	Cask body evaluation for 40 inch drop onto the puncture bar
Thermal 71.73-(c)(3)	2.7.3.1	Maximum component pressures and temperatures
	2.7.3.2	Cask body thermal stresses due to fire accident
	2.7.3.3	Maximum combined stresses
Immersion 71.73-(c)(5) 71.73-(c)(6) 71.61	2.7.4.1	Cask body stresses due to 3 foot water head (1.3 psi)
	2.7.4.2	Cask body stresses due to 50 foot water head (21.7 psi)
	2.7.4.3	Containment vessel stresses due to 290 psi external pressure (pressure directly applies to the containment vessel) Buckling analysis of the containment vessel due to 290 psi external pressure
Basket Evaluation	2.7.5	Structural analysis of the basket due to 30 foot end drop and 30 foot side drop loads
Summary of Accident Condition Structural Analysis	2.7.6	Lists the highest stress intensities in the containment vessel and gamma shield shell and compare with the allowables

Table 2-16
Summary of Individual Load Factors for Hypothetical
Accident Condition of Transport

Run No.	Individual Load Type	Load Used in Analysis	Factor Used for Accident Conditions Load Combinations
IL-1	Bolt preload and lid seating pressure	-	1.0
IL-2	Fabrication Stresses	-	1.0
IL-3	Internal pressure	100 psig	1.0
IL-4	External pressure	25	1.0
IL-5	Thermal stresses at 100°F (hot) environment	-	1.0
IL-6	Thermal stresses at -20°F (cold) environment	-	1.0
IL-8	Cask Horizontal on Skid – 1g Down Gravity	1g	1.0
IL-12	End drop on bottom	1g	49.0 ⁽¹⁾
IL-13	End drop on lid	1g	49.0 ⁽¹⁾
IL-15	Side drop	1g	51.0 ⁽¹⁾
IL-16	CG Over Corner Drop on Front (Lid) Impact Limiter	32g axial, 14g radial	1.0
IL-17	CG Over Corner Drop on Rear (Bottom) Impact Limiter	32g axial, 14g radial	1.0
IL-18	Oblique Impact on Lid End (slapdown)	22g axial, 39g radial	1.0
IL-19	Oblique Impact on Bottom End (slapdown)	22g axial, 39g radial	1.0

Notes:

(1) Taken from Appendix 2.10.8

Table 2-17
Summary of Load Combinations for Hypothetical Accident Condition of Transport

Load Combination	Applicable Individual Load											Combination Number
	IL-1	IL-2	IL-3	IL-4	IL-12	IL-13	IL-15	IL-16	IL-17	IL-18	IL-19	
	Bolt Preload	Fabrication	Internal Pressure	External Pressure	Bottom end Drop	Top end Drop	Side drop	Corner drop Lid	Corner drop Bottom	Oblique drop Lid	Oblique drop Bottom	
30 Ft. End Drop on Bottom End	x	x	x		x							A1
	x	x		x	x							A2
30 Ft. End Drop on Lid End	x	x	x			x						A3
	x	x		x		x						A4
30 Ft. Side Drop	x	x	x				x					A5
	x	x		x			x					A6
30 Ft. CG Over Corner Drop on Bottom End	x	x	x						x			A7
	x	x		x					x			A8
30 Ft. CG Over Corner Drop on Lid End	x	x	x					x				A9
	x	x		x				x				A10
30 Ft. 20° Slap Down Impact on Lid End	x	x	x							x		A11
	x	x		x						x		A12
30 Ft. 20° Slap Down Impact on Bottom End	x	x	x								x	A13
	x	x		x							x	A14
Fire Accident	x	x	x									A15

Table 2-18
Summary of Load Combination Stresses for Hypothetical
Accident Condition of Transport

Load Comb.	Stress Type	Cask Component Nodal Stress Intensity (ksi)						Allowable (ksi)
		Lid	Flange	Inner Shell	Gamma Cylinder	Bottom Plate	Trunnion Region	
30 Ft. End Drop on Bottom End	A1 (Hot)	8.28	14.67	18.23	5.91	7.83	4.04	45.5
	A2 (Cold)	8.52	15.45	19.11	5.56	5.10	3.67	45.5
30 Ft. End Drop on Lid End	A3 (Hot)	11.66	16.62	16.51	5.77	3.56	5.78	45.5
	A4 (Cold)	11.20	17.41	18.36	5.42	7.97	5.42	45.5
30 Ft. Side Drop	A5 (Hot)	27.21	34.79*	15.58	42.37*	25.91	10.81	45.5
	A6 (Cold)	27.19	33.66*	16.14	42.38*	20.89	10.79	45.5
30 Ft. CG Over Corner Drop on Bottom End	A7 (Hot)	8.47	14.07	28.95	15.96	15.70	4.25	45.5
	A8 (Cold)	8.20	14.84	29.84	15.93	15.64	3.81	45.5
30 Ft. CG Over Corner Drop on Lid End	A9 (Hot)	36.19*	29.24	24.65	35.91*	12.40	7.62	45.5
	A10 (Cold)	38.49*	31.80*	25.18	35.87*	12.35	7.47	45.5
30 Ft. 20° Slap Down Impact on Lid End	A11 (Hot)	47.23*	43.45*	20.70	60.94*	10.15	14.77	45.5
	A12 (Cold)	49.20*	42.79*	21.20	60.94*	6.78	14.76	45.5
30 Ft. 20° Slap Down Impact on Bottom End	A13 (Hot)	9.55	13.98	20.26	25.91	24.95	5.76	45.5
	A14 (Cold)	9.06	14.73	20.91	25.94	24.63	5.18	45.5
Fire Accident	A15 (600° F)	8.71	12.65	13.74	7.21	6.95	3.68	45.5

*The stresses which result in factor of safety less than 1.5 are linearized in Table 2-19.

Table 2-19
Linearized Stress Evaluation for Hypothetical Accident
Condition Load Combinations

Load Comb.	Component	Nodal Stress Intensity (ksi)	Linearized Stress Intensity			Allowable (ksi)	Factor of Safety
			Node Nos.	Type	Magnitude (ksi)		
A5 (Hot) (30 Ft. Side Drop)	Flange	34.79	15719-458	P _M	14.71	45.5	3.09
				P _L + P _B	24.47	65.0	2.66
	Gamma Shield Shell	42.37	4886-5589	P _M	5.22	45.5	8.72
				P _L + P _B	16.77	65.0	3.88
A6 (Cold) (30 Ft. Side Drop)	Flange	33.66	15719-458	P _M	14.75	45.5	3.08
				P _L + P _B	24.25	65.0	2.68
	Gamma Shield Shell	43.38	4886-5589	P _M	5.23	45.5	8.70
				P _L + P _B	16.75	65.0	3.88
A9 (Hot) (30 Ft. Corner Drop on Lid)	Lid & Shield	36.19	4537-4548	P _M	9.69	45.5	4.70
				P _L + P _B	27.05	65.0	2.40
	Gamma Shield Shell	35.91	4793-5649	P _M	4.75	45.5	9.58
				P _L + P _B	13.97	65.0	4.65
A10 (Cold) (30 Ft. Corner Drop on Lid)	Lid & Shield	38.49	4537-4548	P _M	9.73	45.5	4.68
				P _L + P _B	27.64	65.0	2.35
	Flange	31.80	3922-5429	P _M	7.22	45.5	6.30
				P _L + P _B	17.95	65.0	3.62
	Gamma Shield Shell	35.87	4793-5649	P _M	4.78	45.5	9.52
				P _L + P _B	13.97	65.0	4.65

Table 2-19
Linearized Stress Evaluation for Accident Condition Load Combinations
 (Concluded)

Load Comb.	Component	Nodal Stress Intensity (ksi)	Linearized Stress Intensity			Allowable (ksi)	Factor of Safety
			Node Nos.	Type	Magnitude (ksi)		
A11 (Hot) (30 Ft. Oblique Drop on Lid) Slap Down	Lid & Shield	47.23	4537-4548	P _M	11.29	45.5	4.03
				P _L + P _B	28.84	65.0	2.25
	Flange	43.45	3920-5434	P _M	18.71	45.5	2.43
				P _L + P _B	33.13	65.0	1.96
	Gamma Shield Shell	60.94	4944-5553	P _M	7.23	45.5	6.29
				P _L + P _B	24.02	65.0	2.71
A12 (Cold) (30 Ft. Oblique Drop on Lid) Slap Down	Lid & Shield	49.20	4537-4548	P _M	11.29	45.5	4.03
				P _L + P _B	29.24	65.0	2.22
	Flange	42.79	3920-5434	P _M	18.79	45.5	2.42
				P _L + P _B	33.14	65.0	1.96
	Gamma Shield Shell	60.94	4944-5553	P _M	7.23	45.5	6.29
				P _L + P _B	24.01	65.0	2.71

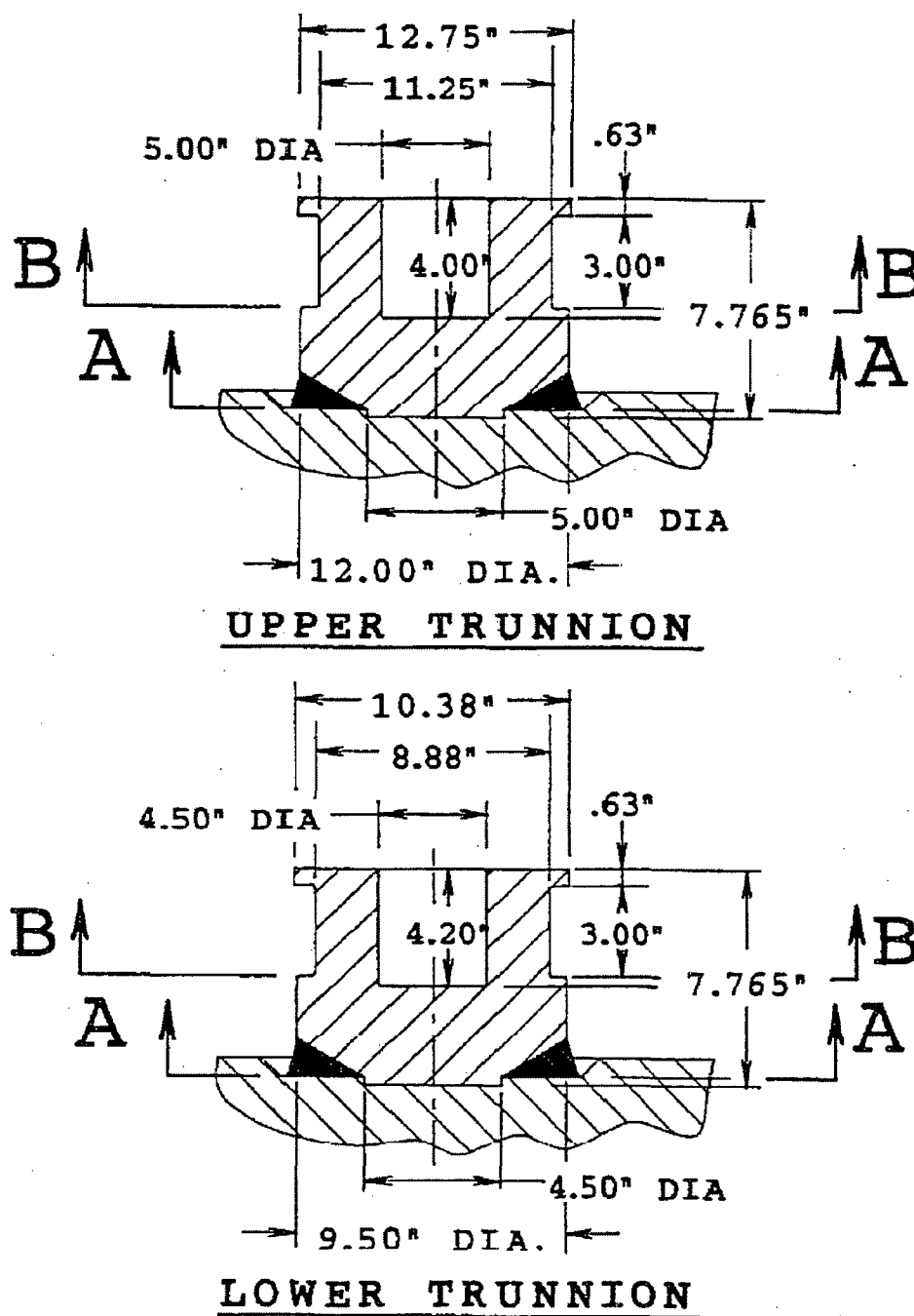


Figure 2-1
Geometry of Upper (front) and Lower (rear) Trunnions

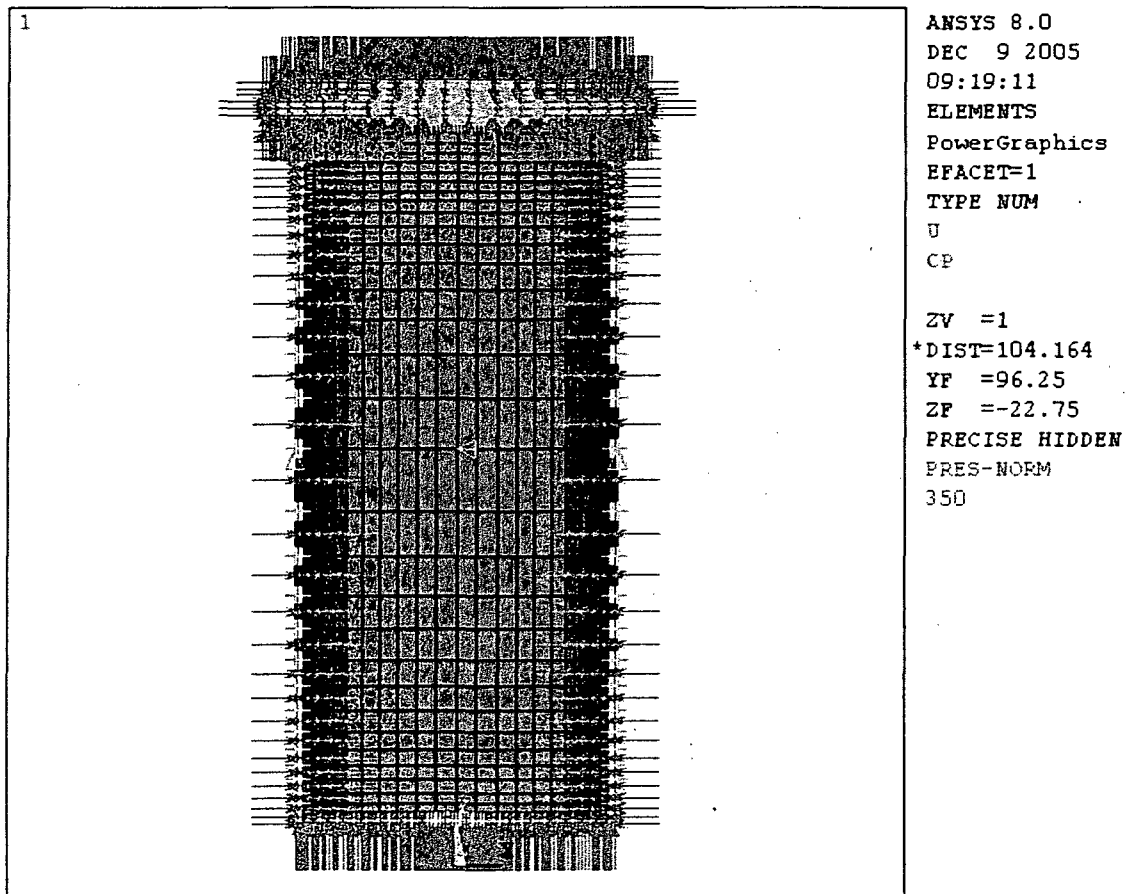


Figure 2-2
290 psig Immersion Analysis Finite Element Model Loads
and Boundary Conditions

Appendix 2.10.1

STRUCTURAL ANALYSIS OF CASK BODY

TABLE OF CONTENTS

	<u>PAGE</u>
2.10.1 STRUCTURAL ANALYSIS OF CASK BODY	2.10.1-1
2.10.1.1 Introduction.....	2.10.1-1
2.10.1.2 ANSYS Analysis	2.10.1-1
2.10.1.3 ANSYS Analysis Results and Report Methodology	2.10.1-21
2.10.1.4 Trunnion Local Stress Analysis Due To Lifting Load	2.10.1-22
2.10.1.5 References	2.10.1-23

LIST OF TABLES

Table 2.10.1-1	Element types, Material Numbers and Real Constants of ANSYS Model Cask Components	2.10.1-24
Table 2.10.1-2	Summary Maximum Nodal Stress Intensities in Cask Components for Individual Load Runs	2.10.1-25
Table 2.10.1-3	6g Lifting Load	2.10.1-26

LIST OF FIGURES

Figure 2.10.1-1	TN-40 Containment Vessel Key Dimensions	2.10.1-27
Figure 2.10.1-2	TN-40 Cask/Lid/Bolt FEM Representation	2.10.1-28
Figure 2.10.1-3	Finite Element Model—Lid	2.10.1-29
Figure 2.10.1-4	Finite Element Model – Containment Flange	2.10.1-30
Figure 2.10.1-5	Finite Element Model – Inner Shell and Bottom Plate	2.10.1-31
Figure 2.10.1-6	Finite Element Model – Gamma Shield Shell	2.10.1-32
Figure 2.10.1-7	Finite Element Model – Gamma Bottom Shield	2.10.1-33
Figure 2.10.1-8	Coupling and Boundary Conditions	2.10.1-34
Figure 2.10.1-9	Bolt Preload – Loading and Displacement Boundary Conditions	2.10.1-35
Figure 2.10.1-10	Fabrication Load – Loading and Displacement Boundary Conditions	2.10.1-36
Figure 2.10.1-11	Internal Pressure – Loading and Displacement Boundary Conditions	2.10.1-37
Figure 2.10.1-12	Thermal Stress 100°F Environment – Loading and Displacement Boundary Conditions	2.10.1-38
Figure 2.10.1-13	Thermal Stress -20°F Environment – Loading and Displacement Boundary Conditions	2.10.1-39
Figure 2.10.1-14	Thermal Stress -40°F Environment – Loading and Displacement Boundary Conditions	2.10.1-40
Figure 2.10.1-15	1g Horizontal – Loading and Displacement Boundary Conditions	2.10.1-41
Figure 2.10.1-16	Transport Tie-Down – Loading and Displacement Boundary Conditions	2.10.1-42
Figure 2.10.1-17	End Drop on Bottom – Loading and Displacement Boundary Conditions	2.10.1-43
Figure 2.10.1-18	End Drop on Lid – Loading and Displacement Boundary Conditions	2.10.1-44
Figure 2.10.1-19	6g Vertical Lifting – Loading and Displacement Boundary Conditions	2.10.1-45
Figure 2.10.1-20	Side Drop, 1g – Loading and Displacement Boundary Conditions	2.10.1-46

Figure 2.10.1-21	Corner Drop on Lid – Loading and Displacement Boundary Conditions	2.10.1-47
Figure 2.10.1-22	Corner Drop on Bottom – Loading and Displacement Boundary Conditions	2.10.1-48
Figure 2.10.1-23	20° Slap Down Impact On Lid End – Loading and Displacement Boundary Conditions	2.10.1-49
Figure 2.10.1-24	20° Slap Down Impact on Bottom End – Loading and Displacement Boundary Conditions	2.10.1-50

2.10.1 STRUCTURAL ANALYSIS OF CASK BODY

2.10.1.1 Introduction

This appendix presents the structural analyses of the TN-40 cask body and the local stress at the trunnion/cask body interface. The cask body includes the inner shell, bottom inner plate, gamma shield shell, bottom shield, shield plate, and the lid outer plate. The methods, models, and assumptions used in analyzing the cask body under various individual loading conditions as specified in 10CFR71.71 and 10CFR71.73 [1] are described. These conditions include both the Normal Conditions of Transport (NCT) and the Hypothetical Accident Conditions (HAC). Stress results are reported at selected locations for each load case. Maximum stresses from this appendix are evaluated in Sections 2.6 and 2.7 where the load combinations as outlined in Regulatory Guide 7.8 [3] are performed and the results are evaluated against the ASME Code [4] and Regulatory Guide 7.6 [5] design criteria, which are described in Section 2.1.2.

Static linear elastic methods are used for the TN-40 cask body structural analyses. The stresses and deformations resulting from the applied loads are generally determined using the ANSYS [6] computer program.

The detailed calculations for the lid bolts are presented in Appendix 2.10.2. Stress evaluations of the lifting devices and tie-down system are described in Section 2.5.

The two analysis methods described in this appendix and used to evaluate the cask body for the specified loading conditions are:

- ANSYS Analysis – Static Linear Elastic Analysis using a 3-D Model
- Bijlaard Trunnion Local Stress Analysis

The Bijlaard [7] analyses are performed to determine the local cask body stresses at trunnion locations where general stresses are also reported from the ANSYS analyses. This permits the localized shell stresses induced by the trunnion loadings to be easily combined with stresses obtained from appropriate ANSYS load cases. The method of combining stress results from individual load cases and their evaluations are discussed in Section 2.6 and Section 2.7 for NCT and HAC loads, respectively.

2.10.1.2 ANSYS Analysis

Cask Geometry Description

The cask body consists of an inner shell and an outer gamma shield shell. The inner shell (and bottom inner plate) is the primary containment boundary of the packaging. Key dimensions of the cask body are shown in Figure 2.10.1-1. The inner shell is 1.5 in. thick cylinder welded to the shell flange and bottom inner plate. The inner shell is shrunk fit into the gamma shield shell. The cask lid is bolted to the shell flange by 48,

1.5 in. diameter, high strength bolts and sealed with two metallic seals. The lid, inner shell, bottom inner plate, and gamma shield shell components are made of low alloy steel forgings and plates. The cask is fitted with an impact limiter at either end. The two impact limiters are held against the cask ends by a set of tie rods connecting them. Two sets of trunnions are welded to the side of the gamma shield shell upper and lower ends for handling and supporting the cask during lifting and handling operations. A basket assembly inside the cask cavity is used to position and support the fuel assemblies. A detailed physical description of the containment components is provided in Chapter 1. Appendix 1.4 contains reference drawings of the TN-40 package on which the analysis models are based.

ANSYS Cask Model

The gamma shield shell, the inner shell and bottom inner plate, the shell flange, and the lid and its shield are modeled utilizing ANSYS eight-node brick elements (SOLID45) as shown in Figures 2.10.1-2 to 2.10.1-7. Due to the cyclic symmetry of the TN-40 body, some nodes in the FEM are rotated into a local cylindrical coordinate system for easy application of node coupling and boundary conditions. This local coordinate system is located at the model axis of symmetry. The lid bolts are modeled using BEAM4 elements. The bolt preload is simulated using pre-strain in the beam elements by their real constants. The nodes at common surfaces between flange and lid are coupled in the model axial direction. The element nodes on the shrunk-fit surfaces between the gamma shield shell and the inner shell are coupled in the radial direction and are shown in Figure 2.10.1-8. Similarly, the nodes on the contacting surface between the bottom shield and the bottom inner plate are coupled in the axial direction. A total of 18,688 elements and 24,354 nodes comprise the ANSYS finite element model of the TN-40 cask. At the cask model cut plane, symmetry boundary conditions are applied. The element types, material numbers and real constants of different components of the model are summarized in Table 2.10.1-1. For various loading conditions, different boundary conditions are used to avoid rigid body motion of the FEM. The loadings and displacement boundary conditions for individual load cases are shown in Figures 2.10.1-9 to -24. To aid clarity, symmetry boundary conditions (UZ) are not shown in these figures.

Material Properties

The materials used for TN-40 Transport Cask and their properties as a function of temperature are listed below [4].

Cask Component	Material	Temperature (°F)	Ultimate Strength (ksi)	Yield Strength (ksi)	Allowable S_m (ksi)	Young's Modulus E (psi)	Thermal Expansion α (in/in/°F)
Containment Inner Shell & Bottom Inner Plate	SA-203 Gr. E or Gr. D	70	65	37	21.7	27.8×10^6	6.27×10^{-6}
		200	65	33.9	19.6	27.1×10^6	6.54×10^{-6}
		300	65	32.7	19.6	26.7×10^6	6.78×10^{-6}
Flange and Lid Outer Plate	SA350 LF3 or SA-203 Gr. E	70	70	37.5	23.3	27.8×10^6	6.27×10^{-6}
		200	70	34.3	22.8	27.1×10^6	6.54×10^{-6}
		300	70	33.2	22.2	26.7×10^6	6.78×10^{-6}
Lid Shield	SA105 or SA516, Gr.70	70	70	36	23.3	29.5×10^6	5.73×10^{-6}
		200	70	33	21.9	28.8×10^6	6.09×10^{-6}
		300	70	31.8	21.3	28.3×10^6	6.43×10^{-6}
Gamma Shield Shell Cylinder & Bottom Shield	SA266 CL 4 or SA516, Gr.70 or SA-105	70	70	36	23.3	29.5×10^6	5.73×10^{-6}
		200	70	33	21.9	28.8×10^6	6.09×10^{-6}
		300	70	31.8	21.3	28.3×10^6	6.43×10^{-6}
Lid Closure Bolt	SA320 Gr. L43	70	125	105	35	27.8×10^6	6.27×10^{-6}
		200	125	99	33	27.1×10^6	6.54×10^{-6}
		300	125	95.7	31.9	26.7×10^6	6.78×10^{-6}

Note: Lower strengths of alternate materials are listed in above table.

Loadings

This analysis evaluates NCT and HAC loadings as specified in 10CFR71. The 20 individual load cases considered in this evaluation are described below.

TN-40 24 Individual Load Cases	
IL-1	Bolt Preload and Lid Seating Pressure
IL-2	Fabrication Stress
IL-3	Internal Pressure (100 psig)
IL-4	External Pressure (25 psig)
IL-5	Thermal Stress Due to Hot Environment (100°F)
IL-6	Thermal Stress Due to Cold Environment (-20°F)
IL-7	Thermal Stress Due to Cold Environment (-40°F)
IL-8	Horizontal Cask Supported by Skid, 1g Down Gravity Load
IL-9	Transport Tie down Load (10g Long., 5g Lat., 2g Vert.)
IL-10	Transport Rail Vibration Load Supported by Skid (0.19g Long., 0.19g Lat., 0.37g Vert.)
IL-11	Transport Rail Shock Load Supported by Skid (4.7g All Directions)
IL-12	End Drop on Bottom -Rear (Bottom) Impact Limiter (1g)
IL-13	End Drop on Lid - Front (Top) Impact Limiter (1g)
IL-14	6G on Front Trunnion Lifting Load (Cask Vertical, 6g Up)
IL-15	Side Drop (1g)
IL-16	CG Over Corner Drop on Lid End (32g Axial, 14g Radial)
IL-17	CG Over Corner Drop on Bottom End (32g Axial, 14g Radial)
IL-18	20° Slap Down Impact on Lid End (22g Axial, 39g Radial)
IL-19	20° Slap Down Impact on Bottom End (22g Axial, 39g Radial)
IL-20	Local Stresses at Upper Trunnion/Cask Body Interface with 1g up - Cask Vertical

The magnitudes of the loads and pressures used in each individual load case analysis are computed as described in the following paragraphs based on the following TN-40 weights:

Component	Calculated Weight (lbs.)	Weight Used (lbs.)
Cask Body	169,796	169,800
Internals	66,693	66,700
Top (Front) Impact Limiter and Top Impact Limiter Spacer	17,489	17,700
Bottom (Rear) Impact Limiter	16,332	16,500
Tie Rods and Bolting Brackets	1,145	1,000*
Total	271,455	271,700

- * This weight is equally divided in two impact limiters in the analysis. i.e.
 Front Impact limiter Weight = 17,700 + 500 = 18,200 LB
 Rear Impact limiter Weight = 16,500 + 500 = 17,000 LB

1. Lid Closure Bolt Preload and Lid Seating Pressure (IL-1)

A bolt axial prestress of 50 ksi, calculated in Appendix 2.10.2, at the bolt shank (1.375 in. diameter) is simulated by specifying an initial strain in BEAM4 elements representing the bolts. The required initial strain value of 0.002108 in./in. (in the bolts) was determined by first calculating the initial strain required to produce an axial stress of 50 ksi (i.e. $\epsilon = \sigma/E = 50E3/26.7E6 = 0.001873$ in./in.). Then, an initial analysis with the calculated strain (0.001873) was conducted and the resulting bolt prestress was backed out. Since, a portion of this strain becomes elastic preload strain in the bolts, and a portion becomes strain in the clamped parts, the backed out prestress from the initial analysis will not produce the desired 50 ksi. The FEM was then updated by multiplying the 0.001873 in./in. strain by the ratio of (desired prestress, 50 ksi / initial analysis prestress), and a second preload analysis was conducted, which resulted in a 50 ksi bolt prestress.

The maximum lid seating pressure required to seat the metallic seals [8] is computed as 1,038,108 lb. This load is calculated based on approximately 2200 lb/in. gasket seating force. Based on the closest nodes in the model to the seal location, the lid seating pressure,

$$p = 1,038,108 / \pi(38.4^2 - 37.35^2) = 4154.5 \text{ psi}$$

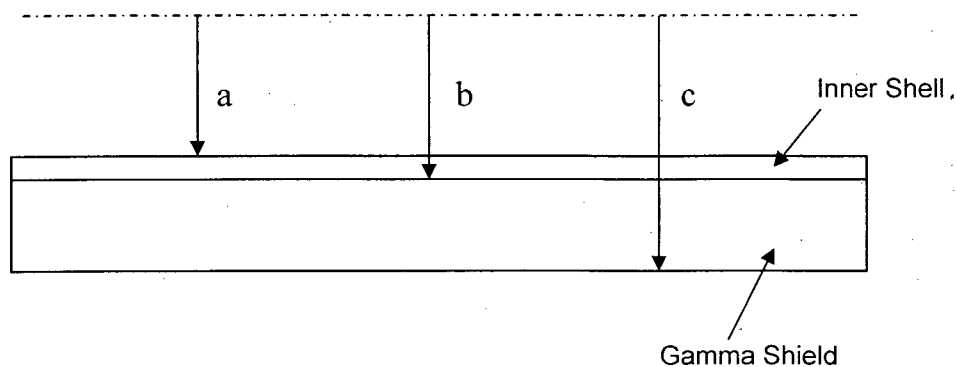
This pressure is applied to the lid and flange seal areas. During the analysis, the cask is supported as shown in Figure 2.10.1-9.

2. Fabrication Stress (IL-2)

The fabrication stresses in the cask are due to the 0.040 in. diametrical interference between the inner shell and the gamma shield shell (Appendix 1.4 drawings). The shrink fit stresses are calculated based on a radial interference of 0.020 in. The interface pressure, p , can be found from the following expression:

$$p = (E\delta/b) [(b^2-a^2)(c^2-b^2)/2b^2(c^2-a^2)] \quad [10]$$

where: $\delta = 0.20 \text{ in.}$ $E = 29.5 \times 10^6 \text{ psi}$
 $a = 36.0 \text{ in.}$ $b = 37.5 \text{ in.}$ $c = 45.5 \text{ in.}$



$$p = (29.5 \times 10^6 \times .02/37.5) [(37.5^2 - 36.0^2) (45.5^2 - 37.5^2)/2 \times 37.5^2 (45.5^2 - 36.0^2)] \\ = 529.1 \text{ psi}$$

Use 530 psi.

In order to model this load, the radial couplings between the inner shell and gamma shield shell are deleted and the interface 530 psi pressure is applied to the two cylinders. The boundary conditions for this loading are shown in Figure 2.10.1-10.

3. Internal Pressure Loading (IL-3)

An internal pressure of 100 psig is applied to the cavity surface as shown in Figure 2.10.1-11. The pressure is applied up to the metallic seal inner radius. The lid closure bolt preload and seal seating loads are removed in this calculation. The cask is supported as shown in Figure 2.10.1-11 for this loading.

4. External Pressure Loading (IL-4)

An external pressure of 25 psig is applied to the outer surface of the cask body. The pressure is applied up to the seal outer radius.

5. Thermal Stress for Hot Environment Condition at 100°F Ambient Temperature (IL-5)

The thermal analysis of the cask body is described in Chapter 3. The thermal model is used to obtain the NCT steady state component temperatures in the cask body. The thermal inputs include 100°F daily averaged ambient air temperature, maximum payload decay heat and maximum solar heat loading. The cask nodal temperatures from the thermal results file are interpolated using an ANSYS macro to determine the nodal temperatures in the structural model. The resulting cask temperature distribution is shown in Figure 2.10.1-12. These temperatures are then used as ANSYS inputs for the thermal stress analysis. Temperature-dependent material properties are used in this analysis. The cask support boundary conditions are also shown in Figure 2.10.1-12.

6. Thermal Stresses for Cold Environment Condition at -20°F Ambient Temperature (IL-6)

The thermal analysis of the cask body is described in Chapter 3. The thermal model is used to obtain the NCT steady-state temperatures in the cask body due to a -20°F daily averaged ambient air temperature. The cask nodal temperatures from the thermal results file are interpolated using an ANSYS macro to determine the nodal temperatures in the structural model. The resulting cask temperature distribution is shown in Figure 2.10.1-13. These temperatures are then used as ANSYS inputs for the thermal stress analysis. Temperature-dependent material properties are used in this analysis. The cask support boundary conditions are also shown in Figure 2.10.1-13.

7. Thermal Stresses for Cold Environment Condition at -40°F Ambient Temperature (IL-7)

The thermal analysis of the cask body is described in Chapter 3. The thermal model is used to obtain the NCT steady-state metal temperatures in the cask body resulting from the -40°F daily averaged ambient air temperature. The cask nodal temperatures from the thermal results file are interpolated using an ANSYS macro to determine the nodal temperatures in the structural model. The resulting cask temperature distribution is shown in Figure 2.10.1-14. These temperatures are then used as ANSYS inputs for the thermal stress analysis. Temperature-dependent material properties are used in this analysis. The cask support boundary conditions are also shown in Figure 2.10.1-14.

8. Cask Supported Horizontally by Skid, 1g down Gravity Load (IL-8)

For the 1g loading, the cask is oriented horizontally, and the cask is secured axially and radially on a transport skid. For the inertial loading, a vertical acceleration of 1g is applied in the global X direction.

The weight of the internals is applied as radial pressure (P_r), the cosine varying pressure is applied around the lower radial portion (0° to 75° range) of the cavity. The pressure is calculated by the following formula, which is developed in Section 2.10.1.2.1:

$$P_r = [g] \frac{W}{LR} \left[\frac{1}{\frac{\sin(\frac{\pi}{2} + \theta)}{(\frac{\pi}{2\theta}) + 1} + \frac{\sin(\frac{\pi}{2} - \theta)}{(\frac{\pi}{2\theta}) - 1}} \right] \times \cos\left(\frac{\pi\theta_i}{2\theta}\right)$$

Where:

- θ = ½ Angle of contact
- θ_i = Circumferential angle pressure is applied
- W = Weight of internals
- L = Length pressure is applied
- R = Radius pressure is applied
- g = Vertical acceleration

For example, a pressure applied at an angle of 7.5° would be calculated as follows:

$$P_r = [1.0] \frac{66,700}{163.0 \times 36} \left[\frac{1}{\frac{\sin(90 + 75)}{(\frac{180}{2 \times 75}) + 1} + \frac{\sin(90 - 75)}{(\frac{180}{2 \times 75}) - 1}} \right] \times \cos\left(\frac{180 \times 7.5}{2 \times 75}\right)$$

$$P_r = 11.367(0.7083)(0.9877) = 7.95 \text{ psi}$$

In addition, radial pressure due to the front impact limiter weight (P_{fr}) is applied along the contacting surfaces of the limiter and the lid/cask wall. This includes the lid and flange radial surfaces. The pressure follows a cosine distribution and is applied from the vertical (Y=180° to Y=105°).

A radial pressure due to the rear impact limiter weight (P_r) is also applied along the contacting surfaces of the limiter and the cask wall. Similar to the front impact limiter, the pressure follows a cosine distribution and is applied from the vertical ($Y=180^\circ$ to $Y=105^\circ$).

Since, resin (10,577 lb.), outer shell (7,453 lb.), trunnions (666 lb.), and aluminum box (1,993 lb.) weights are not included in the FEM, their weight is incorporated in outer gamma cylinder (mat, 6) by increasing its actual density (0.283) to an equivalent density of 0.343 lb/in³. This increased density is used in all subsequent drop and inertia load runs.

During the run, the cask is supported as shown in Figure 2.10.1-15. Since the support saddle and strap are not modeled, displacement boundary conditions are applied to nodes near these locations.

9. Transport Tie-Down Loading (IL-9)

For the tie down loading, the cask is oriented horizontally and secured axially and radially on a transport skid. The input loading conditions used to evaluate the TN-40 cask for transport tie-down loading are obtained from 10CFR71.45. The peak inertia (acceleration) values used are:

Vertical	2 g
Longitudinal	10 g
Lateral	5 g

Two inertial loads are applied in the FEM:

1. A longitudinal 10g acceleration (applied in the axial direction)
2. The resultant of the vertical & lateral accelerations (applied in the radial direction) is calculated as $(2^2 + 5^2)^{1/2} = 5.4g$.

A pressure due to the weight of the front impact limiter (P_{fa}) is applied axially at lid end and calculated as:

$$P_{fa} = 10.0 \times (18,200) / ((3.14159) \times 45.5^2) = 27.98 \text{ psi}$$

In addition, pressure loads due to the weight of the internals are applied to the cask inner surface in the axial and radial directions. The pressure due to the axial load acting on the inside surface of the rear bottom plate (P_{ia}) is calculated by:

$$P_{ia} = 10.0 \times (66,700) / ((3.14159) \times 36.0^2) = 163.82 \text{ psi}$$

Radial pressure (P_r) acting on the lower half of the inner cask surface due to the weight of internals is represented as a cosine varying pressure around the lower radial portion (0° to 75° range) of the cavity as described above.

As an example, pressure applied at an angle of 7.5° would be calculated as follows:

$$P_r = [5.4] \frac{66,700}{163.0 \times 36.0} \left[\frac{1}{\frac{\sin(90+75)}{(\frac{180}{2 \times 75}) + 1} + \frac{\sin(90-75)}{(\frac{180}{2 \times 75}) - 1}} \right] \times \cos\left(\frac{180 \times 7.5}{2 \times 75}\right)$$

$$P_r = 61.380 * (0.7083)(0.9877) = 42.94 \text{ psi}$$

In addition, the radial pressure due to the front impact limiter weight (P_{fr}) is applied along the contacting surfaces of the limiter and the lid/cask wall. This includes the lid and flange radial surfaces. The pressure follows a cosine variation and is applied from the vertical ($Y=180^\circ$ to $Y=105^\circ$).

A radial pressure due to the rear impact limiter weight (P_{rr}) is also applied along the contacting surfaces of the limiter and the cask wall. Similar to the front impact limiter, the cosine varying pressure is applied from the vertical ($Y=180^\circ$ to $Y=105^\circ$).

During the ANSYS analysis, the cask is supported as shown in Figure 2.10.1-16. Since the skid saddles are not modeled, displacement boundary conditions are applied to nodes near the saddle centerline locations. Axial restraint is provided by displacement boundary conditions at the cask bottom (rear) nodes.

10. & 11. Rail Car Vibration and Rail Car Shock Loadings (IL-10 & IL-11)

For the rail car vibration and shock loadings, the same methodology utilized for the transport tie-down loading is applied, with the exception that the inertial loads are based on the following accelerations:

Rail Car Vibration Accelerations [9]:

Vertical	0.37g
Longitudinal	0.19g
Lateral	0.19g

Rail Car Shock Accelerations [9]:

Vertical	4.7g
Longitudinal	4.7g
Lateral	4.7g

12. End Drop on Bottom (Rear) Impact Limiter (IL-12)

The dynamic analysis described in Appendix 2.10.8 determines the inertial load on the TN-40 packaging for both a 1 foot and a 30 foot end drop onto an unyielding surface. This stress evaluation is conducted for a unit load (1g). However, since this is a linear elastic analysis, stresses can be ratioed for the actual g loads when the load

combinations are calculated. The payload and the impact limiters are not included in the FEM. Rather, their loading effects are simulated as distributed pressures applied to the cask at the appropriate locations.

The following inertia loads (pressure) are applied due to a 1g vertical acceleration.

An axial pressure due to the cask internals (P_i) is applied to the bottom inner plate surface:

$$P_i = 1.0 \times 66,700 / ((\pi) \times 36.0^2) = 16.382 \text{ psi}$$

An axial pressure due to the front impact limiter (P_{fl}) is applied to the outer lid surfaces based on the projected area:

$$P_{fl} = 1.0 \times 18,200 / ((\pi) \times 45.5^2) = 2.798 \text{ psi}$$

The bottom nodes of the cask are supported in vertical direction. Loading and displacement boundary conditions are shown in Figure 2.10.1-17.

13. End Drop on Lid (Front) Impact Limiter (IL-13)

An analysis similar to that of bottom end drop is performed for the 1g vertical load. The following loads are applied.

A 1.0 g vertical acceleration of the finite element model simulates the inertial loading.

An axial pressure due to the cask internals (P_i) is applied to the inner lid surface based on:

$$P_i = 1.0 \times 66,700 / ((\pi) \times 36.0^2) = 16.382 \text{ psi}$$

An axial pressure due to the rear impact limiter (P_{rl}) is applied to the outer surface of the cask bottom shield:

$$P_{rl} = 1.0 \times 17,000 / ((\pi) \times 45.5^2) = 2.614 \text{ psi}$$

Loading and displacement boundary conditions are shown in Figure 2.10.1-18.

14. 6g Lifting on Upper Trunnion (IL-14)

The cask is oriented vertically and supported by the 2 upper trunnions. The inertial loading is simulated by applying a 6g vertical acceleration to the finite element model. Note that the impact limiters are not included in this case, as they are removed prior to lifting.

Since the internals are not included in the model, their loading effects are simulated by a distributed pressure (P_i) acting on the inside bottom surface of the cask cavity:

$$P_i = 6.0 \times (66,700) / ((3.14159) \times 36.0^2) = 98.293 \text{ psi}$$

Loading and displacement boundary conditions are shown in Figure 2.10.1-19. This load step is to calculate the globe stress of the cask component and will be used for containment fatigue analysis. The stresses at the trunnion/gamma shield shell interface due to 6g lifting load are calculated in Section 2.10.1.4.

15. Side Drop (IL-15)

The dynamic analyses described in Appendix 2.10.8 determine the inertial loads on the TN-40 packaging for both 1 foot and 30 foot side drops onto an unyielding surface. This stress evaluation assumes a unit load (1g). However, since this is a linear elastic analysis, stresses can be ratioed for the actual g loads when the load combinations are calculated. The payload and the impact limiters are not included in the FEM. Their loading effects are simulated as distributed pressures applied to the cask at the appropriate locations.

The contacting impact limiter forces on the cask and lid are applied as reaction pressures required to balance the inertial forces of the system. Thus, the vessel is in equilibrium under the applied forces. During the side drop, the pressure on the inner surface due to the internals and the reaction pressure on the outer cask surface due to the impact limiters are assumed to vary as a cosine function over a defined arc length.

The loads acting in this case are:

A. Cask Body Inertia

The inertial loading is simulated by applying a 1g vertical acceleration to the finite element model in the global X direction which is perpendicular to the cask axis.

B. Pressure Due to Internals

The radial pressure (P_i) acting on the lower half of the inner shell surface due to the weight of internals is represented as a cosine varying pressure applied around the lower radial portion (0° to 75° range) of the cavity surface.

$$P_i = [g] \frac{W}{LR} \left[\frac{1}{\frac{\sin(\frac{\pi}{2} + \theta)}{(\frac{\pi}{2\theta}) + 1} + \frac{\sin(\frac{\pi}{2} - \theta)}{(\frac{\pi}{2\theta}) - 1}} \right] \times \cos\left(\frac{\pi\theta_i}{2\theta}\right)$$

For example, a pressure applied at an angle of 7.5° would be calculated as follows:

$$P_i = [1.0] \frac{66,700}{163.0 \times 36.0} \left[\frac{1}{\frac{\sin(90 + 75)}{(\frac{180}{2 \times 75}) + 1} + \frac{\sin(90 - 75)}{(\frac{180}{2 \times 75}) - 1}} \right] \times \cos\left(\frac{180 \times 7.5}{2 \times 75}\right)$$

$$P_i = 7.95 \text{ psi}$$

C. Impact Reaction Pressures:

Pressures applied by the rear and front impact limiter reactions on the lower longitudinal half of the outer cask body during impact are computed. These radial pressures are assumed to vary in a cosine distribution around the bottom half of the outer surfaces (0° to 89.5° range) and are calculated just as the internals pressure above. However, the total force (F) applied in the equation is based on the following reactions:

Total cask weight, W = 236,500 lb. Use 237,000 lb. (cask + internals)

Reaction force, Front (lid) = 237,000 x 92.33/183.75
= 118,974 lb.

Reaction force, Rear (bottom) = 237,000 x 91.42/183.75
= 118,026 lb.

The front (lid / cask side) reaction force is divided in the ratio of two lengths: 4.5 in. (R = 41.375") for the lid and 7.5 in. (R = 45.5") for the portion of the cask covered by the impact limiter.

Loading and displacement boundary conditions are shown in Figure 2.10.1-20.

16. 30 Foot CG Over Corner Drop on Lid End (IL-16)

For CG over corner, the cask is inclined at approximately 64° from the horizontal. The dynamic analysis of Appendix 2.10.8 determines the inertial loads for this loading condition. All the applied loads and reaction forces are transformed into axial and normal components. The axial pressure components due to the internals, bottom impact limiter and impact reaction are assumed uniformly distributed. All radial pressure components (i.e. pressure due to internals, rear impact limiter and impact reactions) are assumed to have a cosine variation over a defined arc length.

The forces acting in this case are:

A. Cask Body Inertia

The component accelerations (32g axial & 14g Radial – Appendix 2.10.8) are applied as inertial loads in the axial and radial directions. In addition, a rotational acceleration of 0.148g is applied at the vessel CG to counteract the out-of-balance caused by the component's acceleration resultant. That is, the component translational accelerations applied have been conservatively rounded, which results in a slight resultant moment

(out-of-balance) when the solution is executed. This moment is counteracted by the applied angular acceleration (torque) to preserve static equilibrium.

B. Pressure Due to Internals

Radial pressure (P_{ir}) acting on the lower half of the inner cask wall due to the weight of internals is represented as a cosine varying pressure around the upper radial portion (180° to 105° range) of the cavity.

In addition, an axial pressure is applied, due to the weight of the internals, to the cask inner lid surface:

$$P_{ia} = 32 \times (66,700) / ((3.14159) \times 36.0^2) = 524.2 \text{ psi}$$

C. Pressure Due to Rear Impact Limiter

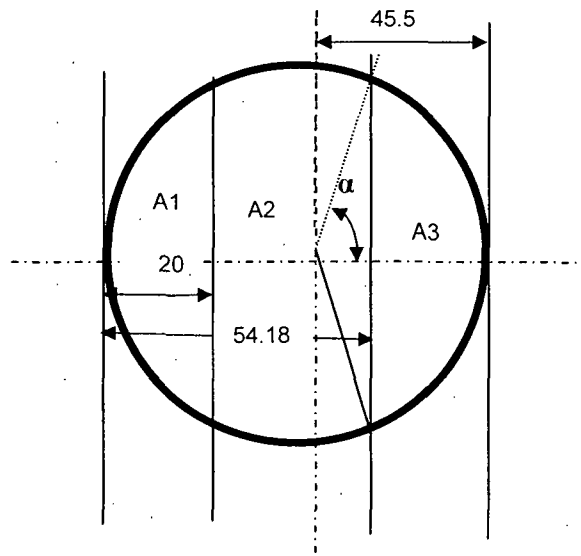
The inertia load of the nonstriking impact limiter is also applied to the cask in two mutually perpendicular directions. The axial component (P_{ra}) is applied as a uniform pressure over the outside surface at the interface with the impact limiter on the bottom end. The pressure applied is calculated as:

$$P_{ra} = 32.0 \times (17,000) / ((3.14159) \times 45.5^2) = 83.7 \text{ psi}$$

The other component (P_{rr}) follows a cosine distribution around the lower half of the outside surface (0° to 75° range) of the cask.

D. Reaction Pressures Due to Front Impact Limiter

The reaction pressure from the striking impact limiter is applied to the cask in two mutually perpendicular directions. The axial component (P_{fa}) is applied as two-step uniform pressure over a portion of the cask interface with the impact limiter on the lid end. The crush footprint of the front impact limiter was projected onto the cask surface based on results obtained from Appendix 2.10.8.



For the axial reaction pressure applied, a total area (4037 in²), for a 360° arc, is calculated as:

$$A = ((\pi) \times 45.5^2) - A_3$$

$$A_3 = \frac{1}{2}(R^2) [2\alpha - \sin 2\alpha] \quad [2]$$

$$\cos \alpha = 8.68/45.5 = 0.1908 \quad \alpha = 79.0 \text{ deg} = 1.3789 \text{ rad.}$$

$$A_3 = \frac{1}{2}(45.5^2) [2 \times 1.3789 - \sin (2 \times 79)] = 2466.9 \text{ in}^2$$

$$\text{Total crushing area, } A = ((\pi) \times 45.5^2) - 2466.9 = 4037 \text{ in}^2$$

Due to the nature of a corner impact the reaction pressure will not be precisely distributed uniformly throughout the crushed area. Instead, the reaction pressures at the center of the crushed area will be higher than those in the peripheral area away from the impact center. It is therefore assumed that the majority weight consisting of the cask plus the rear end impact limiter is to be reacted by an area bounded by 20 in. from the edge of the cask and the weight of internal cargo is to be reacted by the rest of the crushed area. The axial reaction pressure to the cask is therefore applied in two steps: p_1 on area A_1 and p_2 on area A_2 the following formulas are used to calculate p_1 and p_2 :

$$\cos \alpha = 25.5/45.5 = 0.5604 \quad \alpha = 55.91 \text{ deg} = 0.9759 \text{ rad.}$$

$$A_1 = \frac{1}{2}(45.5^2) [2 \times 0.9759 - \sin (2 \times 55.91)] = 1059.3 \text{ in}^2$$

$$A_2 = 4037 - 1059.3 = 2977.3 \text{ in}^2$$

Pressure on area A_1 :

$$p_1 = 32.0 \times (169,800 + 17,000) / 1059.3 \text{ in}^2 = 5,643 \text{ psi}$$

Pressure on area A_2 :

$$p_2 = 32.0 \times (66,700) / 2977.3 \text{ in}^2 = 718 \text{ psi}$$

The radial component pressures follow a cosine distribution around the radial crush foot print from 90.5° to 180° of the cask. The radial reaction pressures are calculated using a modified version of cosine formula. Since the crush footprint is a circular segment, and the pressures are being applied to two separate side surfaces (i.e. lid and upper flange wall). The total force (F) applied in the equation is based on the percentage of the total length to which the specific pressure is applied.

$$P_{fr1} = [g] \times \left[\frac{L}{L_t} \right] \times \left[\frac{F_R}{LR} \right] \times \left[\frac{1}{\frac{\sin(\frac{\pi}{2} + \theta)}{(\frac{\pi}{2\theta}) + 1} + \frac{\sin(\frac{\pi}{2} - \theta)}{(\frac{\pi}{2\theta}) - 1}} \right] \times \cos\left(\frac{\pi(180 - \theta)}{2\theta}\right)$$

The calculated reaction axial and radial pressures due to the crushed impact limiter had to be adjusted and a rotational acceleration 0.148g applied to balance the applied loads. Loading and displacement boundary conditions are shown in Figure 2.10.1-21.

17. 30 Foot CG Over the Corner Drop on Bottom End (IL-17)

For this corner drop, the cask is again inclined at approximately 64° from the horizontal as described in Appendix 2.10.8. The applied loads are transformed into axial and normal components, and are applied using the same methodology adopted for the CG over corner lid drop. All radial pressure components (i.e. pressure due to internals, front impact limiter and impact reactions) are assumed to have a cosine variation. The forces acting in this case are:

A. Cask Body Inertia

The component accelerations (i.e. 32g axial & 14g Radial – Appendix 2.10.8) are applied as translational inertial loads in the axial and radial directions respectively. In addition, a rotational acceleration of 0.1452g is applied at the vessel CG to counter act the out-of-balance and return the model to static equilibrium.

B. Pressure Due to Internals

The radial pressure (P_{ir}) acting on the lower half of the inner cask wall due to the weight of the cask internals is represented as a cosine varying pressure around the lower radial portion (0° to 75° range) of the cavity.

In addition, an axial pressure due to the weight of the internals is applied to the cask inner bottom surface based on:

$$P_{ia} = 32.0 \times (66,700) / ((3.14159) \times 36.0^2) = 524.2 \text{ psi}$$

C. Pressure Due to the Front Impact Limiter

The inertia load of the nonstriking impact limiter is also applied to the cask in two mutually perpendicular directions. The axial component (P_{ia}) is applied as a uniform pressure over the outer surface of the lid. The pressure applied is calculated as:

$$P_{ia} = 32.0 \times (18,200) / ((3.14159) \times 45.5^2) = 89.5 \text{ psi}$$

The other component (P_{ir}) is assumed to follow a cosine distribution around the upper half of the outside surface (105° to 180° range) of the cask.

D. Reaction Pressures Due to Rear Impact Limiter

The reaction pressure from the striking impact limiter is applied to the cask in two mutually perpendicular directions as described in the above Loading Case IL-16.

For the axial reaction pressure applied, the total area, 4,037 in², and areas A1 and A2 are the same as calculated for the corner drop on the lid (Case IL-16).

Pressure on area A1:

$$p_1 = 32.0 \times (169,800 + 18,200) / 1059.3 = 5,679 \text{ psi}$$

Pressure on area A2:

$$p_2 = 32.0 \times (66,700) / 2977.3 = 718 \text{ psi}$$

The radial component pressure (P_{rr}) is assumed to follow a cosine distribution around the radial crush foot print from 0° to 89.5° of the cask. The radial reaction pressures are calculated using a modified version of the cosine distribution, based on the calculated angle of application.

The calculated reaction axial and radial pressures due to crushed impact limiter had to be adjusted and a rotational acceleration 0.1452g applied to balance the applied loads. Loading and displacement boundary conditions are shown in Figure 2.10.1-22.

18. 20° Slapdown Impact on Lid End (IL-18)

For the oblique lid impact, the cask is inclined at approximately 20° from the horizontal as described in Appendix 2.10.8. All the applied loads and reaction forces are transformed into axial and normal components respectively. The axial pressure components due to the internals, bottom impact limiter and impact reaction are assumed to be uniformly distributed in two steps. All radial pressure components (i.e. pressure due to internals, rear impact limiter and impact reactions) are assumed to have a cosine variation over a determined arc length.

The forces acting in this case are:

A. Cask Body Inertia

The component accelerations (i.e. 22g axial & 39g Radial – Appendix 2.10.8) are applied as inertial loads in the axial and radial directions respectively. In addition, a rotational acceleration of 1.113g is applied at the vessel C.G. to counter act the out-of-balance forces and return the model to static equilibrium.

B. Pressure Due to Internals

Radial pressure (P_{ir}) acting on the lower half of the inner cask wall due to the weight of the internals is represented as a cosine varying pressure around the upper radial portion (105° to 180° range) of the cavity.

In addition, the axial pressure due to the weight of the internals is applied to the cask inner lid surface:

$$P_{ia} = 22.0 \times (66,700) / ((3.14159) \times 36.0^2) = 360.4 \text{ psi}$$

C. Pressure Due to Rear Impact Limiter

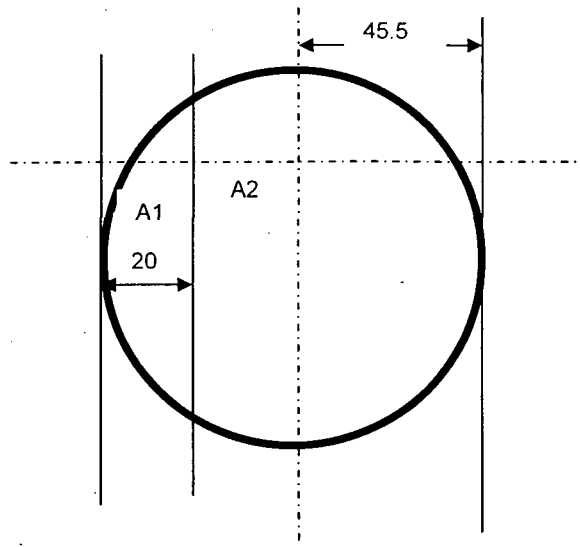
The inertia load of the nonstriking impact limiter is also applied to the cask in two mutually perpendicular directions. The axial component (P_{ra}) is applied as a uniform pressure over the outside surface at the interface with the impact limiter on the bottom end. The pressure applied is calculated as:

$$P_{ra} = 22.0 \times (17,000) / (3.14159) \times 45.5^2 = 57.5 \text{ psi}$$

The radial component (P_{rr}) is assumed to follow a cosine distribution around the lower half of the outside surface (0° to 75° range) of the cask.

D. Reaction Pressures Due to Front Impact Limiter

The axial reaction pressure (P_{ra}) was applied over entire interface with the impact limiter on the lid end as shown by the crush footprint of the front impact limiter by Appendix 2.10.8. A total area of $6,503.88 \text{ in}^2$ (assuming a 360° arc) was assumed and the pressure applied in two pressure steps as calculated below:



For the axial reaction pressure applied, a total area ($6,503.8 \text{ in}^2$), and a 360° arc, is calculated as:

$$A = ((\pi) \times 45.5^2) = 6503.8 \text{ in}^2$$

Axial pressure is applied as two-step (p_1 and p_2) uniform pressures on total area. The cask and impact limiter load is applied on area A1 and the internals load is applied on the remaining area, A2.

$$A1, (\text{as calculated in Load Case IL-16}) = 1059.3 \text{ in}^2$$

$$A2 = 6503.8 - 1059.3 = 5444.5 \text{ in}^2$$

Pressure on area A1:

$$p_1 = 22.0 \times (169,800 + 17,000) / 1059.3 = 3,880 \text{ psi}$$

Pressure on area A2:

$$p_2 = 22.0 \times (66,700) / 5444.5 = 270 \text{ psi}$$

The radial reaction pressures (P_{rr1} and P_{rr2}) are applied to the crush footprint in the radial direction and assume a cosine varying pressure from 90.5° to 180° of the cask. Since the crush footprint is a circular segment, and the pressures are being applied to two separate surfaces (i.e. lid and flange), the total force, F , applied in the equation is based on the percentage of the total length the specific pressure is applied to.

The calculated reaction axial and radial pressures due to the crushed impact limiter are adjusted and a rotational acceleration 1.113g applied to balance the applied loads. Loading and displacement boundary conditions are shown in Figure 2.10.1-23.

19. 20° Slapdown Impact on Bottom End (IL-19)

For the oblique bottom impact, the cask is inclined at approximately 20° from the horizontal. All the applied loads and reaction forces are transformed into axial and normal components respectively. The axial pressure components due to the internals, front impact limiter and impact reaction are assumed uniformly distributed in two steps. All radial pressure components (i.e. pressure due to internals, front impact limiter and impact reactions) are assumed to have cosine variation over a defined arc length.

The forces acting in this case are:

A. Cask Body Inertia

The component accelerations (i.e. 22g axial & 39g Radial – Appendix 2.10.8) are applied as translational inertial loads in the axial and radial directions, respectively. In addition, a rotational acceleration of 1.092g is applied at the vessel C.G. to counteract the out-of-balance and return the model to static equilibrium.

B. Pressure Due to Internals:

Radial pressure (P_{ir}) acting on the lower half of the inner cask wall due to the weight of internals is represented as a cosine varying pressure around the lower radial portion (0° to 75° range) of the cavity.

In addition, an axial pressure due to the weight of the internals is applied to the cask inner lid surface:

$$P_{ia} = 22.0 \times (66,700) / ((3.14159) \times 36.0^2) = 360.4 \text{ psi}$$

C. Pressure Due to Front Impact Limiter

The inertia load of the nonstriking impact limiter is also applied to the cask in two mutually perpendicular directions. The axial component (P_{la}) is applied as a uniform pressure over the outer surface of the lid. The pressure applied is calculated as:

$$P_{la} = 33.0 \times (18,200) / ((3.14159) \times 45.5^2) = 61.6 \text{ psi}$$

The other component (P_{lr}) is assumed to follow a cosine distribution around the upper half of the outside surface (105° to 180° range) of the cask.

D. Reaction Pressures Due to Bottom Impact Limiter

The reaction pressure of the striking impact limiter is applied to the cask in two directions (i.e. axial at the cask base and radial at the cask outer wall). The axial component (P_{ra}) is applied as a uniform pressure in two steps over the entire interface with the bottom impact limiter. The crush footprint of the rear impact limiter is shown in Appendix 2.10.8. For the axial reaction pressure applied, a total projected area of $6,503.8 \text{ in}^2$ (assuming a 360° arc) is assumed and the pressure is applied at the bottom cask surface along the crush footprint.

For the axial reaction pressure applied, areas A1 and A2 are the same as were calculated the oblique drop on the lid.

$$A1 = 1,059.3 \text{ in}^2$$

$$A2 = 5,444.5 \text{ in}^2$$

Pressure on area A1:

$$p_1 = 22.0 \times (169,800 + 18,200) / 1059.3 = 3,904.5 \text{ psi}$$

Pressure on area A2:

$$p_2 = 22.0 \times (66,700) / 5444.5 = 270 \text{ psi}$$

The radial component pressure (P_{rr}) is assumed to follow a cosine distribution around the radial crush footprint from 0° to 89.5° of the cask.

The calculated reaction axial and radial pressures due to the crushed impact limiter are adjusted and a rotational acceleration $1.092g$ applied to balance the applied loads. Loading and displacement boundary conditions are shown in Figure 2.10.1-24.

2.10.1.2.1 Pressure Distribution over Contact Area of Cask for Impact Load in Transverse Direction

The impact load acting in the transverse direction is applied as a load over the contact area between the impact limiter and the outer surface of the cask. The pressure distribution is assumed to be in the longitudinal direction over the 12 inch long impact

limiter contact length and vary with a cosine distribution around the circumference of the cask. For the impact conditions, the angle of contact is dependent upon the amount of crush occurring in the impact limiter. The most severe loads result from impacts on the side of the impact limiter. For these conditions, the contact angle between the impact limiter and the cask outer surface will be approximately 180 degrees. For non-crushing surfaces, a contact angle of 150 degrees (75 degree half angle of contact) is used for the cask impact analysis. The circumferential cosine pressure distribution over a half angle, θ , is calculated as follows:

$$P_i = P_{\max} \cos(\pi\theta_i / 2\theta)$$

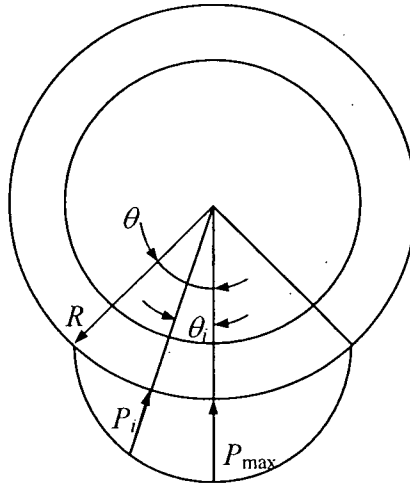
where:

P_i = Pressure load at angle θ_i .

P_{\max} = Peak pressure load, at point of impact, and

θ_i = Angle corresponding to point of interest.

The circumferential pressure distribution is illustrated in the following figure.



Circumferential Pressure Load Distribution

The peak pressure load, P_{\max} , is determined by setting the integral of the vertical pressure components, Q_i , equal to the total transverse impact load, F_t , as follows:

$$\begin{aligned} F_t &= \int_{-\theta}^{\theta} Q_i LR d\theta_i = \int_{-\theta}^{\theta} P_i \cos(\theta_i) LR d\theta_i = \int_{-\theta}^{\theta} P_{\max} \cos\left(\frac{\pi\theta_i}{2\theta}\right) \cos(\theta_i) LR d\theta_i \\ &= \frac{P_{\max} LR}{2} \int_{-\theta}^{\theta} \left[\cos\left(\frac{\pi\theta_i}{2\theta} + \theta_i\right) + \cos\left(\frac{\pi\theta_i}{2\theta} - \theta_i\right) \right] d\theta_i \end{aligned}$$

$$= P_{max} LR \left[\frac{\sin\left(\frac{\pi}{2} + \theta\right)}{\left(\frac{\pi}{2\theta}\right) + 1} + \frac{\sin\left(\frac{\pi}{2} - \theta\right)}{\left(\frac{\pi}{2\theta}\right) - 1} \right]$$

Rearranging terms gives the peak pressure, P_{max} :

$$P_{max} = \frac{F_t}{LR} \left[\frac{\sin\left(\frac{\pi}{2} + \theta\right)}{\left(\frac{\pi}{2\theta}\right) + 1} + \frac{\sin\left(\frac{\pi}{2} - \theta\right)}{\left(\frac{\pi}{2\theta}\right) - 1} \right]^{-1}$$

Therefore, the pressure at any circumferential location is given by:

$$P_i = \frac{F_t}{LR} \left[\frac{\sin\left(\frac{\pi}{2} + \theta\right)}{\left(\frac{\pi}{2\theta}\right) + 1} + \frac{\sin\left(\frac{\pi}{2} - \theta\right)}{\left(\frac{\pi}{2\theta}\right) - 1} \right]^{-1} \cos\left(\frac{\pi\theta_i}{2\theta}\right)$$

where:

$$F_t = g \times W$$

W = Weight of internals or impact limiter

g = Acceleration in the transverse direction

Therefore,

$$P_i = g \frac{W}{LR} \left[\frac{\sin\left(\frac{\pi}{2} + \theta\right)}{\left(\frac{\pi}{2\theta}\right) + 1} + \frac{\sin\left(\frac{\pi}{2} - \theta\right)}{\left(\frac{\pi}{2\theta}\right) - 1} \right]^{-1} \cos\left(\frac{\pi\theta_i}{2\theta}\right)$$

2.10.1.3 ANSYS Analysis Results and Report Methodology

ANSYS linear elastic analyses are performed for the above individual load cases. These individual loads are to be combined and evaluated for normal operating and accident conditions as described in Section 2.10.1.1. A summary of maximum nodal stress intensities in each major cask component under each individual load is presented in Table 2.10.1-2.

2.10.1.4 Trunnion Local Stress Analysis Due To Lifting Load

Method of Analysis

10CFR 71.45(a) [1] requires that any lifting attachment (trunnions) which is a structural part of package must be designed with a minimum safety factor of three against yielding when used to lift the package in the intended manner. The TN-40 trunnion design meets the 10CFR71.45(a) [1] requirements. ASME code allowable is used to evaluate the stress at the trunnion/gamma shell interface. The maximum local membrane (P_1) and local membrane plus secondary ($P_1 + Q$) stress intensities are limited to $1.5 S_m$ and $3.0 S_m$ [4] respectively.

The local stress induced in the Gamma Shield Shell by the trunnions are calculated using "Bijlaard's" method conservatively using 6g. The neutron shield and thin outer shell are not considered to strengthen either the trunnions or the gamma shield shell. The Trunnion is approximated by an equivalent attachment so that the curves of the Reference WRC-107 [7] can be used to obtain the necessary coefficients. These resulting coefficients are inserted into Table 5 of [7]. The stresses are calculated by performing the indicated multiplication in the column entitled "Compute Absolute Values of Stress and Enter Result." The resulting stress is inserted into the stress table at the eight stress locations, i.e., AU, AL, BU, BL, etc. The stresses are calculated by completing Table 5 of Reference [7]. Table 2.10.1-3 contains the computation results for the 6g lifting loads.

Results / Conclusions

The maximum stress intensity on the outside and inside of the gamma shield shell for the lifting loads are calculated in Table 2.10.1-3. The maximum stress intensity calculated in Table 2.10.1-3 are combined with the pressure stress and thermal stress calculated in Table 2.10.1-2. The maximum P_1 and $P_1 + Q$ stress intensities are then listed in the following table and compared with the allowables.

	Stress Intensity P_1 (ksi)	Allowable $1.5 S_m$ (ksi)	Stress Intensity $P_1 + Q$	Allowable $3.0 S_m$ (ksi)
Outside Edge of Gamma Shield Shell	12.4	33.75	20.58	67.5
Inside Edge of Gamma Shield Shell	12.4	33.75	19.97	67.5

2.10.1.5 References

1. 10CFR Part 71, "Packaging and Transportation of Radioactive Material".
2. Roark, "Formulas For Stress and Strain," Fourth Edition.
3. Regulatory Guide 7.8, "Load Combinations for the Structural Analysis of Shipping casks for Radioactive Material" Rev. 1, March 1989.
4. ASME Code Section III, Subsection NB and Appendices, 1989.
5. Regulatory Guide 7.6, "Design Criteria for the Structural Analysis of Shipping Cask Containment Vessels" Rev. 1, March 1978.
6. ANSYS Engineering Analysis System, Users Manual for ANSYS Release 8.0.
7. WRC Bulletin 107, March 1979, "Local Stresses in Spherical and Cylindrical Shells Due to External Loadings".
8. "Prairie Island Independent Spent Fuel Storage Installation Safety Analysis Report", Rev. 10, October 11, 2005.
9. NUREG 766510, "Shock and Vibration Environments for Large Shipping Containers on Rail Cars and Trucks", June 1977.
10. John Harvey, "Theory and Design of Modern Pressure Vessels", Second Edition.

Table 2.10.1-1
Element types, Material Numbers and Real Constants of
ANSYS Model Cask Components

Component	Element Type No.	Material No.	Real Constant No.
Containment Inner Shell	3	1	-
Containment Bottom Plate	3	1	-
Containment Flange	3	2	-
Lid Outer Plate	6	4	-
Lid Shielding Plate	7	3	-
Bolt Shank	2	5	2
Bolt Head	1	5	3
Bolt Thread	2	5	4
Gamma Shield Shell	4	6	-
Gamma Bottom Shield	5	3	-

Table 2.10.1-2
Summary Maximum Nodal Stress Intensities in Cask Components
for Individual Load Runs

(See Figures 2.10.1-3 to 2.10.1-7 for component definition)

Load Case Number	Maximum Nodal Stress Intensity (ksi)				
	Lid	Flange	Inner Shell	Gamma Shield Shell	Gamma Bottom Plate
IL - 1 Bolt Pre-load	8.06	4.90	0.17	0.31	0.02
IL - 2 Fabrication	1.08	13.01	14.45	5.93	3.60
IL - 3 Int. Press.	2.07	2.21	1.54	1.52	4.05
IL - 4 Ext. Press.	0.52	0.55	0.38	0.38	1.02
IL - 5 Therm. 100F	4.02	5.20	4.87	3.21	8.65
IL - 6 Therm. -20F	1.31	3.48	3.43	2.29	5.02
IL - 7 Therm. -40F	1.26	3.13	3.15	2.29	4.27
IL - 8 Gravity 1g	0.26	0.21	0.19	0.32	0.19
IL - 9 Tie-down	1.42	1.35	1.13	1.98	1.29
IL - 10 Vibration	0.11	0.09	0.07	0.13	0.08
IL - 11 Rail Shock	1.75	1.42	1.18	2.11	1.39
IL - 12 End Drop, Bottom 1g	0.12	0.11	0.09	0.08	0.08
IL - 13 End Drop, Top, 1g	0.08	0.14	0.17	0.09	0.18
IL - 14 Lifting -6g	2.81	2.25	1.84	9.58	4.88
IL - 15 Side Drop-1g	0.53	0.71	0.24	0.83	0.38
IL - 16 Corner Drop, Lid	38.83	31.31	12.68	36.16	12.35
IL - 17 Corner Drop, Bottom	3.97	3.89	15.22	15.93	15.58
IL - 18 Oblique Drop, Lid	49.83	45.24	14.55	60.92	7.49
IL - 19 Oblique Drop, Bottom	5.05	3.87	16.68	26.04	24.70

Table 2.10.1-3
6g Lifting Load

Trunnion Loading		Geometry		Cask Loading							
Cask Weight lb	250000		Gamma Shield Thickness (in)	7.295	Longitudinal	6					
			Mean Radius (in)	41.150	Vertical g	0					
Moment Arm (in)	9.22		Trunnion Outer Radius (in)	6.000	Lateral g	0					
Circumferential Trunnion Moment Mc (in lb)	0		Geometry Factor Gamma	5.641							
Longitudinal Trunnion Moment ML (in lb)	-6915000		Geometry Factor Beta	0.1280							
Torsional Trunnion Moment Mt (in lb)	0										
P (lb)	0										
Circumferential Loading Vc (lb)	0										
Longitudinal Loading VL (lb)	-750000										
Reference Figure	Reference Curve from Fig	Multiplier	Absolute Stress (psi)	Au	Al	Bu	Bl	Cu	Cl	Du	DI
3c or 4c	0.97	0.000	0.0	0.0	0.0	0.0	0.0	0.0	0.0	0.0	0.0
1c or 2c-1	0.2	0.000	0.0	0.0	0.0	0.0	0.0	0.0	0.0	0.0	0.0
3a	0.07	0.000	0.0					0.0	0.0	0.0	0.0
1a	0.11	0.000	0.0					0.0	0.0	0.0	0.0
3b	0.26	-4373.360	-1137.1	1137.1	1137.1	-1137.1	-1137.1				
1b or 1b-1	0.068	-148017.489	-10065.2	10065.2	-10065.2	-10065.2	10065.2				
Summation of Phi Stress				11202.3	-8928.1	-11202.3	8928.1	0.0	0.0	0.0	0.0
3c or 4c	0.97	0.000	0.0	0.0	0.0	0.0	0.0	0.0	0.0	0.0	0.0
1c-1 or 2c	0.2	0.000	0.0	0.0	0.0	0.0	0.0	0.0	0.0	0.0	0.0
4a	0.09	0.000	0.0					0.0	0.0	0.0	0.0
2a	0.068	0.000	0.0					0.0	0.0	0.0	0.0
4b	0.07	-4373.360	-306.1	306.1	306.1	-306.1	-306.1				
2b or 2b-1	0.105	-148017.489	-15541.8	15541.8	-15541.8	-15541.8	15541.8				
Summation of Chi Stress				15848.0	-15235.7	-15848.0	15235.7	0.0	0.0	0.0	0.0
Torsional Shear Stress		0.0		0.0	0.0	0.0	0.0	0.0	0.0	0.0	0.0
Circumferential Shear Stress		0.0		0.0	0.0	0.0	0.0				
Longitudinal Shear Stress		-5454.3						5454.3	5454.3	-5454.3	-5454.3
Summation of Tau Stress				0.0	0.0	0.0	0.0	5454.3	5454.3	-5454.3	-5454.3
Stress Intensity Root 1				15848.0	8928.1	11202.3	15235.7	5454.3	5454.3	5454.3	5454.3
Stress Intensity Root 2				11202.3	15235.7	15848.0	8928.1	5454.3	5454.3	5454.3	5454.3
Stress Intensity Root 3				4645.7	6307.6	4645.7	6307.6	10908.5	10908.5	10908.5	10908.5
Max Stress Intensity											
Membrane Stress Intensity Root 1				1137.1	1137.1	306.1	306.1	5454.3	5454.3	5454.3	5454.3
Membrane Stress Intensity Root 2				306.1	306.1	1137.1	1137.1	5454.3	5454.3	5454.3	5454.3
Membrane Stress Intensity Root 3				830.9	830.9	830.9	830.9	10908.5	10908.5	10908.5	10908.5
Max Membrane Stress Intensity											

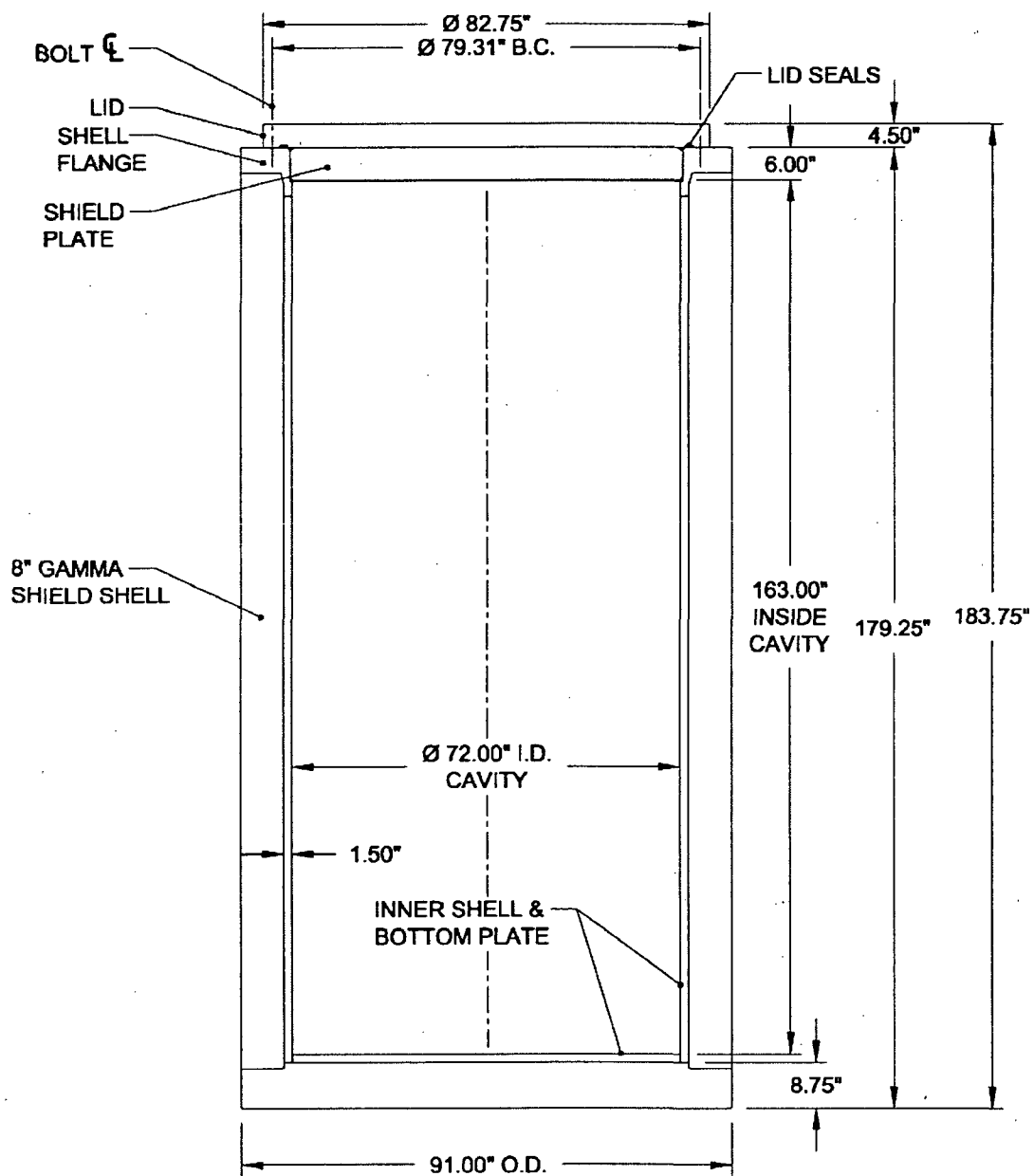


Figure 2.10.1-1
TN-40 Containment Vessel Key Dimensions

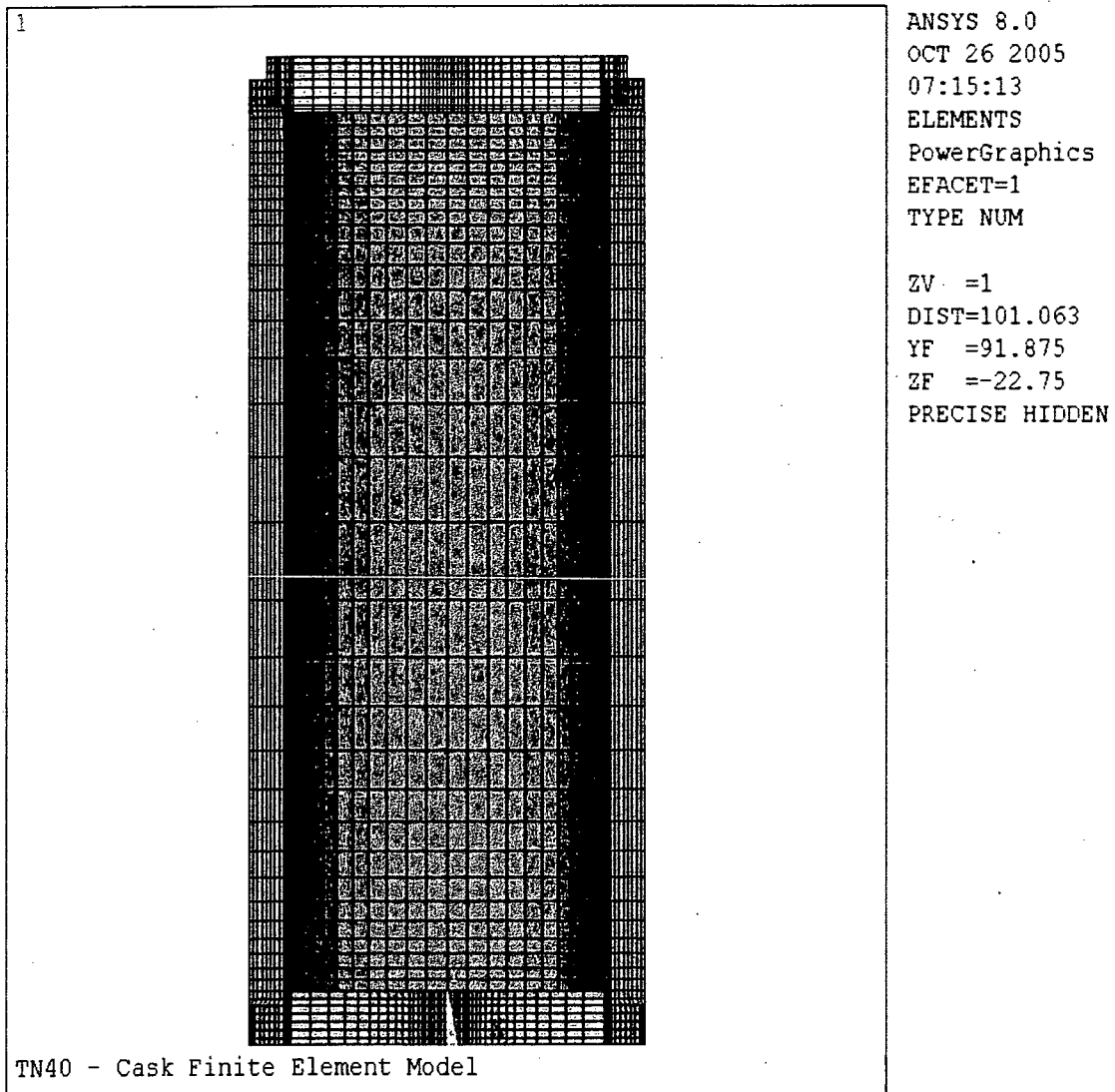


Figure 2.10.1-2
TN-40 Cask/Lid/Bolt FEM Representation

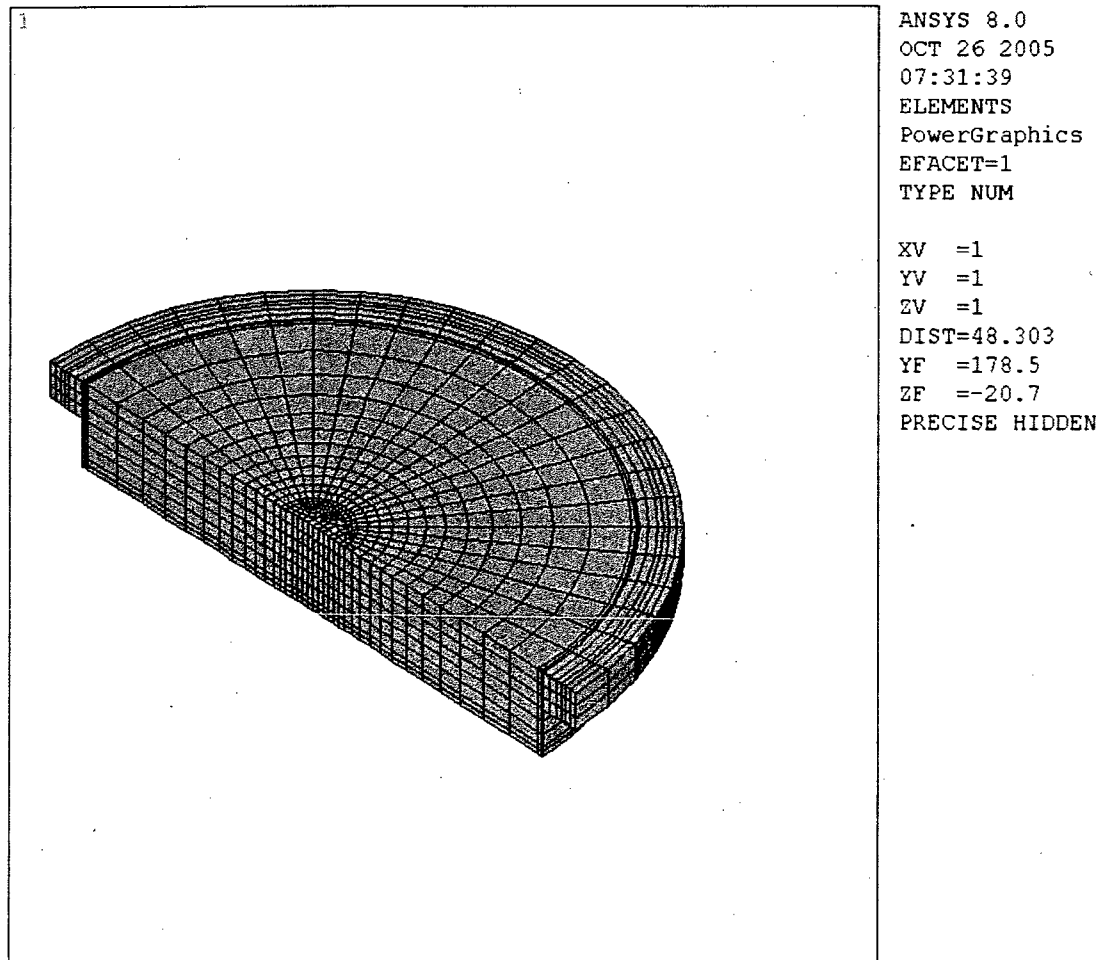


Figure 2.10.1-3
Finite Element Model—Lid

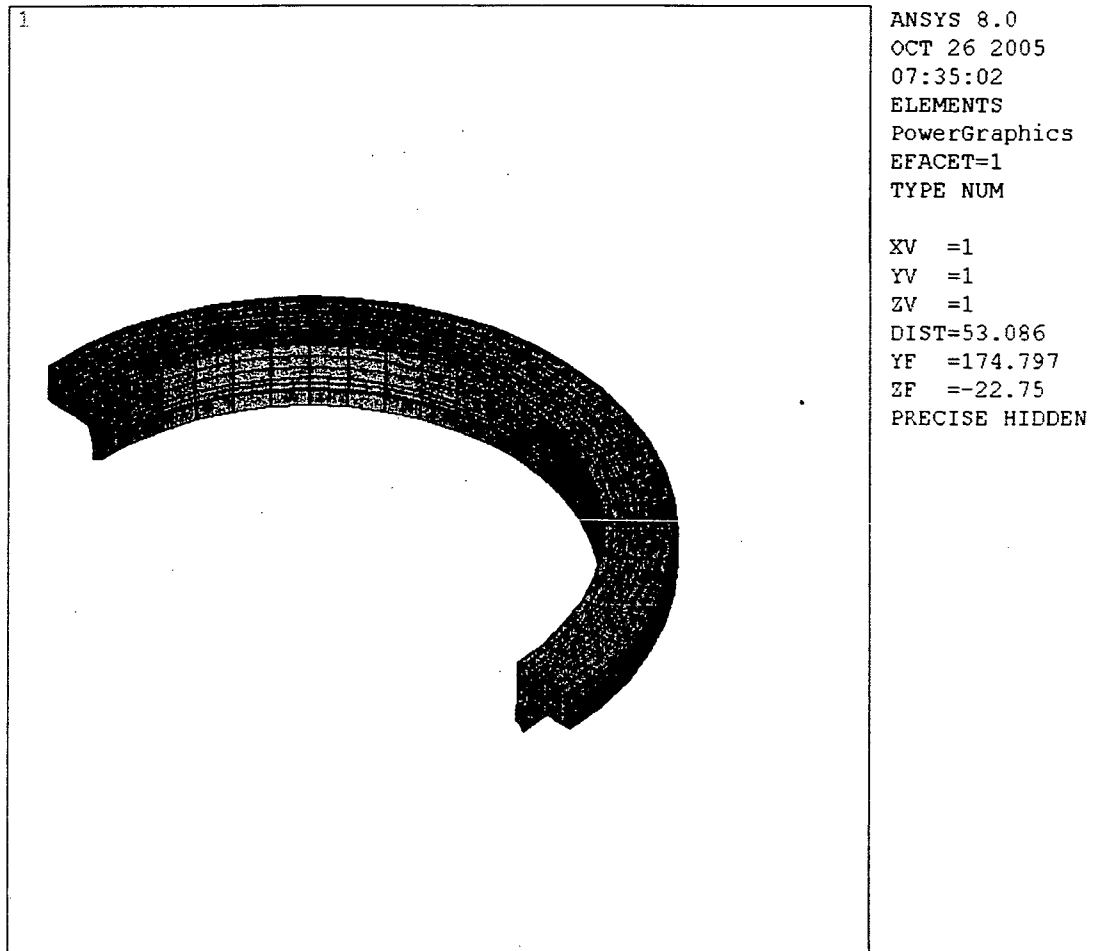


Figure 2.10.1-4
Finite Element Model – Containment Flange

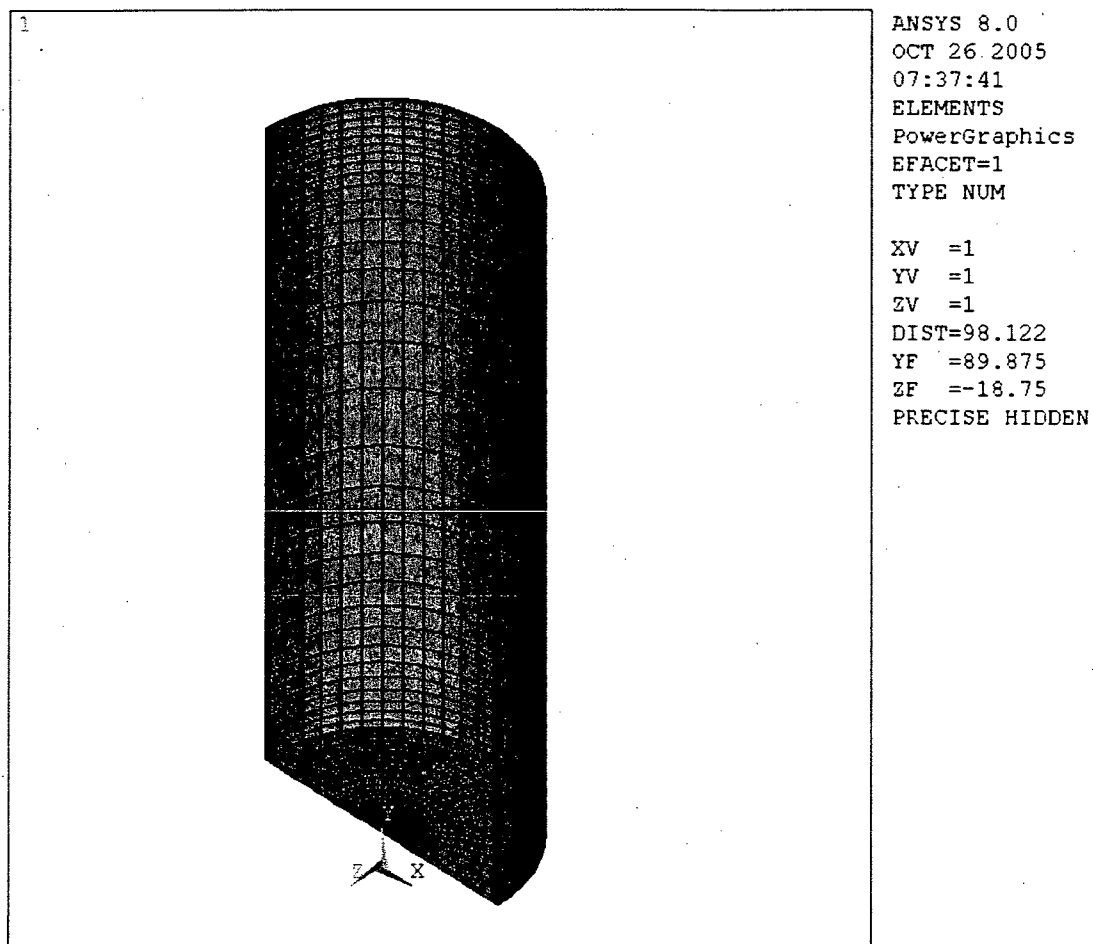


Figure 2.10.1-5
Finite Element Model – Inner Shell and Bottom Plate

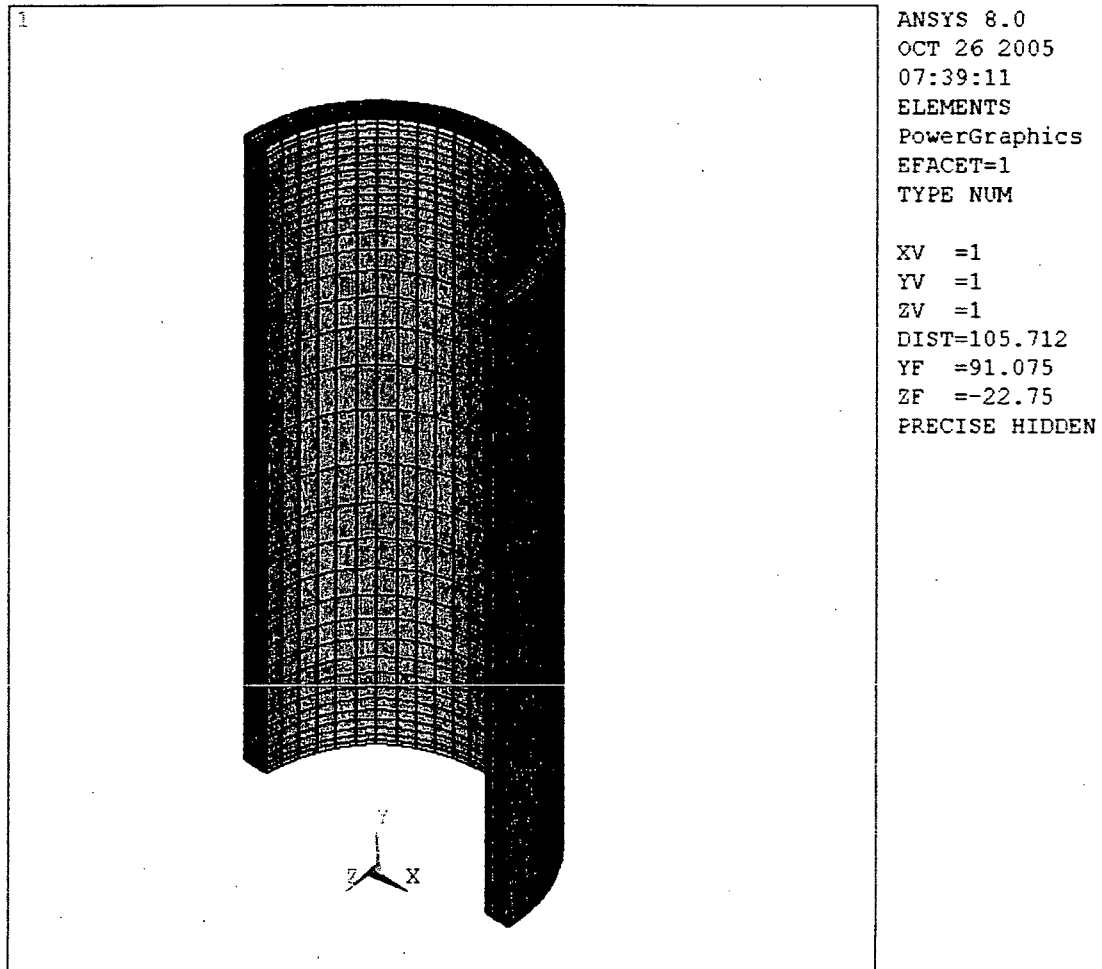


Figure 2.10.1-6
Finite Element Model – Gamma Shield Shell

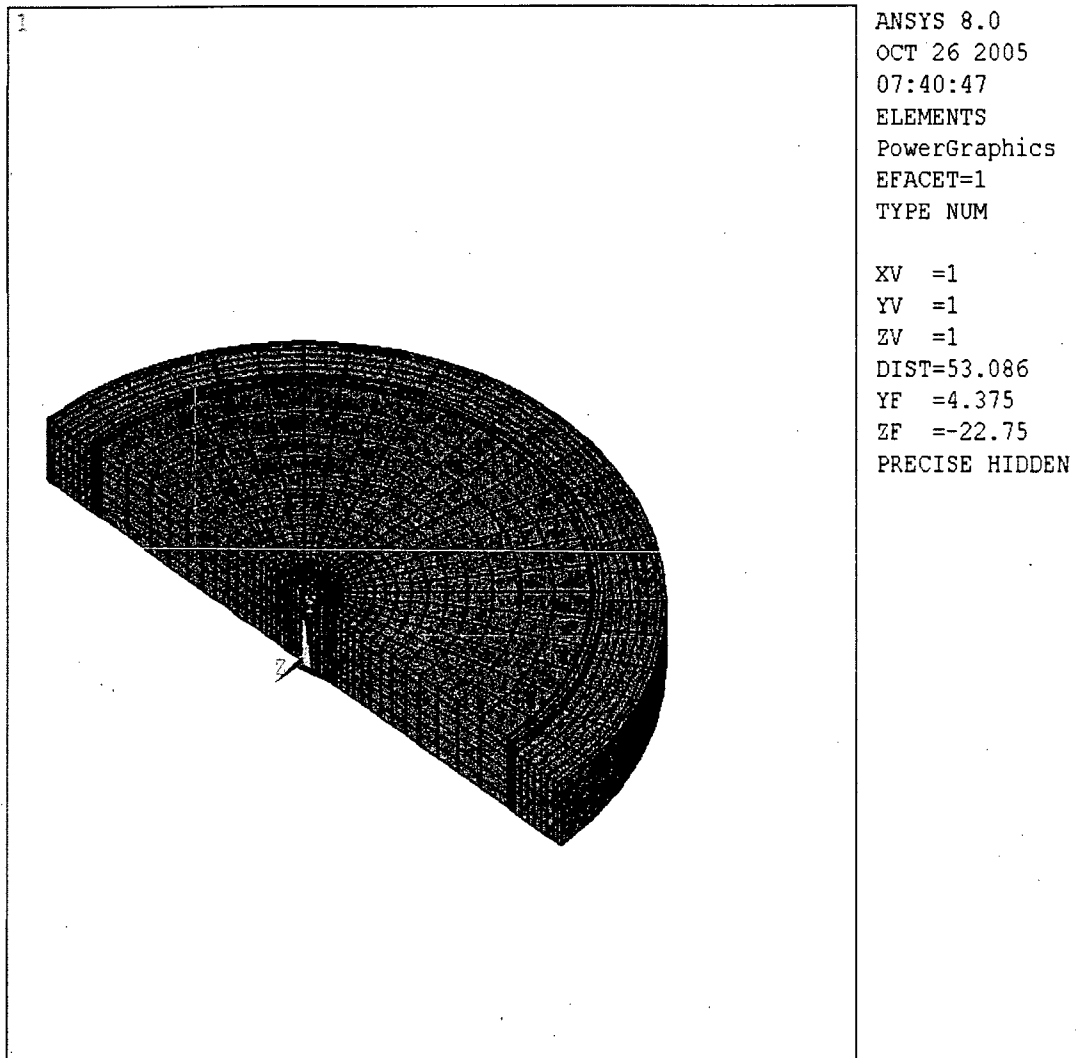


Figure 2.10.1-7
Finite Element Model – Gamma Bottom Shield

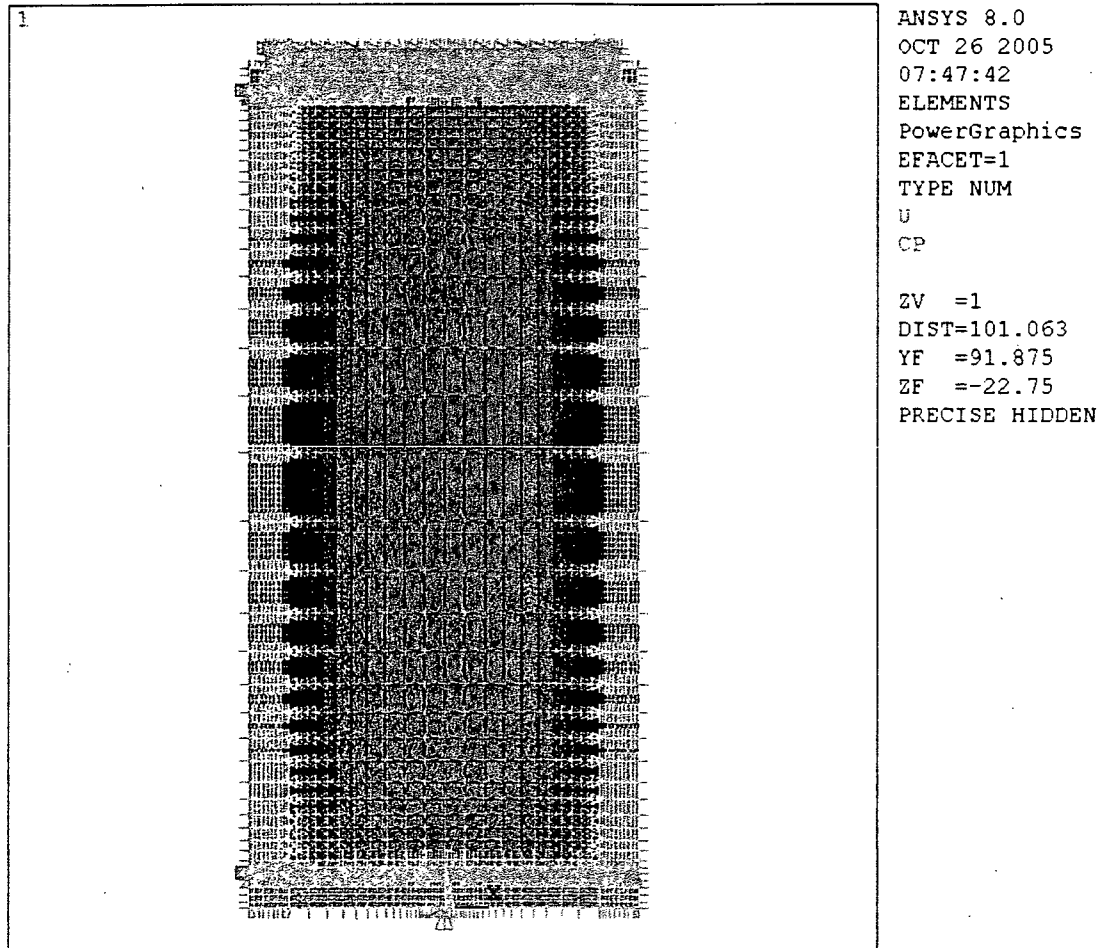


Figure 2.10.1-8
Coupling and Boundary Conditions

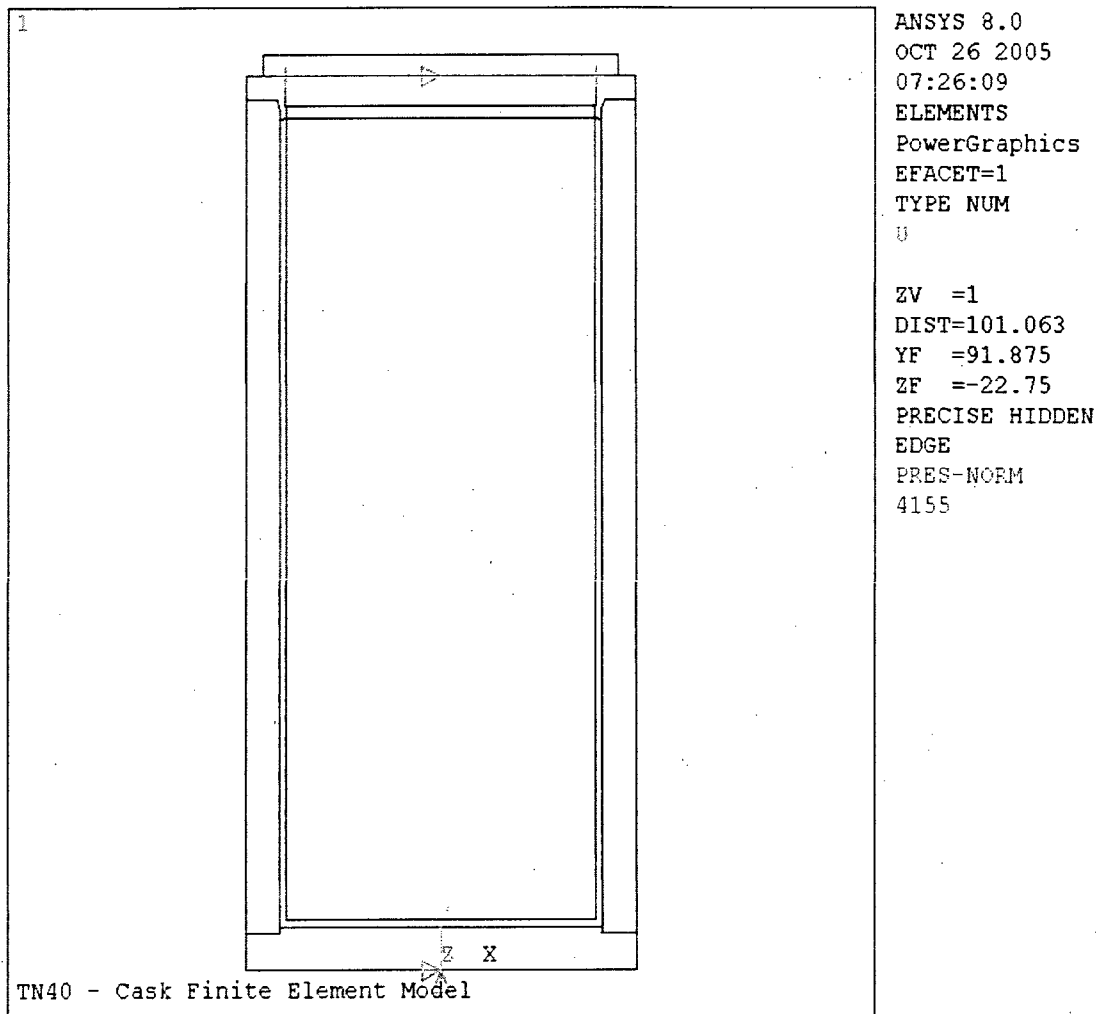


Figure 2.10.1-9
Bolt Preload – Loading and Displacement Boundary Conditions

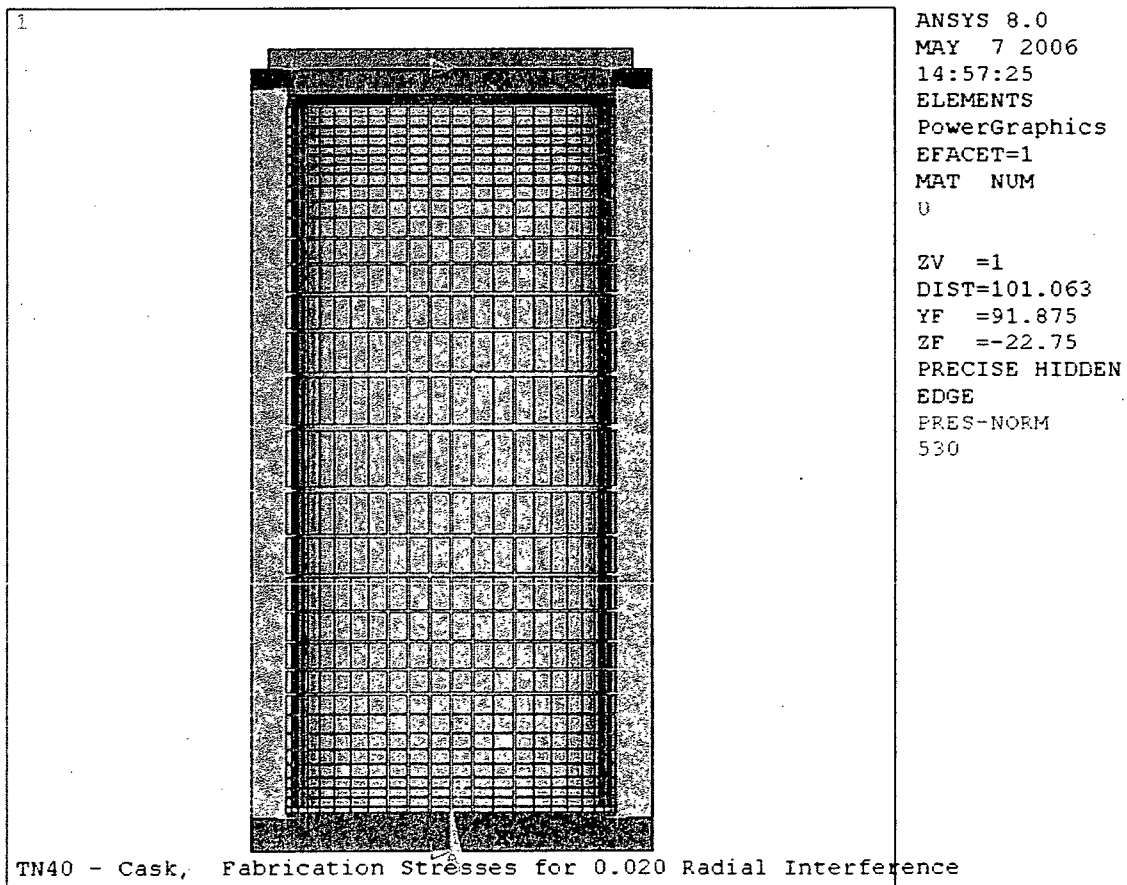


Figure 2.10.1-10
Fabrication Load – Loading and Displacement Boundary Conditions

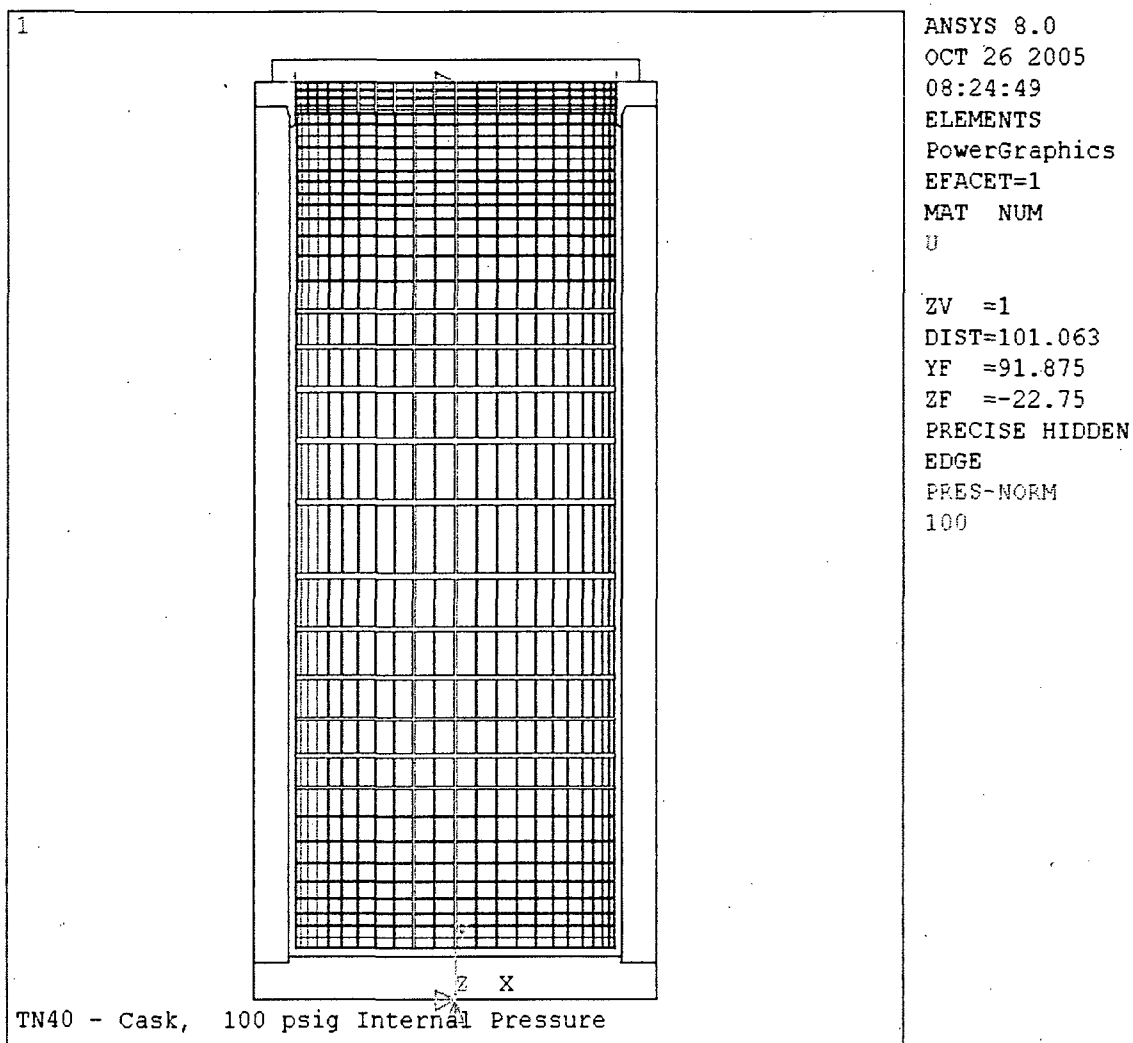


Figure 2.10.1-11
Internal Pressure – Loading and Displacement Boundary Conditions

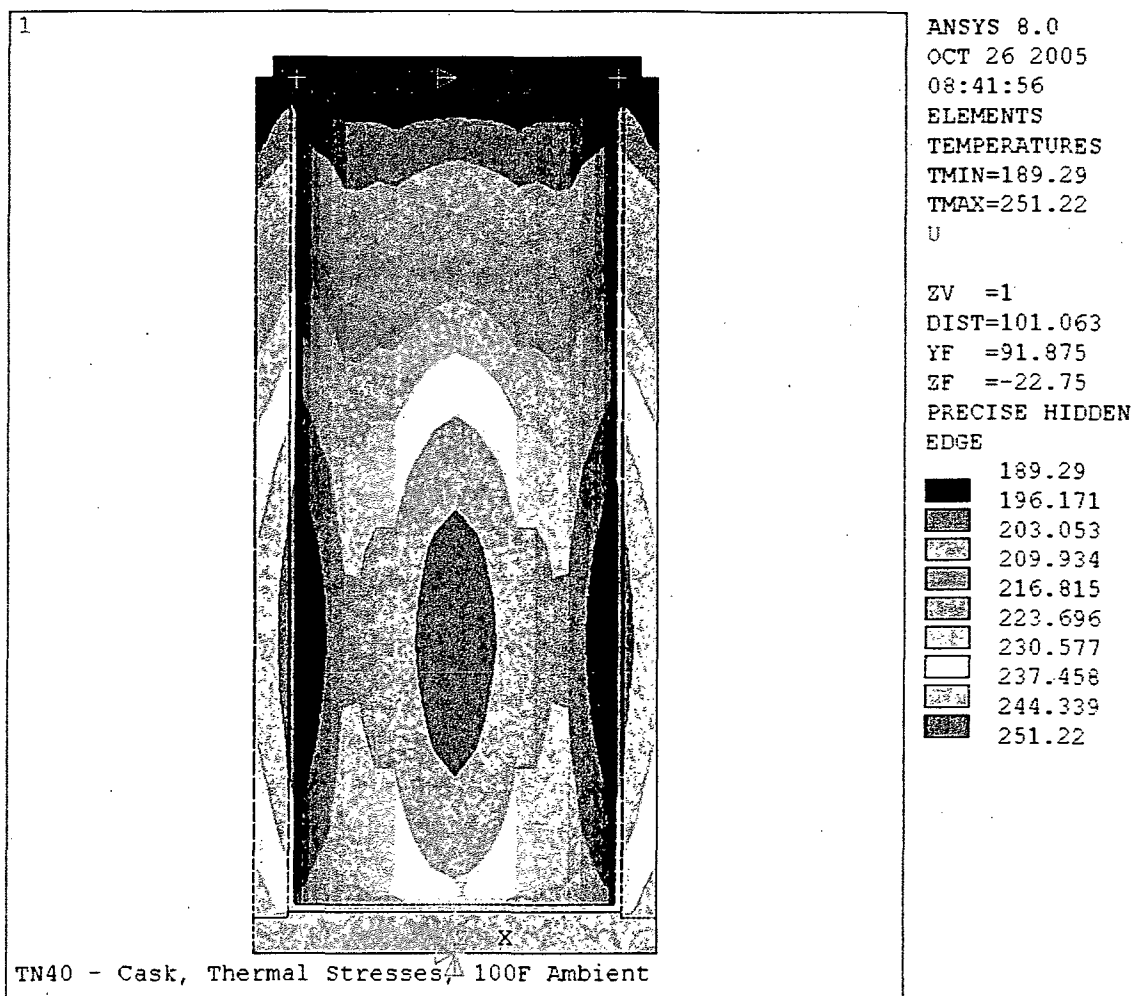


Figure 2.10.1-12
Thermal Stress 100°F Environment – Loading
and Displacement Boundary Conditions

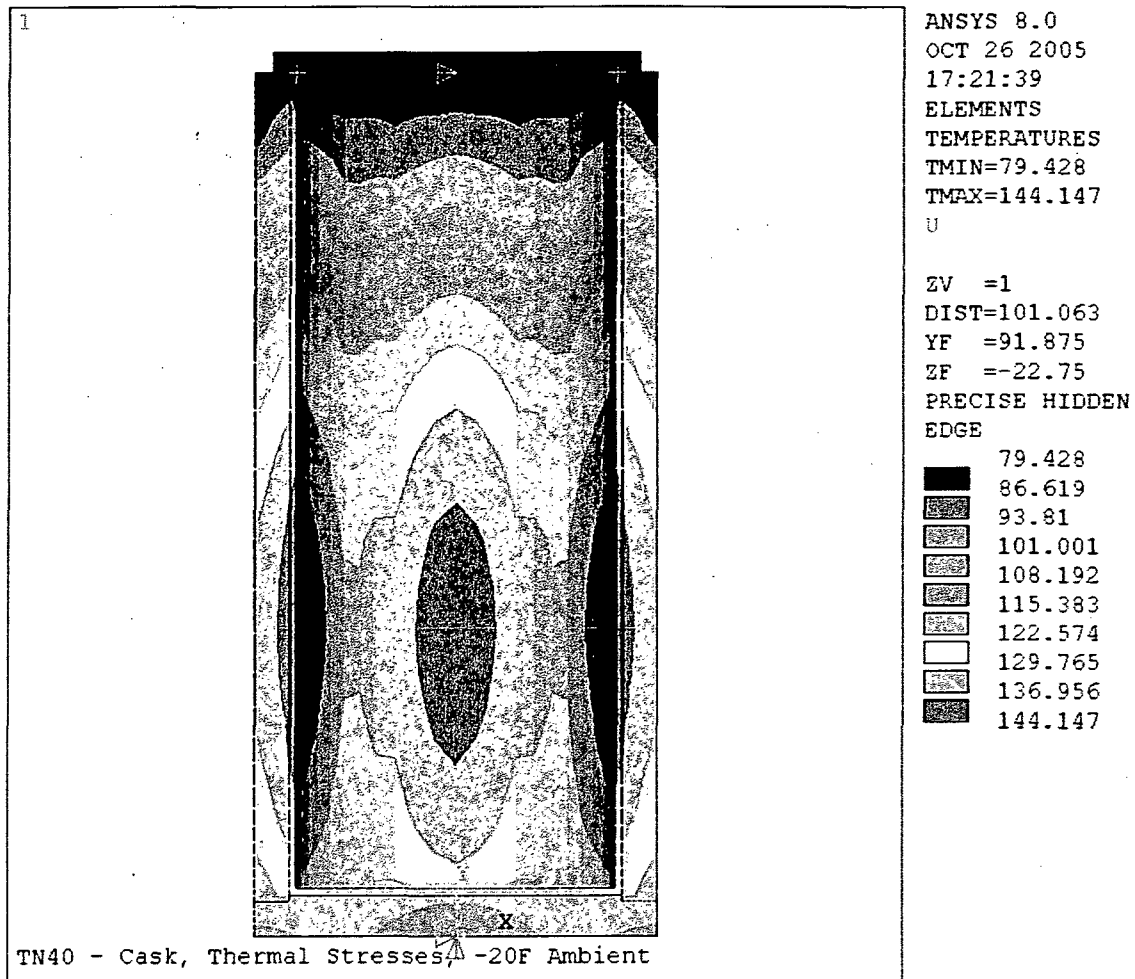


Figure 2.10.1-13
Thermal Stress -20°F Environment – Loading
and Displacement Boundary Conditions

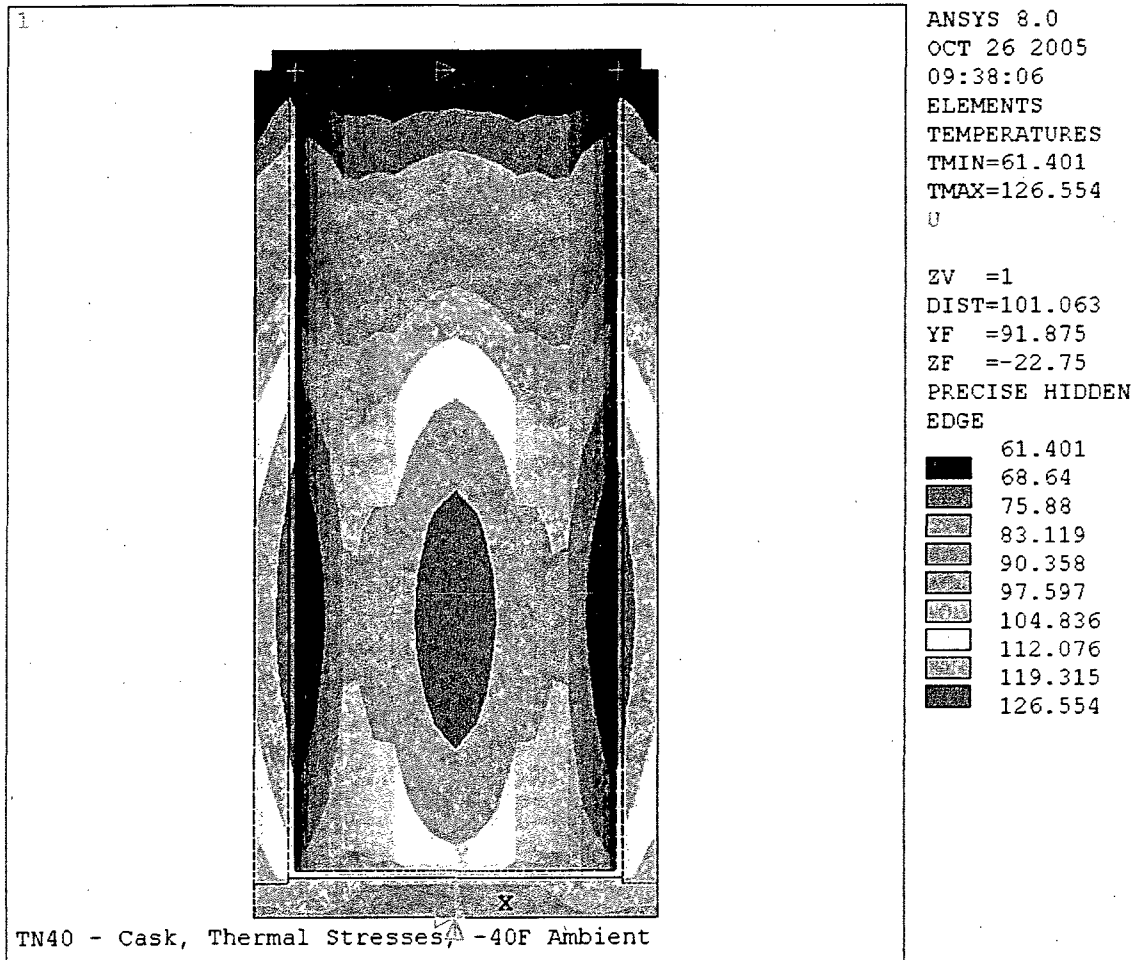


Figure 2.10.1-14
Thermal Stress -40°F Environment – Loading
and Displacement Boundary Conditions

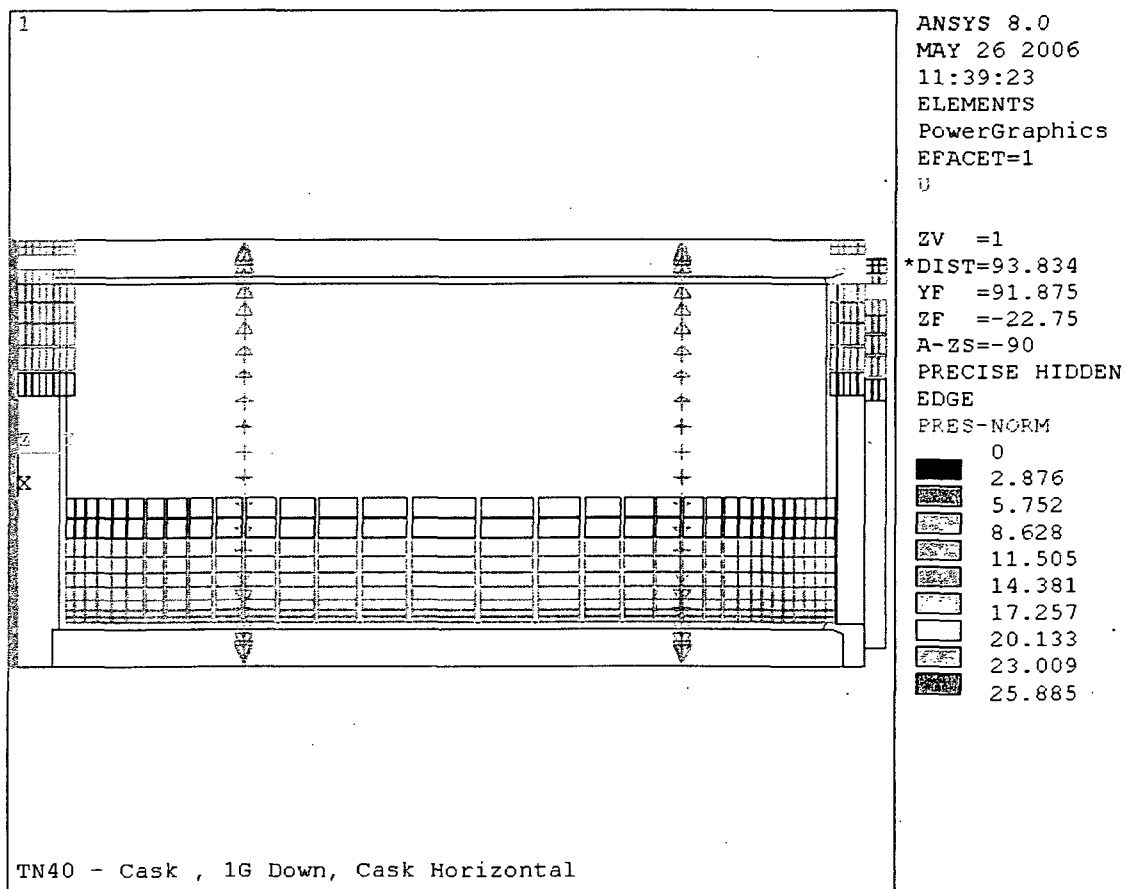


Figure 2.10.1-15
1g Horizontal – Loading and Displacement Boundary Conditions

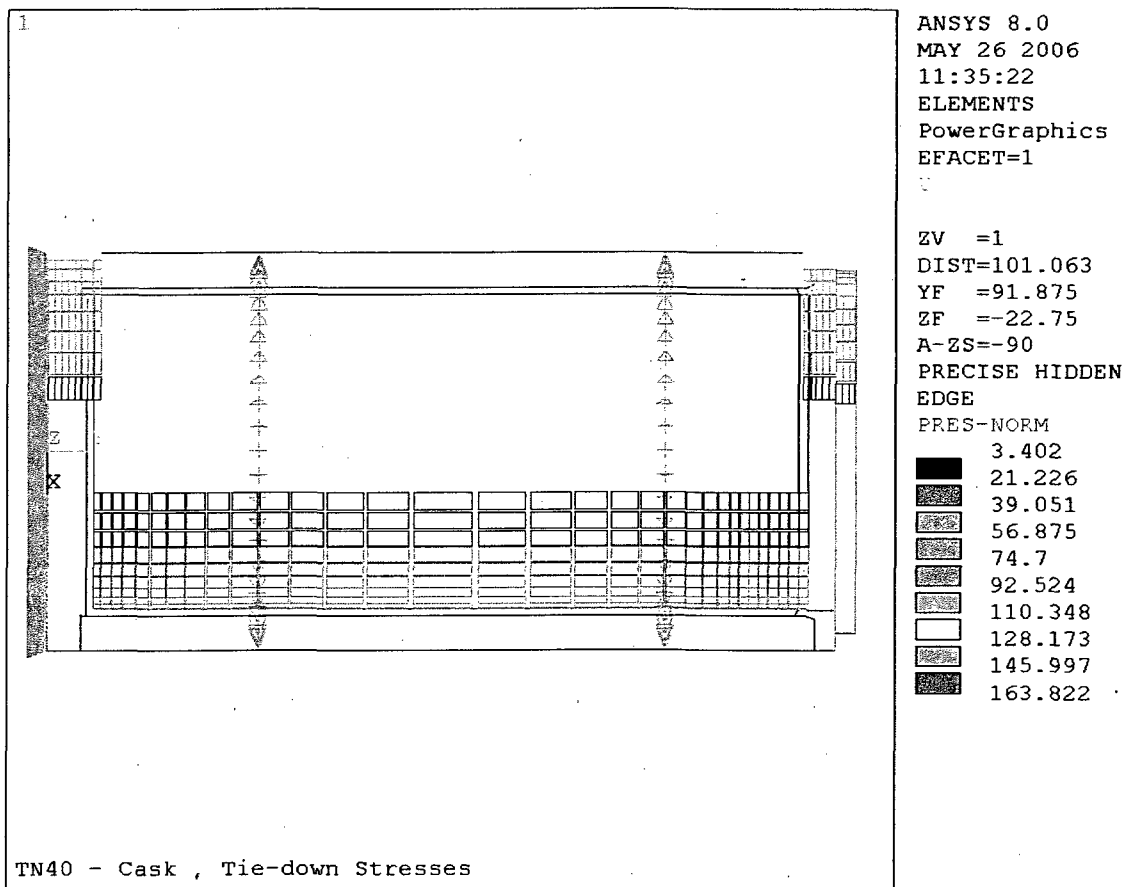


Figure 2.10.1-16
Transport Tie-Down – Loading and Displacement Boundary Conditions

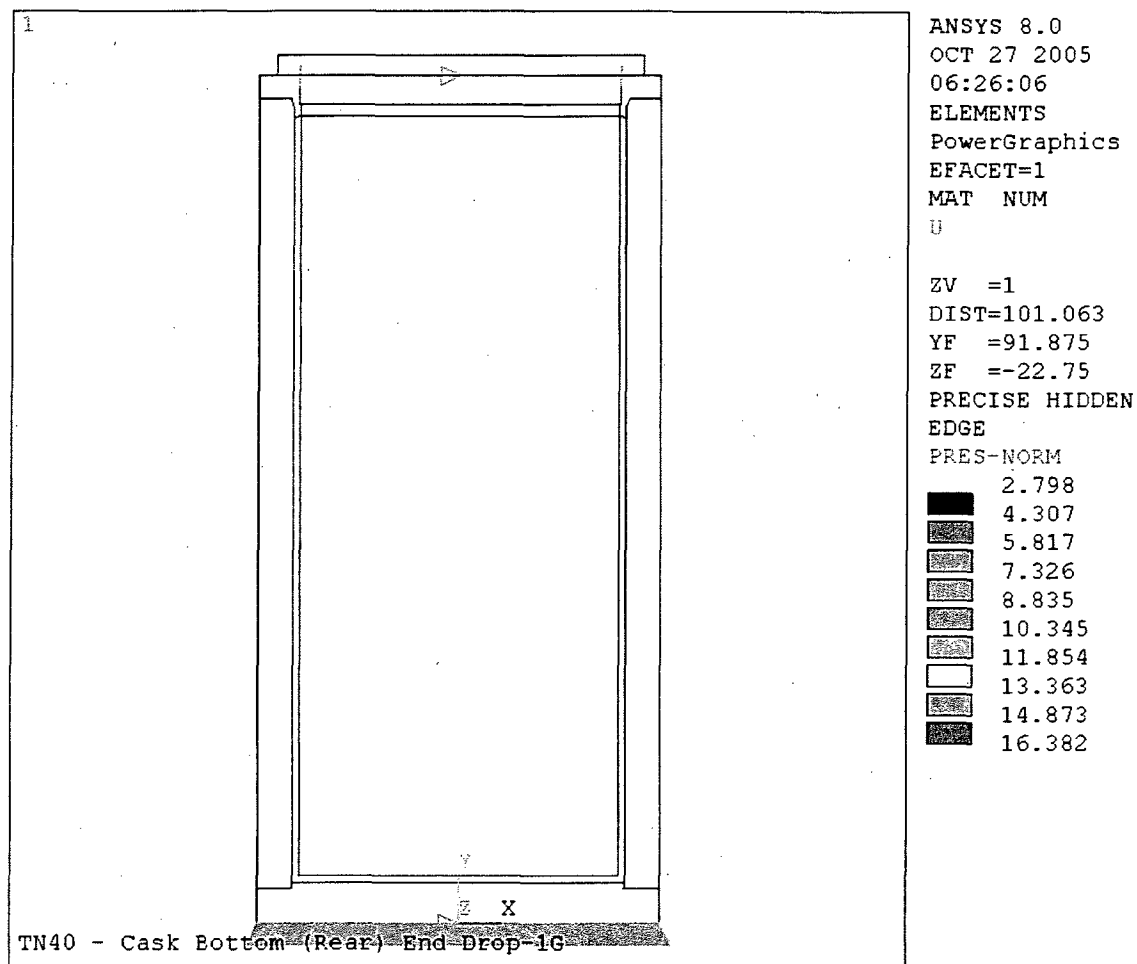


Figure 2.10.1-17
End Drop on Bottom – Loading and Displacement Boundary Conditions

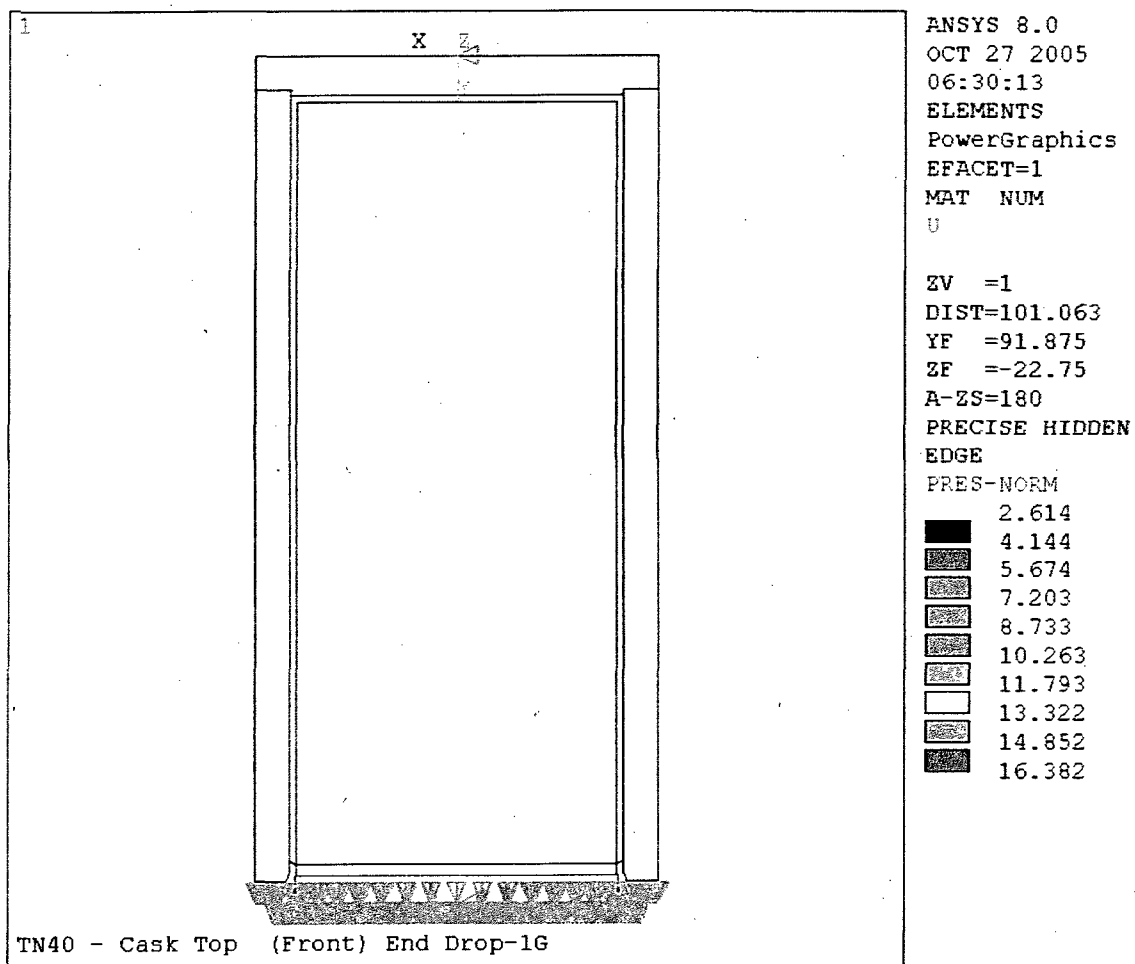


Figure 2.10.1-18
End Drop on Lid – Loading and Displacement Boundary Conditions

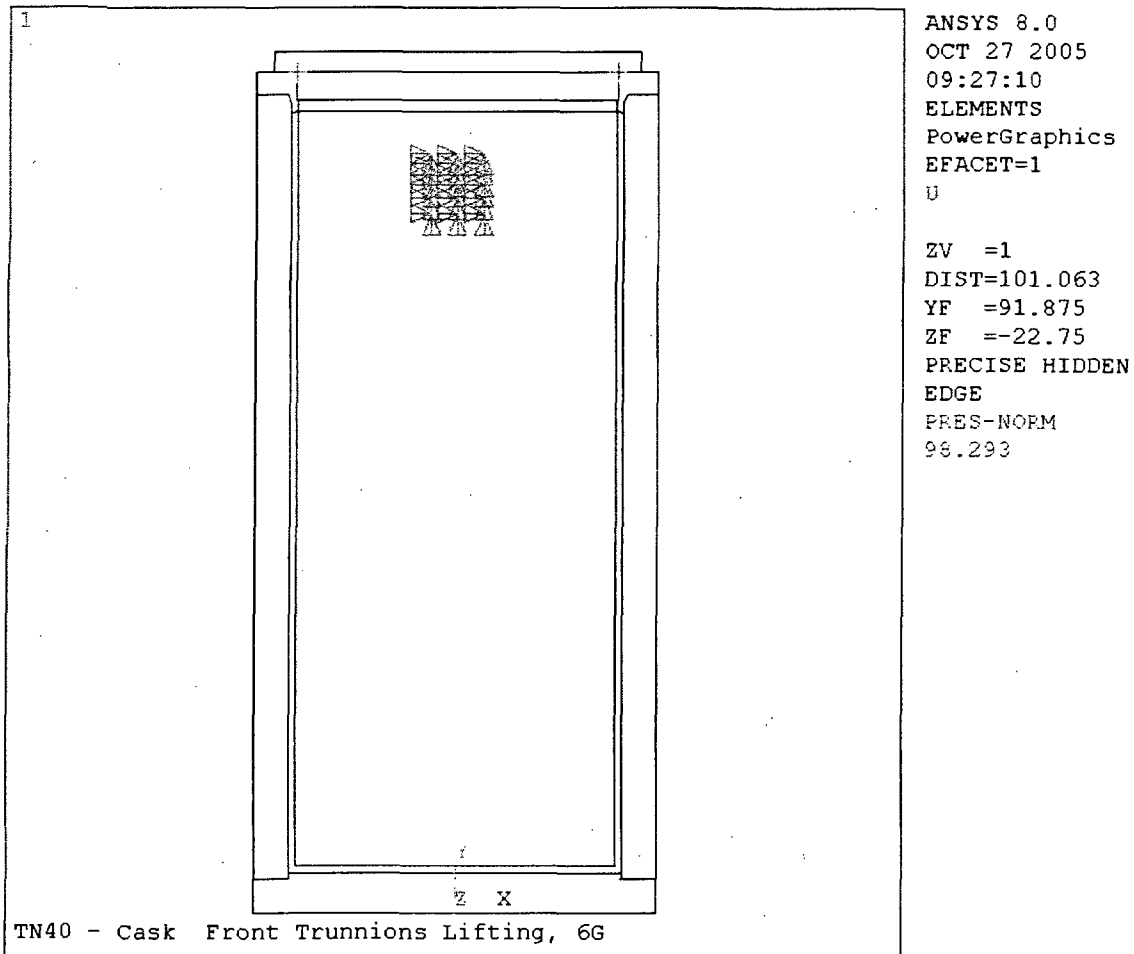


Figure 2.10.1-19
6g Vertical Lifting – Loading and Displacement Boundary Conditions

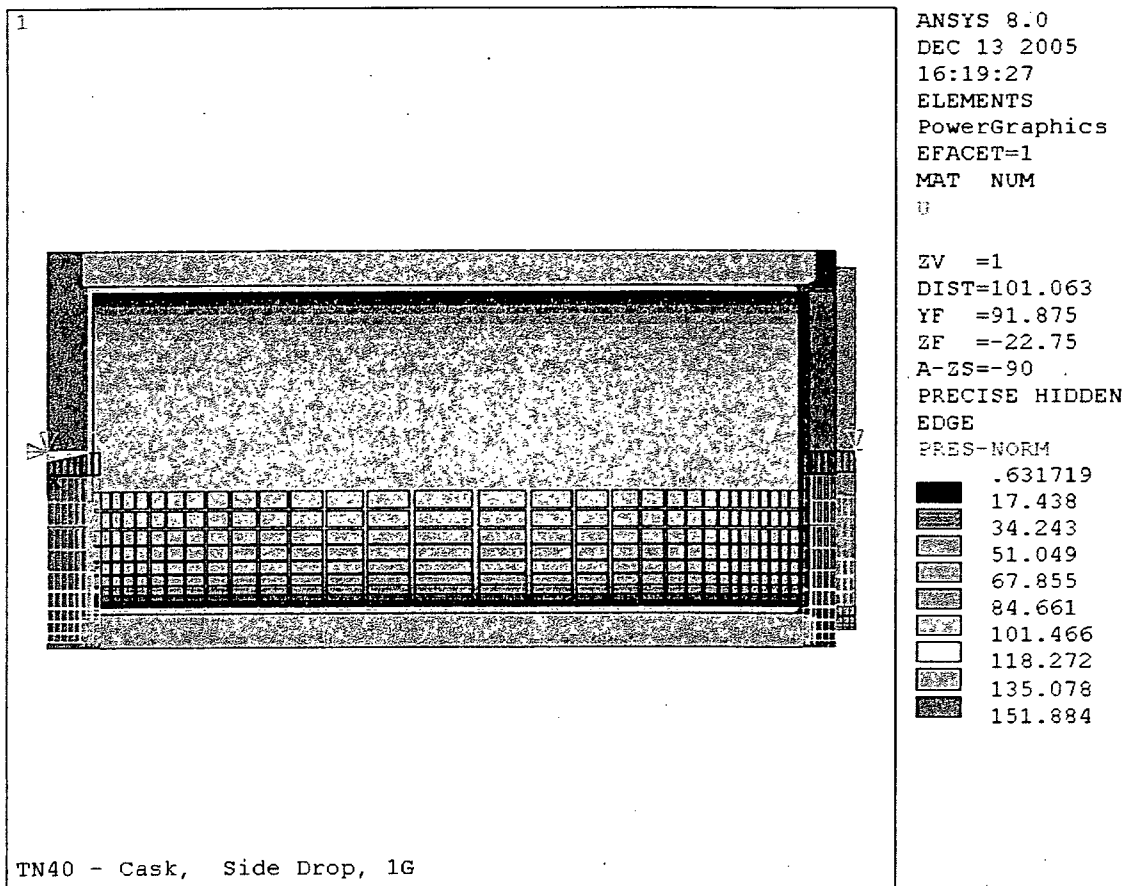


Figure 2.10.1-20
Side Drop, 1g – Loading and Displacement Boundary Conditions

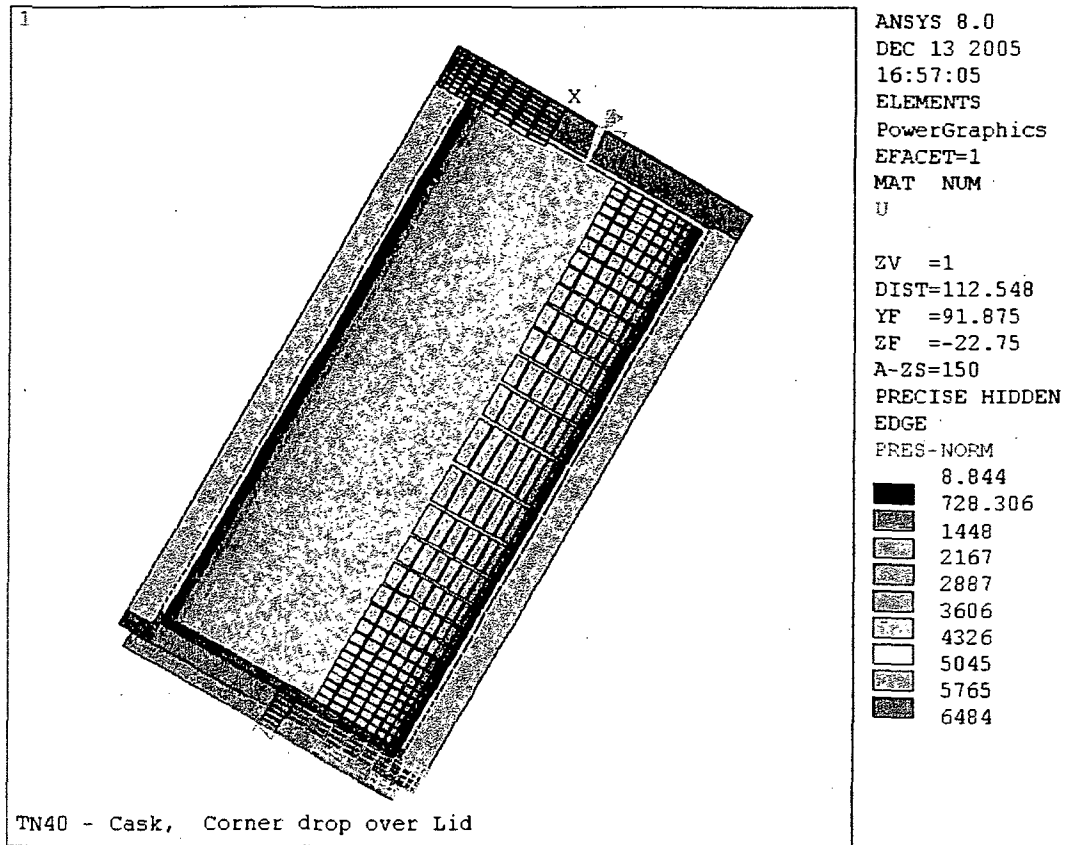


Figure 2.10.1-21
Corner Drop on Lid – Loading and Displacement Boundary Conditions

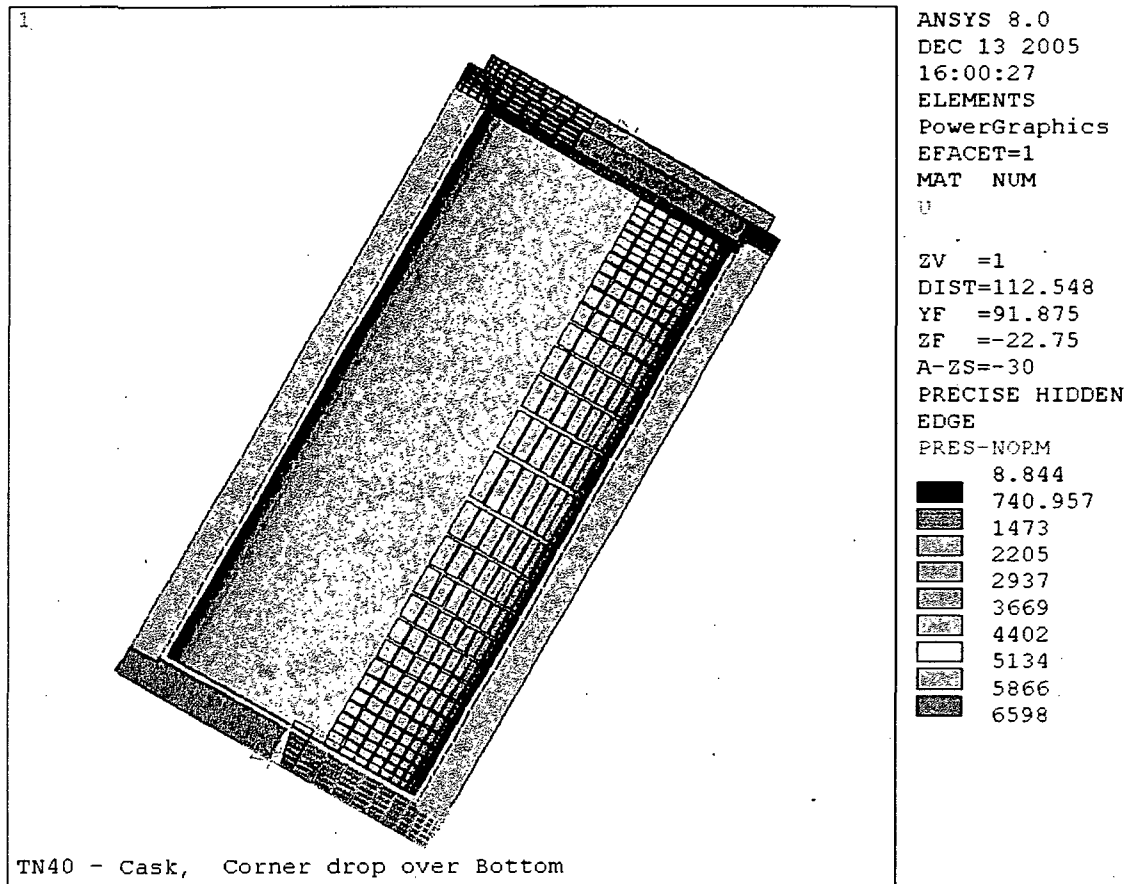


Figure 2.10.1-22
Corner Drop on Bottom – Loading and Displacement Boundary Conditions

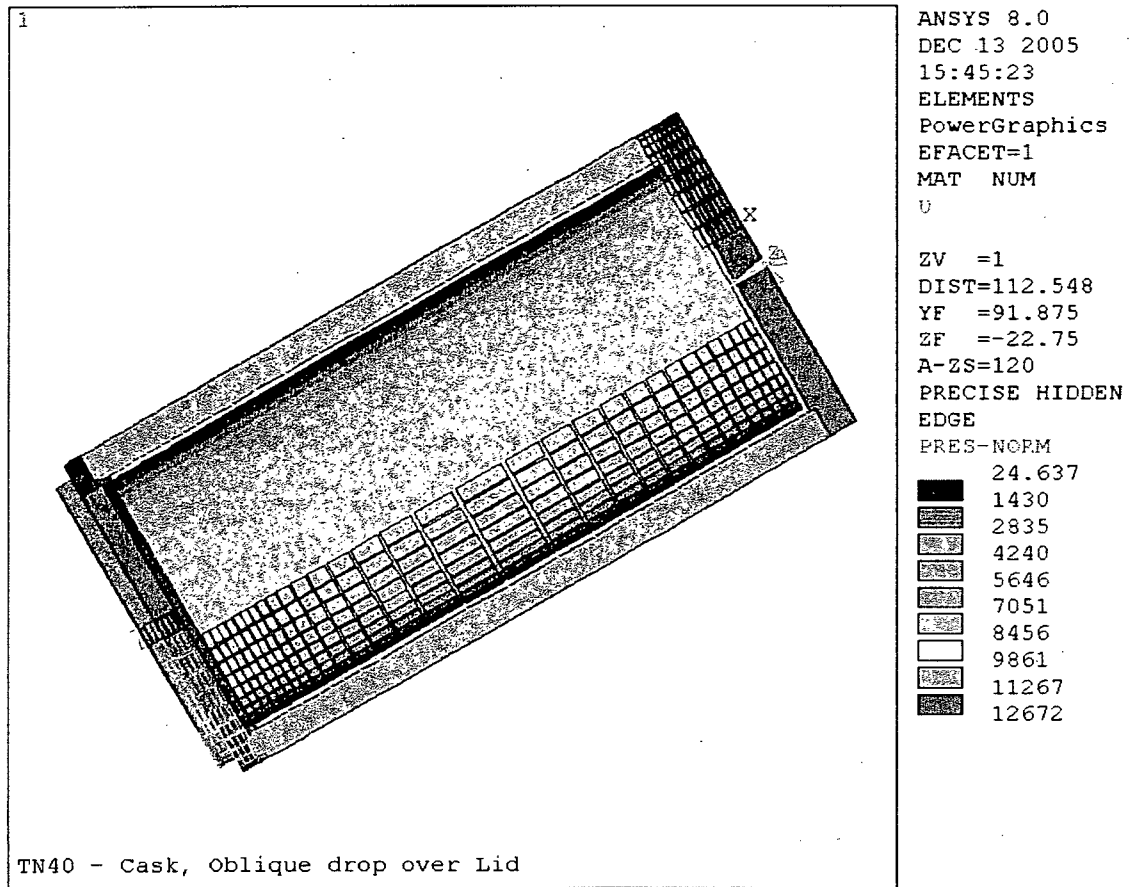


Figure 2.10.1-23
20° Slap Down Impact On Lid End –
Loading and Displacement Boundary Conditions

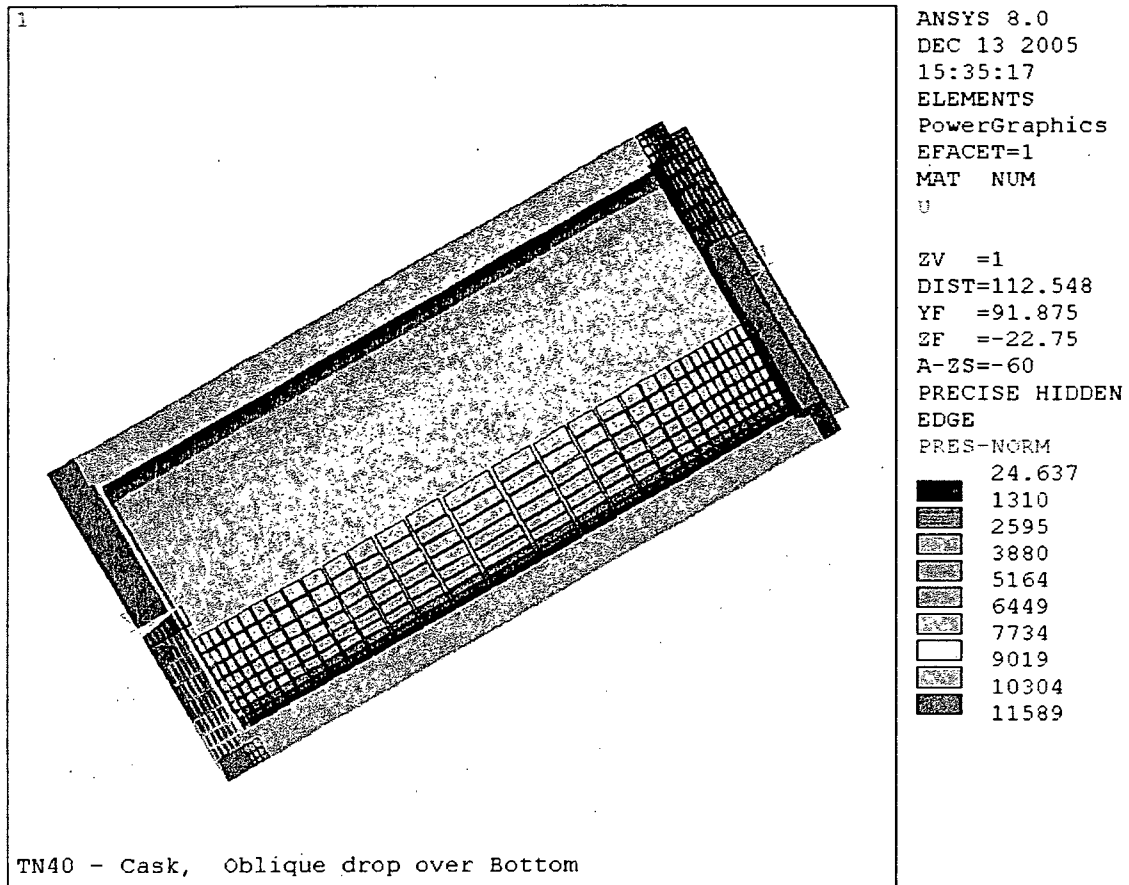


Figure 2.10.1-24
20° Slap Down Impact on Bottom End–
Loading and Displacement Boundary Conditions

APPENDIX 2.10.2

LID BOLT ANALYSIS

TABLE OF CONTENTS

	<u>PAGE</u>
2.10.2 LID BOLT ANALYSIS	2.10.2-1
2.10.2.1 Introduction.....	2.10.2-1
2.10.2.2 Lid Bolt Load Calculations	2.10.2-2
2.10.2.3 Summary of Lid Bolt Loads	2.10.2-8
2.10.2.4 Lid Bolt Load Combinations.....	2.10.2-9
2.10.2.5 Lid Bolt Stress Calculations	2.10.2-11
2.10.2.6 Analysis Results	2.10.2-14
2.10.2.7 Lid Bolt Fatigue Analysis	2.10.2-14
2.10.2.8 Lid Seal Contact Evaluation	2.10.2-18
2.10.2.9 Minimum Engagement Length for Bolt and Flange	2.10.2-19
2.10.2.10 Conclusions	2.10.2-21
2.10.2.11 References	2.10.2-22

LIST OF TABLES

Table 2.10.2-1	Design Parameters For Lid Bolt Analysis	2.10.2-23
Table 2.10.2-2	Bolt Data	2.10.2-24
Table 2.10.2-3	Allowable Stresses In Closure Bolts For Normal Conditions	2.10.2-24
Table 2.10.2-4	Allowable Stresses In Closure Bolts For Accident Conditions	2.10.2-25

LIST OF FIGURES

Figure 2.10.2-1	Lid/Cask Axial Interface	2.10.2-26
Figure 2.10.2-2	TN-40 Transport Cask (CG Over Corner Lid Drop - Hot) Seal Decompression as a Function of Circumferential Location	2.10.2-27

2.10.2 LID BOLT ANALYSIS

2.10.2.1 Introduction

This Appendix evaluates the ability of the cask closure bolt to maintain a leak tight seal under events defined by Normal Conditions Transport (NCT) and the Hypothetical Accident Conditions (HAC). Also evaluated in this section are the bolt thread and internal thread stresses, and lid bolt fatigue. The stress analysis is performed in accordance with NUREG/CR-6007 [1].

The TN-40 cask lid closure arrangement is shown in Figure 2.10.2-1. The 4.5 in. thick lid with a 6.0 in. radiation shield is bolted directly to the shell flange by 48 high strength alloy steel 1.375 in. diameter bolts (with 1 ½ -8UN threaded portion). Close fitting alignment pins ensure that the lid is centered in the vessel. The bolt material is SA-320 Gr. L43 which has a minimum yield strength of 105 ksi at room temperature.

The following ways to minimize bolt forces and bolt failures for shipping casks are taken directly from with Reference [1], page xiii. All of the following design methods are employed in the TN-40 closure system.

- Protect closure lid from direct impact to minimize bolt forces generated by free drops. (use impact limiters)
- Use materials with similar thermal properties for the closure bolts, the lid, and the cask wall to minimize the bolt forces generated by fire accident
- Apply sufficiently large bolt preload to minimize fatigue and loosening of the bolts by vibration.
- Lubricate bolt threads to reduce required preload torque and to increase the predictability of the achieved preload.
- Use closure lid design which minimizes the prying actions of applied loads.
- When choosing a bolt preload, pay special attention to the interactions between the preload and thermal load and between the preload and the prying action.

The following lid bolt evaluations are presented in this section:

- Lid bolt torque
- Bolt preload
- Gasket seating load
- Pressure load
- Temperature load
- Impact load
- Puncture load

- Bearing stress
- Load combinations for NCT and HAC
- Bolt stresses and allowable stresses
- Lid bolt fatigue
- Lid/Cask seal evaluation
- Thread engagement length evaluation

The design parameters of the lid closure, taken from Reference [1] are summarized in Table 2.10.2-1. The lid bolt data and material allowables are presented in Tables 2.10.2-2 through 2.10.2-4. A maximum temperature of 300°F is used in the lid bolt region during NCT and HAC based on results of thermal analyses documented in Chapter 3. The following load cases are considered in the analysis.

1. Preload + Temperature Load (NCT)
2. Pressure Load + 1 Foot Drop (NCT)
3. Pressure + 30 Foot Corner Drop (HAC)
4. Pressure + Puncture Load (HAC)

2.10.2.2 Lid Bolt Load Calculations

2.10.2.2.1 Lid Bolt Torque

The desired maximum preload stress in the lid bolts is 50,000 psi.

For a 1.375" bolt shank, the Tensile Stress Area is 1.485 in² (see Table 2.10.2-2). Therefore,

$$F_a = 50,000 \times \text{Stress Area} = 50,000 \times 1.485 = 74,250 \text{ lb.}$$

The torque required to achieve this preload is (Reference [1], Section 4.0):

$$Q = K D_b F_a = 0.135 (1.375) (74,250) = 13,783 \text{ in. lb.} = 1,149 \text{ ft. lb.}$$

A bolt torque range of 1,100 to 1,150 ft. lb. has been selected. For the minimum torque,

$$F_a = Q/KD_b = 1,100 \times 12 / (0.135 \times 1.375) = 71,111 \text{ lbs}$$

2.10.2.2.2 Bolt Preload

The method used for the following calculation is taken from Reference [1], Table 4.1.

$$F_a = Q/KD_b = 1,150 \times 12 / 0.135(1.375) = 74,343 \text{ lb.}$$

Residual torsional moment is:

$$M_{tr} = 0.5Q = .5(1,150 \times 12) = 6,900 \text{ in. lb.}$$

Residual tensile bolt force,

$$F_{ar} = F_a = 74,343 \text{ lbs}$$

2.10.2.2.3 Gasket Seating Load

Gasket characteristics for the Helicoflex HND 229 seals with an aluminum jacket and a 0.236 seal cross section are taken from Reference [2]. The diameter of the inner seal, D_{is} , is 74.3 in., and the diameter of the outer seal, D_{os} , is 75.9 in. The force to seat the seals is approximately 1399 lbs./in for aluminum jacket [2] and approximately 2198 lbs/in. for a silver jacket [6]. Therefore the total force required to seat the seals is:

$$\text{Inner: } \pi (74.3) (1399) = 326,555 \text{ lbs; } \pi (74.3)(2198) = 513,058 \text{ lbs}$$

$$\text{Outer: } \pi (75.9) (1399) = 333,587 \text{ lbs; } \pi (75.9)(2198) = 524,106 \text{ lbs}$$

$$\text{Total, } F_a = 660,142 \text{ lbs; } F_a = 1,037,164 \text{ lbs}$$

Therefore, the seal seating load is:

$$F_a/48 = 660,142/48 = 13,753 \text{ lb/bolt; } F_a/48 = 1,037,164/48 = 21,608 \text{ lb/bolt}$$

The specified preload has the required force to seat the seals.

2.10.2.2.4 Pressure Loads

The method used for the following calculation is taken from Reference [1], Table 4.3.

Axial force per bolt due to internal pressure is:

$$F_a = \frac{\pi D_{ig}^2 (P_{li} - P_{lo})}{4N_b}$$

D_{ig} for outer seal (conservative) = 75.9 in. Then,

$$F_a = \frac{\pi (75.9^2)(100 - 0)}{4(48)} = 9,426 \text{ lb./bolt}$$

The fixed edge closure lid force is:

$$F_f = \frac{D_{lb}(P_{li} - P_{lo})}{4} = \frac{79.31(100)}{4} = 1,983 \text{ lb. in.}^{-1}$$

The fixed edge closure lid moment is:

$$M_f = \frac{(P_{li} - P_{lo})D_{lb}^2}{32} = \frac{100(79.31^2)}{32} = 19,656 \text{ in. lb. in.}^{-1}$$

The shear bolt force per bolt is:

$$F_s = \frac{\pi E_i t_i (P_{li} - P_{lo}) D_{lb}^2}{2 N_b E_c t_c (1 - N_{ul})} = \frac{\pi (27.8 \times 10^6) (5.0) (100) (79.31)^2}{2 (48) (27.8 \times 10^6) (9.5) (0.7)} = 32,501 \text{ lb./bolt}$$

The lid shoulder takes this shear force, so that $F_s = 0$.

2.10.2.2.5 Temperature Loads

The lid bolt material is SA-320 Grade L43, 1 3/4 Ni 3/4 Cr 1/4 Mo. This is Group E in the thermal coefficients of expansion tables in Reference [5]. Both the lid and flange are made of SA-350 Gr. LF3, 3 1/2 Ni, which is also Group E. Consequently, the bolts, lid and flange have the same coefficient of thermal expansion (6.9×10^{-6} in/in-°F at 300°F). Therefore, heating to the maximum isothermal temperature will not generate bolt stress.

2.10.2.2.6 Impact Loads

The method used for the following calculation is taken from Reference [1], Table 4.5.

The non-prying tensile bolt force per bolt, F_a , is:

$$F_a = \frac{1.34 \sin(xi)(LF)(ai)(W_l + W_c)}{N_b} = \frac{1.34 \sin(xi)(1.1)(ai)(82,000)}{48} = 2,518(ai) \sin(xi) \text{ lb/bolt}$$

Note: $W_l + W_c$ is conservatively assumed to be 82,000 lbs. [Actual weights from Table 2-6 are 13,910 lbs for lid and lid bolts, 14,690 lbs for basket, rails, and shims, and 52,000 lbs for fuel assemblies resulting in a total weight of 80,600 lbs.]

The shear bolt force is:

$$F_s = \frac{\cos(xi)(ai)(W_l)}{N_b} = \frac{82,000(ai) \cos(xi)}{48} = 1,708(ai) \cos(xi) \text{ lb/bolt}$$

The lid shoulder during normal and accident condition drops takes shear force.

Therefore,

$$F_s = 0$$

The fixed-edge closure lid force, F_f , is:

$$F_f = \frac{1.34 \sin(xi)(LF)(ai)(W_l + W_c)}{\pi D_{lb}} = \frac{1.34 \sin(xi)(1.1)(ai)(82,000)}{\pi (79.31)} = 485.1 \sin(xi)(ai) \text{ lb/bolt}$$

The fixed-edge closure lid moment, M_f , is,

$$M_f = \frac{1.34 \sin(\xi)(LF)(a_i)(W_l + W_c)}{8\pi} = \frac{1.34 \sin(\xi)(1.1)(a_i)(82,000)}{8\pi} = 4,809 \sin(\xi)(a_i) \text{ lb/bolt}$$

NCT Impact Loads

Since the bolts are protected by the impact limiter during an end drop, the worst case scenario is taken to be roughly a 63.8° C.G. over corner drop. From the impact limiter 1 foot normal condition analysis (Appendix 2.10.8), the maximum g load for a 1 foot 63.8° C.G. over corner drop is 5g vertical and 3g horizontal.

However, for the lid bolt analysis the following normal condition g-loading is conservatively used:

$$a_i = 10 \text{ gs, and } \xi = 63.8^\circ$$

Therefore,

$$F_a = 2,518 \times 10 \times \sin(63.8^\circ) = 22,594 \text{ lb./bolt}$$

$$F_s = 0 \text{ lb./bolt}$$

$$F_f = 485.1 \times 10 \times \sin(63.8^\circ) = 4,353 \text{ lb./bolt}$$

$$M_f = 4,809 \times 10 \times \sin(63.8^\circ) = 43,151 \text{ lb./bolt}$$

HAC Impact Loads

The loads resulting from a 30 foot, 63.8° corner drop are conservatively taken to be the following (actual loads are 32 g vertical, and 14 g horizontal, given in Appendix 2.10.8).

$$a_i = 38 \text{ g, and } \xi = 63.8^\circ$$

Therefore,

$$F_a = 2,518 \times 38 \times \sin(63.8^\circ) = 85,856 \text{ lb./bolt}$$

$$F_s = 0 \text{ lb./bolt}$$

$$F_f = 485.1 \times 38 \times \sin(63.8^\circ) = 16,540 \text{ lb./bolt}$$

$$M_f = 4,809 \times 38 \times \sin(63.8^\circ) = 163,973 \text{ lb./bolt}$$

2.10.2.2.7 Puncture Loads

The method used for the following calculation is taken from Reference [1], Table 4.7.

The non-prying tensile bolt force per bolt, F_a , is:

$$F_a = \frac{-\sin(\xi)P_{un}}{N_b}$$

where:

$$P_{un} = \text{The smaller of } \begin{cases} 0.75\pi D_{pb}^2 S_{yl} \\ 0.6\pi D_{pb} t_l S_{ul} \end{cases}$$

$$= \text{The smaller of } \begin{cases} 0.75\pi(6^2)(33,200) = 2.816 \times 10^6 \\ 0.6\pi(6)(10.5)(70,000) = 8.31 \times 10^6 \end{cases}$$

$$\Rightarrow P_{un} = 2.816 \times 10^6 \text{ lb}$$

The puncture force is greatest when $\alpha = 90^\circ$. Conservatively neglect the protection provided by the impact limiter. Then,

$$F_a = \frac{-\sin(\alpha) 2.816 \times 10^6}{48} = -58,669 \text{ lb}$$

Since this force is negative (inward acting), the actual resulting bolt force, $F_a = 0$, because the applied load is supported by the cask wall and not the lid bolts. The shear bolt force is:

$$F_s = \frac{\cos(90^\circ) P_{un}}{N_b} \text{ lb/bolt}$$

The lid shoulder during puncture takes shear force. Therefore,

$$F_s = 0$$

The fixed-edge closure lid force, F_f , is:

$$F_f = \frac{-\sin(\alpha) P_{un}}{\pi D_{lb}} = \frac{-\sin(90^\circ) 2.816 \times 10^6}{\pi(79.31)} = -11,302 \text{ lb/bolt}$$

The fixed-edge closure lid moment, M_f , is,

$$M_f = \frac{-\sin(\alpha) P_{un}}{4\pi} = \frac{-\sin(90^\circ) 2.816 \times 10^6}{4\pi} = -224,100 \text{ lb/bolt}$$

2.10.2.2.8 External Pressure Load of 290 psig

An external pressure load of 290 psig is evaluated as shown in Reference [1], Table 4.3.

The axial force per bolt due to internal pressure is,

$$F_a = \frac{\pi D_{lg}^2 (P_{li} - P_{lo})}{4N_b}$$

Where the outer seal diameter, D_{lg} , is

$$D_{lg} = 75.9 \text{ in.}$$

Then,

$$F_a = \frac{\pi(75.9^2)(0 - 290)}{4(48)} = -27,336 \text{ lb./bolt}$$

Since this force is negative (inward acting), the actual resulting bolt force, $F_a = 0$, because the applied load is supported by the cask wall and not the lid bolts.

The fixed edge closure lid force F_f is,

$$F_f = \frac{D_{lb}(P_{li} - P_{lo})}{4} = \frac{79.31(-290)}{4} = -5,750 \text{ lb in.}^{-1}$$

The fixed edge closure lid moment, M_f , is,

$$M_f = \frac{(P_{li} - P_{lo})D_{lb}^2}{32} = \frac{-290(79.31^2)}{32} = -57,004 \text{ in. lb in.}^{-1}$$

The lid shoulder during external pressure takes shear force. Therefore,

$$F_s = 0$$

2.10.2.3 Summary of Lid Bolt Loads

The loads calculated in the previous sections are summarized in the following table.

LID BOLT INDIVIDUAL LOAD SUMMARY

Load Case	Applied Load		Non-Prying Tensile Force, F_a (lb.)	Torsional Moment, M_t (in. lb.)	Prying Force, F_r (lb.in. ⁻¹)	Prying Moment, M_r (in. lb. in. ⁻¹)
Preload	Residual	Maximum Torque	74,343	6,900	0	0
		Minimum Torque	71,111	6,600	0	0
Gasket	Seating Load		21,608	0	0	0
Pressure	100 psig Internal		9,426	0	1,983	19,656
Thermal	300°F		0	0	0	0
Impact	1 Foot Normal Condition Drop		22,594	0	4,353	43,151
	30 foot Accident Condition Drop		85,856	0	16,540	163,973
Puncture	Drop on six inch diameter rod		0	0	-11,302	-224,100
External Pressure	290 psig External		0	0	-5,750	-57,004

2.10.2.4 Lid Bolt Load Combinations

A summary of normal and accident condition load combinations is presented in the following table. The method used for the following combination is taken from Reference [1], Table 4.9.

LID BOLT NORMAL AND ACCIDENT LOAD COMBINATIONS

Load Case	Combination Description	Non-Prying Tensile Force, F_a (lb.)	Torsional Moment, M_t (in. lb.)	Prying Force, F_f (lb.in. ⁻¹)	Prying Moment, M_f (in. lb. in. ⁻¹)
1	Preload + Temperature (Normal Condition)	A. Maximum Torque	74,343	6,900	0
		B. Minimum Torque	71,111	6,600	0
2	Pressure + Normal Impact (Normal Condition)	32,020	0	6,336	62,807
3	Pressure + Accident Impact (Accident Condition)	95,282	0	18,523	183,629
4	Pressure + Puncture (Accident Condition)	9,426	0	-9,319	-204,444
5	Internal & External Pressure	9,426	0	-3,767	37,348

Additional Prying Bolt Force

Since the prying forces applied in load cases 4 and 5 acts inward, normal to the cask lid, an additional prying bolt force, F_{ap} , is generated (Reference [1], Table 2.1). No additional force is generated for the outward loadings however (load cases 1, 2, and 3), because of the gap between the lid and flange at the outer edge. Only load case 4 is considered because it bounds load case 5, above. F_{ap} is calculated in the following way.

$$F_{ap} = -\left(\frac{\pi D_{lb}}{N_b}\right) \left[\frac{\frac{2M_f}{(D_{li} - D_{lb})} - C_1(B - F_f) - C_2(B - P)}{C_1 + C_2} \right],$$

where,

$$C_1 = 1, C_2 = \left(\frac{8}{3(D_{li} - D_{lb})^2} \right) \left[\frac{E_f t_f^3}{1 - N_{ul}} + \frac{(D_{lo} - D_{li}) E_{ff} t_{ff}^3}{D_{lb}} \right] \left(\frac{L_b}{N_b D_b^2 E_b} \right)$$

$$= \left(\frac{8}{3(72.87 - 79.31)^2} \right) \left[\frac{26.7 \times 10^6 (10.5^3)}{1 - 0.3} + \frac{(82.75 - 72.87)(26.7 \times 10^6)(4.5)^3}{79.31} \right] \left(\frac{4.5}{(48)(1.375^2)(26.7 \times 10^6)} \right)$$

$$= 5.309,$$

B is the non-prying tensile bolt force, and P is the bolt preload. Since $F_s = 0$, $F_s < P$, and therefore $B = P$. Parameters B, P, F_f , and M_f are quantities per unit length of bolt circle. Also, the Pressure load is not included because it decreases the magnitude of the applied prying moment, which is less conservative. For the applied inward force,

$$P = B = \frac{F_a N_b}{\pi D_{lb}} = \frac{(74,343)(48)}{\pi(79.31)} = 14,322 \text{ lb. in.}^{-1}$$

$$M_f = \frac{(-224,100)(48)}{\pi(79.31)} = -224,100 \text{ lb. in.}^{-1}, \text{ and } F_f = 0 \text{ lb. in.}^{-1}$$

Therefore,

$$F_{ap} = - \left(\frac{\pi(79.31)}{48} \right) \left[\frac{\frac{2(-224,100)}{(72.81 - 79.31)} - 1(14,322 - 0) - 5.309(14,322 - 14,322)}{1 + 5.309} \right]$$

$$= 45,478 \text{ lb/bolt}$$

It is observed that the additional tensile bolt force due to prying for the puncture is less than the accident impact force. The puncture is therefore not critical for bolt stress evaluation.

Bolt Bending Moment

The method used for the following calculation is taken from Reference [1], Table 2.2.

The maximum bolt bending moment, M_{bb} , generated by the applied load is evaluated as follows:

$$M_{bb} = \left(\frac{\pi D_{lb}}{N_b} \right) \left[\frac{K_b}{K_b + K_f} \right] M_f$$

The terms K_b and K_f are based on geometry and material properties and are defined in Reference [1], Table 2.2. By substituting the values given above,

$$K_b = \left(\frac{N_b}{L_b} \right) \left(\frac{E_b}{D_{lb}} \right) \left(\frac{D_b^4}{64} \right) = \left(\frac{48}{4.5} \right) \left(\frac{26.7 \times 10^6}{79.31} \right) \left(\frac{1.375^4}{64} \right) = 2.006 \times 10^5$$

$$K_f \frac{E_f t_f^3}{3 \left[(1 - N_{ul}^2) + (1 - N_{ul})^2 \left(\frac{D_{lb}}{D_{lo}} \right)^2 \right] D_{lb}} = \frac{26.7 \times 10^6 (10.5^3)}{3 \left[(1 - 0.3^2) + (1 - 0.3)^2 \left(\frac{79.31}{82.75} \right)^2 \right] 79.31}$$

$$= 9.551 \times 10^7$$

Therefore,

$$M_{bb} = \left(\frac{\pi 79.31}{48} \right) \left[\frac{2.006 \times 10^5}{2.006 \times 10^5 + 9.551 \times 10^7} \right] M_f = 0.0109 M_f$$

For load case 2, $M_f = 62,807$ in. lb. Substituting this value into the equation above gives,

$$M_{bb} = 684.6 \text{ in. lb/bolt}$$

2.10.2.5 Lid Bolt Stress Calculations

The method used for the following calculation is taken from Reference [1], Table 5.1.

2.10.2.5.1 Average Tensile Stress

The bolt preload is calculated to withstand the worst case load combination and to maintain a clamping (compressive) force on the closure joint, under both normal and accident conditions. Based upon the load combination it is shown that a positive (compressive) load is maintained on the clamped joint for all load combinations except for the accident condition impact plus pressure load. A more detailed finite element analysis is performed in Section 2.10.2.8 of this Appendix to evaluate closure of the lid during this event. The maximum non-prying tensile force for normal conditions is 74,343 lb, from load case 1.A. (maximum torque preload + temperature load), and the maximum non-prying tensile force for accident conditions is 95,282 lb from load case 3 (accident impact + pressure load). These loads are used to compute bolt stresses below.

NCT:

$$S_{ba} = 1.2732 \frac{F_a}{D_{ba}^2} = 1.2732 \frac{74,343}{1.375^2} = 50,065 \text{ psi} = 50.1 \text{ ksi}$$

HAC:

$$S_{ba} = 1.2732 \frac{95,282}{1.375^2} = 64,166 \text{ psi} = 64.2 \text{ ksi}$$

2.10.2.5.2 Bending Stress

Normal Condition:

$$S_{bb} = 10.186 \frac{M_{bb}}{D_{ba}^3} = 10.186 \frac{684.6}{1.375^3} = 2,682 \text{ psi} = 2.7 \text{ ksi}$$

2.10.2.5.3 Shear Stress

For both normal and accident conditions, the average shear stress caused by shear bolt force F_s is,

$$S_{bs} = 0$$

For normal and accident conditions the maximum shear stress caused by the torsional moment M_t is,

$$S_{bt} = 5.093 \frac{M_t}{D_{ba}^3} = 5.093 \frac{6,900}{1.375^3} = 13,518 \text{ psi} = 13.5 \text{ ksi}$$

2.10.2.5.4 Maximum Combined Stress Intensity

The maximum combined stress intensity is calculated in the following way (Reference [1], Table 5.1).

$$S_{bi} = [(S_{ba} + S_{bb})^2 + 4(S_{bs} + S_{bt})^2]^{0.5}$$

For normal conditions, the combined tension, shear, bending, and residual torsion results in a maximum stress intensity of:

$$S_{bi} = [(50,065 + 2,682)^2 + 4(0 + 13,518)^2]^{0.5} = 59,272 \text{ psi} = 59.3 \text{ ksi}$$

2.10.2.5.5 Stress Ratios

In order to meet the stress ratio requirement, the following relationship must hold for both normal and accident conditions.

$$R_t^2 + R_s^2 < 1$$

Where R_t is the ratio of average tensile stress to allowable average tensile stress, and R_s is the ratio of average shear stress to allowable average shear stress.

For NCT:

$$R_t = 50,065/63,800 = 0.785$$

$$R_s = 13,518/38,280 = 0.353$$

$$R_t^2 + R_s^2 = (0.785)^2 + (0.353)^2 = 0.740 < 1$$

For HAC:

$$R_t = 64,166/87,500 = 0.733$$

$$R_s = 13,518/52,500 = 0.257$$

$$R_t^2 + R_s^2 = (0.733)^2 + (0.257)^2 = 0.603 < 1$$

2.10.2.5.6 Bearing Stress Under Lid Bolt Head

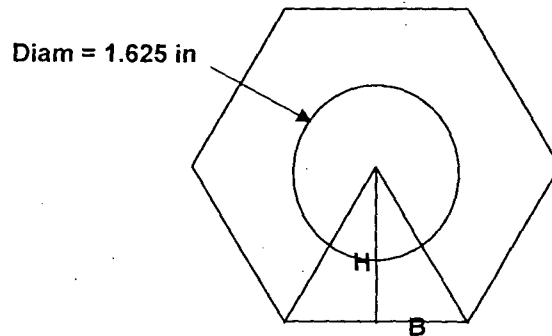
The maximum NCT axial force is 74,343 lb. A bolt hole of 1.625" diameter is used for the shank (Chapter 1, Appendix 1.4 drawings).

$$H = 2.25/2 \text{ in.}$$

$$B = 1.125 \tan(30^\circ) = 0.650 \text{ in.}$$

$$\begin{aligned} \text{Total Area of one triangle} \\ = (1.125)(.650) = .731 \text{ in.}^2 \end{aligned}$$

$$\begin{aligned} \text{Total area under Bolt head - Bolt Hole area} \\ = 6(.731) - (\pi/4)(1.625^2) = 2.31 \text{ in.}^2 \end{aligned}$$



The total bearing area is 2.31 in.² The bearing stress for normal conditions is,

$$\text{Bearing Stress} = 74,343/2.31 = 32,179 \text{ psi} = 32.2 \text{ ksi}$$

The allowable normal condition bearing stress on the lid is taken to be the yield stress of the lid material at 300°F. The lid is manufactured out of SA-350 Grade LF3, which has a yield stress of 33.2 ksi at 300°F.

2.10.2.6 Analysis Results

A summary of the lid bolt stresses calculated above is presented in the following table:

SUMMARY OF STRESSES AND ALLOWABLES

Stress Type	NCT		HAC	
	Stress	Allowable	Stress	Allowable
Average Tensile (ksi)	50.1	63.8	64.2	87.5
Shear (ksi)	13.5	38.3	13.5	52.5
Combined (ksi)	59.3	86.1	Not Required Reference [1]	
Interaction E.Q. $R_t^2 + R_s^2 < 1$	0.740	1	0.603	1
Bearing Allowable (ksi) (S_y of lid material)	32.2	33.2	Not Required Reference [1]	

The calculated bolt stresses are all less than the specified allowable stresses.

2.10.2.7 Lid Bolt Fatigue Analysis

The purpose of the fatigue analysis is to show quantitatively that the fatigue damage to the bolts during NCT is acceptable. This is done by determining the fatigue damage factor for each NCT event. For this analysis it is assumed that the bolts are replaced after 50 round trip shipments. The total cumulative damage or fatigue usage for all events was conservatively determined by adding the usage factors for the individual events. The sum of the individual usage factors was checked to make certain that for the 50 round trip shipments of the TN-40 cask, the total usage factor was less than one. The following sequence of events was assumed for the fatigue evaluation.

1. Operating Preload (Bolt Tensile stress, $S_{ba} = 50,000$ psi, and bolt torsional shear stress, $S_{bt} = 13,518$ psi, corresponding to a bolt torque of 1,150 ft. lb.), with 50 round trip shipments considered.
2. Test pressure
3. Rail vibration / shock
4. Pressure and temperature fluctuations
5. 1 foot normal condition drop

Since the bolt preload stress applied to the TN-40 cask lid bolts is higher than all of the other NCT condition loads, the stress in the bolt will never exceed the bolt preload stress. Consequently, the application and removal of preload is the only real cyclic loading that occurs in the lid bolts. The following analysis is therefore very conservative

since it assumes that the damage factor is the sum of all of the individual event damage factors, and not simply the damage factor for bolt preload.

2.10.2.7.1 Operating Preload

Assuming that the bolts are replaced after 50 round trips, the number of preload cycles is two times the number of trips or 100 cycles.

The maximum normal condition bolt stress intensity is 59.3 ksi (Section 2.10.2.5.4).

2.10.2.7.2 Test Pressure

The ASME code-mandated proof test [10] is $1.25 \times (\text{Design Pressure}) = 125 \text{ psi}$, and will only be performed once.

From Section 2.10.2.2, the 100 psi internal pressure load analysis can be used by scaling the results upward by a factor of 1.25.

$$\begin{aligned} F_a &= 9,426 \times 1.25 = 11,783 \text{ lb / bolt,} \\ F_s &= 0 \times 1.25 = 0 \text{ lb / bolt,} \\ F_f &= 1,983 \times 1.25 = 2,479 \text{ lb / in.} \\ M_f &= 19,656 \times 1.25 = 24,570 \text{ in-lb / in.} \\ M_{bb} &= 0.0109 M_f = 267.8 \text{ in-lb / bolt} \end{aligned}$$

The lid bolt diameter is 1.375 in. Therefore from Reference [1], we get the following:

$$S_{ba} = 1.2732 \frac{F_a}{D_{ba}^2} = 1.2732 \frac{11,783}{1.375^2} = 7,935 \text{ psi}$$

$$S_{bb} = 10.186 \frac{M_{bb}}{D_{ba}^3} = 10.186 \frac{267.8}{1.375^3} = 1,049 \text{ psi}$$

Since internal pressure causes no bolt torsion, and all shear loads are taken by the lid shoulder,

Shear stress:

$$S_{bs} = 0, \text{ and } S_{bt} = 0.$$

Stress Intensity:

$$S.I. = S_{bi} = [(S_{ba} + S_{bb})^2 + 4(S_{bs} + S_{bt})^2]^{0.5} = [(7,935 + 1,049)^2 + 4(0)^2]^{0.5} = 8,984 \text{ psi}$$

2.10.2.7.3 Vibration / Shock

Since the TN-40 Package will be shipped by rail car, the shock and vibration loadings for rail configurations only will be considered.

Rail Car Shock:

Again, assume 50 round trip shipments, averaging 2000 miles each way. Reference [4] reports that there are roughly 9 shock cycles per 100 miles of rail car transport. Therefore the total number of cycles is $2000 \text{ miles} \times 2 \text{ round trip} \times 150 \text{ shipments} \times 0.09 \text{ shocks per mile} = 18,000 \text{ cycles}$.

Reference [4] also specifies a peak shock loading of 4.7 g in the longitudinal direction for rail car transport. Consequently, the bolt force due to rail car shock is

$$(82,000 \text{ lb})(4.7 \text{ g}) / (48 \text{ bolts})(1.485 \text{ in}^2 \text{ per bolt}) = 5,407 \text{ psi}$$

Vibration:

According to Reference [4], the peak vibration load on the deck of a rail car in the longitudinal direction is 0.19 g. This results in a stress of 219 psi, which is negligible for a high strength bolt.

2.10.2.7.4 Pressure and Temperature Fluctuations

The lid bolt material is SA320 GR. L43, 1¼Ni ¾Cr ¼Mo, which is in group E in the coefficients of thermal expansion tables in Reference [5]. The lid and flange are both made of SA 350 GR LF3, 3 ½ Ni, which is also group E. Therefore the lid bolts and all of the materials it contacts have the same coefficient of thermal expansion. Consequently thermal load will cause no stress in the lid bolts.

The pressure fluctuation is conservatively assumed to be the maximum design pressure, 100 psi, which is far greater than the actual operating pressure. Since the stress intensity in the lid bolts is linearly proportional to the internal / external pressure difference, the stress intensity due to 100 psi internal load is,

$$8,984 \text{ psi} \times \frac{100 \text{ psi}}{125 \text{ psi}} = 7,187 \text{ psi}$$

The pressure fluctuation is assumed to occur once per round trip, since there is no payload, and therefore no pressurization, during the return trip. So the total number of cycles of pressure fluctuation is 50.

2.10.2.7.5 1 Foot Normal Condition Drop

The normal condition drop consists of a 1 foot drop in an orientation that results in the most damage. For the side drop the resulting shear load is taken entirely by the lid / flange interface. For the end drop, the load is transferred to the cask body via the impact limiters, protecting the bolts. Therefore the worst case scenario is taken to be roughly a 63.8° C.G. over corner drop.

The lid bolt analysis above conservatively uses a 63.8° corner drop axial acceleration of 10 g to calculate the following bolt loads:

$$\begin{aligned} F_a &= 22,594 \text{ lb/bolt} \\ F_s &= 0 \text{ lb./bolt} \\ F_f &= 4,353 \text{ lb./bolt and} \\ M_f &= 43,151 \text{ lb./bolt} \\ M_{bb} &= 0.0109 M_f = 470 \text{ in-lb / bolt} \end{aligned}$$

The lid bolt diameter is 1.375 in. Therefore, from Reference [1], we get the following

$$S_{ba} = 1.2732 \frac{F_a}{D_{ba}^2} = 1.2732 \frac{22,594}{1.375^2} = 15,215 \text{ psi}$$

$$S_{bb} = 10.186 \frac{M_{bb}}{D_{ba}^3} = 10.186 \frac{470}{1.375^3} = 1,842 \text{ psi}$$

Since internal pressure causes no bolt torsion, and all shear loads are taken by the lid shoulder,

$$\begin{aligned} \text{Shear stress} \\ S_{bs} &= 0, \text{ and } S_{bt} = 0. \end{aligned}$$

$$\begin{aligned} \text{Stress intensity} \\ S.I. = S_{bi} &= [(S_{ba} + S_{bb})^2 + 4(S_{bs} + S_{bt})^2]^{0.5} \\ &= [(15,215 + 1,842)^2 + 4(0)^2]^{0.5} = 17,057 \text{ psi} \end{aligned}$$

Conservatively assume that the cask is dropped once per shipment, resulting in 50 normal condition drops before the lid bolts are changed.

2.10.2.7.6 Damage Factor Calculation

The following damage factors are computed based on the stresses and cyclic histories described above, a fatigue strength reduction factor, K_F , of 4 (Reference [5]), and the fatigue curve shown in Table I-9.4 of Reference [5].

Event	Stress Intensity (psi)	S.I. $\times K_F$ (psi)	S_a (psi)	Cycles		Damage Factor n/N
				n	N	
Operating Preload	59,300	237,200	128,088	100	619	0.16
Test Pressure	8,984	35,936	19,405	1	81,054	0.00
Rail Car Shock	5,407	21,628	23,354	18,000	35,314	0.51
Pressure and Temperature	7,187	28,748	15,524	50	10^6	0.00
1 Foot Normal Condition Drop	17,057	68,228	36,843	50	7,701	0.0065
Σ						0.68

Here, n is the number of cycles, N is taken from Figure I-9.4 of Reference [5], and S_a is defined in the following way:

If one cycle goes from 0 to $+S.I.$, then $S_a = (1/2) \times S.I. \times K_F \times K_E$.

If one cycle goes from $-S.I.$ to $+S.I.$, then $S_a = S.I. \times K_F \times K_E$.

Where K_E is the correction factor for modulus of elasticity, $30 \times 10^6 / 27.8 \times 10^6 = 1.08$ (Reference [5]).

Since the total damage factor is less than one in both cases, the TN-40 cask lid bolts will not fail due to fatigue in either case.

2.10.2.8 Lid Seal Contact Evaluation

The lid seal design was conducted in order to determine the lid/cask seal status when subject to a CG over lid corner impact 30 foot drop.

Section 2.10.2.3 above shows that during accident condition the preload is not enough to maintain a compressive force on the seal. An elastic finite element analysis is performed to determine the status of the lid/cask seal during a CG over corner 30 foot drop. The finite element model from Appendix 2.10.1 is modified to include contact elements (CONTAC52) at the lid/cask axial interface, internal pressure, bolt preload, seal load and 30 foot drop conditions.

2.10.2.8.1 Assumptions

- CG over corner lid impact with internal pressure is the worst case condition.
- The force to seat the seals is 1399 lbs./in [2] and 2198 lbs/in [6]. The total load to seat the seal is 660,142 lbs or 1,037,164 lbs, but 700,000 lbs and 1,040,000 lbs will be used conservatively.
- The maximum allowable decompression of the seal is 0.040" [2].

2.10.2.8.2 Analysis

The finite element model from Appendix 2.10.1 is modified to include contact elements (CONTAC52) at the lid/cask axial interface, internal pressure, bolt preload, seal load and 30 foot drop conditions.

Gap elements (CONTAC52) were used to model the lid/cask axial interface. To get an accurate contact representation a 60 mil axial gap was included radially outwards of Ø77.25" (closest node at Ø78.10") between the lid/cask axial interface. Figure 2.10.2-1 shows the lid/cask axial interface.

A pressure of 100 psi was applied to all internal surfaces. Bolt shank prestrain was calculated based on $\epsilon = \sigma/E$, where σ is the bolt prestress (50 ksi per Section 2.10.2.2 above). The seal loads of 700,000 lbs and 1,040,000 lbs were applied via CONTAC52 elements. The stiffness for the gap element was calculated based on $F=kx$. The accident drop conditions were kept consistent with Appendix 2.10.1.

2.10.2.8.3 Results

Figure 2.10.2-2 plots the decompression of the seal as a function of circumferential location. The maximum decompression is 0.003 in. which is less than the allowable seal decompression of 0.040 in.

From the analysis results presented in the Figures and discussion, it can be concluded that during the CG over corner drop lid impact loading with internal pressure, the metal-to-metal contact exists at the Helicoflex seal. Since a seal exists around the circumference of the TN-40 vessel, the internal contents will not leak during a worst case loading condition.

2.10.2.9 Minimum Engagement Length for Bolt and Flange

For a 1½ – 8UN bolt, the material is SA – 320 GR L43, with

$S_u = 125$ ksi, and

$S_y = 105$ ksi (at room temperature)

The flange material is SA – 350 GR LF3, with

$S_u = 70$ ksi, and

$S_y = 37.5$ ksi (at room temperature)

The minimum engagement length, L_e , for the bolt and flange is (Reference [7], Page 1490),

$$L_e = \frac{2A_t}{3.146K_{n\max} \left[\frac{1}{2} + .57735n(E_{s\min} - K_{n\max}) \right]}$$

where,

A_t = tensile stress area = 1.485 in.²

n = number of threads per inch = 8

$K_{n\max}$ = maximum minor diameter of internal threads = 1.390 in.

$E_{s\min}$ = minimum pitch diameter of external threads = 1.4166 in.

$D_{s\min}$ = minimum major diameter of external threads = 1.4978 in.

Substituting the values given above,

$$L_e = \frac{2(1.485)}{(3.1416)(1.390) \left[\frac{1}{2} + .57735(8)(1.4166 - 1.390) \right]} = 1.09 \text{ in.}$$

$$J = \frac{A_s \times S_{ue}}{A_n \times S_{ui}}, \text{ (Reference [7])}$$

Where, S_{ue} is the tensile strength of external thread material, and S_{ui} is the tensile strength of internal thread material.

A_s = shear area of external threads

$$= 3.1416 n L_e K_{n\max} [1/(2n) + .57735 (E_{s\min} - K_{n\max})]$$

A_n = shear area of internal threads

$$= 3.1416 n L_e D_{s\min} [1/(2n) + .57735(D_{s\min} - E_{n\max})]$$

For the bolt / flange insert connection:

$E_{n\max}$ = maximum pitch diameter of internal threads = 1.4283 in.

Therefore,

$$A_s = 3.1416 (8) (1.09) (1.390) [1 / (2 \times 8) + .57735 (1.4166 - 1.390)] \\ = 2.96 \text{ in.}^2$$

$$A_n = 3.1416 (8) (1.09) (1.4978) [1 / (2 \times 8) + .57735 (1.4978 - 1.4283)] \\ = 4.21 \text{ in.}^2$$

So,

$$J = \frac{2.96(125.0)}{4.21(70.0)} = 1.26$$

Therefore, the minimum required engagement length,

$$Q = J L_e = 1.26 \times 1.09 = 1.37 \text{ in.}$$

The actual minimum engagement length

$$= (6.50 \text{ bolt length} - 4.50 \text{ lid thickness}) = 2.00 \text{ in.} > 1.37 \text{ in.}$$

The above calculation bounds the minimum required engagement length if inserts are used because S_u of inserts is higher than the S_u for the lid thus lowering the J value.

2.10.2.10 Conclusions

- A lid bolt torque range of 1,100 to 1,150 ft. lb. is recommended to achieve the desired preload stress of 50,000 psi.
- Lid bolt stresses meet the acceptance criteria of NUREG/CR-6007 "Stress Analysis of Closure Bolts for Shipping Casks" [1].
- For the recommended preload, a positive (compressive) load is maintained during all load combinations, except for the accident condition impact plus pressure load case.
- Closure of the TN-40 Cask lid is evaluated in Section 2.10.2.8 above and the seal remains closed during a worst case impact.
- The bolt and flange thread engagement length is acceptable.

2.10.2.11 References

1. Stress Analysis of Closure Bolts for Shipping Cask, NUREG/CR-6007, 1992.
2. High Performance Sealing, Metal Seals Helicoflex Catalog, Helicoflex Co., Boonton, N.J., ET 507 E 5930.
3. Draft American Standard Design Basis for Resistance to Shock and Vibration of Radioactive Material Packages Greater than One Ton in Truck Transport, ANSI N14.23.
4. Shock and Vibration Environments for Large Shipping Containers on Rail Cars and Trucks, NUREG 766510.
5. American Society of Mechanical Engineers, ASME Boiler and Pressure Vessel Code, Section III and Appendix, 1989.
6. "Prairie Island Independent Spent Fuel Storage Installation Safety Analysis Report," Rev. 10, 10/11/2005.
7. Machinery Handbook, 26st Ed, Industrial Press, 2000.
8. Baumeister, T., Marks, L. S., Standard Handbook for Mechanical Engineers, 7th Edition, McGraw-Hill, 1967.
9. Design Criteria for the Structural Analysis of Shipping Cask Containment Vessels, U. S. Nuclear Regulatory Commission, Regulatory Guide 7.6, Revision 1, March 1978.
10. ASME Boiler and Pressure Vessel Code, Section III, Division 1, Subsection NB6220, 1989.

Table 2.10.2-1
Design Parameters For Lid Bolt Analysis

- D_b Nominal diameter of closure bolt; 1.375 in.
- K Nut factor for empirical relation between the applied torque and achieved preload is 0.135 for neolube
- Q Applied torque for the preload (in.-lb.)
- D_{lb} Closure lid diameter at bolt circle, 79.31 in.
- D_{lg} Closure lid diameter at the seal (outer), 75.9 in.
- E_c Young's modulus of cask wall material (SA-350, LF3, 300°F), 26.7×10^6 psi
- E_l Young's modulus of lid material (SA-350, LF3, 300°F), 26.7×10^6 psi
- N_b Total number of closure bolts, 48
- N_{ul} Poisson's ratio of closure lid, 0.3, (Reference [8], p. 5-6 use nominal value).
- P_{ei} Inside pressure of cask, 100 psig.
- D_{lo} Closure lid diameter at outer edge, 82.75 in.
- P_{li} Pressure inside the closure lid, 100 psig.
- t_c Thickness of cask wall, $8.0 + 1.5 = 9.5$ in.
- t_l Thickness of lid center, 10.5 in; lid flange, 4.5 in.
- l_b Thermal coefficient of expansion, bolt (SA-320, L43), 6.4×10^{-6} at R.T., 6.9×10^{-6} in. in.⁻¹ °F⁻¹ at 300°F
- l_c Thermal coefficient of expansion, cask (SA-350, LF3) 6.4×10^{-6} at R.T., 6.9×10^{-6} in. in.⁻¹ °F⁻¹ at 300°F
- l_l Thermal coefficient of expansion, lid (SA-350, LF3) 6.4×10^{-6} R.T., 6.9×10^{-6} in. in.⁻¹ °F⁻¹ at 300°F
- E_b Young's modulus of bolt material (SA-320, L43, 300° F), 26.7×10^6 psi
- a_i Maximum rigid-body impact acceleration (g) of the cask
- LF Load Factor to account for any difference between the rigid body acceleration and the acceleration of the contents and closure lid = 1.1
- W_c Weight of contents = 52,000 (fuel) + 14,693 (basket)** = 66,693 lbs.
- W_l Weight of lid = 13,907 lbs.
- $W_c + W_l$ 66,693 + 13,907 = 80,600 lbs., assume 82,000 lbs.
- α_i Impact angle between the cask axis and target surface
- S_{yl} Yield strength of closure lid material (SA-350, LF3, 300° F), 33,200 psi
- S_{ul} Ultimate strength of closure lid (SA-350, LF3, 300° F), 70,000 psi
- S_{yb} Yield strength of bolt material (see Table 2.10.2-3)
- S_{ub} Ultimate strength of bolt material (see Table 2.10.2-4)
- P_{lo} Pressure outside the lid
- L_b Bolt length between the top and bottom surfaces of closure, 4.5 in.
- P_{un} Maximum impact force generated by the puncture bar during a normal impact
- D_{pb} Puncture bar diameter, 6 inches per 10 CFR 71.73 (c) (3)

** Conservatively using higher basket weight for lid bolt analysis

Table 2.10.2-2
Bolt Data

Parameters necessary to use formulas of Reference [1], Table 5.1.

Bolt: 1 1/2" – UN8 – 2A

N : no of threads per inch = 8

p : Pitch = 1/8" = .125 in.

D_b : Nominal Diameter = 1.5 in.

D_{ba} : Bolt diameter for stress calculations in the threaded area
= $D_b - .9743p = 1.5 - .9743(.125) = 1.378$ in

Bolt Thread Stress Area = $\pi/4 (1.378)^2 = 1.491 \text{ in}^2$

Bolt Shank Stress Area = $\pi/4 (1.375)^2 = 1.484 \text{ in}^2$

Table 2.10.2-3
Allowable Stresses In Closure Bolts For Normal Conditions

(MATERIAL: SA-320 Gr. L43)

Temperature (°F)	Yield Stress ¹ (ksi)	Normal Condition Allowables		
		F_{tb} ^{2,4} (ksi)	F_{vb} ^{3,4} (ksi)	$S.I.$ ⁵ (ksi)
100	105.0	70.0	42.0	94.5
200	99.0	66.0	39.6	89.1
300	95.7	63.8	38.3	86.1
400	91.8	61.2	36.7	82.6
500	88.5	59.0	35.4	79.7
600	84.3	56.2	33.7	75.9

Notes:

- Yield stress values are from [5]
- Allowable Tensile stress, $F_{tb} = 2/3 S_y$ [1]
- Allowable shear stress, $F_{vb} = 0.4 S_y$ [1]
- Tension and shear stresses must be combined using the following interaction equation:

$$\frac{\sigma_{tb}^2}{F_{tb}^2} + \frac{\tau_{yb}^2}{F_{yb}^2} \leq 1.0 \quad [1]$$

- Stress intensity from combined tensile, shear and residual torsion loads, $S.I. \leq 0.9 S_y$ [1]

Table 2.10.2-4
Allowable Stresses In Closure Bolts For Accident Conditions

(MATERIAL: SA-320 Gr. L43)

Temperature (°F)	Yield Stress ¹ (ksi)	Accident Condition Allowables		
		$0.6 S_y$ ³ (ksi)	F_{tb} ^{2,4} (ksi)	F_{vb} ^{3,4} (ksi)
100	105.0	63.0	87.5	52.5
200	99.0	59.4	87.5	52.5
300	95.7	57.4	87.5	52.5
400	91.8	55.1	87.5	52.5
500	88.5	53.1	87.5	52.5
600	84.3	50.6	84.3	50.6

Notes:

1. Yield and tensile stress values are from [5], Note that S_u is 125 ksi at all temperatures of interest.
2. Allowable Tensile stress, $F_{tb} = \text{MINIMUM}(0.7 S_u, S_y)$, where $0.7 S_u = 0.7 (125) = 87.5$ ksi [1].
3. Allowable shear stress, $F_{vb} = \text{MINIMUM}(0.42 S_u, 0.6 S_y)$, where $0.42 S_u = 0.42 (125) = 52.5$ ksi [1].
4. Tension and shear stresses must be combined using the following interaction equation:

$$\frac{\sigma_{tb}^2}{F_{tb}^2} + \frac{\tau_{yb}^2}{F_{yb}^2} \leq 1.0 \text{ [1]}$$

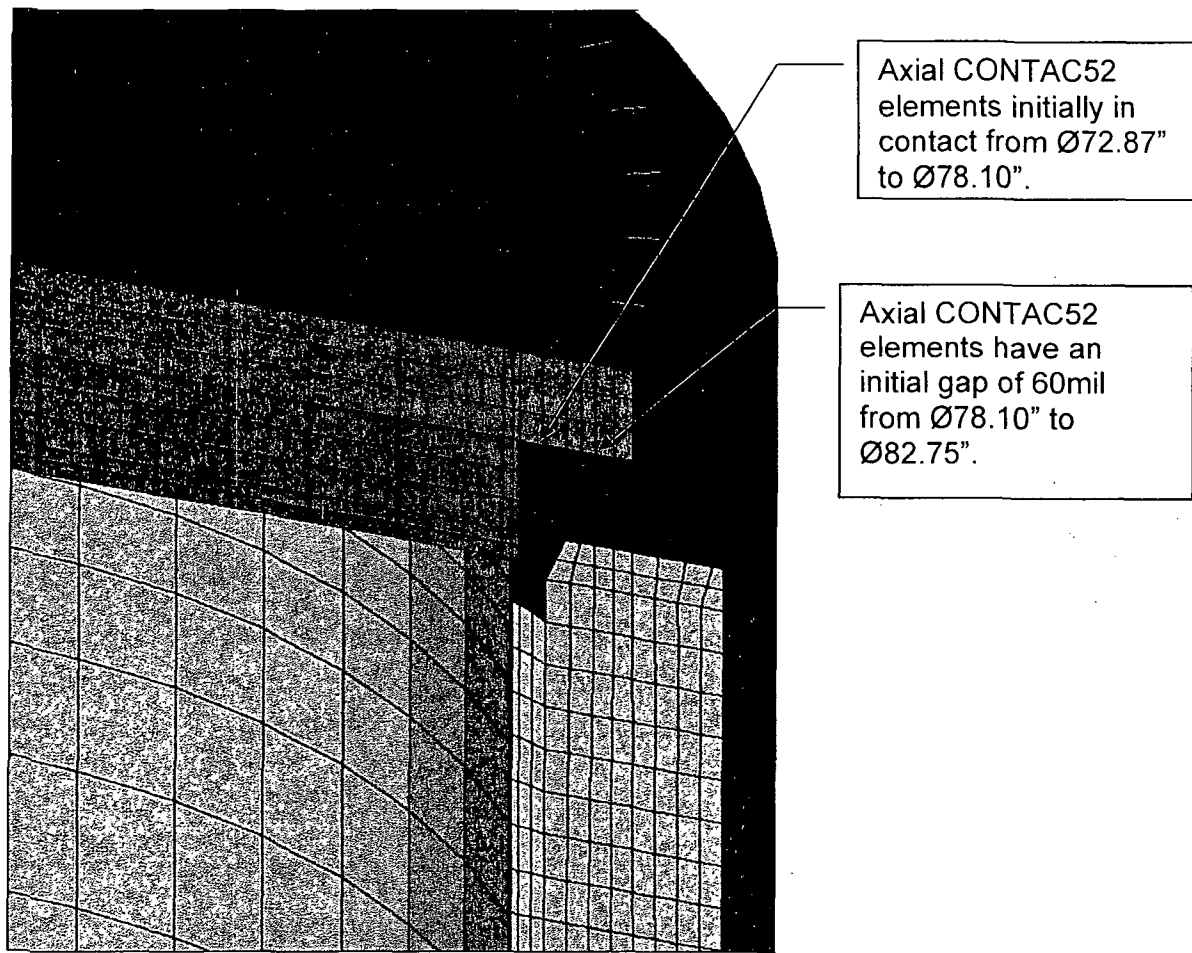


Figure 2.10.2-1
Lid/Cask Axial Interface

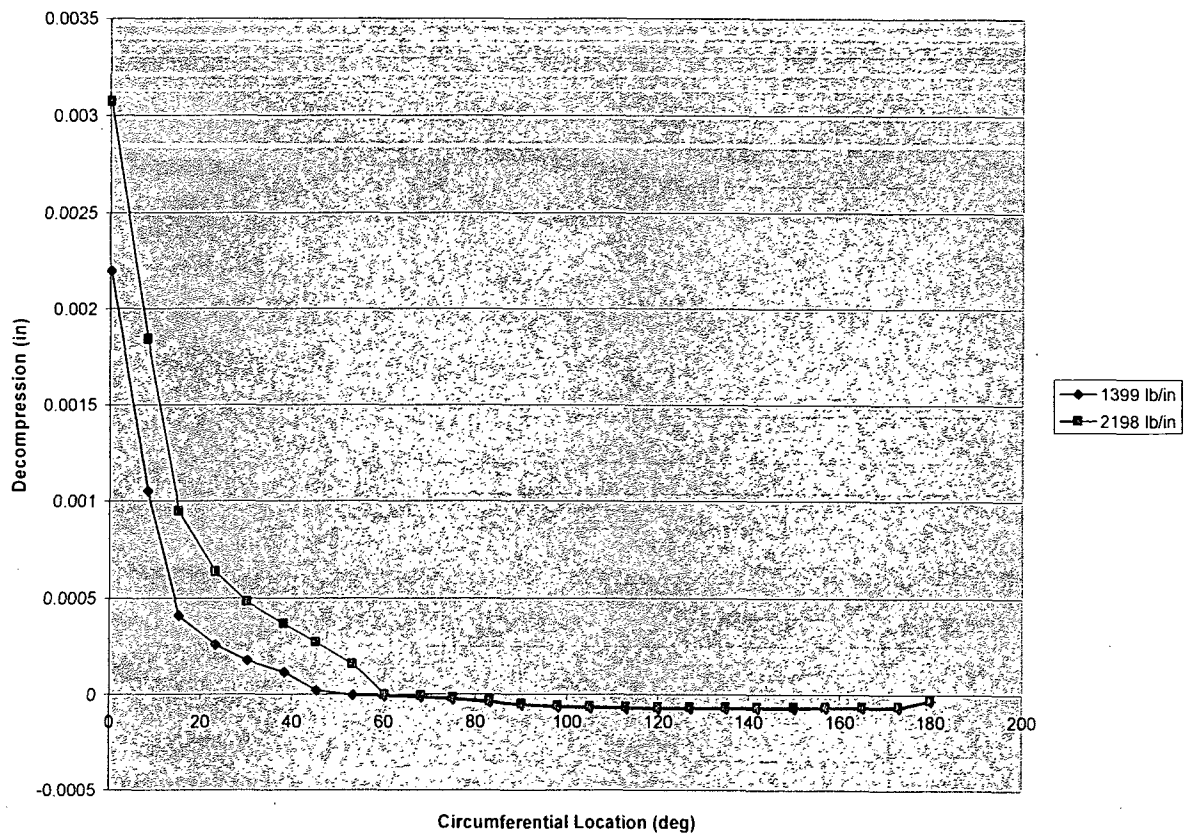


Figure 2.10.2-2
TN-40 Transport Cask (CG Over Corner Lid Drop - Hot)
Seal Decompression as a Function of Circumferential Location

Appendix 2.10.3

STRUCTURAL ANALYSIS OF THE OUTER SHELL

TABLE OF CONTENTS

	<u>PAGE</u>
2.10.3 STRUCTURAL ANALYSIS OF THE OUTER SHELL	2.10.3-1
2.10.3.1 Introduction.....	2.10.3-1
2.10.3.2 Description	2.10.3-1
2.10.3.3 Materials Input Data	2.10.3-1
2.10.3.4 Applied Loads.....	2.10.3-1
2.10.3.5 Method of Analysis	2.10.3-2
2.10.3.6 Analysis Results	2.10.3-4
2.10.3.7 References	2.10.3-6

LIST OF FIGURES

Figure 2.10.3-1 Cask Outer Shell and Connection to Cask Body	2.10.3-7
Figure 2.10.3-2 Finite Element Model - Boundary Conditions.....	2.10.3-8

2.10.3 STRUCTURAL ANALYSIS OF THE OUTER SHELL

2.10.3.1 Introduction

This section presents the structural analysis of the outer shell of the TN-40 package. The outer shell consists of a cylindrical shell section and closure plates at each end which connect the shell to the cask body. The shell is evaluated for Normal Condition of Transport (NCT) that includes internal pressure, normal handling/tiedown loads and 1 foot end/side drops. Maximum membrane and membrane plus bending stress intensities due to the pressure difference, handling/tiedown loads and 1 foot end/side drop loads are determined. These stresses are compared to the allowable stress limits in Chapter 2 to assure that the design criteria are met.

2.10.3.2 Description

The outer shell is constructed from low-alloy carbon steel and is welded to the outer surface of the gamma shield shell. The cylindrical shell section is 0.5 in. thick and the closure plates are 0.75 inches thick. Pertinent dimensions are shown in Figure 2.10.3-1 and Drawing 10421-71-3 in Appendix 1.4.1.

2.10.3.3 Materials Input Data

The outer shell cylindrical section and closure plates are SA-516 Gr 55. The material properties are taken from the ASME Code [1]. The yield strength of the material is also obtained from the ASME Code [1] at a temperature of 250°F. The temperature is a conservative value as compared to the calculated maximum temperature of 214°F given in Chapter 3, Table 3-1.

2.10.3.4 Applied Loads

It is assumed that a pressure of 25 psig may be applied to the inside of the outer shell during NCT. However, the external pressure load on the shell is reacted by the resin-filled aluminum containers inside the shell and thus does not create significant stresses in the shell.

The handling loads acting on the outer shell are a result of lifting. The lifting load includes a 3g factor as specified in 10CFR71 [2]. The weight or inertia g load includes the weight of the outer shell, neutron resin, and aluminum containers. The 2g vertical, 5g lateral and 10g longitudinal acceleration tiedown loads are applied when the cask is oriented horizontally to ensure it is not damaged during transport. The most severe NCT loads are the 1 foot end drop and side drops. The drop accelerations are 12g and 16g for the NCT end drop and side drop, respectively. These values are taken from Table 2.10.8-7. The load cases considered consist of the following:

- Cask in the Vertical Orientation
 - Stress due to 25 psig internal pressure
 - Stress due to 25 psig internal pressure and 3g inertia load (lifting)
 - Stress due to 25 psig internal pressure and 1 foot end drop (12g)
- Cask in the Horizontal Orientation
 - Stress due to 25 psig internal pressure
 - Stress due to 25 psig internal pressure, 2g vertical, 5g lateral and 10g longitudinal forward acceleration
 - Stress due to 25 psig internal pressure, 2g vertical, 5g lateral and 10g longitudinal backward acceleration
 - Stress due to 25 psig internal pressure and 1 foot side drop (16g)

2.10.3.5 Method of Analysis

ANSYS Model

A finite element model is built for the structural analysis of the outer shell and closure plates. The outer shell and closure plates are modeled with ANSYS Solid 45 elements [3]. The basic geometry of the outer shell and weld sizes used for analysis are shown in Figure 2.10.3-1. The finite element model is shown in Figure 2.10.3-2.

Cask in the Vertical Orientation

- Stress due to 25 psig internal pressure

An internal pressure of 25 psig is used as the maximum pressure acting on the inner surface of the outer shell. The maximum shell stress intensity for this load case is 5.02 ksi.

- Stress due to 25 psig internal pressure and 3g inertia load (lifting – cask in the vertical orientation)

The weight of the resin and aluminum containers is modeled as an additional pressure on the bottom inner surface. The added pressure load is 9.31 psi per g. The effect of the outer shell dead weight is accounted for by using a 3g gravitational load in the longitudinal direction. The maximum stress intensity for this load case is 6.57 ksi.

- Stress due to 25 psig internal pressure and 1 foot end drop (12g) (cask in the vertical orientation)

The weight of the resin and aluminum containers is modeled as an additional pressure on the bottom inner surface. The effect of the outer shell dead weight is accounted for by using a 12g gravitational load in the longitudinal direction using the same added pressure per g as used for the lifting case. The maximum shell stress intensity for this load case is 17.0 ksi.

Cask in the Horizontal Orientation

- Stresses due to 25 psig internal pressure

The stress due to 25 psig internal pressure is the same in both horizontal and vertical orientations (5.02 ksi).

- Stress due to 25 psig internal pressure, 2g vertical, 5g lateral, and 10g longitudinal forward acceleration.

The vertical and lateral accelerations are combined such that $g = (2.0^2 + 5.0^2)^{1/2} = 5.4g$. When the cask is in horizontal orientation, it is assumed that the weight of the outer shell, resin, and aluminum containers of the top 140° is supported by gamma shield, and the remaining weight of the outer shell, resin, and aluminum containers (220°) is uniformly distributed over the 152.5 in. length and over 180° arc.

For the loading due to 10g longitudinal forward acceleration, the weight of the resin and aluminum boxes is modeled as an additional pressure on the forward (lid side) inner surface of the outer shell.

The effect of the outer shell dead weight is accounted for by using a 10g gravitational load in the longitudinal direction. The maximum shell stress intensity for this load case is 17.64 ksi.

- Stress due to 25 psig internal pressure, 2g vertical, 5g lateral accelerations, and 10g longitudinal backward acceleration.

The loading due to 25 psig internal pressure, 2g vertical, and 5g lateral and 10g longitudinal backward acceleration is the same as it is in the previous case.

The effect of the outer shell dead weight is accounted for by using a 10g gravitational load in the longitudinal direction. The maximum stress intensity for this load case is 17.54 ksi.

- Stress due to 25 psig internal pressure and 1 foot side drop (16g)

When calculating the stress due to a 16g inertia load, it is assumed that the weight of the outer shell, resin, and aluminum containers of the top 140° is supported by the gamma shield, and the remaining weight of the outer shell, resin, and aluminum containers (220°) is uniformly distributed over the 152.5 in. length and over 180° arc.

The maximum stress intensity for this load case is 11.62 ksi.

Based on the above calculations the shell stress intensities are summarized in the following table:

2.10.3.6 Analysis Results

Loading	Stress Intensities (ksi)
25 psig Internal Pressure	5.02
25 psig + 3g Down (Cask in Vertical Orientation)	6.57
25 psig + 12g Down (Vertical End Drop)	17.00
25 psig + 2g vertical and 5g Lateral + 10g Longitudinal (Forward) (Cask in Horizontal Orientation)	17.64
25 psig + 2g vertical and 5g Lateral + 10g Longitudinal (Backward) (Cask in Horizontal Orientation)	17.54
25 psig + 16g Down (Side Drop)	11.62

All the above calculated maximum stress intensities are less than the allowable stress of 27.0 ksi (1.5 S_m , SA-516 GR.55, at 250°F).

Weld stress intensities are also calculated at the locations noted in Figure 2.10.3-1. These values are shown below.

Weld Location (Figure 2.10.3-1)	Max. Stress Intensity (ksi)
25 psig Internal Pressure	
Location 1	2.38
Location 2	5.02
Location 3	4.78
Location 4	2.31
25 psig Internal Pressure + Lifting Load	
Location 1	7.34
Location 2	7.43
Location 3	3.93
Location 4	2.38
25 psig Internal Pressure + End Drop Loads	
Location 1	13.86
Location 2	11.21
Location 3	1.40
Location 4	13.87
25 psig Internal Pressure + Forward Acceleration Loads	
Location 1	13.39
Location 2	2.30
Location 3	11.03
Location 4	13.95
25 psig Internal Pressure + Backward Acceleration Loads	
Location 1	14.27
Location 2	11.02
Location 3	2.02
Location 4	13.11
25 psig Internal Pressure + Side Drop Loads	
Location 1	9.40
Location 2	8.93
Location 3	8.50
Location 4	9.19

The weld stress intensities are less than the allowable stress of 16.5 ksi ($0.3S_u$, SA-516 GR.55, at 250° F).

2.10.3.7 References

1. ASME Boiler and Pressure Vessel Code, Section III, Division 1, Appendices, 1989.
2. 10 CFR 71 Packaging and Transportation of Radioactive Material.
3. ANSYS Engineering Analysis System, Users Manual for ANSYS Release 8.0.

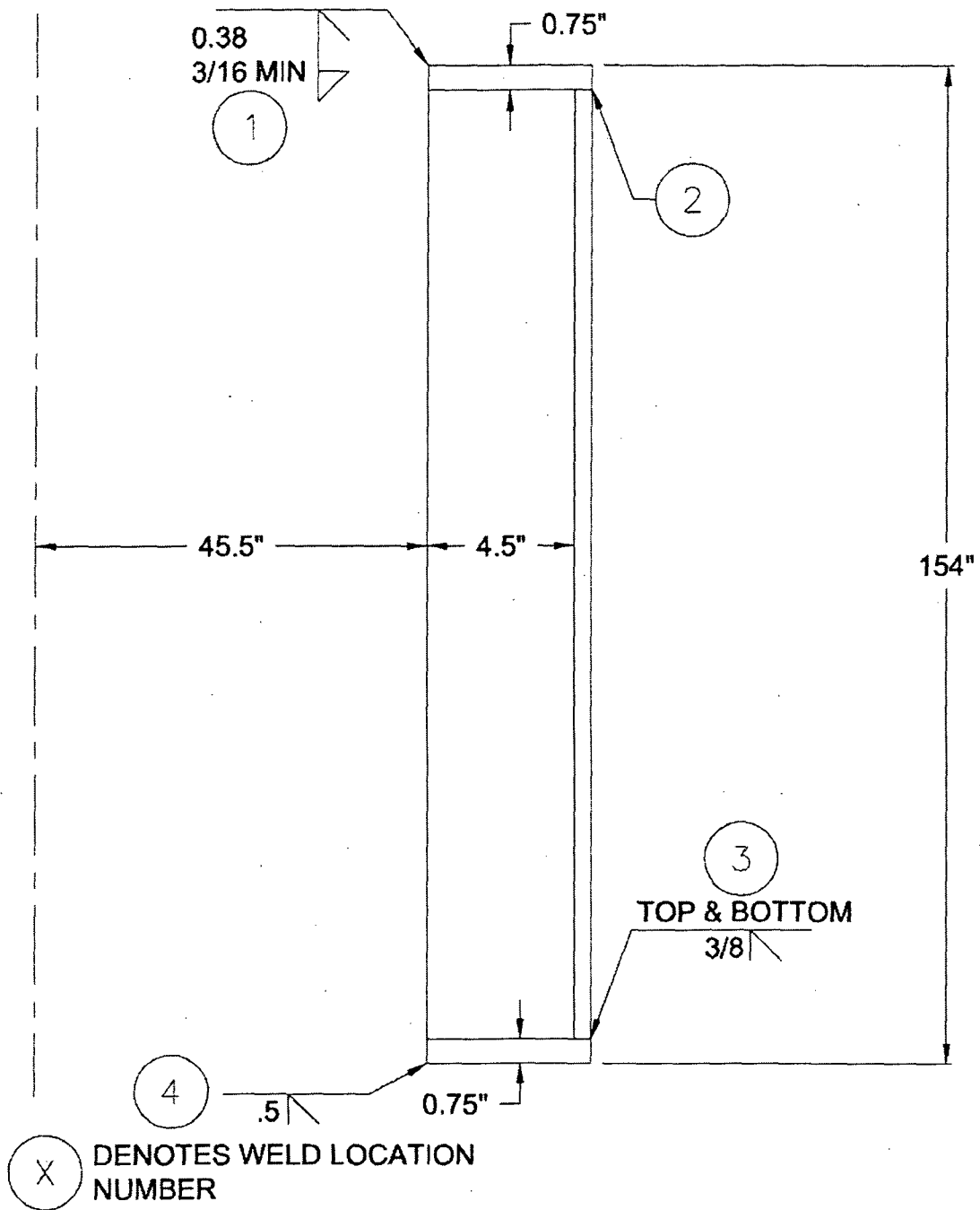


Figure 2.10.3-1
Cask Outer Shell and Connection to Cask Body

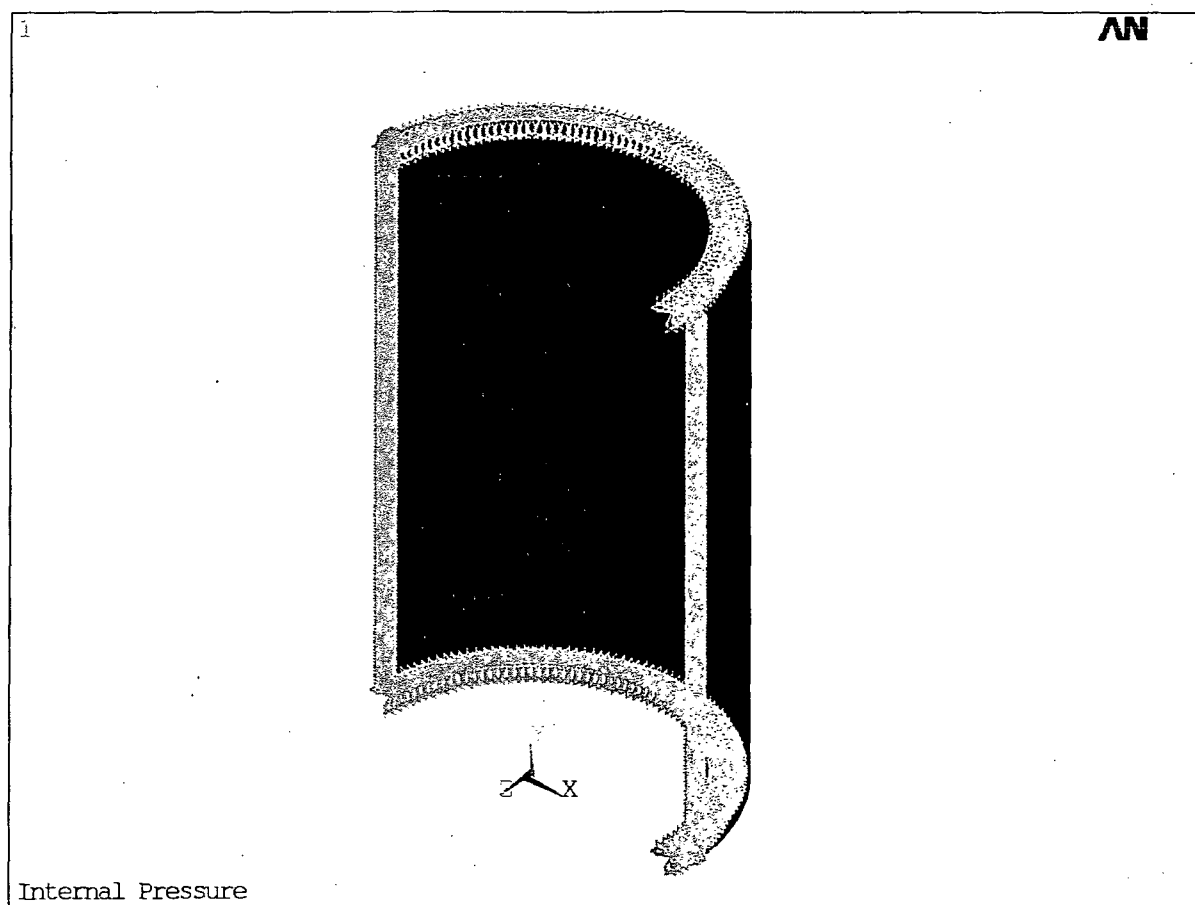


Figure 2.10.3-2
Finite Element Model - Boundary Conditions

APPENDIX 2.10.4 FRACTURE TOUGHNESS EVALUATION OF THE TN-40 CASK

TABLE OF CONTENTS

	<u>PAGE</u>
2.10.4 FRACTURE TOUGHNESS EVALUATION OF THE TN-40 CASK	2.10.4-1
2.10.4.1 Introduction.....	2.10.4-1
2.10.4.2 Fracture Toughness Requirements of The Cask.....	2.10.4-1
2.10.4.3 Fracture Toughness Evaluation of Cask Components and Welds	2.10.4-3
2.10.4.4 Methodology.....	2.10.4-3
2.10.4.5 Loadings.....	2.10.4-3
2.10.4.6 Material Fracture Toughness.....	2.10.4-3
2.10.4.7 Fracture Toughness Criteria.....	2.10.4-5
2.10.4.8 Stress Intensity Factor Calculations	2.10.4-5
2.10.4.9 Conclusions.....	2.10.4-5
2.10.4.10 NDE Inspection Plan	2.10.4-6
2.10.4.11 References	2.10.4-7

LIST OF TABLES

Table 2.10.4-1	Summary Stress Components - Normal Conditions of Transport	2.10.4-8
Table 2.10.4-2	Summary Stress Components – Hypothetical Accident Conditions.....	2.10.4-9
Table 2.10.4-3	Summary Stress Intensity Factors for Normal Condition of Transport Loadings.....	2.10.4-10
Table 2.10.4-4	Summary Stress Intensity Factors for Hypothetical Accident Condition Loadings	2.10.4-11

LIST OF FIGURES

Figure 2.10.4-1 Critical Locations for Stress and Fracture Evaluation 2.10.4-12

Figure 2.10.4-2 Charpy V-Notch Test Results for SA-266 Forging 2.10.4-13

2.10.4 FRACTURE TOUGHNESS EVALUATION OF THE TN-40 CASK

2.10.4.1 Introduction

This appendix documents the fracture toughness evaluation of the TN-40 cask.

2.10.4.2 Fracture Toughness Requirements of The Cask

The TN-40 cask material is a ferritic steel (penetration covers are stainless steel) and is therefore subject to fracture toughness requirements in order to assure ductile behavior at the lowest service temperature (LST) of -20°F .

The inner shell and bottom inner plate are fabricated from SA-203 Gr. D or E plate material, 1.5 inches thick. The shell flange is 4.6 inches thick, fabricated from SA-350 Gr. LF3 forging material and the lid outer plate is 4.5 inches thick, fabricated from either SA-350 Gr. LF3 or SA-203 Gr. E material. The 1.5 inch lid closure bolts are fabricated from SA320 Grade L43, Class1 material.

By interpolating between values provided in NUREG/CR-3826 [1] and NUREG/CR-1815 [2], the nil ductility transition temperatures (T_{NDT}) of the containment boundary materials are:

- Inner Shell and bottom inner plates (1.5 in.): -80°F
- Shell Flange (4.6 in.): -137°F
- Lid Outer Plate (4.5 in.): -125°F

The fracture toughness requirements of the lid closure bolts meet the criteria of ASME Code, Section III, Subsection NB (Para. NB-2333) [3]. Charpy v-notch testing is performed at -20°F . The acceptance criterion is that the material exhibits at least 25 mils lateral expansion (Table NB-2333-1). All the lid closure bolt materials meet the NB-2300 criteria.

The 1.5in. plate material which forms the inner shell and inner bottom plate meets the NUREG fracture arrest criteria.

Drop weight and Charpy test measurements of the shell flange and lid outer plate from 24 TN-40 casks are shown in the table below.

Measured Data for Shell Flange and Lid Outer Plate

Cask #	SHELL FLANGE				LID OUTER PLATE			
	Measured T_{NDT} (°F)	Charpy Test Result			Measured T_{NDT} (°F)	Charpy Test Result		
		Test Temp. (°F)	Ave. Energy (ft-lbs)	Ave. Lateral Expansion (mils)		Test Temp. (°F)	Ave. Energy (ft-lbs)	Ave. Lateral Expansion (mils)
1	≤ -80	-20	107	73	≤ -80	-20	88	60
2	≤ -80	-20	107	73	≤ -80	-20	84	75
3	≤ -80	-20	107	73	≤ -80	-20	97	67
4	≤ -80	-20	118	79	≤ -80	-20	95	60
5	≤ -80	-20	102	67	≤ -80	-20	101	73
6	≤ -80	-20	102	67	≤ -80	-20	68	51
7	≤ -80	-20	112	77	≤ -80	-20	62	51
8	-90	-30	107	88	-110	-50	110	79
9	-90	-30	107	88	-110	-50	110	79
10	-90	-30	107	88	-110	-50	110	79
11	-90	-30	107	88	-110	-50	110	79
12	-90	-30	107	88	-110	-50	110	79
13	-112	-52	150	92	-126	-67	180	93
14	-112	-52	150	92	-126	-67	180	93
15	-112	-52	150	92	-126	-67	180	93
16	-112	-52	150	92	-126	-67	180	93
17	-112	-52	150	92	-126	-67	180	93
18	-134	-83	143	63	-136	-83	106	60
19	-134	-83	143	63	-136	-83	106	60
20	-134	-83	143	63	-136	-83	106	60
21	-136	-83	126	61	≤ -80	-20	259	96
22	-136	-83	126	61	≤ -80	-20	259	96
23	-136	-83	126	61	≤ -80	-20	259	96
24	-136	-83	126	61	≤ -80	-20	259	96

From the measured data for the TN-40 cask containment boundary material described above, one can observe that the actual T_{NDT} of some of the lid outer plate and shell flange material does not meet the NUREG fracture arrest criteria. Therefore, a fracture mechanics evaluation is performed for all the applicable cask components (including non-containment boundary components).

2.10.4.3 Fracture Toughness Evaluation of Cask Components and Welds

A fracture toughness evaluation of the TN-40 cask components and welds based on a service temperature of -20°F is performed. The evaluation includes the following:

- Methodology
- Loadings
- Material fracture toughness
- Fracture toughness criteria
- Stress Intensity Factor calculations
- Conclusions
- NDE Inspection Plan

2.10.4.4 Methodology

The allowable flaw sizes were determined using linear elastic fracture mechanics (LEFM) methodology from Section XI of ASME Code [4]. Flaws in the welds, if they occur, are welding defects, rather than initiated cracks. There is no active mechanism for crack initiation and growth at any of the weld locations since all the containment welds are volumetrically examined by RT and/or UT examination to assure no weld defects are present.

2.10.4.5 Loadings

Figure 2.10.4-1 shows the selected locations on the cask numbered 1 through 10 for fracture toughness analysis. Stresses are linearized at these critical locations for maximum tensile membrane and bending stresses. Tables 2.10.4-1 and Title 2.10.4-2 list the maximum membrane and bending stresses at these selected locations under NCT and HAC.

2.10.4.6 Material Fracture Toughness

The shell flange is basically a forged cylinder, nominally 4.6 inches thick by 9 inches long, made from SA-350 Gr. LF-3 material. The welding of the flange to the shell may be performed using SAW, FCAW, or GTAW processes. The lid outer plate is either a forged disc or a plate, nominally 4.5 inches thick with an 82.75 inch diameter, made from either SA-350 Gr. LF3 or SA-203 Gr. E material.

The Charpy impact testing data for twenty four TN-40 casks are tabulated above. The tabulated data shows a dispersion in the absorbed energy values mainly due to the flange and lid material being supplied by different material suppliers.

The electrodes used in the shell flange and lid outer plate weldments have a high nickel content. The high alloy content of the electrodes and their typical usage in applications where good toughness is required indicate that the expected fracture toughness values for the weld filler material is as good or better than that of the base material.

The gamma shield shell is a forged cylinder, nominally 8 inches thick by 167 inches long. The bottom shield is nominally 8.75 inches thick and 91 inches in diameter. These components are made from SA-266 Class 4, SA-516 Gr. 70 or SA-105 material. Similarly, the 6 in. thick lid shield plate is made from SA-516 Gr. 70 or SA-105. The welding at the top flange and bottom plate may be performed using SAW, FCAW, or SMAW processes.

All these materials are enveloped by the low fracture toughness material SA-266 forging. Therefore, it is conservative to use fracture toughness of the SA-266 forging for the fracture toughness evaluations of the TN40 components.

Reference [5] is a very thorough review of correlation between a range of ferritic steel material strength levels and Charpy impact energies. Figure 2.10.4-2 (reproduced from Figure 4-5 of Reference [5]) corresponds to Charpy V-notch impact test results for a normalized SA-266 forging. The actual data points are shown along with a smoothed line that connects the average value at each test temperature. This data demonstrates that a lower bound Charpy impact value of 18 ft-lbs is appropriate for an exposure temperature of -20°F. The various correlations between K_{Ic} and K_{Id} given in Table 4-2 of Reference [5] are compared at the 18 ft-lb level. Using the equation for yield strength for 36 to 50 ksi in transition in Table 4-2 of Reference [5], the Charpy impact measurement may be transformed into a fracture toughness value:

$$K_{Id} = [5E(C_v)]^{1/2} = 50,289 \text{ psi} \cdot (\text{in})^{1/2} = 50 \text{ ksi} \cdot (\text{in})^{1/2}$$

Where

K_{Id} = Dynamic Fracture Toughness (based on crack arrest), $\text{psi} \cdot (\text{in})^{1/2}$
 E = Modulus of Elasticity, 28.1×10^6 psi (conservatively use 300°F)
 C_v = Charpy Impact Measurement, 18 ft-lbs

For conservatism, the above calculated K_{Id} was reduced to $47 \text{ ksi} \cdot (\text{in})^{1/2}$ for fracture toughness evaluations of the TN-40 Cask components (containment and non-containment boundary) and welds.

Both the FCAW and SMAW electrodes used in the gamma shield weldments are alloyed with manganese, nickel, chromium, and vanadium. They are essentially matching filler metals for alloys such as ASME SA-533 Gr. B, the most commonly used reactor pressure vessel steel. The higher alloy content of the FCAW and SMAW electrodes and their typical usage in applications where good toughness is required indicate that the expected fracture toughness values for the FCAW and SMAW weld fillers are as good as or better than that of the SA-266 material. Use of the fracture properties from the wrought material for locations at or near the weld joints is conservative.

2.10.4.7 Fracture Toughness Criteria

Using the rule of Section XI, IWB-3613 [4], the limiting fracture toughness values are reduced by a factor of $\sqrt{10}$ for the NCT and $\sqrt{2}$ for the HAC, to define the limiting allowable $K_{allowable}$. That is,

$$K_{allowable} \leq K_{ia}/(\sqrt{10}) = 47/(\sqrt{10}) = 14.86 \text{ ksi}\sqrt{\text{in}} \text{ for normal conditions}$$

$$K_{allowable} \leq K_{ic}/(\sqrt{2}) = 47/(\sqrt{2}) = 33.23 \text{ ksi}\sqrt{\text{in}} \text{ for accident conditions}$$

Where:

K_{ia} = the available fracture toughness based on crack arrest for the corresponding crack tip temperature

K_{ic} = the available fracture toughness based on crack initiation for the corresponding crack tip temperature

Because of the dynamic loading (1-foot and 30-foot drops), it is appropriate to use the K_{ia} value (47 ksi-in^{1/2}) calculated above for K_{ia} and K_{ic} for the following normal and accident condition fracture toughness evaluations.

2.10.4.8 Stress Intensity Factor Calculations

The total applied stress intensity K_I (applied) is determined from the membrane and bending stresses. For purpose of analysis, the postulated surface flaws are oriented in both the axial and circumferential directions. The surface crack depth is assumed as 15% of component thickness. However, the maximum crack depth is limited to 1/2 inch. The crack length is assumed to be 10 times the crack depth. The assumed crack sizes are such that they can be readily spotted by visual examination. Compared to surface cracks, same size subsurface cracks are less critical. The results of the applied stress intensity K_I calculations for normal and accident conditions are shown in Tables 2.10.4-3 and -4, respectively.

2.10.4.9 Conclusions

Based on the results of fracture analysis of TN-40 cask components and welds with the postulated surface crack sizes, it is concluded that there is no potential of fracture failure due to NCT and HAC transport loadings. The postulated surface flaw sizes are such that they can be readily detected by a visual inspection.

Note that the gamma shield shell is not part of the containment boundary. Cracks postulated in the gamma shield shell will not propagate into the containment boundary due to the geometry of the cask. If the gamma shield shell were to fracture along the length or around the circumference or around the weld between the gamma shield shell and top flange, there is no credible mechanism that would result in the gamma shielding separating from the containment vessel. The top shield plate is welded to the lid and is

captured by the containment vessel. Therefore, if the weld were to completely fail, the shield plate would still remain inside the containment boundary and would not lose its shielding capability. Therefore, even if a fracture were to occur in the gamma shield shell or the weld between the gamma shield and top flange or top shield plate or weld between top shield plate and lid, there would be no safety significance, since containment would be maintained, and shielding would remain in place. The one exception is in the region of the weld of the gamma shield shell to the bottom plate. In this region, if the weld were to completely fail, the bottom plate could become detached and have an impact on the shielding capability of the cask. However, the bottom trunnions are independently welded to the gamma shield shell and the bottom shield plate and these additional attachment points (welds) would resist detachment of the bottom shield plate from the cask.

2.10.4.10 NDE Inspection Plan

The results of the fracture toughness analysis show that the flaws in the gamma shield shell and top and bottom shield plates which would result in unstable crack growth or brittle fracture are larger than those generally observed in forged steel and plate components. No special examination requirements on the gamma shield shell, top and bottom shield plates are, therefore, required.

The flaw sizes in the welds that could result in brittle fracture at -20°F will be detected by NDE methods and repaired.

The liquid penetrant or magnetic particle method will be in accordance with Section V, Article 6 of ASME Code [4].

2.10.4.11 References

1. NUREG/CR-3826, "Recommendations for Protecting against Failure by Brittle Fracture in Ferritic Steel Shipping Containers Greater than Four Inches Thick", April 1984.
2. NUREG/CR-1815, Recommendations for Protecting Against Failure by Brittle Fracture in Ferritic Steel Shipping Containers up to Four Inches Thick.
3. American Society of Mechanical Engineers, ASME Boiler and Pressure Vessel Code Section III, Subsection NB, 1989.
4. American Society of Mechanical Engineers, ASME Boiler and Pressure Vessel Code Section V and Section XI, 1989.
5. SIR-98-110, Rev. 0, "Allowable Flaw Evaluation of Transnuclear TN-32 Cask", Structural Integrity Associates, Inc. 1998.

Table 2.10.4-1
Summary Stress Components - Normal Conditions of Transport

Cask Location from Figure 2.10.4-1	Max. Stress Type*	Membrane Stress (ksi)			Bending Stress (ksi)		
		S _x (Rad.)	S _y (Tang.)	S _z (Axial)	S _x (Rad.)	S _y (Tang.)	S _z (Axial)
1. Weld	S _y (N11)	0.03	1.74	-0.61	0.08	0.10	0.35
	S _z (N11)	0.01	0.73	-0.53	0.24	0.04	0.31
2. Weld	S _y (N11)	-1.54	0.37	-0.50	0.87	0.42	0.50
	S _z (N11)	-1.51	0.23	-0.33	0.86	0.40	0.51
3. Weld	S _y (N11)	1.23	1.51	0.80	0.24	0.50	1.11
	S _z (N11)	3.26	0.71	1.36	0.77	0.68	1.37
4. Bottom Shield	S _x (N11)	-0.50	-1.03	-0.14	3.59	1.03	1.52
	S _y (N11)	0.25	1.54	-0.21	0.87	1.41	0.01
	S _z (N11)	-2.12	-1.32	1.55	2.13	1.45	2.24
5. Gam. Shield Shell-Mid	S _y (N10)	-0.40	3.21	1.90	0.33	2.20	2.20
	S _z (N10)	-0.41	3.21	1.89	0.35	2.15	2.23
6. Gam. Shield Shell-End	S _y (N10)	-0.40	3.45	1.55	0.34	2.06	2.62
	S _z (N10)	-0.44	-1.32	1.39	2.62	1.98	4.29
7. Flange	S _x , S _y (N9)	0.23	0.17	0.13	3.15	1.46	1.55
	S _z (N9)	-0.06	0.51	2.54	2.21	1.32	2.57
8. Shield Plate	S _x (N11)	0.38	-0.01	-0.41	1.42	1.24	0.10
	S _y (N11)	0.27	0.80	-0.37	1.12	1.64	0.14
	S _z (N11)	-0.20	-0.99	0.34	0.27	0.22	0.12
9. Lid Outer Plate	S _x (N11)	0.26	-0.04	0.67	2.03	0.46	0.78
	S _y (N11)	0.44	1.06	2.16	0.30	1.36	1.46
	S _z (N11)	0.62	1.37	2.98	1.28	0.32	0.48
10. Inner Shell & Bottom Inner Plate	S _x (N7)	-0.64	-3.29	-4.00	2.91	1.23	0.25
	S _y (N7)	-0.66	-1.0	3.32	2.59	1.27	0.60
	S _z (N7)	-0.71	-1.51	3.71	2.20	1.06	0.53

* S_y – Tangential StressS_z – Axial Stress

Table 2.10.4-2
Summary Stress Components – Hypothetical Accident Conditions

Cask Location from Figure 2.10.4-1	Max. Stress Type*	Membrane Stress (ksi)			Bending Stress (ksi)		
		S _x (Rad.)	S _y (Tang.)	S _z (Axial)	S _x (Rad.)	S _y (Tang.)	S _z (Axial)
1. Weld	S _y , S _z (A13)	0.14	3.99	-0.71	0.98	0.56	0.78
2. Weld	S _y (A12)	-1.66	3.34	-1.89	2.21	0.93	0.90
	S _z (A12)	-0.21	-0.35	-0.45	0.07	0.10	0.07
3. Weld	S _y (A12)	-10.52	0.51	-3.80	2.59	1.04	1.86
	S _z (A12)	0.40	-1.52	-0.18	1.17	0.41	0.04
4. Bottom Shield	S _x (A5)	-5.20	-7.31	0.34	8.92	3.68	2.08
	S _y (A5)	-1.32	2.27	-0.94	3.20	3.17	1.50
	S _z (A5)	-7.01	-7.71	2.74	5.57	4.00	3.67
5. Gam. Shield Shell-Mid	S _y (A11)	-0.43	4.32	2.62	0.41	1.13	1.22
	S _z (A11)	-0.43	4.32	2.62	0.41	1.13	1.22
6. Gam. Shield Shell-End	S _y (A11)	1.12	4.53	0.01	2.16	3.81	5.62
	S _z (A11)	1.06	0.10	1.19	1.17	1.02	3.79
7. Flange	S _x , S _y (A11)	-0.03	4.67	-0.35	0.11	1.10	0.27
	S _z (A11)	0.06	6.46	3.95	0.28	1.47	3.08
8. Shield Plate	S _x , S _y (A12)	-4.77	-3.98	-0.76	16.55	11.82	0.38
	S _z (A12)	-2.74	-1.52	8.99	8.26	6.40	10.92
9. Lid Outer Plate	S _x (A12)	0.26	6.55	-3.35	2.14	0.15	3.34
	S _y (A12)	-3.74	4.45	-2.70	11.50	5.87	2.79
	S _z (A12)	1.01	5.45	2.93	0.07	3.14	0.22
10. Inner Shell & Bottom Inner Plate	S _x (A8)	0.78	-7.65	-7.35	6.87	1.82	1.19
	S _y , S _z (A8)	1.98	5.40	7.16	4.72	2.13	0.40

* S_y – Tangential StressS_z – Axial Stress

Table 2.10.4-3
Summary Stress Intensity Factors for Normal Condition of Transport Loadings

Component	Thick., t (in)	Crack depth, a (in)	Crack length, l (in)	Max. Stress Type (1)	Critical Crack Direction (1)	Stress Intens. Factor (ksi-√in)	Allow. Stress Intens. Factor (ksi-√in)	Factors of Safety
1. Weld	1.25	0.1875	1.875	S _Y	Axial	1.52	14.86	9.77
2. Weld	0.5	0.075	0.75	S _Y	Axial	0.37	14.86	>10
3. Weld	0.75	0.1125	1.125	S _Z	Hoop	1.59	14.86	9.35
4. Bottom Shield	8.75	0.500	5.00	S _Z	Hoop	4.73	14.86	3.15
5. Gam. Shield Shell-Mid	8.0	0.500	5.00	S _Y	Axial	6.89	14.86	2.16
6. Gam. Shield Shell-End	8.0	0.500	5.00	S _Z	Hoop	7.18	14.86	2.07
7. Flange	4.6	0.500	5.00	S _Z	Hoop	6.32	14.86	2.36
8. Shield Plate	6.0	0.500	5.00	S _Y	Axial	2.92	14.86	5.10
9. Lid Outer Plate	4.5	0.500	5.00	S _Z	Hoop	5.65	14.86	2.64
10. Inner Shell & Bottom Inner Plate	1.5	0.225	2.25	S _Z	Hoop	3.86	14.86	3.86

(1) S_Y – Hoop Stress – Results in Axial crack S_Z – Axial Stress – Results in Hoop crack

Table 2.10.4-4
Summary Stress Intensity Factors for Hypothetical Accident Condition Loadings

Component	Thick., t (in)	Crack depth, a (in)	Crack length, l (in)	Max. Stress Type ⁽¹⁾	Critical Crack Direction ⁽¹⁾	Stress Intens. Factor (ksi-√in)	Allow. Stress Intens. Factor (ksi-√in)	Factors of Safety
1. Weld	1.25	0.1875	1.875	S _Y	Axial	3.74	33.23	8.90
2. Weld	0.5	0.075	0.75	S _Y	Axial	2.17	33.23	>10
3. Weld	0.75	0.1125	1.125	S _Z	Hoop	0.97	33.23	>10
4. Bottom Shield	8.75	0.500	5.00	S _X	Tang.	10.71	33.23	3.10
5. Gam. Shield Shell-Mid	8.0	0.500	5.00	S _Y	Axial	7.08	33.23	4.69
6. Gam. Shield Shell-End	8.0	0.500	5.00	S _Y	Axial	9.85	33.23	3.37
7. Flange	4.6	0.500	5.00	S _Y	Axial	10.36	33.23	3.20
8. Shield Plate	6.0	0.500	5.00	S _Z	Hoop	25.04	33.23	1.33
9. Lid Outer Plate	4.5	0.500	5.00	S _Y	Axial	15.65	33.23	2.12
10. Inner Shell & Bottom Inner Plate	1.5	0.225	2.25	S _Z	Hoop	7.51	33.23	4.42

- (1) S_Y: Hoop Stress – Results in Axial crack
S_Z: Axial Stress – Results in Hoop crack
S_X: Radial Stress – Results in Tangential Crack

APPENDIX 2.10.5

STRUCTURAL ANALYSIS OF THE TN-40 BASKET

TABLE OF CONTENTS

	<u>Page</u>
2.10.5 STRUCTURAL ANALYSIS OF THE TN-40 BASKET	2.10.5-1
2.10.5.1 Introduction	2.10.5-1
2.10.5.2 TN-40 Fuel Basket Stress Analysis	2.10.5-3
2.10.5.3 TN-40 Fuel Basket Buckling Analysis	2.10.5-9
2.10.5.4 References	2.10.5-12

LIST OF TABLES

Table 2.10.5-1	Material Properties for TN-40 Fuel Basket	2.10.5-13
Table 2.10.5-2	Basket Structural Allowable Stresses, NCT	2.10.5-14
Table 2.10.5-3	Basket Structural Allowable Stresses, HAC	2.10.5-14
Table 2.10.5-4	NCT 0° Side Drop, Basket Stress Analysis Results	2.10.5-15
Table 2.10.5-5	NCT 45° Side Drop, Basket Stress Analysis Results	2.10.5-16
Table 2.10.5-6	NCT 90° Side Drop, Basket Stress Analysis Results	2.10.5-17
Table 2.10.5-7	HAC 0° Side Drop, Basket Stress Analysis Results	2.10.5-18
Table 2.10.5-8	HAC 45° Side Drop, Basket Stress Analysis Results	2.10.5-19
Table 2.10.5-9	HAC 90° Side Drop, Basket Stress Analysis Results	2.10.5-20
Table 2.10.5-10	Shear Stress in Basket Fusion Welds For HAC Drop	2.10.5-20
Table 2.10.5-11	Fuel Basket Buckling Analysis Results	2.10.5-21

LIST OF FIGURES

Figure 2.10.5-1	Typical TN-40 Basket Fuel Compartment Plate	2.10.5-22
Figure 2.10.5-2	TN-40 Basket Finite Element Model Including Drop Orientations	2.10.5-23
Figure 2.10.5-3	Basket Finite Element Model Displacement Constraints – 0° Side Drop	2.10.5-24
Figure 2.10.5-4	Basket Finite Element Model Displacement Constraints – 30° Side Drop	2.10.5-25
Figure 2.10.5-5	Basket Finite Element Model Displacement Constraints – 45° Side Drop	2.10.5-26
Figure 2.10.5-6	Basket Finite Element Model Displacement Constraints – 60° Side Drop	2.10.5-27
Figure 2.10.5-7	Basket Finite Element Model Displacement Constraints – 90° Side Drop	2.10.5-28
Figure 2.10.5-8	Basket Finite Element Model Temperature Boundary Condition.....	2.10.5-29
Figure 2.10.5-9	Basket Finite Element Model Applied Pressures – 0° Drop, NCT	2.10.5-30
Figure 2.10.5-10	Basket Finite Element Model Applied Pressures – 45° Drop, NCT	2.10.5-31
Figure 2.10.5-11	Basket Finite Element Model Applied Pressures – 90° Drop, NCT	2.10.5-32
Figure 2.10.5-12	NCT 45° Side Drop - S.S. Plates - Membrane plus Bending Stress Intensity	2.10.5-33
Figure 2.10.5-13	NCT 45° Side Drop – Al. Plates - Membrane plus Bending Stress Intensity	2.10.5-34
Figure 2.10.5-14	NCT 45° Side Drop – Al. Periphery Plates - Membrane plus Bending Stress Intensity.....	2.10.5-35
Figure 2.10.5-15	NCT 45° Side Drop – Al. Outer Plates - Membrane plus Bending Stress Intensity	2.10.5-36
Figure 2.10.5-16	Thermal Stress Analysis Finite Element Model - Configuration 1	2.10.5-37
Figure 2.10.5-17	Thermal Stress Analysis Finite Element Model - Configuration 2	2.10.5-38

LIST OF FIGURES - Cont'd

Figure 2.10.5-18	Thermal Stress Analysis - Configuration 1 – Maximum Aluminum Stress Intensity	2.10.5-39
Figure 2.10.5-19	Thermal Stress Analysis - Configuration 1 - Maximum Stainless Steel Stress Intensity.....	2.10.5-40
Figure 2.10.5-20	Thermal Stress Analysis - Configuration 2 – Maximum Aluminum Stress Intensity	2.10.5-41
Figure 2.10.5-21	Thermal Stress Analysis - Configuration 2 – Maximum Stainless Steel Stress Intensity.....	2.10.5-42
Figure 2.10.5-22	Fuel Basket Buckling Analysis Finite Element Model Node Couplings	2.10.5-43
Figure 2.10.5-23	Basket Buckling Analysis Loading Boundary Conditions – 0° Side Drop	2.10.5-44
Figure 2.10.5-24	Basket Buckling Analysis Loading Boundary Conditions – 30° Side Drop	2.10.5-45
Figure 2.10.5-25	Basket Buckling Analysis Loading Boundary Conditions – 45° Side Drop	2.10.5-46
Figure 2.10.5-26	Basket Buckling Analysis Loading Boundary Conditions – 60° Side Drop	2.10.5-47
Figure 2.10.5-27	Basket Buckling Analysis Loading Boundary Conditions – 90° Side Drop	2.10.5-48
Figure 2.10.5-28	Fuel Basket Deformation at Buckling Load – 0° Side Drop.....	2.10.5-49
Figure 2.10.5-29	Fuel Basket Deformation at Buckling Load – 30° Side Drop.....	2.10.5-50
Figure 2.10.5-30	Fuel Basket Deformation at Buckling Load – 45° Side Drop.....	2.10.5-51
Figure 2.10.5-31	Fuel Basket Deformation at Buckling Load – 60° Side Drop.....	2.10.5-52
Figure 2.10.5-32	Fuel Basket Deformation at Buckling Load – 90° Side Drop.....	2.10.5-53

2.10.5 STRUCTURAL ANALYSIS OF THE TN-40 BASKET

2.10.5.1 Introduction

This appendix presents the structural analysis of the TN-40 fuel support basket. The basket is a welded assembly of stainless steel boxes and is designed to accommodate 40 PWR fuel assemblies. The fuel compartment stainless steel box sections are attached together locally by cylindrical stainless steel plugs that pass through the aluminum and Boral[®] plates and are fusion welded to both adjacent box sections. The basket contains 40 compartments for proper spacing and support of the fuel assemblies.

The basket structure is open at each end and therefore, longitudinal fuel assembly loads are applied directly to the cask body and not to the fuel basket structure. The fuel assemblies are laterally supported by the stainless steel structural tubes, and the basket is laterally supported by the cask inner shell.

The deformations and stresses induced in the basket structure due to the applied lateral loads are determined using the ANSYS computer program [1]. The most severe loadings for which the basket is evaluated are the 30 foot Hypothetical Accident Condition (HAC) side drop and end drop accidents. The basket is also evaluated for 1 foot side drop and end drop loads under the Normal Conditions of Transport (NCT). The g-loads and drop orientations used for the basket structural analysis are described in Appendix 2.10.8. The dynamic load factor is calculated in Appendix 2.10.6. The inertial loads of the fuel assemblies are applied as equivalent pressures on the stainless steel box interior surfaces. Quasi-static stress analyses are performed with applied loads in equilibrium with the reactions at the periphery of the basket. The calculated stresses in the basket structure are compared with the stress limits to demonstrate that the established design criteria are met.

2.10.5.1.1 TN-40 Fuel Basket Geometry

The details of the TN-40 basket are shown on TN Drawing Nos. 10421-71-8 and -9 in Chapter 1, Appendix 1.4.1. As described above, the basket structure consists of an assembly of stainless steel boxes or cells joined by fusion welded steel plugs and separated by aluminum and neutron poison material (Boral[®] sheets). The stainless, aluminum and Boral[®] wall between fuel compartments is effectively a sandwich panel. The 304 stainless steel members are the primary structural components. The aluminum provides the heat conduction path from the fuel assemblies to the cask inner shell, and the neutron poison material provides the necessary criticality control.

A representative basket wall panel between fuel compartments is shown in Figure 2.10.5-1. The panel plates are welded together at discrete locations (2 attachments every 8 inches) along their length. The adjacent fuel compartment stainless steel walls are fusion welded to cylindrical plugs that pass through holes in the Boral[®] and aluminum plates. This method of construction forms a very strong honeycomb-like

structure of boxes. The nominal open dimension of each fuel compartment cell or box is 8.05 in. \times 8.05 in. which provides a minimum of 1/8 in. clearance around the fuel assemblies. The pitch of the cells is approximately 8.85 in. The overall basket length (160 in.) is less than the cask cavity length to allow for loading the fuel assemblies, thermal expansion and tolerance stackup.

Several of the aluminum conductor plates are continuous across the diameter of the basket to provide uninterrupted heat conduction paths. Other shorter plates are provided between and perpendicular to these continuous plates. Some of the aluminum plates are as short as one cell width.

Structural rails oriented parallel to the axis of the cask are attached to the inner cavity wall of the cask body to establish and maintain basket orientation, to prevent twisting of the basket assembly, and to support the edges of those plates adjacent to the rails which would otherwise be free to slide tangentially around the cask cavity wall under lateral inertial loadings.

2.10.5.1.2 Fuel Basket Analysis Overview

The fuel basket is evaluated for NCT and HAC impact and thermal loads. The basket stress analysis is performed using a finite element method for the side drop and thermal load cases and analytical calculations for the end drop load cases. Buckling of the basket plates when subjected to lateral impact loads is evaluated using a nonlinear finite element buckling analysis. Stress and buckling analyses are provided in Sections 2.10.5.2 and 2.10.5.3 respectively.

2.10.5.1.3 Weight

The total weight of the TN-40 basket is 14,693 lb., and the total weight of all 40 fuel assemblies is 52,000 lb. A value of 1,300 lb. is assumed for the weight of each fuel assembly. Under lateral inertial loading each assembly is assumed to be uniformly supported across the width and along the length of the tube wall. The inertia of the basket structure (weight of the basket \times g-load) is also included in the analysis.

2.10.5.1.4 Temperature

Thermal analyses are performed to obtain the temperature distributions in the basket for various conditions. These analyses are presented in Chapter 3. The model temperature distribution is shown in Figure 2.10.5-8. Thermal stresses induced in the fuel basket by the applied temperature distributions are evaluated in Section 2.10.5.2.4.

2.10.5.2 TN-40 Fuel Basket Stress Analysis

2.10.5.2.1 Approach

Bounding inertial loads of 20g and 75g are applied for the NCT and HAC transport cask free drop cases respectively. These inertial loads are taken from the impact limiter analyses provided in Appendices 2.10.8. 0°, 45° and 90° azimuth orientations are analyzed in order to bound all possible drop orientations.

Nonlinear analyses with bilinear material properties and small deflections were performed in ANSYS [1] for the critical azimuth side drop orientations. The membrane and membrane plus bending stresses were compared against S_m and $1.5 S_m$ stress criteria values [2] for the NCT cask drop. The membrane and membrane plus bending stresses were compared against $0.7 S_u$ and $0.9 S_u$ elastic-plastic analysis stress criteria values [2] for the HAC cask drop.

The TN-40 transport cask geometry is described in Section 2.10.5.1.1 and depicted in detail in the design drawings provided in Chapter 1, Appendix 1.4.1 (Drawings 10421-71-8 and -9). Nominal dimensions are used in the analyses that follow.

Side drop impact analyses using finite element methods are provided in Section 2.10.5.2.2 and the analytical analysis for the end drop impact is provided in Section 2.10.5.2.3. The thermal stress analysis of the fuel basket is provided in Section 2.10.5.2.4.

2.10.5.2.2 Basket Finite Element Analysis for Side Impact Loads

A. Finite Element Model Description

A three-dimensional finite element model of the fuel basket is constructed using shell elements. The overall finite element model of the fuel basket is shown in Figure 2.10.5-2. The fuel tubes, aluminum structural plates, aluminum outer plates and periphery plates are included in the model. For conservatism, the strength of Boral® plates in the basket is neglected by excluding these from the finite element model. However, their weight is accounted for by increasing the structural aluminum plate material densities.

Because of the large number of plates in the basket and large size of the basket, certain modeling approximations were necessary. In view of continuous support of fuel compartment tubes by the peripheral rails along the entire basket length during a side drop, only an 8.0 inch long slice of the basket and rail is modeled. At the two cut faces of the model, symmetry boundary conditions are applied ($U_Y = ROTX = ROTZ = 0$). The displacement constraints for the 0°, 45°, and 90° side drop angles are shown in Figures 2.10.5-3, 2.10.5-5, and 2.10.5-7 respectively. For clarity, symmetry displacement constraints are not shown.

The nodes between the steel tubes including the intermediate aluminum plates are coupled together in the out-of-plane direction so that they will bend in unison under surface pressure or other lateral loading to simulate through the thickness support provided by Boral® plates. The aluminum plates are coupled together at their intersection. The fusion welds, connecting the fuel compartments and plates, are modeled with short pipe elements connected at each end to adjacent fuel compartment boxes in all directions.

B. Material Properties and Design Criteria

The stainless steel boxes and rails are constructed from SA-240, Gr. 304 stainless steel. The aluminum plates, outer plates and basket periphery plates are constructed from SB-209, 6061-T651 aluminum alloy. A bilinear stress-strain curve for SA-240 Type 304 stainless steel and SB-209 Type 6061-T651 aluminum alloy ($E_p/E = 0.05$) is used for the basket plates.

Table 2.10.5-1 lists the material properties used in all analyses of the TN-40 fuel basket. Tables 2.10.5-2 and 2.10.5-3 summarize the stress criteria for the NCT and HAC events respectively.

C. Side Drop Loading Conditions

The basket structure is analyzed for 0°, 45° and 90° azimuth side drops. Due to the basket structure symmetry, these orientations of side drops are assumed to envelop all other possible drop orientations.

A fuel assembly weight of 1,300 lb. is used in the analysis. A uniform fuel weight distribution is assumed over 144 inches, which is the active fuel length. An 8.0 inch sector of the basket assembly is modeled. The weight of the Boral® plates is accounted for by increasing the density of the aluminum plates. The Boral® plate's stiffness is conservatively neglected in the analysis.

Temperatures at the cross section where the maximum temperatures occur in the basket are used, which are taken from the normal transfer condition (100°F) thermal analysis presented in Chapter 3. Figure 2.10.5-8 shows the temperature contour used in all analyses.

The load resulting from the fuel assembly weight is applied as pressure on the fuel compartment plates of the basket. For the 0° orientation, the pressure acts only on the horizontal plates, and for the 90° orientation, the pressure acts only on the vertical plates. For the 45° orientation, the pressure was divided into components that act on both horizontal and vertical plates of the basket. The pressures for all orientations are calculated below for 20g and 75g accelerations.

0° and 90° Drop Orientations

$$\text{Pressure for 1g, } p = \text{Fuel assembly weight} / (\text{Panel span} \times \text{Panel length}) \\ = 1300 \text{ lb.} / (8.14 \text{ in.} \times 144 \text{ in.}) = 1.109 \text{ psi}$$

$$\text{Pressure for 20g} = 20 \times 1.109 = 22 \text{ psi}$$

$$\text{Pressure for 75g} = 75 \times 1.109 = 83 \text{ psi}$$

45° Orientation

$$\text{Pressure for 1g} = p \cos 45^\circ \\ = 1.109 \times 0.7071 = 0.7842$$

$$\text{Pressure for 20g} = 22 \times 0.7071 = 16 \text{ psi}$$

$$\text{Pressure for 75g} = 83 \times 0.7071 = 59 \text{ psi}$$

The load distributions for the 0°, 45° and 90° analyses for the NCT drops are shown in Figures 2.10.5-9 to 2.10.5-11, respectively. The load distribution for the 0°, 45° and 90° HAC drop analyses are similar to those shown in Figures 2.10.5-9 to 2.10.5-11, except that the applied pressures are scaled up to 75g accordingly.

The acceleration applied in each run are as follows.

Orientation	Inertial Load (g)	a_x (g)	a_y (g)	a_z (g)
0°	20	20	0	0
	75	75	0	0
45°	20	14.14	0	-14.14
	75	53.03	0	-53.03
90°	20	0	0	-20
	75	0	0	-75

D. Side Drop Analysis and Results

NCT Side Drop Analysis and Results

Nonlinear analyses with bilinear material properties and small deflections were performed using ANSYS [1] for the 0°, 45°, and 90° drop orientations. Loads corresponding to 20g were applied in all analyses. It was confirmed that no area in the model was plastically deformed; hence all the analyses were linear elastic analyses.

The nodal stress intensity distribution in the stainless steel boxes, aluminum plates, aluminum periphery plates and aluminum outer plates are computed by ANSYS. The membrane plus bending stress intensity distributions for the NCT 45° azimuth drops are shown in Figures 2.10.5-12 through 2.10.5-15 as representative sample of the resulting stresses. The shell middle surface nodal stress intensity is the membrane stress intensity and the top or bottom surface stress intensity is the membrane plus bending stress intensity. Allowable stress / stress at each node for membrane and membrane plus bending stresses at the temperature for that node are calculated. The location

where allowable stress / stress is at a minimum (the location with minimum factor of safety) is determined. The results are summarized in Tables 2.10.5-4 through 2.10.5-6.

The limiting stress ($P_m + P_b + Q$) in the stainless steel plates for normal conditions, 10.15 ksi (maximum thermal stress is 1.45 ksi from Section 2.10.5.2.4), is also lower than the criteria 59.6 ksi ($3 S_m$ at 310° F). The limiting stress ($P_m + P_b + Q$) in the aluminum plates for normal conditions, 5.01 ksi (maximum thermal stress is 0.84 ksi from Section 2.10.5.2.4), is also lower than the criteria, 10.0 ksi ($3 S_m$ at 440° F).

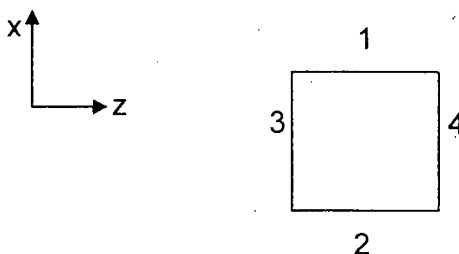
HAC Side Drop Analysis and Results

Nonlinear analyses with bilinear material properties and small deflection were performed in ANSYS [1] for the 0°, 45°, and 90° drop orientations. Loads corresponding to 75g were applied in all analyses. The nodal stress intensity distributions throughout the fuel basket are qualitatively similar to those shown in Figures 2.10.5-12 through 2.10.5-15, except with higher stress amplitudes.

Allowable stress / stress at each node for membrane and membrane plus bending stresses at the temperature for that node are calculated. The location where allowable stress / stress is at a minimum (the location with minimum factor of safety) is determined. The results are summarized in Tables 2.10.5-7 through 2.10.5-9.

Maximum Relative deflection of the Basket

The maximum relative deflections in the critical fuel compartment during the 75g side drops of 0°, 45°, and 90° orientations are summarized in the following table.



Maximum Relative Deflection of the Basket

Orientation	Total Deflection at Locations (in)				Relative Deflection	
	1 (ux)	2 (ux)	3 (uz)	4 (uz)	$\delta_1 - \delta_2$ (ux)	$\delta_3 - \delta_4$ (uz)
0 degree	-0.051	-0.028	-0.0001	0.0009	-0.023	-0.0008
45 degree	-0.025	-0.028	0.037	0.022	0.003	0.015
90 degree	-0.0014	-0.0007	0.052	0.029	-0.0007	0.023

It is seen that the maximum total relative deflection in the critical box is in the order of 0.023 in. It should be noted that this is the deflection at 75g; permanent deformation will be significantly less.

Shear Loads in Fusion Welds during Side Drop Impacts

All of the NCT and HAC side drop analyses were post-processed to compute shear stresses in the pipe elements which represent the fusion welds. Table 2.10.5-6 summarizes the maximum shear stresses in the welds due to NCT side drop. Table 2.10.5-10 summarizes the maximum shear stresses in the welds due to HAC side drop.

2.10.5.2.3 Fuel Basket End Drop Analysis

During an end drop, the fuel assemblies and fuel compartments are forced against the bottom or top of the TN-40 cask. It is important to note that, for any vertical or near vertical loading, the fuel assemblies react directly against the bottom or top end of the cask and not through the basket structure as in lateral loading. It is the weight of the basket that causes axial compressive stress during an end drop. Axial compressive stresses are conservatively computed first by assuming that all of the basket weight is reacted by the compartment tubes during an end drop and second, that all of the basket weight is reacted by the aluminum plates. A conservative basket weight of 15.0 kips (actual weight is 14.693 kips) is used in the end drop stress calculations.

Stainless Steel Basket Components

Assuming that all of the weight is supported by the stainless steel fuel compartments we have,

$$\begin{aligned}\text{Area of Steel Baskets} &= 40 \times [(w + 2t)^2 - w^2] \\ &= 40 \times [(8.05 + 2 \times 0.09)^2 - 8.05^2] = 117.2 \text{ in}^2\end{aligned}$$

$$\begin{aligned}\text{Stress in steel baskets at 1g loading} &= P / A \\ &= 15,000 / 117.2 = 128.0 \text{ psi}\end{aligned}$$

Therefore, the stress generated in the stainless fuel compartments is summarized as follows.

	Axial Stress (ksi)	Allowable Stress (P_m) at 450°F (ksi)
NCT (20g)	2.56	18.1
HAC (75g)	9.60	44.8

The maximum stress ($P_m + P_b + Q$) for normal condition, 4.01 ksi (maximum thermal stress is 1.45 ksi from Section 2.10.5.2.4), is also lower than the criteria 54.3 ksi (3 S_m).

Aluminum Basket Plates

The weight is assumed to be totally supported by the aluminum basket plates.

Area of aluminum basket plate – 340.9 in.²

$$\begin{aligned}\text{Stress in Aluminum Basket Plates at 1g loading} &= P / A \\ &= 15000 / 340.9 = 44.0 \text{ psi}\end{aligned}$$

Therefore, the stress generated in the aluminum basket plates is summarized as follows.

	Axial Stress (ksi)	Allowable Stress (P_m) at 450°F (ksi)
NCT (20g)	0.88	3.1
HAC (75g)	3.30	8.6

The maximum stress ($P_m + P_b + Q$) for normal condition, 1.72 ksi (maximum thermal stress is 0.84 ksi from Section 2.10.5.2.4), is also lower than the criteria 9.2 ksi ($3 S_m$).

2.10.5.2.4 Fuel Basket Thermal Stress Analysis

An elastic ANSYS [1] finite element analysis was conducted on the basket to evaluate the thermal stresses in the stainless steel and aluminum plates. Two different areas in the basket were analyzed, the first configuration included two 0.25 inch thick aluminum plates and the second configuration included one 0.5 inch thick aluminum plate. The finite element models for both configurations are shown in Figures 2.10.5-16 and 2.10.5-17.

The stainless steel plates are connected by pipe elements representing the stainless steel bar and fusion welds. The aluminum plates are connected to the stainless steel bar via gap elements. A gap of 0.0 inches is used. The actual nominal gap is 0.06 inches.

Elastic material properties described in Section 2.10.5.2.2.B are used, and a uniform temperature of 450°F is applied.

The maximum stress intensities in the aluminum plates for configuration 1 and 2 are 0.84 ksi and 0.60 ksi respectively. The maximum stress intensities in the steel plates for configuration 1 and 2 are 1.45 ksi and 1.03 ksi respectively. The nodal stress intensity distributions in the stainless steel and aluminum plates are shown in Figures 2.10.5-18 through 2.10.5-21 for both configurations.

2.10.5.2.5 Basket Stress Analysis Conclusions

Stresses in the stainless steel plates, aluminum plates, aluminum periphery plates, and aluminum rails are calculated for the NCT and HAC cask drop cases. The results for the side drop analysis are summarized in Tables 2.10.5-4 through 2.10.5-6 and Tables 2.10.5-7 through 2.10.5-9 for the NCT and HAC cases respectively. The results for the end drop analysis are summarized in the tables in Section 2.10.5.2.3. The stresses in the stainless steel and aluminum plates are given in Section 2.10.5.2.4. All stresses meet the stress criteria discussed in Section 2.10.5.2.2.B for both NCT and HAC evaluations.

2.10.5.3 TN-40 Fuel Basket Buckling Analysis

2.10.5.3.1 Analysis Approach

Two techniques are available in the ANSYS program [1] for predicting the buckling load and buckling mode shape of a structure: nonlinear buckling analysis and eigenvalue (or linear) buckling analysis. Nonlinear buckling analysis is a more accurate approach since it can include features such as initial imperfections, material plastic behavior, gaps and large deflection response. This technique employs a nonlinear static analysis with gradually increasing loads to seek the load level at which structure becomes unstable.

Eigenvalue buckling analysis predicts the theoretical buckling strength of an ideal linear elastic structure. However, imperfections and nonlinearities prevent most real-world structures from achieving their theoretical elastic buckling strength. Thus, eigenvalue buckling analysis often yields unconservative results and is not recommended in actual engineering analysis [1]. Furthermore, this analysis is linear and can not account for the material plastic behavior.

An ANSYS nonlinear finite element analysis of the basket is conducted using large displacement and stress stiffening options with bilinear material properties to evaluate the plastic buckling loads. The five critical azimuth drop orientations analyzed are:

- 0° (load applied in the direction parallel to the basket vertical plates)
- 30° (load applied at 30° relative to the basket vertical plate direction)
- 45° (load applied at 45° relative to the basket vertical plate direction)
- 60° (load applied at 60° relative to the basket vertical plate direction)
- 90° (load applied in the direction perpendicular to basket vertical plates)

In order to calculate the buckling load, a three-dimensional finite element model of an 8 inch thick section of the basket is created. Figure 2.10.5-2 shows the model and the drop orientations.

The nodes between the steel baskets including the intermediate aluminum plates are coupled together in the out-of-plane direction so that they will bend in unison under surface pressure or other lateral loading to simulate through the thickness support

provided by Boral® plates. The aluminum plates are coupled together at their intersection. The fusion welds, connecting the fuel compartments and plates, are modeled by coupling nodes in all directions. The node couplings are shown in Figure 2.10.5-22.

At the two cut faces, symmetry boundary conditions are applied ($U_Y = ROTX = ROTZ = 0$). The displacement constraints for the 0°, 30°, 45°, 60° and 90° side drop angles are shown in Figures 2.10.5-3 through 2.10.5-7. For clarity, symmetry displacement constraints are not shown.

2.10.5.3.2 Buckling Analysis Loading Conditions

The basket structure was analyzed for 0°, 30°, 45°, 60° and 90° side drops. Due to basket structure symmetry, these side drop azimuth orientations envelop all possible buckling modes.

Temperatures at the cross section where the maximum temperature occurred for the basket are taken from the NCT maximum environment of 100°F (Chapter 3). Figure 2.10.5-8 shows the temperature contour used in all analyses.

The load resulting from the fuel assembly weight is applied as pressure on the fuel compartment plates of the basket. For the 0° orientation, the pressure acts only on the horizontal plates, and for the 90° orientation, the pressure acted only on the vertical plates. But for the 30°, 45°, and 60° orientations, the pressure is divided into components that act on both horizontal and vertical plates of the basket. The pressures for the various orientations are calculated below for a 200g acceleration.

0° and 90° Drop Orientations

$$\begin{aligned}\text{Pressure for 1g, } p &= \text{Fuel assembly weight} / (\text{Panel span} \times \text{Panel length}) \\ &= 1300 \text{ lb.} / (8.14 \text{ in.} \times 144 \text{ in.}) = 1.109 \text{ psi} \\ \text{Pressure for 200g} &= 200 \times 1.109 = 222 \text{ psi}\end{aligned}$$

30° Orientation

$$\begin{aligned}\text{Horizontal pressure for 1g} &= p \sin 30^\circ \\ &= 1.109 \times 0.5 = 0.5545 \text{ psi} \\ \text{Horizontal pressure for 200g} &= 222 \times 0.5 = 111 \text{ psi} \\ \text{Vertical pressure for 1g} &= p \cos 30^\circ \\ &= 1.109 \times 0.866 = 0.9604 \text{ psi} \\ \text{Vertical pressure for 200g} &= 222 \times 0.866 = 192 \text{ psi}\end{aligned}$$

45° Orientation

$$\begin{aligned}\text{Pressure for 1g} &= p \cos 45^\circ \\ &= 1.109 \times 0.7071 = 0.7842 \text{ psi} \\ \text{Pressure for 200g} &= 222 \times 0.7071 = 157 \text{ psi}\end{aligned}$$

60° Orientation

$$\begin{aligned}\text{Horizontal pressure for 1g} &= p \sin 60^\circ \\ &= 1.109 \times 0.866 = 0.9604 \text{ psi} \\ \text{Horizontal pressure for 200g} &= 222 \times 0.866 = 192 \text{ psi} \\ \text{Vertical pressure for 1g} &= p \cos 60^\circ \\ &= 1.109 \times 0.5 = 0.5545 \text{ psi} \\ \text{Vertical pressure for 200g} &= 222 \times 0.5 = 111 \text{ psi}\end{aligned}$$

The acceleration applied in each run are as follows.

Orientation	Inertial Load (g)	a_x (g)	a_y (g)	a_z (g)
0°	200g	200	0	0
30°	200g	173.21	0	-100.00
45°	200g	141.42	0	-141.42
60°	200g	100.00	0	-173.21
90°	200g	0	0	-200

The pressure load distributions for the 0°, 30°, 45°, 60° and 90° analyses are shown in Figures 2.0.5-23 through 2.10.5-27.

2.10.5.3.3 Buckling Analysis and Results

A maximum load of 200g was applied to each analysis. The automatic time stepping option AUTOTS was activated. This option lets the program decide the actual size of the load sub-step for a converged solution. The last load step with a converged solution is the buckling load of the model.

The ANSYS input, buckling loads and factors of safety for 0°, 30°, 45°, 60° and 90° side drops are summarized in the Table 2.10.5-11. Displacement patterns, at the last converged sub-step (buckling load) for the five cases are shown in Figures 2.10.5-28 through 2.10.5-32. It may be seen that the displacements are not excessive at the last converged load step.

2.10.5.3.4 Buckling Analysis Conclusions

Since the computed buckling loads for the TN-40 fuel basket are greater, with reasonable factors of safety, than the maximum applied 75g deceleration, the basket will not fail in buckling during the accident condition side drop event.

2.10.5.4 References

1. ANSYS Engineering Analysis System User's Manual, Rev. 8.0.
2. ASME Boiler and Pressure Vessel Code, 1989, Section III, Subsection NB, NF & Appendices; Section VIII, Divs I & 2.
3. "Aluminum Standards and Data", The Aluminum Association, Inc., 1976.

Table 2.10.5-1
Material Properties for TN-40 Fuel Basket

Part	Material	Temperature (°F)	S _y (psi)	S _u (psi)	E (psi×10 ⁶)	α _m (in/in/°F)	Density (lb/in ³)
Al Plates	SB-209, 6061-T651	70	35,000	42,000	10.0	-	0.1085
		300	27,400	31,700	9.2	13.22×10 ⁻⁶	0.1085
		400	13,300	17,700	8.7	13.52×10 ⁻⁶	0.1085
		500	4,375	7,000	8.1	13.82×10 ⁻⁶	0.1085
Steel Boxes and Rails	SA-240, Gr. 304	70	30,000	75,000	28.3	-	0.29
		300	22,500	66,000	27.0	9.0×10 ⁻⁶	0.29
		400	20,700	64,400	26.5	9.19×10 ⁻⁶	0.29
		500	19,400	63,500	25.8	9.37×10 ⁻⁶	0.29
Outer Plates	SB-209, 6061-T651	70	35,000	42,000	10.0	-	0.098
		300	27,400	31,700	9.2	13.22×10 ⁻⁶	0.098
		400	13,300	17,700	8.7	13.52×10 ⁻⁶	0.098
		500	4,375	7,000	8.1	13.82×10 ⁻⁶	0.098
Al Periphery Plates	SB-209, 6061-T651	70	35,000	42,000	10.0	-	0.098
		300	27,400	31,700	9.2	13.22×10 ⁻⁶	0.098
		400	13,300	17,700	8.7	13.52×10 ⁻⁶	0.098
		500	4,375	7,000	8.1	13.82×10 ⁻⁶	0.098

Notes:

- Material Properties are obtained from ASME code Section III Appendices [2]. Aluminum material properties at elevated temperatures are taken from aluminum standards and data [3].
- 5% of the elastic modulus used as the tangent modulus
- Since the Boral[®] plates were not included in the analysis, the weight of the plates is included in the weight of the aluminum plates. The density of the aluminum plates is adjusted to match the total weight of the Boral[®] and aluminum plates.

Table 2.10.5-2
Basket Structural Allowable Stresses, NCT

Material	Temperature (°F)	P_m (S_m or S) (psi)	$P_m + P_b$ ($1.5S_m$ or $1.5S$) (psi)
SB-209, 6061-T651	70	14,000	21,000
	300	11,300	16,950
	400	4,400	6,600
	500	1,750	2,625
SA-240, Gr. 304	70	20,000	30,000
	300	20,000	30,000
	400	18,700	28,050
	500	17,500	26,250

Notes:

- S_m obtained from ASME code Section VIII, Division 2; S obtained from Section III or the lower of $S_u/4$ or $2/3 S_y$

Table 2.10.5-3
Basket Structural Allowable Stresses, HAC

Material	Temperature (°F)	P_m ($0.7 S_u$) (psi)	$P_m + P_b$ ($0.9 S_u$) (psi)
SB-209, 6061-T651	70	29,400	37,800
	300	22,190	28,530
	400	12,390	15,930
	500	4,900	6,300
SA-240, Gr. 304	70	52,500	67,500
	300	46,200	59,400
	400	45,080	57,960
	500	44,450	57,150

Table 2.10.5-4
NCT 0° Side Drop, Basket Stress Analysis Results

Component	Stress* Location	Stress Category	Stress (20g) (ksi)	Temperature (°F)	Allowable Stress (ksi)
S.S. Boxes and Rails	Max Stress	P_m	5.8	310	19.9
		$P_m + P_b$	6.7	310	29.8
	Min F.S.	P_m	5.8	333	19.6
		$P_m + P_b$	6.7	310	29.8
Aluminum Plates	Max Stress	P_m	4.5	316	10.2
		$P_m + P_b$	4.7	316	15.3
	Min F.S.	P_m	4.5	316	10.2
		$P_m + P_b$	2.9	437	5.1
Aluminum Periphery Plates	Max Stress	P_m	1.3	298	11.3
		$P_m + P_b$	1.9	339	12.9
	Min F.S.	P_m	1.1	326	9.5
		$P_m + P_b$	1.9	339	12.9
Aluminum Outer Plates	Max Stress	P_m	0.8	288	11.4
		$P_m + P_b$	1.7	288	17.2
	Min F.S.	P_m	0.8	288	11.4
		$P_m + P_b$	1.7	288	17.2

* Max Stress: Report the maximum stress of the component
 Min F.S.: Report the stress at the location which has the minimum factor of safety

Table 2.10.5-5
NCT 45° Side Drop, Basket Stress Analysis Results

Component	Stress* Location	Stress Category	Stress (20g) (ksi)	Temperature (°F)	Allowable Stress (ksi)
S.S. Boxes and Rails	Max Stress	P_m	4.6	351	19.3
		$P_m + P_b$	6.9	317	29.7
	Min F.S.	P_m	4.6	351	19.3
		$P_m + P_b$	6.9	317	29.7
Aluminum Plates	Max Stress	P_m	3.3	308	10.8
		$P_m + P_b$	4.5	251	17.8
	Min F.S.	P_m	3.2	316	10.2
		$P_m + P_b$	3.7	440	5.0
Aluminum Periphery Plates	Max Stress	P_m	0.9	298	11.3
		$P_m + P_b$	2.5	323	14.6
	Min F.S.	P_m	0.8	326	9.5
		$P_m + P_b$	2.5	323	14.6
Aluminum Outer Plates	Max Stress	P_m	0.9	251	11.8
		$P_m + P_b$	1.4	251	17.8
	Min F.S.	P_m	0.9	251	11.8
		$P_m + P_b$	1.4	251	17.8

* Max Stress: Report the maximum stress of the component
 Min F.S.: Report the stress at the location which has the minimum factor of safety

Table 2.10.5-6
NCT 90° Side Drop, Basket Stress Analysis Results

Component	Stress* Location	Stress Category	Stress (20g) (ksi)	Temperature (°F)	Allowable Stress (ksi)
S.S. Boxes and Rails	Max Stress	P_m	5.5	365	19.2
		$P_m + P_b$	8.7	308	29.8
	Min F.S.	P_m	5.5	365	19.2
		$P_m + P_b$	8.7	308	29.8
Aluminum Plates	Max Stress	P_m	3.9	316	10.2
		$P_m + P_b$	4.6	367	10.0
	Min F.S.	P_m	3.8	320	9.9
		$P_m + P_b$	4.2	440	5.0
Aluminum Periphery Plates	Max Stress	P_m	0.5	288	11.4
		$P_m + P_b$	2.2	328	14.1
	Min F.S.	P_m	0.4	337	8.8
		$P_m + P_b$	1.9	360	10.7
Aluminum Outer Plates	Max Stress	P_m	0.7	251	11.8
		$P_m + P_b$	0.9	251	17.8
	Min F.S.	P_m	0.7	251	11.8
		$P_m + P_b$	0.9	251	17.8

Shear Stress In Basket Fusion Welds For NCT Drop

	Basket Side Drop Orientation	Maximum Shear Stress (ksi)	Shear Stress** Allowable (ksi)
NCT Drop	0°	13.0	14.0
	45°	12.8	14.0
	90°	12.9	14.0

* Max Stress: Report the maximum stress of the component
 Min F.S.: Report the stress at the location which has the minimum factor of safety

** See Table 2-5 of Chapter 2 for basket stress limits.

Table 2.10.5-7
HAC 0° Side Drop, Basket Stress Analysis Results

Component	Stress* Location	Stress Category	Stress (75g) (ksi)	Temperature (°F)	Allowable Stress (ksi)
S.S. Boxes and Rails	Max Stress	P_m	24.7	310	46.1
		$P_m + P_b$	29.2	310	59.3
	Min F.S.	P_m	24.7	310	46.1
		$P_m + P_b$	29.2	310	59.3
Aluminum Plates	Max Stress	P_m	16.7	316	20.6
		$P_m + P_b$	17.3	245	30.7
	Min F.S.	P_m	16.7	316	20.6
		$P_m + P_b$	8.6	437	12.3
Aluminum Periphery Plates	Max Stress	P_m	4.7	298	22.3
		$P_m + P_b$	7.3	339	23.7
	Min F.S.	P_m	4.3	326	19.6
		$P_m + P_b$	7.3	339	23.7
Aluminum Outer Plates	Max Stress	P_m	3.1	288	22.5
		$P_m + P_b$	6.4	288	29.0
	Min F.S.	P_m	3.1	288	22.5
		$P_m + P_b$	6.4	288	29.0

* Max Stress: Report the maximum stress of the component
 Min F.S.: Report the stress at the location which has the minimum factor of safety

Table 2.10.5-8
HAC 45° Side Drop, Basket Stress Analysis Results

Component	Stress* Location	Stress Category	Stress (75g) (ksi)	Temperature (°F)	Allowable Stress (ksi)
S.S. Boxes and Rails	Max Stress	P_m	16.7	351	45.6
		$P_m + P_b$	29.0	308	59.3
	Min F.S.	P_m	16.7	351	45.6
		$P_m + P_b$	29.0	308	59.3
Aluminum Plates	Max Stress	P_m	12.3	308	21.4
		$P_m + P_b$	15.4	382	18.3
	Min F.S.	P_m	12.2	313	20.9
		$P_m + P_b$	14.1	415	14.5
Aluminum Periphery Plates	Max Stress	P_m	3.4	298	22.3
		$P_m + P_b$	8.6	323	25.6
	Min F.S.	P_m	3.1	326	19.6
		$P_m + P_b$	8.6	323	25.6
Aluminum Outer Plates	Max Stress	P_m	3.5	251	23.7
		$P_m + P_b$	5.3	251	30.5
	Min F.S.	P_m	3.5	251	23.7
		$P_m + P_b$	5.3	251	30.5

* Max Stress: Report the maximum stress of the component
 Min F.S.: Report the stress at the location which has the minimum factor of safety

Table 2.10.5-9
HAC 90° Side Drop, Basket Stress Analysis Results

Component	Stress* Location	Stress Category	Stress (75G) (ksi)	Temperature (°F)	Allowable Stress (ksi)
S.S. Boxes and Rails	Max Stress	P_m	21.1	316	46.0
		$P_m + P_b$	25.7	308	59.3
	Min F.S.	P_m	21.1	316	46.0
		$P_m + P_b$	25.7	308	59.3
Aluminum Plates	Max Stress	P_m	14.4	316	20.6
		$P_m + P_b$	17.1	367	20.1
	Min F.S.	P_m	14.1	320	20.2
		$P_m + P_b$	15.4	403	15.6
Aluminum Periphery Plates	Max Stress	P_m	2.0	288	22.6
		$P_m + P_b$	8.4	328	25.1
	Min F.S.	P_m	1.6	337	18.6
		$P_m + P_b$	7.3	358	21.2
Aluminum Outer Plates	Max Stress	P_m	2.6	251	23.7
		$P_m + P_b$	3.5	251	30.5
	Min F.S.	P_m	2.6	251	23.7
		$P_m + P_b$	3.5	251	30.5

- * Max Stress: Report the maximum stress of the component
 Min F.S.: Report the stress at the location which has the minimum factor of safety

Table 2.10.5-10
Shear Stress in Basket Fusion Welds For HAC Drop

	Basket Side Drop Orientation	Maximum Shear Stress (ksi)	Shear Stress** Allowable (ksi)
HAC Drop	0°	14.3	26.67
	45°	14.4	26.67
	90°	14.4	26.67

- ** See Table 2-5 of Chapter 2 for basket stress limits.

Table 2.10.5-11
Fuel Basket Buckling Analysis Results

Basket Side Drop Orientation	Maximum Load used in Analyses			Last Converged Load (g)	Actual Max. Load (g)	Factor of Safety
	Maximum Acceleration (g)	Vertical Pressure (psi)	Horizontal Pressure (psi)			
0°	200	222	0	145.44	75	1.94
30°	200	192	111	88.54	75	1.18
45°	200	157	157	92.54	75	1.23
60°	200	111	192	92.54	75	1.23
90°	200	0	222	115.15	75	1.54

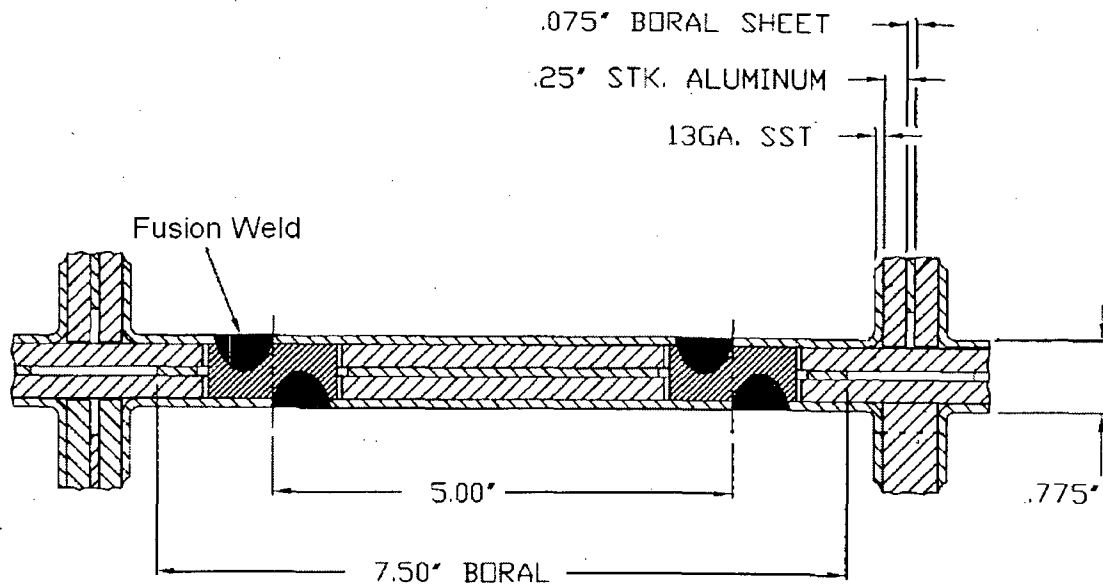


Figure 2.10.5-1
Typical TN-40 Basket Fuel Compartment Plate

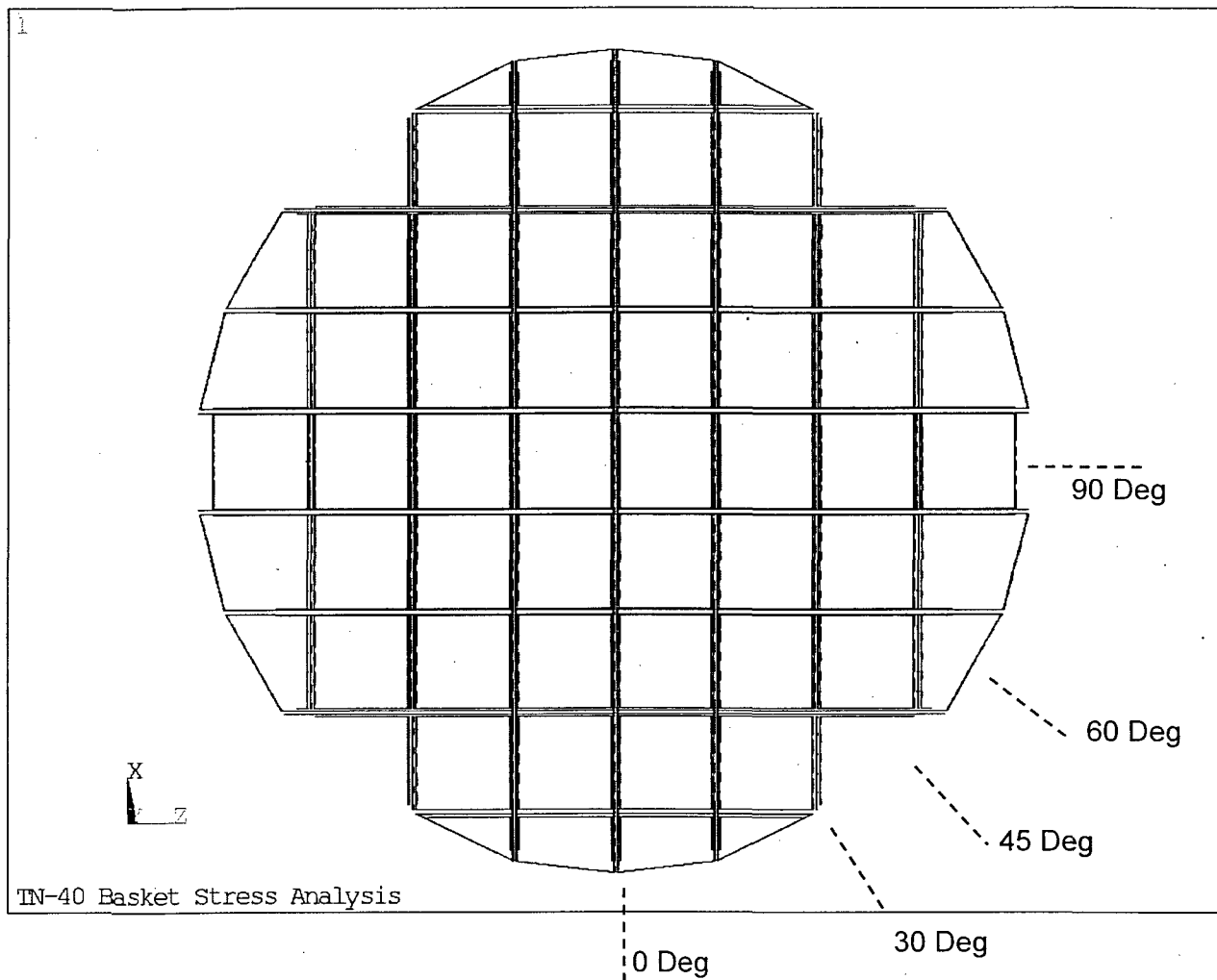


Figure 2.10.5-2
TN-40 Basket Finite Element Model Including Drop Orientations

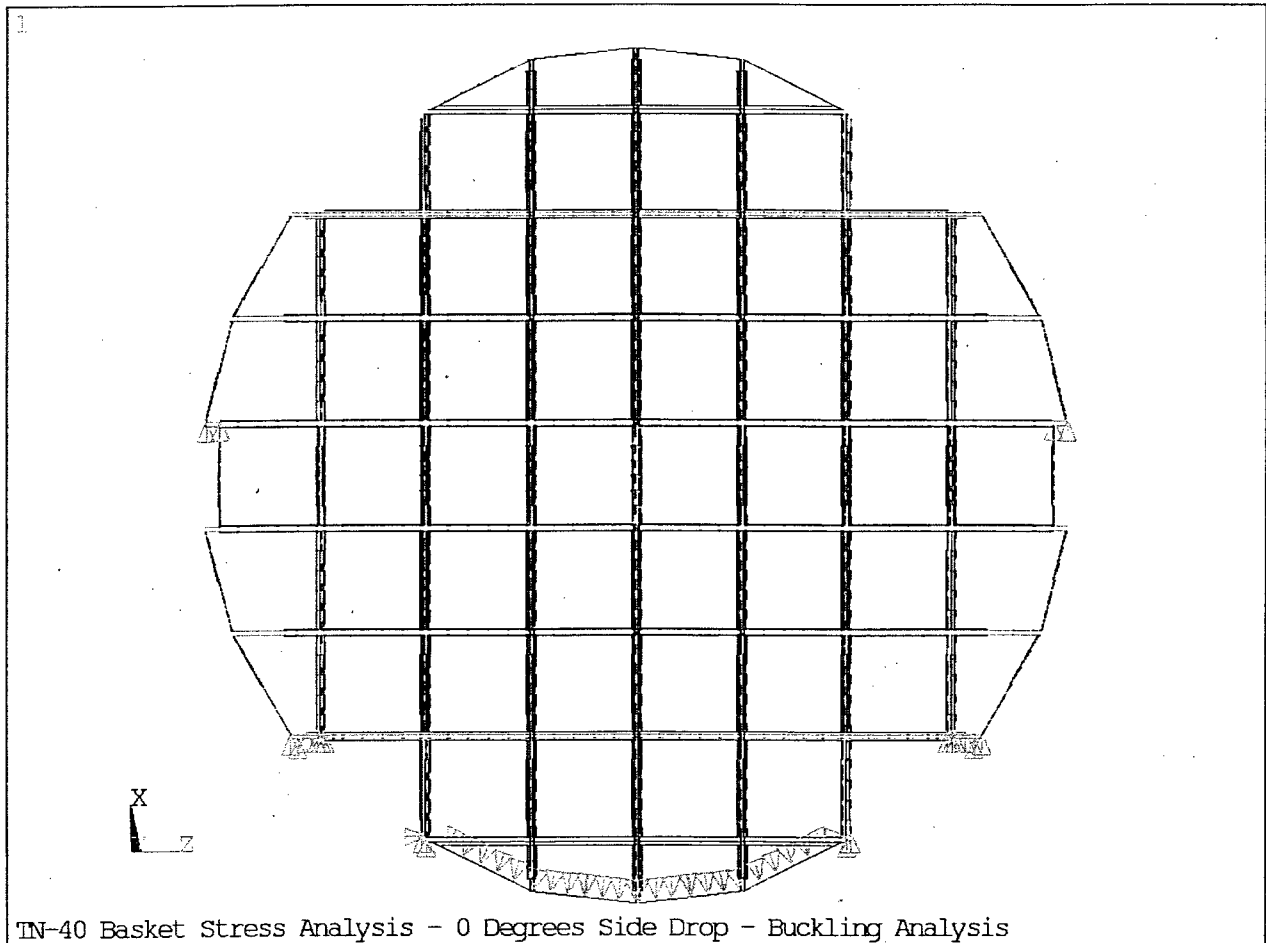


Figure 2.10.5-3
Basket Finite Element Model Displacement Constraints – 0° Side Drop

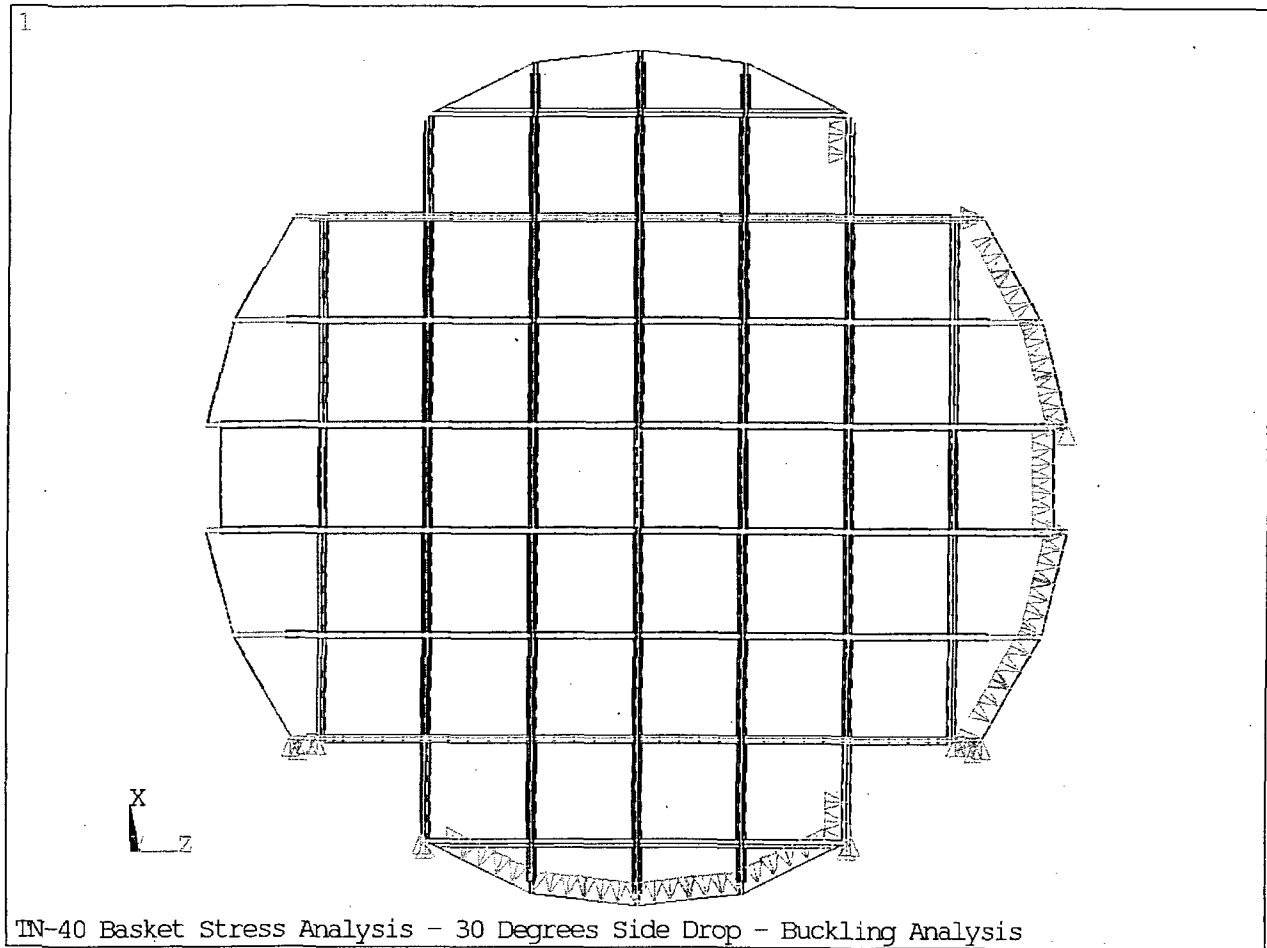


Figure 2.10.5-4
Basket Finite Element Model Displacement Constraints – 30° Side Drop

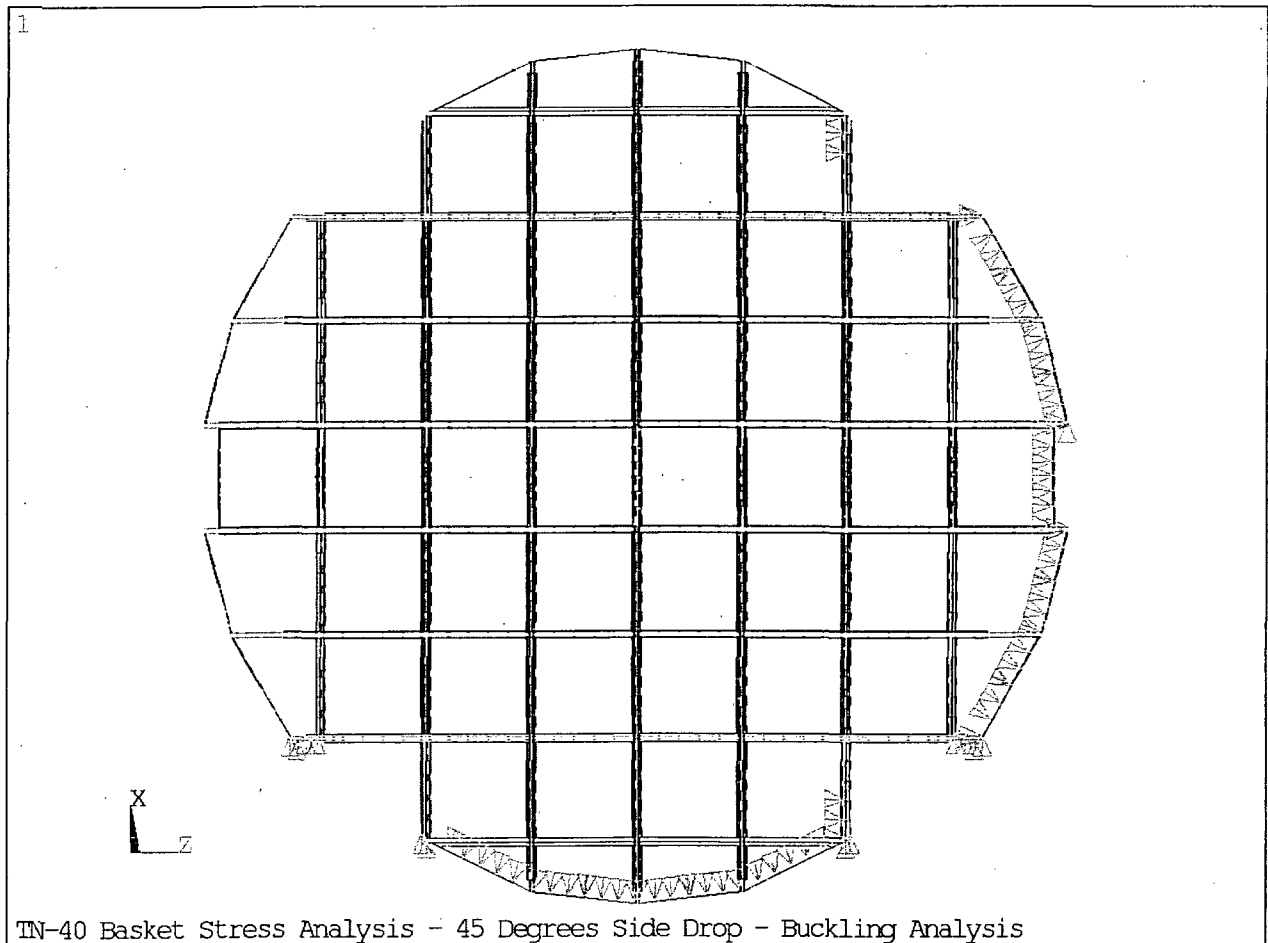


Figure 2.10.5-5
Basket Finite Element Model Displacement Constraints – 45° Side Drop

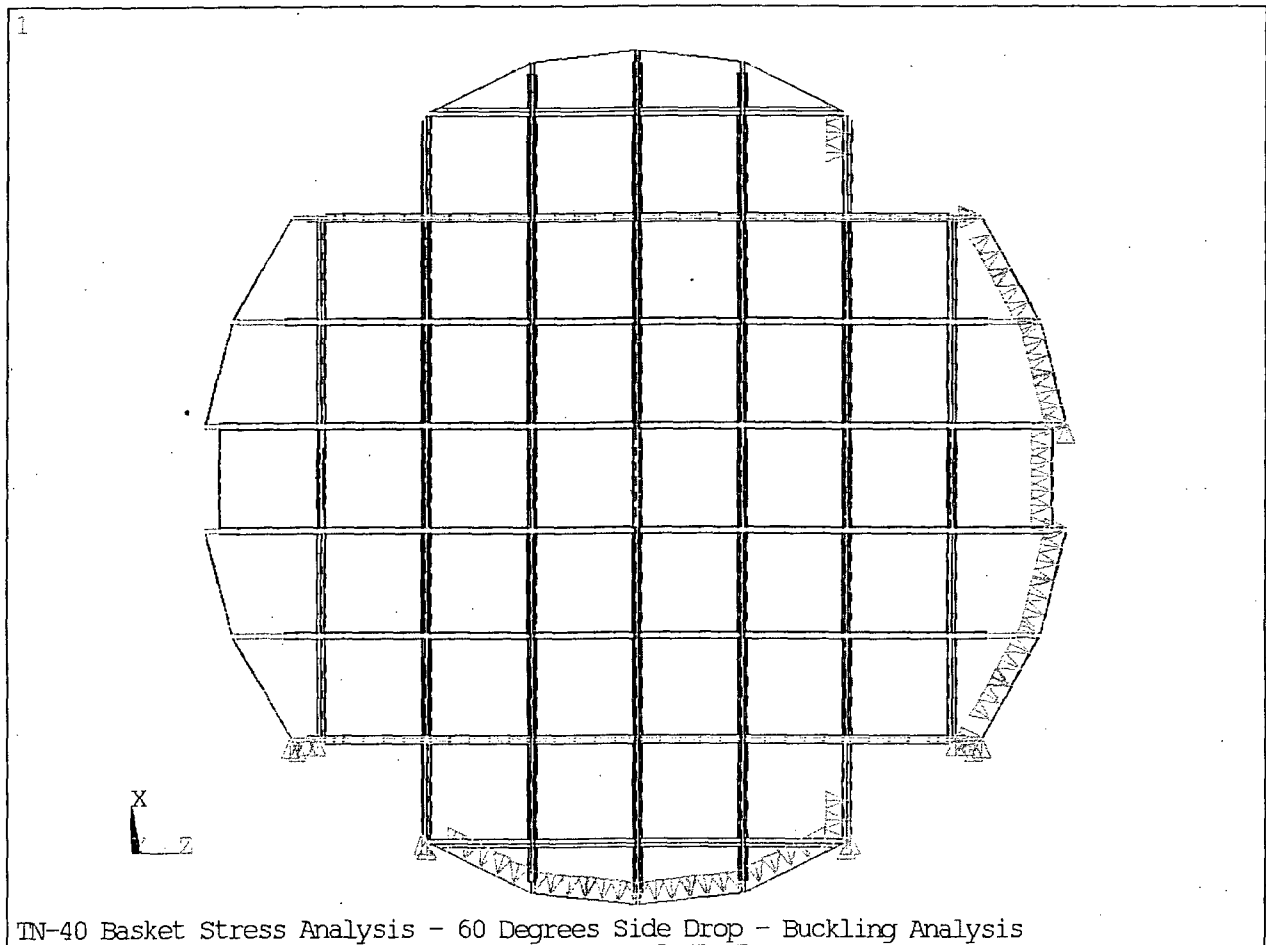


Figure 2.10.5-6
Basket Finite Element Model Displacement Constraints – 60° Side Drop

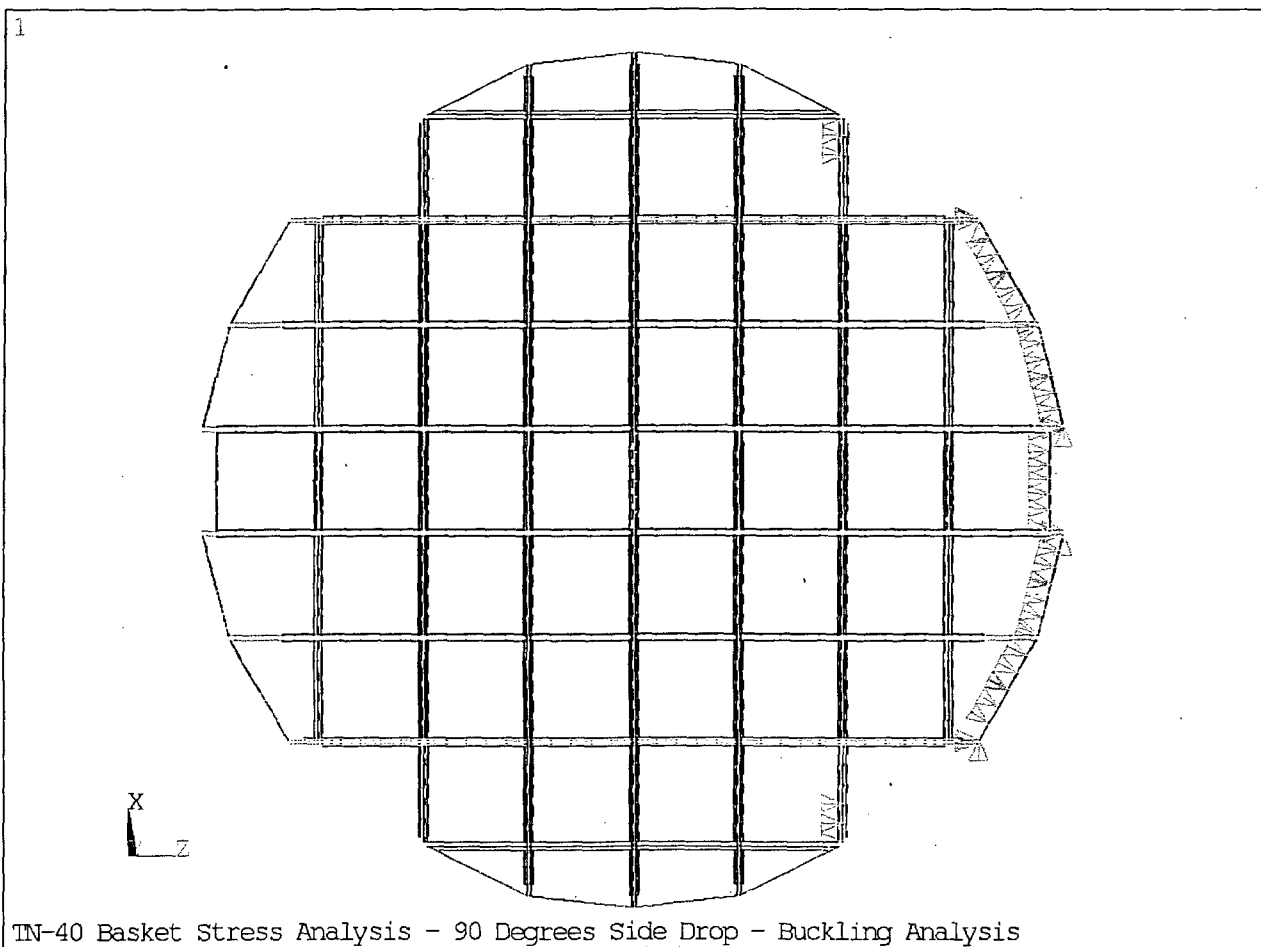


Figure 2.10.5-7
Basket Finite Element Model Displacement Constraints – 90° Side Drop

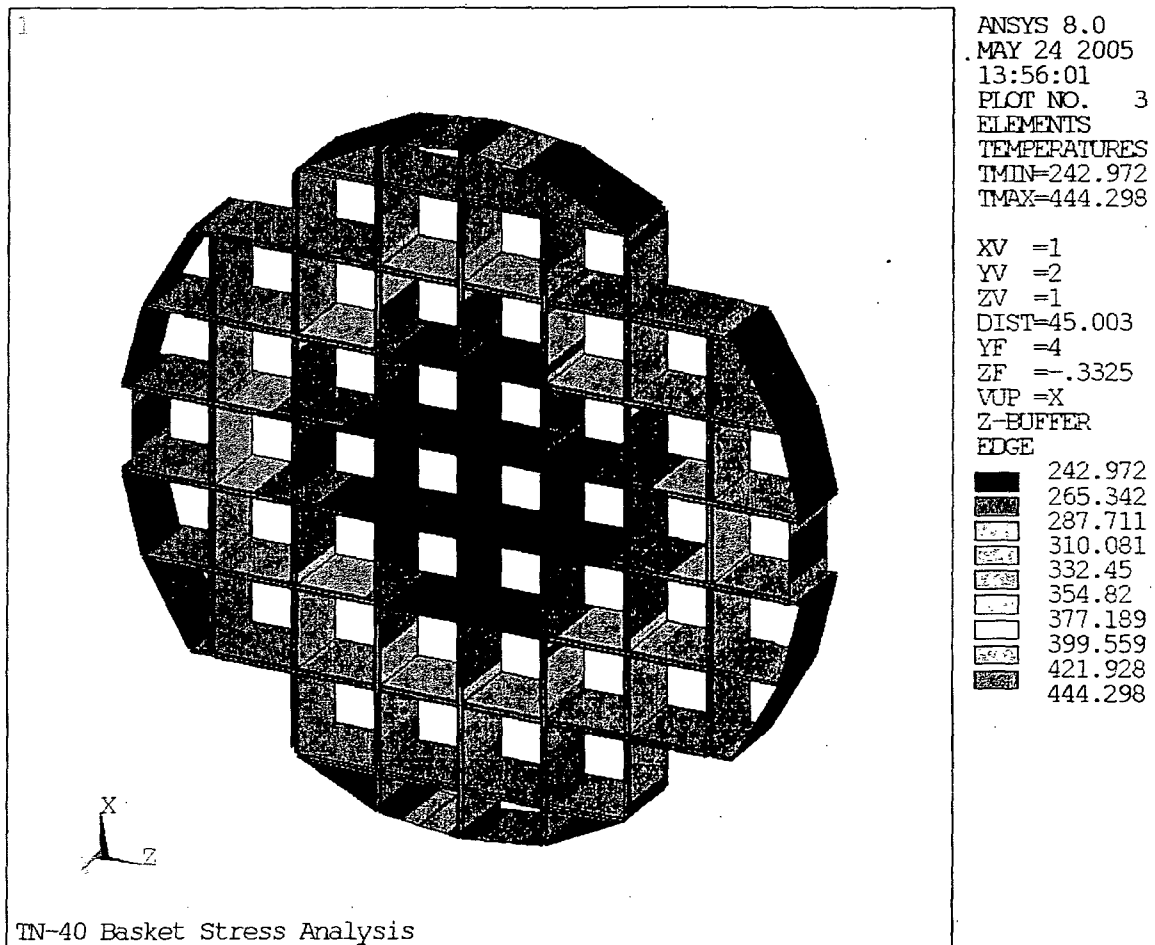


Figure 2.10.5-8
Basket Finite Element Model Temperature Boundary Condition

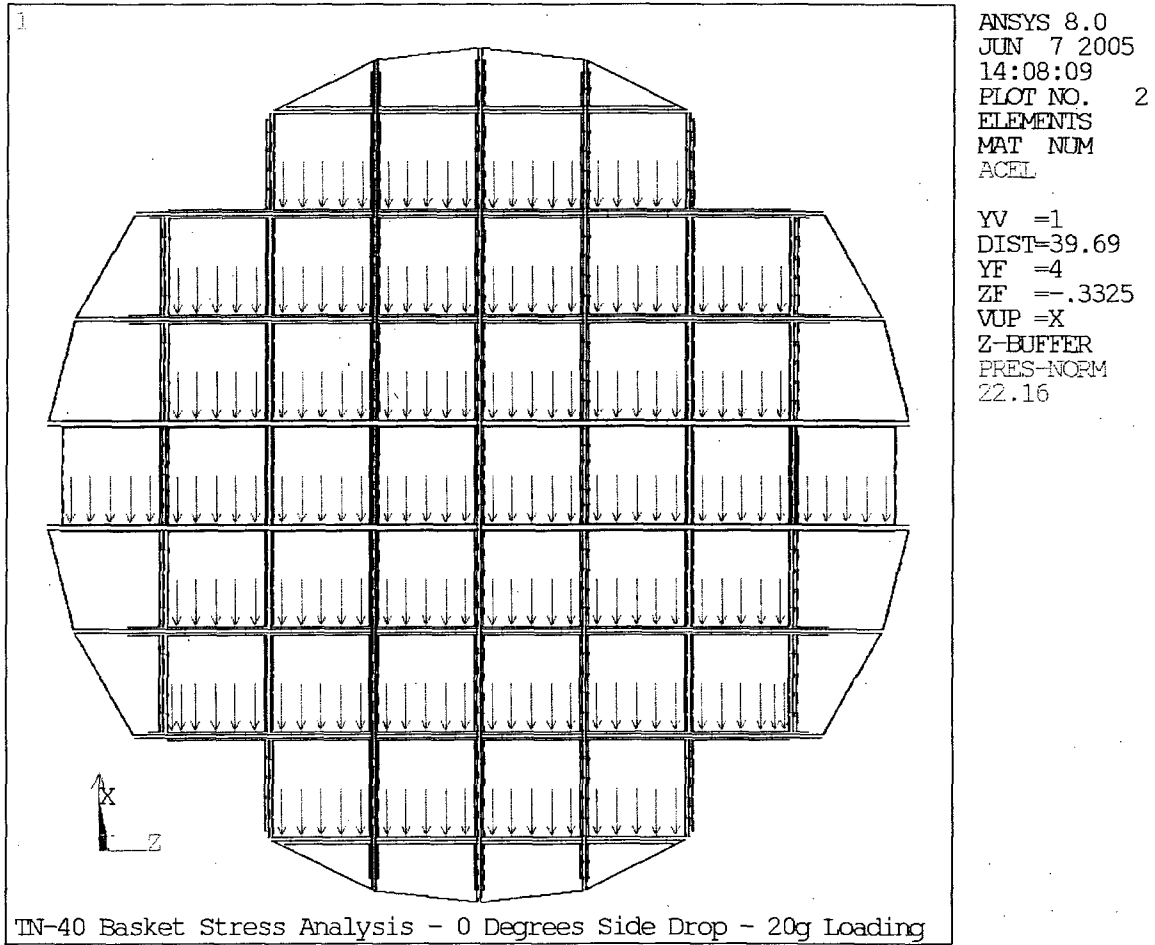


Figure 2.10.5-9
Basket Finite Element Model Applied Pressures – 0° Drop, NCT

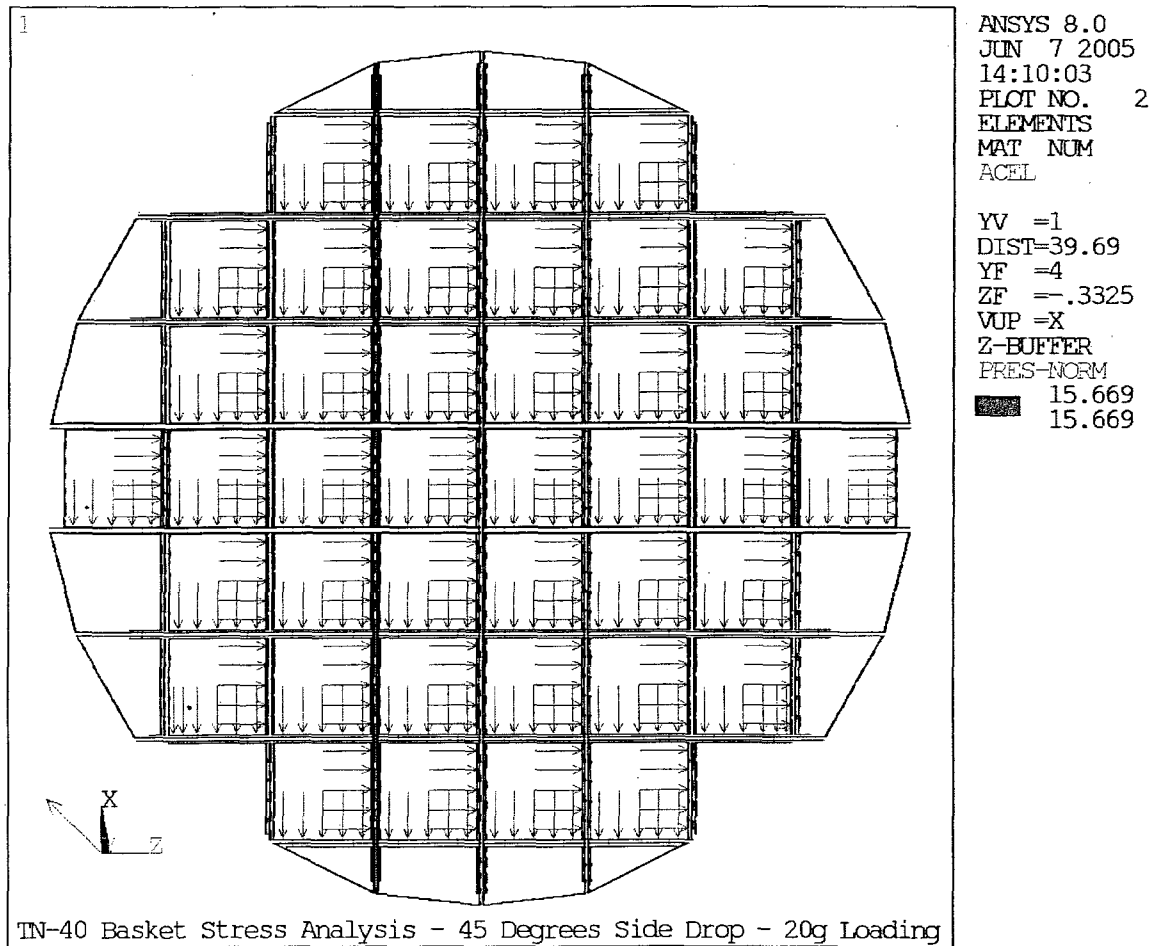


Figure 2.10.5-10
Basket Finite Element Model Applied Pressures - 45° Drop, NCT

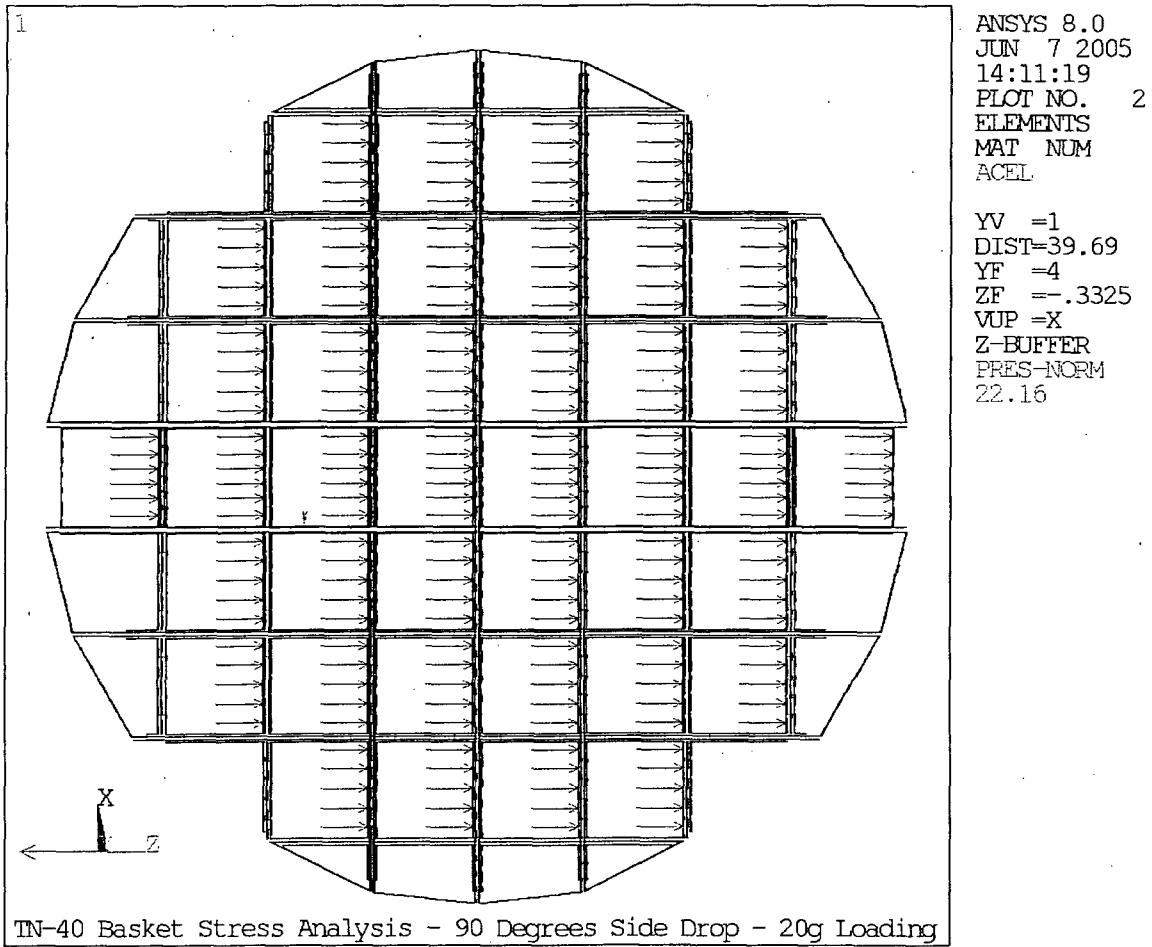


Figure 2.10.5-11
Basket Finite Element Model Applied Pressures – 90° Drop, NCT

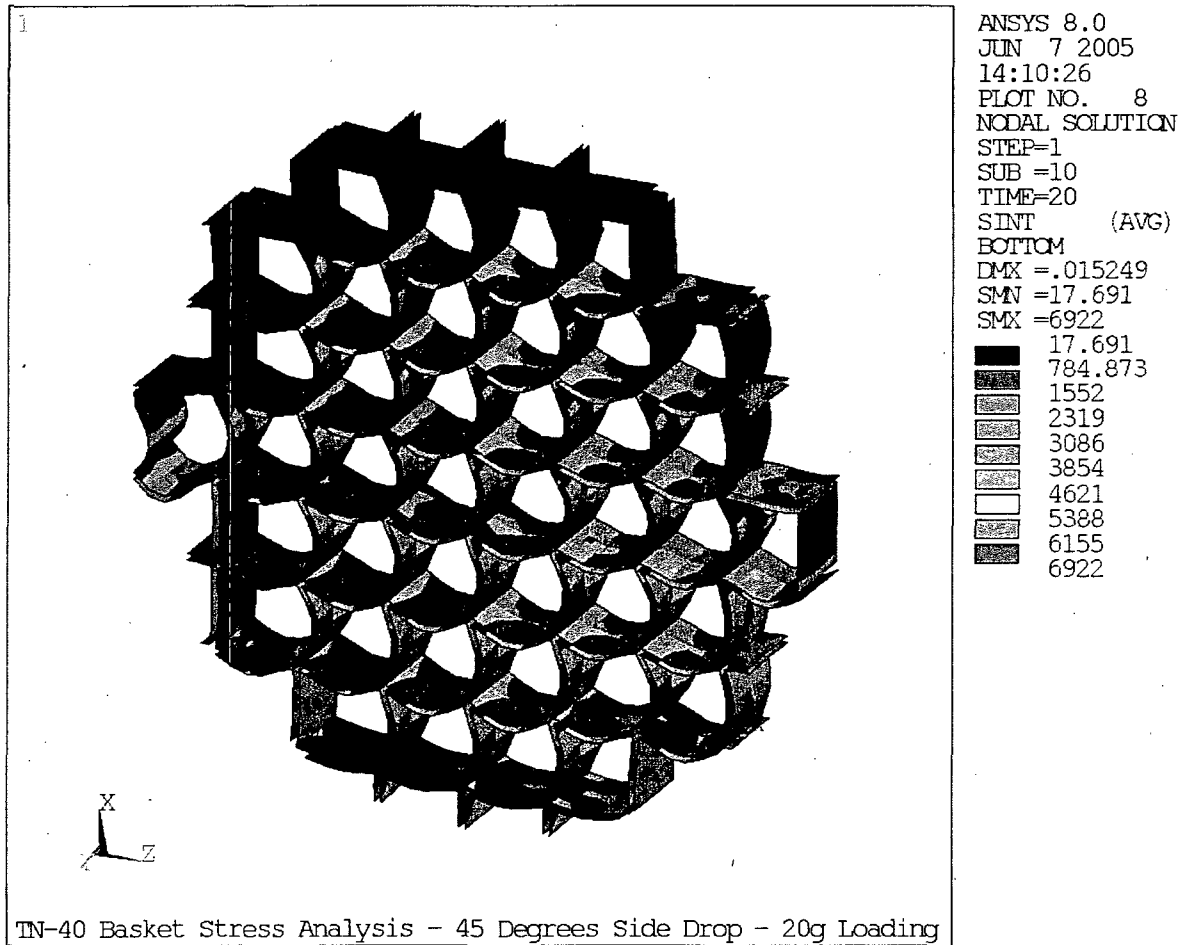


Figure 2.10.5-12
NCT 45° Side Drop - S.S. Plates - Membrane plus Bending Stress Intensity

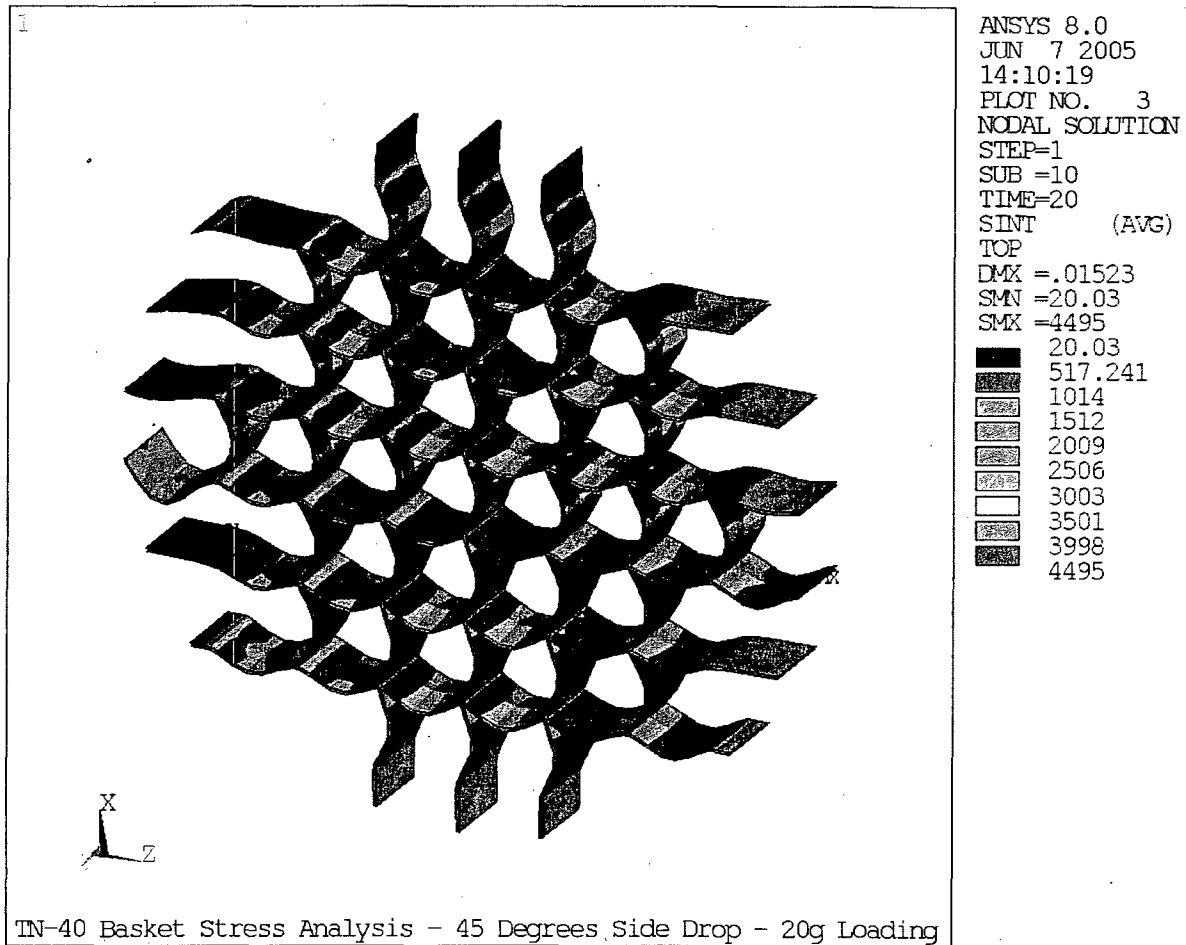


Figure 2.10.5-13
NCT 45° Side Drop – Al. Plates - Membrane plus Bending Stress Intensity

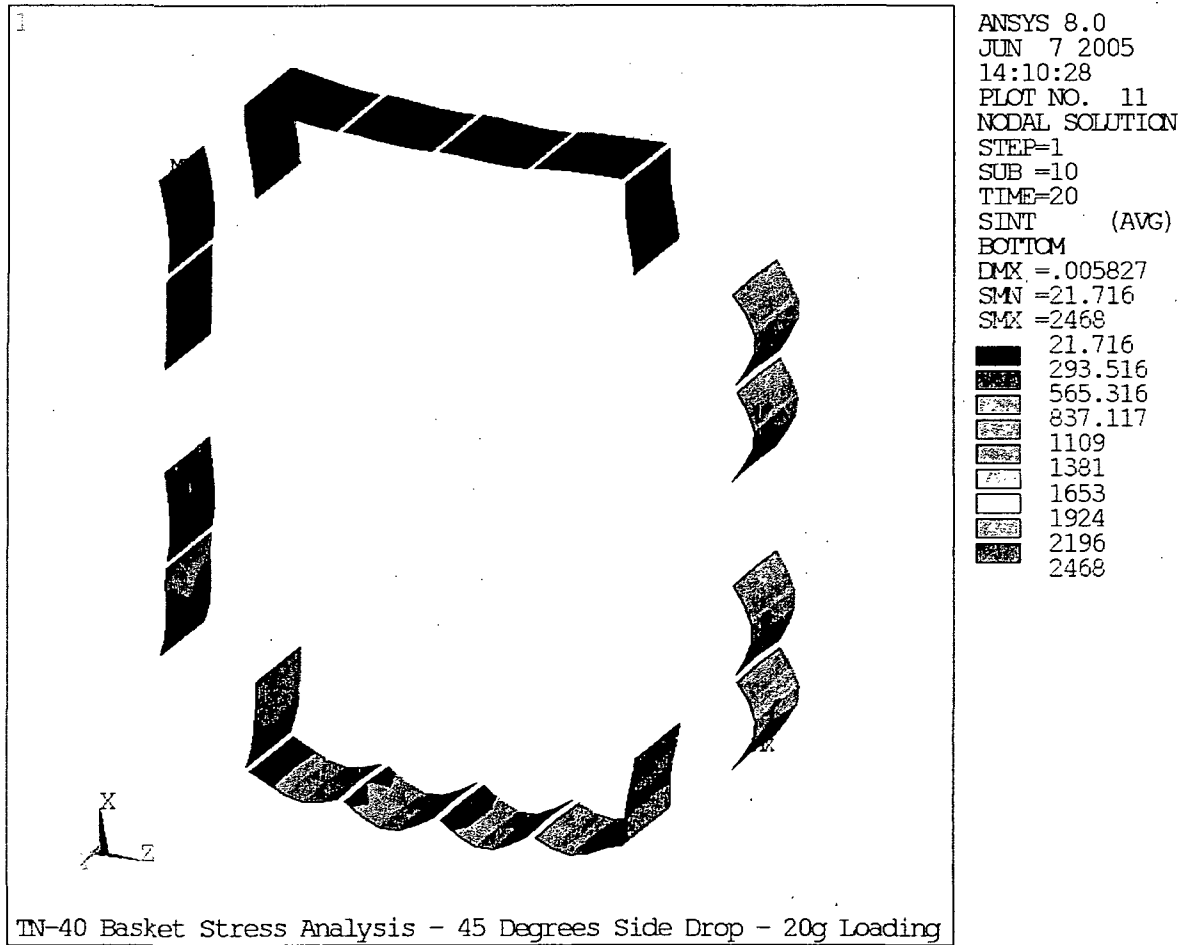


Figure 2.10.5-14
NCT 45° Side Drop – Al. Periphery Plates -
Membrane plus Bending Stress Intensity

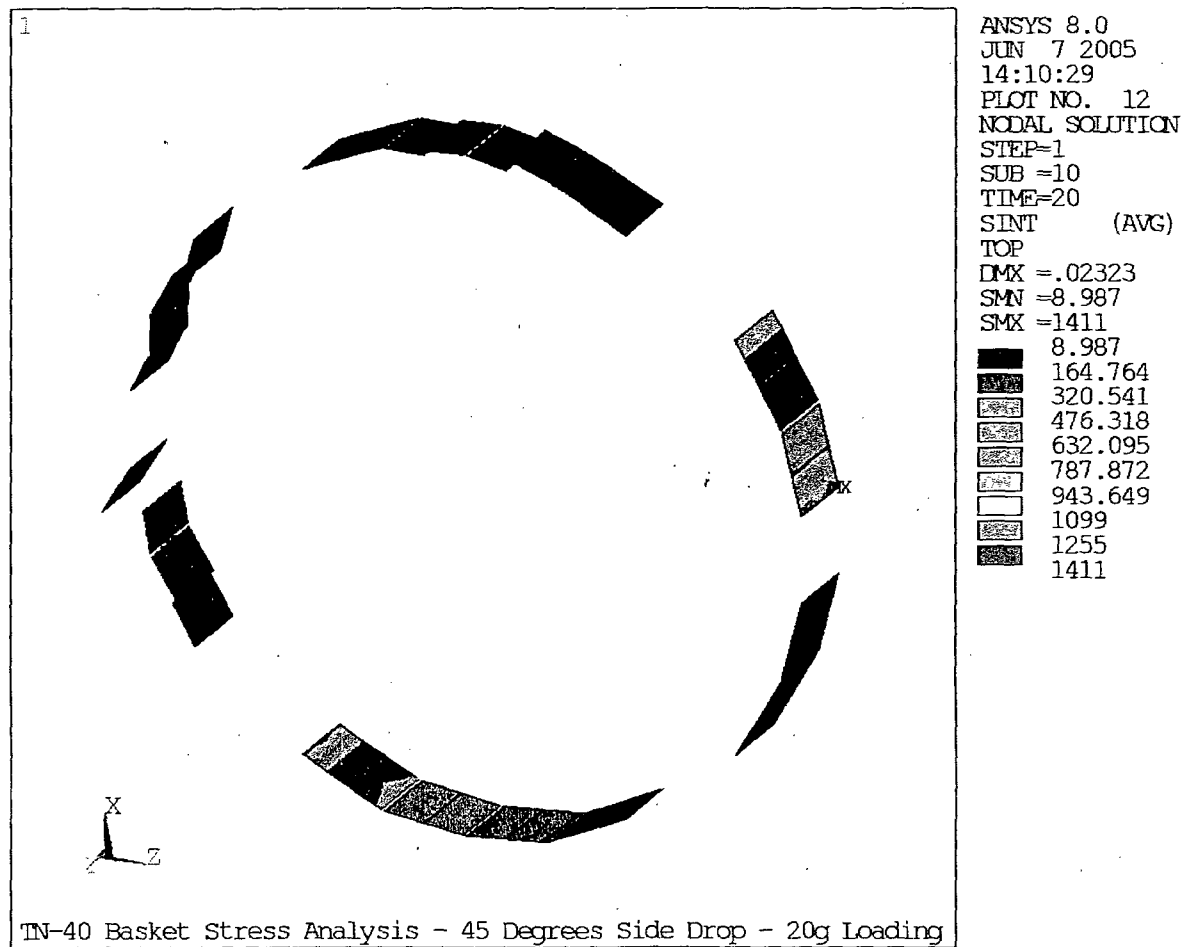


Figure 2.10.5-15
NCT 45° Side Drop – Al. Outer Plates - Membrane plus Bending Stress Intensity

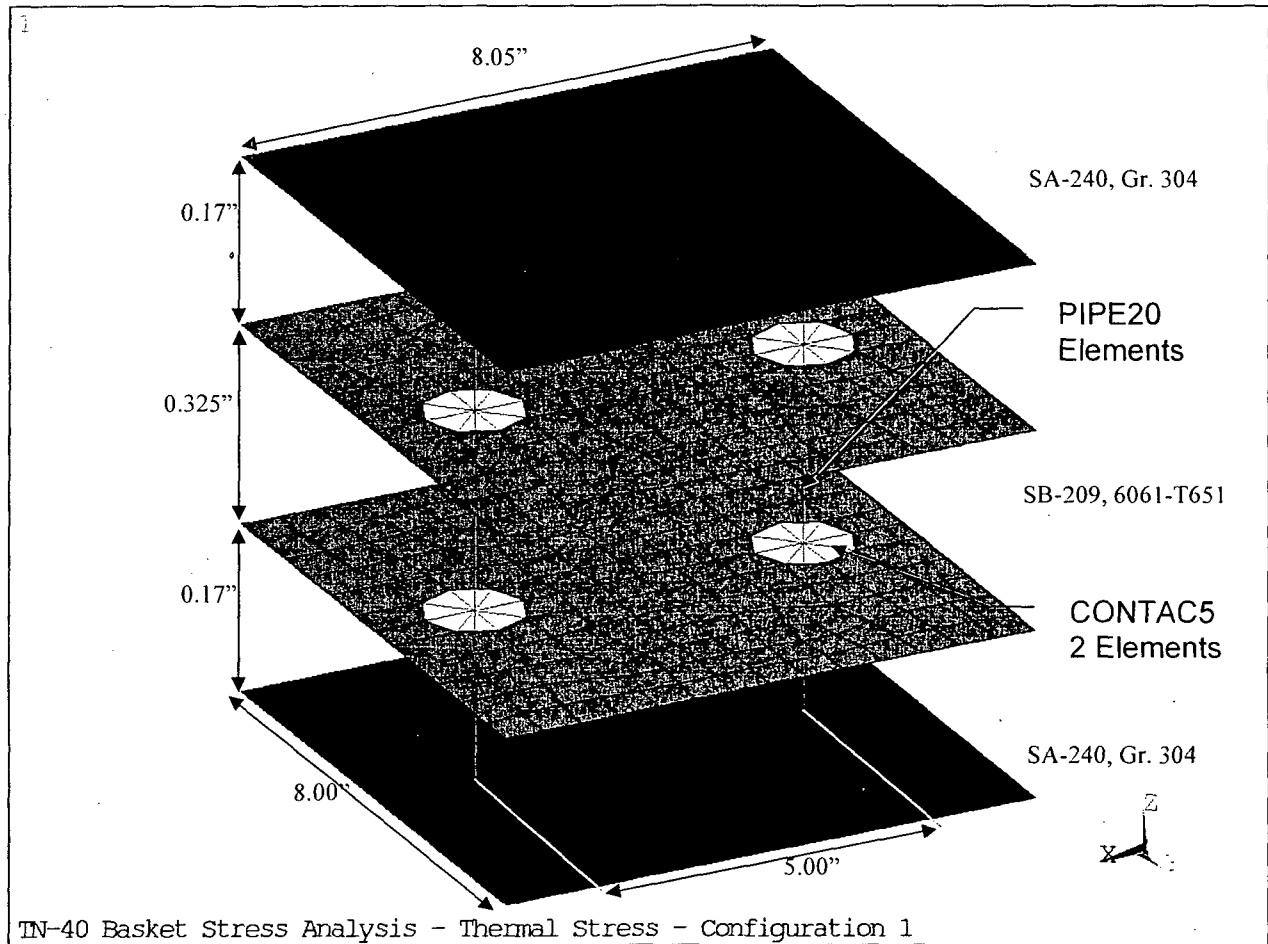


Figure 2.10.5-16
Thermal Stress Analysis Finite Element Model - Configuration 1

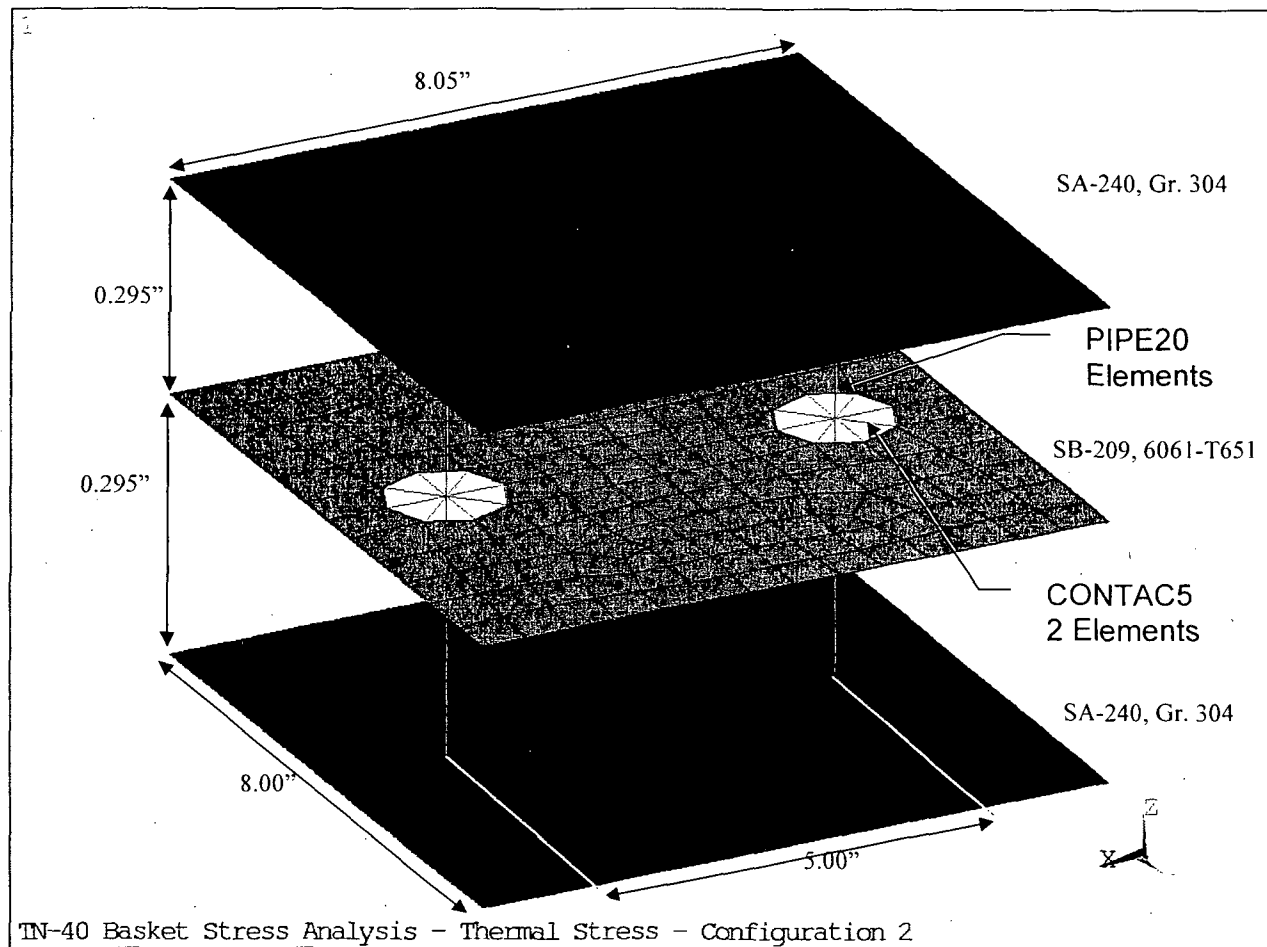


Figure 2.10.5-17
Thermal Stress Analysis Finite Element Model - Configuration 2

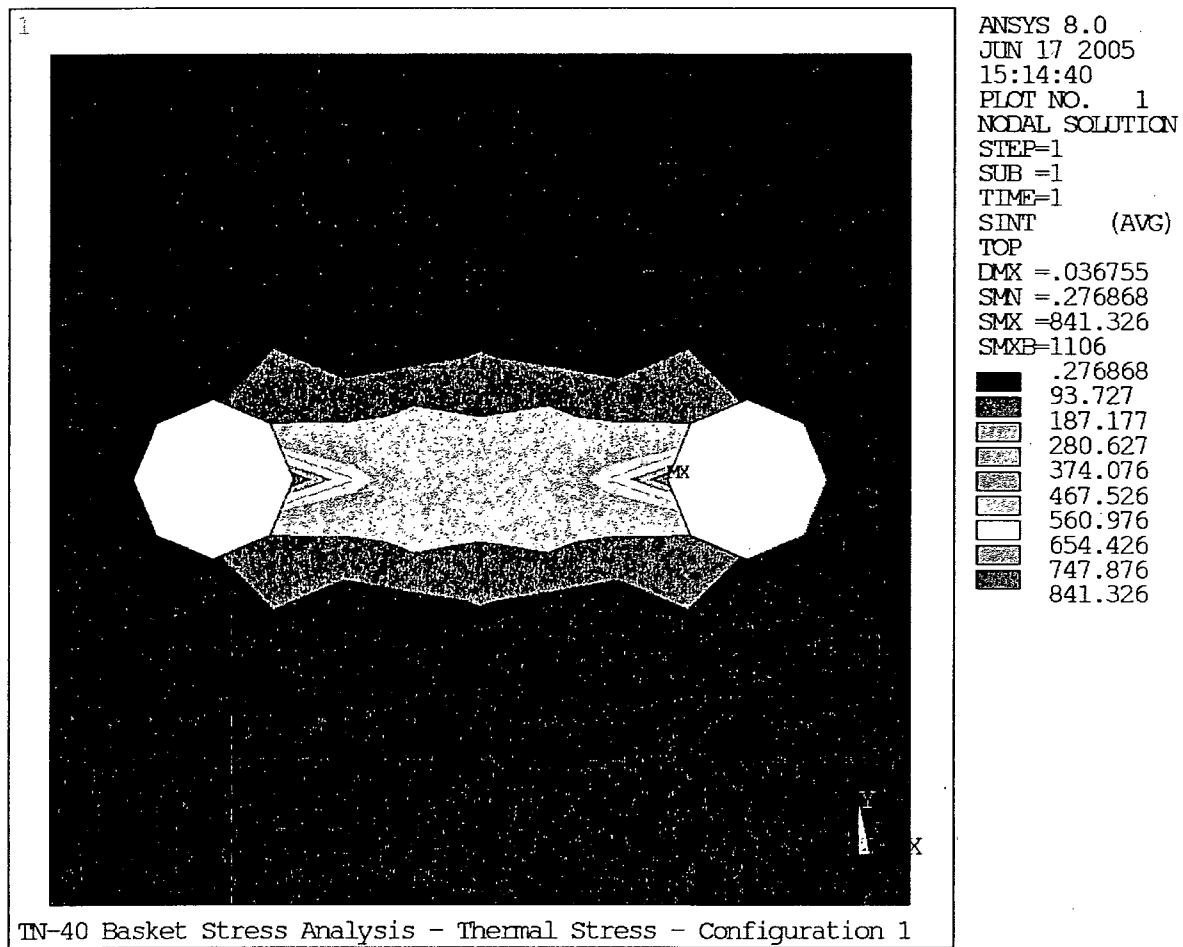


Figure 2.10.5-18
Thermal Stress Analysis - Configuration 1 - Maximum Aluminum Stress Intensity

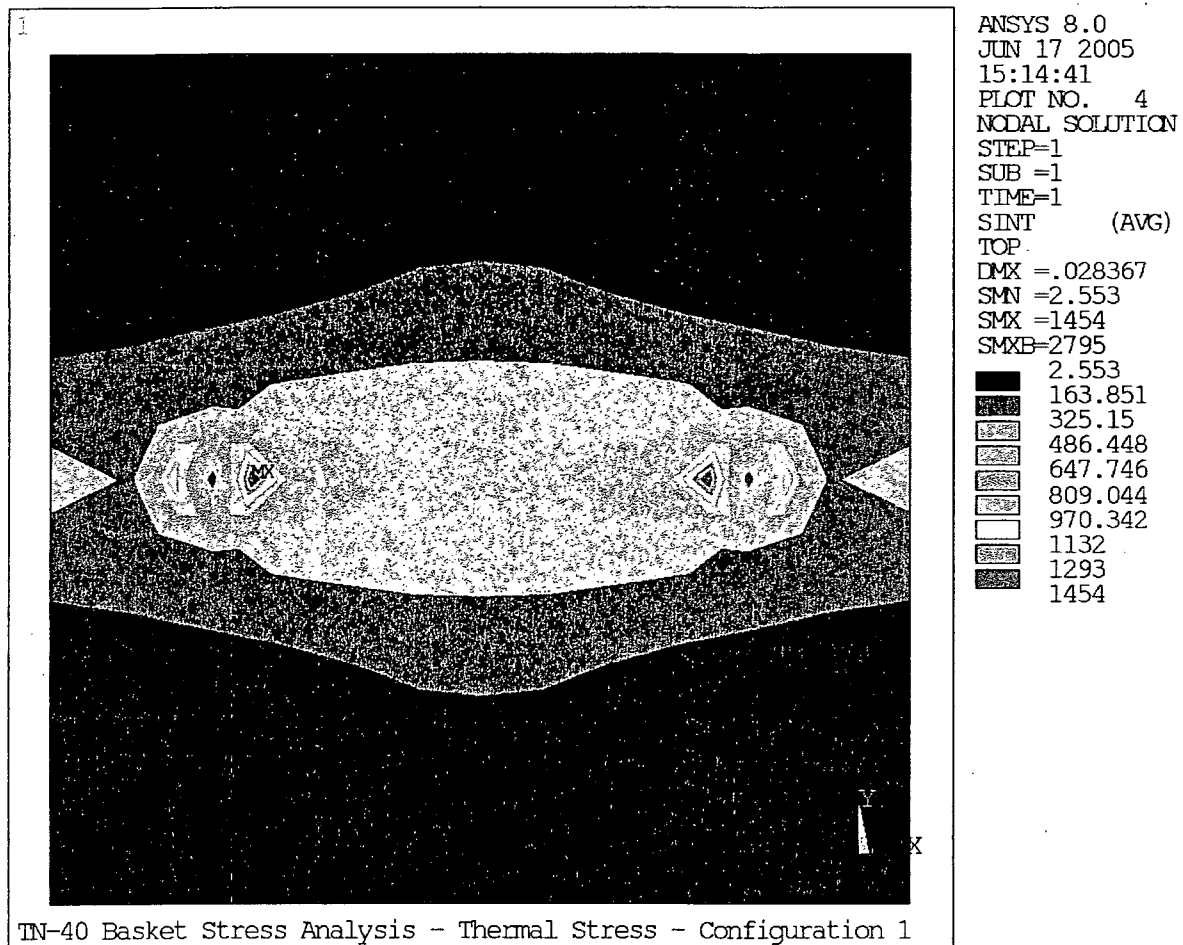


Figure 2.10.5-19
Thermal Stress Analysis - Configuration 1 -
Maximum Stainless Steel Stress Intensity

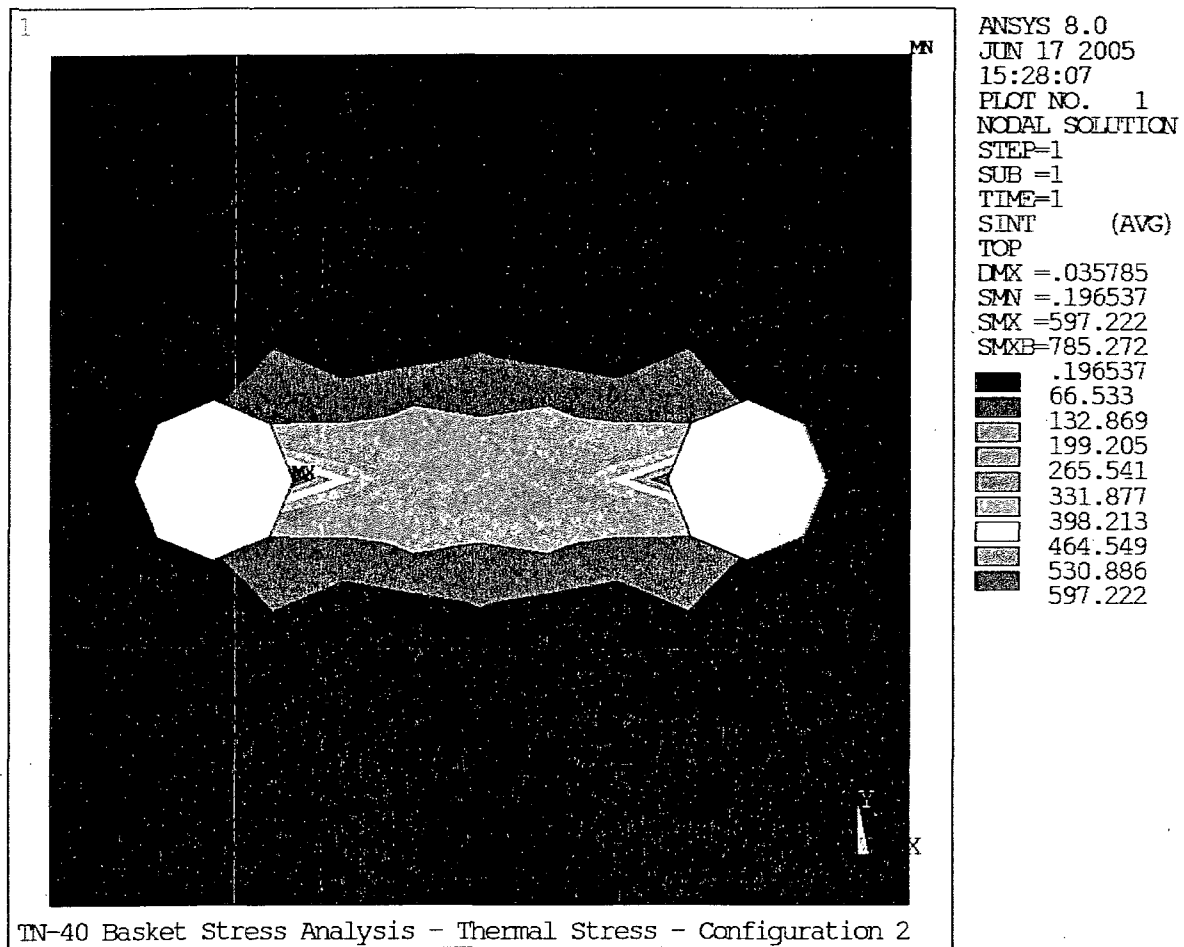


Figure 2.10.5-20
Thermal Stress Analysis - Configuration 2 - Maximum Aluminum Stress Intensity

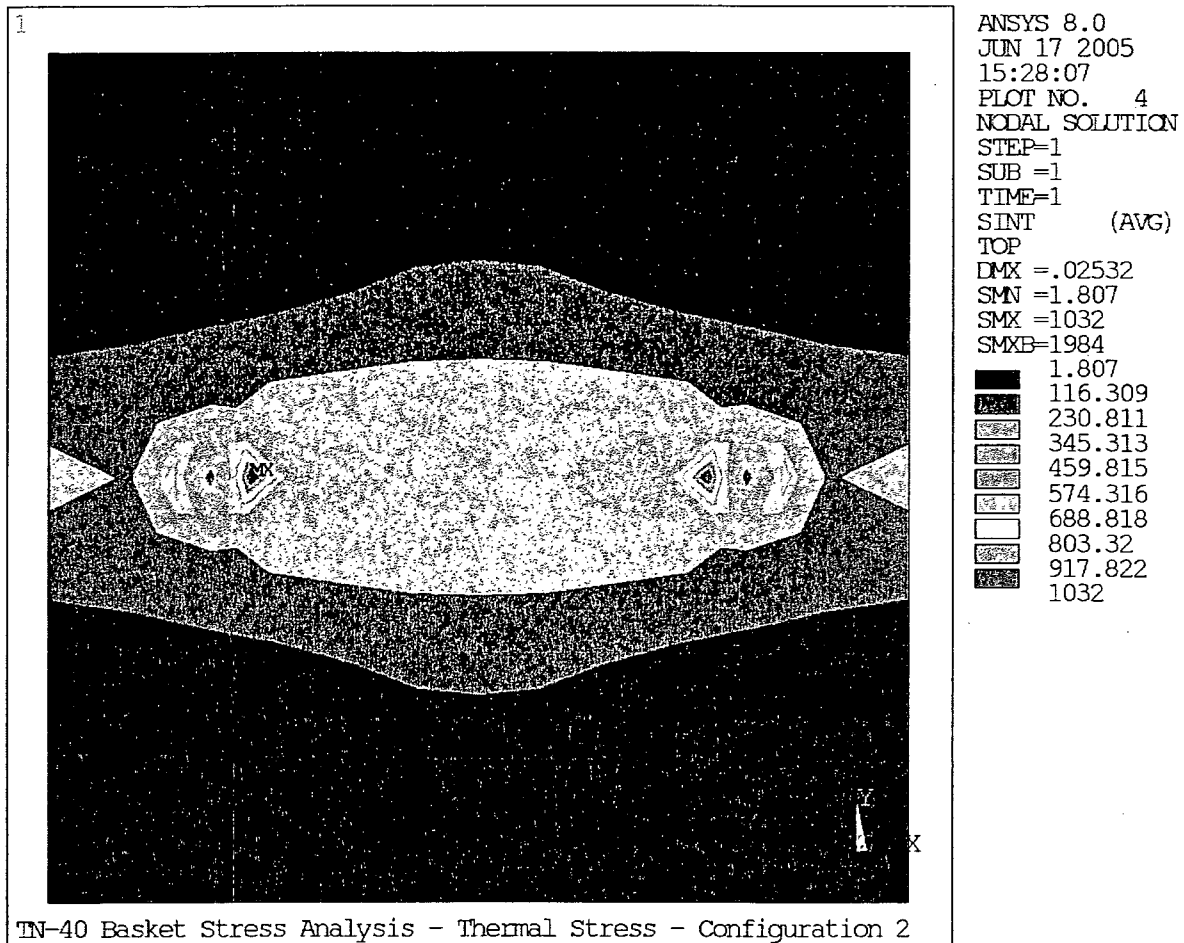


Figure 2.10.5-21
Thermal Stress Analysis - Configuration 2 -
Maximum Stainless Steel Stress Intensity

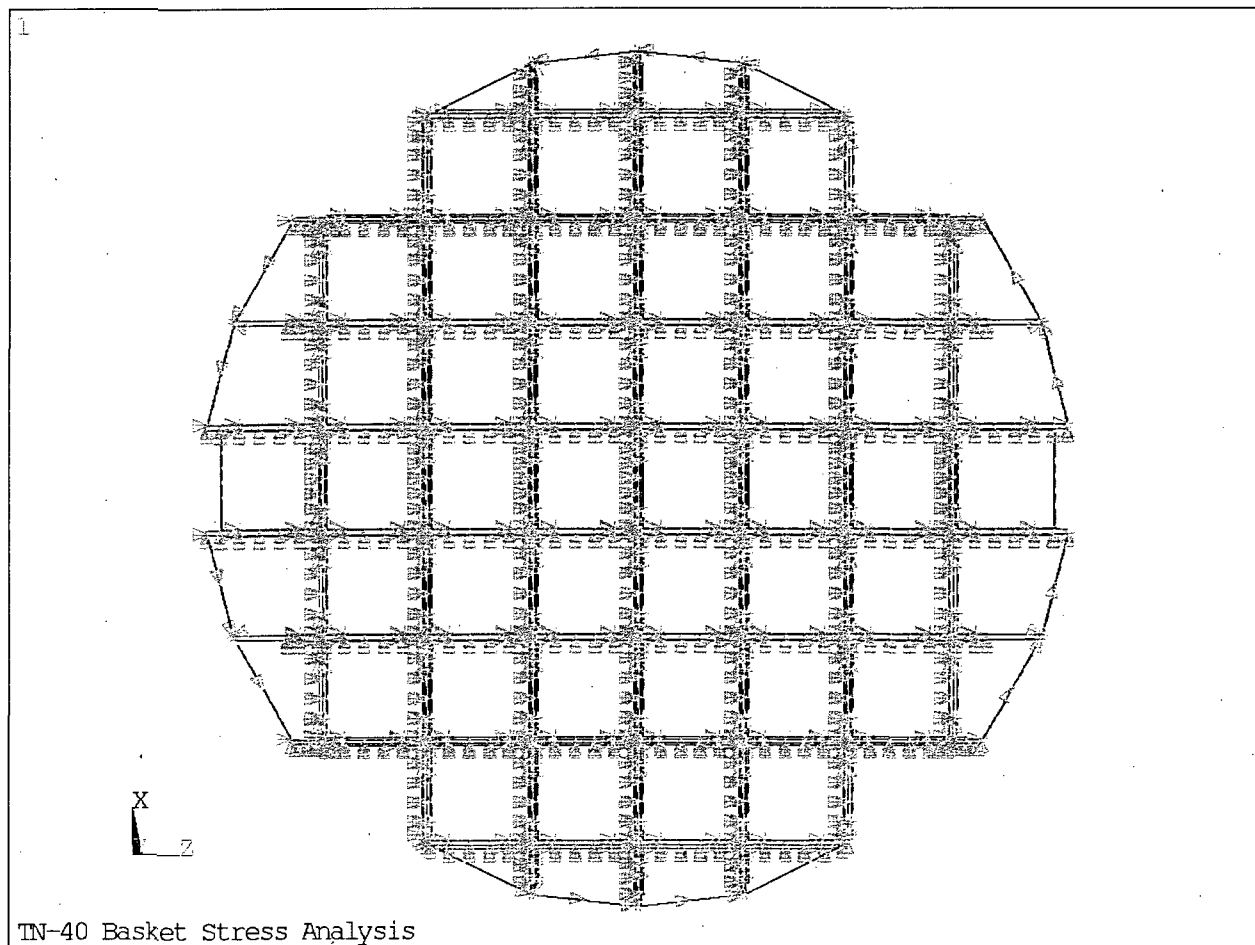


Figure 2.10.5-22
Fuel Basket Buckling Analysis Finite Element Model Node Couplings

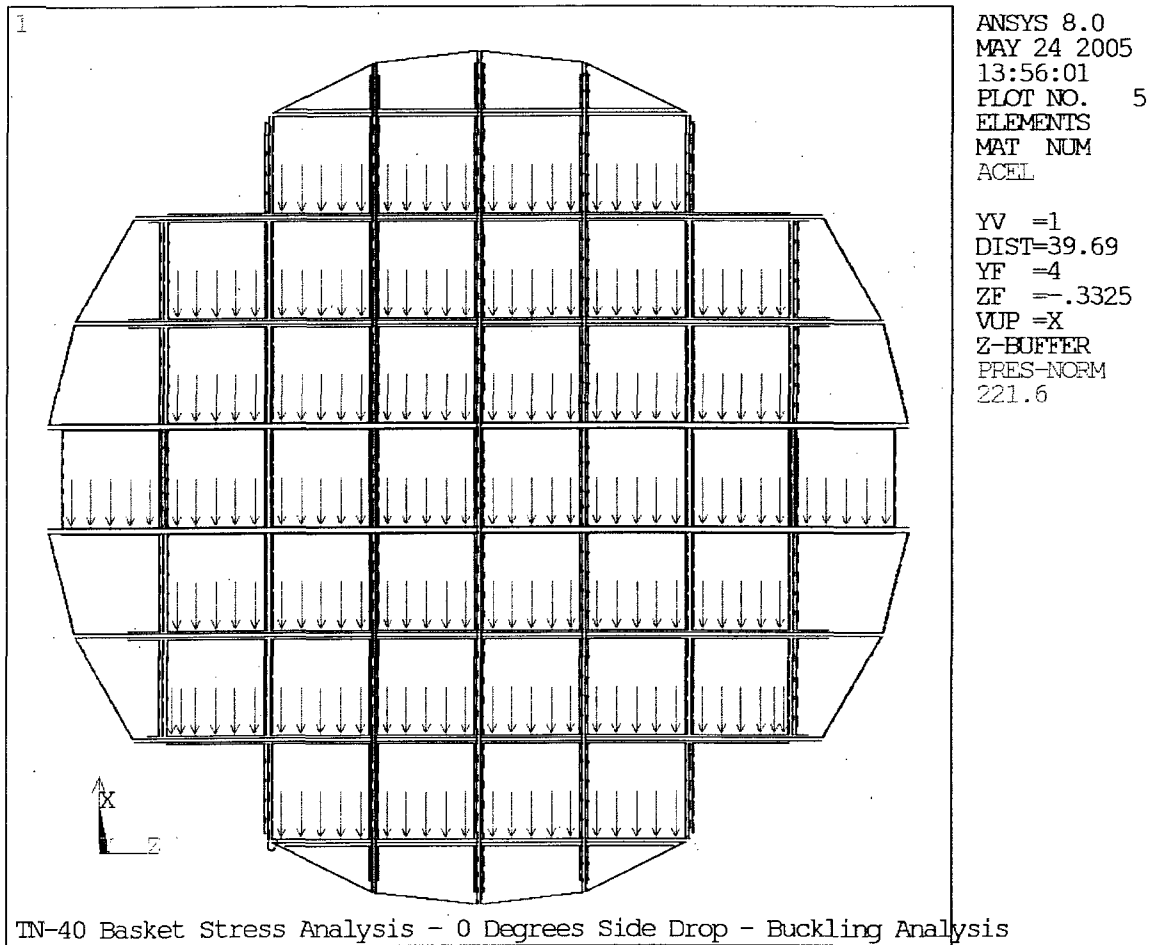


Figure 2.10.5-23
Basket Buckling Analysis Loading Boundary Conditions – 0° Side Drop

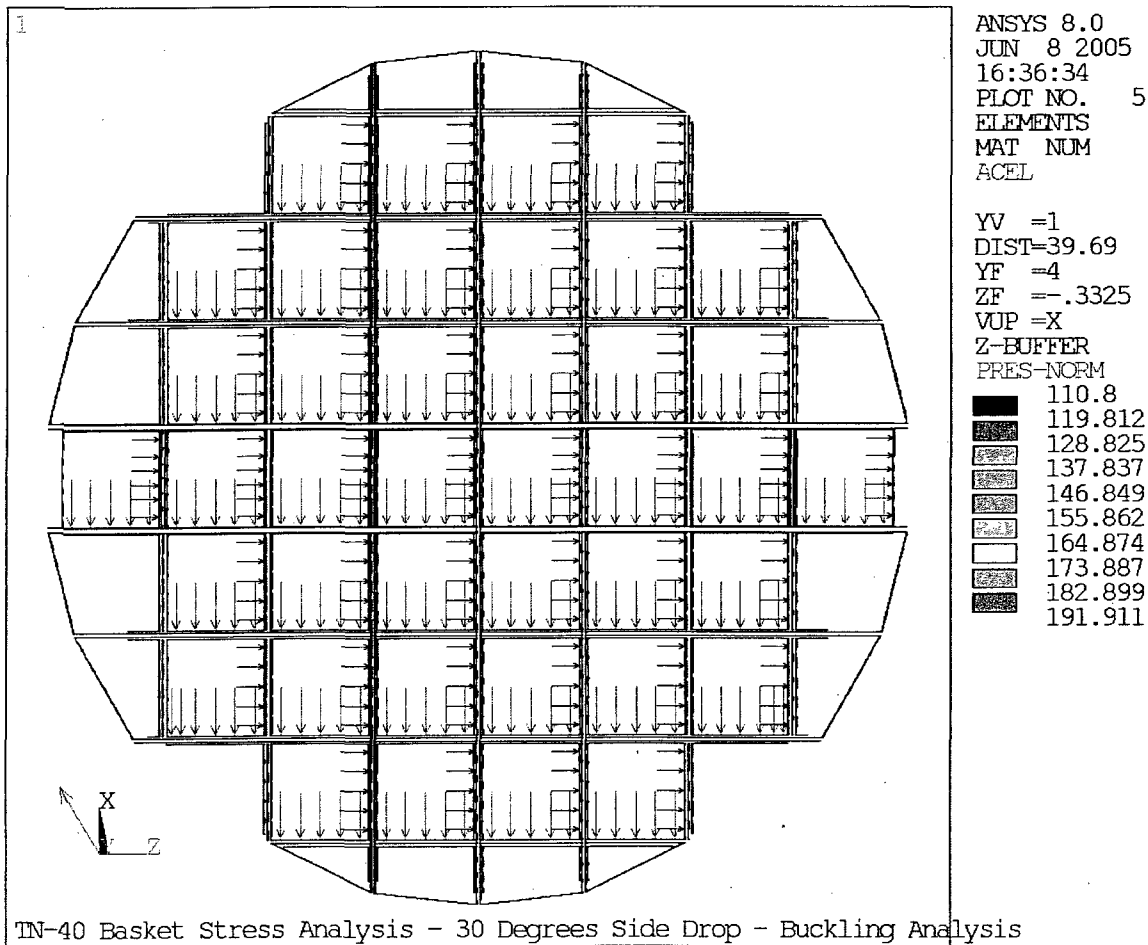


Figure 2.10.5-24
Basket Buckling Analysis Loading Boundary Conditions – 30° Side Drop

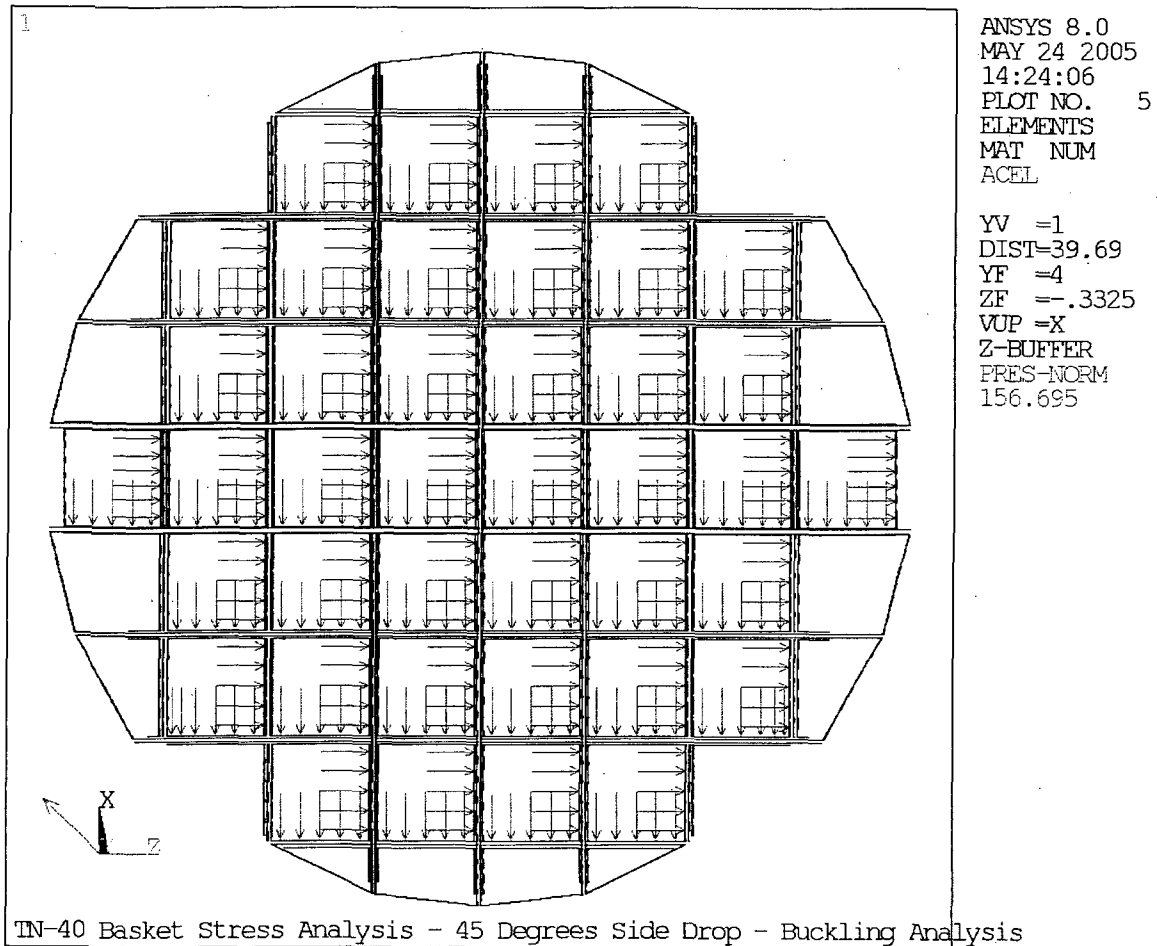


Figure 2.10.5-25
Basket Buckling Analysis Loading Boundary Conditions – 45° Side Drop

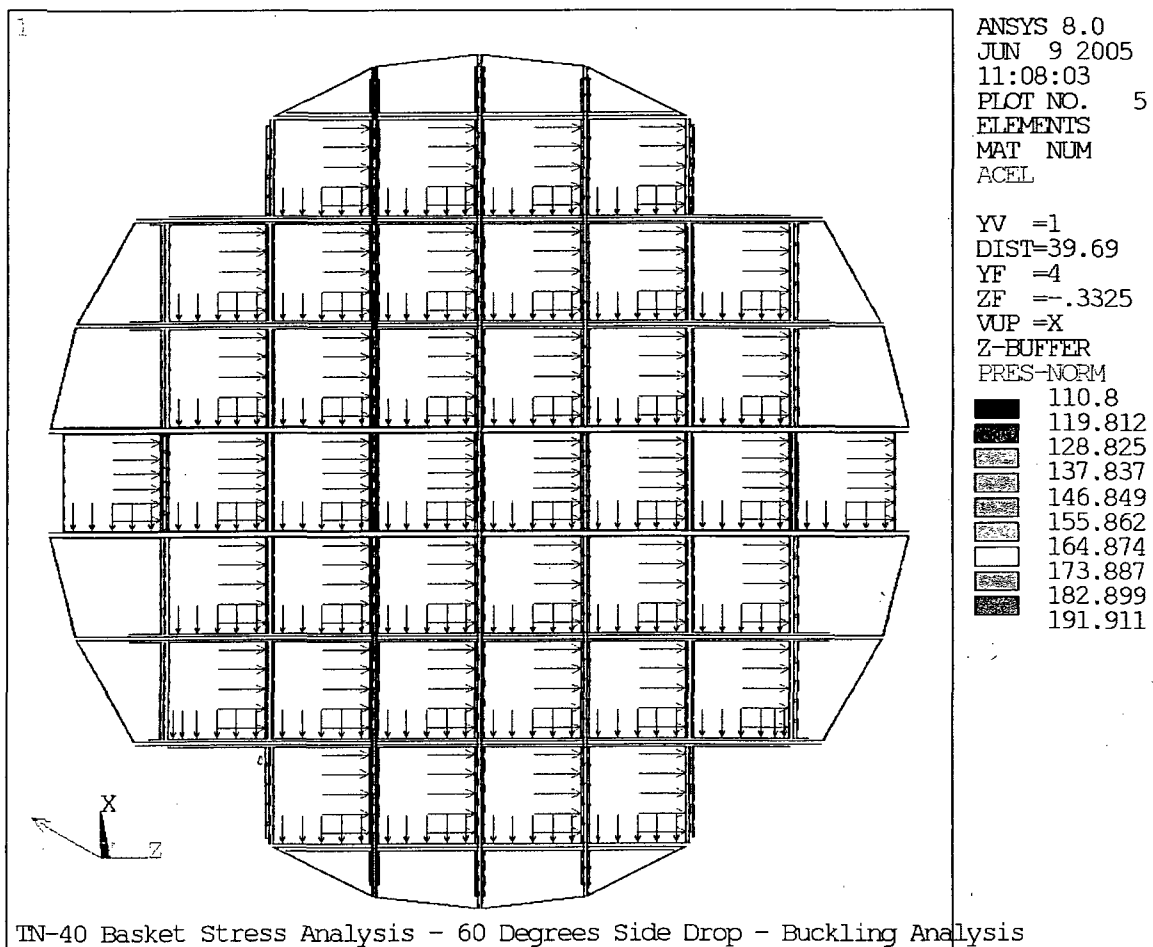


Figure 2.10.5-26
Basket Buckling Analysis Loading Boundary Conditions – 60° Side Drop

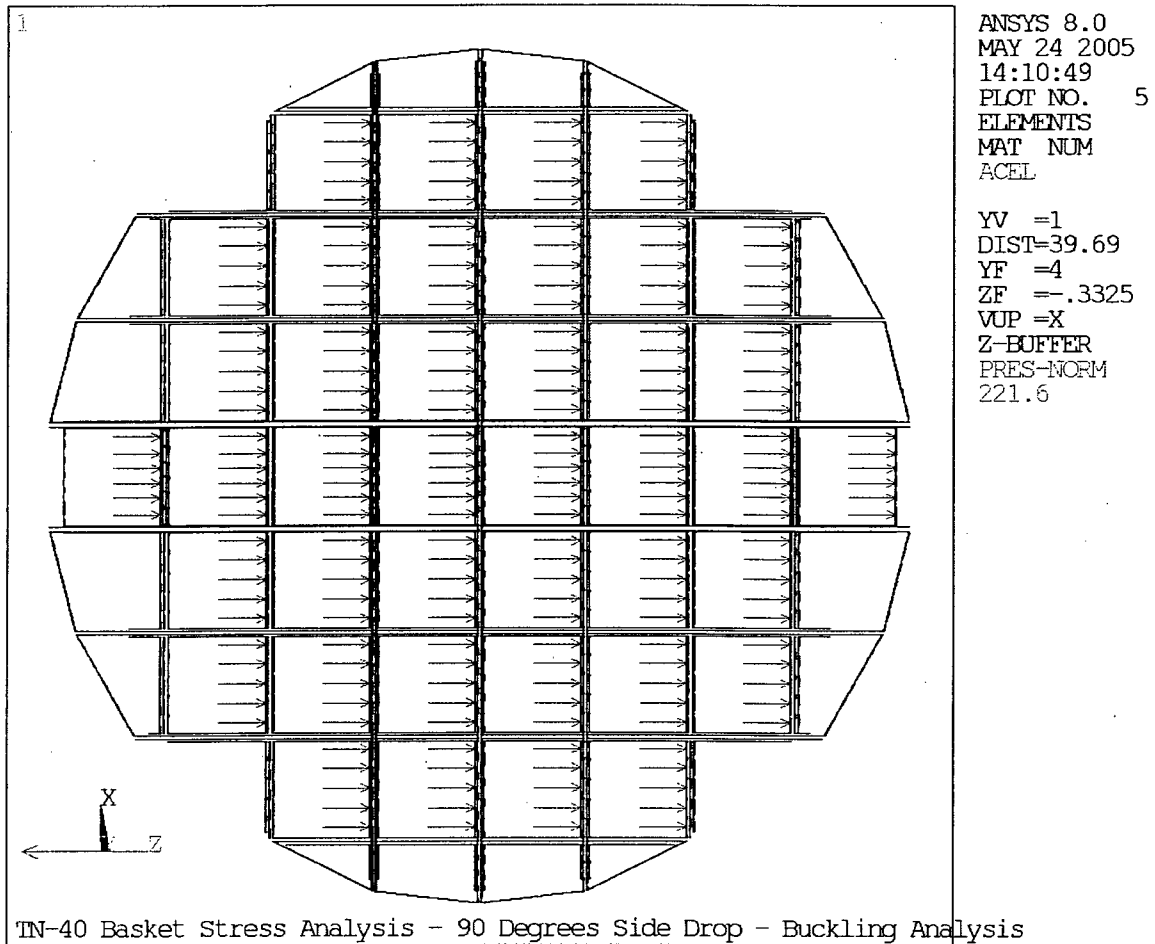


Figure 2.10.5-27
Basket Buckling Analysis Loading Boundary Conditions – 90° Side Drop

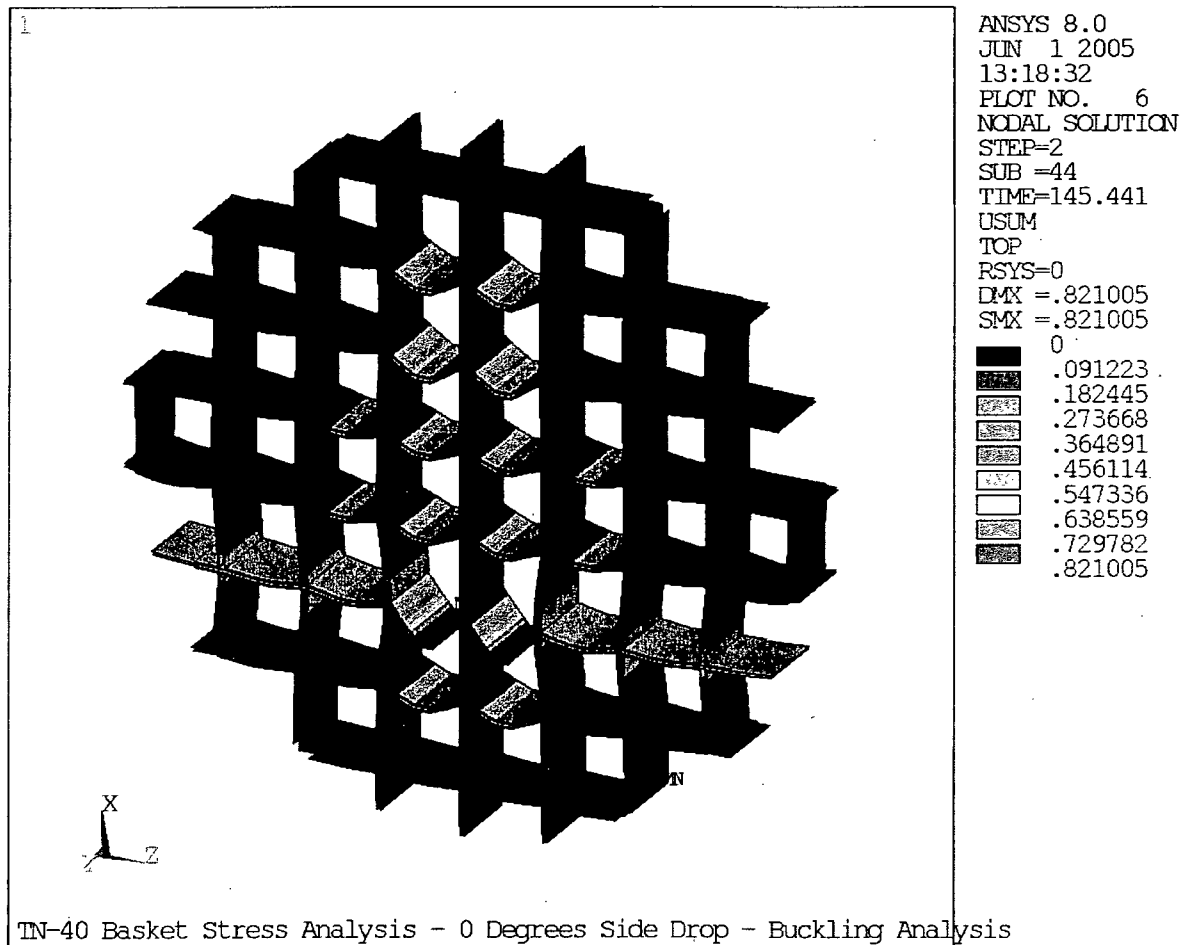


Figure 2.10.5-28
Fuel Basket Deformation at Buckling Load – 0° Side Drop

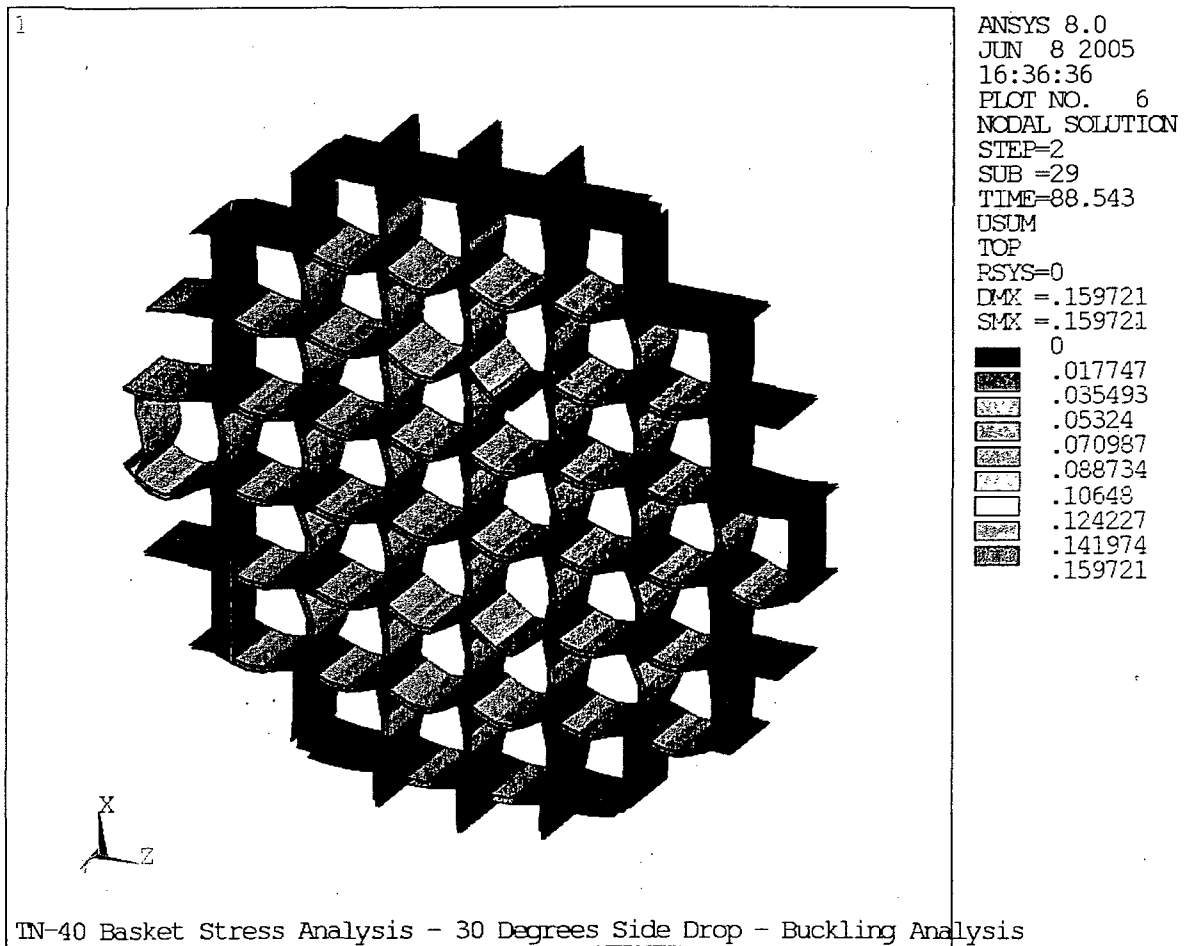


Figure 2.10.5-29
Fuel Basket Deformation at Buckling Load – 30° Side Drop

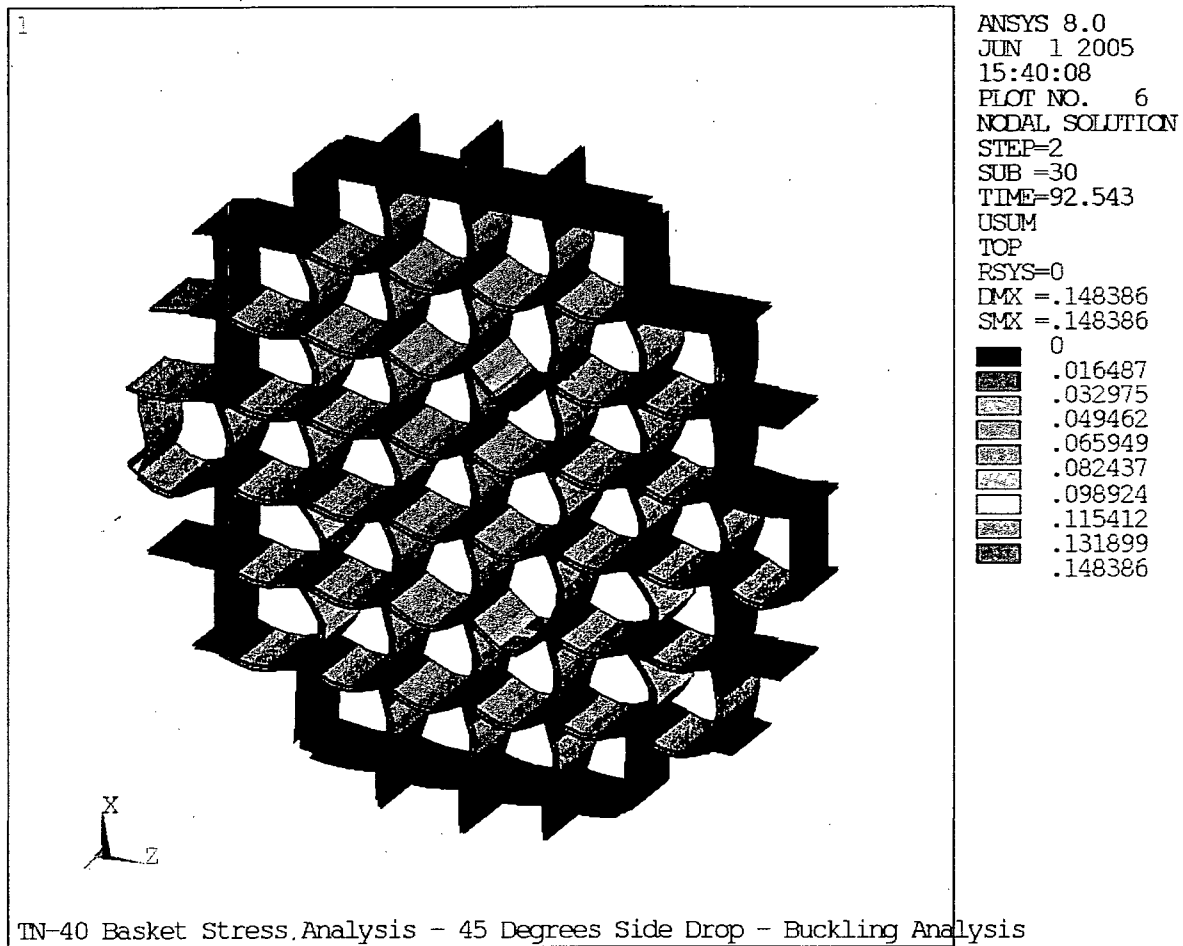


Figure 2.10.5-30
Fuel Basket Deformation at Buckling Load – 45° Side Drop

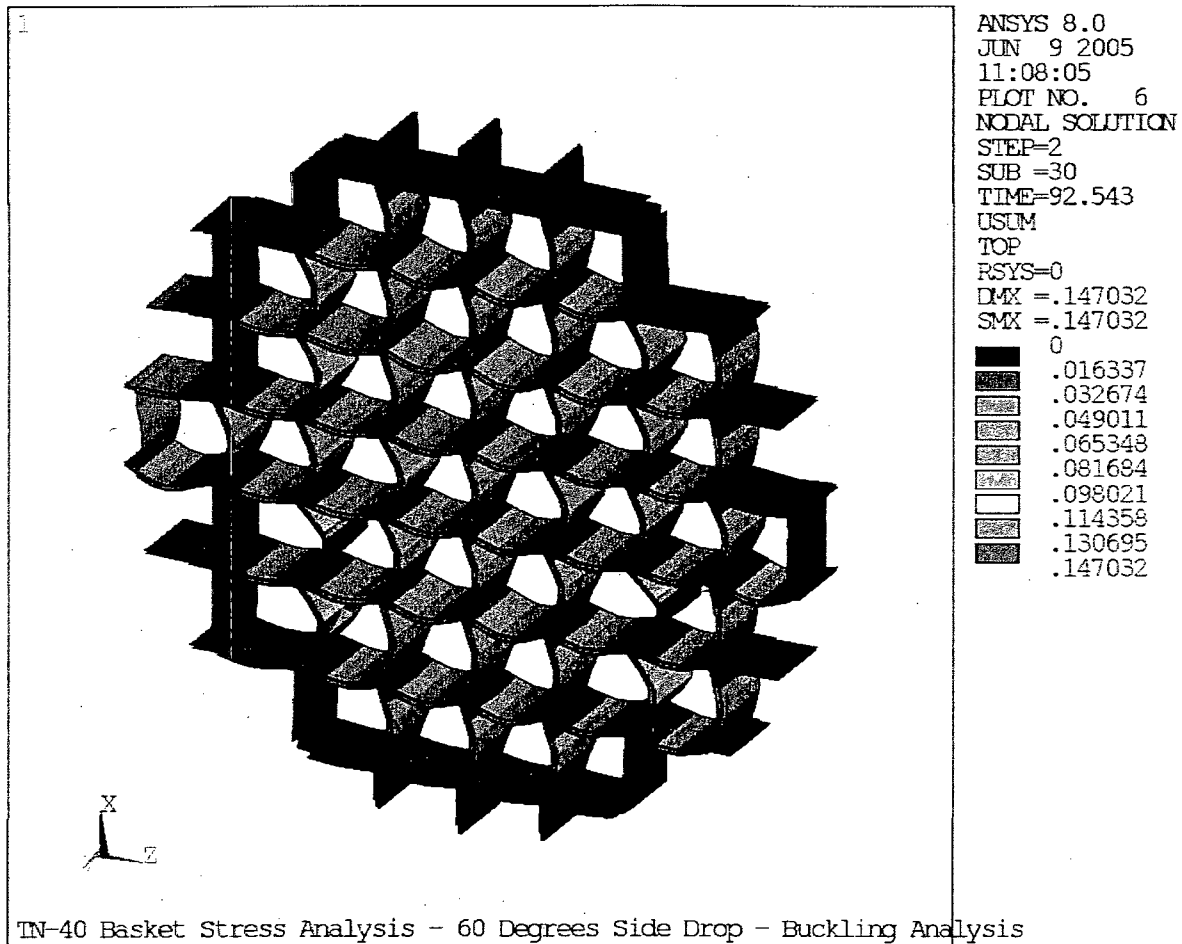


Figure 2.10.5-31
Fuel Basket Deformation at Buckling Load – 60° Side Drop

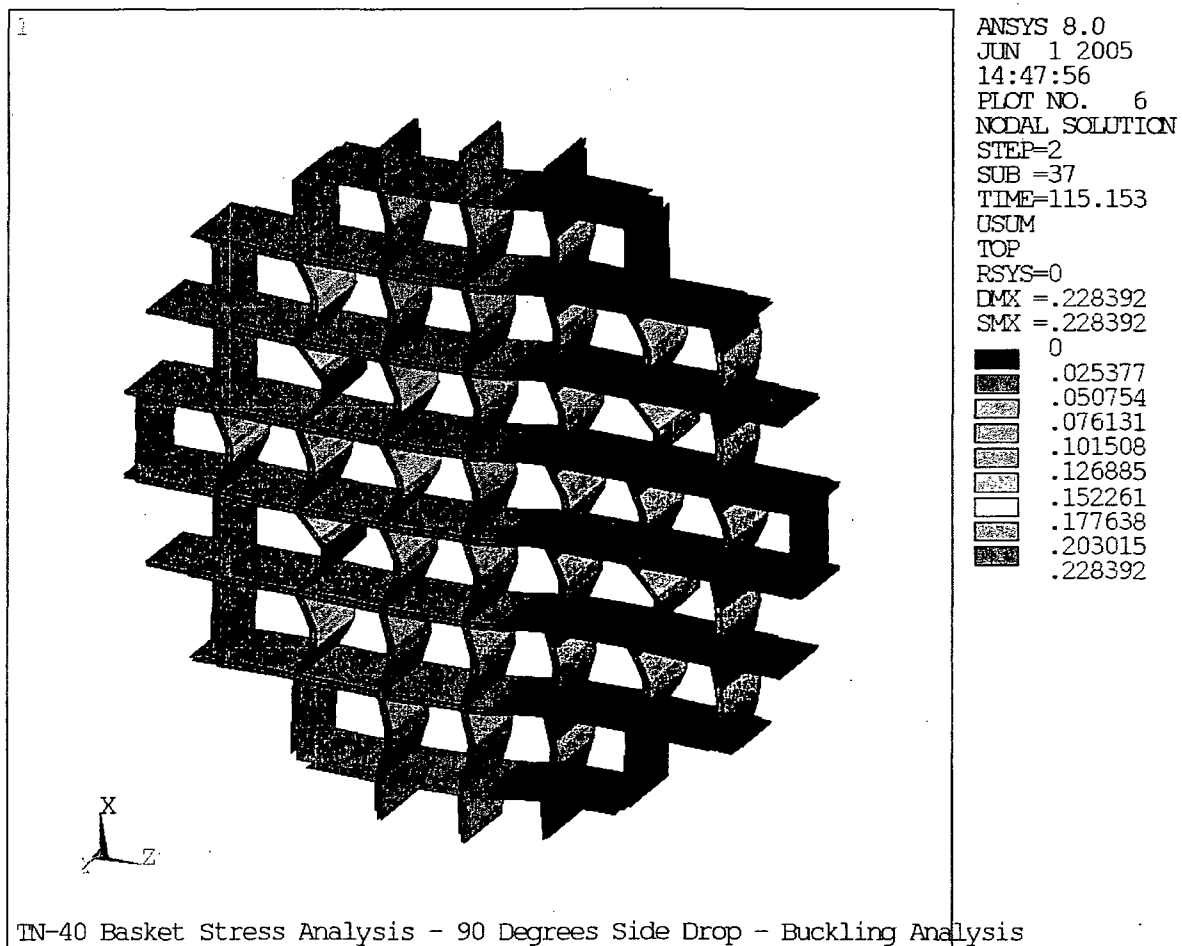


Figure 2.10.5-32
Fuel Basket Deformation at Buckling Load – 90° Side Drop

Appendix 2.10.6

DYNAMIC LOAD FACTOR FOR BASKET DROP ANALYSIS

TABLE OF CONTENTS

	<u>PAGE</u>
2.10.6 DYNAMIC LOAD FACTOR FOR BASKET DROP ANALYSIS	2.10.6-1
2.10.6.1 Introduction	2.10.6-1
2.10.6.2 Modal Analysis of Basket Side Drop Loading Condition	2.10.6-1
2.10.6.3 Frequency of Basket due to Basket End Drop Loading Condition	2.10.6-3
2.10.6.4 Dynamic Load Factor Calculations	2.10.6-3
2.10.6.5 References	2.10.6-5

LIST OF FIGURES

Figure 2.10.6-1	TN-40 Basket Finite Element Model	2.10.6-6
Figure 2.10.6-2	Displacement Boundary Condition - 0° Side Drop	2.10.6-7
Figure 2.10.6-3	0° Side Drop - 1st Mode	2.10.6-8
Figure 2.10.6-4	45° Side Drop - 1st Mode	2.10.6-9
Figure 2.10.6-5	90° Side Drop - 1st Mode	2.10.6-10
Figure 2.10.6-6	DLF Calculation Relationship	2.10.6-11
Figure 2.10.6-7	TN-68 Cask 1/3 Scale Impact Limiter Testing – Acceleration Time History for End Drop	2.10.6-12
Figure 2.10.6-8	TN-68 Cask 1/3 Scale Impact Limiter Testing – Acceleration Time History for Side Drop	2.10.6-13

2.10.6 DYNAMIC LOAD FACTOR FOR BASKET DROP ANALYSIS

2.10.6.1 Introduction

This appendix presents the modal analysis of the TN-40 fuel basket. The TN-40 basket is analyzed for 30 foot end drop and side drop accidents in Appendix 2.10.5 using equivalent static methods. The equivalent static loads for the drop evaluations of the TN-40 basket are determined by multiplying the peak rigid body accelerations (analyzed in Appendix 2.10.8) by the corresponding dynamic load factor (DLF). The DLF is a function of the rise time of the applied load, the duration of the load, the shape of the load, and the modal frequencies of the structure. The purpose of this analysis is to determine the fundamental frequencies of the basket which have the most significant effect on the response of the basket to the 30 foot side impact. Using the fundamental frequencies of the basket structure, the DLF is determined from the curve shown in Figure 2.10.6-6 which is taken from the NUREG/CR-3966 [1]. The results give the DLFs for a half-sine-wave as a function of the ratio of the impulse duration to the natural period of the structure. The half sine wave is used because it gives a reasonable approximation of the actual load experienced by the cask during a drop event.

2.10.6.2 Modal Analysis of Basket Side Drop Loading Condition

Finite Element Model

Modal analyses were run using the ANSYS [2] finite element model described in Appendix 2.10.5. The model was modified such that the fuel weight is included as mass instead of pressure. The basket finite element model is shown on Figure 2.10.6-1.

Material Properties

The stainless steel boxes are constructed of SA-240, Gr. 304 stainless steel. The aluminum plates, outer plates and basket periphery plates are constructed of SB-209, 6061-T651 aluminum alloy. The calculated maximum temperature in the basket is 444°F (Chapter 3, Table 3-1), material properties at 450°F are used. The following material properties are used in the analysis [5][6].

For SA-240, Gr. 304 at 450°F:

$$\begin{aligned} E &= 26.15 \times 10^6 \text{ psi} \\ \nu &= 0.3 \\ \rho &= 0.29/386.4 \text{ lbm/in}^3 \end{aligned}$$

For SB-209, 6061-T651 at 450°F:

$$\begin{aligned} E &= 8.4 \times 10^6 \text{ psi} \\ \nu &= 0.3 \\ \rho &= 0.098/386.4 \text{ lbm/in}^3 \end{aligned}$$

The density of the aluminum plates was adjusted to match the total weight of the Boral[®] and aluminum plates:

$$\begin{aligned}\rho &= \rho_{AL} \times (W_{AL} + W_{Boral}^{\text{®}}) / (W_{AL}) \\ &= (0.098 / 386.4) \times (5402.6 + 579.5) / (5402.6) \\ &= 2.81 \times 10^{-4} \text{ lbm/in}^3\end{aligned}$$

The weight of the fuel (1300 lbs) was added to the bottom or right surface of the steel basket depending on the drop orientation.

$$\text{For } 0^\circ \text{ and } 90^\circ \text{ Side Drop} \rightarrow \rho = \rho_{st} + [(1300 / 386.4) \times (8 / 144) / (8 \times 8.14 \times 0.09)] = 0.033 \text{ lbm/in}^3$$

$$\text{For } 45^\circ \text{ Side Drop} \rightarrow \rho = \rho_{st} + [0.7071 (1300 / 386.4) \times (8 / 144) / (8 \times 8.14 \times 0.09)] = 0.023 \text{ lbm/in}^3$$

Boundary Conditions

The bottom half of the basket perimeter is constrained in the direction parallel to the drop angle and the entire perimeter is constrained in the perpendicular direction. These boundary conditions were chosen to eliminate modes of vibration that are incompatible with the physics of the drop. For instance, side to side modes are not important because they are restrained by the basket wall and more importantly, because they will have no modal weight in the drop direction and therefore will not be activated by the drop. Typical boundary conditions for the 0° modal analysis are shown on Figure 2.10.6-2.

Results of the Modal Analysis

The first five frequencies for each drop angle are summarized in the following table. The deformed shapes of the first mode of each drop are shown in Figures 2.10.6-3 to 2.10.6-5.

Results Summary - Natural Frequencies

Mode	Frequency (Hz)		
	0° Drop	45° Drop	90° Drop
1	148.3	165.9	148.7
2	151.3	166.1	148.7
3	154.0	168.3	151.4
4	159.0	171.5	152.2
5	161.0	171.9	154.3

2.10.6.3 Frequency of Basket due to Basket End Drop Loading Condition

The fundamental natural frequency of a simply supported cylindrical shell under axial vibration simplifies to that of a uniform beam, free axially at both ends. The fundamental natural frequency of a uniform beam free at both ends, under longitudinal vibrations is as follows [4].

$$f_1 = \frac{\lambda_1}{2\pi l} \left(\frac{E}{\mu} \right)^{\frac{1}{2}}$$

Where $\lambda_1 = \pi$

The average mass density, μ , is calculated the following way, the stiffness of the aluminum and Boral® plates are ignored:

Total weight for steel components = 6,608.8 lbs

Total volume for steel components = 6,608.8 / 0.29 = 22,789.0 in.³

Total weight for aluminum/ Boral® components = 8,083.7 lbs

Average weight density = (6,608.8 + 8,083.7) / 22,789 = 0.645 lb in.⁻³

Average mass density, $\mu = 0.645 / 386.4 = 0.00167$ lbm. in.⁻³

$l = 160$ in.

Therefore,

$$f_1 = \frac{\pi}{2\pi(160)} \left(\frac{26.15 \times 10^6}{0.00167} \right)^{\frac{1}{2}} = 391.0 \text{ Hz}$$

The stiffness of the aluminum and Boral® plates are ignored which will increase the natural frequencies.

2.10.6.4 Dynamic Load Factor Calculations

The DLF is computed for the end and side drops. The TN-40 impact limiter design is similar to the TN-68 design, therefore, the impact duration from the TN-68 1/3 model drop test (Appendix 2.10.9, Reference [3]) is used.

The DLF calculation procedure in Reference [1] is based on the natural time period T (or 1/natural frequency) of the structure, and the duration and shape of the impact impulse.

The DLF of the TN-40 basket are based on a half sine wave shape impulse and cask impact impulse durations (t) of 0.045 and 0.060 sec [3].

The DLF calculated for side and end drops are shown in the following table, using Figure 2.10.6-6 and the lowest natural frequency calculated in Sections 2.10.6.2 and 2.10.6.3.

Dynamic Load Factor Calculations

Drop Orientation	Natural Frequency (Hz)	Natural Time Period, T (Sec.)	Impulse Duration ⁽¹⁾ , t (Sec)	Ratio t/T	DLF (from Figure 2.10.6-6)
End Drop	391.0	0.0026	0.045	17.3	< 1.1
Side Drop	148.3	0.0067	0.060	8.95	< 1.1

Notes:

- (1) Impact durations from the TN68 1/3 scale impact limiter testing are 0.015 and 0.02 sec for end and side drops, respectively. These are equivalent to 0.045 and 0.06 sec for the full scale impact limiter. The time history of the TN68 1/3 Scale impact limiter End and Side Drop are shown in Figures 2.10.6-7 and 2.10.6-8 (Reproduced from Figures 2.10.9-15 and 2.10.9-18 of TN68 Transport SAR [3])

2.10.6.5 References

1. NUREG/CR-3966, "Methods for Impact Analysis of Shipping Containers", 11/1987.
2. ANSYS Engineering Analysis System User's Manual, Rev. 8.0.
3. *TN-68 Transport Packaging Safety Analysis Report*, Rev. 4, NRC Docket 71-9293
4. Blevins, Robert D., "Formulas for Natural Frequency and Mode Shape", Krieger Publishing Company, Florida, 1995.
5. ASME Boiler and Pressure Vessel Code, 1989, Section III & Appendices; Section VIII, Divs 1 & 2.
6. "Aluminum Standards and Data", The Aluminum Association, Inc., 1976.

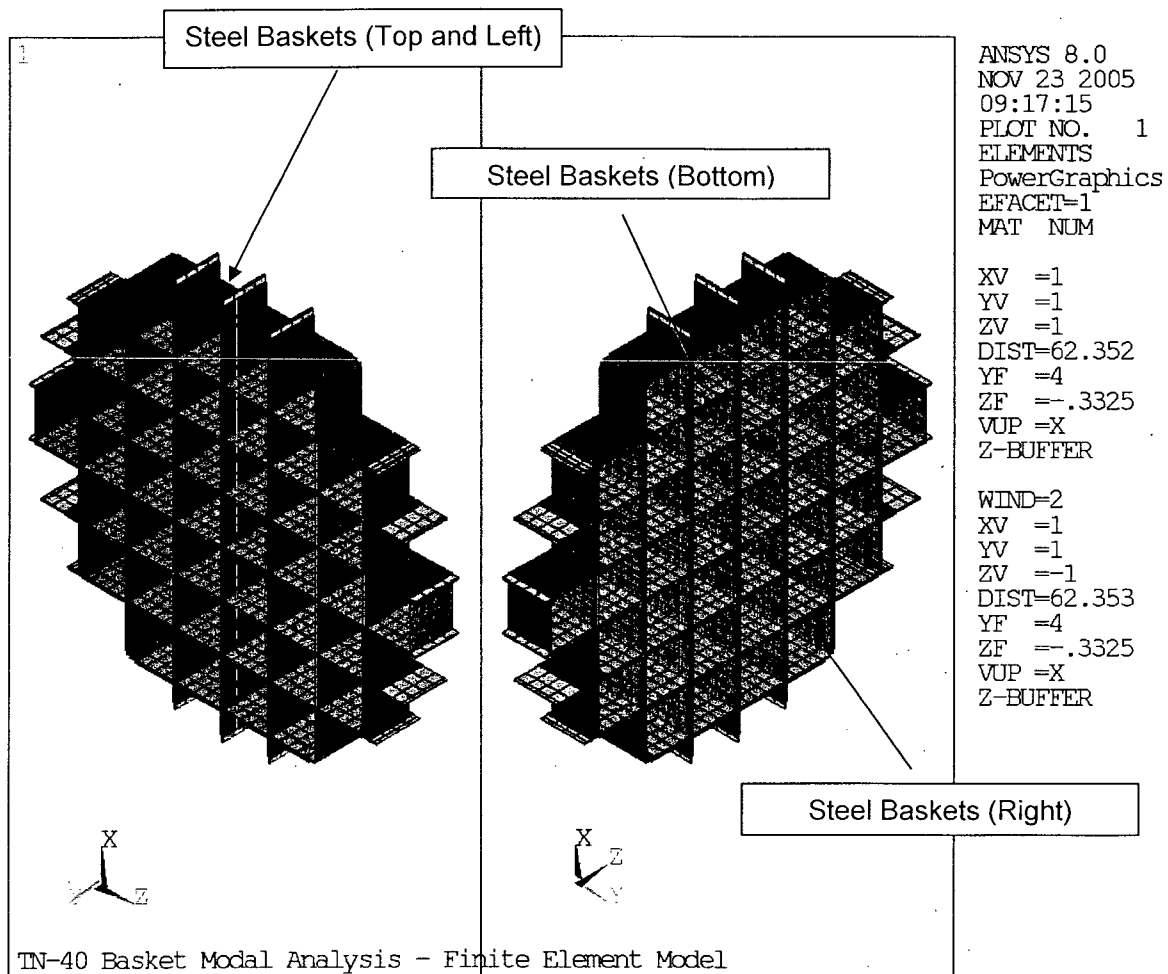


Figure 2.10.6-1
TN-40 Basket Finite Element Model

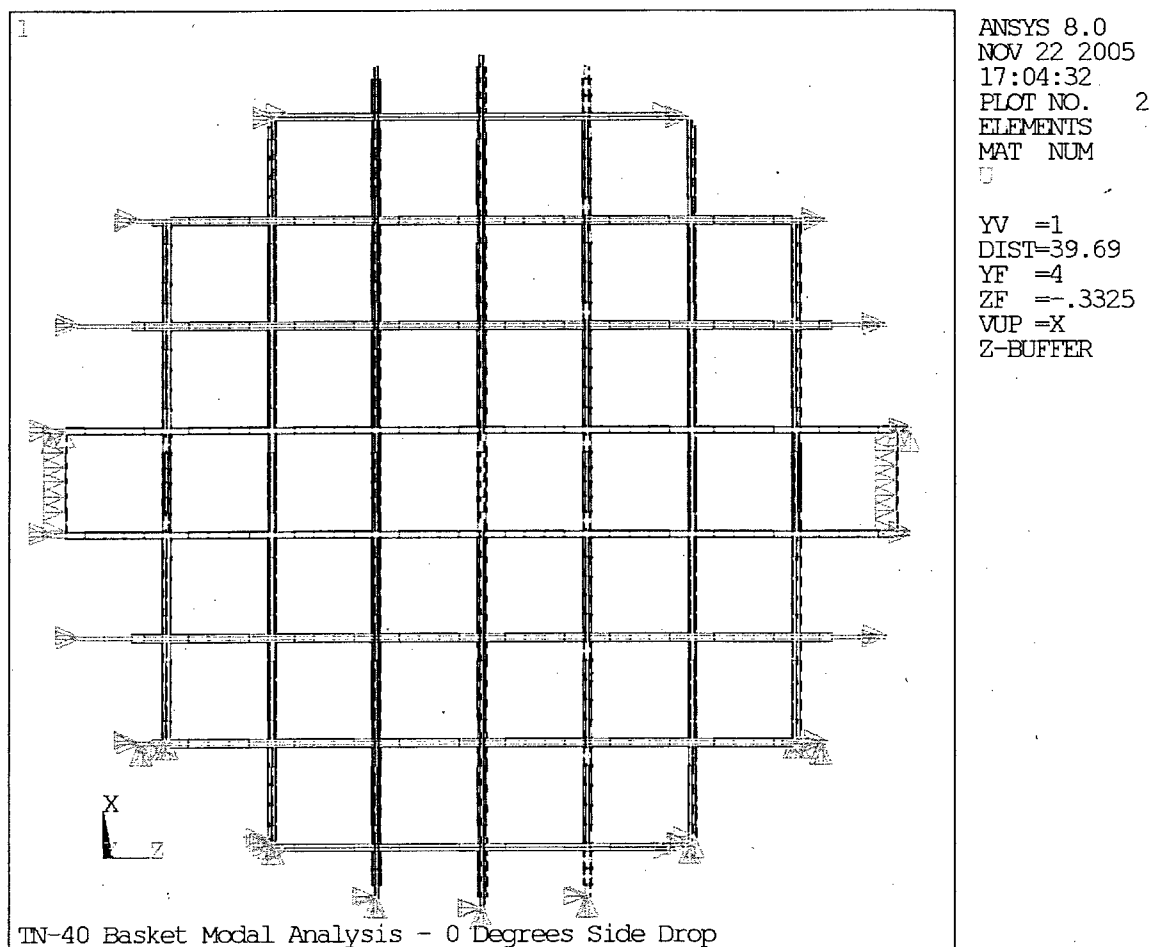


Figure 2.10.6-2
Displacement Boundary Condition - 0° Side Drop

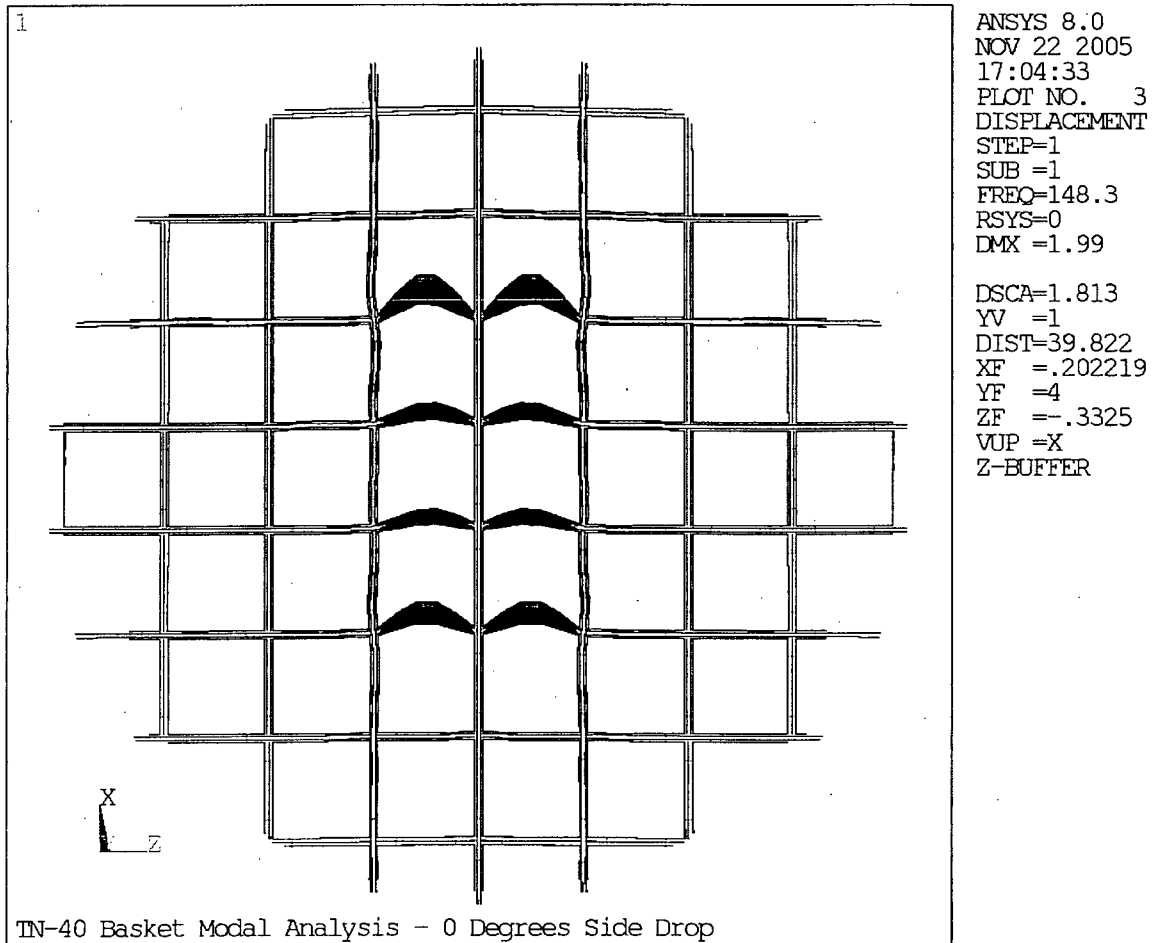


Figure 2.10.6-3
0° Side Drop - 1st Mode

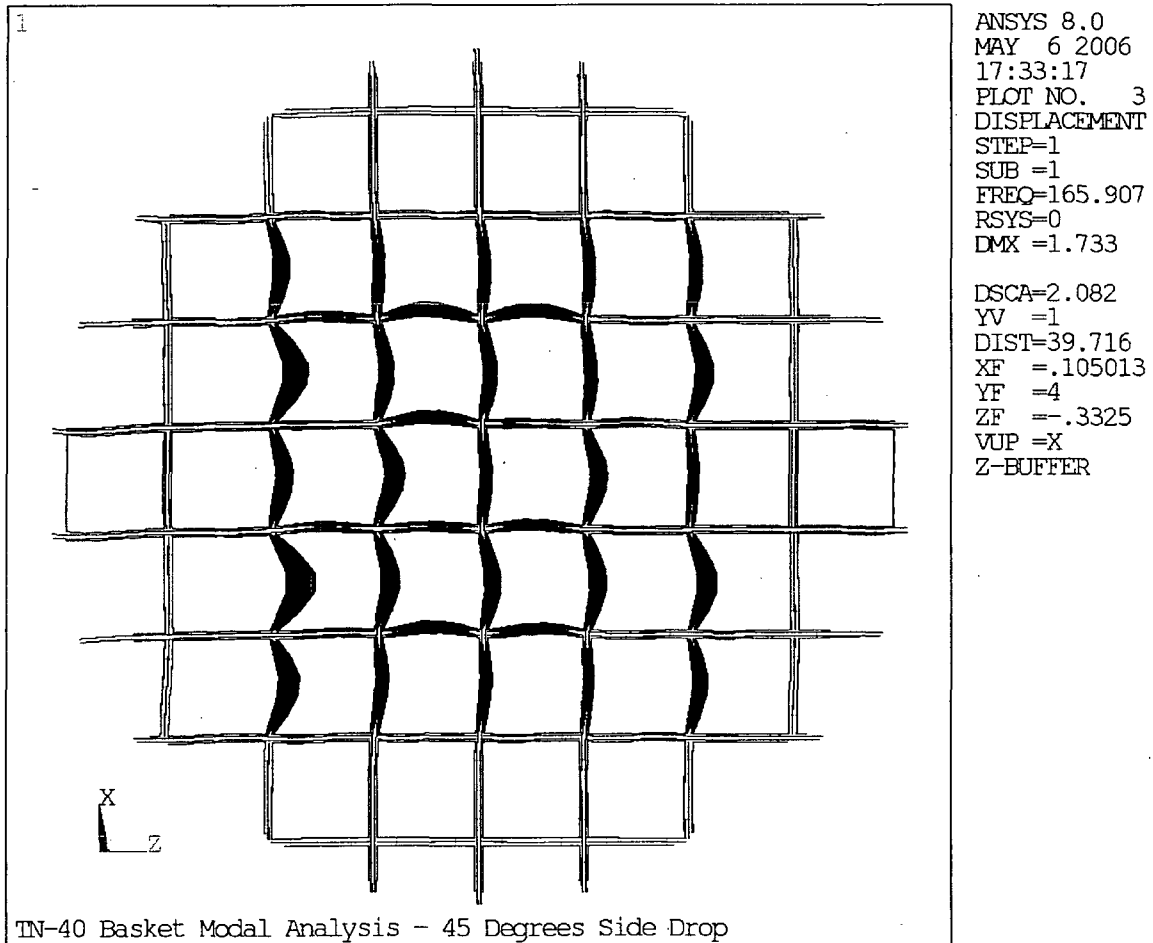


Figure 2.10.6-4
45° Side Drop - 1st Mode

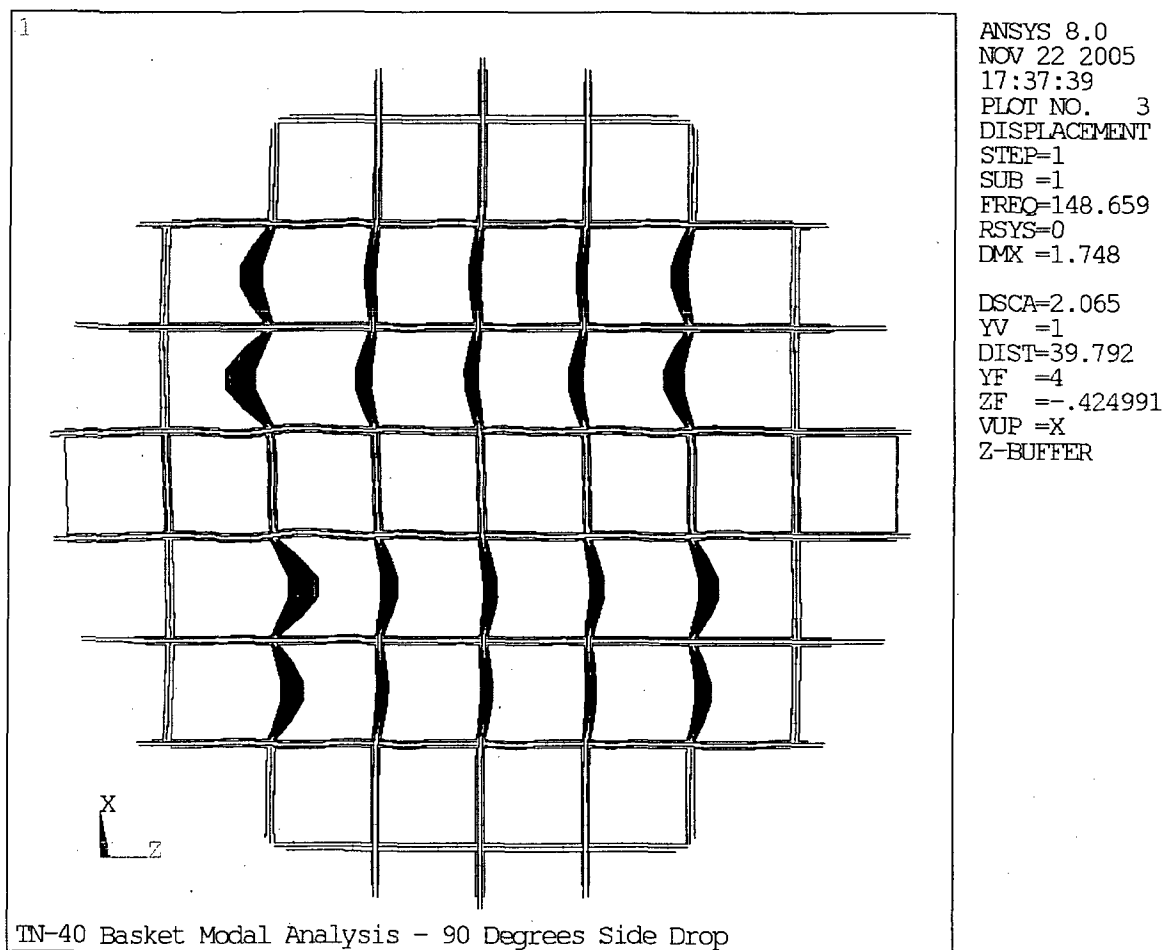
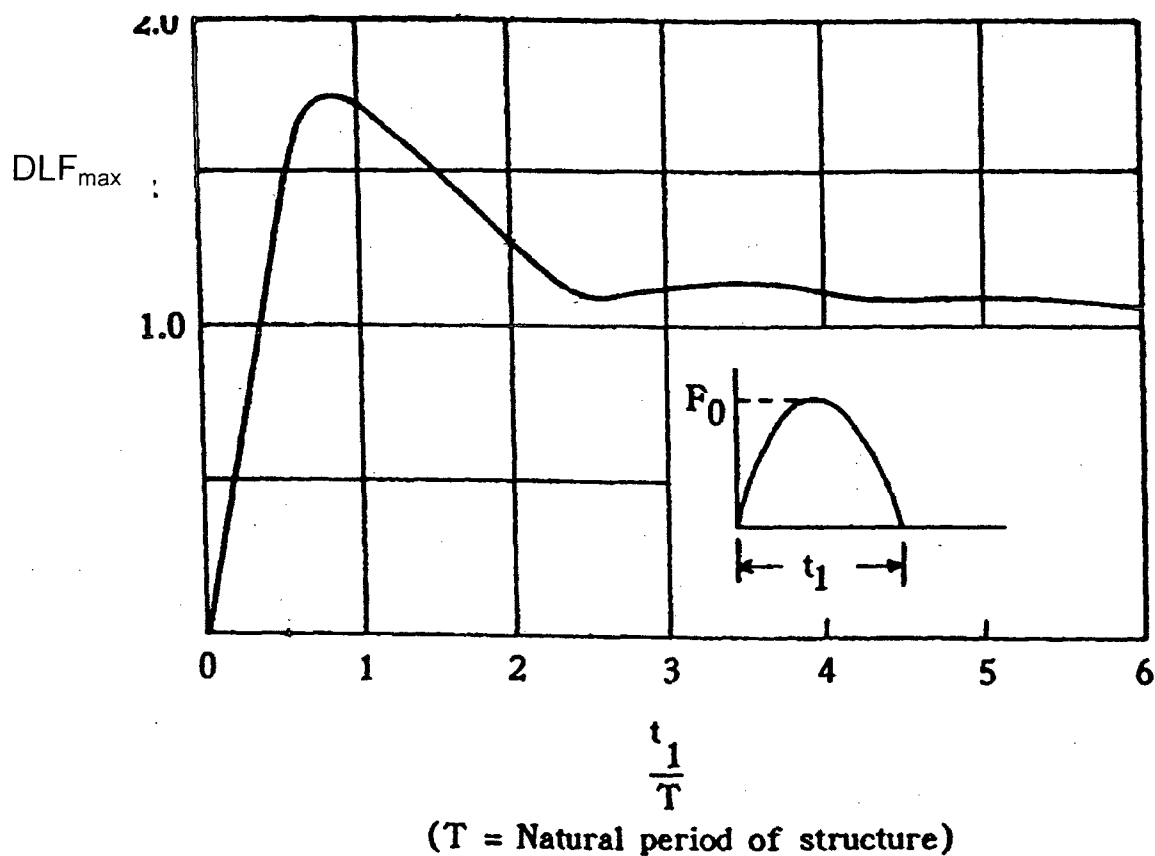


Figure 2.10.6-5
90° Side Drop - 1st Mode



(Reproduced from Reference [1])

Figure 2.10.6-6
DLF Calculation Relationship

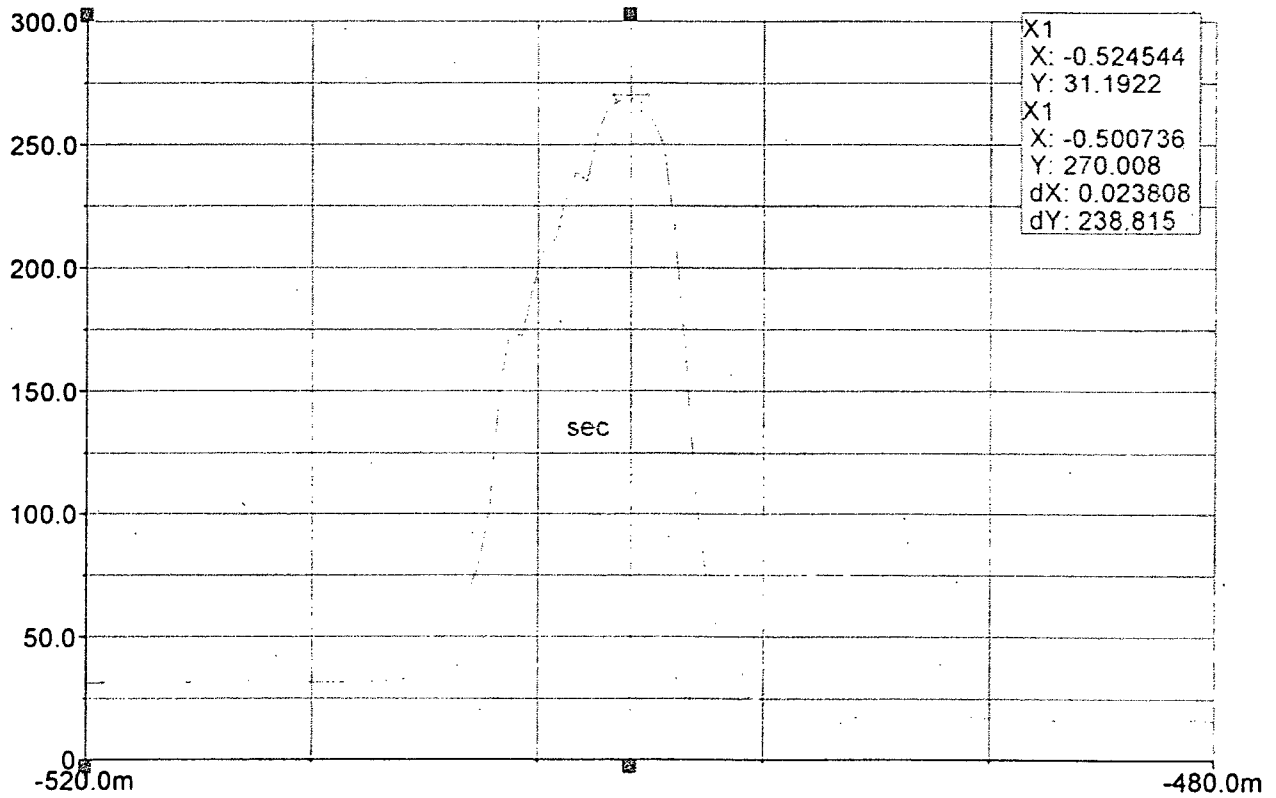


Figure 2.10.6-7
TN-68 Cask 1/3 Scale Impact Limiter Testing -
Acceleration Time History for End Drop

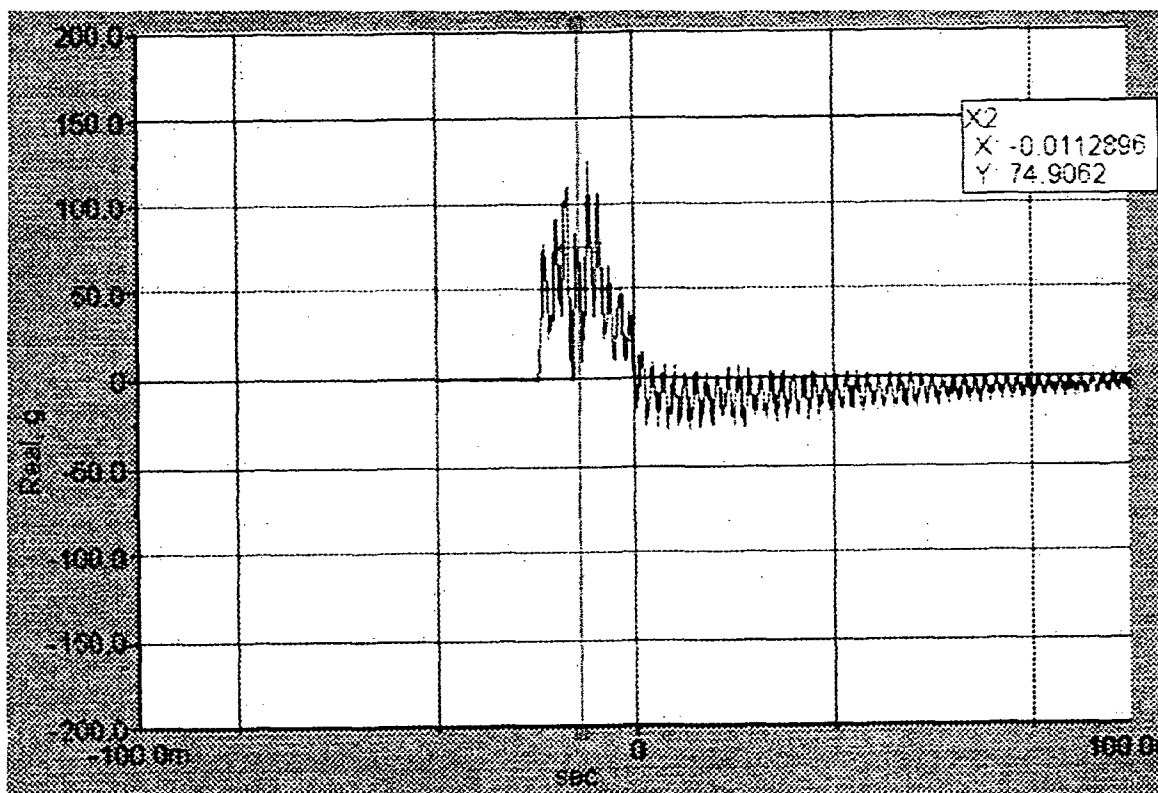


Figure 2.10.6-8
TN-68 Cask 1/3 Scale Impact Limiter Testing -
Acceleration Time History for Side Drop

Appendix 2.10.7
STRUCTURAL EVALUATION OF THE FUEL ROD
CLADDING UNDER ACCIDENT IMPACT

PROPRIETARY INFORMATION WITHHELD
UNDER 10CFR2.390

APPENDIX 2.10.8 STRUCTURAL EVALUATION OF THE IMPACT LIMITERS

TABLE OF CONTENTS

	<u>Page</u>
2.10.8 STRUCTURAL EVALUATION OF THE IMPACT LIMITERS	2.10.8-1
2.10.8.1 Introduction	2.10.8-1
2.10.8.2 Design Description	2.10.8-1
2.10.8.3 Design Criteria	2.10.8-3
2.10.8.4 Analysis of the HAC 30 Foot Free Drop	2.10.8-3
2.10.8.5 Analysis for One Foot Drop Normal Condition of Transport.....	2.10.8-7
2.10.8.6 Impact Limiter Attachment Analysis	2.10.8-8
2.10.8.7 Summary of ADOC Results Used for Structural Analysis ..	2.10.8-20
2.10.8.8 Summary Description of ADOC Computer Code	2.10.8-21
2.10.8.9 References.....	2.10.8-32

LIST OF TABLES

Table 2.10.8-1	Mechanical Properties of Wood and Wood Adhesive	2.10.8-33
Table 2.10.8-2	Typical Wood Material Properties	2.10.8-33
Table 2.10.8-3	First Impact Maximum Inertia g-Load versus Initial Angle of Impact for 30 Foot Drop, Using Maximum Wood Crush Stress Properties	2.10.8-34
Table 2.10.8-4	First Impact Maximum Inertia g-Load versus Initial Angle of Impact for 30 Foot Drop, Using Minimum Wood Crush Stress Properties	2.10.8-35
Table 2.10.8-5	Maximum Impact Limiter Deformation versus Initial Angle of Impact, for 30 Foot Drop, using the Maximum Wood Properties	2.10.8-36
Table 2.10.8-6	Maximum Impact Limiter Deformation versus Initial Angle of Impact, for 30 Foot Drop, using the Minimum Wood Properties	2.10.8-37
Table 2.10.8-7	Maximum Inertial g-Load during 1 Foot Drop.....	2.10.8-38
Table 2.10.8-8	Maximum Impact Limiter Deformation versus Initial Angle of Impact for 1 Foot Drop.....	2.10.8-39
Table 2.10.8-9	Loading Used in Cask Body Analysis, Appendix 2.10.1 versus Maximum g-Loads Predicted by ADOC Program.....	2.10.8-40
Table 2.10.8-10	Loading Used in Basket Structural Analysis, Appendix 2.10.5 versus Maximum g-Load Predicted by ADOC Program.....	2.10.8-41

LIST OF FIGURES

Figure 2.10.8-1	Impact Limiter Geometry.....	2.10.8-42
Figure 2.10.8-2	Sample Force/Deflection Curve for Balsa	2.10.8-43
Figure 2.10.8-3	Sample Force/Deflection Curve for Redwood	2.10.8-44
Figure 2.10.8-4	ADOC Computer Model for TN-40 Transport Package.....	2.10.8-45
Figure 2.10.8-5	TN-40 Package Geometry during Impact for Wood Strain Computation	2.10.8-46
Figure 2.10.8-6	Geometry of Packaging	2.10.8-47
Figure 2.10.8-7	Packaging at Time, t	2.10.8-48
Figure 2.10.8-8	Geometry of Impact Limiter Parameters	2.10.8-49
Figure 2.10.8-9	Definition of Limiter Deformation.....	2.10.8-50
Figure 2.10.8-10	Crush Pattern in Impact Limiter	2.10.8-51
Figure 2.10.8-11	Impact Limiter Segments	2.10.8-52
Figure 2.10.8-12	Strain Computation for Crush Pattern I.....	2.10.8-53
Figure 2.10.8-13	Strain Computation for Crush Pattern II.....	2.10.8-54
Figure 2.10.8-14	Strain Computation for Crush Pattern III.....	2.10.8-55
Figure 2.10.8-15	Wood Stress-Strain Curve	2.10.8-56
Figure 2.10.8-16	Impact Limiter Free Body Diagram during 20° Slap Down....	2.10.8-57
Figure 2.10.8-17	Impact limiter Lifting Lug Geometry	2.10.8-58
Figure 2.10.8-18	Cask Geometry during Tip-Over Event.....	2.10.8-59

2.10.8 STRUCTURAL EVALUATION OF THE IMPACT LIMITERS

2.10.8.1 Introduction

This appendix presents the details of the structural analysis of the TN-40 impact limiters. The impact limiters are designed to absorb the kinetic energy resulting from the one (1) foot and thirty (30) foot normal condition of transport (NCT) and hypothetical accident condition (HAC) free drop events specified by 10 CFR 71 [5]. Redwood and balsa wood are used as the primary energy absorption material(s) in the impact limiters. A sketch of the impact limiter is shown in Figure 2.10.8-1. A functional description of the impact limiters is given in Section 2.10.8.2. The impact limiter design criteria are described in Section 2.10.8.3.

A computer model of the TN-40 Packaging was developed to perform system dynamic analyses during impacts of 30 foot HAC and 1 foot NCT drops. The model was developed for use with the ADOC (Acceleration Due To Drop On Covers) [6] computer code described in detail in Section 2.10.8.8 which determines the deformation of the impact limiters, the forces on the cask and the cask deceleration due to impact of the package on an unyielding surface. Numerous cases were run to determine the effects of the wood properties and the impact angle. A description of the computer model, input data, analysis results and conclusions for the 30 foot HAC condition and one foot NCT free drops are given in Sections 2.10.8.4 and 2.10.8.5 respectively. The analysis of the impact limiter attachments is described in Section 2.10.8.6. A summary of results for all drop orientations is provided in Section 2.10.8.7. The forces and accelerations used in the cask body and basket structural analysis are presented in detail in Appendix 2.10.1 and Appendix 2.10.5 respectively. The accelerations are given in Tables 2.10.8-9 and -10 (loading values calculated in this appendix are increased for conservatism). Planned testing programs on the TN-40 wood-filled limiters are discussed in Appendix 2.10.9.

2.10.8.2 Design Description

The impact limiters absorb energy during impact events by crushing of balsa and redwood. The size, location and orientation of each wood block is selected to provide protection for the cask during all NCT and HAC drop events.

The top and bottom impact limiters are nearly identical. Each has an outside diameter of 144 inches and a height of 50 inches. The bottom impact limiter has pockets to accommodate the lower trunnions. The inner and outer shells are SA-240 Type 304 stainless steel joined by radial gussets of the same material. The gussets limit the stresses in and deflection of the 0.25 in. thick steel outer cylinder and end plates due to pressure differentials caused by elevation and temperature changes during normal transport and provide wood confinement during impact. The metal structure positions, supports, confines and protects the wood energy absorption material. The metal structure contributes to the energy absorbing capability of the impact limiter. However, the contribution to a side drop or oblique angles is negligible because contact starts at a

single point with the unyielding surface (target) and initiates buckling of a single gusset. After the drop event is complete, relatively few gussets are buckled. The strength of the steel shell is conservatively omitted from the impact limiter analysis.

The region of the impact limiter which is adjacent to the cask ends is filled with balsa wood and redwood mostly oriented with the grain direction parallel to the axis of the cask as shown in Figure 2.10.8-1. The materials and grain orientations are selected to provide acceptably low deceleration to limit stresses in the cask during the 30 foot HAC impact end drop. A 2.50 inch layer of balsa wood with the grain perpendicular to the axis of the cask is provided on the outer face of the impact limiter to minimize decelerations after a one foot NCT end drop.

A 8.75 inch wide ring of redwood (consisting of 12 segments or blocks of wood) is located in the sides of the pie shaped compartments which surround the end of the cylindrical surface of the cask with the grain direction oriented radially. This ring of redwood absorbs most of the kinetic energy during a side drop. Redwood was selected for this portion of the impact limiter because of its high crush strength and hence the ability of a small amount of wood to absorb a large amount of energy in a relatively short crush distance.

The corners of the pie-shaped compartments are filled with redwood. A 34.75 inch section of redwood is located around the outer corner of the impact limiter. The grain is oriented radially. The primary function of the redwood block is energy absorption during a 30 foot corner drop.

All wood blocks used in the impact limiters are composed of individual boards glued together with a Phenol Resorcinol Adhesive or equivalent. This adhesive is selected for its superior strength and moisture resistance. The wood blocks are assembled and glued together in accordance with an approved QA procedure. Minimum properties of the adhesive are listed in Table 2.10.8-1. Ranges of shear and tensile strengths of each type of wood are also listed. The adhesive is significantly stronger than any of the wood used in the limiter in terms of shear and tensile strength. Therefore the boards or blocks of wood will not fail along the glue joints.

The other mechanical properties of the wood used in the analysis are shown in Table 2.10.8-2. The crush strength properties used cover the range of density and moisture content specified in the fabrication specification. During fabrication, wood samples are tested for density and moisture content in accordance with an approved sampling plan. If the density or moisture content are not within the specified range, the wood blocks from which samples are taken are rejected.

During the end drop, all of the wood in the central part of the impact limiter that is directly "backed-up" by the cask body will crush. The wood in the corners and sides of the limiter will tend to slide along the side of the cask since it is not supported or backed-up by the body and it will not crush or absorb energy as effectively as the wood that is backed-up. During the side or oblique drop the wood backed up by the cask will

crush, while the wood beyond the end of the cask body will have a tendency to slide around the end of the cask. The analyses assume that the effectiveness of the portion of the wood that is not backed-up is 20%. Effectiveness is defined as the actual crush force developed at the target by this material divided by the theoretical force required to crush the material. The analysis also assumes a range of wood crush strengths. When determining maximum deceleration, the maximum crush strengths are used. When determining crush depth, the minimum wood crush strengths are used.

Each impact limiter is attached to the cask using four attachment bolts and the two limiters are attached to each other by thirteen tierods. The attachments have been sized to withstand the loads transmitted during a low angle drop slap down. This analysis is described in Section 2.10.8.6 of this Appendix.

2.10.8.3 Design Criteria

The outside dimensions of the impact limiter are sized to be within federal and state highway height and width restrictions. The balsa and redwood distribution and densities have been selected to limit the maximum cask body inertia loads due to the one foot NCT drop and the thirty foot HAC drop so that the design criteria specified for the cask and basket (Section 2.1) are met.

The welded stainless steel structure of the impact limiter is designed so that the wood is maintained in position and is confined during crushing of the impact limiters. The outer shell and gussets are designed to buckle and crush during impact. Local failure of the shell is allowed during impact limiter crushing. The welded stainless steel shell and its internal gussets are designed to withstand pressure differences and normal handling and transport loads with stresses limited to the material yield strength.

The impact limiters are designed to remain attached to the cask body during all NCT and HAC drop events.

2.10.8.4 Analysis of the HAC 30 Foot Free Drop

2.10.8.4.1 Approach

The kinetic energy due to the HAC 30 foot drop is absorbed by crushing of the impact limiters mounted on the ends of the cask. The limiters contain materials, i.e. balsa and redwood, which provide controlled deceleration of the packaging by crushing between the target surface and the cask body.

The applicable regulation, 10CFR71.73 [5], requires that the packaging be oriented for the drop so that it strikes the target in a position for which maximum damage is expected. Dynamic impact analyses were performed for different packaging orientations using the ADOC computer code described in Section 2.10.8.8. This computer code has been validated by comparing its dynamic results with those from hand calculations for relatively simple problems, comparing its calculated

force-deflection curves with those obtained from static crush tests, and by correlating dynamic results with actual measured cask behavior on other programs.

2.10.8.4.2 Assumptions and Boundary Conditions

The assumptions and boundary conditions are as follows:

1. The cask body is assumed to be rigid and absorbs no energy. This assumption is realistic since the design criteria of Section 2.1.2 limit metal deformations to small values. All of the impact energy is therefore assumed to be absorbed by the impact limiters.
2. The crushable material is one of several anisotropic materials. The different wood regions are modeled individually.
3. The crush strengths of the wood sections are obtained from the properties parallel to and perpendicular to the grain based on the orientation of the cask at impact.
4. Each wood region is modeled as a one dimensional elastic, perfectly plastic material up to a specific locking strain. After reaching the locking strain, the stress increases linearly with the additional strain. The wood properties (modulus of elasticity, average crush strength, locking modulus, and locking strain) are taken from force-deflection curves of sample blocks of wood. Typical force-deflection curves for balsa and redwood are shown in Figures 2.10.8-2 and 2.10.8-3. Since the locking strain varies from sample to sample, conservatively low locking strains of 80% for balsa and 60% for redwood are used.
5. The crush properties of the wood are based on the initial angle of impact and do not change during the drop event being evaluated.
6. The cask and impact limiters are axisymmetric bodies.
7. The crushing resistance of the impact limiter shell and gussets have a negligible effect on the crush strength of the limiter and, therefore, a negligible effect on the impact forces and inertia loads.

2.10.8.4.3 Packaging Dynamic Computer Model

Figure 2.10.8-4 illustrates the computer model used for all packaging orientations. Regions I, II, and III in the model are used to delineate regions where different impact limiter materials are used. It should be noted that the properties of the three regions have been designed by choosing wood types and orientations to accommodate the crush requirements of the drop orientations. The crushable materials of Regions I, II, and III are selected to control the decelerations resulting from end, corner, and side drop orientations, respectively. Table 2.10.8-2 tabulates the wood properties that were used to describe the wood stress-strain behavior in the analysis.

A portion of the impact limiter crushable material is backed up by the cask body as it crushes against the impact surface. The remaining material overhangs the cask body and is not backed up. Backed up regions project vertically from the target footprint to the cask body, while unbacked regions do not project vertically to the cask. The effectiveness of the energy absorbing crushable material varies depending on whether it is backed up by the cask or is unsupported. Two cases are analyzed to bound impact limiter performance. In one case, the non-backed up material is assumed to be 20% effective and maximum wood crush strength is used (maximum of the possible range based on specified density). In the other case, the non-backed up material is also assumed to be 20% effective but the minimum wood strength is used. Evaluating impact limiter performance in this way results in a range of deceleration values, crush forces and crush depths. This, in combination with close control of wood properties during procurement, assures that the effects of wood property variations (including temperature effects) are bounded by the analyses.

2.10.8.4.4 Analysis Results Predicted by ADOC

The peak inertia loadings or cask body decelerations (in terms of g's) versus initial angle of impact are presented in Tables 2.10.8-3 and 2.10.8-4 for the 30 foot drop. The 30 foot dimension is defined to be the distance from the impact surface to the lowest point of the impact limiter. The center of gravity (CG) of the cask is thus much higher than 30 feet. The values of maximum crush depth for each 30 foot drop orientation are shown in Tables 2.10.8-5 and 2.10.8-6. Since the TN-40 package CG is within a few inches of the geometric package center and the impact limiters are nearly identical, these tables are valid for impacts on either end.

2.10.8.4.5 Wood Strain Computation

During the low angle drops (5° to 40°) the method used by ADOC to compute the strain in the wood segments is overly conservative. Consequently, the maximum strains achieved during certain impacts with drop orientations between 5° and 40° are recomputed. The average wood strains are only recomputed for the minimum wood property cases since strains generated using minimum wood properties bounds the maximum wood property strain for a given drop orientation. The Figure 2.10.8-5 depicts the geometry of the package during impact.

Given the impact angle θ and the crush depth Δ , computed by ADOC, the crush depths a and b shown in Figure 2.10.8-5 can be calculated. The impact limiter strain is then taken to be the average of a and b divided by the impact limiter radial thickness, 25.50 inches. The recomputed strains are provided in Tables 2.10.8-5 and 2.10.8-6, identified by *.

2.10.8.4.6 Trunnion Clearance during Low Angle Drops

In this section the clearance between the impact target and the outer edge of the trunnions is computed in order to assure that the trunnions are not damaged or cause

large accelerations during a near 0° drop. The trunnion clearance is only computed for the minimum wood property case since crush depths are always smaller when maximum wood properties are used.

Trunnion Clearance during 0° Side Drop

The maximum crush depth Δ_{sd} during a side drop event (using minimum wood properties) is:

$$\Delta_{sd} = 15.87 \text{ in.}$$

The trunnion clearance δ_{sd} is then:

$$\begin{aligned}\delta_{sd} &= 71.75 \text{ in. (impact limiter outer radius)} - 15.87 \text{ in.} - 104.50 / 2 \text{ in. (trunnion radius)} \\ &= 3.63 \text{ in.}\end{aligned}$$

Trunnion Clearance during 5° Drop

The maximum crush depth Δ_{5° during a side drop event (using minimum wood properties) is:

$$\Delta_{5^\circ} = 18.89 \text{ in.}$$

The angle of the cask at the time of the maximum crush depth, θ_{5° is:

$$\theta_{5^\circ} = 90^\circ - 88.61^\circ = 1.39^\circ$$

The trunnion clearance δ_{5° is then:

$$\begin{aligned}\Delta_{5^\circ} &= 71.75 \text{ in. (impact limiter outer radius)} - [18.89 \text{ in.} - 37.25 \sin(1.39^\circ)] \\ &\quad - 104.50 / 2 \text{ in. (trunnion radius)} = 1.51 \text{ in.}\end{aligned}$$

Trunnion Clearance during 10° Drop

The maximum crush depth Δ_{10° during a side drop event (using minimum wood properties) is:

$$\Delta_{10^\circ} = 18.15 \text{ in.}$$

The angle of the cask at the time of the maximum crush depth, θ_{10° is:

$$\theta_{10^\circ} = 90^\circ - 88.24^\circ = 1.76^\circ$$

The trunnion clearance δ_{10° is then,

$$\delta_{10^\circ} = 71.75 \text{ in. (impact limiter outer radius)} - [18.15 \text{ in.} - 37.25 \sin(1.76^\circ)] \\ - 104.50 / 2 \text{ in. (trunnion radius)} = 2.49 \text{ in.}$$

Trunnion Clearance during 15° Drop

The maximum crush depth Δ_{15° during a side drop event (using minimum wood properties) is:

$$\Delta_{15^\circ} = 20.06 \text{ in.}$$

The angle of the cask at the time of the maximum crush depth, θ_{15° is:

$$\theta_{15^\circ} = 90^\circ - 76.79^\circ = 13.21^\circ$$

The trunnion clearance δ_{15° is then:

$$\delta_{15^\circ} = 71.75 \text{ in. (impact limiter outer radius)} - [20.06 \text{ in.} - 37.25 \sin(13.21^\circ)] \\ - 104.50 / 2 \text{ in. (trunnion radius)} = 7.95 \text{ in.}$$

Based on the above calculations, there is adequate clearance between the trunnion outer edge and the impact target during low angle 30 foot drops.

2.10.8.5 Analysis for One Foot Drop Normal Condition of Transport

This section describes the analysis of the TN-40 packaging for the one foot NCT drop. The TN-40 cask is lifted vertically and is transported horizontally. End and side drop orientations are therefore considered to be credible NCT drop events. Any other drop orientation will cause the cask to tip over onto its side, which is clearly an accident. The accident analyses in Section 2.10.8.4 bound any possible tipping accident. Therefore, the one foot drop analysis is performed for end and side drop orientations. A one foot, 63.8° CG over corner drop is also analyzed to show that the NCT side and end drops are critical with respect to acceleration and deformation.

The packaging kinetic energy is absorbed by crushing of the impact limiters. The dynamic system model of Section 2.10.8.4 was used to perform the side drop (0°) analysis using the ADOC computer program described in Section 2.10.8.8. The end drop analysis was performed assuming that the energy would be absorbed by the soft balsa wood (oriented in the weak direction) in the outer end of the limiter. This is an accurate way to determine g loads on an end drop since the g values can be calculated by the expression $F = Ma$ where F is the crush stress times the area and M is the package weight divided by the acceleration of gravity g .

The inertial load results of these one foot drop analyses are presented in Table 2.10.8-7. Again, two extreme cases are considered. The upper bound stiffness case assumes maximum wood crush strength and the lower bound stiffness case assumes minimum wood strength. Stress analyses in Section 2.10.1 are conservatively

performed for the case(s) with maximum inertia loads resulting from upper bound stiffness cases.

The maximum crush depths for each of the 1 foot drop orientations are presented in Table 2.10.8-8.

2.10.8.6 Impact Limiter Attachment Analysis

The impact limiter attachments are designed to keep the impact limiters attached to the cask body during all NCT and HAC events. The loading that has the highest potential for detaching the impact limiter is the slap down or secondary impact after a shallow angle 30 foot drop. During this impact, the crushing force on the portion of the impact limiter beyond the cask body (the non backed-up area) tends to pull the limiter away from the cask. The end and corner drops are not critical cases for the impact limiter attachments since the impact force tends to push the impact limiter onto the cask in these orientations.

2.10.8.6.1 Tie Rod Stress Analysis

For the tie rod evaluation, maximum wood crush strengths of 2010 psi for balsa and 6500 psi for redwood are assumed. The maximum wood properties produce the highest overturning moment on the limiter. Based on the dynamic analysis performed using the ADOC code, the most severe slap down impact occurs after a shallow angle oblique impact.

The worst case loading applied to the impact limiter attachments occurs during a low angle (20°) slap down event. The maximum lateral force due to 20° second (slap down) impact is 12,500 kips at a distance of 82.3 inches from the package C.G. This load is conservatively set higher than the actual force of 12,210 kips computed by the ADOC analysis. Only the thirteen 1.5 inch diameter tie rods react the moment applied during the 20° slap down drop. This assumption is considered conservative because the impact limiter attachment bolts will also take some of this load.

The maximum moment applied to the impact limiter attachments is conservatively determined ignoring the mass of the impact limiter which tends to reduce the attachment forces. A free body diagram of the impact limiter is shown in Figure 2.10.8-16. It is conservatively assumed that the impact limiter pivots about the edge of the cask. The resultant of the external impact force on the limiter is offset 5.16 in. from the resultant of the cask reaction force. Therefore, the net moment applied to the limiter is $12.50 \times 10^6 \times 5.16$ or 6.45×10^7 in lb in the counterclockwise direction. There is also a frictional force that acts to pull the impact limiter away from the cask. Assuming a frictional coefficient of 0.42 between the cask and limiter and between the limiter and impact surface, the magnitude of this force is:

$$F_f = \mu R = (0.42)(1.25 \times 10^7) = 5.25 \times 10^6 \text{ lbs.}$$

The crush depth on the side is 5.62 inches. The resultant moment due to friction is:

$$M_f = (5.25 \times 10^6)(26.50 - 5.62) = 1.0962 \times 10^8 \text{ in lbs. (clockwise)}$$

The total moment is therefore 4.512×10^7 in lbs in the clockwise direction. Assume that only the tie rods hold the impact limiters in place, and that the impact limiter will tend to pivot around the edge of the cask. The force distribution among the tie rods will be linearly proportional to their distance from the pivot point. There are two different angular orientations of the impact limiter that are of interest. The first orientation is the angle that causes the highest stress in the single tie rod brackets, and the second is the angle that causes the highest stress in the double tie rod brackets.

Orientation 1 Stress Analysis

During a slapdown impact event in orientation 1, the target surface crushes the impact limiters at the double tie rod bracket located at 270° (Appendix 1.4.1 of Chapter 1, Drawing 10421-71-40). The angular location of each tie rod bracket from vertical (perpendicular to the target surface) is computed in the following way. The tie rods are numbered clockwise 1 through 13 starting from the first tie rod located just above the 270° mark.

Tie Rod Number	Tie Rod Bracket Type	Angular Location Calculation (For Orientation 1)	Angular Location
1	Double	$180^\circ + \arctan[4.31/(124.00/2)] =$	184°
2	Single	$180^\circ + 30^\circ =$	210°
3	Double	$180^\circ + 90^\circ - \arctan[4.31/63.00] =$	266°
4	Double	$180^\circ + 90^\circ + \arctan[4.31/63.00] =$	274°
5	Single	$180^\circ + 120^\circ =$	300°
6	Single	$180^\circ + 150^\circ =$	330°
7	Single	$180^\circ + 180^\circ =$	360°
8	Single	$180^\circ + 210^\circ =$	390°
9	Single	$180^\circ + 240^\circ =$	420°
10	Double	$180^\circ + 270^\circ - \arctan[4.31/63.00] =$	446°
11	Double	$180^\circ + 270^\circ + \arctan[4.31/63.00] =$	454°
12	Single	$180^\circ + 330^\circ =$	510°
13	Double	$360^\circ + 180^\circ - \arctan[4.31/(124.00/2)] =$	536°

The vertical distance from the target surface to each tie rod is computed as follows.

Tie Rod Number	Tie Rod Bracket Type	Vertical Distance Calculation (in.) (For Orientation 1)	Vertical Distance (in.)
1	Double	$[4.31^2 + (124/2)^2]^{1/2} \cos(184^\circ) + 91.00/2 =$	-16.50
2	Single	$(124.00/2) \cos(210^\circ) + 91.00/2 =$	-8.19
3	Double	$[4.31^2 + 63.00^2]^{1/2} \cos(266^\circ) + 91.00/2 =$	41.09
4	Double	$[4.31^2 + 63.00^2]^{1/2} \cos(274^\circ) + 91.00/2 =$	49.90
5	Single	$(124.00/2) \cos(300^\circ) + 91.00/2 =$	76.50
6	Single	$(124.00/2) \cos(330^\circ) + 91.00/2 =$	99.19
7	Single	$(124.00/2) \cos(360^\circ) + 91.00/2 =$	107.50
8	Single	$(124.00/2) \cos(390^\circ) + 91.00/2 =$	99.19
9	Single	$(124.00/2) \cos(420^\circ) + 91.00/2 =$	76.50
10	Double	$[4.31^2 + 63.00^2]^{1/2} \cos(446^\circ) + 91.00/2 =$	49.90
11	Double	$[4.31^2 + 63.00^2]^{1/2} \cos(454^\circ) + 91.00/2 =$	41.09
12	Single	$(124.00/2) \cos(510^\circ) + 91.00/2 =$	-8.19
13	Double	$[4.31^2 + (124/2)^2]^{1/2} \cos(536^\circ) + 91.00/2 =$	-16.50

In the table above, negative vertical distances correspond to tie rods that are below the crush line of the impact limiter. Therefore, these tie rods are conservatively considered to be ineffective and do not carry any of the prying load.

The tie rod farthest away from the target surface (tie rod 7) is assumed to carry the maximum tensile force, F_{\max} . All other tie rods are assumed to carry a tensile force linearly proportional to their distance from the target surface. Therefore, each tie rod will carry the following prying moment.

Tie Rod Number	Tie Rod Bracket Type	Tensile Force in Orientation 1 (lb.)	Moment Arm (in.)	Moment (in.lb.)
1	Double	0	-	0
2	Single	0	-	0
3	Double	$(41.09/107.50) F_{\max}$	41.09	$15.71 F_{\max}$
4	Double	$(49.90/107.50) F_{\max}$	49.90	$23.16 F_{\max}$
5	Single	$(76.50/107.50) F_{\max}$	76.50	$54.44 F_{\max}$
6	Single	$(99.19/107.50) F_{\max}$	99.19	$91.53 F_{\max}$
7	Single	F_{\max}	107.50	$107.50 F_{\max}$
8	Single	$(99.19/107.50) F_{\max}$	99.19	$91.53 F_{\max}$
9	Single	$(76.50/107.50) F_{\max}$	76.50	$54.44 F_{\max}$
10	Double	$(49.90/107.50) F_{\max}$	49.90	$23.16 F_{\max}$
11	Double	$(41.09/107.50) F_{\max}$	41.09	$15.71 F_{\max}$
12	Single	0	-	0
13	Double	0	-	0
			Total Moment =	$477.18 F_{\max}$

Equating this total moment with M_{tot} computed above and solve for F_{max} :

$$477.18 F_{max} = 4.512 \times 10^7 \text{ in.lb.} \Rightarrow F_{max} = 4.512 \times 10^7 / 477.18 = 94,556 \text{ lb.}$$

The minimum tensile area of the 1½ inch diameter tie rod is at the threads and is 1.490 in². The maximum allowable stress is lesser of $0.7S_u$ or S_y (Level D, Bolted joint, F1335.1, [4]). The maximum impact limiter surface temperature at bracket attach to tie-rod is around 120°F (Chapter 3, Figure 3-10), conservatively 200°F is used for the material allowable. The tie rod material is A193 Grade B7, which has an ultimate strength, S_u , of 125 ksi [4] at 200°F and a yield strength of $S_y = 98$ ksi [4] at 200°F. Therefore, the allowable is smaller of $0.7 \times 125 \text{ ksi} = 87.5 \text{ ksi}$ or $S_y = 98 \text{ ksi}$. So for orientation 1, the maximum tie rod tensile stress is $94,556 / 1.490 = 63.5 \text{ ksi}$, which is less than $0.7 S_u = 87.5 \text{ ksi}$.

Orientation 2 Stress Analysis

During a slapdown impact event in orientation 2, the target surface crushes the impact limiters at the double tie rod bracket located at 0° (Appendix 1.4, Drawing 10421-71-40). The angular locations of each tie rod bracket from vertical (perpendicular to the target surface) are computed in the following way. The tie rods are numbered clockwise 1 through 13 starting from the first tie rod located just above the 270° mark.

Tie Rod Number	Tie Rod Bracket Type	Angular Location Calculation (For Orientation 2)	Angular Location
1	Double	$90^\circ + \arctan[4.31/(124.00/2)] =$	94°
2	Single	$90^\circ + 30^\circ =$	120°
3	Double	$90^\circ + 90^\circ - \arctan[4.31/63.00] =$	176°
4	Double	$90^\circ + 90^\circ + \arctan[4.31/63.00] =$	184°
5	Single	$90^\circ + 120^\circ =$	210°
6	Single	$90^\circ + 150^\circ =$	240°
7	Single	$90^\circ + 180^\circ =$	270°
8	Single	$90^\circ + 210^\circ =$	300°
9	Single	$90^\circ + 240^\circ =$	330°
10	Double	$90^\circ + 270^\circ - \arctan[4.31/63.00] =$	356°
11	Double	$90^\circ + 270^\circ + \arctan[4.31/63.00] =$	364°
12	Single	$90^\circ + 330^\circ =$	420°
13	Double	$360^\circ + 90^\circ - \arctan[4.31/(124.00/2)] =$	446°

Compute the vertical distance from the target surface to each tie rod as follows.

Tie Rod Number	Tie Rod Bracket Type	Vertical Distance Calculation (in.) (For Orientation 2)	Vertical Distance (in.)
1	Double	$[4.31^2 + (124/2)^2]^{1/2} \cos(94^\circ) + 91.00/2 =$	41.16
2	Single	$(124.00/2) \cos(120^\circ) + 91.00/2 =$	14.50
3	Double	$[4.31^2 + 63.00^2]^{1/2} \cos(176^\circ) + 91.00/2 =$	-17.50
4	Double	$[4.31^2 + 63.00^2]^{1/2} \cos(184^\circ) + 91.00/2 =$	-17.50
5	Single	$(124.00/2) \cos(210^\circ) + 91.00/2 =$	-8.19
6	Single	$(124.00/2) \cos(240^\circ) + 91.00/2 =$	14.50
7	Single	$(124.00/2) \cos(270^\circ) + 91.00/2 =$	45.50
8	Single	$(124.00/2) \cos(300^\circ) + 91.00/2 =$	76.50
9	Single	$(124.00/2) \cos(330^\circ) + 91.00/2 =$	99.19
10	Double	$[4.31^2 + 63.00^2]^{1/2} \cos(356^\circ) + 91.00/2 =$	108.49
11	Double	$[4.31^2 + 63.00^2]^{1/2} \cos(364^\circ) + 91.00/2 =$	108.50
12	Single	$(124.00/2) \cos(420^\circ) + 91.00/2 =$	76.50
13	Double	$[4.31^2 + (124/2)^2]^{1/2} \cos(446^\circ) + 91.00/2 =$	49.84

In the table above, negative vertical distances correspond to tie rods that are below the crush line of the impact limiter. Therefore, these tie rods are conservatively considered to be ineffective and not carry any of the prying load.

The set of tie rods farthest away from the target surface (tie rods 10 and 11) are assumed to carry the maximum tensile force, F_{\max} . All other tie rods are assumed to carry a tensile force linearly proportional to their distance from the target surface. Therefore, each tie rod will carry the following prying moment.

Tie Rod Number	Tie Rod Bracket Type	Tensile Force In Orientation 2 (lb.)	Moment Arm (in.)	Moment (in.lb.)
1	Double	$(41.16/108.50) F_{\max}$	41.16	$15.61 F_{\max}$
2	Single	$(14.50/108.50) F_{\max}$	14.50	$1.94 F_{\max}$
3	Double	0	-	0
4	Double	0	-	0
5	Single	0	-	0
6	Single	$(14.50/108.50) F_{\max}$	14.50	$1.94 F_{\max}$
7	Single	$(45.50/108.50) F_{\max}$	45.50	$19.08 F_{\max}$
8	Single	$(76.50/108.50) F_{\max}$	76.50	$53.94 F_{\max}$
9	Single	$(99.19/108.50) F_{\max}$	99.19	$90.68 F_{\max}$
10	Double	F_{\max}	108.50	$108.50 F_{\max}$
11	Double	F_{\max}	108.50	$108.49 F_{\max}$
12	Single	$(76.50/108.50) F_{\max}$	76.50	$53.94 F_{\max}$
13	Double	$(49.81/108.50) F_{\max}$	49.81	$22.89 F_{\max}$
			Total Moment =	$477.01 F_{\max}$

Equating this total moment with M_{tot} computed above and solve for F_{max} :

$$477.01 F_{max} = 4.512 \times 10^7 \text{ in.lb.} \Rightarrow F_{max} = 4.512 \times 10^7 / 477.01 = 94,589 \text{ lb.}$$

The minimum tensile area of the 1½ inch diameter tie rod is at the threads and is 1.490 in². So for orientation 2, the maximum tie rod tensile stress is 94,589. / 1.490 = 63.5 ksi, which is less than 0.7 S_u = 87.5 ksi.

2.10.8.6.2 Tie Rod Bracket Analysis

Tie Rod Bracket And Impact Limiter Gusset Allowable Stress

The material used for the tie rod brackets and impact limiter gussets is A-240 Type 304. The allowable stress for the brackets and impact limiter gussets is S_u or 71 ksi [4] at 200°F.

Tie Rod Bracket / Impact Limiter Weld

For ¼ inch fillet welds, the throat width is $0.25 \sin(45^\circ) = 0.1768 \text{ in.}$

Single bracket:

$$\text{Area of weld} = 0.1768 \times 2(13 + 6) = 6.718 \text{ in.}^2$$

$$\sigma_{weld} = 94,589 / 6.718 = 14,080 \text{ psi} < 71,000 \text{ psi}$$

Double bracket:

$$\text{Area of weld} = 0.1768 \times 2(11 + 21.62) = 11.534 \text{ in.}^2$$

$$\sigma_{weld} = 2 \times 94,589 / 11.534 = 16,402 \text{ psi} < 71,000 \text{ psi}$$

Impact limiter gussets

Since the gussets are fillet welded on both sides to the top plate of the impact limiter, the cross sectional area of the gusset is the critical tensile area. Assume the tensile force from the tie rods acts over a length of the gusset equal to 150% of the length of the bracket reinforcement pad.

Single bracket:

$$\text{Active tensile area of gusset} = (0.19 \text{ in.})(1.5 \times 6.00 \text{ in.}) = 1.710 \text{ in.}^2$$

$$\sigma_{gusset} = 94,589 / 1.710 = 55,315 \text{ psi} < 71,000 \text{ psi}$$

Double bracket:

$$\text{Active tensile area of gusset} = (0.19 \text{ in.})(1.5 \times 11.00 \text{ in.}) = 3.135 \text{ in.}^2$$

$$\sigma_{gusset} = 2 \times 94,589 / 3.135 = 60,344 \text{ psi} < 71,000 \text{ psi}$$

Fillet weld / side plate

Single bracket:

$$\text{Throat width} = 2 \times 0.31 (45^\circ) = 0.438 \text{ in.}$$

$$\text{Stress Area} = 5 \times 2 \times 0.438 = 4.384 \text{ in.}^2$$

$$\sigma_{\text{weld}} = 94,589 / 4.384 = 21,576 \text{ psi} < 71,000 \text{ psi}$$

Double bracket:

$$\text{Throat width} = 2 \times 0.31 \sin (45^\circ) = 0.438 \text{ in.}$$

$$\text{Stress Area} = 2(2)(.25) \sin (45^\circ) + 2(5)(.438) = 5.087 \text{ in.}^2$$

$$\sigma_{\text{weld}} = 2 \times 94,589 / 5.087 = 37,189 \text{ psi} < 71,000 \text{ psi}$$

Shear stress in 2 inch top plate (allowable shear stress 0.42 S_u)

Single bracket:

$$\text{Shear Area} = 2 \times (7.00 \text{ in.} - 1.75 \text{ in.}) = 10.5 \text{ in.}^2$$

$$\tau = 94,589 / 10.5 = 9,008 \text{ psi} < 29,820 \text{ psi}$$

Double bracket:

$$\text{Shear Area} = 2 \times (7.00 \text{ in.} - 1.75 \text{ in.}) = 10.5 \text{ in.}^2$$

$$\tau = 2 \times 94,589 / 10.5 = 18,017 \text{ psi} < 29,820 \text{ psi}$$

2.10.8.6.3 Lifting Lug Analysis

The weights of the top and bottom impact limiters are 16,338 lb and 16,332 lb respectively. For the following analysis conservatively use a weight of 16,450 lb. per impact limiter. Each impact limiter is supported by two lifting lugs. The material used for the lifting lugs is also A-240 Type 304. The temperature at outer surface of impact limiter is around 120°F (Chapter 3, Figure 3-10), conservatively 150°F is used for the lifting lug analysis. The allowable shear stress is $0.5S_y = 13.75 \text{ ksi}$. The allowable primary plus bending is $S_y = 27.5 \text{ ksi}$ [4].

A 60° angle between the slings and horizontal is assumed. This allows the slings to clear the impact limiter. The loading is taken to be 3 times the weight of the impact limiter. The lifting lugs are on the impact limiter CG. Figure 2.10.8-17 shows the geometry of the impact limiter lifting lugs.

The tension in the lifting sling is,

$$T = \frac{2 \times 16,450}{2} \frac{1}{\sin(60^\circ)} = 28,492 \text{ lbs}$$

The normal stress σ_n in the lifting lug is conservatively computed in the following way:

$$\begin{aligned}\text{Normal Force } F_n &= 28,492 \sin(30^\circ) = 14,246 \text{ lb} & \text{Normal Area, } A &= (1)(5-1.5) = 3.5 \text{ in.}^2 \\ \text{Normal Stress } \sigma_n &= 14,246/3.5 = 4,070 \text{ psi}\end{aligned}$$

The bending stress σ_b in the lifting lug is computed in the following way.

$$\text{Moment of Inertia, } I = (1/12)(1)(5^3) = 10.42 \text{ in.}^4 \quad F_b = 28,492 (\cos(30^\circ)) = 24,675 \text{ lb}$$

$$\sigma_b = \frac{2.5(2.5)(24,675)}{10.42} = 14,800 \text{ psi}$$

The shear stress τ in the lug is conservatively computed as follows.

$$\begin{aligned}\text{Shear Area} &= 2 \times (2.5 - 0.75)(1) = 3.50 \text{ in.}^2 \\ \tau &= 28,492/3.50 = 8,141 \text{ psi.}\end{aligned}$$

The total stress intensity is,

$$\text{S.I.} = \sqrt{(4,070 + 14,800)^2 + 4(8,141)^2} = 24,924 \text{ psi.} < 27,500 \text{ psi.}$$

The stresses in the lifting lug weld are computed as follows.

$$\begin{aligned}\text{Stress Area, } A_{lug} &= (0.375) \sin(45^\circ)(5 \times 2 + 1 \times 2) = 3.18 \text{ in}^2 \\ \text{Normal Stress } \sigma_n &= 14,246/3.18 = 4,480 \text{ psi} \\ \text{Moment of inertia, } I_{weld} &= (2/12)(0.375) \sin(45^\circ)(5^3) + (2/12)(1)[0.375 \sin(45^\circ)]^3 \\ &\quad + 2[0.375 \sin(45^\circ)](1)(2.5^2) = 8.84 \text{ in}^4.\end{aligned}$$

$$\begin{aligned}\sigma_b &= \frac{2.5(2.5)(24,675)}{8.84} = 17,446 \text{ psi} \\ \tau &= 24,675 / 3.18 = 7,759 \text{ psi}\end{aligned}$$

$$\text{S.I.} = \sqrt{(4,480 + 17,446)^2 + 4(7,759)^2} = 26,862 \text{ psi.} < 27,500 \text{ psi.}$$

2.10.8.6.4 Impact Limiter Attachment Bolt and Bracket Analysis

The thirteen tie rods attached to both impact limiters are designed to hold the impact limiter on the cask during all drop scenarios without the aid of the attachment bolts. The purpose of the eight attachment bolts and brackets is to hold the top impact limiter on the cask body during a tip over event immediately following a near 90° corner drop.

After a high angle corner drop (45° to 90°) the crushing of the impact limiter (from inside where the cask contacts the impact limiter) on the bottom (impact side) could cause the tie rods to become loose. In the event that the tie rods become loose, and the package tips over (second impact) the attachment bolts will hold the top impact limiter in place.

The following calculation shows that the attachment bolts and brackets are structurally adequate to withstand the load corresponding to a tip over (second impact) event. Four 1½ – 8UN bolts are used to attach the top impact limiter to the cask in the event of a 30 foot corner drop where the impact limiter crushing exceeds 12.00 inches from the inside where the cask tips over (immediately after a corner drop) when the top impact limiter's inertia would tend to pull it off the cask.

During the tip over, after a corner drop, simple energy conservation laws are used to determine the maximum axial acceleration that the top impact limiter could experience. All of the potential energy of the package in the CG over corner drop impact position is assumed to be converted into rotational energy (the CG over corner drop impact position yields the highest potential energy). This is conservative since some of the potential energy in the package is converted to vertical translational energy. Figure 2.10.8-18 shows the height of the center of gravity of the package in the impact position, H_1 , and after the tip over, H_2 .

The axial distance from the bottom of the bottom impact limiter to the CG is given by:

$$91.42 \text{ in. (distance from bottom of cask to CG)} + 38.00 \text{ in. (thickness of impact limiter)} \\ = 129.42 \text{ in.}$$

The weight of the TN-40 Transport Package is $W = 271,455 \text{ lb.}$ For this analysis, a weight of 272,000 lb is conservatively used. Therefore, the potential energy change of the package during tip over ΔPE is therefore:

$$\Delta PE = W \Delta H = 272,000 \text{ lb.} \times (148.10 - 72.00) = 2.070 \times 10^7 \text{ in. lb.}$$

Where, ΔH is the change in height of the package during tip over. This energy is assumed to be converted entirely into rotational energy of the package ΔKE which is equal to the following:

$$\Delta KE = \frac{1}{2} I \omega^2$$

Where I is the moment of inertia of the package about the pivot point, and ω is the rate of rotation of the cask after tip over. The moment of inertia of the TN-40 transport package about its center of gravity, I_{CG} , is $3.393 \times 10^6 \text{ lbf.in.sec}^2$ [Section 2.2]. Therefore the moment of inertia of the package about the pivot point is:

$$I = I_{CG} + m r^2 = 3.393 \times 10^6 + (272,000/386.4) \times 148.10^2 = 1.883 \times 10^7 \text{ lbf.in.sec}^2.$$

Then,

$$\Delta PE = \Delta KE = \frac{1}{2} I \omega^2 \\ \Rightarrow \omega^2 = 2 \Delta PE / I = 2 \times 2.070 \times 10^7 / 1.883 \times 10^7 = 2.2 \text{ rad}^2 / \text{sec}^2$$

The axial centripetal acceleration a associated with this angular velocity is:

$$a = r \omega^2 = 270.62 \times 2.2 = 595.4 \text{ in. sec.}^{-2}$$

Here, r is the distance from the pivot point to the end of the top impact limiter ($r = [260.87^2 + 72^2]^{1/2} = 270.62$ in). The corresponding g-load is $a / g = 595.4/386.4 = 1.54$ g.

Therefore, for analysis purpose, assume that the top impact limiter experiences 1.6 g during tip over. A conservative weight of 16,500 lb is used for the top impact limiter. Therefore, the tensile force applied to the four bolts is:

$$16,500 \times 1.6 = 26,400 \text{ lbs.}$$

The tensile force per bolt is,

$$26,400 / 4 = 6,600 \text{ lb/bolt}$$

Attachment Bolt Stress Analysis

The Stress area for a 1½ – 8UN bolt is 1.4899 in² [3]. Therefore the tensile stress is $6,600 / 1.4899 = 4,430$ psi.

The impact limiter bolt material is A540 Class 2 with allowable stress equal to the smaller of $0.7 S_u = 108.5$ ksi ($S_u = 155$ ksi at 250°F [4]) or $S_y = 131.55$ ksi [4] at 250°. The above calculated stress of 4430 psi is well below the allowable stress of 108.5 ksi.

Attachment Bolt Bracket Stress Analysis

The geometry of the TN-40 impact limiter attachment bolt is provided in Drawing 10421-71-44 in Chapter 1, Appendix 1.4.1. The load applied to the bracket by the bolt is counteracted by shear force in the fillet weld between the bracket and the outer shell. The resulting shear stress in the weld is calculated in the following way. The throat area of the weld A_t is:

$$A_t = 0.75 \cos(45^\circ) = 0.530 \text{ in.}$$

The weld shear area is $7 \times 0.530 = 3.712$ in² (weld length is 7 inches, so that the bolt holes are not welded over).

The shear stress per bracket, τ , is:

$$\tau = 6,600 / 3.712 = 1,778 \text{ psi.}$$

The bracket material is A516 Grade 70. Therefore the allowable shear stress is $0.42 S_u$ or 29.4 ksi ($S_u = 70$ ksi at 250°F [4]), which is well above the calculated shear stress.

The bending stress in the bolting bracket is computed assuming that only the 5 inch tall plate carries the bending load. The moment of inertia of the plate is:

$$I = \frac{10 \times 0.75^3}{12} = 0.3516 \text{ in.}^4$$

The applied moment is:

$$M = 6,600 \times 2.66 = 17,556 \text{ in. lb.}$$

$$\sigma = \frac{Mc}{I} = \frac{17,556 \times (0.75/2)}{0.3516} = 18,724 \text{ psi.} < 70,000 \text{ psi.}$$

2.10.8.6.5 Impact Limiter Shell Stress Analysis

Using the geometry of the TN-40 impact limiter bolt bracket and gusset plate/bolting boss from drawings 10421-71-43 and 10421-71-44, in Chapter 1, Appendix 1.4.1, a stress analysis is performed on the impact limiter bolt connection. The material used for the gusset plate is A-240 Type 304 with $S_y = 23.75$ ksi, and $S_u = 68.5$ ksi [4] at 250°F. Conservatively assuming the entire load is carried by the gusset plate/welds and that the ¼ inch thick impact limiter plate does not bear any of the bolt load the corresponding stresses are analyzed. The length of the moment arm acting on the gusset plate and bottom gusset plate weld is measured from the bolting boss center (where the load is applied) to the termination of the gusset plate at the side impact limiter plate which is 7.16 inches. Referring to the bolt load calculated in section 2.10.8.6.4 the applied moment on the gusset plate and attachment weld is:

$$6,600 \text{ lb}(7.16 \text{ inches}) = 47,256 \text{ in lb}$$

Similarly the moment arm for the gusset plate/bolting boss interface is measured from the center of the bolting boss to the gusset plate/bolting boss connection which results in an applied moment of:

$$6,600 \text{ lb}(1.5 \text{ inches}) = 9,900 \text{ in lb}$$

Since both welds have the same stress area and moment of inertia, the bottom weld is the limiting case for analysis. The stress area and moment of inertia for the bottom weld are:

$$\text{Stress Area} = 0.25 \sin(45^\circ)(2(3.5 + 0.375)) = 1.37 \text{ in}^2$$

Moment of inertia,

$$I_{\text{weld}} = (2/12)(0.25) \sin(45^\circ)(3.5^3) + (2/12)(0.25)[0.25 \sin(45^\circ)]^3 \\ + 2[0.25 \sin(45^\circ)](0.25)(3.5^2) = 1.67 \text{ in}^4$$

The corresponding shear and bending stresses in the bottom weld are then

$$\text{Shear Stress, } \tau = 6,600 / 1.37 = 4,818 \text{ psi} < 0.42 S_u (28,770 \text{ psi})$$

$$\text{Bending Stress, } \sigma_b = \frac{Mc}{I} = \frac{47,256 \times \left(\frac{3.5}{2}\right)}{1.67} = 49,520 \text{ psi} < S_u (68,500 \text{ psi})$$

Using a similar analysis for the gusset plate gives a stress area and moment of inertia of

$$\text{Stress Area} = 0.375(3.5) = 1.3125 \text{ in}^2$$

and

$$\text{Moment of inertia, } I_{\text{plate}} = (1/12)(0.375)(3.5^3) = 1.34 \text{ in}^4$$

The corresponding shear and bending stresses in the gusset plate are then

$$\text{Shear Stress, } \tau = 6,600 / 1.3125 = 5,029 \text{ psi} < 0.42 S_u (28,770 \text{ psi})$$

$$\text{Bending Stress, } \sigma_b = \frac{Mc}{I} = \frac{47,256 \times \left(\frac{3.5}{2}\right)}{1.34} = 61,715 \text{ psi} < S_u (68,500 \text{ psi})$$

2.10.8.6.6 Attachment Bolt Torque

Assume a bolt force, F_a , of 6,600. The torque required is:

$$Q = K D_b F_a = 0.1 \times 1.5 \times 6,600 = 990 \text{ in.lb.} = 82.5 \text{ ft.lb.}$$

Where F_a is the bolt force, Q is the applied torque, K is the nut factor (0.1 with lubrication), and D_b is the nominal bolt diameter.

For a bolt torque of 60 ft. lb.,

$$F_a = \frac{Q}{K D_b} = \frac{60 \times 12}{0.1 \times 1.5} = 4,800 \text{ lb.}$$

For a bolt torque of 80 ft. lb.,

$$F_a = \frac{Q}{K D_b} = \frac{80 \times 12}{0.1 \times 1.5} = 6,400 \text{ lb.}$$

Therefore, the maximum tensile stress in the bolt due to pretension is $6,400/1.4899 = 4,296$ psi which is less than $0.7S_u = 108.5$ ksi.

2.10.8.7 Summary of ADOC Results Used for Structural Analysis

Cask Structural Analysis, g-Load and Drop Orientation

In order to determine the cask stresses, the maximum g-loads from ADOC runs are converted to forces and applied as quasistatic loadings on the cask body. A detailed ANSYS finite element model of the TN-40 cask is used to perform this analysis.

Only the loads corresponding to the most critical normal and accident condition free drop orientations are used in the cask body analysis in Appendix 2.10.1. For the 30 foot accident condition drops, g-loads corresponding to four different angles are evaluated, and for the 1 foot normal condition drops, g-loads corresponding to two different angles are evaluated. The orientations evaluated in Appendix 2.10.1 are as follows.

Drop Height (Normal / Accident)	Orientation Analyzed
30 Foot Accident Condition Drop	0° Side Drop
	20° Slap Down
	63.8° C.G. Over Corner Drop
	90° End Drop
1 Foot Normal Condition Drop	0° Side Drop
	90° End Drop

The g-loads corresponding to these drop orientations are provided in Tables 2.10.8-3, 2.10.8-4, and 2.10.8-7.

The thirty foot side drop is evaluated because it produces the highest normal transverse g-load. The 20°, thirty foot slap down is analyzed because it produces a high normal as well as rotational g-load at the ends of the cask (second impact). Stresses in the cask and lid bolts are most sensitive to g-loads applied in the 63.8° (CG over corner) direction. Consequently, the thirty foot CG over corner drop is evaluated. The highest axial g-load occurs during a 90°, thirty foot end drop, and is therefore also evaluated.

For the normal condition one foot drops, the 0° side drop, and the 90° end drop are bounding, since they produce the highest normal g-loads in the transverse and axial directions respectively. The g-loads from other drop angles are small and generate insignificant rotational inertia g-loads due to much lower impact velocity.

The g-loads predicted by ADOC and used in the cask body analysis are shown in Table 2.10.8-9.

Basket Structural Analysis, g-Load and Drop Orientation

The loading conditions considered in the evaluation of the fuel basket consist of inertial loads resulting from normal handling (1 foot drop) and hypothetical accident (30 foot) drops. The inertial loads of significance for the basket analysis are those that act transverse to the cask and basket structural longitudinal axes, so that the loading from the fuel assemblies is applied normal to the basket plates and is transferred to the cask wall by the basket. The side drop will result in the highest inertia load due to the fuel assemblies impacting the basket. For example, the transverse g-load (normal) resulting from maximum wood properties, 0° side drop is 51 g, and the maximum transverse g-load (normal) resulting from 5° slap down second impact is about 27 g. The rotational g-loads from slap down impact have a very small effect on the basket because the cask stiffness is much greater than the basket stiffness and the basket is enveloped by the cask. Any rotational bending affect will be absorbed by the cask body. Therefore, the basket structure is analyzed for 1 foot and 30 foot side drops. For clarity, the basket structure is also analyzed for 1 foot and 30 foot end drops to show a large margin of safety.

Table 2.10.8-10 lists the g-loads (including dynamic load factors calculated in Appendix 2.10.6) used for the basket structural analysis.

2.10.8.8 Summary Description of ADOC Computer Code

One of the accident conditions which must be evaluated in the design of transport packagings to be used for the shipment of radioactive material is a free drop from a thirty-foot height onto an unyielding surface (10CFR71). The packaging must be dropped at an orientation that results in the most severe damage. Impact limiters are usually provided on the packaging to cushion the effects of such impact on the containment portion of the packaging. The limiters are usually hollow cylindrical cups which encase each end of the containment and are filled with an energy absorbing material such as wood.

A computer code, ADOC (Acceleration due to Drop On Covers), has been written to determine the response of a packaging during impact. The analysis upon which this code is based is discussed in this section. The overall analysis of the packaging response is discussed in Section 2.10.8.8.1, and the methods used to compute the forces in the limiters as they crush are presented in Section 2.10.8.8.2.

2.10.8.8.1 General Formulation

The general formulation used to compute the response of the packaging as it impacts with a rigid target is discussed in this section. The assumptions upon which the analysis is based are first presented followed by a detailed development of the equations of motion used to calculate the packaging dynamic behavior. This is followed by a discussion of the numerical methods and the computer code used to implement the analysis. A significant part of the development is concerned with the prediction of

forces developed in the impact limiters as the impact occurs. This aspect of the evaluation is discussed in Section 2.10.8.8.2.

Assumptions

The cask body is assumed to be rigid and axisymmetric. Therefore, all of the energy absorption occurs in the impact limiters which are also assumed to have an axisymmetric geometry. Several assumptions are made in calculating the forces which develop in the limiters as they crush. These are discussed in Section 2.10.8.8.2. Since the packaging is axisymmetric, its motion during impact will be planar. The vertical, horizontal, and rotational components of the motion of the packaging center of gravity (CG) are used to describe this planar motion.

Equations of Motion

A sketch of the packaging at the moment of impact is shown on Figure 2.10.8-6. The packaging is dropped from a height H , measured from the lowest point on the packaging to the target. The packaging is oriented during the drop, and at impact, so that the centerline is at an angle r with respect to the horizontal. At the instant of impact, the packaging has a vertical velocity of

$$V_0 = \sqrt{2gH} \quad (1)$$

Where g is the gravitational constant.

At some time t after first impact, the packaging has undergone vertical u , horizontal x , and rotational ρ displacements. The location of the packaging at this time is shown on Figure 2.10.8-7. One or both of the limiters have been crushed as shown. The resulting deformations (and strains) in the limiters result in forces which the limiters exert on the packaging, thereby decelerating it. These forces, and their points of application on the packaging, are shown on Figure 2.10.8-7 as F_{v1} , F_{v2} , and F_h . The method used to calculate these forces and the points of application are provided in Section 2.10.8.8.2, below.

The three equations of motion of the cask are:

$$M\ddot{u} + F_{v1} + F_{v2} - W = 0, \quad (2)$$

$$M\ddot{x} - F_h = 0, \text{ and} \quad (3)$$

$$J\ddot{\rho} - F_{v1}x_{v1} + F_{v2}x_{v2} + F_h y_h = 0. \quad (4)$$

Where M is the mass of packaging, J is the polar moment of inertia of the packaging about its CG, W is the packaging weight, and $\ddot{}$ denotes acceleration. At impact ($t = 0$), all of the initial conditions are zero except that $u =$ the vertical velocity.

Computer Solution

The computer code is written to compute the motion of the packaging during impact. The solution is obtained by numerically integrating the equations of motion (equations 2, 3, and 4) from the time of impact, $t = 0$, to a specified maximum time, t_{max} . The integrations are carried forward in time at a specified time increment, Δt . Parametric studies indicate that a time increment of 1 msec is sufficiently small so that further reduction of the time increment does not affect the results. Solutions are usually carried out to about 150 msec for the near horizontal drops and to about 50 msec for the near vertical drops. The significant motions of the packaging normally occur within these time periods.

A standard fourth order Runge Kutta numerical integration method is used to perform the numerical integrations. The following procedure is used to carry the solution from time t_i to time t_{i+1} . Note that at time t_i the displacements and velocities of the three degrees of freedom describing the motion of the CG of the packaging are known.

1. Calculate the deformation of each of the limiters based on the packaging geometry and the motion of the package CG (see Section 2.10.8.8.2).
2. Calculate the forces which the limiters exert on the packaging body using the deformation of the limiters and their stress-strain characteristics (see Section 2.10.8.8.2).
3. Use Equations 2, 3, and 4 to calculate the accelerations during the time interval. Use the Runge Kutta equations to calculate the location and velocity of the cask CG at time t_{i+1} .
4. Go to step (1) to repeat the process until time t_{max} .
5. Generate the output.

Output from the code consists of:

- Problem title, packaging geometry, drop conditions, and integration data.
- Limiter geometric and material property data.
- History of packaging CG motion and amount of crushing in each of the limiters.
- Force history data.
- Plot of acceleration histories.
- Plot of maximum limiter deformations.

2.10.8.8.2 Forces in Limiters

The methods used to calculate the forces F_{v1} , F_{v2} , and F_h in the limiter at a given crush depth are discussed in this section. These calculations are used to perform steps (1)

and (2) above. The limiter geometry and material specification is discussed first. The general methodology used to calculate the forces are then presented which is followed with a detailed development of the equations used to calculate the force-displacement relationships.

Limiter Geometry

A sketch of the model of a limiter is shown on Figure 2.10.8-8. Regions I, II and III are used to delineate regions where different materials are used. It should be noted that the properties of the three regions are designed to accommodate the crush requirements of the three significant drop orientations. The properties of regions I, II and III are selected to control the decelerations resulting from vertical, corner, and shallow drop orientations, respectively. The properties used to describe the stress-strain behavior of each of the three materials are discussed below. The dimensions A and B may vary for the limiters at each end of the packaging, but R_0 and R_i are taken to be the same for both limiters. The same material properties are used for each of the limiters.

General Approach

The ideal energy absorbing material is one that has a stress-strain curve that has a large strain region where the stress is constant. Such a material absorbs the maximum energy while minimizing force (which determines the magnitude of the deceleration). Wood, foam, and honeycomb materials exhibit such behavior and are prime candidates for impact limiter crushable material. If the constant stress region of the stress-strain curve is of primary interest, the forces may be calculated as the crush stress times the area of the surface defined by the intersection of the target and the impact limiter. This approach assumes that the crush stress, which acts normal to the crush surface, is not influenced by stresses acting in directions parallel to the crush surface (i.e., the confining stresses). This assumption is made in the computer code. The crush stress used as input to the code is selected to represent that value which is consistent with the degree of confinement afforded by the impact limiter geometry for the drop orientation considered.

Therefore, the crushable material is modeled in the code with a one dimensional (oriented normal to the crush surface) stress-strain law. The properties of the stress-strain law are selected to represent the degree of confinement provided by stresses acting in the other two dimensions. The properties of the crushable material are not modified as the packaging rotates but are selected to represent the material properties for the initial crush direction of the material.

A portion of the "crushed" area of the limiter is often not backed up by the packaging body (i.e., a projection of a point in this non backed up area normal to the target (impact surface) does not intersect the cask body). The user must specify the percentage of these forces which are to be included in the calculation. The confinement provided by the overall construction of the limiter will determine the extent to which these non backed up forces are actually effective. The computer code does not perform any

computations which would allow the user to judge the adequacy of the selected percentage of non backed up forces which are counted.

The evaluation of the impact area and its centroid (required to locate the impact forces) is computationally complicated because of the many variations possible in the manner in which the target intersects the limiter. This problem is resolved by dividing the surface of the limiter into many small segments. The segment is located relative to the target at each computation. If the segment's original location is below the target, then it has crushed and it contributes a force equal to the stress times its area projected on the target. The location of this force is also known. The strain at the segment may also be evaluated so that the peak strains may be determined and stresses may be evaluated for strains which fall outside of the constant crush stress region of the stress-strain law.

The forces must be calculated at each time that the solution for the packaging response is computed. The problem, therefore, is to determine the forces acting on the limiters given the current location of the packaging center of gravity. The solution for the location of the packaging center of gravity is discussed in Section 2.10.8.8.1. The procedure used to perform these computations is as follows (each of the steps is detailed below).

1. Define the location of the target relative to the limiters from the current location of the packaging center of gravity relative to the target.
2. Divide the surface of the limiter into segments and calculate the strain in a one-dimensional element spanning the distance between the center of the segment and the packaging body.
3. Compute the stress in the element from the stress-strain relationship. Multiply the stress by the area of the element projected onto the target.
4. After all of the segments on the limiter are evaluated, sum the segment forces and moments of the forces to find the total force and moment acting on the packaging.
5. Calculate the horizontal force and moment of the horizontal force.
6. Use equations 2, 3, and 4 to extend the solution to the next time step. The new solution consists of the location of the packaging CG at the new time. The above steps are then repeated. This process is continued until the specified maximum time is reached.

Details of Force Computations

Details of each of the six steps outlined above are given in this section. Note that the location of the packaging CG is known at the beginning of this computational sequence.

Deformation of the Limiter

The first step in the computation is to evaluate the location of the limiters relative to the target given the location of the packaging CG relative to the target. The limiter position relative to the target is defined by the six variables, D_1 through D_6 , as shown on Figure 2.10.8-9. The location of the cask at first contact is shown in Figure 2.10.8-9a with the subscript 0 added to the D 's indicating initial values. The initial values of these parameters (when the lowest corner of the packaging first contacts) are found from the following geometric considerations.

$$\begin{aligned} D_{10} &= 2R_0 \cos \theta, \\ D_{20} &= 0, \\ D_{30} &= B_1 \sin \theta, \\ D_{40} &= D_{30} + D_{10} + L \sin \theta + B_2 \sin \theta, \\ D_{50} &= D_{40} - D_{10}, \\ D_{60} &= D_{30} + L \sin \theta, \end{aligned} \tag{5}$$

At a given time t the packaging CG has displaced vertically u horizontally x and has rotated ρ and reached the position shown in Figure 2.10.8-8b. Each of the six points have then fallen by an amount:

$$\Delta D = u + l [\sin \theta - \sin(\theta - \rho)] + r [\cos \theta - \cos(\theta - \rho)] \tag{6}$$

Where l is the axial distance CG to point (+CG to top), and r is the radial distance CG to point (+CG to impact).

Then the corner deformation, D_2 , at time, $t + l$, becomes

$$D_{2(t+1)} = D_{2t} + \Delta D_2.$$

Where

$$\begin{aligned} l_1 &= l_2 = -yL^* - B_1, \\ l_3 &= -yL^*, \\ l_4 &= l_5 = (l - y)L^* + B_2, \\ l_6 &= (l - y)L^*, \\ r_1 &= r_4 = -R_0, \text{ and} \\ r_2 &= r_3 = r_5 = r_6 = R_0. \end{aligned}$$

To facilitate the computation of strains in the limiter, the position of the limiter relative to the impact surface is classified as shown in Figure 2.10.8-10. There are three possible locations of the impact surface relative to the limiter. The task is therefore to define which of the three patterns apply, and to determine the parameters ϕ and Δ in terms of the variables D_1 through D_6 , just determined.

These deformations are next related to the three types of crush patterns for the bottom limiter shown on Figure 2.10.8-10. Crush pattern I applies when

$$D_1 < 0; D_2 < 0; D_3 > 0. \quad (8)$$

Then,

$$\Delta = -\frac{D_2}{\cos \phi}, \text{ and} \quad (9)$$

$$\phi = \cos^{-1} \frac{D_3 - D_2}{B_1}$$

Crush pattern II applies when

$$D_1 > 0; D_2 < 0; D_3 > 0. \quad (10)$$

Then,

$$\Delta = -\frac{D_2}{\cos \phi}, \text{ and} \quad (11)$$

$$\phi = \cos^{-1} \frac{D_3 - D_2}{B_1}$$

Crush pattern III applies when:

$$D_1 > 0; D_2 < 0; D_3 < 0. \quad (12)$$

Then,

$$\Delta = \frac{D_2}{\sin \phi}, \text{ and} \quad (13)$$

$$\phi = \sin^{-1} \frac{D_1 - D_2}{2R_0}$$

The same set of equations applies to the top limiter if D_1 , D_2 , D_3 , and B_1 are replaced with D_4 , D_5 , D_6 , and B_2 in equations (8) through (13).

Strains in Limiters

The next step in the computation is to calculate strains in the limiters given the deformation defined above. The limiters are first divided into segments as shown in Figure 2.10.8-11. The number of segments used for the bottom NB and the sides NS are input by the user. Locations on the surface of the limiters are described in terms of the (R, Z, β) coordinate systems shown on the figure. Strains in the segments along the sides of the limiters are calculated based on the location of the center of the segment (R_0, Z, β) . The segments at the bottom are divided into two pieces: one for $R < R_i$ (i.e. in Region 1) and the second for $R > R_i$. A strain is calculated for each of these two pieces for each segment along the bottom surface.

The strains ε are calculated as the deformation of the point normal to the crush surface δ divided by the undeformed distance of the point from the surface of the limiter to the outer container q , again measured normal to the crush surface. Therefore:

$$\varepsilon = \delta / q \quad (14)$$

Different equations govern each of these parameters for each of the three crush patterns as shown on Figure 2.10.8-10.

The geometry for crush pattern I is shown on Figure 2.10.8-12. Forces resulting from deformation of the side elements are neglected for this crush pattern. It may be shown that the deformation is:

$$\delta = \Delta \cos\phi + (R \cos\beta - R_0) \sin\phi \quad (15)$$

The undeformed length of the element is taken measured to the plane of the packaging bottom so that

$$q = A1 \cos\phi \quad (16)$$

The geometry for crush pattern II is shown on Figure 2.10.8-13. The deformation of the points on the bottom (a) and along the side (b) may be represented with the same equation

$$\delta = \Delta \cos\phi + (R \cos\beta - R_0) \sin\phi - Z/\cos\phi \quad (17)$$

The original length of the element depends on the intersection of the projection of the point on the impact surface with the outline of the limiter. These points are shown on Figure 2.10.8-13. The lengths are:

$$q_1 = \frac{A - Z}{\cos\phi}$$

$$\begin{aligned}
 q_2 &= \frac{X}{\sin \phi}, \\
 q_3 &= \frac{B-Z}{\cos \phi}, \text{ and} \\
 q_4 &= \left[(R_0^2 - R^2 \sin^2 \beta)^{1/2} + R \cos \beta \right] \sin \phi.
 \end{aligned}
 \tag{18}$$

Where $X = R \cos \beta + (R^2 \cos^2 \beta - R^2 + R_1^2)^{1/2}$.

The deformation for crush pattern III is shown on Figure 2.10.8-14. Deformations of points on the bottom of the limiter are neglected for this crush pattern. The deformation is

$$\delta = \frac{\Delta - Z / \tan \phi - R_0(1 - \cos \beta)}{\sin \phi}$$

The original length is measured to R_i so that:

$$q = \frac{R_0 - R_i}{\sin \phi}. \tag{20}$$

Segment Stress

The stresses in the elements are calculated from the above strains. As mentioned above, three sets of stress-strain laws are input to the code, one for each of the regions defined in Figure 2.10.8-8.

The location of the center of the segment on the surface of the limiter is used to determine which of the three stress-strain laws is to be used. The model may be viewed as a set of one dimensional rods which run from the center of the segment, normal to the target, to another boundary of the limiter. The entire rod is given the properties which the limiter material has at the beginning point of the rod (i.e., the intersection with the target).

The stress-strain law used for the materials is shown on Figure 2.10.8-15. Each of the seven parameters shown on the figure is input to the code for each of the three regions of the limiter. The arrows on the figure indicate the load-unload paths used in the model. The step in the crush strength is built into the stress-strain law so that two crushable materials in series may be modeled. The two crush strengths should be specified as the actual crush strengths of the two materials. The first locking strain ϵ_L should be specified as the locking strain of the weaker material times the length of the weaker material divided by the total specimen length. The higher locking strain ϵ_L

should be specified as the first locking strain plus the locking strain of the stronger material times its length and divided by the specimen length.

As stated above, the properties of the limiter material are not varied as the limiter crushes and the packaging rotates. Limiter materials such as wood exhibit anisotropic material properties. This must be accounted for when the properties are input to the code based on the anticipated direction of crushing. Most of the anisotropic wood data is based on tests performed in the elastic range. The following relationship has been used to represent wood properties for a loading which is applied at an angle α with respect to the wood grain:

$$P = \frac{P_1 \cos^4 \alpha + P_2 \sin^4 \alpha}{\cos^4 \alpha + \sin^4 \alpha} \quad (21)$$

Where P is the property of interest at angle α , and P_1 and P_2 are properties parallel and perpendicular to grain.

Evaluation of Forces

The stresses determined above are multiplied by the area of the segment projected onto the crush surface. The areas of the sidewall segments are (see Figure 2.10.8-11):

$$A_s = \frac{2R_0 B \cos(\theta - \rho)}{(NB)(NS) \tan \beta} \quad (22)$$

The area of the bottom segments is divided into two parts, one in region I and the other in region II. These areas are:

$$A_b = \frac{4R_0 L_b \sin(\theta - \rho)}{NB} \quad (23)$$

Where, $L_b = (R_i^2 - R_c^2)^{1/2}$ for region 1, and $L_b = (R_0^2 - R_c^2)^{1/2} - (R_i^2 - R_c^2)^{1/2}$ for region II.

These forces are summed for all of the elements to determine the total force acting on the packaging. The forces are also multiplied by their moment arms about the packaging CG to calculate the total moment acting on the packaging. The point on the segment is first projected, normal to the target, to evaluate whether or not it intersects the packaging body. If the projection does not intersect the packaging body, only a percentage of the force is included in the summation. The user specifies the percentage to be used.

Horizontal Force

A horizontal force develops at the limiter/target interface. This force is only considered for the bottom limiter (i.e., the first to impact) since the packaging is always close to horizontal when the top impact limiter is in contact.

The horizontal force F_h is first calculated as that required to restrain horizontal motion of the tip of the limiter.

The horizontal acceleration $\ddot{\Delta}_H$ at the tip of the bottom limiter (point 2 on Figure 2.10.8-9) may be related to the CG motion of the packaging by:

$$\ddot{\Delta}_H = \ddot{x} - \ddot{\rho}[(\gamma L + B_1)\cos\phi + R_0 \sin\phi] \quad (24)$$

Where $\phi = \frac{\pi}{2} - \theta + \rho$.

Equating Δ_H to zero would result in no acceleration of the tip in the horizontal direction and provides the solution for x in terms of ρ .

Substituting this solution for x into Equation (3) results in an expression for the horizontal force F_h required to restrict horizontal acceleration of the tip, in terms of the rotational acceleration ρ . Finally, equation 4 is used to eliminate ρ with the following result.

$$F_h = \frac{M_v W [(\gamma L + B_1)\cos\phi + R_0 \sin\phi]}{J_g + W [(\gamma L + B_1)\cos\phi + R_0 \sin\phi]^2} \quad (25)$$

Where M_v is the moment due to vertical forces, which is equal to $F_{v1}X_{v1} - F_{v2}X_{v2}$, and W is the packaging weight.

This force is restricted to:

$$F_h < \mu F_{v1} \quad (26)$$

Where μ is the coefficient of friction specified by user.

2.10.8.9 References

1. Federal Specification MMM-A-188b.
2. Dreisback, J.F., Balsa Wood and Its Properties, Columbia Graphs, Columbia, CT 1952.
3. Marks Standard Handbook for Mechanical Engineers, Eighth Edition, pg. 6-124.
4. American Society Of Mechanical Engineers, ASME Boiler And Pressure Vessel Code, Section III, Appendices, 1989.
5. 10 CFR 71, "Packaging And Transportation Of Radioactive Material."
6. Transnuclear ADOC Computer Program, Rev. 1.

Table 2.10.8-1
Mechanical Properties of Wood and Wood Adhesive

Minimum Properties of Adhesive [1]	
Shear Strength by Compression Loading	2,800 lb in ²
Shear Strength by Tension Loading	340 lb in ²
Properties of Heavy Balsa (10-12 lb ft³) [2]	
Shear Strength Parallel to Grain	315-385 psi max.
Tensile Strength Perpendicular to Grain	140-160 psi
Properties of Redwood [3]	
Shear Strength Parallel to Grain	940 psi
Tensile Strength Perpendicular to Grain	240 psi

Table 2.10.8-2
Typical Wood Material Properties

Property	High Density Balsa	Redwood
Density	10-12 lb ft ³	18.7-27.5 lb ft ³
Parallel to Grain		
Crush Stress	1560-2010 psi	5000-6500 psi
Locking Strain	0.8	0.6
Unloading Modulus	32,000 psi	1,247,000 psi
Locking Modulus	10 × (max. crush stress)	10 × (max. crush stress)
Perpendicular to Grain		
Crush Stress	300-420 psi	750-975 psi
Locking Strain	0.8	0.6
Unloading Modulus	32,000 psi	1,247,000 psi
Locking Modulus	10 × (max. crush stress)	10 × (max. crush stress)

Table 2.10.8-3
First Impact Maximum Inertia g-Load versus Initial Angle of Impact
for 30 Foot Drop, Using Maximum Wood Crush Stress Properties

Impact Angle, 30 Foot Drop	Maximum g-Load During First Impact (Bottom), Maximum Wood Properties			
	Axial	Transverse		
	CG	Top	Bottom	CG
0°	4	51	50	51
5°	7	$g_{nor} = 27^*$ $g_{rot} = 52^*$	$g_{nor} = 24$ $g_{rot} = 35$	27
10°	10	$g_{nor} = 27^*$ $g_{rot} = 51^*$	$g_{nor} = 27$ $g_{rot} = 39$	27
15°	15	$g_{nor} = 28^*$ $g_{rot} = 52^*$	$g_{nor} = 32$ $g_{rot} = 44$	32
20°	22	$g_{nor} = 27^*$ $g_{rot} = 49^*$	$g_{nor} = 39$ $g_{rot} = 51$	39
30°	26	$g_{nor} = 33^*$ $g_{rot} = 57^*$	$g_{nor} = 32$ $g_{rot} = 35$	33
40°	21	3	39	18
45°	27	3	36	19
50°	29	8	25	17
60°	29	8	15	11
63.8°	32	8	14	11
70°	38	8	12	10
80°	44	4	7	5
90°	49	3	1	2

* Maximum acceleration occurred during second impact.

Table 2.10.8-4
First Impact Maximum Inertia g-Load versus Initial Angle of Impact
for 30 Foot Drop, Using Minimum Wood Crush Stress Properties

Impact Angle, 30 Foot Drop	Maximum g-Load During First Impact (Bottom), Minimum Wood Properties			
	Axial	Transverse		
	CG	Top	Bottom	CG
0°	3	39	38	39
5°	5	$g_{nor} = 25^*$ $g_{rot} = 47^*$	$g_{nor} = 21$ $g_{rot} = 29$	28
10°	8	$g_{nor} = 23^*$ $g_{rot} = 45^*$	$g_{nor} = 22$ $g_{rot} = 35$	23
15°	12	$g_{nor} = 22^*$ $g_{rot} = 42^*$	$g_{nor} = 26$ $g_{rot} = 36$	26
20°	19	$g_{nor} = 23^*$ $g_{rot} = 43^*$	$g_{nor} = 32$ $g_{rot} = 44$	32
30°	21	$g_{nor} = 27^*$ $g_{rot} = 48^*$	$g_{nor} = 26$ $g_{rot} = 28$	27
40°	20	4	37	20
45°	24	3	32	17
50°	25	6	22	14
60°	26	7	13	10
63.8°	29	7	13	10
70°	38	7	12	10
80°	46	6	8	7
90°	37	4	1	2

* Maximum acceleration occurred during second impact

Table 2.10.8-5
Maximum Impact Limiter Deformation versus Initial Angle of Impact,
for 30 Foot Drop, using the Maximum Wood Properties

Impact Limiter Deformation using Maximum Wood Properties				
Impact Angle 30 ft Drop	First Impact (bottom)		Second Impact (top)	
	Maximum Wood Crush Depth (in.)	Maximum Wood Strain	Maximum Wood Crush Depth (in.)	Maximum Wood Strain
0°	13.58	0.462	13.42	0.451
5°	13.17	0.442	16.17	0.562
10°	15.75	0.529	15.52	0.537
15°	18.72	0.617	15.16	0.521
20°	22.26	< 0.389*	15.50	0.531
30°	29.77	< 0.463*	19.00	< 0.311*
40°	41.17	0.387	-	-
45°	37.09	0.440	-	-
50°	35.18	0.541	-	-
60°	33.00	0.593	-	-
63.8°	30.88	0.566	-	-
70°	30.63	0.615	-	-
80°	21.46	0.468	-	-
90°	10.23	0.275	-	-

*Value computed using more accurate method than ADOC. All other strain values not noted are taken from the ADOC results files which are very conservative.

Table 2.10.8-6
Maximum Impact Limiter Deformation versus Initial Angle of Impact,
for 30 Foot Drop, using the Minimum Wood Properties

Impact Limiter Deformation using Minimum Wood Properties				
Impact Angle 30 ft Drop	First Impact (bottom)		Second Impact (top)	
	Maximum Wood Crush Depth (in.)	Maximum Wood Strain	Maximum Wood Crush Depth (in.)	Maximum Wood Strain
0°	15.87	0.552	15.72	0.546
5°	14.72	0.503	18.89	0.669***
10°	17.19	0.586	18.15	0.640
15°	20.06	0.400*	17.80	0.625
20°	23.48	0.389*	18.07	0.574*
30°	31.78	0.463*	20.88	0.311*
40°	33.66	0.837	-	-
45°	41.25	0.486	-	-
50°	39.30	0.603	-	-
60°	37.13	0.672**	-	-
63.8°	34.60	0.644	-	-
70°	33.47	0.681	-	-
80°	23.95	0.532	-	-
90°	13.16	0.353	-	-

* Value computed using more accurate method than ADOC. All other strain values not noted are taken from the ADOC results files which are very conservative.

** The maximum strain is slightly higher ($0.672 - 0.630 = 0.042$) than the maximum locking strain of 0.630 (in Region II). However, the region of maximum wood strain is very small and will therefore, not affect the impact acceleration or wood mechanical properties significantly.

*** The maximum strain is slightly higher than the maximum locking strain of 0.651 (in Region III). However, the region of maximum wood strain is very small and will therefore, not affect the impact acceleration or wood mechanical properties significantly.

Table 2.10.8-7
Maximum Inertial g-Load during 1 Foot Drop

Impact Angle, 1 foot Drop	Maximum g-Load During First Impact, Maximum Wood Properties			
	Axial	Transverse		
	CG	Top	Bottom	CG
90°	12	0	0	0
0°	1	16	16	16
63.8°	5	2	3	3

Impact Angle, 1 foot Drop	Maximum g-Load During First Impact, Minimum Wood Properties			
	Axial	Transverse		
	CG	Top	Bottom	CG
90°	9	1	0	0
0°	1	12	12	12
63.8°	5	2	3	2

Table 2.10.8-8
Maximum Impact Limiter Deformation versus
Initial Angle of Impact for 1 Foot Drop

Maximum Wood Properties

Impact Angle 1 ft Drop	First Impact		Second Impact	
	Maximum Wood Crush Depth (in.)	Maximum Wood Strain	Maximum Wood Crush Depth (in.)	Maximum Wood Strain
90°	1.17	0.032	-	-
0°	2.77	0.038	2.75	0.038
63.8°	10.71	0.177	-	-

Minimum Wood Properties

Impact Angle 1 ft Drop	First Impact		Second Impact	
	Maximum Wood Crush Depth (in.)	Maximum Wood Strain	Maximum Wood Crush Depth (in.)	Maximum Wood Strain
90°	1.71	0.046	-	-
0°	3.06	0.050	3.05	0.049
63.8°	12.06	0.202	-	-

Table 2.10.8-9
Loading Used in Cask Body Analysis, Appendix 2.10.1
versus Maximum g-Loads Predicted by ADOC Program

Accident Conditions (30 Foot Drops)		
Drop Orientation	Max. g-Load from ADOC	Input Loading Used in FEA
End Drop on Lid and Bottom	49g Axial	49g Axial
Side Drop	51g Transverse	51g Transverse
CG over Corner Drop on Lid And Bottom (63.8°)	32g Axial	32g Axial
	14g Transverse	14g Transverse
20° Slap Down on Top Impact Limiter	22g Axial	22g Axial
	39g Transverse (normal)	39g Transverse (normal)

Normal Conditions (1 Foot Drops)		
Drop Orientation	Max. g-Load from ADOC	Input Loading Used in FEA
90° End Drop on Lid and Bottom	12g Axial	12g Axial
0° Side Drop	16g Transverse	16g Transverse

Table 2.10.8-10
Loading Used in Basket Structural Analysis, Appendix 2.10.5
versus Maximum g-Load Predicted by ADOC Program

Accident Conditions (30 Foot Drops)		
Drop Orientation	Maximum g-Load, from ADOC	Input g-Load Used in Basket Structural Analysis, Including Dynamic Load Factor
90° End Drop	49 g Axial	75 g Axial (Conservatively Using Higher g-load)
0° Side Drop	51 g Transverse	75 g Transverse (Conservatively Using Higher g-load)

Normal Conditions (1 Foot Drops)		
Drop Orientation	Maximum g-Load from ADOC	Input g-Load Used in Basket Structural Analysis, Including Dynamic Load Factor
90° End Drop	12 g Axial	20 g Axial
0° Side Drop	16 g Transverse	20 g Transverse

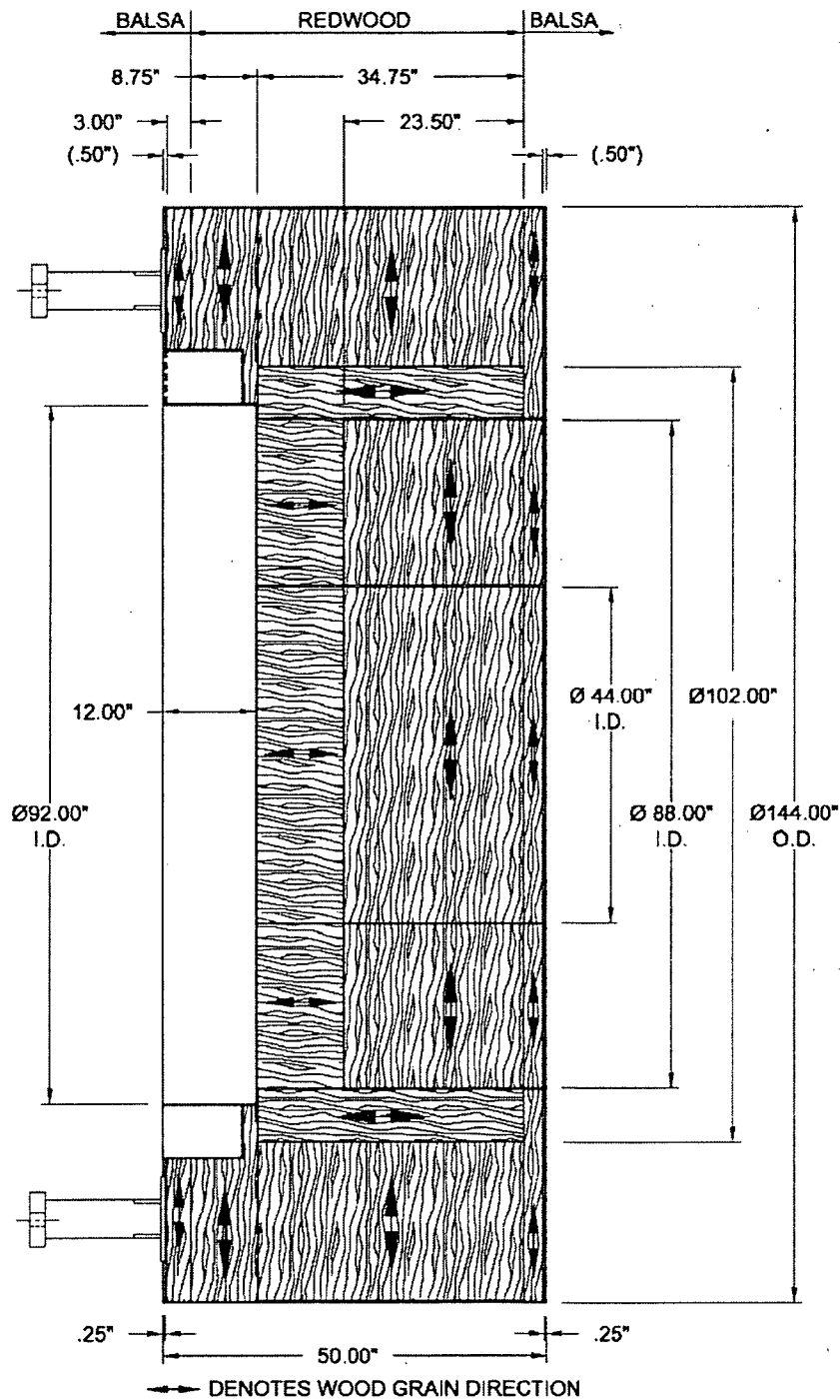


Figure 2.10.8-1
Impact Limiter Geometry

SAMPLE SIZE : 2.0"DIA × 2.0" HT.
WOOD DENSITY : 6.03 LBS/FT³

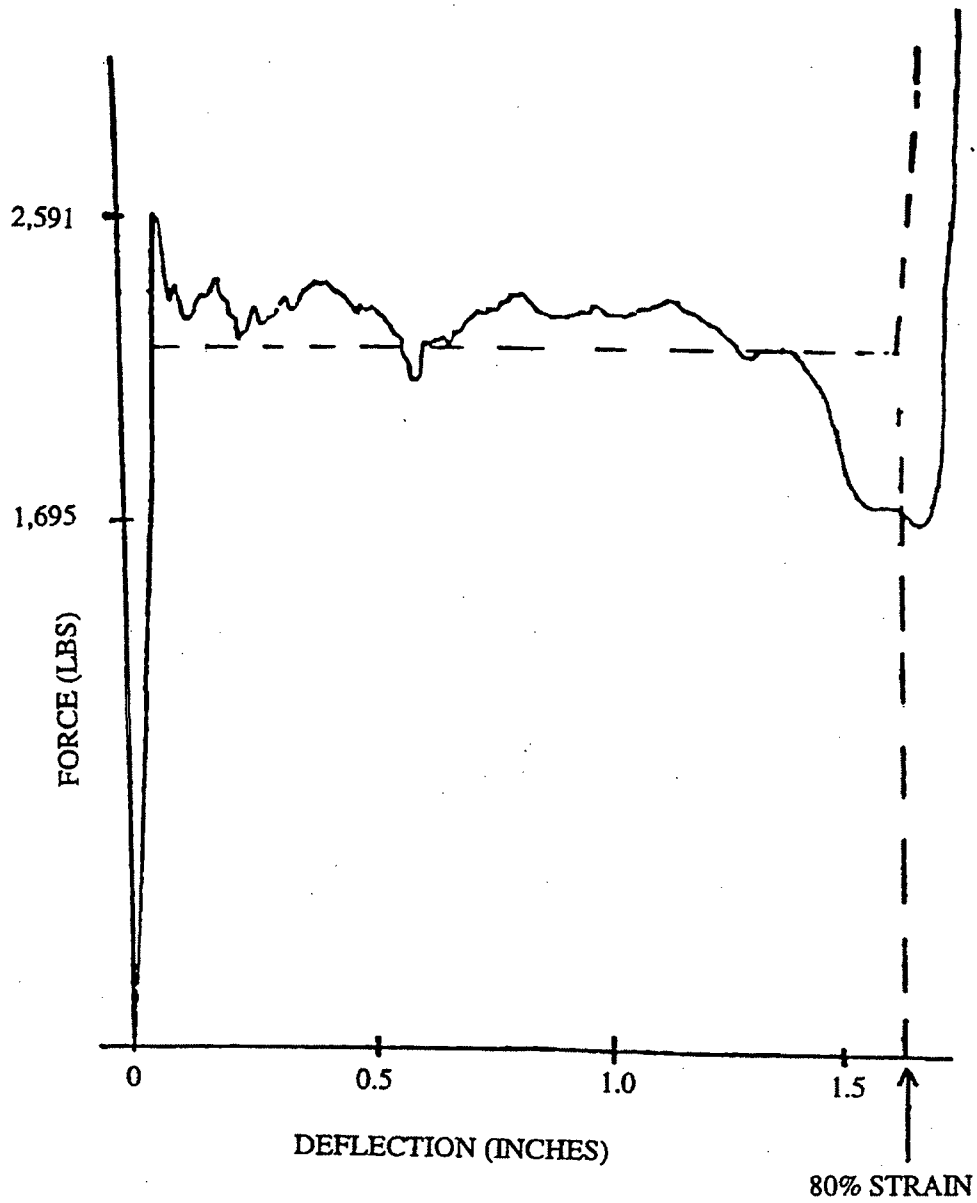


Figure 2.10.8-2
Sample Force/Deflection Curve for Balsa

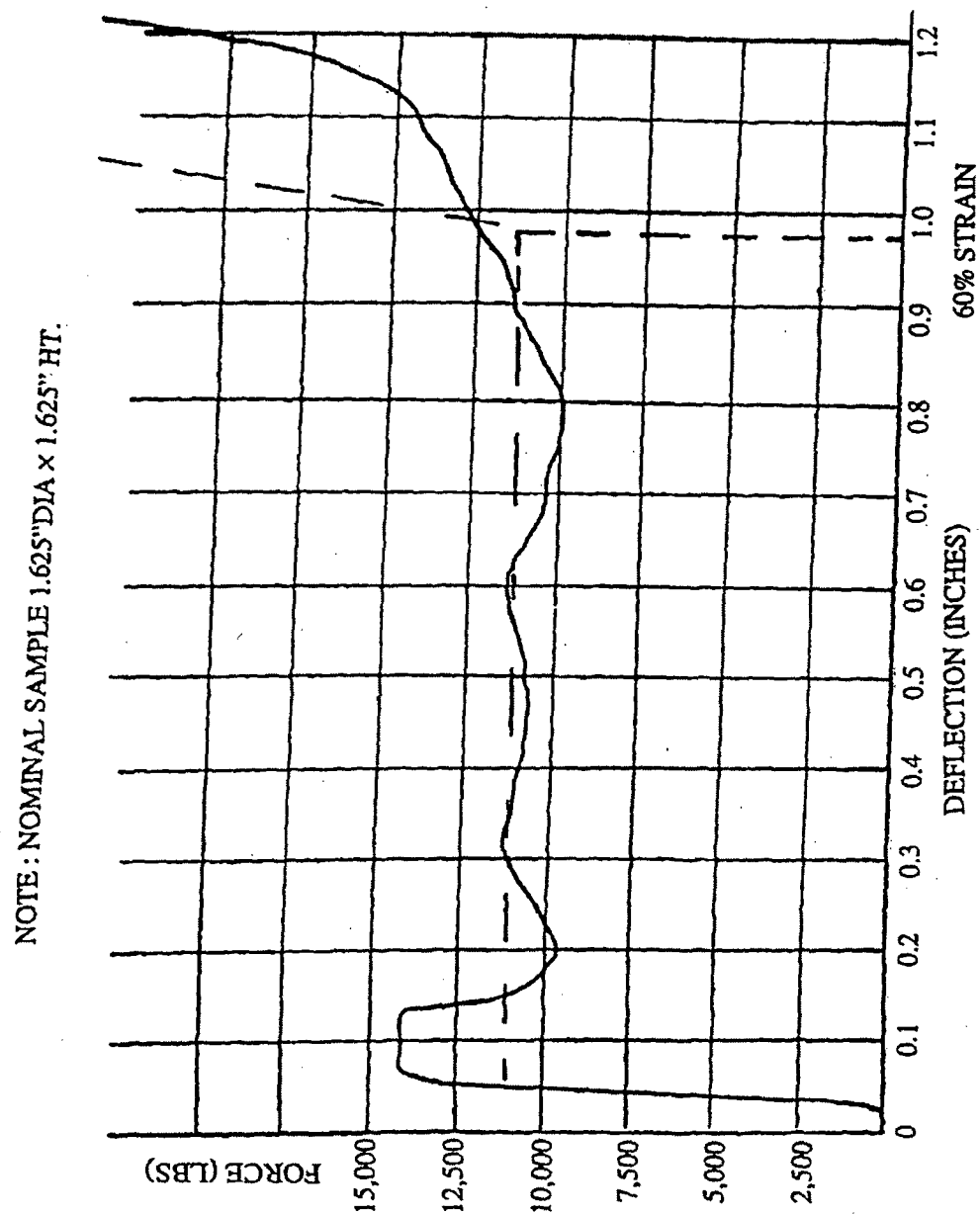
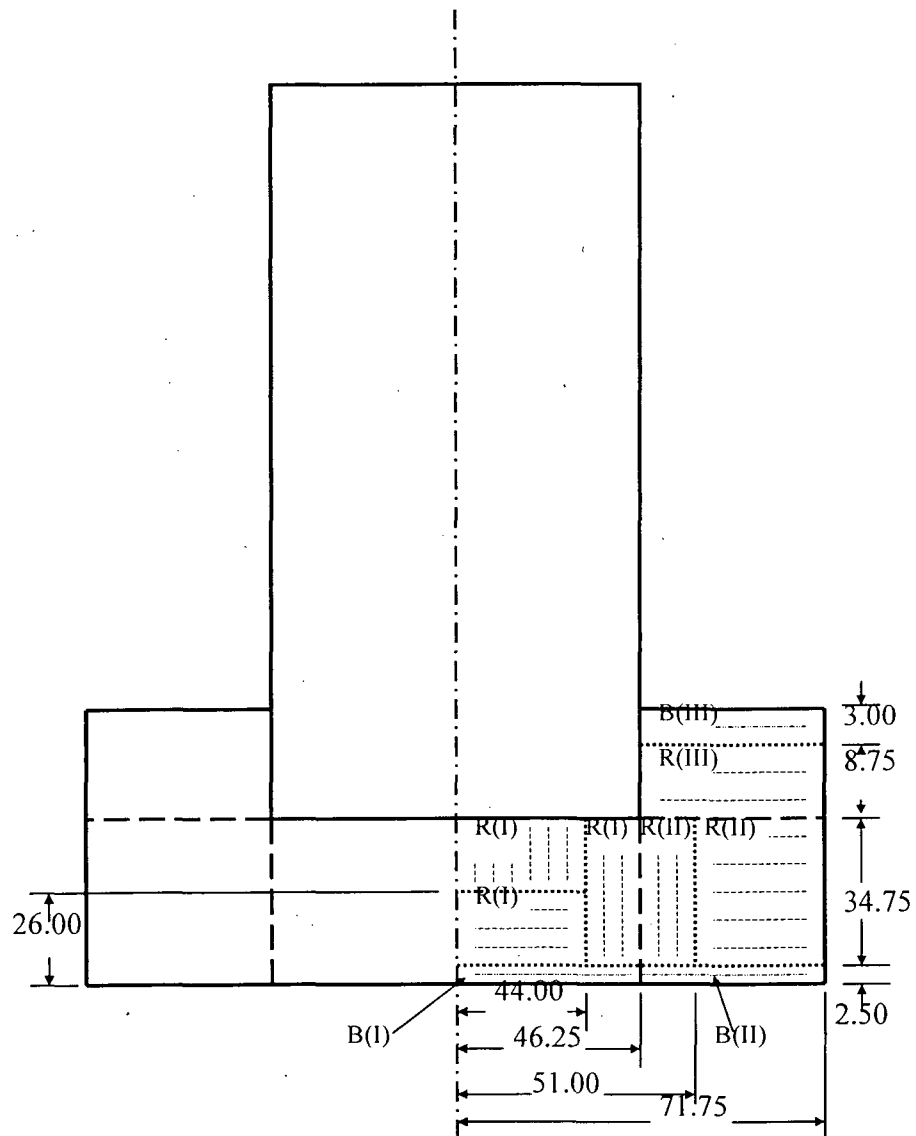


Figure 2.10.8-3
Sample Force/Deflection Curve for Redwood



B regions are bolsa.
R regions are redwood.
Dashed lines indicate grain orientation.

Figure 2.10.8-4
ADOC Computer Model for TN-40 Transport Package

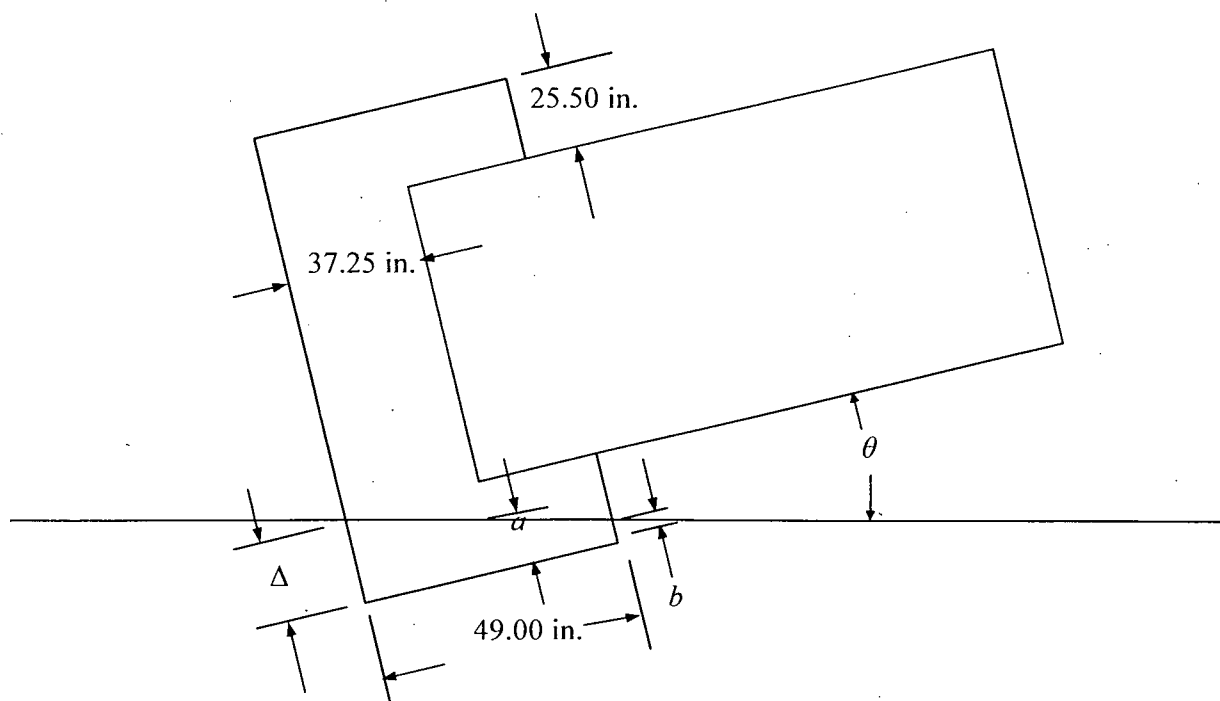


Figure 2.10.8-5
TN-40 Package Geometry during Impact for Wood Strain Computation

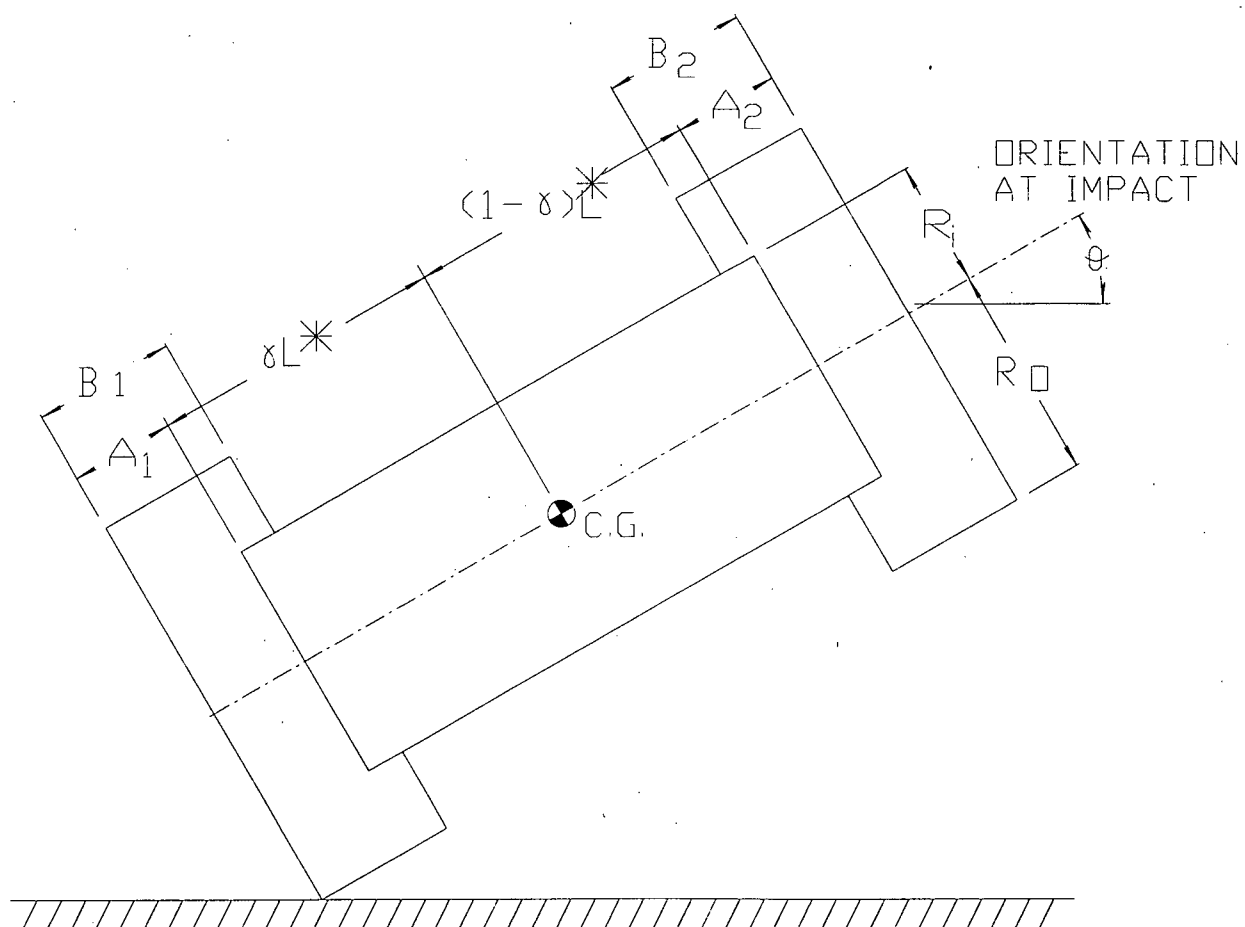


Figure 2.10.8-6
Geometry of Packaging

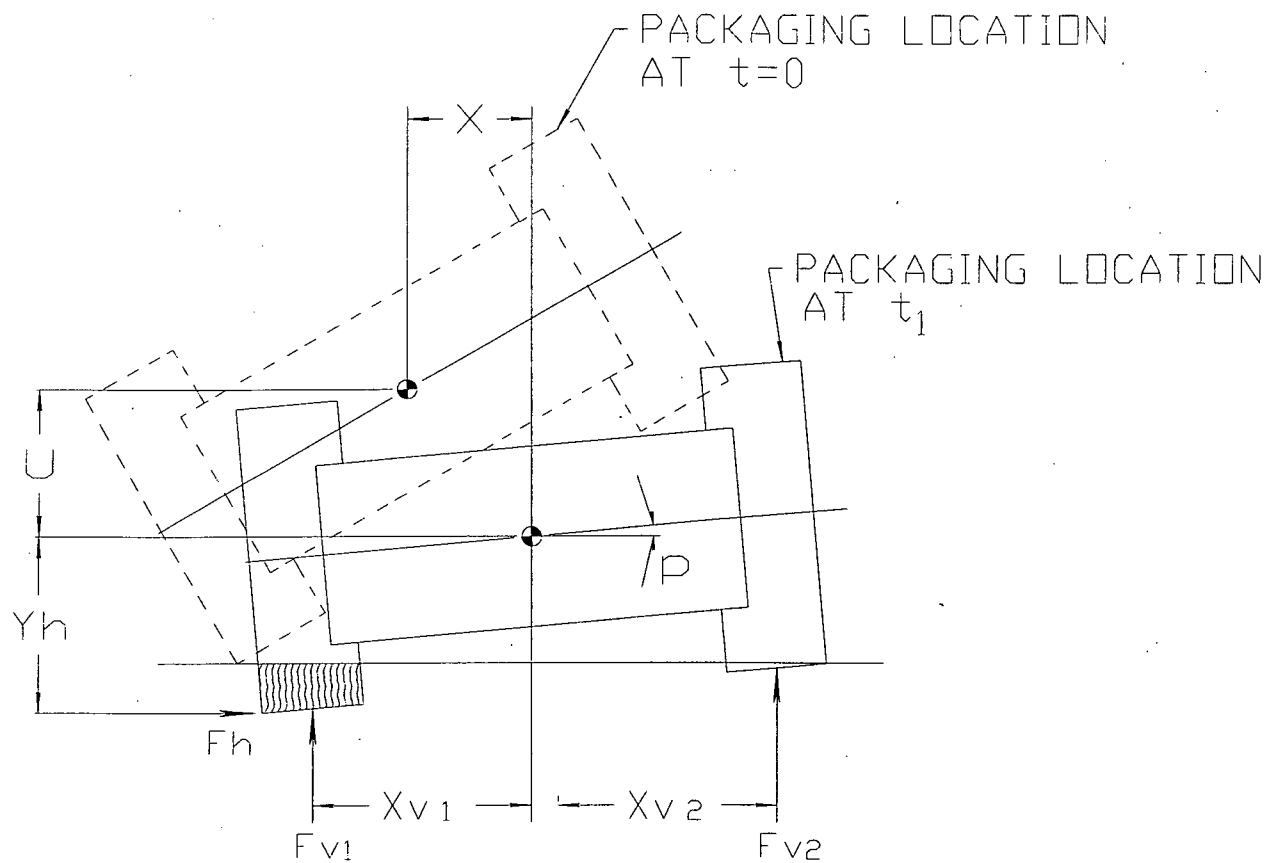


Figure 2.10.8-7
Packaging at Time, t

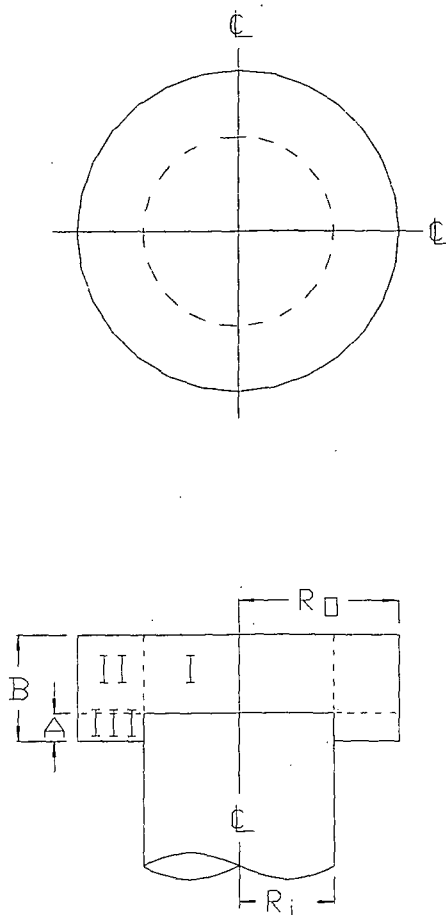
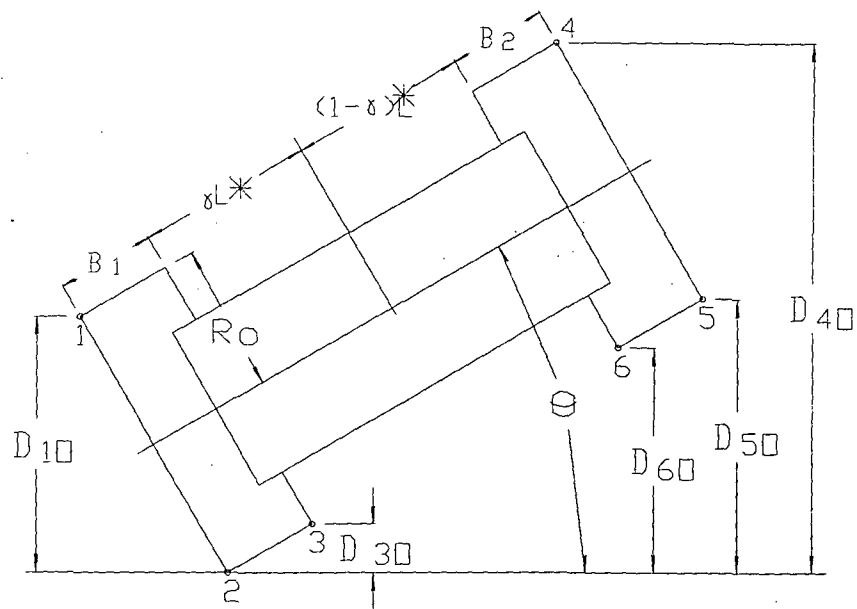
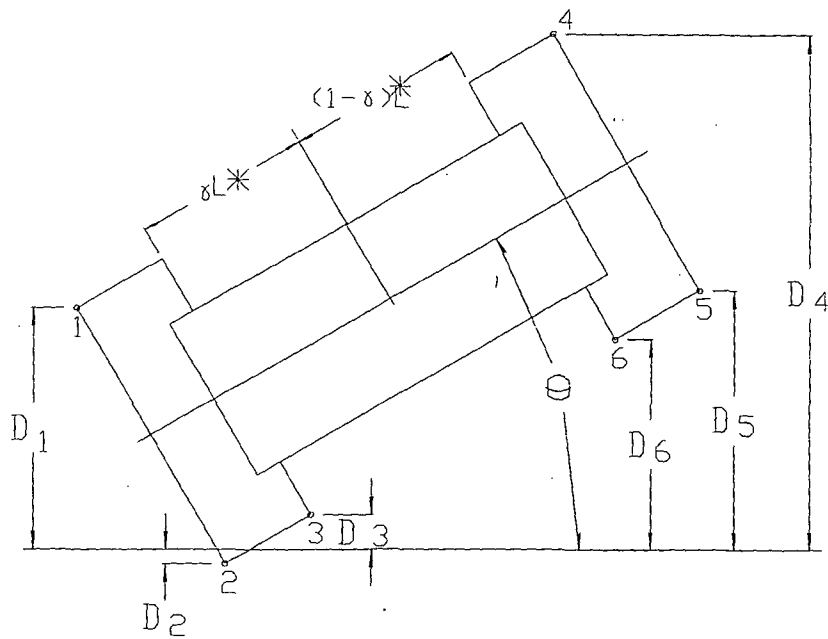


Figure 2.10.8-8
Geometry of Impact Limiter Parameters

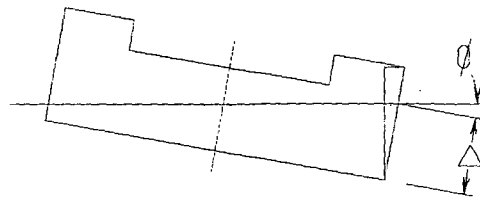


a) IMPACT LIMITER PARAMETERS AT FIRST IMPACT

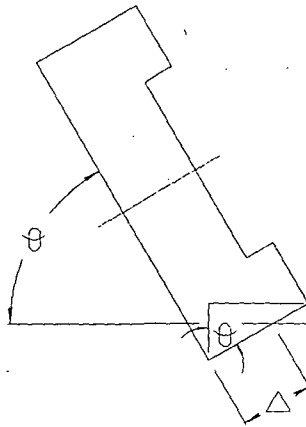


b) IMPACT LIMITER PARAMETER - GENERAL

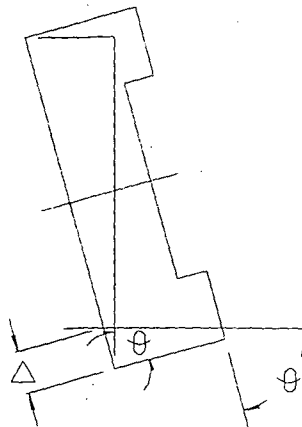
Figure 2.10.8-9
Definition of Limiter Deformation



a) CRUSH PATTERN I



b) CRUSH PATTERN II



c) CRUSH PATTERN III

Figure 2.10.8-10
Crush Pattern in Impact Limiter

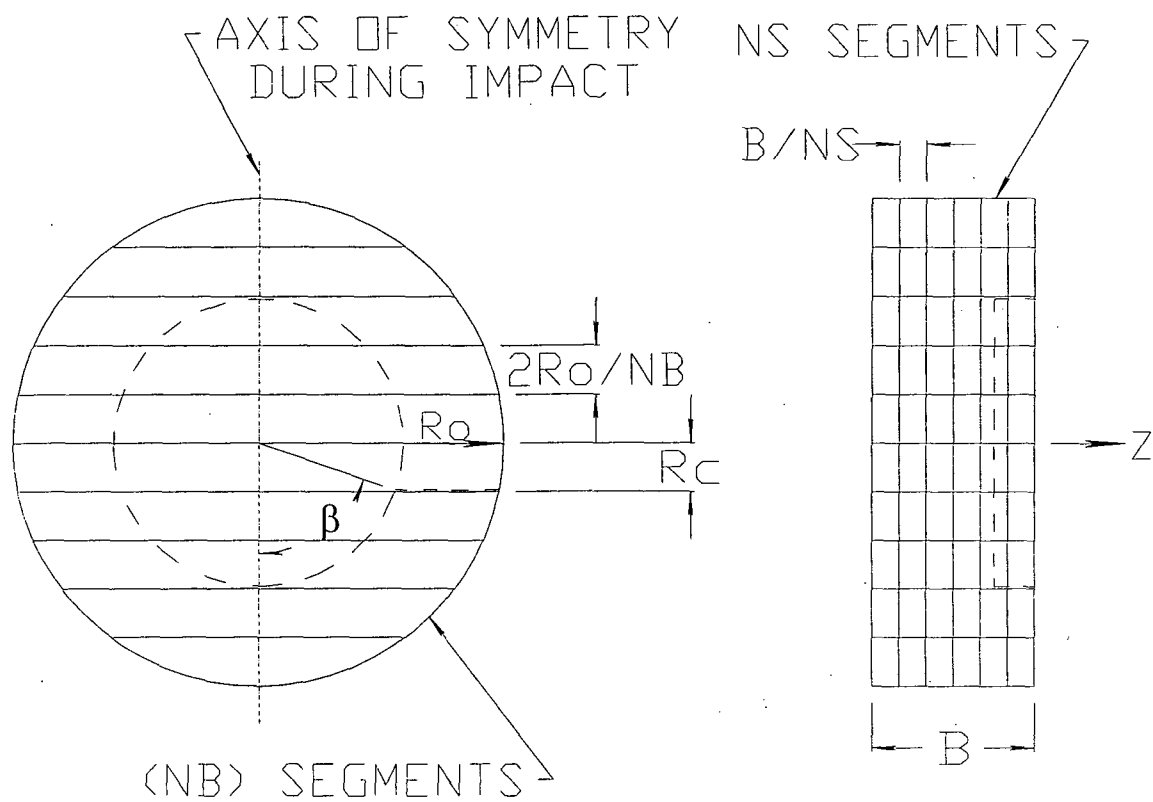


Figure 2.10.8-11
Impact Limiter Segments

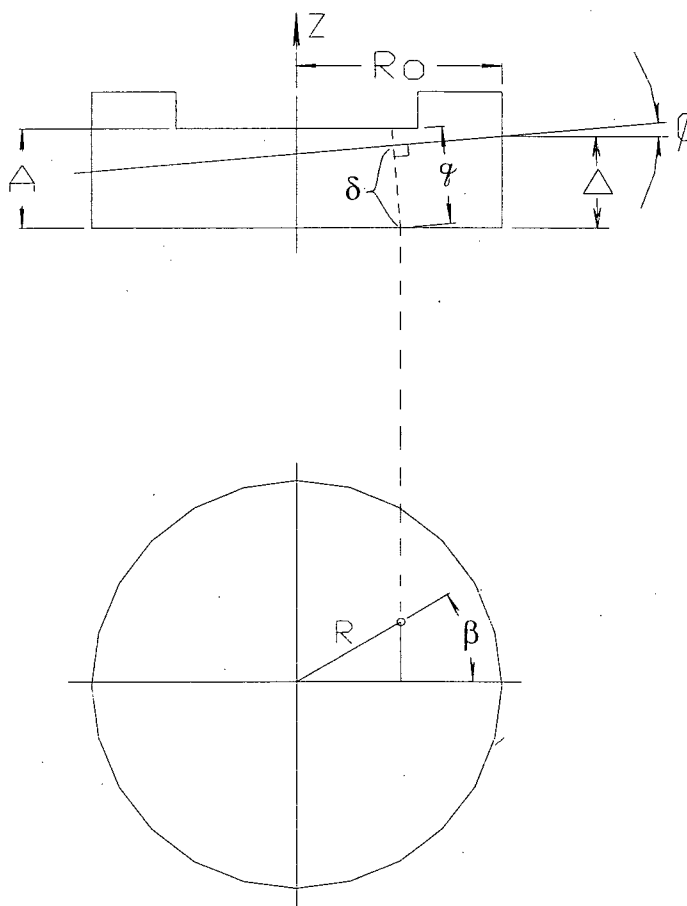


Figure 2.10.8-12
Strain Computation for Crush Pattern I

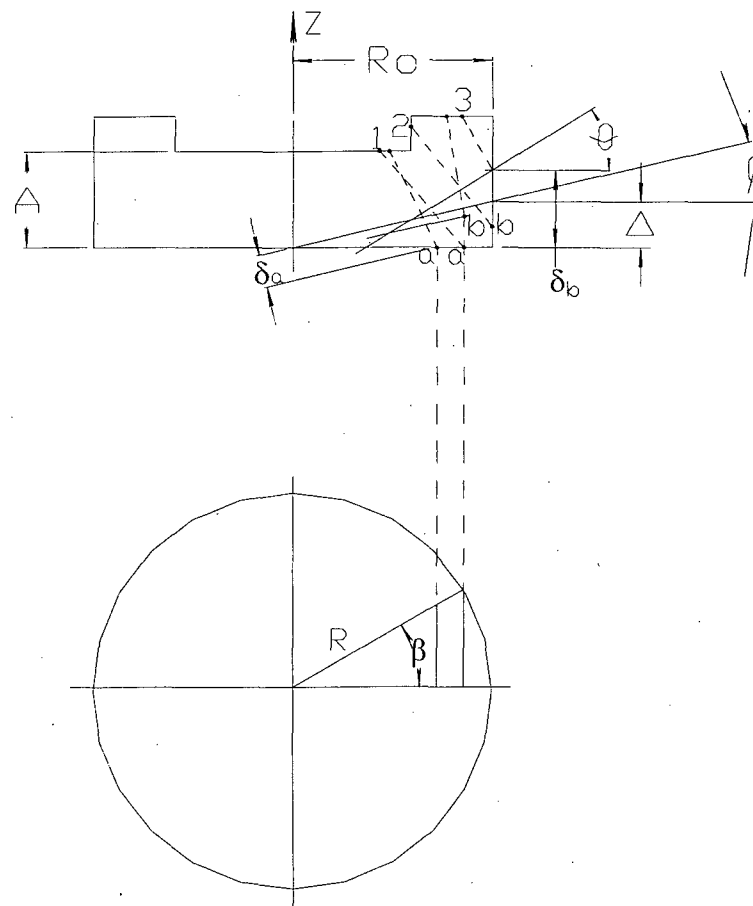


Figure 2.10.8-13
Strain Computation for Crush Pattern II

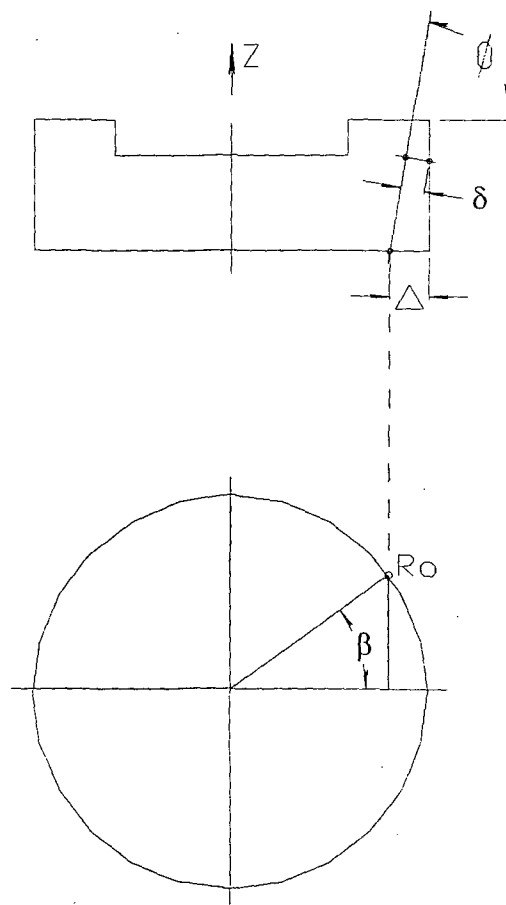


Figure 2.10.8-14
Strain Computation for Crush Pattern III

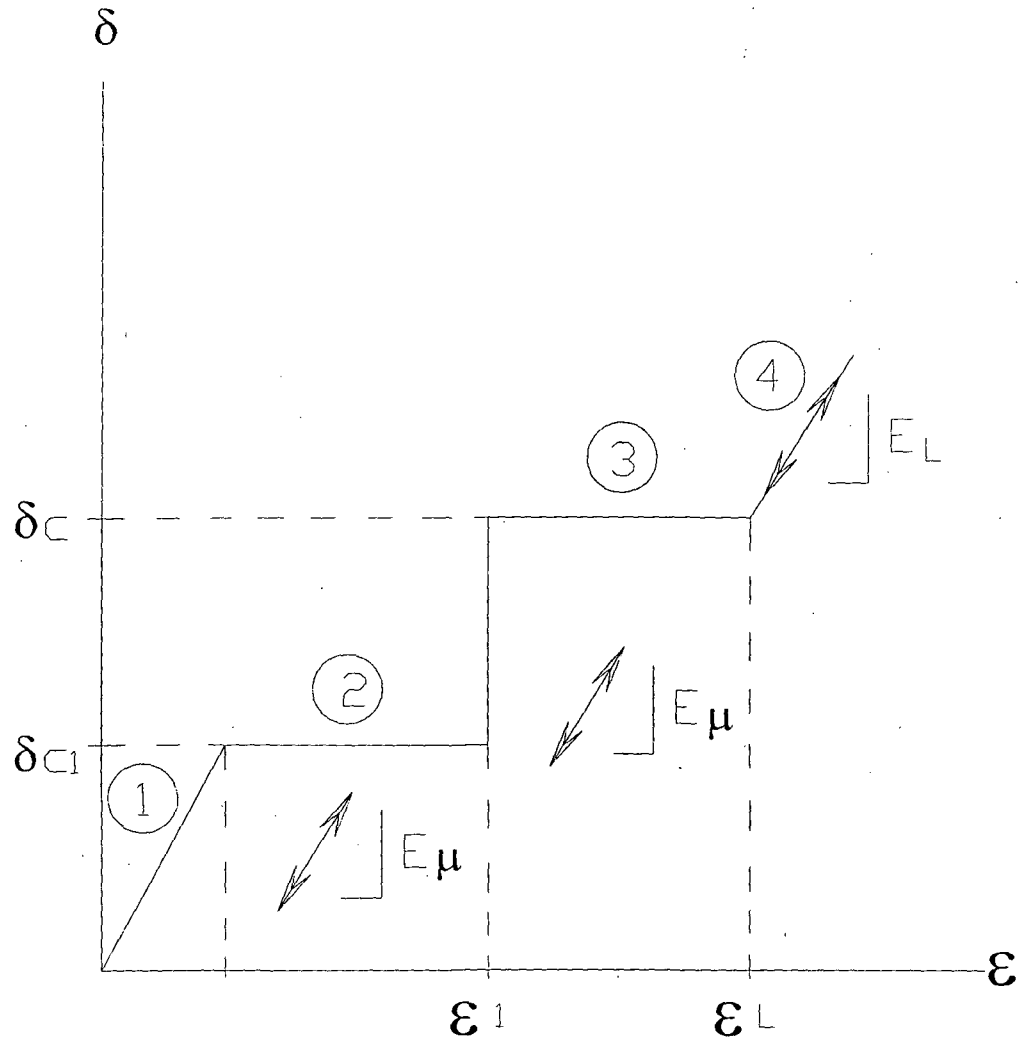
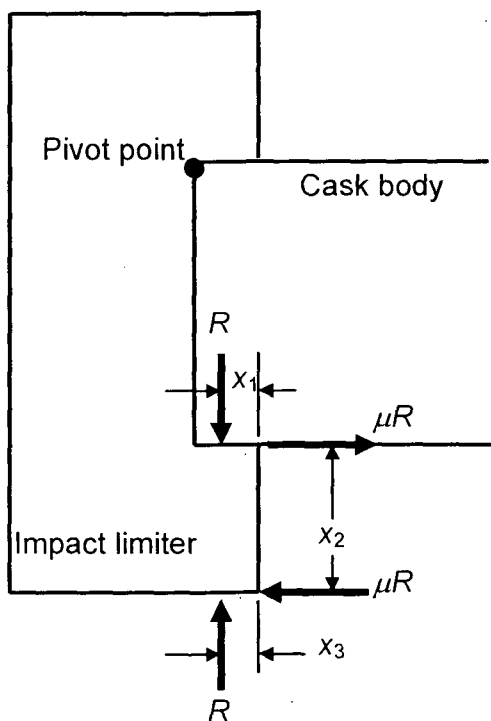


Figure 2.10.8-15
Wood Stress-Strain Curve



Where:

$$R = 12,500 \text{ kips}$$

$$\mu = 0.42$$

$$x_1 = 12.00/2 = 6.00 \text{ in.}$$

$$x_2 = (\text{I.L. o.d.} - \text{Cask o.d.})/2 - \text{crush depth} \\ = (144.00 - 91.00)/2 - 5.62 = 20.88 \text{ in.}$$

$$x_3 = 12.00 \text{ in.} - 11.16 \text{ in.} = 0.84 \text{ in.}$$

Figure 2.10.8-16
Impact Limiter Free Body Diagram during 20° Slap Down

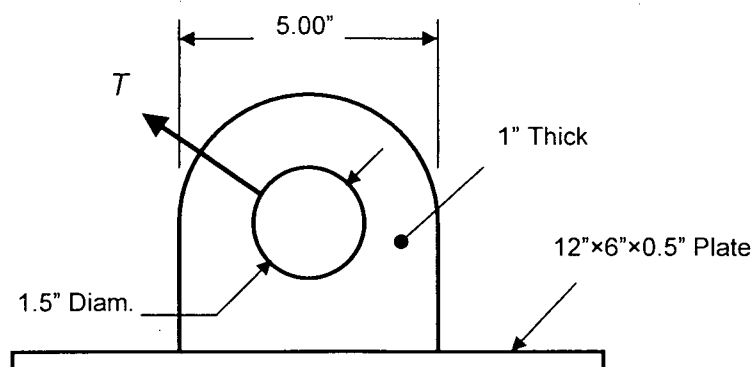


Figure 2.10.8-17
Impact limiter Lifting Lug Geometry

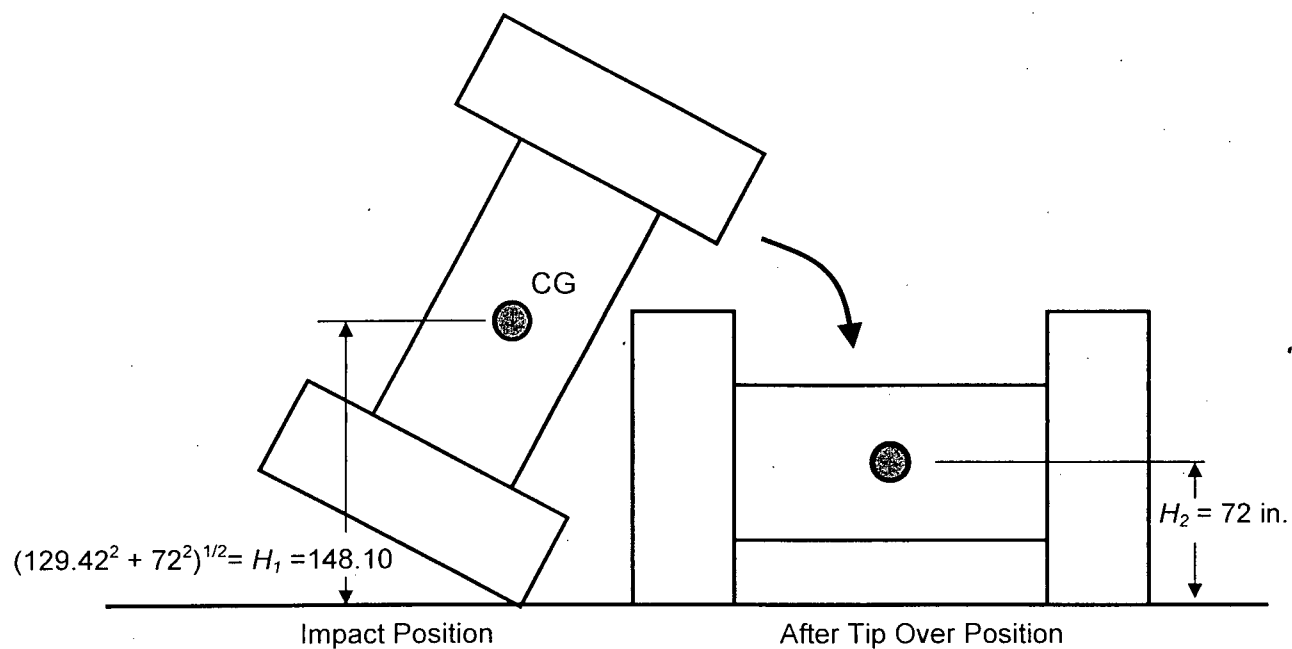


Figure 2.10.8-18
Cask Geometry during Tip-Over Event

APPENDIX 2.10.9

IMPACT LIMITER TEST SPECIFICATION

TABLE OF CONTENTS

	<u>Page</u>
2.10.9 IMPACT LIMITER TEST SPECIFICATION	2.10.9-1
2.10.9.1 Introduction	2.10.9-1
2.10.9.2 Technical Requirements	2.10.9-1
2.10.9.2.1 General Requirements.....	2.10.9-1
2.10.9.2.2 Test Package.....	2.10.9-1
2.10.9.2.3 Test Description.....	2.10.9-2
2.10.9.2.4 Test Facility	2.10.9-3
2.10.9.2.5 Instrumentation Calibration.....	2.10.9-3
2.10.9.2.6 Test Data	2.10.9-3
2.10.9.2.7 Instrumentation and Data Recording Equipment	2.10.9-5
2.10.9.2.8 Test Conditions.....	2.10.9-6

LIST OF FIGURES

Figure 2.10.9-1	TN-40 Scale Model 0° Side Drop Test Setup.....	2.10.9-7
Figure 2.10.9-2	TN-40 Scale Model C.G. Over Corner Drop Test Setup	2.10.9-8
Figure 2.10.9-3	TN-40 Scale Model 20° Slap Down Test Setup	2.10.9-9
Figure 2.10.9-4	TN-40 Scale Model 90° End Drop Test Setup	2.10.9-10
Figure 2.10.9-5	TN-40 Scale Model 90° Puncture Drop Test Setup	2.10.9-11
Figure 2.10.9-6	Accelerometer Locations on the Test Cask Dummy Model ..	2.10.9-12

2.10.9 IMPACT LIMITER TEST SPECIFICATION

2.10.9.1 Introduction

The following sections describe the requirements for dynamic testing of a one-third scale model of the TN-40 impact limiters, including general requirements, test descriptions, instrumentation, and data recording. Figures 2.10.9-1 through 2.10.9-6 provide illustrations of test setups and accelerometer locations.

2.10.9.2 Technical Requirements

2.10.9.2.1 General Requirements

The purpose of conducting this test is to demonstrate that the TN-40 Impact Limiters absorb the energy of a 30 foot drop of a loaded TN-40 package.

Performance of the test program will:

- a. Verify the impact limiters are not dislodged from the cask as a result of the drop.
- b. Demonstrate the effectiveness of the impact limiter tie rods, attachment bolts, and stainless steel covers.
- c. Provide data on the deformation of the impact limiters due to the drop.
- d. Provide data on the acceleration experienced by the test package during impact.
- e. Provide data on the impact limiter damage caused by a 40 inch drop on a 2 in. diameter puncture bar.

2.10.9.2.2 Test Package

The test package consists of a 1/3 scale model of the TN-40 transport package with impact limiters on each end. The impact limiters are attached to each other by thirteen 0.5 inch diameter tie rods, snug tight, and to the cask with four 0.5 inch bolts.

The test package weights approximately 10,100 lb. and has maximum dimensions of approximately 87.0 inches long by 48.0 inches in diameter.

The test package is equipped with lifting lugs to facilitate lifting.

2.10.9.2.3 Test Description

General

All drops shall be performed using a quick release mechanism to assure that the correct drop orientation is maintained until the moment of impact. The drops are to be performed in the order given below.

0° Side Drop

The test package shall be dropped from a height of 30 feet (impact surface to the lowest point on the test package) at an impact angle of 0° as shown in Figure 2.10.9-1, so that the centerline of the package is parallel to the impact surface.

C. G. Over Corner Drop

After the results of the previous drop have been recorded, replace any damaged attachment hardware. Reattach the lifting straps so that when suspended, the undamaged portion of the impact limiters face downward. Adjust the lifting straps so that the test package is suspended at an angle of 64° as shown in Figure 2.10.9-2.

20° Slap Down

Install new impact limiters. The test model shall be dropped from a height of 30 feet (impact surface to the lowest point on the test package) at an impact angle of 20° as shown in Figure 2.10.9-3. After the test cask and impact limiters have been examined and impact limiter deformation measured, an impact limiter (#2 of Figure 2.10.9-2 or #4 of Figure 2.10.9-3 depending on evaluation of damage) shall be placed in a cooler to begin cooling to -20°F.

90° End Drop

Immediately prior to the drop, the impact limiter that has been cooled in a -20°F chamber for at least 24 hours shall be installed. The test package shall be dropped from a height of 30 feet (impact surface to the lowest point on the test package) at an impact angle of 90° with the chilled impact limiter impacting the test surface as shown in Figure 2.10.9-4.

90° Drop onto puncture bar

After the test cask and impact limiters have been examined and impact limiter deformation measured, the test package shall be dropped onto the puncture bar from a height of 40 inches (top of puncture bar to the lowest point on the test article). The impact angle for the puncture drop test shall be 90° as shown in Figure 2.10.9-5. The puncture bar shall be positioned so that it will impact the bottom of the test article at the centerline of the package.

2.10.9.2.4 Test Facility

The impact surface is to be an unyielding surface. This requirement can be met by ensuring that the drop pad has a mass of at least 10 times the test package mass and by covering the upper surface of the pad with a steel plate.

A vertical mild steel pin is to be rigidly attached to the test pad for the puncture test(s). The pin must be 2 in. dia. with the corners rounded to 0.083 in.

The test facility must have the ability to drop the test article from a height of 30 feet, measured from the lowest point on the test article, onto the impact surface.

2.10.9.2.5 Instrumentation Calibration

All instrumentation (excluding cameras) shall be calibrated against certified standards having known relationships to national standards. Instrument calibrations shall be performed in accordance with written procedures and calibration results shall be recorded. The instruments used in the test shall have current calibrations. The instrument description, calibration, and other pertinent information shall be included in the test procedure and test data.

All instrumentation intended for use in the test program shall be identified in the test procedures. Information describing the operating range, response, performance limitations, sensitivity, and accuracy of these instruments shall be provided.

2.10.9.2.6 Test Data

All required test data shall be recorded on data sheets, samples of which shall be included in the test procedures. Each data sheet must identify the test conditions and other pertinent data.

Test data is classified into three categories:

- a. Data taken to verify that desired test conditions exist at the time of the test.
- b. Data taken during the test.
- c. Data taken after the test.

Data Taken Before Each Test

The following as-built values should be provided:

- a. Test article dimensions and weights.
- b. Required torque on impact limiter attachment bolts.
- c. As-built C.G. data.

The following data should be provided before the test:

- a. Weight the test cask and each impact limiter with an accuracy of $\pm 0.05\%$.
- b. Locate the center of gravity of an assembled test package within ± 0.5 inches accuracy.
- c. Provide color photographs of the test arrangement.
- d. Have current calibration data for all instrumentation used in the test.
- e. Provide an angular orientation of the test article relative to the impact surface ($\pm 1.0^\circ$).
- f. Provide the measured height from the lowest point on the test article to the impact surface or puncture bar (+ 1.0 – 0.0 inch).
- g. Provide atmospheric condition data, i.e. ambient temperature, wind speed, etc., immediately prior to release of the test article.
- h. Torque values of the impact limiter attachment bolts.
- i. Provide the length of time and the temperature at which the chilled impact limiter is cooled.
- j. The date and time the chilled impact limiter was removed from the chiller. If the impact limiter is not immediately installed on the dummy test model, it shall be insulated to minimize temperature change.

Data Taken During Each Test

The following information shall be measured and recorded during each test:

- a. Impact accelerations measured by accelerometers attached to the test article.
- b. Test article behavior on video tape.
- c. Date and time of test.
- d. Identification of personnel performing the test.
- e. Observations of damage or unexpected behavior of the test article.

Data Taken After Each Test

The following information shall be measured and recorded after each test:

- a. Observations and photographs of test article damage other than to the impact limiters.

- b. Measurement of deformation to each impact limiter to fully describe the extent of damage. These measurements shall include: depth of internal and external crushing on each impact limiter, overall thickness of each impact limiter after each test, width of the impact footprint, measurement of damage to impact pad, and any other measurements deemed necessary by the Transnuclear representative at the time of the test.
- c. Photographs of the impact limiter deformation and damage.

2.10.9.2.7 Instrumentation and Data Recording Equipment

The instrumentation shall include as a minimum:

- a. Accelerometers
- b. Still photo cameras
- c. Videotape cameras
- d. Scale for measuring weight of test article
- e. Torque wrench
- f. Thermometer, or other temperature measuring device

Accelerometer Measurements

Accelerometers will be mounted to brackets around the exterior of the test cask dummy body at 0°, 90°, 180°, and 270° orientations at the approximate center of gravity location and adjacent to each impact limiter. The locations of the accelerometers are shown in Figure 2.10.9-6.

For the 0° side drop test, the accelerometers will be oriented to measure accelerations in the drop impact direction.

For the 90° end drop test, the accelerometers will be oriented to measure accelerations in the axial (drop) direction.

For both 20° slap down, the accelerometers will be oriented to measure accelerations in both axial and radial directions.

Data will be collected by accelerometers having a frequency response of at least 10,000 Hz. The lowest natural vibration frequencies of the test cask, which are excited during the test, are much lower than this. These body vibrations involve small displacements (low stresses) at high frequencies, which excite the accelerometers and tend to mask the low frequency rigid body acceleration. This low frequency acceleration is masked, because both low frequency rigid body and high frequency natural vibration accelerations superimpose and the net acceleration is recorded. Filtering the data is necessary to remove these high frequency accelerations. A cutoff filter will be used to

eliminate data above a specified cutoff frequency. The cutoff frequency used to filter the data will be set at a value slightly below the significant natural frequency of the test body (roughly 560 Hz).

Still Photographs

Still Photographs shall be taken to obtain a pictorial record of all changes to the test body, impact limiters, instrumentation, and target surface as a result of each test. Photographs shall be taken:

Before Impact:

- a. Test Body
- b. Both Impact Limiters (if used before, show orientations of prior damage relative to the test body)
- c. Hoist and release devices with test package attached.

After Impact:

- a. Test Body
- b. Both Impact Limiters (New damage, as well as changes to old damage due to this test)
- c. Impact limiter attachments (Tie rods and bolts)
- d. Contact footprint on target surface

Motion Pictures

Motion Pictures of the drops shall be taken with stadia boards and a dimensional reference in the camera view.

Two video tape cameras shall be used to provide a front and side view of the entire drop sequence.

2.10.9.2.8 Test Conditions

The tests shall be performed at a time of day when the ambient temperature is stable, under bright conditions that are suitable for photography. The test shall not be performed at wind speeds that could affect the attitude of the test model.

The impact limiter used for the 90° end drop test shall be cooled for at least 24 hours at a temperature of -20°F. The time between when the impact limiter is removed from the cooler to when the test article is dropped shall be minimized.

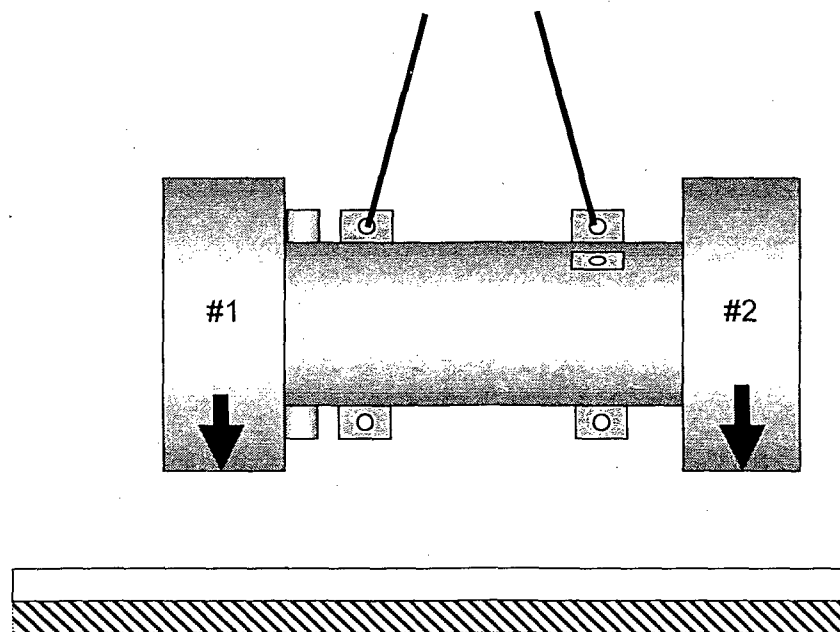


Figure 2.10.9-1
TN-40 Scale Model 0° Side Drop Test Setup

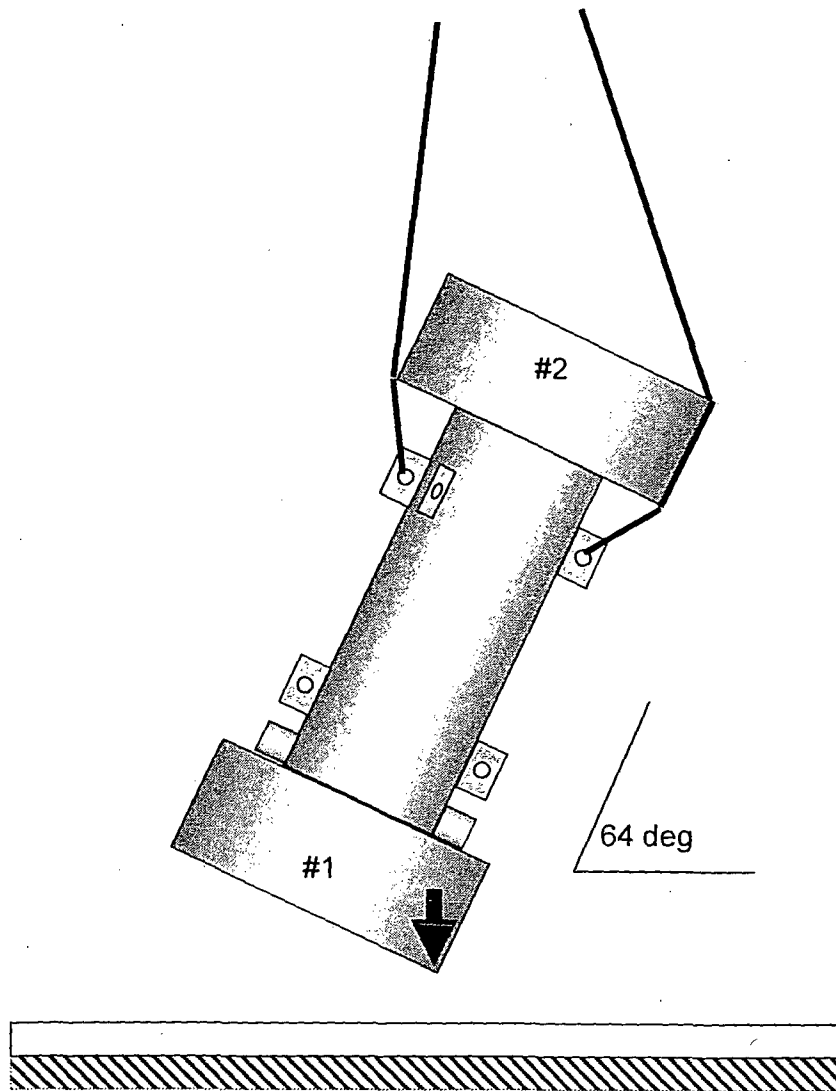


Figure 2.10.9-2
TN-40 Scale Model C.G. Over Corner Drop Test Setup

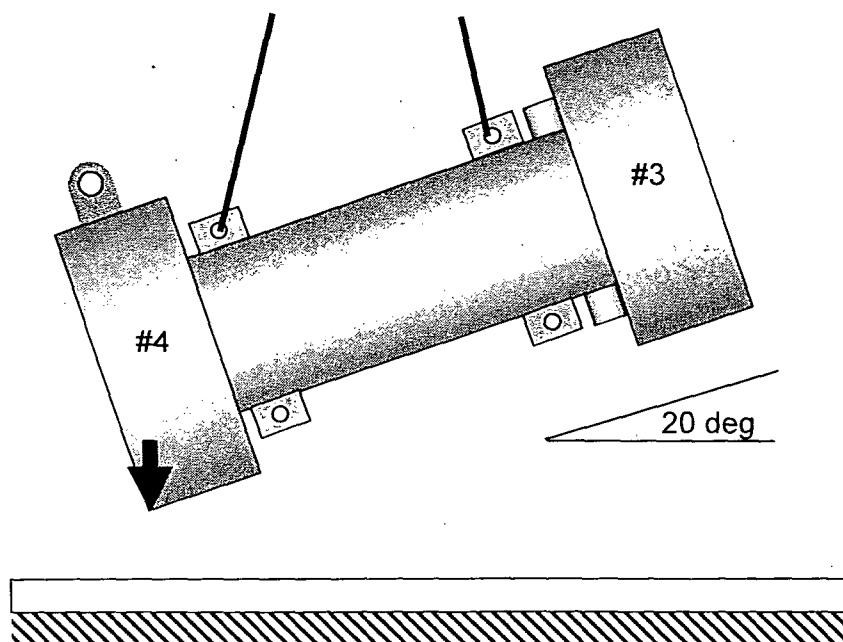


Figure 2.10.9-3
TN-40 Scale Model 20° Slap Down Test Setup

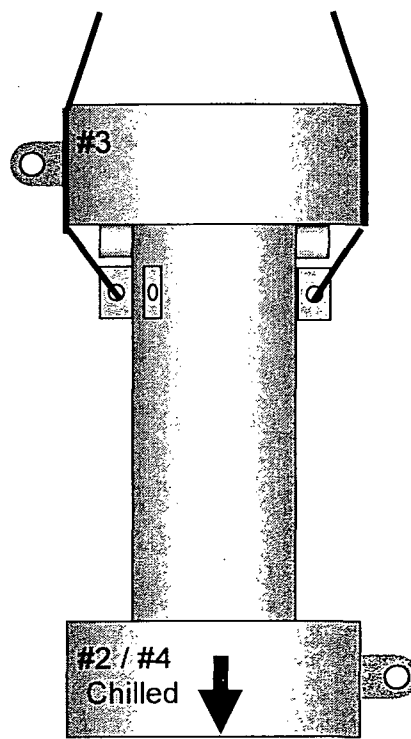


Figure 2.10.9-4
TN-40 Scale Model 90° End Drop Test Setup

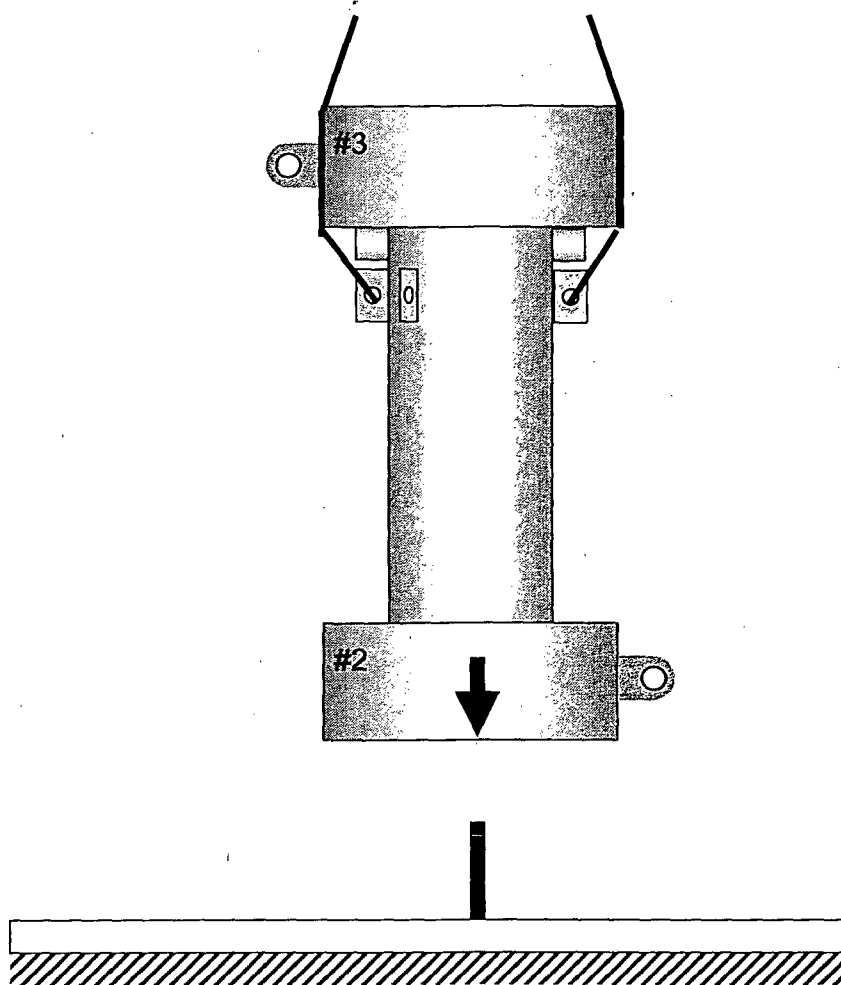


Figure 2.10.9-5
TN-40 Scale Model 90° Puncture Drop Test Setup

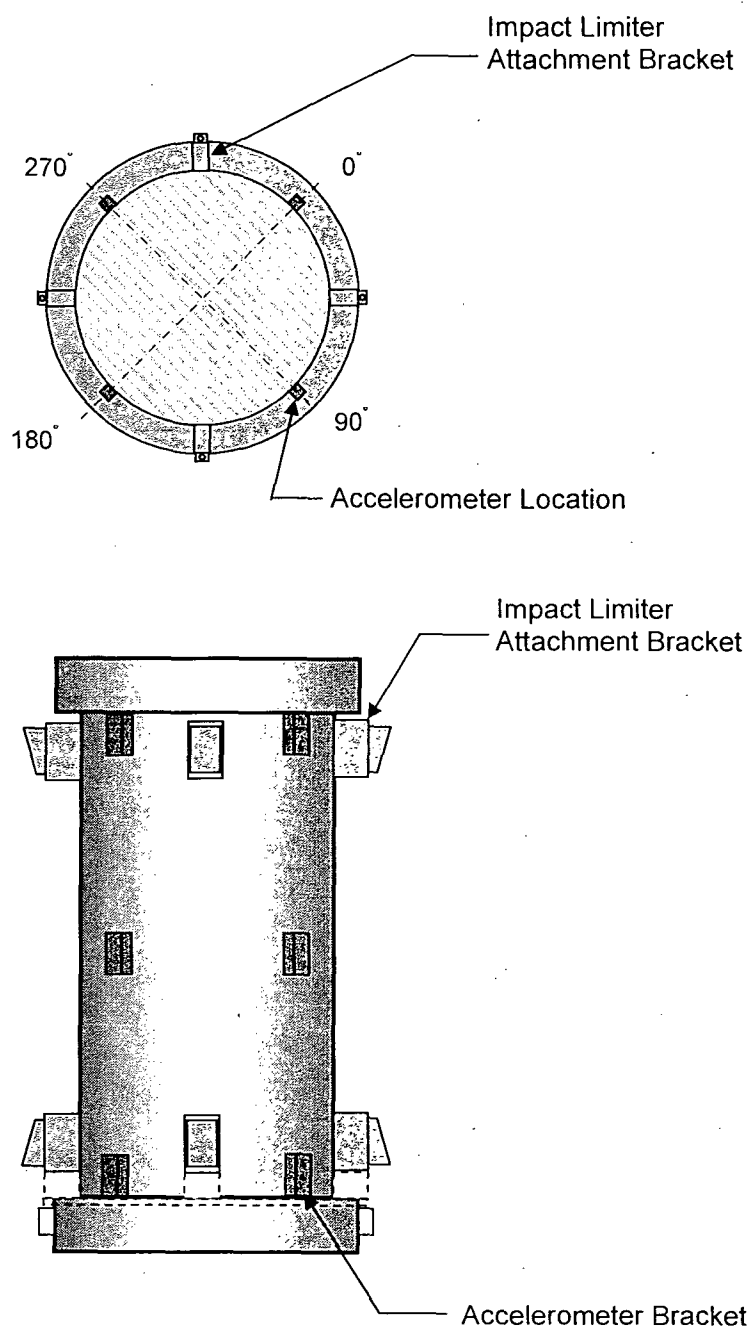


Figure 2.10.9-6
Accelerometer Locations on the Test Cask Dummy Model

CHAPTER 3 THERMAL EVALUATION

TABLE OF CONTENTS

	<u>PAGE</u>
3.0 THERMAL EVALUATION	3-1
3.1 Discussion	3-1
3.2 Summary of Thermal Properties of Materials	3-3
3.3 Technical Specifications for Components.....	3-8
3.4 Thermal Evaluation for Normal Conditions of Transport.....	3-8
3.4.1 Thermal Models	3-8
3.4.2 Maximum Temperatures	3-13
3.4.3 Maximum Accessible Surface Temperature in the Shade.....	3-13
3.4.4 Minimum Temperatures	3-14
3.4.5 Maximum Internal Pressure	3-14
3.4.6 Maximum Thermal Stresses	3-14
3.4.7 Evaluation of Cask Performance for Normal Conditions of Transport.....	3-14
3.5 Thermal Evaluation for Hypothetical Accident Conditions	3-14
3.5.1 Fire Accident Evaluation	3-15
3.5.2 Boundary conditions for the HAC	3-15
3.5.3 Crushed Impact Limiter Models.....	3-15
3.5.4 Summary of Results.....	3-17
3.5.5 Evaluation of Package Performance During and after the HAC Fire	3-17
3.6 References	3-18
3.7 Appendices.....	3-20

LIST OF TABLES

Table 3-1	NCT Component Temperatures In The TN-40 Package.....	3-21
Table 3-2	Temperature Distribution In The TN-40 Package (Low Ambient Temperature, Max Decay Heat).....	3-22
Table 3-3	Maximum HAC Transient Temperatures During Fire Accident	3-23

LIST OF FIGURES

Figure 3-1	Schematic Of The Cask Body.....	3-24
Figure 3-2	Thermal Model 90 Degree Radial Cross Section.....	3-25
Figure 3-3	Finite Element Model Of TN-40 Transport Cask	3-26
Figure 3-4	Finite Element Model Of The TN-40 Transport Cask, Details	3-27
Figure 3-5	Finite Element Model Of The TN-40 Basket Cross Section	3-28
Figure 3-6	Finite Element Model Of The TN-40 Basket, Details	3-29
Figure 3-7	Finite Element Model Of The TN-40 Basket Compartment Weld Joint Details	3-30
Figure 3-8	Details of Impact Limiters.....	3-31
Figure 3-9	Mesh Of Finite Element Model.....	3-32
Figure 3-10	Temperature Distribution In The TN-40 Cask, NCT, 100° F	3-33
Figure 3-11	Temperature Distributions In The TN-40 Cask, Fuel & Resin NCT, 100° F	3-34
Figure 3-12	Temperature Distributions In The TN-40 Cask, Impact Limiters & Rail Normal Conditions Of Transport NCT, 100° F	3-35
Figure 3-13	Temperature Distributions In The TN-40 Cask Low Ambient Temperatures	3-36
Figure 3-14	Maximum Temperature Distribution in the TN-40 Cask HAC, End of Fire / Smoldering	3-37
Figure 3-15	Maximum Temperature Distribution in the TN-40 Cask HAC, Cool-Down Period.....	3-38

3.0 THERMAL EVALUATION

3.1 Discussion

The TN-40 packaging is designed to passively reject decay heat under Normal Conditions of Transport (NCT) and Hypothetical Accident Conditions (HAC) while maintaining packaging temperatures and pressures within specified limits. Objectives of the thermal analyses performed for this evaluation include:

- Determination of maximum and minimum temperatures with respect to cask materials limits to ensure components perform their intended safety functions
- Determination of temperature distributions to support the calculation of thermal stresses
- Determination of the cask cavity gas temperature to support containment pressure calculations
- Determination of the maximum fuel cladding temperature

Chapter 2 presents the principal design bases for the TN-40 packaging.

The design features of the TN-40 basket are described in Section 1.2. The basket is a welded assembly of stainless steel fuel compartment boxes separated by aluminum and poison plates which form a sandwich panel. The panel consists of two 0.25 in. thick aluminum plates which sandwich a poison plate 0.075 in. thick. The aluminum provides heat conduction paths from the fuel assemblies to the basket peripheral plates. The poison material provides the necessary criticality control. This method of construction forms a very strong honeycomb-like structure of cell liners which provide compartments for 40 fuel assemblies. The aluminum basket rails are bolted to the inner shell and provide a conduction path from the basket to the inner shell. These thermal design features of the basket allow the heat generated by the fuel assemblies to be conducted efficiently from the basket to the shell.

A thermal design feature of the cask is the conduction path created by the aluminum boxes that contain the neutron shielding material as described in Section 1.2. The neutron shielding material is provided by a resin compound cast into long slender aluminum boxes placed around the gamma shield shell and enclosed within a steel outer shell. The aluminum boxes are designed to fit tightly against the steel shell surfaces, thus improving the heat transfer across the neutron shield.

The design of the steel-encased wood impact limiters is described in Section 1.2. These components are included in the thermal analysis because of their contribution as a thermal insulator. The impact limiters provide protection to the lid and bottom regions from the external heat load applied during the HAC thermal event.

A personnel barrier prevents access to the outer surfaces of the cask body. The barrier, which consists of a stainless steel mesh attached to stainless steel tubing, will enclose the cask body between the impact limiters, and have an open area of approximately 80%.

Several thermal design criteria are established for the TN-40 to ensure the package meets all its functional and safety requirements. These are:

- Containment of radioactive material and gases is a major design requirement. Seal temperatures must be maintained within specified limits to satisfy the NCT leak tight containment requirement. A maximum temperature limit of 536°F (280°C) is set for the metallic seals (double metallic O-rings) in the containment vessel lid [11].
- To maintain the stability of the neutron shield resin, a maximum allowable NCT temperature of 300°F (149°C) is set for the neutron shield [15].
- In accordance with 10CFR71.43(g) [1] the maximum temperature of accessible package surfaces in the shade is limited to 185°F (85°C).
- Maximum fuel cladding temperature limits of 400°C (752°F) for NCT and 570°C (1058°F) for HAC are set for the fuel assemblies with an inert cover gas as concluded in Reference [14].
- A temperature limit of 230°F is set for wood to prevent excessive reduction in structural properties at elevated temperatures [17].

The NCT ambient temperature range is -20 to 100°F (-29 to 38°C) per 10CFR71.71(b) [1]. In general, all the thermal criteria are associated with maximum temperature limits and not minimum temperatures. All materials can be subjected to the minimum environment temperature of -40°F (-40°C) without adverse effects as required by 10CFR71.71 (c)(2) [1].

The TN-40 thermal analysis is conservatively based on a maximum total heat load of 22 kW from 40 fuel assemblies and with a maximum of 0.55 kW per fuel assembly, even though the maximum total heat load is limited to 21 kW. A peak power factor of 1.2 and an active length of 144 in. are considered for calculation of the decay heat profile of the fuel assemblies as described in Section 3.4.1.3. A description of the detailed NCT analyses is provided in Section 3.4 and HAC analyses in Section 3.5. A summary of the NCT analysis results is provided in Table 3-1. The thermal evaluation concludes that for this thermal design heat load, all design criteria are satisfied.

3.2 Summary of Thermal Properties of Materials

The analyses use interpolated values when appropriate for intermediate temperatures where the temperature dependency of a specific parameter is significant. The interpolation assumes a linear relationship between the reported values.

Thermal radiation at the external surfaces of the packaging is considered. The thermal analysis assumes that the cask and impact limiter external surfaces are painted white. Reference [7] gives an emissivity between 0.92 to 0.96 and a solar absorptivity between 0.09 to 0.23 for white paints. To account for dust and dirt and to bound the problem, the thermal analysis uses a solar absorptivity of 0.3 and an emissivity of 0.9 for the white painted surfaces. After a fire, the cask surface will be partially covered in soot (absorptivity = 0.95, Reference [7]). The HAC thermal analysis conservatively assumes an absorptivity of 1.0 and an emissivity of 0.9 for the cool-down period.

1. PWR Fuel Assembly

The effective thermal conductivity is calculated using the bounding values, maximum pellet to clad gap and minimum clad thickness, for the PWR fuel assemblies that may be transported in this cask. The fuel conductivity analysis, including the specific heat and density, is presented in Appendix 3.7.1.

Temperature (°F)	k_{axial} (Btu/hr-in-°F)	Temperature (°F)	k_{trans} (Btu/hr-in-°F)	Temperature (°F)	$C_{p, eff}$ (Btu/lbm-°F)
212	0.0558	136	0.0161	80	0.0593
392	0.0587	233	0.0177	260	0.0654
572	0.0623	330	0.0193	692	0.0726
752	0.0673	428	0.0210	1502	0.0778
932	0.0738	526	0.0228	$\rho_{eff} = 0.135 \text{ lb/in}^3$	
		624	0.0246		
		722	0.0263		
		821	0.0281		
		920	0.0298		
		1019	0.0317		

2. 6061 Aluminum (used for basket and rails)

Properties are taken from ASME Section III [3]. The specific heat

$$C_p, \text{ shown is calculated from: } c_p = \frac{k}{\rho \alpha}$$

where: $\rho = 0.098 \text{ lbm/in.}^3$ [3]
 α = thermal diffusivity [3]
 K = thermal conductivity [3]

Al 6061	Thermal Conductivity, k	Specific heat, C _p
Temperature (°F)	(Btu/hr-in-°F)	(Btu/lbm-°F)
70	8.008	0.213
100	8.075	0.215
150	8.167	0.218
200	8.250	0.221
250	8.317	0.223
300	8.383	0.226
350	8.442	0.228
400	8.492	0.230

3. Poison Plates

As a conservative measure, this analysis assumes the Boral[®] plates do not conduct or store heat. A virtual conductivity of 1×10^{-8} is given to the elements representing Boral[®] in the ANSYS [5] model.

4. Stainless Steel Type 304/304L (used for fuel compartments) [3]

The stainless steel specific heat is calculated as described above for 6061 Aluminum.

SA 240, Type 304	Thermal Conductivity, k	Specific heat, C _p
Temperature (°F)	(Btu/hr-in-°F)	(Btu/lbm-°F)
70	0.717	0.114
100	0.725	0.114
150	0.750	0.117
200	0.775	0.119
250	0.800	0.121
300	0.817	0.122
350	0.842	0.124
400	0.867	0.126
450	0.883	0.127
500	0.908	0.128
550	0.925	0.129
600	0.942	0.130
650	0.967	0.131
700	0.983	0.132
750	1.000	0.132
800	1.017	0.132
$\rho = 0.29 \text{ lbm/in}^3$ [13]		

5. Low Alloy Steel SA 203, Gr E and SA-350, Grade LF3 containment shell) [3]

Steel specific heat is calculated as described above for 6061 Aluminum.

SA 203, Gr. E SA 350, LF3	Thermal Conductivity, k	Specific heat, C_p
Temperature (°F)	(Btu/hr-in-°F)	(Btu/lbm-°F)
70	1.958	0.102
100	1.967	0.105
200	1.967	0.111
300	1.950	0.116
400	1.925	0.122
500	1.892	0.127
600	1.850	0.132
700	1.800	0.137
800	1.750	0.144
$\rho = 0.284 \text{ lbm/in}^3$ [13]		

6. Helium (used for gaps within the cask cavity) [12]

Helium	Thermal Conductivity, k
Temperature (°F)	(Btu/hr-in-°F)
-100	0.0055
-10	0.0064
80	0.0072
260	0.0086
440	0.0102
620	0.0119
980	0.0148
1340	0.0175

For the transient analyses, the thermal mass is relatively small and neglected. The density and specific heat are not used.

7. SA-516 Grade 70 Carbon Steel (gamma shield shell, outer shell and lid) [3]

Steel specific heat is calculated as described above for 6061 Aluminum.

SA 266, Cl. 4 SA 516, Gr. 70 or 55 SA 105	Thermal Conductivity, k	Specific heat, C _p
Temperature (°F)	(Btu/hr-in-°F)	(Btu/lbm-°F)
70	2.925	0.103
100	2.892	0.105
200	2.800	0.112
300	2.692	0.117
400	2.575	0.123
500	2.458	0.127
600	2.333	0.132
700	2.217	0.138
800	2.100	0.145
900	1.983	0.153
1000	1.867	0.162
1100	1.742	0.170
1200	1.625	0.182
1300	1.500	0.204
1400	1.367	0.408
$\rho = 0.284 \text{ lbm/in}^3$ [13]		

8. Air [12]

Temperature °F	Thermal Conductivity (Btu/hr-in-° F)
-100	0.0009
80	0.0013
260	0.0016
440	0.0019
620	0.0022
980	0.0028
1340	0.0033

For the transient analyses, the thermal mass is relatively small and neglected. The density and specific heat are not used.

The following correlations are used to calculate the properties of air to be used in the calculations described in Section 3.4.1.4

Specific Heat (kJ/kg-K) [6]	Dynamic Viscosity (N-s/m ²) [6]	Conductivity (W/m-K) [6]
$c_p = \sum [A(N)T^N]$ A(0)= 0.103409E+1 A(1)= -0.2848870E-3 A(2)= 0.7816818E-6 A(3)= -0.4970786E-9 A(4)= 0.1077024E-12	$\mu = \sum [B(N)T^N]$ For $250 \leq T < 600$ K B(0)= -9.8601E-1 B(1)= 9.080125E-2 B(2)= -1.17635575E-4 B(3)= 1.2349703E-7 B(4)= -5.7971299E-11 For $600 \leq T < 1050$ K B(0)= 4.8856745 B(1)= 5.43232E-2 B(2)= -2.4261775E-5 B(3)= 7.9306E-9 B(4)= -1.10398E-12	$k = \sum [C(N)T^N]$ C(0)= -2.276501E-3 C(1)= 1.2598485E-4 C(2)= -1.4815235E-7 C(3)= 1.73550646E-10 C(4)= -1.066657E-13 C(5)= 2.47663035E-17

9. Neutron Shielding (Polyester Resin) [4]

Thermal Conductivity (Btu/hr-in-° F)	Specific Heat (Btu/lbm-° F)	Density (lb/in ³)
0.0083	0.311	0.057

10. Wood

Thermal Conductivity (Btu/hr-in-° F)	
Min.	Max.
0.0019	0.0135

Thermal conductivity values bound values given in Reference [2] for moisture contents up to 30% and specific gravities between 0.08 and 0.80. These values also bound the conductivity parallel and perpendicular to the grain for NCT conditions. Wood conductivity parallel to the grain is 2.0 to 2.8 times higher than the conductivity across the grain [2]. The maximum wood conductivity, used during the fire accident condition, is taken to be 2.8 times that of the bounding maximum conductivity across the grain to maximize heat conductance from fire toward the cask during fire period. The maximum wood conductivity during fire is:

$$K = (2.8)(0.0135 \text{ Btu/hr-in-}^\circ\text{F}) = 0.0378 \text{ Btu/hr-in-}^\circ\text{F}$$

During the transient analyses the thermal mass of the wood is conservatively neglected.

3.3 Technical Specifications for Components

The cask components for which a thermal technical specification is necessary are the seals.

The seals used in the packaging are the Helicoflex seals (double metallic O-rings). The seals will have a minimum and maximum temperature rating of -40°F and 536°F respectively.

3.4 Thermal Evaluation for Normal Conditions of Transport

The NCT ambient conditions are used for the determination of the maximum fuel cladding temperature, TN-40 component temperatures, containment pressure and thermal stresses. These steady state environmental conditions correspond to the maximum daily averaged ambient temperature of 100°F and the 10CFR Part 71.71(c)(1) [1] insolation averaged over a 24 hour period.

3.4.1 Thermal Models

A finite element model is developed using the ANSYS computer code [5]. ANSYS is a comprehensive thermal, structural and fluid flow analysis package. It is a finite element analysis code capable of solving steady-state and transient thermal analysis problems in one, two or three dimensions. Heat transfer via a combination of conduction, radiation and convection can be modeled by ANSYS. The three-dimensional geometry of the cask is modeled. All cask components including the gaps are modeled by SOLID70 conducting elements.

To determine temperatures of components within the cask body and basket during NCT a finite element model of the basket and cask is developed. The model has 90 degree symmetry and includes the complete cask length. The cask model includes the impact limiters, trunnions, neutron shield, cask shells, cask bottom plate, cask lid, basket, and fuel assemblies (see Figures 3-1 through 3-9). The model simulates the effective thermal properties of the fuel with a homogenized material occupying the volume within the basket where the 144 inch active length of the fuel is stored. The inner shell and gamma shield shell are assembled with an interference fit. This assures thermal contact at the shell interface. The thermal interface conductance increases with contact pressure and decreases with rougher surface finish. At a minimal contact pressure of 5 psi, Reference [15] considers a conductance of 375 Btu/hr-ft². For conservatism, a 0.01 in. gap with conductivity of 0.0243 Btu/hr-in-°F is considered between the inner shell and the gamma shield shell to represent the interference fit between these shells. A 0.125 in. gap is modeled between the bottom shield and the bottom inner plate. Also, a 0.01 in. axial gap is assumed between the lid outer plate and the shell flange and the lid outer plate and the shield plate. The neutron shielding consists of 60 long resin-filled aluminum containers placed between the gamma shield shell and outer shell. The aluminum containers are confined between these shells, and butt against the adjacent shells. For conservatism, an air gap of 0.01 in. at thermal equilibrium is assumed to be

present between the aluminum resin boxes and the adjacent shells. Radiation across these gaps is neglected. Locations of the gaps in the finite element plots of the model are shown in Figure 3-4, Figure 3-6, and Figure 3-7. Figure 3-9 shows the finite element model mesh.

3.4.1.1 Basket Model

The basket model is an integrated part of the finite element model which reflects the structure of the basket. The basket structure is composed of 40 stainless steel boxes (8.05 in. square) with two 0.25 in thick aluminum plates and one 0.075 in. thick poison plate placed between adjacent boxes. The boxes are held together by welded stainless steel plugs which pass through the aluminum and poison plates. The plug welding design causes the aluminum and poison plates to be tightly sandwiched between adjacent box sides, (see Figure 3-7). The basket portion of the thermal model simulates the conduction paths provided by the aluminum plates, the stainless steel boxes and the fuel (modeled as a homogenous material). Virtually no thermal conductance is credited to the Boral[®] poison material.

Aluminum plates (0.38 in. thick) are welded to the basket periphery to increase the surface area for heat transfer while providing some structural support for the basket. These peripheral plates are sized and formed to be in relatively close contact to the inner shell surface at thermal equilibrium. However, the thermal model assumes a 0.10 in gap between these plates and the inner shell surface. The aluminum rails, bolted to the inner shell, are sized so that heat is conducted from the basket periphery across a small gap. All decay heat is transferred from the basket to the inner shell across a helium gap via conduction. Other modes of heat transfer are conservatively neglected. Figures 3-5 and 3-6 show the basket model with the gaps.

Good surface contact is expected between adjacent components within the basket structure. However to bound the heat conductance uncertainty between adjacent components, the following gaps at thermal equilibrium are assumed:

- a. 0.01 in. gap between the weld plugs and adjacent stainless steel fuel compartments.
- b. 0.16 in. gap between the small aluminum rail and the basket plate.
- c. 0.09 in. gap between the small conduction plate of the large rail and the basket plate.
- d. 0.01 in gap between each adjacent basket plate.
- e. 0.10 in gap between the peripheral aluminum basket plates and the inner shell.

The finite element model of the basket includes a representation of the spent nuclear fuel that is based on a fuel effective conductivity model. The decay heat of the fuel with a peaking factor of 1.2 was applied directly to the fuel elements. The maximum fuel temperature reported is based on the results of the temperature distribution in the fuel

region of the model. Fuel assembly is modeled as a homogenized material. The effective properties for the homogenized fuel assemblies are described in Appendix 3.7.1.

The gas temperature within the basket is calculated using the temperatures at the hottest cross section of the basket. For simplicity and conservatism, it is assumed to be the average value of the maximum basket plate and cask inner shell temperatures.

3.4.1.2 Impact Limiter Model

Similar to the basket model, the impact limiters are an integrated part of the finite element model which determines the maximum wood temperature and the surface temperature of the impact limiters during NCT.

The redwood and balsa within the impact limiters are modeled as a homogenized region containing bounding material properties.

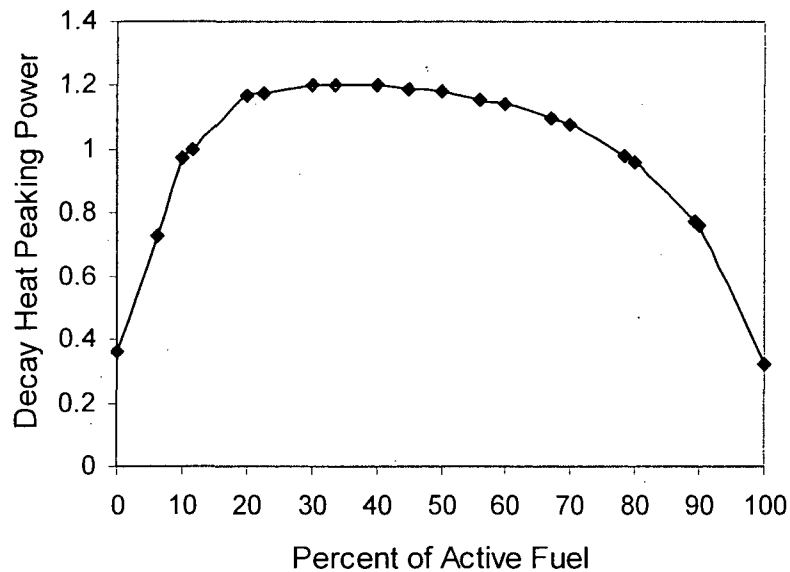
To bound the heat conductance uncertainty between adjacent packaging components the following gaps at thermal equilibrium are assumed:

- a. 0.01 in. axial gap between the impact limiter spacer and the cask lid.
- b. 0.01 in. axial gap between the impact limiter spacer and the shell flange.
- c. 0.0625 in. axial gap between the impact limiter spacer and the top impact limiter.
- d. 0.0625 in. axial gap between the bottom shield and the bottom impact limiter.

All heat transfer across the gaps is by gaseous conduction. Other modes of heat transfer are neglected. The finite element plot of the impact limiter model is shown in Figure 3-8.

3.4.1.3 Decay Heat Load

The decay heat load corresponds to a total heat load of 22 kW from 40 assemblies (0.55 kW/assy). A typical heat flux profile for spent PWR fuel with an axial peaking factor of 1.2 was used to distribute the decay heat load in the axial direction within the active fuel length. This heat flux profile is shown below. Within the basket model, the decay heat load is applied as volumetric heat generation in the elements that represent the homogenized fuel.



3.4.1.4 Heat Dissipation

Heat is dissipated from the surface of the packaging by a combination of radiation and natural convection.

Heat dissipation by natural convection from various surfaces is described by the following equations using an average Nusselt number [6]:

For horizontal cylinders:

$$h_c = \frac{Nu \, k}{D} \quad \text{with}$$

D = diameter of the horizontal cylinder

k = air conductivity

$$Nu^T = 0.772 \, \overline{C}_l \, Ra^{1/4} \quad \overline{C}_l = 0.515 \quad \text{for gases [6]}$$

$$Nu_l = \frac{2f}{\ln(1 + 2f / Nu^T)} \quad \text{Nusselt number for fully laminar heat transfer with}$$

$$f = 1 - \frac{0.13}{(Nu^T)^{0.16}}$$

$$Nu_t = \overline{C}_t \, Ra^{1/3}$$

Nusselt number for fully turbulent heat transfer with

$$\overline{C}_t = 0.14 \left(\frac{1 + 0.0107 \, Pr}{1 + 0.01 \, Pr} \right) \quad \text{for horizontal cylinders [6]}$$

$$Nu = [(Nu_l)^m + (Nu_t)^m]^{1/m} \quad \text{with } m = 10 \quad \text{for } 10^{-10} < Ra < 10^7$$

$$Ra = Gr Pr \quad ; \quad Gr = \frac{g \beta (T_w - T_\infty) D^3}{\nu^2}$$

For vertical flat plates:

$$h_c = \frac{Nu k}{L} \quad \text{with}$$

L = height of the vertical plate
k = air conductivity

$$Nu^T = \bar{C}_l Ra^{1/4} \quad \bar{C}_l = 0.515 \quad \text{for gases [6]}$$

$$Nu_l = \frac{2.0}{\ln(1 + 2.0 / Nu^T)} \quad \text{Nusselt number for fully laminar heat transfer}$$

$$Nu_t = C_l^V Ra^{1/3} \quad \text{Nusselt number for fully turbulent heat transfer with}$$

$$C_l^V = \frac{0.13 Pr^{0.22}}{(1 + 0.61 Pr^{0.81})^{0.42}}$$

$$Nu = [(Nu_l)^m + (Nu_t)^m]^{1/m} \quad \text{with } m = 6 \quad \text{for } 0.1 < Ra < 10^{12}$$

$$Ra = Gr Pr \quad ; \quad Gr = \frac{g \beta (T_w - T_\infty) L^3}{\nu^2}$$

Heat transfer from the surface of the package by radiation to the ambient environment is given by

$$h_r = \varepsilon F_{12} \left[\frac{\sigma (T_1^4 - T_2^4)}{T_1 - T_2} \right] \text{ Btu/hr} \cdot \text{ft}^2 \cdot ^\circ\text{F}$$

Where:

- ε = surface emissivity,
- F_{12} = view factor from surface to ambient environment,
- σ = $0.1714 \times 10^{-8} \text{ Btu/hr} \cdot \text{ft}^2 \cdot ^\circ\text{R}^4$,
- T_1 = surface temperature, $^\circ\text{R}$, and
- T_2 = ambient temperature, $^\circ\text{R}$.

The total heat transfer coefficient $H_t = h_r + h_c$, is applied as a boundary condition on the outer surfaces of the finite element model.

3.4.1.5 Solar Heat Load

The total insolation for a 12-hour period in a day is 1475 Btu/ft² for curved surfaces and 738 Btu/ft² for flat surfaces not transported horizontally as per 10CFR Part 71.71(c)(1) [1]. This insolation is averaged over a 24-hr period (daily averaged value) and applied as a constant steady state value to the external surfaces of the thermal models. A solar absorptivity of 0.30 is used for the painted outer surfaces of the packaging. Daily averaging of the solar heat load is justified based on the large thermal inertia of the TN-40 transport package.

3.4.2 Maximum Temperatures

Steady state thermal analyses are performed using the maximum decay heat load of 0.55 kW per assembly (22 kW total per cask), 100°F ambient temperature and the maximum insolation. The temperature distribution within the cask body and basket is shown in Figure 3-10. The temperature distributions as calculated in the fuel assemblies and the neutron shield are shown in Figure 3-11. The temperature distributions within the impact limiter wood and basket rail are shown in Figure 3-12. A summary of the calculated cask component temperatures is listed in Table 3-1.

3.4.3 Maximum Accessible Surface Temperature in the Shade

The analysis shows that without the personnel barrier, the maximum accessible cask surface temperature at 100°F ambient in the shade is 208°F and exceeds the limit of 185°F. Therefore, a personnel barrier is required for transport operation at the maximum design basis transportation heat load of 21 kW per cask.

The accessible surfaces of the TN40 packaging consist of the personnel barrier and outermost vertical and radial surfaces of the impact limiters. The personnel barrier surrounds the cask body between impact limiters and has an open area of at least 80%.

The presence of the barrier has negligible effect on heat transfer between the cask surface and the environment. Convection is not affected because distance between the barrier and cask and the 80% open area of the barrier ensures the airflow around the cask is not restricted. Radiant heat transfer to or from the cask surface is not significantly affected because the 80% opening of the barrier allows the cask to "see" the ambient environment and the distance between the cask and the barrier ensures the screen is very close to ambient temperature. Thus, the 20% of the barrier that the cask sees is also very close to the ambient temperature.

The personnel barrier limits the accessible packaging surfaces to only the impact limiter surfaces. The NCT model with full insolation at 100° F ambient temperature shows that the accessible surface temperature of the impact limiters does not exceed 115° F. The maximum accessible surface temperature of the impact limiters at 100° F ambient in the shade is 106° F. Accessible surfaces of the packaging therefore, remain below the design criteria of 185° F (85° C).

3.4.4 Minimum Temperatures

Under the minimum temperature condition of -40°F (-40°C) ambient, the resulting packaging component temperatures will approach -40°F if no credit is taken for the decay heat load. Since the package materials, including containment structures and the seals, continue to function at this temperature, the minimum temperature condition has no adverse effect on the performance of the TN-40.

Temperature distributions at ambient temperatures of -40°F and -20°F with maximum decay heat and no insulation are determined. Table 3-2 lists the results of the analyses and the temperature distribution are shown in Figure 3-13.

3.4.5 Maximum Internal Pressure

The maximum NCT internal pressure is calculated in Chapter 4.

3.4.6 Maximum Thermal Stresses

The maximum NCT thermal stresses are calculated in Chapter 2.

3.4.7 Evaluation of Cask Performance for Normal Conditions of Transport

The thermal analysis of NCT demonstrates that the TN-40 cask design meets all applicable requirements as documented in Table 3-1. The maximum temperatures calculated using conservative assumptions are well below specified limits. The maximum temperature of any containment structural component is less than 251° F (122° C). The maximum seal temperature (195° F, 91° C) during NCT is well below the 536° F (280° C) long-term limit specified for continued seal function. The maximum neutron shield temperature is below 300° F (149° C) and no degradation of the neutron shielding is expected. The predicted maximum fuel cladding temperature (495° F, 257° C) is well within allowable fuel temperature limit of 752° F (400° C).

3.5 Thermal Evaluation for Hypothetical Accident Conditions

The TN-40 cask is evaluated under the HAC sequence of 10CFR71.73 [1]. The top impact limiter protects the TN-40 cask lid containing the lid and port seals from the thermal accident environment. Analytical models are developed as discussed in Sections 3.5.2 and 3.5.3 to demonstrate that seal temperatures are below their material temperature limits during HAC.

3.5.1 Fire Accident Evaluation

The fire thermal evaluation is performed primarily to demonstrate the containment integrity of the TN-40. This is assured as long as the metallic seals in the lid remain below 536°F and the cask cavity pressure is less than 100 psig. A full-length, 90 degree symmetric cask model as described in Section 3.4.1 is used for the evaluation. The model is modified to represent two crushed impact limiters as described in Section 3.5.3

Reference [8] reports an average convective heat transfer coefficient of 4.5 Btu/hr-ft²-°F for a railroad tank car fire test. The same parameter is utilized for the HAC fire accident evaluation.

3.5.2 Boundary conditions for the HAC

The boundary conditions described in Section 3.4.1. are modified for the HAC fire. During the pre-fire and post-fire phases, convection and radiation from the external surface of the model replicate the NCT analysis (100° F ambient). During the fire phase, a constant convective heat transfer coefficient of 4.5 Btu/hr-ft²-°F is used. All gaps are removed during the fire and restored immediately after the fire. This assumption is conservative in that it ensures maximum heat transfer into the cask during the fire and minimum heat transfer from the cask during the post-fire cooling period. As required by 10CFR71.73 [1], a 30 minute 1,475° F temperature fire with an emittance of 0.9 and a surface absorptivity of 0.8 is applied to the model. An emissivity of 0.9 and an absorptivity of unity are used for the cask external surfaces after the fire accident condition in order to bound the problem.

A detailed description of the model including the method used to calculate the maximum fuel cladding temperature and the average cavity gas temperature is provided in Section 3.4.1. The decay heat load used in this analysis corresponds to a conservative total heat load of 22 kW from 40 assemblies (0.55 kW/assy) with a peaking factor of 1.2 even though the design basis total heat load for transportation condition is 21 kW per cask.

3.5.3 Crushed Impact Limiter Models

In order to maximize the effect of the fire on cask components during and after the fire accident, the impact limiter finite element model developed in Section 3.4.1.2 is modified to reflect deformation due to a 30 foot drop. The maximum amount of crush experienced by the impact limiter in a given direction is assumed to occur everywhere on the limiter. Crushed impact limiter configurations based on side, corner and slap down drops are considered:

1. A crushed impact limiter corresponding to the side drop resulting in the shortest radial distance between the fire ambient and the cask surface. The maximum radial deformation of top and bottom impact limiters is 13.42 in. and 13.58 in. respectively. The impact limiters are thus modeled with a uniform

diameter of 117.2 in. (144-2x13.42) for the top impact limiter and 116.8 in. (144-2x13.58) for the bottom impact limiter to bound the maximum damage at any angular location.

2. A crushed impact limiter corresponding to the corner and end drops resulting in the shortest axial distance between the fire ambient and the cask surface. The maximum axial deformation (17.6 in) occurs for the corner drop. The impact limiters are modeled with a uniform axial length of 20.4 in (38-17.6).

Although the impact limiters are locally deformed during the 30 foot drop, they remain firmly attached to the cask. Under exposure to the thermal accident environment the wood at the periphery of the impact limiter would char but not burn. Hence, the steel encased wood impact limiters still protect the lid of the cask from the external heat load applied during the HAC fire.

Although unlikely, the worst-case damage due to a hypothetical puncture conditions based on 10CFR71.73(c)(3) [1] may result in the tearing off the outer steel skin of the front impact limiter, crushing the wood out of the damaged area, and exposing the partially contained wood to the hypothetical fire conditions.

A study of fire performance of wood at elevated temperatures and heat fluxes [16] shows that the surface temperature for the rapid spontaneous ignition of wood is between 330° C and 600° C (626° F and 1,112° F). Based on standard fire test (ASTM E119, 1988) reported in [16], if a thick piece of wood is exposed to fire temperatures between 815° C and 1,038° C (1,500° F and 1,900° F), the outermost layer of wood is charred. At a dept of 13mm (~0.5") from the active charzone, the wood is only 105° C (220° F). This behavior is due to the low conductivity of wood and fire retardant characteristics of char. It is also shown that the char forming rate under high temperature fire conditions is between 37 mm/hr for soft woods and 55 mm/hr for hard woods. Redwood has a char rate of 46 mm/hr [16].

The thickness of Redwood at the center of the TN-40 cask impact limiter is 34.75 inches (883 mm), see Drawing 10421-71-42, Rev. 0, Section 1.4.1. Considering the char rate for Redwood, it takes about 19 hours until the char reaches 13 mm above the inner surface of the center cover plate. At that moment, the maximum char temperature would be imposed at the impact limiter inner surface.

$$(\text{Redwood thickness} - 13) / \text{char rate} = \frac{(883 - 13)}{46} = 18.9 \text{ hr}$$

It takes another 17 minutes until the last 13 mm of Redwood is charred.

$$(\text{thickness of last portion of hot Redwood}) / \text{char rate} = \frac{13}{46} = 0.28 \text{ hr} = 17.0 \text{ min}$$

During the last 17 minutes, the inner surface of the impact limiter is exposed to the high temperature of charring wood. The impact of charring wood on the cask is maximized if charring occurs immediately after fire for 17 minutes.

To bound the problem and remain conservative, it is considered in the finite element model that the inner surface of the impact limiter inner cover is exposed to 1,112°F maximum char wood temperature for 30 minutes immediately after the end of fire. No heat dissipation is considered for the open surface of the torn wood segment after the period, assuming conservatively that this surface is entirely covered with a thin layer of low conductivity wood char.

Considering the size of wood segments and location of seals, the worst case scenario occurs when a middle segment of wood (ID 44" to OD 88", 90 degree) is torn. Nevertheless, the effects of a torn side segment (ID 88" OD 144", 30 degree) are also evaluated.

3.5.4 Summary of Results

The three investigated accident cases described in Section 3.5.3 show that the maximum component temperatures are bounded by the case of deformed impact limiter with torn middle segment. Table 3-3 presents the bounding maximum temperatures of the cask components during and after the fire event for deformed and torn impact limiter. The bounding values calculated for the maximum seal and the fuel cladding temperatures are 325°F and 529°F, respectively. The transient average cavity gas temperature peaks at 387°F. For conservatism, an average cavity gas temperature of 441°F is considered for calculating the cavity pressure. The corresponding peak cavity pressure assuming 100% fuel failure is evaluated in Chapter 4 and is less than 100 psig. The temperature distributions in the packaging for HAC are shown in Figure 3-14 and Figure 3-15.

3.5.5 Evaluation of Package Performance During and after the HAC Fire

It is concluded that the TN-40 maintains containment during the postulated sequential drop, puncture, and fire accident. The neutron shield will off-gas during the fire event. A pressure relief valve is provided on the outer shell to prevent the pressurization of the outer shell. The shielding integrity of the neutron shielding is assumed to be lost after the fire event and the resulting accident dose rates have been evaluated in Chapter 5. The maximum seal temperature is well below the 536° F long-term limit specified for continued seal function and the fuel cladding temperature is below the limit of 1058° F (570° C) defined in [14].

3.6 References

1. Code of Federal Regulations, 10CFR71, "Packaging and Transportation of Radioactive Materials".
2. *Wood Handbook: Wood as an Engineering Material*, U.S. Department of Agriculture, Forest Service, March 1999.
3. *ASME Boiler and Pressure Vessel Code*, American Society of Mechanical Engineers, Section III and Appendices, 1989.
4. *TN-24 Dry Storage Cask Topical Report*, Transnuclear, Inc., Revision 2A, Hawthorne, NY, 1989.
5. ANSYS Engineering Analysis System, *User's Manual for ANSYS Release 8.0*, and 8.1 ANSYS, Inc., Canonsburg, PA.
6. Rohsenow, M. W., Cho, Y. I., and Hartnett, J. P., *Handbook of Heat Transfer*, 3rd Edition, 1998.
7. Siegel, Howell, "Thermal Radiation Heat Transfer," 4th Edition, 2002.
8. Gregory et al., *Thermal Measurements in a Series of Large Pool Fires*, SAND85-0196, TTC-0659, Sandia National Laboratories, 1987.
9. NUREG/CR-0497, *A Handbook of Materials Properties for Use in the Analysis of Light Water Reactor Fuel Rod Behavior*, MATPRO - Version 11 (Revision 2), EG&G Idaho, Inc., TREE-1280, August 1981.
10. Baumeister & Marks, *Standard Handbook for Mechanical Engineers*, Seventh Edition, McGraw-Hill Book Co., New York, 1969.
11. Helicoflex High Performance Sealing Catalog, Carbone Lorraine, Helicoflex Components Division, ET 507 E 5930.
12. W. M. Rohsenow, J. P. Hartnett, "Handbook of Heat Transfer Fundamentals," 2nd Edition, 1985.
13. Perry, Chilton, *Chemical Engineer's Handbook*, 5th Edition, McGraw-Hill, Inc. New York, 1973.
14. USNRC, SFPO, "Cladding Consideration for the Transportation and Storage of Spent Fuel," Interim Staff Guidance ISG-11, Rev. 3.
15. Prairie Island independent Spent Fuel Storage Installation Safety Analysis Report, Revision 10.

16. Mitchell S. Sweet, *Fire Performance of Wood: Test Methods and Fire Retardant Treatments*, Fire Safety of Wood Products, USDA Forest Service.
<http://www.fpl.fs.fed.us/documents/pdf1993/sweet93a.pdf>.
17. NUREG/CR-0322, Effects of Temperature on the Energy Absorbing Characteristics of Redwood, Von Riesemann, Gues, SAND77-1589, Sandia Lab.

3.7 Appendices

Appendix 3.7.1 Effective Fuel Properties for the Fuel Assembly

Table 3-1
NCT Component Temperatures In The TN-40 Package

Component	Normal Transport		
	Maximum (°F)	Minimum* (°F)	Allowable Range(°F)
Outer Shell	214	-40	**
Radial Neutron Shield	229	-40	-40 to 300
Inner Shell	251	-40	**
Basket Rail	257	-40	**
Basket Plate	444	-40	**
Gamma Shield Shell	248	-40	**
Fuel Cladding	495	-40	752 max.
Impact Limiter Wood	224	-40	230
Lid O-ring Seal	195	-40	-40 to 536
Average Cavity Gas*	345	-40	N/A

* Assuming no credit for decay heat and a daily average ambient temperature of -40°F

** The components perform their intended safety function within the operating range.

+ A conservative value of 348° F is used for calculating MNOP.

Table 3-2
Temperature Distribution In The TN-40 Package
(Low Ambient Temperature, Max Decay Heat)

<u>Component</u>	Maximum Component Temperature (°F)	
	-40 °F Ambient Temperature	-20 °F Ambient Temperature
Outer Shell	88	106
Aluminum Boxes	102	120
Resin	102	120
Gamma Shield Shell	123	140
Inner Shell	127	144
Basket Rails	133	151
Fuel Cladding	386	401
Cask Bottom Plate	101	119
Lid O-ring Seal	68	86
Basket (Fuel Compartments)	330	346

Table 3-3
Maximum HAC Transient Temperatures During Fire Accident

<u>Component</u>	<u>Maximum Transient Temperature (°F)</u>	<u>Allowable Range (°F)</u>
Impact Limiter Outer Surface	1431 (end of fire)	**
Outer Shell Surface	1084 (end of fire)	**
Lid O-ring Seal	325 (one hour after fire)	536
Gamma Shield Shell	694 (end of fire)	**
Cask Rail / Shim	330 (one hour after fire)	**
Inner Shell	403 (end of fire)	**
Basket (Fuel Compartment)	480 (20 hours after fire)	**
Fuel Cladding	529 (26 hours after fire)	1058
Average Cavity Gas	387 (10.2 hours after fire)	**

* An average cavity gas temperature of 441° F is considered for calculating of cavity gas pressure in Chapter 4 for conservatism.

** The components perform their intended safety function within the operating range.

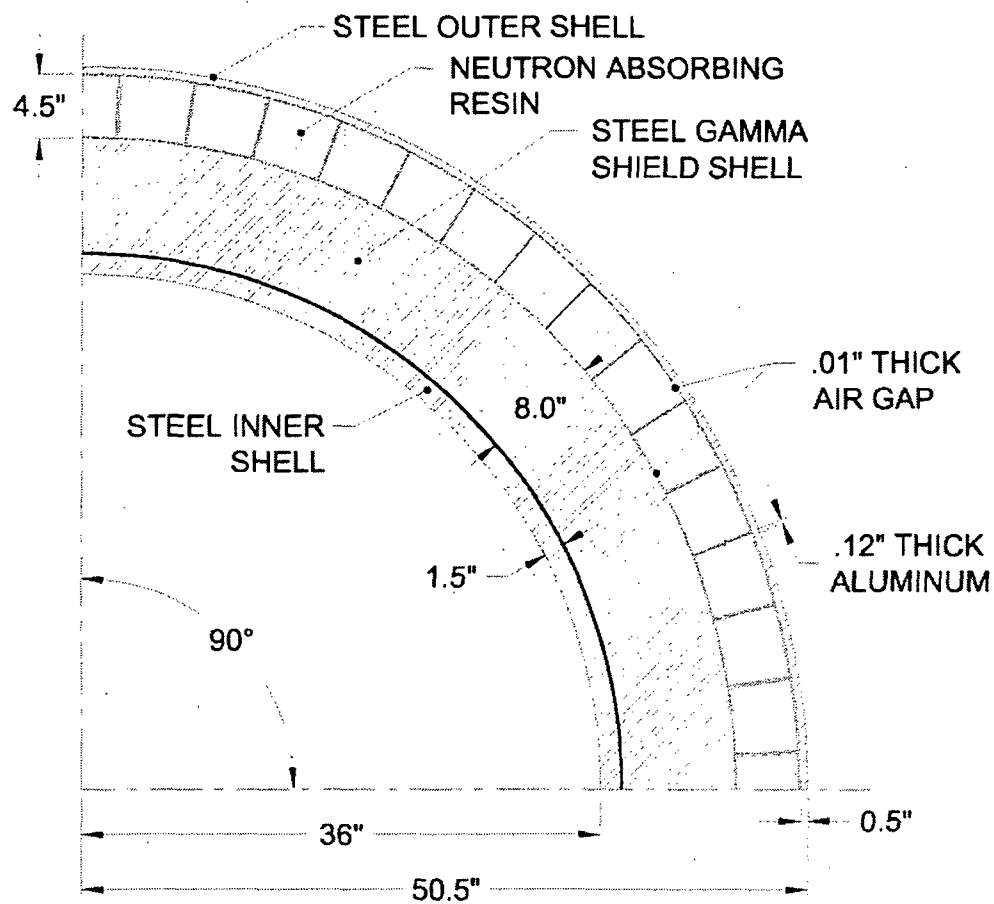


Figure 3-1
Schematic Of The Cask Body

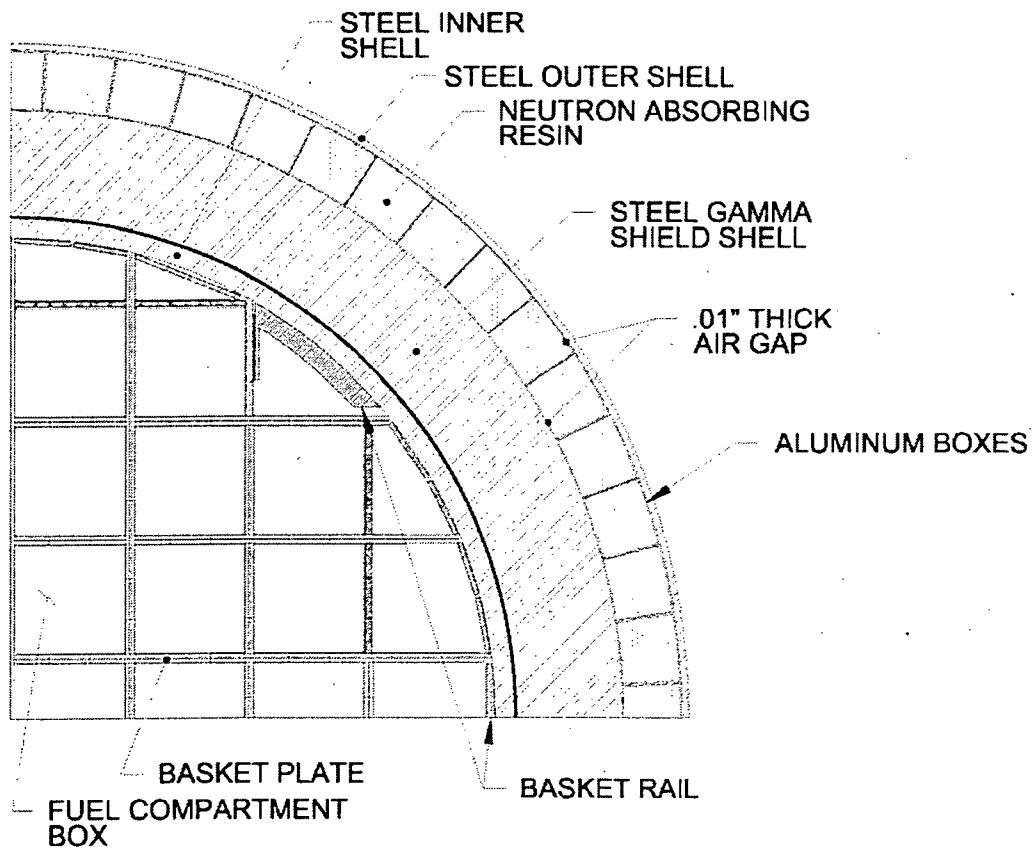


Figure 3-2
Thermal Model
90 Degree Radial Cross Section

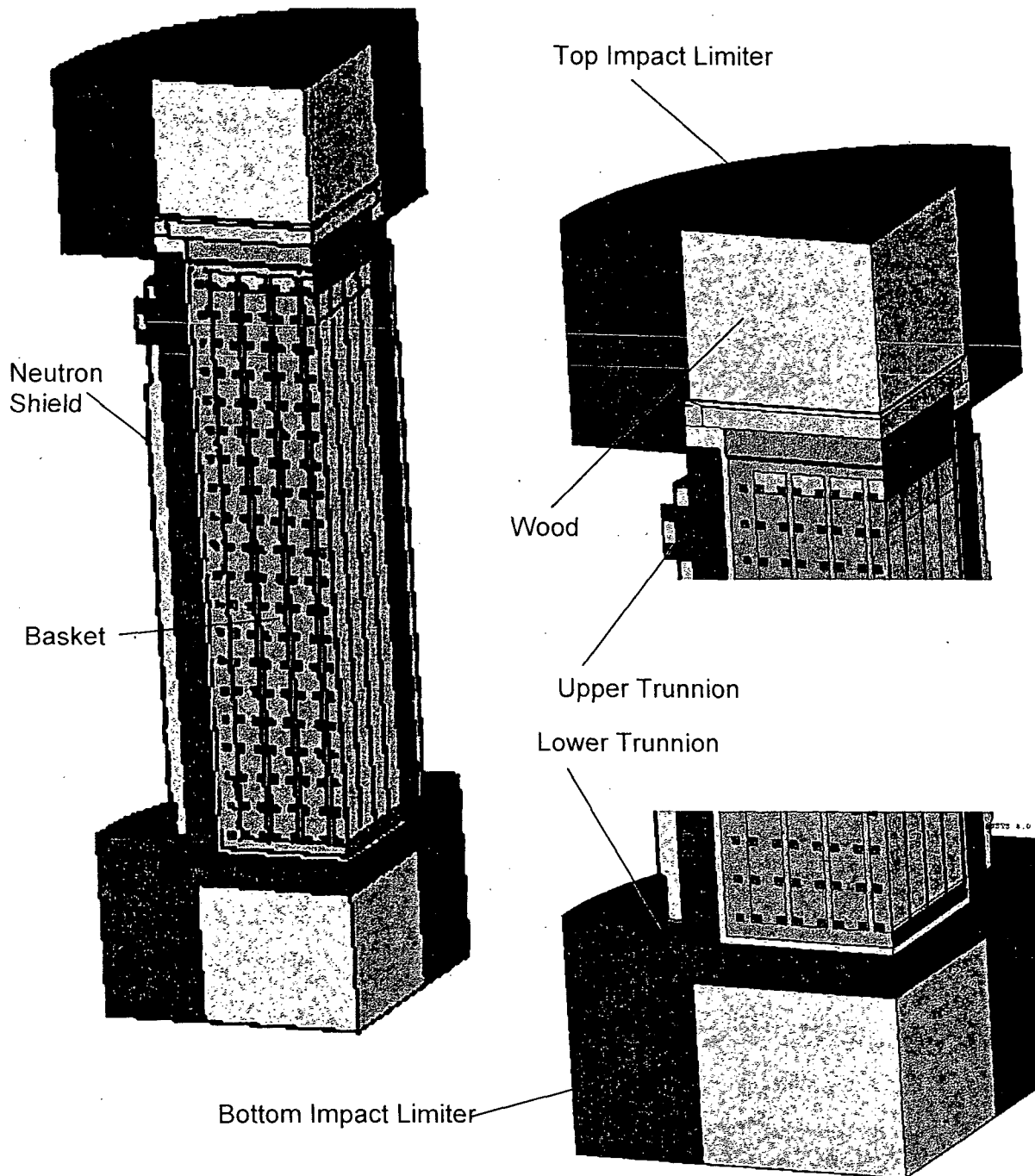


Figure 3-3
Finite Element Model Of TN-40 Transport Cask

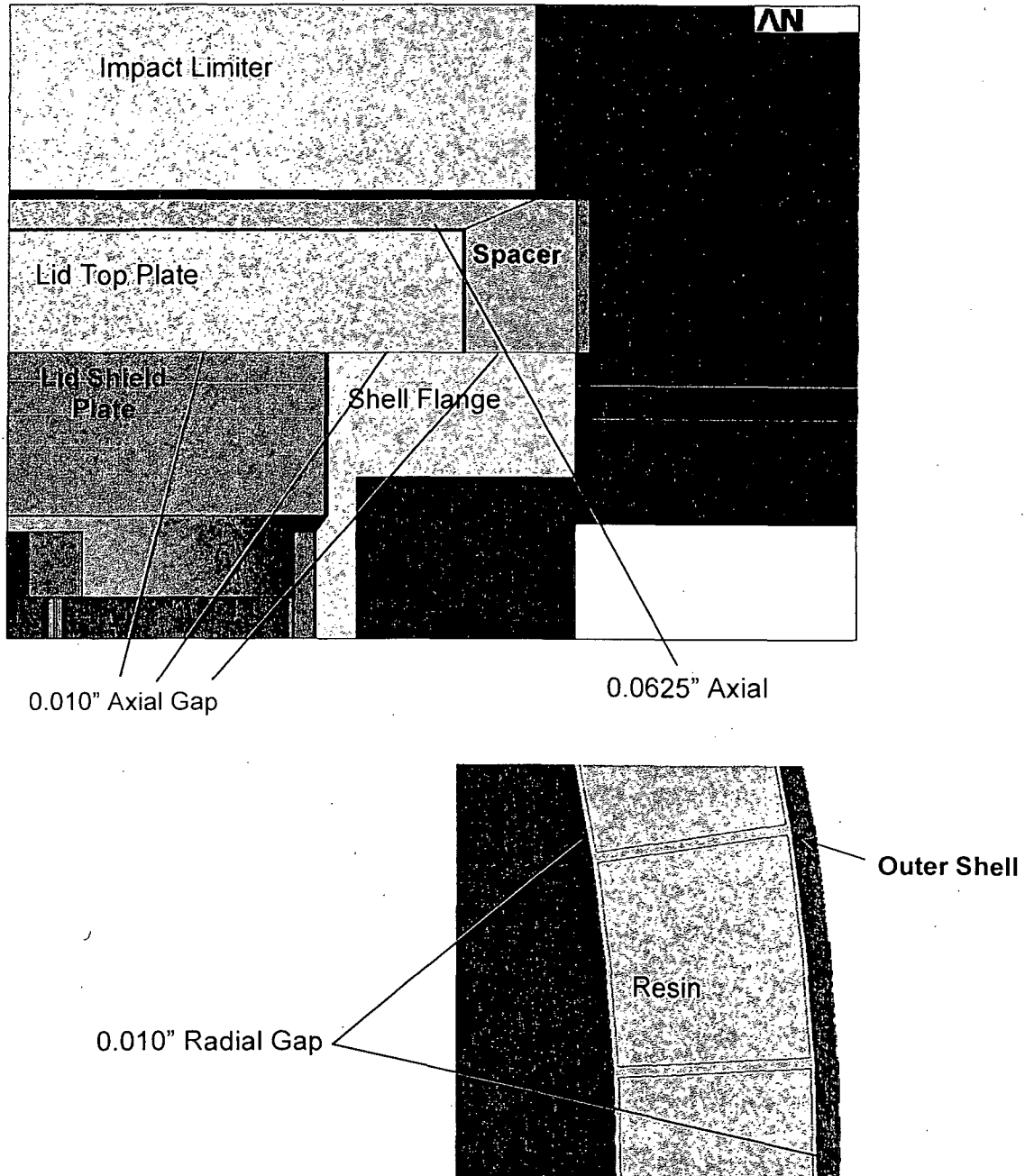


Figure 3-4
Finite Element Model Of The TN-40 Transport Cask, Details

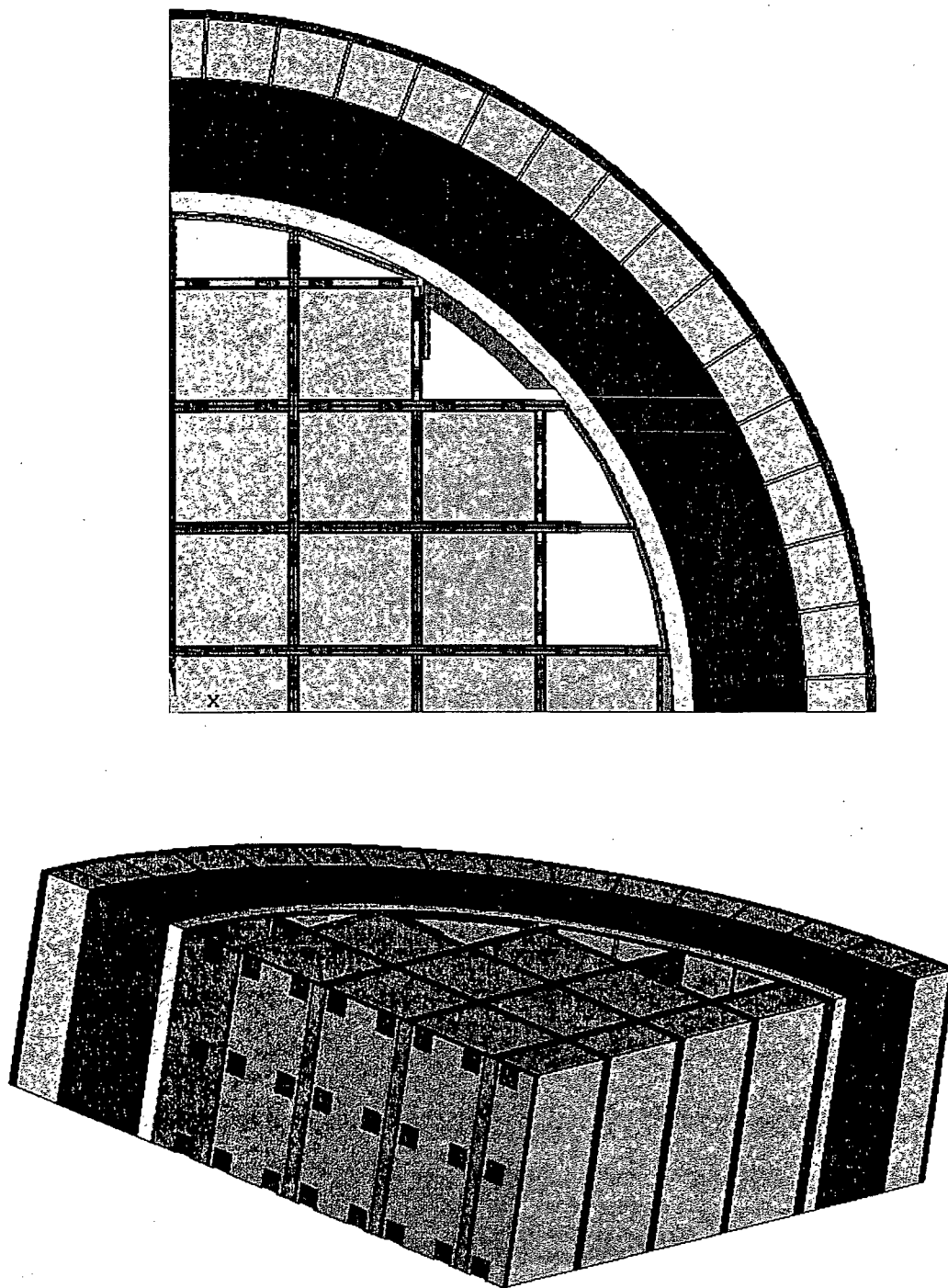
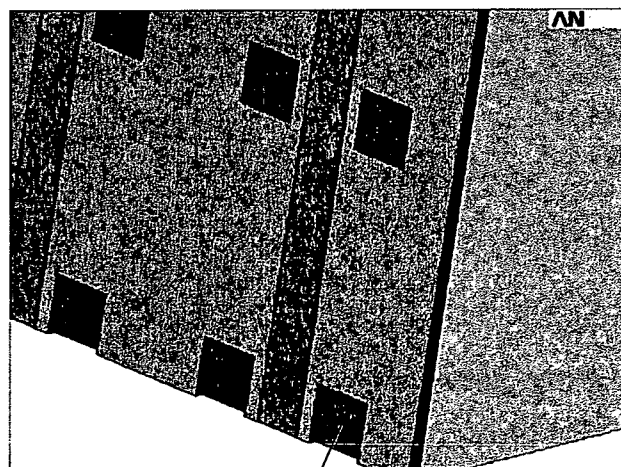
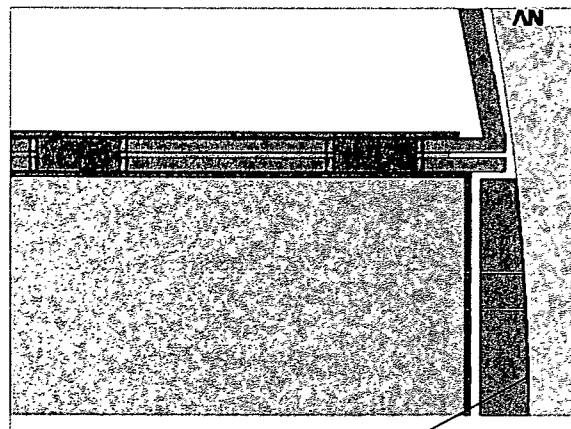


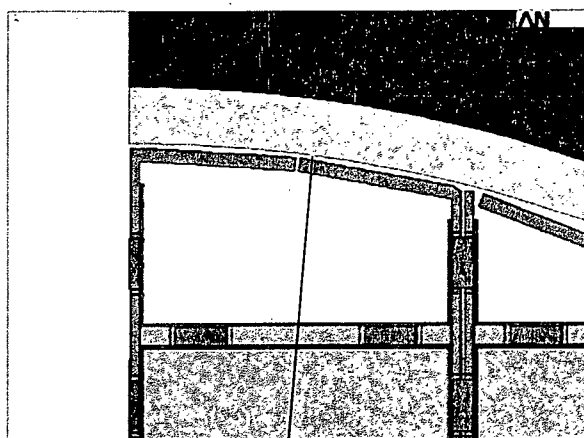
Figure 3-5
Finite Element Model Of The TN-40 Basket Cross Section



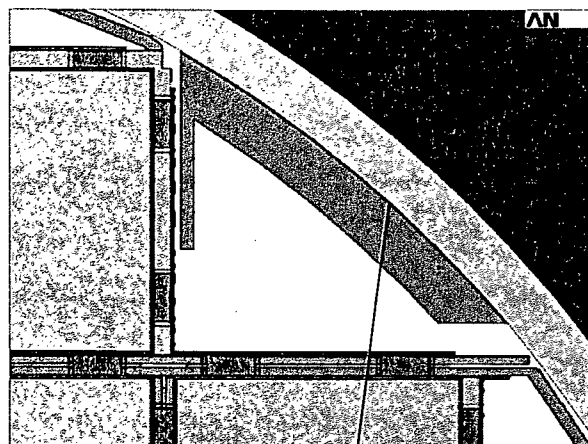
Hole sq. 1.63"
Weld Plug sq. 1.38" Centered



0.020" Radial Gap



0.10" Minimum Gap
Between Inner Shell
and Aluminum Plates



0.020" Radial Gap

Figure 3-6
Finite Element Model Of The TN-40 Basket, Details

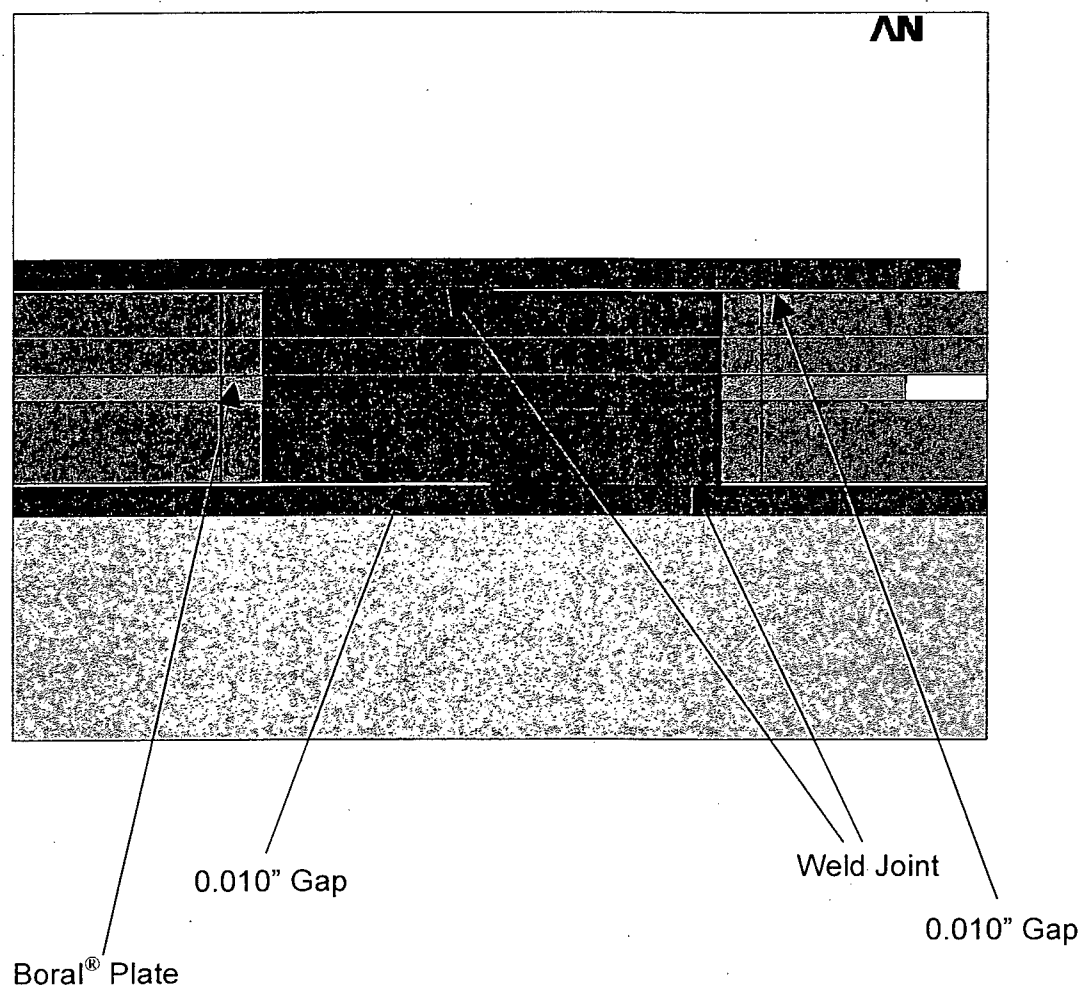
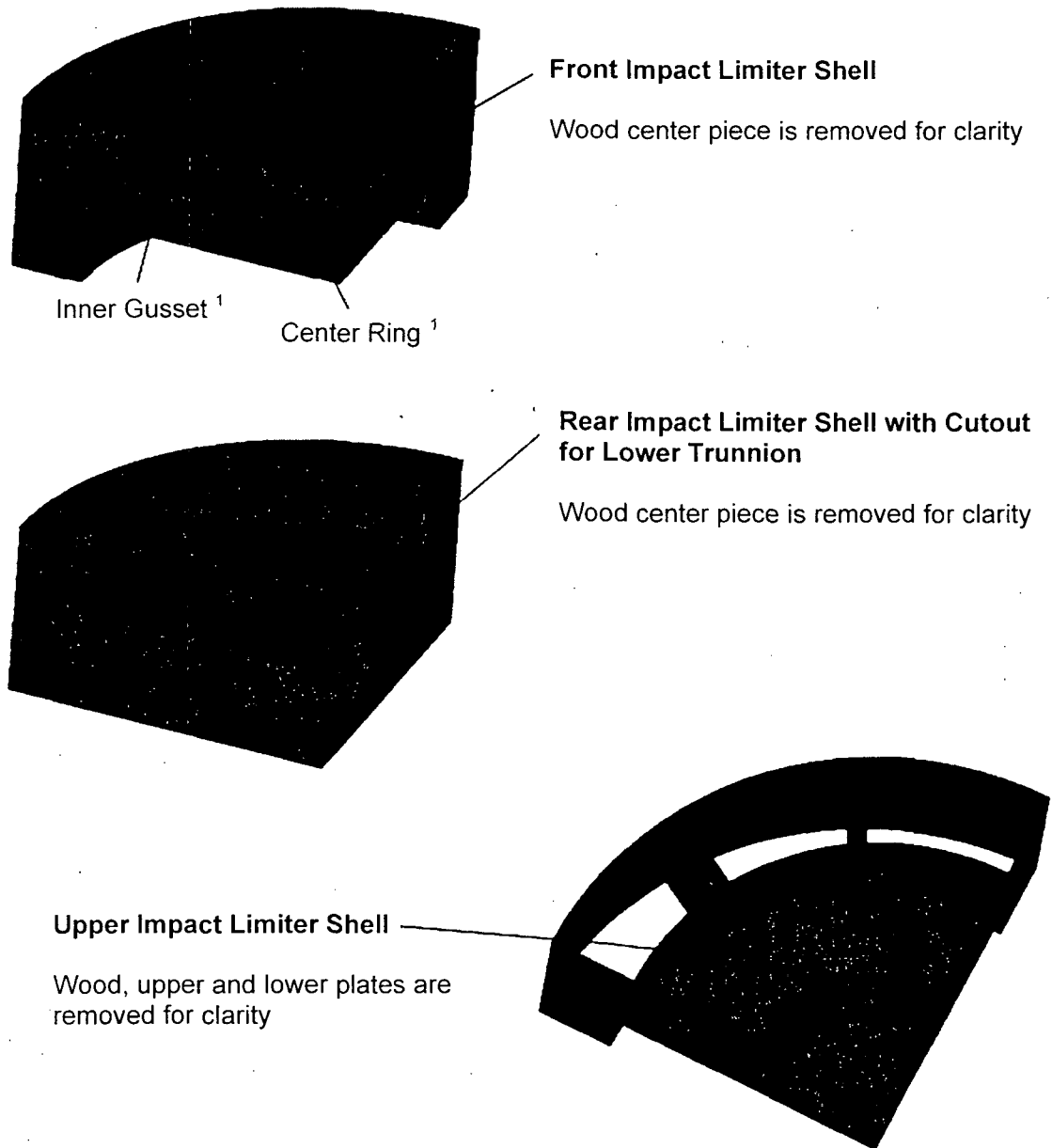


Figure 3-7
Finite Element Model Of The TN-40 Basket Compartment
Weld Joint Details



¹ Center ring and inner gussets are not included in the model for normal transport conditions. These features are considered only for accident conditions.

Figure 3-8
Details of Impact Limiters

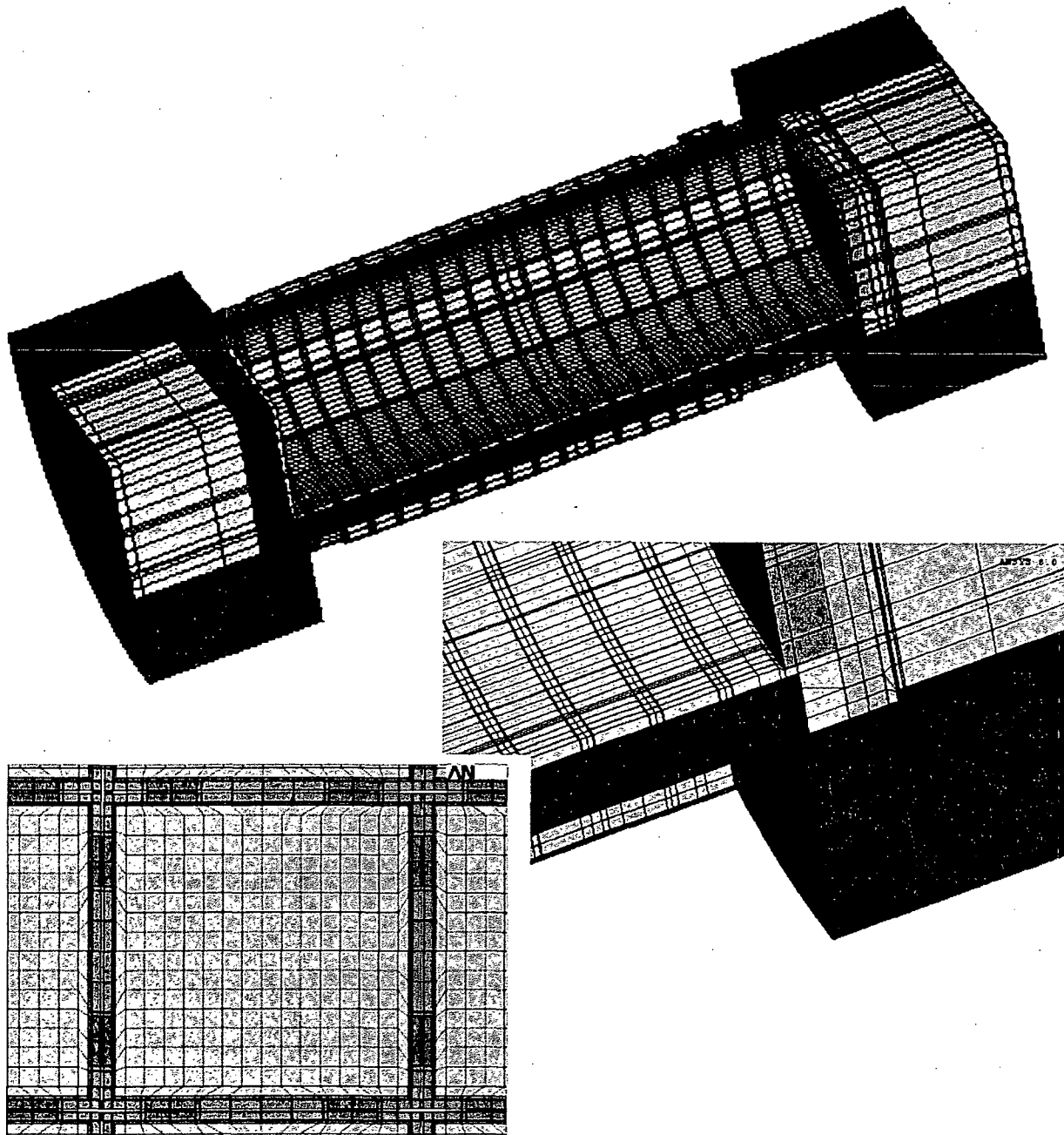


Figure 3-9
Mesh Of Finite Element Model

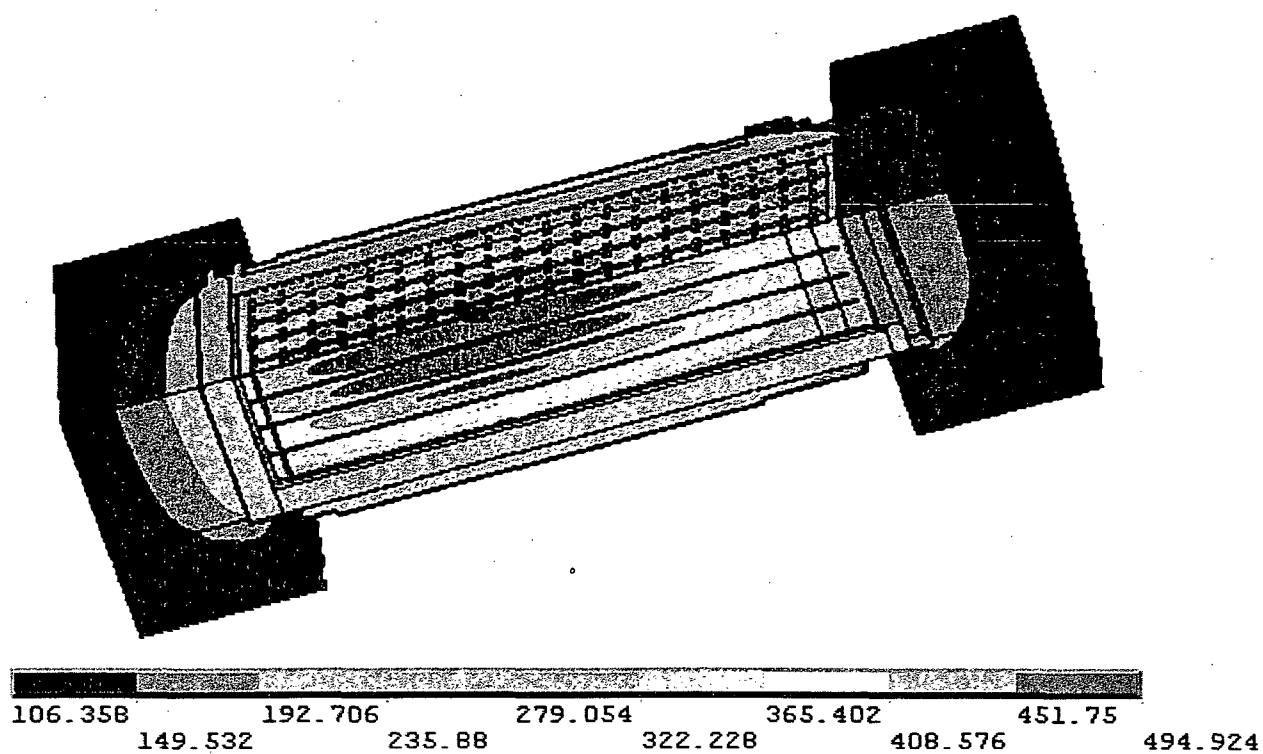
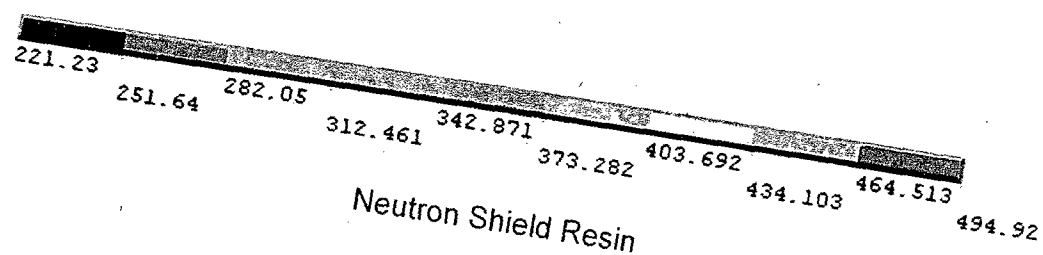
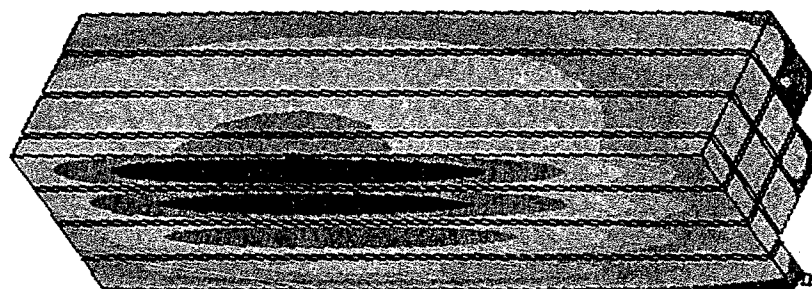


Figure 3-10
Temperature Distribution In The TN-40 Cask, NCT, 100° F

Fuel Assemblies



Neutron Shield Resin

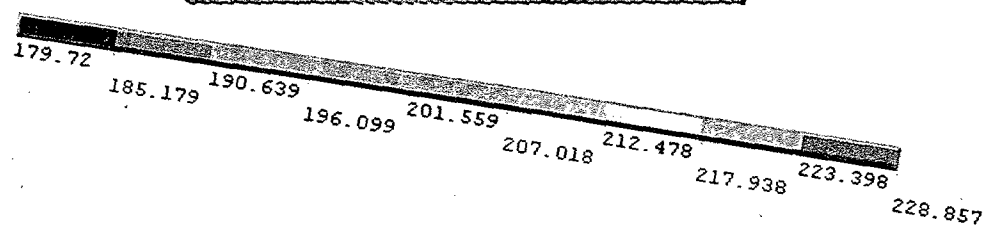
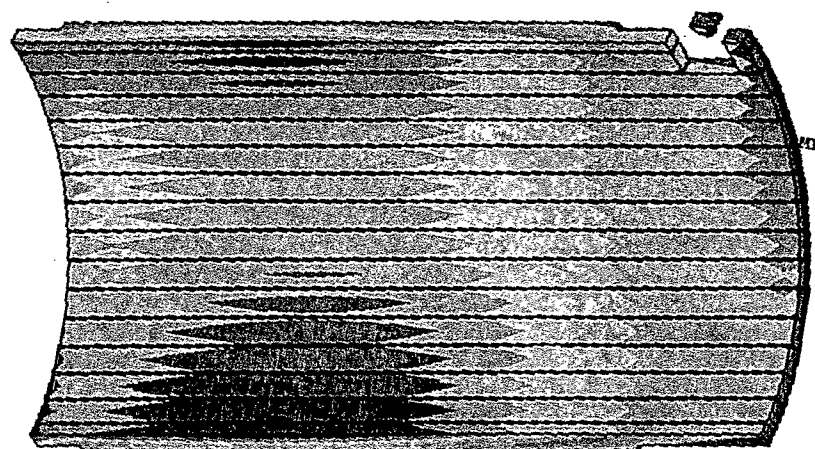
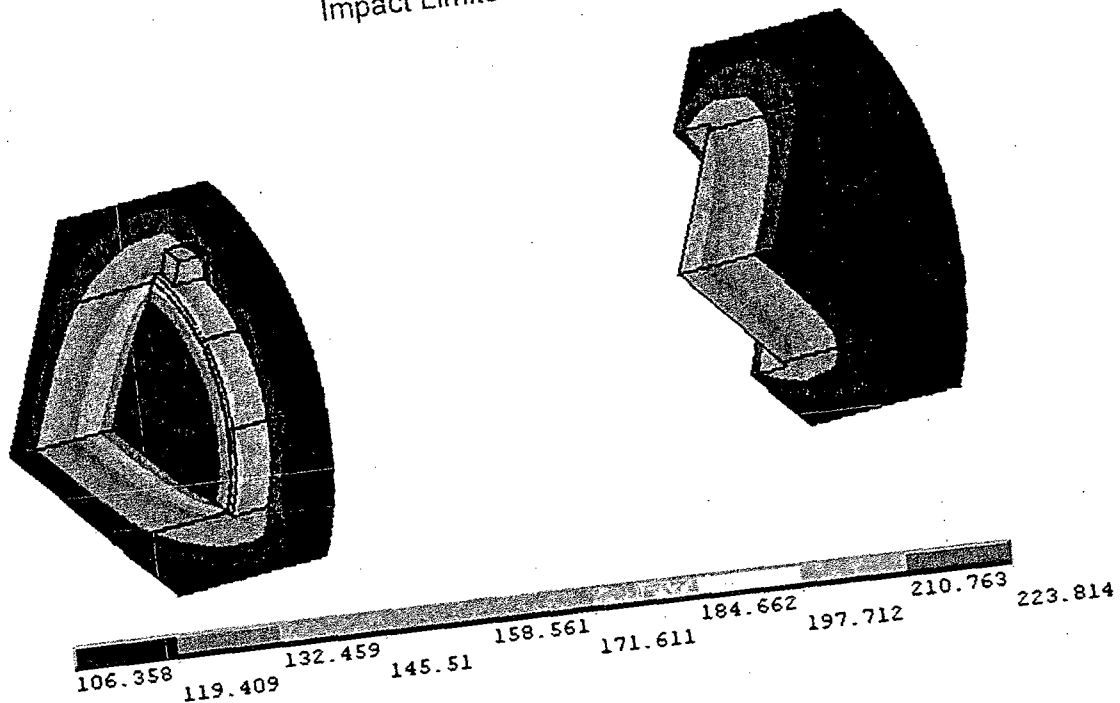


Figure 3-11
Temperature Distributions In The TN-40 Cask, Fuel & Resin NCT, 100° F.

Impact Limiter Wood



Large and Small Basket Rails

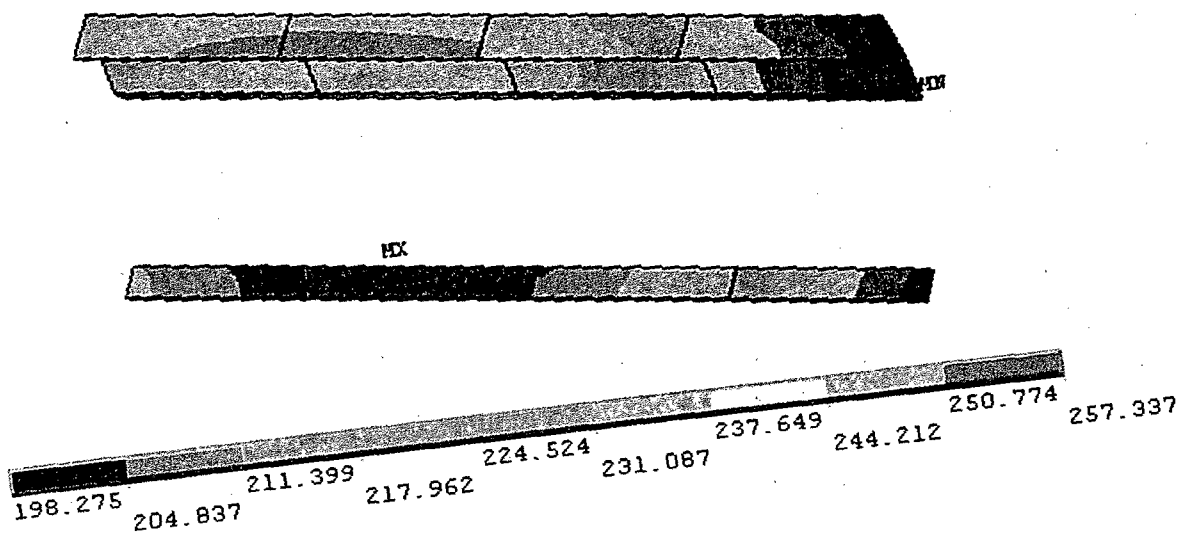


Figure 3-12
Temperature Distributions In The TN-40 Cask, Impact Limiters & Rail
Normal Conditions Of Transport NCT, 100° F

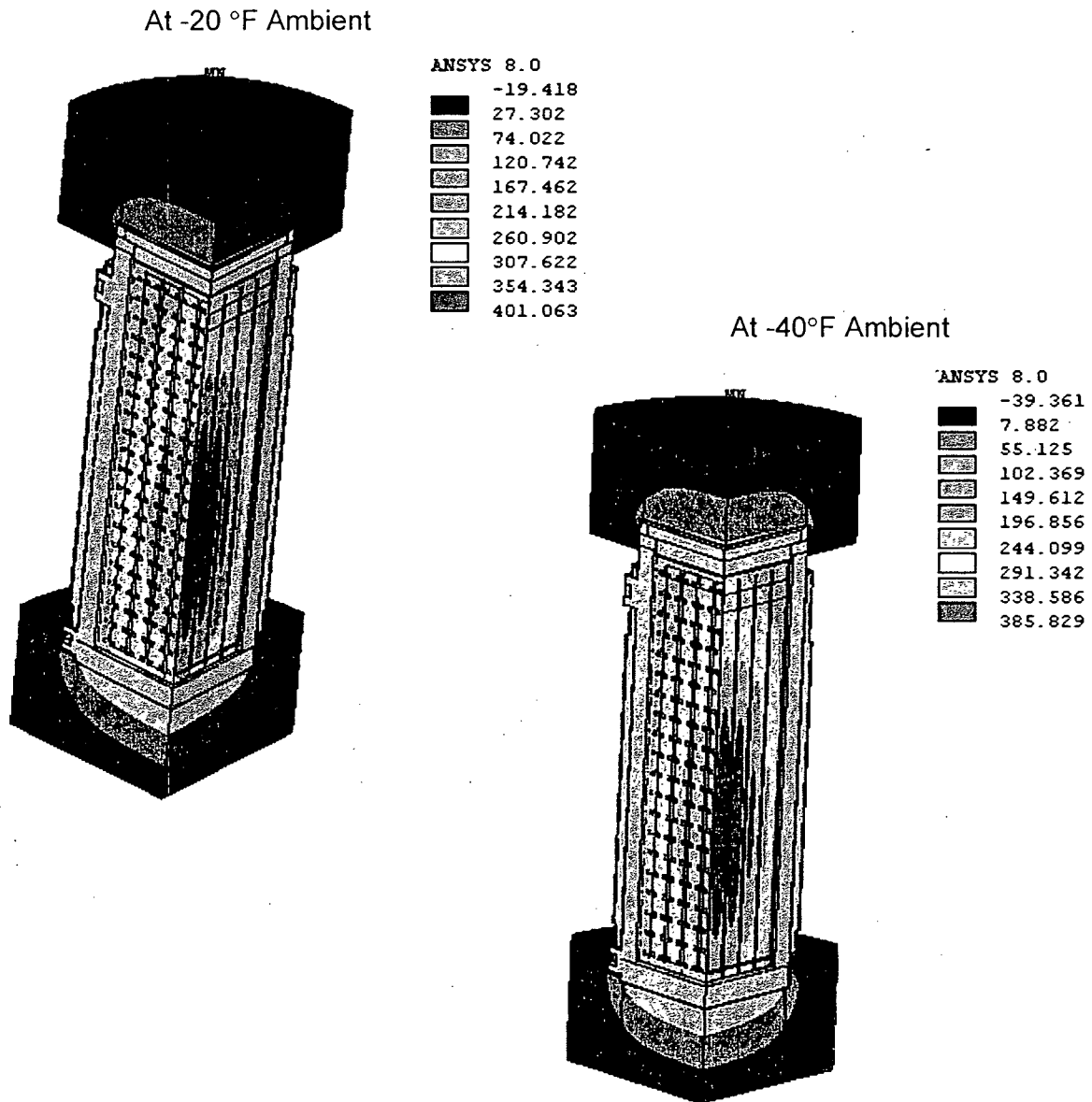
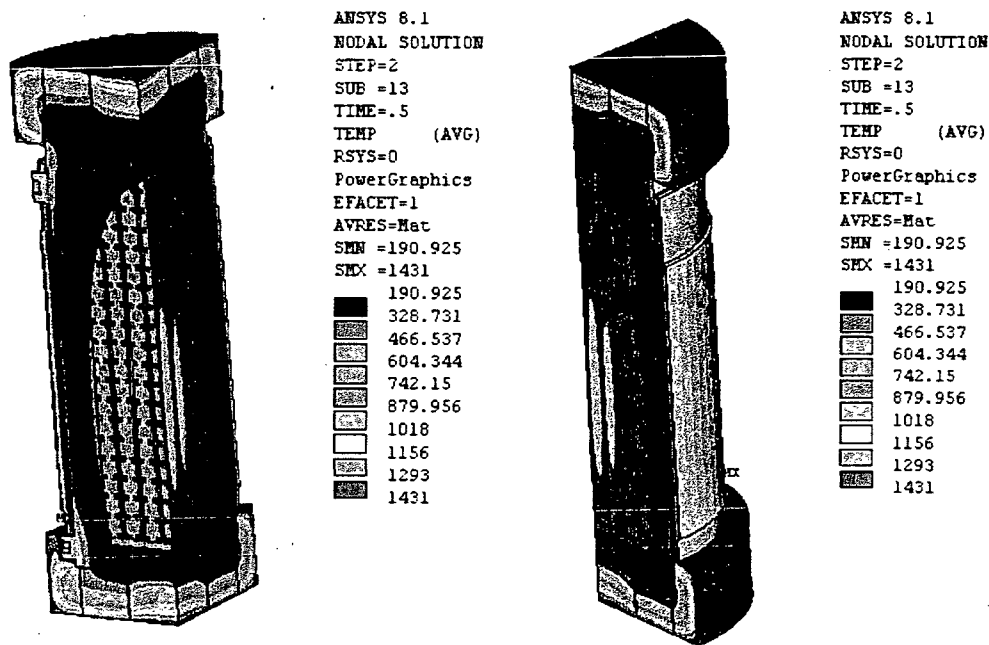
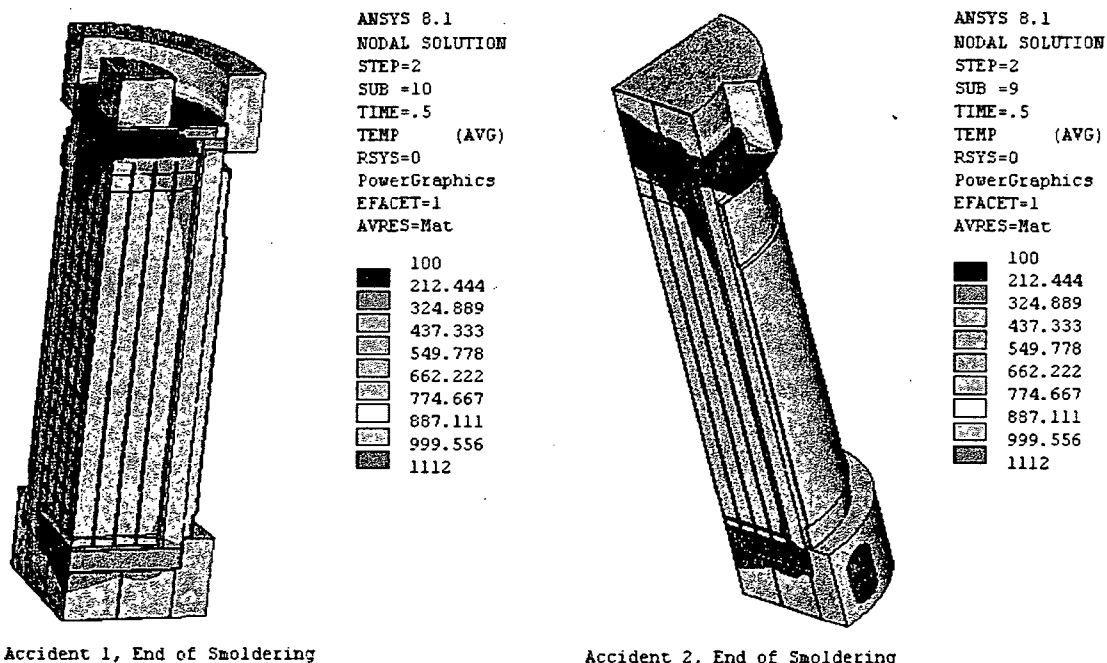


Figure 3-13
Temperature Distributions In The TN-40 Cask
Low Ambient Temperatures



Distribution at the End of the Fire

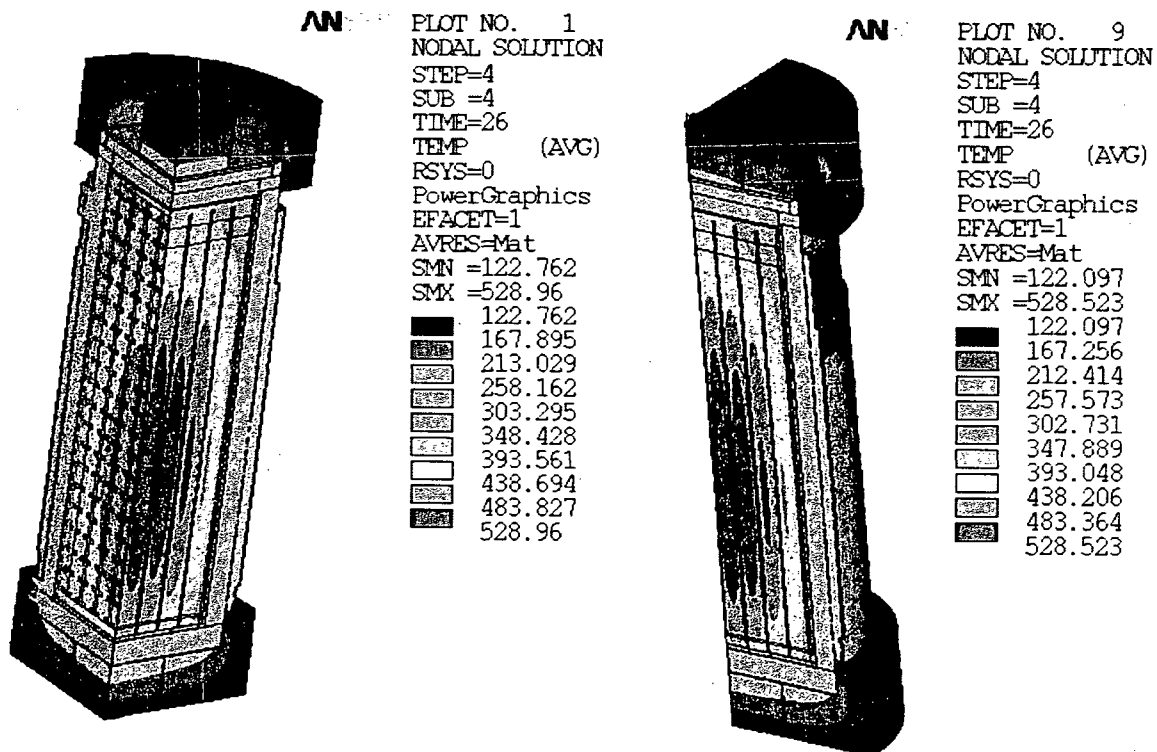


Accident 1, End of Smoldering

Accident 2, End of Smoldering

Distribution at the End of the Wood Smoldering

Figure 3-14
Maximum Temperature Distribution in the TN-40 Cask
HAC, End of Fire / Smoldering



Distribution in Cool-Down Period 26 hours after the End of Fire

Figure 3-15
Maximum Temperature Distribution in the TN-40 Cask
HAC, Cool-Down Period

APPENDIX 3.7.1

EFFECTIVE THERMAL PROPERTIES FOR THE FUEL ASSEMBLY

TABLE OF CONTENTS

	<u>Page</u>
3.7.1 EFFECTIVE THERMAL PROPERTIES FOR THE FUEL ASSEMBLY	3.7.1-1
3.7.1.1 Discussion	3.7.1-1
3.7.1.2 14 x 14 PWR Fuel Geometry Parameters.....	3.7.1-1
3.7.1.3 Summary of Material Properties	3.7.1-1
3.7.1.4 Thermal Model.....	3.7.1-3
3.7.1.4.1 Transverse Effective Conductivity	3.7.1-3
3.7.1.4.2 Finite Element Model	3.7.1-4
3.7.1.4.3 Axial Effective Conductivity	3.7.1-5
3.7.1.5 Effective Density and Specific Heat	3.7.1-5
3.7.1.6 Conclusion	3.7.1-6
3.7.1.7 References	3.7.1-7

LIST OF FIGURES

Figure 3.7.1-1	Finite Element Model Of WE 14 X 14 Assembly (1/4 Symmetry)	3.7.1-8
Figure 3.7.1-2	Typical Boundary Conditions Based On FE Model Of WE14 X 14.....	3.7.1-9
Figure 3.7.1-3	Typical Temperature Distributions For FE Model Of WE 14 X 14.....	3.7.1-10

3.7.1 EFFECTIVE THERMAL PROPERTIES FOR THE FUEL ASSEMBLY

3.7.1.1 Discussion

In order to determine the effective fuel assembly thermal conductivity, effective fuel density, and effective specific heat, the 14x14 PWR fuel assemblies to be transported in the TN-40 cask were reviewed to select the fuel assembly or parameters that would provide the most conservative (lowest) effective thermal conductivity. Use of these properties would conservatively predict bounding maximum temperatures for the TN-40 cask.

Effective conductivity values in the axial and transverse directions are calculated separately. The transverse fuel effective conductivity is determined by creating a two-dimensional finite element model of the fuel assembly centered within a basket compartment using the ANSYS computer code [5]. The outer surfaces, representing the fuel compartment walls, are held at a constant temperature, and a decay heat is applied to the fuel pellets within the model. A steady state solution of the model determines the maximum fuel assembly temperature. The two-dimensional model is described in Section 3.7.1.4.

3.7.1.2 14 x 14 PWR Fuel Geometry Parameters

The fuel assemblies to be transported in the TN-40 cask are WE14x14 Standard, WE14x14 OFA, Exxon Standard, Exxon High Burnup, and Exxon TOPROD.

The bounding values for the gap between the pellet and the clad (maximum gap of 0.0048 in.) and for the clad thickness (minimum of 0.0225 in.) are used for this evaluation. These values give the minimum transverse effective conductivity.

The material properties used to calculate the effective fuel properties are listed in Section 3.7.1.3.

3.7.1.3 Summary of Material Properties

a. UO_2 [3]

Temperature (°C)	k (cal/s-cm-°C)	Temperature (°F)	k (Btu/hr-in-°F)
25	0.025	77	0.503
100	0.021	212	0.423
200	0.018	392	0.362
300	0.015	572	0.302
500	0.0132	932	0.266
700	0.0123	1292	0.248
800	0.0124	1472	0.250

Temperature (°C)	Cp (cal/g-°C)	Temperature (°F)	Cp (Btu/lbm-°F)
0	0.056	32	0.056
100	0.063	212	0.063
200	0.0675	392	0.068
400	0.0722	752	0.072
1200	0.079	2192	0.079

The density of fuel pellets (UO_2) is $10.96 \text{ g/cc} = 0.396 \text{ lbm/in}^3$ [3]

b. Zircaloy-4 [2]

Temperature (K)	k (W/m-K)	Temperature (°F)	k (Btu/hr-in-°F)
373.2	13.6	212	0.655
473.2	14.3	392	0.689
573.2	15.2	572	0.732
673.2	16.4	752	0.790
773.2	18.0	932	0.867
873.2	20.1	1112	0.968

Temperature (K)	Cp (J/kg-K)	Temperature (°F)	Cp (Btu/lbm-°F)
300	281	80	0.067
400	302	260	0.072
640	331	692	0.079
1090	375	1502	0.090

The density of Zircaloy is $6.56 \text{ g/cm}^3 = 0.237 \text{ lbm/in}^3$, as defined in Reference [3].

Table B-3.11 of Reference [2] lists the measured emissivity values for fuel cladding. For ease of calculation a temperature independent emissivity of 0.80 is set for zircaloy-4.

$$\epsilon_{\text{zirc}} = 0.80$$

c. Helium (used for gaps within the cask cavity) [6]

Helium	Thermal Conductivity, k
Temperature (°F)	(Btu/hr-in-°F)
-100	0.0055
-10	0.0064
80	0.0072
260	0.0087
440	0.0102
620	0.0119
980	0.0148
1340	0.0175

For the transient analyses, the thermal mass is relatively small and neglected. The density and specific heat are not used.

d. Stainless Steel

A hemispherical emissivity of 0.46 is reported in [7] for 304 stainless steel samples. For conservatism an emissivity of 0.3 is considered in this calculation for the link elements representing the stainless compartment walls to create the radiation superelement.

3.7.1.4 Thermal Model

3.7.1.4.1 Transverse Effective Conductivity

The purpose of the effective conductivity in the transverse direction of a fuel assembly is to relate the temperature drop of a homogeneous heat generating square to the temperature drop across an actual assembly cross section for a given heat load. The isotropic effective thermal conductivity of a heat generating square, such as the fuel assembly, can be calculated from the following equation from [4]:

$$k_{trans} = \frac{q''' a^2}{(T_c - T_o)} (0.29468) \quad (1)$$

q''' = volumetric heat generation rate (Btu/hr-in.³)

a = half of the compartment width = 8.05 in./2 = 4.025 (in.)

T_c = maximum center temperature (peak cladding temperature) (°F)

T_o = wall temperature (°F)

The volumetric heat generation rate is:

$$q''' = \frac{Q}{4 a^2 L_a} \quad (2)$$

Q = decay heat load per assembly = 0.675 kW¹ = 2,303.3 Btu/hr

L_a = active fuel length = 144 (in.)

Substituting equation (2) in (1) gives:

$$k_{trans} = \frac{Q}{4 L_a (T_c - T_o)} (0.29468) \quad (3)$$

In determining the temperature dependent effective fuel conductivities an average temperature, equal to $(T_c + T_o)/2$, is used for the fuel temperature.

¹ 0.675 kW is the decay heat load per assembly for the TN-40 storage cask [1]. For transportation, maximum heat load per assembly in TN-40 cask is limited to 0.55 kW. The effective transverse conductivity is relatively insensitive to decay heat load.

3.7.1.4.2 Finite Element Model

A discrete finite element model of the fuel assembly in the TN-40 fuel compartment is developed using the ANSYS computer code [5]. This two-dimensional quarter-symmetry model of the fuel assembly simulates heat transfer by radiation and convection and includes the geometry of the fuel rods and guide tubes. Helium is used as the fill gas in the fuel assembly. A fuel assembly decay heat load of 0.675 kW is used for heat generation. An active length of 144 in. (366 cm) is assumed. Radiation between the fuel pellet and cladding is conservatively neglected. The fuel assembly is centered within the fuel compartment.

The fuel components were modeled using PLANE55 elements. No convection is considered within the fuel assembly model. Heat transfer from the fuel rods to the fuel compartment walls is through conduction and radiation.

Radiation between the fuel rods, the guide tubes, and the fuel compartment walls was simulated using the radiation super-element processor (/AUX12). LINK32 elements were used to define radiating surfaces to create the radiation super-element. The LINK32 elements were unselected prior to the solution of the model. The model was run with a series of isothermal boundary conditions applied to the outermost nodes representing fuel compartment walls.

LINK32 elements were located at symmetry axes to make an enclosure for creating the radiation super-element. A very low emissivity (0.001) is given to the LINK32 elements lying on the symmetry axes to minimize their effect on overall radiation heat transfer.

The conductivity of helium is considered for the back fill gas for transport conditions.

The thermal properties used are as described in Section 3.7.1.3, and the fuel assembly geometry is described in Section 3.7.1.2. Figure 3.7.1-1 shows the details of the finite element model. A typical boundary condition is shown in Figure 3.7.1-2. A typical temperature distribution is shown in Figure 3.7.1-3.

The maximum fuel assembly temperatures resulting from the 2D analysis are shown in the table below. The reaction solution (Q_{react}) equals the decay heat load per active length of the fuel assembly. Since the model is quarter-symmetric, the applied decay heat load is:

$$Q = 4 \times Q_{react} \times L_a \quad (4)$$

Substituting equation (4) in equation (3) gives the effective fuel conductivity in the transverse direction.

$$k_{trans} = \frac{Q_{react}}{(T_c - T_o)} (0.29468)$$

Several computational runs were made using isothermal boundary temperatures ranging from 100 to 1000°F. The results of the finite element analysis and the effective fuel assembly conductivity calculation using the equation above are:

T ₀ (°F)	T _c (°F)	T _{avg} (°F)	Q _{react} (Btu/hr-in)	k _{eff} (Btu/hr-in-°F)
100	173	136	3.9753	0.0161
200	266	233	3.9753	0.0177
300	361	330	3.9753	0.0193
400	456	428	3.9753	0.0210
500	551	526	3.9753	0.0228
600	648	624	3.9753	0.0246
700	744	722	3.9752	0.0263
800	842	821	3.9753	0.0281
900	939	920	3.9753	0.0298
1000	1037	1019	3.9754	0.0317
Q (Btu/hr) / kW		2290	0.671	

3.7.1.4.3 Axial Effective Conductivity

The axial fuel assembly conductivity can be calculated by taking credit for the conduction paths provided by the fuel cladding, the guide tube and the helium in the fuel compartment. However, in accordance with [8], the axial effective conductivity calculated here is limited to the conductivity of the cladding. The axial conductivity provided by the fuel pellets conservatively neglected.

The effective conductivity is determined by weighting the cladding conductivity by its fractional area to the fuel compartment area:

$$k_{axial} = \frac{\text{cladding area}}{4a^2} \times \text{cladding conductivity}$$

$$a = \text{half of compartment width} = 8.05''/2 = 4.025''$$

$$\text{Zr-4 Cladding: } A_{Zr} = 179 \frac{\pi}{4} ((0.422)^2 - (0.422 - 2 \times 0.0225)^2) = 5.05 \text{ in}^2$$

The results are summarized in Section 3.7.1.6.

3.7.1.5 Effective Density and Specific Heat

Volume average density and weight average specific heat are calculated to determine the effective density and specific heat for the fuel assembly. The equations to determine the effective density and specific heat are shown below.

$$\rho_{eff} = \frac{\sum \rho_i V_i}{V_{assembly}} = \frac{\rho_{UO_2} V_{UO_2} + \rho_{Zr_4} V_{Zr_4}}{4a^2 L_a}$$

$$C_{p,eff} = \frac{\sum \rho_i V_i C_{Pi}}{\sum \rho_i V_i} = \frac{\rho_{UO_2} V_{UO_2} C_{P,UO_2} + \rho_{Zr_4} V_{Zr_4} C_{P,Zr_4}}{\rho_{UO_2} V_{UO_2} + \rho_{Zr_4} V_{Zr_4}}$$

The results are summarized in Section 3.7.1.6.

3.7.1.6 Conclusion

The minimum temperature-dependent effective conductivities, density, and specific heat have been calculated for the 14 x 14 PWR fuel to be transported in the TN-40 cask and are summarized below:

Temperature (°F)	Axial Conductivity, k_{axial} (Btu/hr-in-°F)	Temperature (°F)	Transverse Conductivity, k_{trans} (Btu/hr-in-°F)	Temperature (°F)	Specific Heat, $C_{p,eff}$ (Btu/lb-°F)
212	0.0558	136	0.0161	80	0.0593
392	0.0587	233	0.0177	260	0.0654
572	0.0623	330	0.0193	692	0.0726
752	0.0673	428	0.0210	1502	0.0778
932	0.0738	526	0.0228	$\rho_{eff} = 0.135 \text{ lb/in}^3$	
		624	0.0246		
		722	0.0263		
		821	0.0281		
		920	0.0298		
		1019	0.0317		

3.7.1.7 References

1. Prairie Island Independent Spent Fuel Storage Installation Safety Analysis Report, Revision 10.
2. NUREG/CR-0497, A Handbook of Materials Properties for Use in the Analysis of Light Water Reactor Fuel Rod Behavior, MATPRO - Version 11 (Revision 2), EG&G Idaho, Inc., TREE-1280, August 1981.
3. Oak Ridge National Laboratory, RSIC Computer Code Collection, "SCALE, A Modular Code System for Performing Standardized Computer Analysis for Licensing Evaluation for Workstations and Personal Computers", NUREG/CR-0200, Rev. 6, ORNL/NUREG/CSD-2/V3/R6.
4. SANDIA Report, SAND90-2406, "A Method for Determining the Spent Fuel Contribution to Transport Cask Containment Requirements", 1992.
5. ANSYS, Inc., ANSYS Engineering Analysis System User's Manual for ANSYS Revision 8.0 and 8.1, Cannonsburg, PA.
6. W.M. Rohsenow, J.P. Harnett, "Handbook of Heat Transfer Fundamentals," 2nd Edition, 1985.
7. Azzazy Technology Inc., "Emissivity Measurements of 304 Stainless Steel," Report Number ATI-2000-09-601, 2000.
8. NUREG-1536, "Standard Review Plan for Dry Cask Storage Systems - Final Report," 1997.

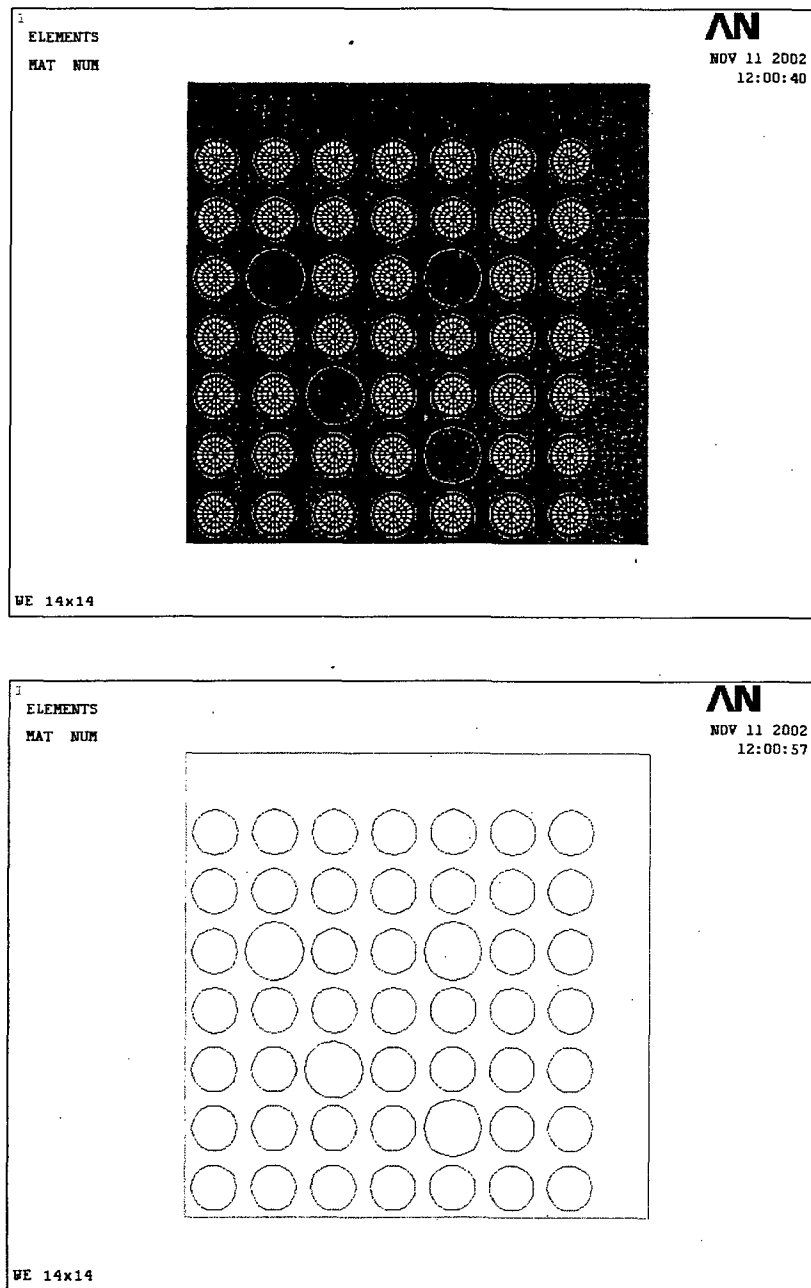


Figure 3.7.1-1
Finite Element Model Of WE 14 X 14 Assembly (1/4 Symmetry)

Heat Generating Boundary Conditions

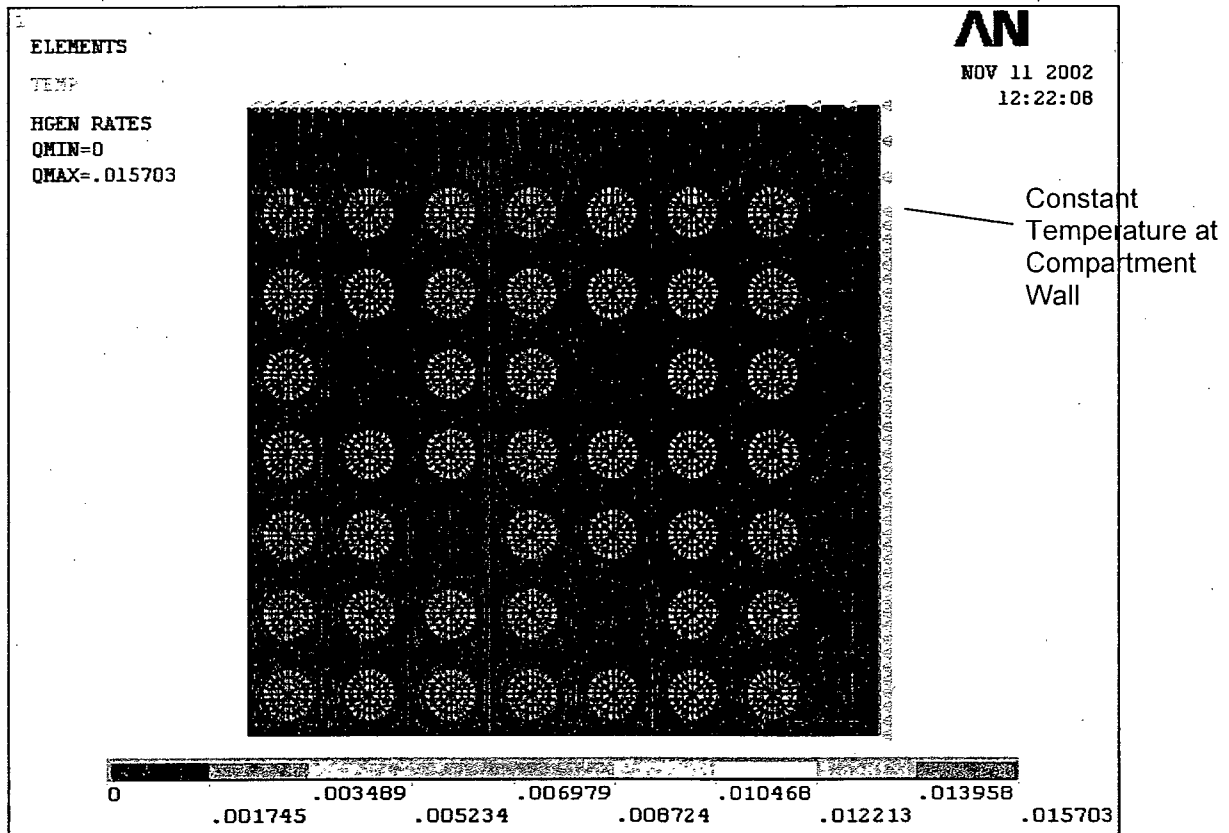


Figure 3.7.1-2
Typical Boundary Conditions Based On FE Model Of WE 14 X 14

ANSYS 8.0

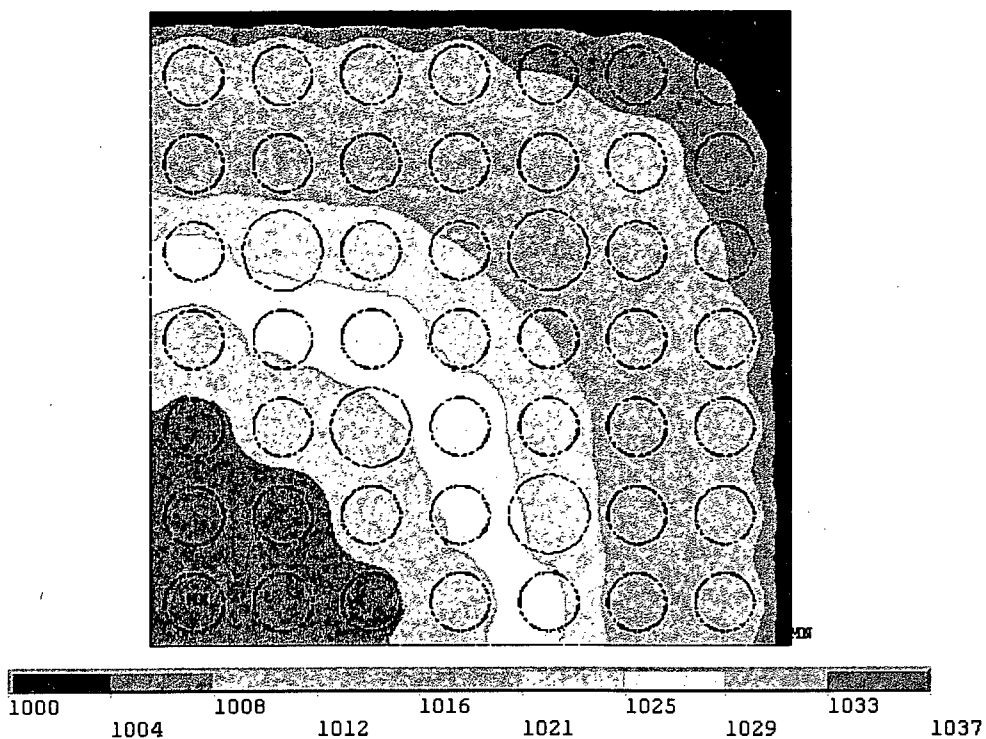


Figure 3.7.1-3
Typical Temperature Distributions For FE Model Of WE 14 X 14

CHAPTER 4 CONTAINMENT

TABLE OF CONTENTS

	<u>PAGE</u>
4.0 CONTAINMENT	4-1
4.1 Containment Boundary	4-1
4.1.1 Containment Vessel	4-1
4.1.2 Containment Penetrations.....	4-1
4.1.3 Seals and Welds	4-2
4.1.4 Closure.....	4-2
4.2 Requirements For Normal Conditions Of Transport.....	4-3
4.2.1 Containment of Radioactive Material	4-3
4.2.2 Pressurization of Containment Vessel	4-8
4.2.3 Containment Criterion	4-10
4.3 Containment Requirements for Hypothetical Accident Conditions	4-10
4.3.1 Source Terms	4-11
4.3.2 Containment of Radioactive Material	4-11
4.3.3 Containment Criterion	4-11
4.4 Special Requirements.....	4-13
4.5 References	4-14

LIST OF TABLES

Table 4-1	Radionuclide Inventory And A_2 Values	4-15
Table 4-2	Activity Concentration By Source	4-16
Table 4-3	Normal Conditions of Transport And Hypothetical Accident Conditions Effective A_2 Values	4-17
Table 4-4	Normal Condition of Transport And Hypothetical Accident Conditions Permissible Leakage Rates From the TN-40	4-18
Table 4-5	Total Moles Of Fission Gas For a WE 14x14 Std. Assembly	4-19
Table 4-6	Cask Gas Mixtures Under Normal Conditions of Transport and Hypothetical Accident Conditions	4-20

LIST OF FIGURES

Figure 4-1	TN-40 Containment Boundary Components	4-21
Figure 4-2	Lid, Vent Port And Drain Port Metal Seals	4-22

4.0 CONTAINMENT

4.1 Containment Boundary

The containment boundary components consist of the inner shell and bottom inner plate, shell flange, lid outer plate, and vent / drain port covers. Also, included are the associated seals and bolts. The containment boundary is shown in Figure 4-1. The construction of the containment boundary is shown on Drawings 10421-71-3, 4 and 5 provided in Appendix 1.4. The containment vessel prevents leakage of radioactive material from the cask cavity. It also maintains an inert atmosphere (helium) in the cask cavity. Helium assists in heat removal and provides a non-reactive environment to protect fuel assemblies against fuel cladding degradation which might otherwise lead to gross rupture.

4.1.1 Containment Vessel

The TN-40 containment vessel consists of an inner shell which is a welded carbon steel cylinder and is welded to a carbon steel bottom inner plate and a shell flange forging. The vessel closure is a carbon steel lid with bolts, vent cover with bolts, and drainport cover with bolts. The lid outer plate thickness is 4.5 in. The overall containment vessel length is 170.5 in. with a wall thickness of 1.5 in. The cylindrical cask cavity has a diameter of 72.0 in. and a length of 163 in.

The containment shell and bottom inner plate materials are SA-203 Grade D or E and the shell flange is SA-350 Grade LF3. The lid outer plate material is SA-203 Grade E or SA-350 Grade LF3.

The cask design, fabrication and testing are performed under Transnuclear's Quality Assurance Program which conforms to the criteria in Subpart H of 10CFR71 [2].

The materials of construction meet the requirements of Section III, Subsection NB-2000 and Section II, Material Specifications [3] or the corresponding ASTM Specifications. The containment vessel is designed to the ASME Code, Section III, Subsection NB, Article 3200 to the maximum practicable extent. The containment vessel is fabricated and examined in accordance with NB-2500, NB-4000 and NB-5000. Also, weld materials conform to NB-2400 and the material specification requirements of Section II, Part C of ASME B&PV. The containment vessel is hydrostatically tested in accordance with the requirements of the ASME B&PV Code, Section III, Article NB-6200.

Alternatives to the ASME Code are specified in SAR Section 2.11.

4.1.2 Containment Penetrations

There are two penetrations through the containment vessel, both in the lid. One is the drain port and the other is the vent port. A double seal mechanical closure is provided for each penetration. Each penetration incorporates a bolted cover.

4.1.3 Seals and Welds

The containment boundary welds consist of the circumferential welds attaching the bottom inner plate and the shell flange to the inner shell. Also, the longitudinal weld(s) on the rolled plate, closing the cylindrical inner shell, and the circumferential weld(s) attaching the rolled shells together are containment welds.

Double metallic seals (O-rings) are utilized on the lid and the two lid penetrations. Helicoflex HND [1] or equivalent seals may be used. The seals are shown in Figure 4-2. The Helicoflex metallic face seals of the lid and lid penetrations possess long-term stability and have high corrosion resistance. These high performance metallic seals consist of an inner spring, a lining, and a jacket. The spring is Nimonic 90 or equivalent material. The lining and jacket are stainless steel and aluminum, respectively. Additionally, all metallic seal seating surfaces are stainless steel for improved surface control.

The internal spring and lining maintain the necessary rigidity and sealing force, and provide some elastic recovery capability. The outer aluminum jacket provides a ductile material that ensures leak tightness. The jacket also provides a connecting sheet between the inner and outer seals. Holes in this sheet allow for attachment screws and for communication between the overpressure port (OP) cover and the space between the seals. This sheet, which is approximately 0.020 in. thick, has insufficient strength to transmit radial forces great enough to overcome the axial compressive forces on the seals. The OP seal is a single metallic seal of the same design, Helicoflex HN200 or equivalent.

The lid and penetration seals described above are contained in grooves in the lid or port covers. A high level of sealing over the transport period is assured by utilizing seals in a deformation-controlled design. The deformation of the seals is constant since bolt loads assure that the mating surfaces remain in contact. The seal deformation is set by the original O-ring cross section and the depth of the groove. The specified preload has the required force to seat the seals as calculated in Appendix 2.10.2.2.3.

The spring is made of Nimonic 60 or equivalent material which ensures the seal will not be affected by relaxation and thus the seal can be maintained at the specified temperatures for extended periods.

Helicoflex metallic seals (Reference [1]) are all capable of limiting leak rates to less than 1×10^{-7} ref cm³/sec. After loading for transport, all lid and cover seals are leak tested in accordance with ANSI N14.5. The acceptable total cask leakage (both inner and outer seals combined) is 1×10^{-4} ref cm³/sec.

4.1.4 Closure

The containment vessel contains an integrally-welded bottom closure and a bolted and flanged top closure (lid). The outer lid plate is attached to the shell flange with 48 bolts.

The bolt torque required to seal the metallic seals located in the lid and maintain containment under normal and accident conditions is provided in Drawing 10421-71-1 provided in Appendix 1.4. The closure bolt analysis is presented in Appendix 2.10.2.

As previously mentioned, the lid contains two penetrations which are sealed by flanged cover plates fastened to the lid by 8 bolts each. The bolt torque required to seal the metallic seals in the penetration covers and maintain containment under normal and accident conditions is provided in Drawing 10421-71-1 provided in Appendix 1.4.

4.2 Requirements For Normal Conditions Of Transport

In accordance with 10 CFR 71.51, a Type B package must be designed, constructed and prepared for shipment so that "no loss or dispersal of radioactive contents, as demonstrated to a sensitivity of 10^{-6} A₂ per hour" will occur under the tests specified in 10 CFR 71.71 for normal conditions of transport.

The guidelines of ANSI N14.5 [6] were used to determine the leakage test criteria which demonstrate that the TN-40 meets the "no-loss" requirements of 10 CFR 71.51.

4.2.1 Containment of Radioactive Material

4.2.1.1 Source Terms

Three sources are considered to determine the releasable airborne material from the TN-40 cask [4].

- Residual activity on the cask interior surfaces as a result of loading operations (and, if applicable, previous shipments);
- Fission and activation-product activity associated with corrosion-deposited material (crud) on the fuel assembly surfaces, and
- Radionuclides within the individual fuel rods comprising the fuel assemblies.

The first source, residual contamination on the interior surfaces of the cask is neglected. Reference [4] indicates that this is negligible as compared to the crud deposition on the fuel rods.

The second source, crud, is basically the radioactive "flaky" material that is formed on the outside surface of the fuel rods due to the radioactive and corrosive environment of the PWR reactor. This material can be loosely bound to the fuel rod surface and may be dislodged during transportation and be available for release from the cask.

The third source is from the fuel itself. A breach in the fuel cladding may allow radionuclides to be released from the fuel to the interior of the cask. There are three types of radionuclides releases associated with the breaches in the fuel rod cladding: gaseous, volatiles and fuel fines.

For conservatism, it is assumed that crud spallation and cladding breaches occur instantaneously after fuel loading and closure operations. Therefore, all radioactivity is readily available for release if a leak occurs.

The containment analysis is based on the void volume within the TN-40 cask. The void volume is estimated below:

$$\text{Cavity Volume} = 6.64\text{E}+05 \text{ in.}^3$$

$$\text{Basket Volume} = 1.05\text{E}+05 \text{ in.}^3$$

$$\text{Fuel Assembly Volume} = 1.64\text{E}+05 \text{ in.}^3 \text{ for 40 assemblies}$$

TN-40 Cask Void Volume:

$$\begin{aligned} \text{Cask Void Volume} &= 6.64\text{E}+05 \text{ in.}^3 - 1.05\text{E}+05 \text{ in.}^3 - 1.64\text{E}+05 \text{ in.}^3 \\ &= 3.95\text{E}+05 \text{ in.}^3 \\ &= 6.46\text{E}+06 \text{ cm}^3 \end{aligned}$$

Source Activity from the Fuel

The fuel transported in the TN-40 transport packaging has a maximum assembly average initial enrichment of 3.85 wt% U-235, 45,000 MWD/MTU bundle average exposure and a minimum of 15 - 25 year cooling time provided the fuel acceptance criteria of Section 1.2.3 have been met. As discussed in Chapter 5, Section 5.2, numerous SAS2H [8] evaluations were performed to determine the design basis fuel for shielding. These SAS2H analyses were also evaluated to determine the bounding fuel parameters for the containment analysis. The bounding SAS2H evaluation was performed for the 14 x 14 Westinghouse standard fuel assembly with 39,000 MWD/MTU burnup, enrichment of 3.3 wt. % U-235 and a cooling time of 15 years. It is assumed that 40 design basis fuel assemblies are loaded in the TN-40 cask transport packaging. The radionuclide inventory consists of activity from iodine, fission products that contribute greater than 0.1% of the design basis fuel activity and actinides that contribute greater than 0.01% of the design basis activity. Tritium is also included although it contributes slightly less than 0.1% of the design basis activity. The radionuclide inventory is presented in Table 4-1.

Source Activity from Release of Volatiles

The source activity concentration inside the TN-40 due to the release of volatiles, $C_{\text{volatiles}}$, is calculated using the following equation [4].

$$C_{\text{volatiles}} = \{N_A f_B A_V f_V\} / V$$

where: N_A = number of assemblies,
 f_B = fraction of rods that develop cladding breaches,
 A_V = specific activity of volatiles in the fuel assembly, Ci/assembly,
 f_V = fraction of volatiles in a fuel rod released if a fuel rod develops a cladding breach, and
 V = void volume inside the containment vessel, cm^3

Table 4-2 presents the results of this calculation.

Source Activity from Release of Gaseous Isotopes

The source activity concentration inside the TN-40 cask due to the release of gaseous isotopes, C_{gases} , is calculated using the following equation [4].

$$C_{\text{gases}} = \{N_A f_B A_G f_G\} / V$$

where: N_A = number of assemblies,
 f_B = fraction of rod that develop cladding breaches,
 A_G = specific activity of gases in the fuel assembly, Ci/assembly,
 f_G = fraction of gases in a fuel rod released if a fuel rod develops a cladding breach, and
 V = void volume inside the containment vessel, cm^3 .

Table 4-2 presents the results of this calculation.

Source Activity from Release of Fuel Fines

The source activity concentration inside the TN-40 due to the release of fuel fines, C_{fines} , is calculated using the following equation [4].

$$C_{\text{fines}} = \{N_A f_B A_F f_F\} / V$$

where: N_A = number of assemblies,
 f_B = fraction of rod that develop cladding breaches,
 A_F = specific activity of fuel fines in the assembly, Ci/assembly,
 f_F = fraction of fuel fines released if a fuel rod develops a cladding breach, and
 V = void volume inside the containment vessel, cm^3 .

Table 4-2 presents the calculated concentration of fuel fines inside the TN-40 for normal transport conditions.

Source Activity due to Crud Spallation

The fuel transported in the TN-40 transport packaging may be cooled a minimum of 15 to 25 years (provided the fuel acceptance criteria of Section 1.2.3 have been met). The activity density that results inside of the TN-40 as a result of crud spallation, C_{crud} , is calculated using the equation below [4].

$$C_{\text{crud}} = \{ f_C S_C N_R N_A S_{AR} \} e^{-\lambda t} / V$$

where:

- f_C = crud spallation factor,
- V = free volume inside the containment vessel, cm^3 ,
- S_C = crud surface activity, Ci/cm^2 ,
- N_R = number of fuel rods per assembly,
- N_A = number of assemblies in the cask,
- S_{AR} = surface area per rod, cm^2 , and
- $e^{-\lambda t}$ = decay factor ($\lambda = 0.693/5.27$ and $t = 15$ yr).

The surface area of the 14 x 14 fuel rods calculated for this containment analysis is presented below.

$$S_{AR} = (\pi d l) + \frac{1}{4}(2 \pi d^2)$$

where:

- d = rod outer diameter = 0.422 in = 1.07 cm (from Table 5-3), and
- l = rod length = 152 in = 386.1 cm (from Table 5-3)

substituting and solving:

$$S_{AR} = 1.30\text{E}+03 \text{ cm}^2 / \text{rod}$$

4.2.1.2 Determination of A_2 Values

The A_2 value of a mixture of radioactive nuclides is determined as follows:

$$A_{2 \text{ mixture}} = [\sum (f_i / A_{2i})]^{-1}$$

where: f_i is the fraction of total activity due to isotope i , and
 A_{2i} is the A_2 value for isotope i .

Using the methodology of 10 CFR 71 and Reference [4], the A_2 values are determined for each source (Table 4-1). The data provided in Table 4-1 (radionuclide inventory and A_2 values) and Table 4-2 (source activity) are combined to determine an effective A_2 for the TN-40 (Table 4-3).

4.2.1.3 Determination of Permissible Leakage Rates

To determine the leakage rates, the four sources are combined to form the total source term:

$$C_{\text{total}} = C_{\text{crud}} + C_{\text{volatiles}} + C_{\text{gases}} + C_{\text{fines}}$$

From Reference [6], the permissible release rate, R, from the TN-40 is:

$$R = L \times C$$

where:

L = volumetric gas leakage rate (cm³/s),

C = curies per unit volume of the radioactive material that passes through the leak path, and

R = $A_2 \times 2.78 \times 10^{-10}$ /second for normal transport conditions.

For normal conditions, the permissible leakage rate is 1.50E-04 cm³/sec (Table 4-4). This value is converted to units of ref-cm³/sec by first calculating the equivalent hole size. From ANSI N14.5 [6]:

L_u = upstream volumetric leakage rate, cc/sec = 1.50E-04 cm³/sec

F_c = coefficient of continuum flow conductance per unit pressure, cm³/atm-sec

F_m = coefficient of free molecular flow conductance per unit pressure, cm³/atm-sec

P_u = fluid upstream pressure, atm abs = 2.50 atm abs (conservative value)

P_d = fluid downstream pressure, atm abs = 1.0 atm abs

D = leakage hole diameter, cm

a = leakage hole length, cm = 0.5 cm (assuming leak path length is on the order of the metal seal width)

μ = fluid viscosity, cP = 0.028 cP

T = fluid absolute temperature, 222°C = 495 K (average cavity gas temperature a conservative value based on Table 3-1)

M = molecular weight, g/g-mol = 4 g/g-mol (from ANSI N14.5, Table B.1)

P_a = average stream pressure = $\frac{1}{2} (P_u + P_d)$, atm abs = 1.75 atm abs

$$L_u = (F_c + F_m)(P_u - P_d)(P_a/P_u) \text{ cm}^3/\text{sec}$$

where:

$F_c = (2.49 \times 10^6 \times D^4) / (a\mu) \text{ cm}^3/\text{atm-sec}$, and

$F_m = \{3.81 \times 10^3 \times D^3 \times (T/M)^{0.5}\} / \{aP_a\} \text{ cm}^3/\text{atm-sec}$.

Substituting:

$$\begin{aligned}
 F_c &= (2.49 \times 10^6 \times D^4) / (0.5 \times 0.028) = 1.78 \times 10^8 D^4 \\
 F_m &= \{3.81 \times 10^3 \times D^3 \times (495/4)^{0.5}\} / \{0.5 \times 1.75\} = 4.84 \times 10^4 D^3 \\
 L_u &= (F_c + F_m)(P_u - P_d)(P_a/P_u) \text{ cm}^3/\text{sec} \\
 1.50 \times 10^{-4} &= (F_c + F_m)(2.50 - 1.0)(1.75 / 2.50) \\
 1.50 \times 10^{-4} &= (F_c + F_m)(1.05) \\
 F_c + F_m &= 1.43 \times 10^{-4}
 \end{aligned}$$

Solving the equations above for D, yields a hole diameter of 8.87×10^{-4} cm.

This equivalent hole size, is then used to calculate the reference air rate at standard conditions. Assuming all upstream test conditions correspond to standard conditions:

$$L_u = (F_c + F_m)(P_u - P_d)(P_a/P_u) \text{ cm}^3/\text{sec}$$

where:

$$\begin{aligned}
 P_u &= \text{air upstream pressure, atm abs} = 1.00 \text{ atm abs} \\
 P_d &= \text{air downstream pressure, atm abs} = 0.01 \text{ atm abs} \\
 \mu &= \text{air viscosity, cP} = 0.0185 \text{ cP (from ANSI N14.5, Table B.1)} \\
 T &= \text{air ref temperature} = 298^\circ \text{K} \\
 M &= \text{molecular weight air, g/g-mol} = 29 \text{ g/g-mol (from ANSI N14.5, Table B.1)} \\
 P_a &= \text{average stream pressure} = \frac{1}{2}(P_u + P_d), \text{ atm abs} = 0.505 \text{ atm}
 \end{aligned}$$

Substituting:

$$\begin{aligned}
 F_c &= \{2.49 \times 10^6 \times (8.87 \times 10^{-4})^4\} / (0.5 \times 0.0185) = 1.66 \times 10^{-4} \\
 F_m &= \{3.81 \times 10^3 \times (8.87 \times 10^{-4})^3 \times (298/29.0)^{0.5}\} / \{0.5 \times 0.505\} = 3.37 \times 10^{-5} \\
 L_{std} &= (F_c + F_m)(P_u - P_d)(P_a/P_u) \text{ cm}^3/\text{sec} \\
 L_{std} &= (1.66 \times 10^{-4} + 3.37 \times 10^{-5})(1.0 - 0.01)(0.505 / 1.0) \\
 L_{std} &= 1.0 \times 10^{-4} \text{ ref cm}^3/\text{s}
 \end{aligned}$$

4.2.2 Pressurization of Containment Vessel

The TN-40 cask cavity is drained, dried and evacuated prior to backfilling with helium at the end of fuel loading operations. If the TN-40 cask contains design basis fuel and has been in storage for a short period prior to shipment (i.e., thermal equilibrium is reached), the cask cavity temperature with 100°F ambient air and maximum solar load is 401°F. The maximum normal operating pressure during storage is 2.2 atm abs [5].

Similarly, during normal transport conditions, the maximum cavity gas temperature is 348°F (176°C) under hot environment conditions. The maximum initial cavity pressure just prior to shipment (assuming no fuel rod failure) is 2.0 atm abs. The operational procedure guidelines for conducting these activities are provided in Chapter 7.

Cavity Gas Mixtures

The determination of fission gases is based on the grams of fission gases from SAS2H / ORIGEN -S computer runs [8], which utilizes fuel with 45,000 MWD/MTU bundle average exposure, 3.8 U-235 wt% initial bundle average enrichment and 15 year cooled. The gases which are considered following irradiation are: iodine (I), krypton (Kr), and xenon (Xe). The bulk of the fission gases remain trapped in the fuel pellet. The release fraction of 0.3 is applied to these gases. Table 4-5 presents the total moles of fission gas for the fuel assembly.

In addition to the fission gasses, gas due to helium from rod pre-pressurization is included. From Reference [5] the free gas volume after irradiation is 9.04 m³/cask at standard temperature and pressure. Therefore the mass of free gas can be determined as:

$$\begin{aligned} n &= VP/RT \\ &= 9.04 \text{ m}^3 \times (1 \text{ atm} \times (1 \text{ bar}/0.9869 \text{ atm})) / ((0.08314 \text{ bar m}^3/\text{kg mole } ^\circ\text{K} \times 273^\circ\text{K}) \\ &= 4.036\text{E-}01 \text{ kg mole/cask.} \end{aligned}$$

The mass of free He gas (pre-pressurization), therefore, can be determined by subtracting the irradiation generated gas (Table 4-5) from the total free gas:

$$0.4036 - 0.3119 = 0.0917 \text{ Kg mole/cask.}$$

The third and final component of gas is helium from cask backfilling operations which is estimated from the ideal gas law below and shown in Table 4-6:

$$\begin{aligned} n &= VP / RT \\ &= 6.46 \text{ m}^3/\text{cask} \times (2.2 \text{ atm} \times (1 \text{ bar}/0.9869 \text{ atm})) / ((0.08314 \text{ bar m}^3/\text{kg mole } ^\circ\text{K} \times 449^\circ\text{K}) \\ &= 3.858\text{E-}01 \text{ kg mole/cask.} \end{aligned}$$

The cavity gas mixture (assuming 3% fuel rod failure) is 97.7% helium (from cask backfill operations and from rod pre-pressurization) with the balance consisting of xenon (2.0%), krypton (0.2%), iodine (0.1%). These results are presented in Table 4-6. This gas mixture is not explosive.

Maximum Normal Operating Pressure (MNOP)

The mechanisms contributing to containment pressurization are ideal gas heating and release of fission gas from the fuel rods. The maximum normal operating pressure is

calculated using the recommendation of NUREG-1617 [7] which uses the following conditions:

- 30% release rate of fission gas from fuel pellets into the gap between the fuel pellets and the cladding.
- 3% failure rate of fuel rod cladding.
- maximum cavity gas temperature of 348°F (176°C) under hot environment conditions.
- the gas volume (plenum and pellet to cladding volume) inside the fuel rods is conservatively neglected when calculating the cask free volume.

The fuel assemblies release a total of 0.0121 Kg-mole (9.35E-03+2.756E-03, Table 4-6). The pressures are calculated below:

$$P_{3\% \text{ rod failure}} = (0.0121 \text{ Kg-moles/cask} \times 0.08314 \text{ bar m}^3/\text{Kg mole } ^\circ\text{K} \times 449^\circ\text{K}) / (6.46 \text{ m}^3)$$

$$P_{3\% \text{ rod failure}} = 0.070 \text{ bars} = 0.069 \text{ atm abs}$$

$$\text{MNOP} = P_{\text{initial}} + P_{3\% \text{ rod failure}}$$

$$\text{MNOP} = 2.0 \text{ atm abs} + 0.069 \text{ atm abs} = 2.07 \text{ atm abs} = 30.4 \text{ psia}$$

Therefore, the maximum normal operating pressure for the TN-40 is 30.4 psia (15.7 psig). Casks designs with MNOP greater than 5.0 psig must be subjected to a structural pressure test in accordance with 10 CFR 71.85(b). The test pressure must be at least 1.5 times MNOP. The TN-40 will be subjected to a hydrostatic test at a pressure of 25 psig. This test is described in Chapter 8.

4.2.3 Containment Criterion

As will be demonstrated in Section 4.3.3, the reference leak rate for normal conditions, 1.0E-04 ref cm³/s, is a significantly lower rate than the accident leakage rate. However, the acceptance criterion for the fabrication verification leak test of the TN-40 containment boundary shall be conservatively set at 1.0E-05 ref cm³/s. The acceptance criterion for the periodic verification leak test shall be set at 1.0E-04 ref cm³/s.

4.3 Containment Requirements for Hypothetical Accident Conditions

The containment requirement under hypothetical accident conditions are specified by 10 CFR 71.51(a)(2). It states "there would be no escape of krypton-85 exceeding 10 A₂ in 1 week, no escape of other radioactive material exceeding a total amount A₂ in 1 week." It is assumed for purposes of the accident condition evaluation that 100% of the fuel rods fail thereby releasing all of the available fission gas in the fuel rod gas gap to the cask cavity.

Calculation of the fission gas inventory is discussed in Section 4.2.1.1.

4.3.1 Source Terms

Similar to normal transport conditions described in Section 4.2.1, the following equations from NUREG/CR-6487 [4] are used to determine the source term available for release.

$$\begin{aligned}
 C_{\text{volatiles}} &= \{N_A f_B A_V f_V\} / V \\
 C_{\text{gases}} &= \{N_A f_B A_G f_G\} / V \\
 C_{\text{fines}} &= \{N_A f_B A_F f_F\} / V \\
 C_{\text{crud}} &= \{f_C S_C N_R N_A S_{AR}\} e^{-\lambda t} / V \\
 C_{\text{total}} &= C_{\text{crud}} + C_{\text{volatiles}} + C_{\text{gases}} + C_{\text{fines}}
 \end{aligned}$$

Table 4-1 shows the design basis radionuclide inventory corresponding to one fuel assembly for the containment evaluation. Table 4-2 shows the activity concentration from each of the sources available for release from inside the TN-40. The release fractions for the radionuclides are taken from NUREG/CR-6487. Under hypothetical accident conditions, the cladding of 100% of the fuel rods is assumed to fail ($f_B=1.0$).

4.3.2 Containment of Radioactive Material

The TN-40 is designed to meet the hypothetical accident requirements of 10 CFR 71.51. The A_2 values are calculated using the methodology of 10 CFR 71.71 and NUREG/CR-6487. The A_2 values are provided in Tables 4-1 and 4-3.

4.3.3 Containment Criterion

The allowable leak rates under hypothetical accident conditions are calculated using the methodology of NUREG/CR-6487 and previously presented in Section 4.2.1.3. The permissible leak rate under hypothetical accidents is $4.11\text{E-}02 \text{ cm}^3/\text{sec}$ (Table 4-4). This value is converted to units of $\text{ref-cm}^3/\text{sec}$ by first calculating the equivalent hole size. The equations of ANSI N14.5 (also see section 4.2.1.3) are used:

$$L_u = (F_c + F_m)(P_u - P_d)(P_a/P_u) \text{ cm}^3/\text{sec at } T_u, P_u$$

where:

$$\begin{aligned}
 L_u &= 4.11\text{E-}02 \text{ cm}^3/\text{sec} \\
 P_u &= 5.50 \text{ atm abs (conservative value)} \\
 P_d &= 1.0 \text{ atm abs} \\
 a &= 0.5 \text{ cm} \\
 \mu &= 0.030 \text{ cP} \\
 T &= 531^\circ\text{F} (= 277^\circ\text{C} = 550 \text{ K}) \text{ conservative value} \\
 M &= 4 \text{ g/mol (from ANSI N14.5, Table B.1)} \\
 P_a &= 3.25 \text{ atm abs}
 \end{aligned}$$

Substituting into the equations of ANSI N14.5:

$$F_c = (2.49 \times 10^6 \times D^4) / (0.5 \times 0.030) = 1.66 \times 10^8 D^4$$

$$F_m = \{3.81 \times 10^3 \times D^3 \times (550/4)^{0.5}\} / \{0.5 \times 3.25\} = 2.75 \times 10^4 D^3$$

$$L_u = (F_c + F_m)(P_u - P_d)(P_a/P_u)$$

$$4.11 \times 10^{-2} = (F_c + F_m)(5.50 - 1.0)(3.25 / 5.50)$$

$$F_c + F_m = 1.55 \times 10^{-2}$$

Solving the equations above for D, yields a hole diameter of 3.07×10^{-3} cm.

This equivalent hole size, is then used to calculate the reference air rate at standard conditions. Assuming all upstream test conditions correspond to standard conditions:

$$L_u = (F_c + F_m)(P_u - P_d)(P_a/P_u) \text{ cm}^3/\text{sec at } T_u, P_u$$

where:

$$P_u = 1.0 \text{ atm abs}$$

$$P_d = 0.01 \text{ atm abs}$$

$$D = 3.07 \times 10^{-3} \text{ cm}$$

$$a = 0.5 \text{ cm}$$

$$\mu = 0.0185 \text{ cP (from ANSI N14.5, Table B.1)}$$

$$T = 298^\circ \text{K}$$

$$M = 29.0 \text{ g/mol (from ANSI N14.5, Table B.1)}$$

$$P_a = 0.505 \text{ atm abs}$$

$$L_u = (F_c + F_m)(P_u - P_d)(P_a/P_u) \text{ cm}^3/\text{sec}$$

$$F_c = \{2.49 \times 10^6 \times (3.07 \times 10^{-3})^4\} / (0.5 \times 0.0185) = 2.40 \times 10^{-2}$$

$$F_m = \{3.81 \times 10^3 \times (3.07 \times 10^{-3})^3 \times (298/29.0)^{0.5}\} / \{0.5 \times 0.505\} = 1.40 \times 10^{-3}$$

$$L_{std} = (F_c + F_m)(P_u - P_d)(P_a/P_u) \text{ cm}^3/\text{sec}$$

$$L_{std} = (2.40 \times 10^{-2} + 1.40 \times 10^{-3})(1.0 - 0.01)(0.505 / 1.0)$$

$$L_{std} = 1.27 \times 10^{-2} \text{ ref cm}^3/\text{s}$$

Because the reference leak rate for normal conditions is lower than that for accident conditions, the leak test criterion developed in Section 4.2.1.3 demonstrates that the containment criteria for both normal and accident conditions are met.

The structural and thermal consequences of hypothetical accident loading conditions do not adversely affect the performance of the containment boundary structure or seals.

The impact limiters remain in place on the cask after the hypothetical accident as concluded in Appendix 2.10.8 for the 30 foot drop orientations. During the hypothetical accident the impact limiters provide insulation for the seals of the penetrations underneath them, including the lid seal, vent and drain ports, and the OP port.

Chapter 3 Table 3-3 lists the maximum temperature of the seals during a hypothetical thermal accident. Temperatures are shown for those areas protected by the insulating effect of the impact limiters, and other areas exposed directly to the accident temperatures environment. None of these temperatures exceeds the seal limit of 536°F. The pressure inside the cask cavity also remains well below the design pressure of 100 psig as shown below (assuming 100% fuel rod failure).

$$P_{HAC} = P_{initial} + P_{100\% \text{ rod failure}}$$

$$P_{initial} = (2.0 \text{ atm abs})(500 \text{ K} / 449 \text{ K}) = 2.23 \text{ atm abs}$$

$$P_{100\% \text{ rod failure}} = (0.404 \text{ kgmole/cask} \times 0.08314 \text{ bar}\cdot\text{m}^3/\text{kgmole K} \times 500 \text{ K}) / (6.46 \text{ m}^3)$$

$$P_{100\% \text{ rod failure}} = 2.6 \text{ bar} = 2.57 \text{ atm abs}$$

$$P_{HAC} = 2.23 + 2.57 = 4.80 \text{ atm abs} = 70.6 \text{ psia} = 55.9 \text{ psig}$$

The cavity gas mixture under accident conditions is presented in Table 4-6. The cavity gas mixture (assuming 100% fuel rod failure) consists of 60.5 % helium (from cask backfill operations and from rod pre-pressurization), 34.3% xenon, 3.4% krypton, 1.5% iodine. This gas mixture is not explosive.

4.4 Special Requirements

Per the requirements of 10 CFR 71.63 [2], "shipments containing plutonium must be made with the contents in solid form, if the contents contain greater than 0.74 TBq (20 Ci) of plutonium," TN-40 transport packaging has plutonium in the solid form in the fuel rods of spent fuel assemblies and therefore meets this requirement.

4.5 References

1. High Performance Sealing Metal Seals Catalogue, Helicoflex Co., Boonton, NJ, ET 507E5930.
2. 10 CFR 71, "Packaging and Transportation of Radioactive Materials."
3. ASME Boiler and Pressure Vessel Code, 1989 Code without Addenda.
4. NUREG/CR-6487, "Containment Analysis for Type B Packages used to Transport Various Contents," Lawrence Livermore National Laboratory, 1996.
5. TN40 SAR, "Prairie Island Independent Spent Fuel Storage Installation Safety Analysis Report," Rev. 10.
6. ANSI N14.5-1997, "American National Standard for Radioactive Material – Leakage Tests on Packages for Shipment," February 1998.
7. NUREG-1617, "Standard Review Plan for Transportation Packages for Spent Nuclear Fuel," March 2000.
8. SCALE-4.4, "Modular Code System for Performing Standardized Computer Analyses for Licensing Evaluation for Workstations and Personal Computers," CCC-545, ORNL.

Table 4-1
Radionuclide Inventory And A₂ Values

Nuclide	A _i ¹ (Ci/assy)	FA Fraction	A ₂ Value (Ci)	FA / A ₂ (Ci ⁻¹)
Crud				
co60	4.54	1.0000	11.0	9.09E-02
Total - Crud	4.54	1.0000	11.0	1/Sum(FA/A ₂)
Volatiles				
cs137 ²	72300	0.7381	16	4.61E-02
cs134	555	0.0057	19	2.98E-04
sr90	25100	0.2562	8.1	3.16E-02
Total - Volatiles	97955	1.0000	12.8	1/Sum(FA/A ₂)
Gases				
i129	0.02	8.9E-06	Unlimited	0.00E+00
kr 81	4.66E-08	2.7E-11	1100	2.44E-14
kr 85	1630	0.9406	270	3.48E-03
rb 87	9.72E-06	5.6E-09	Unlimited	0.00E+00
h 3	103	0.0594	1100	5.40E-05
Total - Gases	1733	1.0000	283	1/Sum(FA/A ₂)
Fines				
pu238	1380	0.0217	0.027	8.05E-01
pu239	137	0.0022	0.027	7.99E-02
pu240	217	0.0034	0.027	1.27E-01
pu241	31600	0.4975	1.6	3.11E-01
am241	1140	0.0179	0.027	6.65E-01
am243	14.1	0.0002	0.027	8.22E-03
cm243	6.5	0.0001	0.027	3.79E-03
cm244	1130	0.0178	0.054	3.29E-01
np239	14.1	0.0002	11	2.02E-05
eu154	959	0.0151	16	9.44E-04
eu155	150	0.0024	81	2.92E-05
pm147	1500	0.0236	54	4.37E-04
sm151	165	0.0026	270	9.62E-06
y 90	25100	0.3952	8.1	4.88E-02
Total - Fines	63512.7	1.0000	0.420	1/Sum(FA/A ₂)

Hypothetical Accident (Gases)

i129	1.55E-02	1.5E-04	Unlimited	0.00E+00
kr 81	4.66E-08	4.5E-10	1100	4.11E-13
rb 87	9.72E-06	9.4E-08	Unlimited	0.00E+00
h 3	1.03E+02	0.9998	1100	9.09E-04
Total - Gases	1.03E+02	1.0000	1100	1/Sum(FA/A ₂)

¹ Values are based on a 14x14 WE STD fuel assembly (39,000 MWD/MTU burnup, 3.3 wt% U-235 initial bundle average enrichment, and 15 year cooled).

² Ba137m contributes about 21% to the total design basis activity. Ba137m is a daughter of Cs137 with a half life of 2.6 min. In accordance with 10CFR71 Appendix A Note III, this radionuclide is evaluated with the parent nuclide.

Table 4-2
Activity Concentration By Source

Source	Fraction available for release from the fuel rod ⁽¹⁾ ($f_V / f_G / f_F / f_C$)	Fraction of rods that develop cladding breach ⁽¹⁾	Activity Concentration in TN-40 cask (Ci/cm ³) ^(2,3)
Normal Transport Conditions			
Volatiles	2E-04	0.03	3.64E-06
Gases	0.3	0.03	9.65E-05
Fines	3E-05	0.03	3.54E-07
Crud ⁽⁴⁾	0.15	not applicable	4.21E-06
Hypothetical Accident Conditions			
Volatiles	2E-04	1.0	1.21E-04
Gases	0.3	1.0	1.91E-04
Gases - Kr-85 only	0.3	1.0	3.03E-03
Fines	3E-05	1.0	1.18E-05
Crud	1.0	not applicable	2.81E-05

¹ Values taken from NUREG/CR-6487 [4].

² 40 assemblies per cask.

³ Cavity free volume is equal to 6.46E+06 cm³

⁴ Crud source is based on a surface area of 1.30E+03 cm² / rod and an initial surface activity of 1.40E-04 Ci/cm² at the time of discharge. At discharge, typically, fuel crud is composed of isotopes of cobalt, manganese, chromium and iron. After a 15 year cooling time, the only isotope of radiological significance is Co-60. A decay factor of 0.14 is included in the values listed above.

Table 4-3
Normal Conditions of Transport And Hypothetical
Accident Conditions Effective A_2 Values

		Fraction	Effective A_2	FA / A_2
i	C_i (C_i/cm^3)	FA	(C_i)	(C_i^{-1})
Normal Conditions of Transport				
V, Volatiles	3.64E-06	3.47E-02	12.8	2.71E-03
G, Gases	9.65E-05	9.22E-01	283	3.26E-03
F, Fines	3.54E-07	3.38E-03	0.420	8.03E-03
C, Crud	4.21E-06	4.02E-02	11.0	3.66E-03
Total	1.05E-04	1.00E+00	56.6	1/Sum(FA/A_2)
Hypothetical Accident Conditions				
V, Volatiles	1.21E-04	3.44E-01	12.8	2.69E-02
G, Gases	1.91E-04	5.43E-01	1100	4.93E-04
F, Fines	1.18E-05	3.35E-02	0.420	7.96E-02
C, Crud	2.81E-05	7.97E-02	11.0	7.25E-03
Total	3.52E-04	1.00E+00	8.8	1/Sum(FA/A_2)

Table 4-4
Normal Condition of Transport And Hypothetical Accident Conditions
Permissible Leakage Rates From the TN-40

Case	Effective A_2 (Ci)	Allowable Release Rate	Allowable Release Rate (Ci/sec)	Concentration C_i (Ci/cm ³)	Permissible Leakage Rate (cm ³ /sec)	Permissible Std Leakage Rate (ref cm ³ /sec)
NCT	56.6	$A_2 \times 10^{-6}$ per hour	1.57E-08	1.05E-04	1.50E-04	1.0E-04
HAC	8.8	A_2 per week	1.45E-05	3.52E-04	4.11E-02	1.27E-02
Kr-85 (HAC)	270	10 A_2 per week	4.46E-03	3.03E-03	1.48E+00	Note 1

Note (1): Hypothetical accident conditions without Kr-85 are bounding. This value is not calculated.

Table 4-5
Total Moles Of Fission Gas For a WE 14x14 Std. Assembly

WE 14x14 std - Design Basis Fuel for Containment		45 GWD/MTU 3.8% U-235 15 yrs decay				
		<u>SAS2H / ORIGEN-S (g/assembly)</u>	<u>Release Fraction</u>	<u>m (kg_{release} / assembly)</u>	<u>M (molar mass)</u>	<u>m/M (kgmole_{release} / cask)</u>
Actinides	he4	9.030E-01	0.3	2.709E-04	4	2.709E-03
					Total He:	2.709E-03
Fission Products	h 3	1.210E-02	0.3	3.630E-06	3	4.840E-05
					Total H:	4.840E-05
	i127	2.370E+01	0.3	7.110E-03	127	2.239E-03
	i129	1.000E+02	0.3	3.000E-02	129	9.302E-03
					Total I:	1.154E-02
	kr 80	3.160E-05	0.3	9.480E-09	80	4.740E-09
	kr 82	4.170E-01	0.3	1.251E-04	82	6.102E-05
	kr 83	2.100E+01	0.3	6.300E-03	83	3.036E-03
	kr 84	6.470E+01	0.3	1.941E-02	84	9.243E-03
	kr 85	4.760E+00	0.3	1.428E-03	85	6.720E-04
	kr 86	1.010E+02	0.3	3.030E-02	86	1.409E-02
					Total Kr:	2.711E-02
	xe128	1.760E+00	0.3	5.280E-04	128	1.650E-04
	xe129	1.350E-02	0.3	4.050E-06	129	1.256E-06
	xe130	5.100E+00	0.3	1.530E-03	130	4.708E-04
	xe131	2.130E+02	0.3	6.390E-02	131	1.951E-02
	xe132	6.390E+02	0.3	1.917E-01	132	5.809E-02
	xe134	8.460E+02	0.3	2.538E-01	134	7.576E-02
	xe136	1.320E+03	0.3	3.960E-01	136	1.165E-01
					Total Xe:	2.705E-01
					<u>Total:</u>	<u>3.119E-01</u>

Table 4-6
Cask Gas Mixtures Under Normal Conditions of Transport
and Hypothetical Accident Conditions

	NCT (3% rod failure) (Kg-mole/cask)	HAC (100% rod failure) (Kg-mole/cask)
<u>Fission Products</u>		
I	3.46E-04	1.15E-02
Kr	8.13E-04	2.71E-02
Xe	8.11E-03	2.70E-01
He	<u>8.13E-05</u>	<u>2.71E-03</u>
Subtotal	9.35 E-03	3.09 E-03
<u>Pre-pressurization</u>		
He	2.75E-03	9.167E-02
<u>Helium Backfill</u>		
He	3.858E-01	3.858E-01
<u>Total</u>	3.979E-01	7.894E-01
% Mass of Gases		
<u>Fission Products</u>		
I	0.1%	1.5%
Kr	0.2%	3.4%
Xe	2.0%	34.3%
He	-	0.3%
<u>Pre-pressurization</u>		
He	0.7%	11.6%
<u>Helium Backfill</u>		
He	97.0%	48.9%
<u>Total</u>	100.0%	100.0%

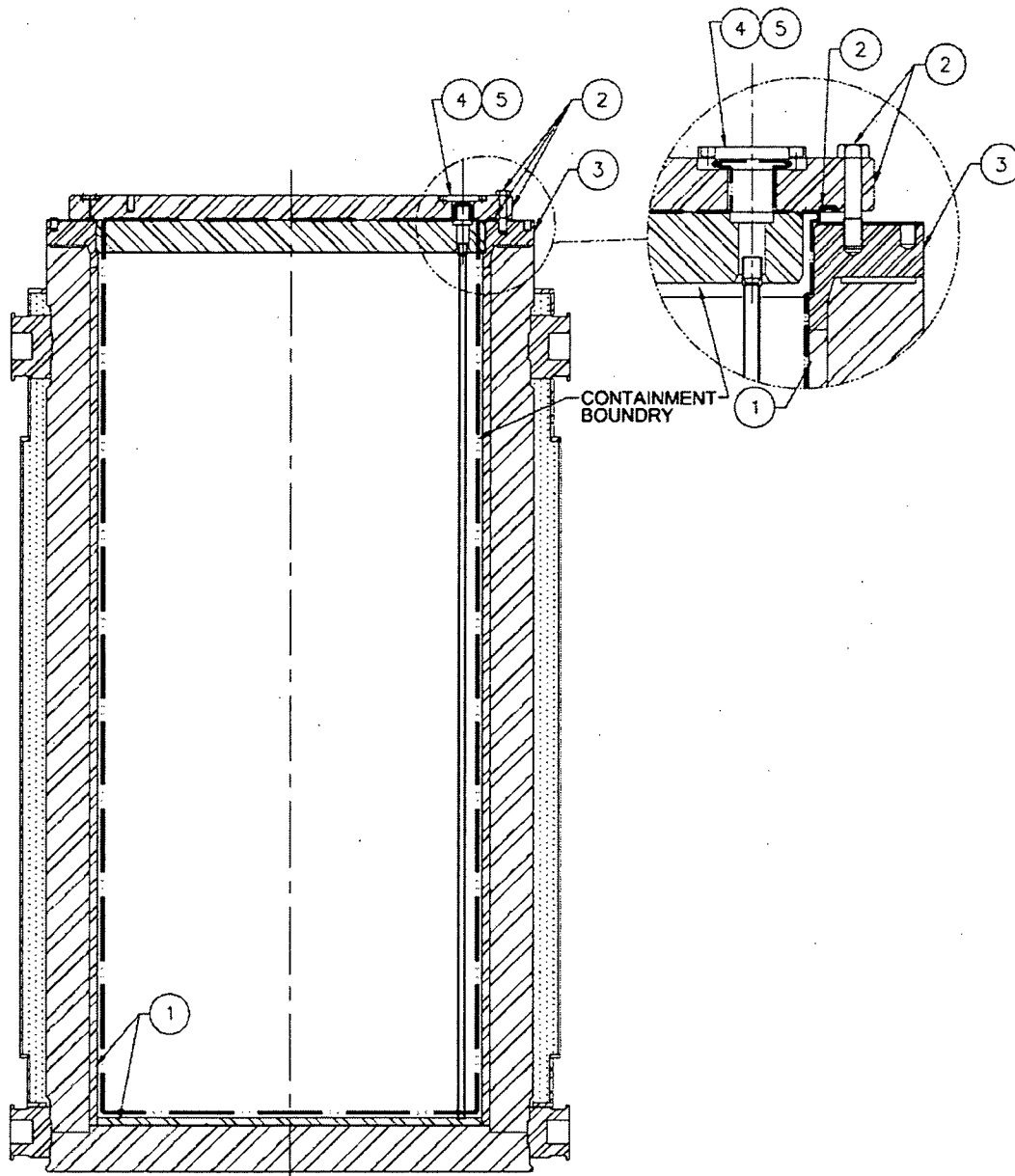


Figure 4-1
TN-40 Containment Boundary Components

Notes to Figure 4-1:

1. Figure not to scale. Features exaggerated for clarity.
2. Phantom lines (— · · — · · — ·) indicate containment boundary.
3. Containment boundary components are listed below:
 - 1 Inner shell.
 - 2 Lid outer plate, closure bolts and inner o-rings.
 - 3 Shell flange.
 - 4 Vent port cover plate, bolts and seals.
 - 5 Drain port cover plate, bolts and seals (not shown).

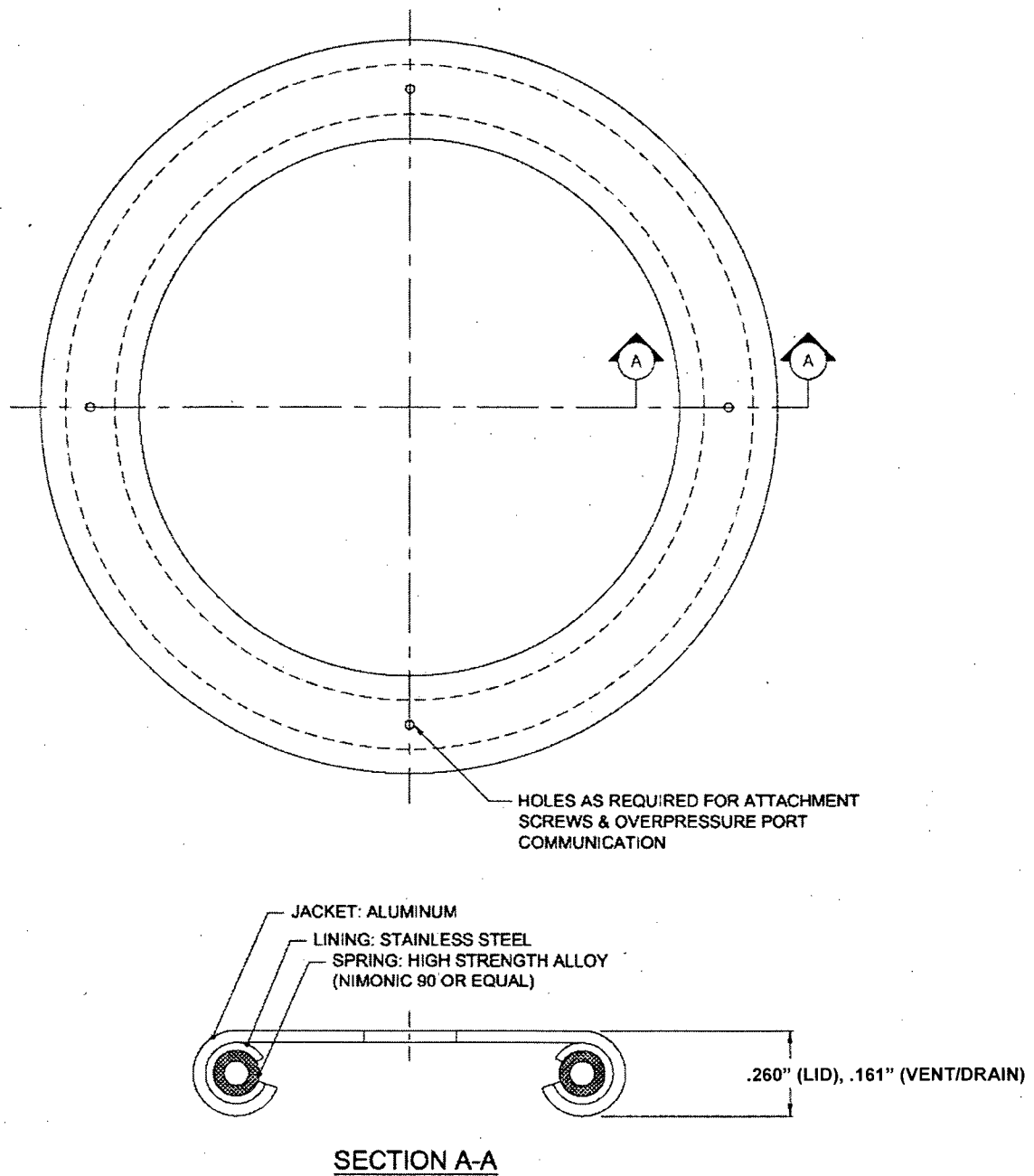


Figure 4-2
Lid, Vent Port And Drain Port Metal Seals

CHAPTER 5 SHIELDING EVALUATION

TABLE OF CONTENTS

	<u>PAGE</u>
5.0 SHIELDING EVALUATION	5-1
5.1 Discussion And Results	5-1
5.2 Source Specification	5-2
5.2.1 Axial Source Distribution	5-3
5.2.2 Gamma Source	5-3
5.2.3 Neutron Source	5-4
5.2.4 Source Conversion Factors	5-4
5.2.5 Fuel Qualification	5-5
5.3 Model Specification	5-6
5.3.1 Description of Radial and Axial Shielding Configuration	5-6
5.3.2 Shield Regional Densities	5-7
5.4 Shielding Evaluation	5-7
5.5 References	5-10
5.6 Input File Listing	5-11
5.6.1 SAS2H/ORIGEN-S Input File	5-11
5.6.2 MCNP Neutron Model Input File	5-13
5.6.3 MCNP Primary Gamma Input File	5-30

LIST OF TABLES

Table 5-1	TN-40 Cask Shield Materials	5-50
Table 5-2	Summary Of TN-40 Dose Rates	5-51
Table 5-3	PWR Fuel Assembly Design Characteristics	5-52
Table 5-4	Westinghouse 14 X 14 STD Fuel Assembly Hardware Characteristics	5-53
Table 5-5	Material Compositions For Fuel Assembly Hardware Materials.....	5-54
Table 5-6	Source Distribution	5-55
Table 5-7	TPA Gamma Source.....	5-55
Table 5-8	Fuel Qualification Table	5-56
Table 5-9	Minimum Cooling (Years) Required To Meet Radiation and Decay Heat Limits.....	5-57
Table 5-10	Estimated 2 Meter Side Dose Rates (MREM/HR)	5-58
Table 5-11	Decay Heat Output (kW PER CASK).....	5-59
Table 5-12	Axial Source Term Peaking Summary	5-60
Table 5-13	Fuel Assembly Materials Input For MCNP	5-61
Table 5-14	Package Materials Input for MCNP.....	5-63
Table 5-15	Flux-to-Dose Rate Conversion Factors For Gamma.....	5-64
Table 5-16	Flux-Dose-Rate Conversion Factors For Neutron.....	5-65
Table 5-17	Average End Dose Rates As A Function Of Railcar Length	5-66

LIST OF FIGURES

Figure 5-1	Cask Shielding Configuration.....	5-67
Figure 5-2	Axial Burnup Profile For Design Basis Fuel	5-68
Figure 5-3	Side View Of TN-40 Transport MCNP Model.....	5-69
Figure 5-4	Detail Views Of TN-40 Transport MCNP Model.....	5-70
Figure 5-5	Plan View Of TN-40 Transport MCNP Model Basket Structure	5-71
Figure 5-6	Details Of Lattice Unit Cell And Rails/Outer SST	5-72
Figure 5-7	Summary of TN-40 Side NCT Dose Rates	5-73
Figure 5-8	Dose Rates Above the Neutron Shield	5-74

5.0 SHIELDING EVALUATION

5.1 Discussion And Results

Shielding for the TN-40 package is provided mainly by the cask body. The cask body is made up of the containment vessel, the gamma shielding and the lid. For the neutron shielding, a borated polyester resin compound surrounds the gamma shield shell radially. Additional shielding is provided by the steel outer shell surrounding the resin layer and by the steel and aluminum structure of the fuel basket.

For transport, wood filled impact limiters are installed on either end of the cask and provide additional shielding for the ends and some radial shielding for the areas at either end of the radial neutron shield. Figure 5-1 shows the configuration of the package shielding. Table 5-1 lists the compositions of the shielding materials.

The fuel assemblies acceptable for transport in the TN-40 are listed in Section 1.2.3. Using the SAS2H/ORIGEN-S modules of SCALE [1], source terms are calculated. The bounding design basis fuel for dose rate has an initial enrichment of 2.35 wt% and a total maximum bundle-average burnup of 42,000 MWD/MTU with a 24.4 year decay time.

The Westinghouse 14x14 standard fuel assembly contains the maximum heavy metal weight (Section 1.2.3) which results in bounding neutron and gamma source terms and is therefore identified as the most conservative fuel assembly. Section 5.2 describes the source specification and Section 5.4 describes the shielding analysis performed for the TN-40 cask. The shielding analysis models are described in Section 5.3.

Normal Conditions of Transport (NCT) are modeled with the neutron shielding and impact limiters on TN-40 intact. This shielding calculation is performed using the Monte Carlo computer code MCNP [5]. Dose rates on the side, top and bottom of the TN-40 package are calculated for the various sources described in Section 5.2 and summed to give a total gamma and neutron dose rate.

Hypothetical Accident Conditions (HAC) assume that the neutron shield and the impact limiters are removed. This evaluation bounds the accident conditions since it is shown in Chapter 2 and Chapter 3 that the neutron shielding may be lost but the impact limiters remain on the cask during HAC. Shielding calculations for the HAC are also performed using MCNP.

The expected maximum dose rates (for NCT and HAC) from the TN-40 package are provided in Table 5-2. Although this dose rate evaluation is performed using design basis fuel, evaluations were performed to determine that 15 year minimum cooled fuel is also acceptable for certain burnup and enrichment combinations. These evaluations were performed to determine the fuel assembly parameters of burnup, percent initial enrichment and cooling time that would result in decay heat and radiological sources that would meet the decay heat requirements (Chapter 3), source terms for containment

(Chapter 4) and radiological sources that provide dose rates less than the current design basis fuel mentioned above and thus would be acceptable for transport in the TN-40 package. Section 5.2 describes these evaluations in more detail.

5.2 Source Specification

There are five principal sources of radiation associated with transport of spent nuclear fuel that are of concern for radiation protection:

- Primary gamma radiation from spent fuel,
- Primary neutron radiation from spent fuel (both alpha-n reactions and spontaneous fission),
- Gamma radiation from activated fuel structural materials and fuel inserts,
- Capture gamma radiation produced by attenuation of neutrons by shielding material of the cask, and
- Neutrons produced by sub-critical fission in fuel.

The TN-40 package is designed to transport Westinghouse 14 x 14 class PWR fuel assemblies. The fuel assemblies acceptable for transport in the TN-40 are described in Section 1.2.3. The various fuel assembly designs were separated according to fuel assembly array, the maximum metric tons of uranium, and the number of guide /instrument tubes. These parameters are the significant contributors to the SAS2H/ORIGEN-S model. The largest uranium loading results in the largest source term at the design basis enrichment and burnup, thus the Westinghouse 14 x 14 standard is the bounding assembly type.

Table 5-3 provides characteristics of the design basis fuel assembly used in the source term analyses. The SAS2H/ORIGEN-S modules of the SCALE code are used to generate gamma and neutron source terms for the bounding Westinghouse 14 x 14 standard assembly. Source terms were generated for initial enrichments ranging from 2.00 wt% to 3.85 wt% U235 and the fuel is irradiated for a constant time of 400 effective full power days per cycle. Burnup values range from 17 GWD/MTU to 45 GWD/MTU using a specific radiation power between about 15 and 25 MW/assembly. A conservative operating cycle history is utilized with a 30 day down time between cycles. Details of the analyses are given in Section 5.2.5.

The source terms are generated for the fuel assembly active fuel region, the plenum region, and the end fitting regions. The fuel assembly hardware materials and masses on a per assembly basis are listed in Table 5-4. Table 5-5 provides the material composition of fuel assembly hardware materials. Cobalt impurities are included in the SAS2H model.

The masses for the materials in the top end fitting, the plenum, and the bottom fitting regions are multiplied by 0.1, 0.2 and 0.2, respectively [4]. These factors are used to correct for the spatial and spectral changes of the neutron flux outside of the active fuel.

zone. The material compositions of the fuel assembly hardware are included in the SAS2H/ORIGEN-S model on a per assembly basis.

5.2.1 Axial Source Distribution

PWR plant operations data for over twenty 14 x 14 fuel assemblies with approximately 36 to 42 GWD/MTU burnup are averaged into a typical profile, shown as maximum profile in Figure 5-2. Also shown in Figure 5-2 is the axial profile from Reference [3] for 38-42 GWD/MTU burnup. The third profile shown in Figure 5-2 is a bounding profile used in this analysis.

The conservative axial profile containing 12 axial zones is utilized in the shielding evaluation. The top and bottom 17% of the assembly are divided into two zones each and the middle 66% divided into 8 approximately equal zones. The peaking factors range from 0.700 at the bottom and top, to a maximum of 1.16 just below the middle. The gamma source is directly proportional to the burnup and the neutron source is proportional to the fourth power of the burnup. This data is presented in Table 5-12.

5.2.2 Gamma Source

The gamma source terms for the design basis spent fuel assembly is provided in Table 5-6. Table 5-6 presents the source terms for a Westinghouse 14 x 14 standard assembly with an initial enrichment of 2.35 wt%, maximum average burnup of 42,000 MWD/MTU, 24.4 year decay with a 13 year cooled TPA insert.

The gamma source spectra are presented in the 18-group structure consistent with the SCALE 27n-18 γ cross section library. The conversion of the source spectra from the default ORIGEN-S energy grouping to the SCALE 27n-18 γ energy grouping is performed directly through the ORIGEN-S code. The SAS2H/ORIGEN-S input file for this fuel assembly is provided in Section 5.6.

The gamma source for the fuel assembly hardware is primarily from the activation of cobalt. This activation contributes primarily to SCALE Energy Groups 36 and 37. The gamma source for the plenum region, the top fitting region and the bottom fitting region is provided in Table 5-6.

The spent fuel assemblies may contain irradiated fuel inserts (BPRA, TPA) which also provide a gamma source which is primarily from activated cobalt. The gamma source from a TPA corresponding to maximum host assembly burnup of 125,000 MWD/MTU and cooled for 13 years is shown in Table 5-7. This gamma source is added to the irradiated fuel gamma source in the plenum and top end fitting regions.

An axial burnup profile has been developed as discussed in Section 5.2.1 above. Table 5-12 provides design axial gamma peaking factors that were utilized in the MCNP shielding model.

5.2.3 Neutron Source

Table 5-6 provides the total neutron source for the design basis fuel assembly under the irradiation/decay history described above in 5.2. The neutron source is comprised mainly of Cm-244 and for the MCNP analyses, the default Cm-244 energy spectrum was utilized.

The neutron source is not linearly dependent with burnup, and therefore calculations were performed to determine the axial neutron source distribution (Section 5.2.1). The axial neutron peaking factors are shown in Table 5-12.

5.2.4 Source Conversion Factors

The following equation defines how the absolute tallies are calculated:

$$\dot{D} = T \cdot S \cdot C_{BU} \cdot \frac{1000 \text{ mrem}}{1 \text{ rem}}$$

Where,

\dot{D} is the absolute dose rate in mrem/hr,
T is the MCNP tally result in rem/hr per particle/sec,
S is the source strength in source particle/sec, and
 C_{BU} is the axial burnup normalization constant.

In the above relationship the constants multiplied against the tally result, T, define the tally multiplier. Therefore, the tally conversion factor, C_T , is defined below.

$$C_T = S \cdot C_{BU} \cdot \frac{1000 \text{ mrem}}{1 \text{ rem}}$$

The source strength must be scaled appropriately by the axial burnup normalization constant. For the axial profile the cumulative density of the burnup profile is 1.049 (Table 5-12). This corresponds to the C_{BU} for the gamma source. Using the fourth power approximation the neutron C_{BU} is 1.367 (Table 5-12).

Neutron Source Term

$$\begin{aligned} C_T &= [2.630\text{E}+08 \text{ neutron/sec/assy} \times 40 \text{ assy}] \times 1.367 \times 1000 \text{ mrem/rem} \\ &= 1.438\text{E}+13 \text{ neutron-mrem/rem-sec} \end{aligned}$$

Gamma Source Term

$$\begin{aligned} C_T &= [1.787\text{E}+15 \text{ gamma/sec/assy} \times 40 \text{ assy}] \times 1.049 \times 1000 \text{ mrem/rem} \\ &= 7.50\text{E}+19 \text{ gamma-mrem/rem-sec} \end{aligned}$$

5.2.5 Fuel Qualification

As stated previously, an evaluation was performed to determine the fuel assembly parameters of burnup, percent initial enrichment and cooling time that would result in dose rates and decay heats less than the design basis fuel mentioned above and thus would be acceptable for transport in the TN-40 cask.

These analyses were carried out using the SAS2H depletion module from the SCALE computer software and MCNP. For all SAS2H calculations the latest SCALE 44 group ENDF/B-V (44groupndf5) library was used. MCNP calculations used the default cross section libraries.

An MCNP model was utilized to calculate a response function at 2 meters from the transportation vehicle. The response function is simply a source-to-dose conversion function. In essence the dose rate at 2 meters is calculated for each gamma energy group of the source as calculated by SAS2H. For neutrons, since a bounding energy spectrum is used, the response function calculated is just a total source to dose factor.

The response function is then utilized with SAS2H models to estimate the 2 meter side dose rate as a function of different burnup, enrichment and cooling time combinations. Other information, such as the decay heat per fuel assembly and the cooling time are also collected.

The calculated dose rate and decay heat along with the cooling time are then utilized according to the steps above to determine the bounding radiological source term. The final design basis radiological source term was generated by adding the TPA source term to the fuel/hardware source term. The cooling times calculated are reduced to a simplified look up table as a function of spent fuel parameters to summarize the loading parameters for the TN-40 transport package and are shown in Table 5-8.

Table 5-9 shows the results of the evaluation which define the spent fuel assembly cooling times to meet radiological and decay heat limits necessary for burnups ranging from 17 GWD to 45 GWD and enrichments between 2.0 wt% and 3.85 wt%. The TN-40 package containing fuel assemblies with parameters defined in this table will meet the dose rate and thermal criteria for transport. Table 5-10 shows the estimated dose rates and Table 5-11 shows the calculated decay heat corresponding to the cooling times shown in Table 5-9. All assemblies producing a decay heat of less than 21 kW per package or 525 watts per assembly are radiation (dose rate) limited. A fuel qualification table (FQT) for loading purposes based on this evaluation is provided in Table 1-2 (also shown in Table 5-8). The FQT is generated by conservatively rounding the cooling times shown in Table 5-9 up to the nearest value greater than 15 years.

5.3 Model Specification

The Monte Carlo computer code MCNP [5] is used for calculating the gamma and neutron doses in this analysis.

5.3.1 Description of Radial and Axial Shielding Configuration

Two base models were constructed. The first model corresponds to the neutron transport problem and the second is the gamma. Variance reduction was accomplished by means of importance zoning followed by weight windows. The importance function was created to balance the particles (per volume) throughout the problem geometry. The process used to do this was an iterative approach starting with basic attenuation factors for the shielding materials. The neutron importance function developed was also applied to the secondary gammas.

The test importance functions were then run in conjunction with the weight window generator. The weight windows calculated were inserted into the final MCNP runs. Weight windows were only used in the gamma cases.

The models were used to calculate both the axial and radial dose rates. The impact limiters and radial neutron shielding were removed for the HAC evaluation.

Sections 5.3.1.1 and 5.3.1.2 describe the shielding model (for the vicinity immediately around the cask) developed for the TN-40 under NCT and HAC.

5.3.1.1 NCT Radial and Axial Shielding Configuration

One shielding configuration is used for the TN-40 NCT design. The model is a complete three dimensional simulation of the TN-40 transportation package. The 72 inch diameter interior cavity of the cask is modeled with a discrete representation of the basket and fuel structure. Each fuel assembly is divided into four axial zones. The bottom zone represents the lower end fittings, the middle zone the active fuel region and the upper zones represent the plenum and upper end fittings, respectively. The axial locations of the plenum and the end fittings of the fuel assembly are similar to those provided in Reference [8]. The modeled active fuel length is 144 inches and the plenum length is 7.14 inches. The modeled bottom end fitting and top end fitting lengths are 3.08 inches and 3.5 inches, respectively. The fuel, end fittings and plenum are homogenized within the each assembly envelope and the axial length of their respective zones.

The basket structure is modeled as a 0.755 inch thick grid of aluminum and steel panels. The neutron poison material is conservatively neglected. The periphery of the basket is modeled by several peripheral basket universes to best represent the geometry. The TN-40 package model is illustrated in Figures 5-3 through 5-6.

The impact limiters are modeled as wood surrounded by a 0.25 in. thick steel shell. The interior steel gussets are conservatively neglected. The wood is modeled mostly as redwood except two areas, as shown in drawings 10421-71-41 and -42 (Appendix 1.4.1), which are modeled as balsa. An aluminum spacer utilized under the top impact limiter is included in the model.

The TN-40 cask body is modeled using the appropriate materials and dimensions shown in the drawings in Appendix 1.4.1.

Voids are neglected within the fuel assembly. The voids within the cask cavity are modeled.

5.3.1.2 HAC Radial and Axial Shielding Configuration under Hypothetical Accident Conditions

For the HAC evaluation, it is conservatively assumed that the top and bottom impact limiters are destroyed and are no longer attached to the cask. Also, the neutron shield is assumed to be removed. The remaining model utilizes the same regional densities and shield thickness as the model for NCT.

5.3.2 Shield Regional Densities

For the MCNP model, four source areas, shown in Figure 5-3, are utilized: fuel zone, plenum, top and bottom end fitting. The sources are uniformly homogenized over the cross section and the appropriate zone length. The fuel basket is discreetly represented by the stainless steel and aluminum plates that bound the fuel assemblies.

The radial resin and aluminum boxes are homogenized into a single composition based on the mass of each component. Measured dose rates around the TN-24P [7], the TN-40, and the TN-32 casks have shown no streaming effects because of the aluminum boxes. This is because the neutrons will not generally travel in a direct path, but scatter, such that the majority of the neutrons will not be able to travel through the aluminum box wall for the full 4.5 inches of resin box thickness. The materials input for the MCNP model is listed in Table 5-13 and Table 5-14.

5.4 Shielding Evaluation

Dose rates around the TN-40 package are determined by choosing the most conservative source and using it within a three dimensional MCNP model. Dose rates were estimated both axially and radially outside the cask. Several tallies were used to accomplish this. All tallies are either surface (F2) or volume flux (F4) tallies and are converted into dose rates using energy dependent dose conversion factors listed in Tables 5-15 and Table 5-16 [6]. The tallies are further scaled by the source conversion factors described in Section 5.2.4. The tally locations were chosen to best evaluate the external dose rate requirements of 10 CFR 71.47(b). Tally segmentation was used to analyze the surface dose rates for any spatial peaking. This was done both axially and

radially. The segments were typically 20 to 25 cm in dimension. Note that dose rates were calculated at several locations from the ends of the cask to assess hypothetical occupational exposure using surface average tallies as a function of railcar length. Also, local tallies were implemented to calculate the dose rates around the trunnions and above the neutron shield. The MCNP shielding evaluation accounts for subcritical neutron multiplication. An initial enrichment of 3.0% wt U-235 was utilized in the MCNP input file to provide a conservative subcritical multiplication source.

For the dose calculation around the TN-40, the source is divided into four separate regions: fuel, plenum, top end fitting, and bottom end fitting. The model is utilized in two separate computer runs consisting of contributions from the following sources:

- Primary gamma radiation from the active fuel and from activated hardware within the top end fitting, plenum region and bottom end fitting (axial and radial directions).
- Neutron radiation from the active fuel region and secondary gamma radiation from neutron interactions.

The sources in the active fuel region (gamma and neutron) are modeled as uniform radially but vary axially. The sources in the structural hardware regions (plenum, top end fitting, and bottom end fitting) are modeled as uniform both radially and axially. The results from the individual runs are summed to provide the total gamma, neutron and total dose for the package.

The statistical uncertainties are generally less than 5% for the majority of tallies except for local tally bins and the accident results. For the accident the neutron end dose rates have the highest relative error around 10%. The statistical uncertainties associated with the neutron dose rates on the top and bottom impact limiter surface are high, but since they contribute less than 1% (less than 0.1 mrem/hr) to the total dose this is acceptable.

The terminology for the dose locations is as follows. On the side of the cask results are reported on the surface of the cask ("contact"), at vertical planes extending up from a 10 feet wide rail car ("vertical planes"), at the diameter of the impact limiters to represent the top and bottom of the package ("top/bottom"), 1 meter from the steel cask body (1 meter accident) and 2 meters from the vertical planes.

The results indicate peaking near the top and bottom of the cask and streaming in the upper trunnion/above the neutron shield regions. These results are expected due to the reduced shielding in these areas. It was determined that the normal conditions peak external surface dose rate of 239 mrem/hr occurs just above the neutron shield. This is approximately a factor of 6 times higher than the average on the cask surface. The localized peaking at the top of the cask is due to the absence of the neutron shield at the top. Neutron streaming was observed through the trunnion itself. However, the total dose rates just outside the trunnion were nearly the same as those averaged around the entire circumference of the cask.

Table 5-2 presents the maximum calculated dose at contact, at the vehicle's outer edge (assumed 10 ft wide vehicle), and at 2 m from the vehicle's outer edge. The calculated total dose rates at the various dose points around the side of the package are illustrated in Figures 5-7 through 5-8.

For the HAC, Table 5-2 also presents the maximum calculated doses at 1 m from the cask body.

The dose rates for an individual at the end of the rail car are presented in Table 5-17. These results are presented as a function of the length of the rail car.

On average the dose rates are dominated by the neutron source term. The results indicate that typically the total dose rates are comprised of 33% primary gamma, 14% (n, γ) and 53% neutron. However, the primary gamma source produces the majority of the dose rate at the ends of the package; the average contribution from primary gamma is approximately 81%. This is a direct result of the neutron shielding from the wood in the impact limiters. As expected, the accident dose rates are produced mostly from the neutron (94%) source due to loss of neutron shielding material and impact limiter.

Typical average (130 cm above and below the active fuel midplane) contact dose rates on the side of the cask are approximately 38 mrem/hr (54% neutron). At 2 meters from the side of the cask the average dose rate is approximately 8.6 mrem/hr which is comprised of 4.5 mrem/hr neutron, 1.0 mrem/hr (n, γ) and 3.1 mrem/hr gamma. On the ends, the total contact dose rates are less than 7 mrem/hr with less than a 0.1 mrem/hr contribution from neutrons.

The dose rate analysis was performed using MCNP, MCNP4C2 [5]. Selected inputs for MCNP are included in Section 5.6.

5.5 References

1. SCALE 4.4, "Modular Code System for Performing Standardized Computer Analyses for Licensing Evaluation for Workstations and Personal Computers," CCC-545, ORNL.
2. ORNL/TM-11018, "Standard- and Extended-Burnup PWR and BWR Reactor Models for the ORIGEN2 Computer Code," Oak Ridge National Laboratory, December 1989.
3. NUREG/CR-6801 (ORNL/TM-2001/273), March 2003, "Recommendations for Addressing Axial Burnup in PWR Burnup Credit Analyses."
4. Luksic, 'Spent Fuel Assembly Hardware: Characterization and 10 CFR 61 Classification for Waste Disposal,' PNL-6906, UC-85, June 1989.
5. MCNP4C2, "Monte Carlo N-Particle Transport Code System," Los Alamos National Laboratory, CCC 701, RSIC, June 2001.
6. "American National Standard for Calculation and Measurement of Direct and Scattered Gamma Radiation from LWR Nuclear Power Plants", ANSI/ANS-6.6.1-1977, American Nuclear Society, Illinois, 1977.
7. EPRI-NP-5128, "The TN-24P PWR Spent-Fuel Storage Cask: Testing and Analyses," prepared by Pacific Northwest Laboratory, Virginia Power Company and EG&G Idaho National Engineering Laboratory, April 1987.
8. DOE/ET/47912-3 Vol. III, "Domestic Light Water Reactor Fuel Design Evolution," Prepared for U. S. Department of Energy Savannah River Operations Office, September 1981.

5.6 Input File Listing

5.6.1 SAS2H/ORIGEN-S Input File

```
=sas2h    parm='halt02,skipshipdata'
NSP W STD (14x14) 410 kgU 2.35 w/o 42 GWD/MTU
44groupndf5  latticecell
'
' =====
' FUEL MATERIAL SPECIFICATION 1=FUEL ALWAYS, 2=CLAD ALWAYS, 3=MOD ALWAYS
' =====
'
'      %TD      T (K)    ... Uranium wt%
uo2  1  0.9555      840    92235  2.35  92238  97.6183  92234  0.02092  92236  0.01081  END
zirc4      2      1.0      620    end
h2o        3  den=0.733    1.0    558    end
boron      3  den=0.733    600-6  558    end
'
' =====
' CASK MATERIAL COMPOSITIONS, START AT 6
' =====
'
' homogenized basket/cavity
'      VF=partial dens/homo dens of fuel
zr          6  den=0.349    end
fe          6  den=0.248    end
al          6  den=0.261    end
'
' primary cask shielding
fe          7  den=7.85     end
'
' neutron shielding resin and aluminum
al          8  den=0.482    end
c           8  den=0.499    end
o           8  den=0.592    end
h           8  den=0.07171  end
b           8  den=0.01491  1.0  293  5010  19.7  5011  80.3  end
'
end comp
'
' =====
' FUEL PIN PARAMETERS
' =====
'
'      pitch  fuelod  mfuel  mmod  cladod  mclad  cladid  mgap
squarepitch  1.41224  0.929386  1      3  1.07188  2    0.948436  0  end
' more data szf=1.2 end
'
' =====
' FUEL ASSEMBLY PARAMETERS
' =====
'
' npin/assm=179  fuelength=365.76  ncycles=2  nlib/cyc=1  printlevel=5
lightel=35      inplevel=1  numinstr=1  ortube=0.53594
srtube=0.474218  end
'
' =====
' FUEL IRRADIATION in MW/BASIS and DAYS
' =====
'
```

```

power=21.5250    burn=400    down=30    end
power=21.5250    burn=400    down=3652   end
,
, =====
, LIGHT ELEMENT SECTION (KG/BASIS)
, =====
,
H 1.08E-3 Li 4.10E-4 B 4.38E-4 C 5.50E-2 N 3.40E-2 O 5.52E+1 F 4.39E-3
Na 6.15E-3 Mg 8.20E-4 Al 4.10E-2 Si 9.30E-2 P 1.78E-2 S 5.61E-3 Cl 2.17E-3
Ca 8.20E-4 Ti 4.50E-2 V 2.90E-3 Cr 2.59E+0 Mn 1.68E-1 Fe 6.49E+0 Co 3.26E-2
Ni 3.49E+0 Cu 7.44E-3 Zn 1.65E-2 Zr 8.16E+1 Nb 2.98E-1 Mo 1.65E-1 Ag 4.10E-5
Cd 1.03E-2 In 8.20E-4 Sn 1.34E+0 Gd 1.03E-3 Hf 6.50E-3 W 2.49E-3 Pb 4.10E-4
,
, =====
, RADIAL GEOMETRY OF CASK
, =====
,
end
end
,
, =====
, END CARD TO TERMINATE SAS RUN
, =====
,
end
=ORIGENS
0$$$ A8 26 A11 71 E 1$$$ 1 1T
decay 24.0 24.4 26.0 28.0 30.0 32.0 35.0 40.0 45.0 50.0 YEARS
3$$$ 21 A3 1 A30 18 A33 18 T
T
56$$$ 0 10 A13 -1 5 E T
60** 24.0 24.4 26.0 28.0 30.0 32.0 35.0 40.0 45.0 50.0
61** F1 65$$$ A25 1 E
65$$$ A10 1 A31 1 A52 1 E
81$$$ 2 0 26 1 E 82$$$ F2
83** 1.00E+07 8.00E+06 6.50E+06 5.00E+06 4.00E+06 3.00E+06 2.50E+06
      2.00E+06 1.66E+06 1.33E+06 1.00E+06 8.00E+05 6.00E+05 4.00E+05
      3.00E+05 2.00E+05 1.00E+05 5.00E+04 1.00E+04 T
24 YEAR COOLING WE STD 14X14 410KGU
24.4 YEAR COOLING WE STD 14X14 410KGU
26 YEAR COOLING WE STD 14X14 410KGU
28 YEAR COOLING WE STD 14X14 410KGU
30 YEAR COOLING WE STD 14X14 410KGU
32 YEAR COOLING WE STD 14X14 410KGU
35 YEAR COOLING WE STD 14X14 410KGU
40 YEAR COOLING WE STD 14X14 410KGU
45 YEAR COOLING WE STD 14X14 410KGU
50 YEAR COOLING WE STD 14X14 410KGU
56$$$ F0 6T
end

```

5.6.2 MCNP Neutron Model Input File

```

TN-40 TRAN NEUTRON UNIFORM 42GWD/2.35%/24.4Y NORMAL RUN 10/12/05
c
c      10      20      30      40      50      60      70
c      |      |      |      |      |      |      |
c 34567890123456789012345678901234567890123456789012345678
c
c ** This model changes the DBF per Prairie Island comments **
c ** Subcritical fission using MCNP **
c
c The following general design parameters are applied throughout this model:
c
c 1. Uniform loading (modeled as two zones)
c 2. Homogenized fuel; discrete steel box and basket aluminm
c 3. Trunnions and impact limiters included
c 4. Assumed burnup profile based on PI plant data
c 5. Generic neutron source spectrum using builtin MCNP spectrum
c 6. 10CFR71 acceptance criteria for dose locations
c 7. Approximated periphery basket (including rails and outer SST inserts)
c 8. Fuel enrichment 3.0 wt. % assumed
c 9. Resin boxes modeled as homogenized Al box & resin mix
c 10. Conservative Boral credit modeled as aluminum around fuel tubes
c
c
c =====
c =
c =                      CELL CARDS                      =
c =
c =====
c
1      0      -11:+12:+13      imp:p=0.0E+00 imp:n=0.0E+00
c
c fuel lattice
c
c center fuel assys
2011 10 -2.45 (-275:+276:-277:+278)      u=11 imp:p=1.0E+00 imp:n=1.0E+00      $
boral gap
2021 0      (-295:+296:-297:+298) &
      +211 -212 +213 -214      u=11 imp:p=1.0E+00 imp:n=1.0E+00      $
void around fuel
2031 6 -7.940 (-211:+212:-213:+214) &
      +271 -272 +273 -274      u=11 imp:p=1.0E+00 imp:n=1.0E+00      $
steel liner
2041 10 -2.702 (-271:+272:-273:+274) &
      +275 -276 +277 -278      u=11 imp:p=1.0E+00 imp:n=1.0E+00      $
aluminum sandwich
2061 0      +295 -296 +297 -298 -205      u=11 imp:p=1.0E+00 imp:n=1.0E+00      $
void gap
2051 4 -2.595 +295 -296 +297 -298 +205 -208 u=11 imp:p=1.0E+00 imp:n=1.0E+00      $
bottom end fitting
2071 1 -3.949 +295 -296 +297 -298 +208 -250 u=11 imp:p=1.0E+00 imp:n=1.0E+00      $
fuel
2081 2 -1.543 +295 -296 +297 -298 +250 -255 u=11 imp:p=1.0E+00 imp:n=1.0E+00      $
plenum
2091 3 -1.970 +295 -296 +297 -298 +255 -260 u=11 imp:p=1.0E+00 imp:n=1.0E+00      $
top end fitting
2101 0      +295 -296 +297 -298 +260      u=11 imp:p=1.0E+00 imp:n=1.0E+00      $
void gap

```

```

c
c periphery fuel assys
2012 10 -2.45 (-275:+276:-277:+278) u=12 imp:p=1.0E+00 imp:n=1.0E+00 $
boral gap
2022 0 (-295:+296:-297:+298) &
+211 -212 +213 -214 u=12 imp:p=1.0E+00 imp:n=1.0E+00 $
void around fuel
2032 6 -7.940 (-211:+212:-213:+214) &
+271 -272 +273 -274 u=12 imp:p=1.0E+00 imp:n=1.0E+00 $
steel liner
2042 10 -2.702 (-271:+272:-273:+274) &
+275 -276 +277 -278 u=12 imp:p=1.0E+00 imp:n=1.0E+00 $
aluminum sandwich
2052 4 -2.595 +295 -296 +297 -298 -208 u=12 imp:p=1.0E+00 imp:n=1.0E+00 $
bottom end fitting
2062 0 +295 -296 +297 -298 -205 u=12 imp:p=1.0E+00 imp:n=1.0E+00 $
void gap
2072 1 -3.949 +295 -296 +297 -298 +208 -250 u=12 imp:p=1.0E+00 imp:n=1.0E+00 $
fuel
2082 2 -1.543 +295 -296 +297 -298 +250 -255 u=12 imp:p=1.0E+00 imp:n=1.0E+00 $
plenum
2092 3 -1.970 +295 -296 +297 -298 +255 -260 u=12 imp:p=1.0E+00 imp:n=1.0E+00 $
top end fitting
2102 0 +295 -296 +297 -298 +260 u=12 imp:p=1.0E+00 imp:n=1.0E+00 $
void gap
c
c
c empty compartment and periphery basket
2013 10 -2.702 (-275:+276:-277:+278) u=2 imp:p=1.0E+00 imp:n=1.0E+00 $
boral gap
2043 10 -2.702 (-271:+272:-273:+274) &
+275 -276 +277 -278 u=2 imp:p=1.0E+00 imp:n=1.0E+00 $
aluminum sandwich
2073 0 +271 -272 +273 -274 u=2 imp:p=1.0E+00 imp:n=1.0E+00 $
empty basket
241 10 -2.702 +272:-273 u=5 imp:p=1.0E+00 imp:n=1.0E+00 $
solid aluminum
245 0 -272 +273 u=5 imp:p=1.0E+00 imp:n=1.0E+00 $
empty assy
251 10 -2.702 -271:-273 u=6 imp:p=1.0E+00 imp:n=1.0E+00 $
basket
255 0 +271 +273 u=6 imp:p=1.0E+00 imp:n=1.0E+00 $
empty assy
261 10 -2.702 -271:+274 u=7 imp:p=1.0E+00 imp:n=1.0E+00 $
basket
265 0 +271 -274 u=7 imp:p=1.0E+00 imp:n=1.0E+00 $
empty assy
271 10 -2.702 +272:+274 u=8 imp:p=1.0E+00 imp:n=1.0E+00 $
basket
275 0 -272 -274 u=8 imp:p=1.0E+00 imp:n=1.0E+00 $
empty assy
299 0 -292 +291 -294 +293 u=9 imp:p=1.0E+00 imp:n=1.0E+00 &
lat=1 fill=-1:8 -5:5 0:0
c
c x coords
c -1 0 1 2 3 4 5 6 7 8
c
9 9 9 9 9 9 9 9 9 9 $ -5
9 9 9 2 2 2 2 9 9 9 $ -4
9 7 8 12 12 12 12 7 8 9 $ -3

```

```

9  2 12 11 11 11 11 12 2 9 $ -2
9  2 12 11 11 11 11 12 2 9 $ -1
9 12 11 11 11 11 11 11 12 9 $ 0
9  2 12 11 11 11 11 12 2 9 $ 1
9  2 12 11 11 11 11 12 2 9 $ 2
9  6  5 12 12 12 12  6  5 9 $ 3
9  9  9  2  2  2  2  9  9 9 $ 4
9  9  9  9  9  9  9  9  9 9 $ 5
c
c cavity cells
23  0      +201 -261 -2990      fill=9      imp:p=1.0E+00 imp:n=1.0E+00
24  6 -7.940 +201 -261 +2990 -299      imp:p=1.0E+00 imp:n=1.0E+00 $
outer SST inserts
2771 10 -2.702 +201 -261 +299 -282 -2991      imp:p=1.0E+00 imp:n=1.0E+00 $
these are the rails
2772 10 -2.702 +201 -261 +299 -282 +2991 -2992      imp:p=1.0E+00 imp:n=1.0E+00
2773 10 -2.702 +201 -261 +299 -282 +2992 -2993      imp:p=1.0E+00 imp:n=1.0E+00
2774 10 -2.702 +201 -261 +299 -282 +2993 -2994      imp:p=1.0E+00 imp:n=1.0E+00
2775 10 -2.702 +201 -261 +299 -282 +2994 -2995      imp:p=1.0E+00 imp:n=1.0E+00
2776 10 -2.702 +201 -261 +299 -282 +2995 -2996      imp:p=1.0E+00 imp:n=1.0E+00
2778 10 -2.702 +201 -261 +299 -282 +2996      imp:p=1.0E+00 imp:n=1.0E+00
c
c main shield shell cells
301  5 -7.821 (261 -511 -801):&
      (802 801 282 -311):(419 -201 -802) imp:p=1.0E+00 imp:n=1.0E+00
302  5 -7.821 (511 -512 -801):&
      (802 801 311 -312):(418 -419 -802) imp:p=1.0E+00 imp:n=1.0E+00
303  5 -7.821 (512 -513 -801):&
      (802 801 312 -313):(417 -418 -802) imp:p=1.0E+00 imp:n=1.0E+00
304  5 -7.821 (513 -514 -801):&
      (802 801 313 -314):(416 -417 -802) imp:p=1.0E+00 imp:n=1.0E+00
305  5 -7.821 (514 -515 -801):&
      (802 801 314 -315):(415 -416 -802) imp:p=1.0E+00 imp:n=1.0E+00
306  5 -7.821 (515 -516 -801):&
      (802 -516 315 -316):(414 -415 -802) imp:p=1.0E+00 imp:n=1.0E+00
307  5 -7.821 (802 -516 316 -317):(413 -414 -802) imp:p=1.0E+00 imp:n=1.0E+00
308  5 -7.821 (802 -516 317 -318):(412 -413 -802) imp:p=1.0E+00 imp:n=1.0E+00
309  5 -7.821 (802 -516 318 -319):(411 -412 -802) imp:p=1.0E+00 imp:n=1.0E+00
310  5 -7.821 (802 -516 319 -320):(410 -411 -802) imp:p=1.0E+00 imp:n=1.0E+00
c
c top of lid
501  5 -7.821 +516 -517 -521      imp:p=1.0E+00 imp:n=1.0E+00
502  5 -7.821 +517 -518 -521      imp:p=1.0E+00 imp:n=1.0E+00
503  5 -7.821 +518 -519 -521      imp:p=1.0E+00 imp:n=1.0E+00
504  5 -7.821 +519 -520 -521      imp:p=3.0E+00 imp:n=3.0E+00
505 10 -2.702 +520 -522 -320      imp:p=3.0E+00 imp:n=3.0E+00 $ A1
impact limiter spacer on top
c
c top impact limiters
601  0      (+622 -750 +320 -651)      imp:p=1.0E+00 imp:n=1.0E+00
602  0      (+622 -750 +651 -672)      imp:p=1.0E+00 imp:n=1.0E+00
603  8 -.125 (+750 -752 +320 -651)      imp:p=1.0E+00 imp:n=1.0E+00
604  8 -.125 (+750 -752 +651 -672)      imp:p=1.0E+00 imp:n=1.0E+00
605 10 -2.702 (+516 -518 +521 -318)      imp:p=1.0E+00 imp:n=1.0E+00
606 10 -2.702 (+518 -520 +521 -318):&
      (+516 -520 +318 -320)      imp:p=3.0E+00 imp:n=3.0E+00
607  9 -.387 (+522 -721 -651):&
      (+752 -522 +320 -651)      imp:p=3.9E+00 imp:n=3.9E+00
608  9 -.387 (+752 -721 +651 -672):&
      (+721 -722 -672)      imp:p=4.2E+00 imp:n=4.2E+00

```

609	9	-.387	+722	-723	-672			imp:p=4.4E+00	imp:n=4.4E+00
610	9	-.387	+723	-724	-672			imp:p=4.1E+00	imp:n=4.1E+00
611	9	-.387	+724	-725	-672			imp:p=4.5E+00	imp:n=4.5E+00
612	9	-.387	+725	-726	-672			imp:p=5.1E+00	imp:n=5.1E+00
613	9	-.387	+726	-727	-672			imp:p=6.5E+00	imp:n=6.5E+00
614	9	-.387	+727	-728	-672			imp:p=8.4E+00	imp:n=8.4E+00
615	9	-.387	+728	-729	-672			imp:p=1.0E+01	imp:n=1.0E+01
616	9	-.387	+729	-730	-672			imp:p=1.3E+01	imp:n=1.3E+01
617	9	-.387	+730	-731	-672			imp:p=1.5E+01	imp:n=1.5E+01
618	9	-.387	+731	-732	-672			imp:p=2.0E+01	imp:n=2.0E+01
619	9	-.387	+732	-733	-672			imp:p=2.8E+01	imp:n=2.8E+01
620	9	-.387	+733	-734	-672			imp:p=4.0E+01	imp:n=4.0E+01
621	9	-.387	+734	-735	-672			imp:p=6.5E+01	imp:n=6.5E+01
622	8	-.125	+735	-762	-672			imp:p=1.0E+02	imp:n=1.0E+02
623	6	-7.940	+762	-736	-672			imp:p=1.0E+02	imp:n=1.0E+02
c									
632	0		+622	-750	+651	+672	-810	imp:p=1.1E+01	imp:n=1.1E+01
634	8	-.125	+750	-752	+651	+672	-810	imp:p=6.3E+00	imp:n=6.3E+00
638	9	-.387	+752	-723	+651	+672	-810	imp:p=5.5E+00	imp:n=5.5E+00
640	9	-.387	+723	-725		+672	-810	imp:p=6.2E+00	imp:n=6.2E+00
642	9	-.387	+725	-727		+672	-810	imp:p=9.4E+00	imp:n=9.4E+00
644	9	-.387	+727	-729		+672	-810	imp:p=1.4E+01	imp:n=1.4E+01
646	9	-.387	+729	-731		+672	-810	imp:p=2.2E+01	imp:n=2.2E+01
648	9	-.387	+731	-733		+672	-810	imp:p=4.0E+01	imp:n=4.0E+01
650	9	-.387	+733	-735		+672	-810	imp:p=9.1E+01	imp:n=9.1E+01
652	8	-.125	+735	-762		+672	-810	imp:p=2.4E+02	imp:n=2.4E+02
653	6	-7.940	+762	-736		+672	-810	imp:p=2.4E+02	imp:n=2.4E+02
c									
662	0		+622	-750	+651	+810	-811	imp:p=2.4E+01	imp:n=2.4E+01
664	8	-.125	+750	-752	+651	+810	-811	imp:p=1.5E+01	imp:n=1.5E+01
668	9	-.387	+752	-723	+651	+810	-811	imp:p=1.2E+01	imp:n=1.2E+01
672	9	-.387	+723	-727		+810	-811	imp:p=1.7E+01	imp:n=1.7E+01
676	9	-.387	+727	-731		+810	-811	imp:p=3.2E+01	imp:n=3.2E+01
680	9	-.387	+731	-735		+810	-811	imp:p=1.2E+02	imp:n=1.2E+02
682	8	-.125	+735	-762		+810	-811	imp:p=6.2E+02	imp:n=6.2E+02
683	6	-7.940	+762	-736		+810	-811	imp:p=6.2E+02	imp:n=6.2E+02
c									
c side neutron shield									
851	7	-1.690	+602	-621	+650	-651	+861	imp:p=1.0E+00	imp:n=1.0E+00
852	7	-1.690	+602	-621	+651	-670	+861	imp:p=1.0E+00	imp:n=1.0E+00
853	5	-7.821	+621	-622	+320	-671		imp:p=1.0E+00	imp:n=1.0E+00
854	5	-7.821	+601	-602	+320	-671		imp:p=1.0E+00	imp:n=1.0E+00
855	5	-7.821	+601	-622	+671	-672	+861	imp:p=1.0E+00	imp:n=1.0E+00
856	7	-1.690	+602	-621	+320	-650	+861	imp:p=1.0E+00	imp:n=1.0E+00
857	7	-1.690	+602	-621	+670	-671	+861	imp:p=1.0E+00	imp:n=1.0E+00
c									
c bottom impact limiters									
c									
701	8	-.125	(+751	-601	+320	-651	-875):&		
			(+751	-601	+320	-651	876)	imp:p=1.0E+00	imp:n=1.0E+00
702	8	-.125	(+751	-601	+651	-672	-875):&		
			(+751	-601	+651	-672	876)	imp:p=1.0E+00	imp:n=1.0E+00
7031	9	-.387	(+410	-751	+320	-651) &		
			(-875:876:-879)					imp:p=1.0E+00	imp:n=1.0E+00
7032	9	-.387	(+716	-410	-651)			imp:p=2.3E+00	imp:n=2.3E+00
7041	9	-.387	(+716	-751	+651	-672)	&		
			(-875:876:-879)					imp:p=1.0E+00	imp:n=1.0E+00
7042	9	-.387	(+715	-716	-672)			imp:p=2.5E+00	imp:n=2.5E+00
705	9	-.387	+714	-715	-672			imp:p=2.5E+00	imp:n=2.5E+00
706	9	-.387	+713	-714	-672			imp:p=2.8E+00	imp:n=2.8E+00

707	9	-.387	+712	-713	-672		imp:p=3.2E+00	imp:n=3.2E+00
708	9	-.387	+711	-712	-672		imp:p=3.4E+00	imp:n=3.4E+00
709	9	-.387	+710	-711	-672		imp:p=4.0E+00	imp:n=4.0E+00
710	9	-.387	+709	-710	-672		imp:p=5.0E+00	imp:n=5.0E+00
711	9	-.387	+708	-709	-672		imp:p=6.5E+00	imp:n=6.5E+00
712	9	-.387	+707	-708	-672		imp:p=8.0E+00	imp:n=8.0E+00
713	9	-.387	+706	-707	-672		imp:p=9.8E+00	imp:n=9.8E+00
714	9	-.387	+705	-706	-672		imp:p=1.4E+01	imp:n=1.4E+01
715	9	-.387	+704	-705	-672		imp:p=1.9E+01	imp:n=1.9E+01
716	9	-.387	+703	-704	-672		imp:p=2.9E+01	imp:n=2.9E+01
717	9	-.387	+761	-703	-672		imp:p=2.9E+01	imp:n=2.9E+01
718	8	-.125	+702	-761	-672		imp:p=6.7E+01	imp:n=6.7E+01
719	6	-7.940	+701	-702	-672		imp:p=6.7E+01	imp:n=6.7E+01
c								
721	0		+753	-601	+672	-810 & (-875:876:-877:878)	imp:p=5.4E+00	imp:n=5.4E+00
722	8	-.125	+751	-753	+672	-810 & (-875:876:-877:878)	imp:p=5.4E+00	imp:n=5.4E+00
724	9	-.387	+715	-751	+672	-810 & (-875:876:-877:878:-879)	imp:p=4.3E+00	imp:n=4.3E+00
726	9	-.387	+713	-715	+672	-810	imp:p=4.5E+00	imp:n=4.5E+00
728	9	-.387	+711	-713	+672	-810	imp:p=6.1E+00	imp:n=6.1E+00
730	9	-.387	+709	-711	+672	-810	imp:p=9.5E+00	imp:n=9.5E+00
732	9	-.387	+707	-709	+672	-810	imp:p=1.6E+01	imp:n=1.6E+01
734	9	-.387	+705	-707	+672	-810	imp:p=2.3E+01	imp:n=2.3E+01
736	9	-.387	+761	-705	+672	-810	imp:p=5.2E+01	imp:n=5.2E+01
738	8	-.125	+702	-761	+672	-810	imp:p=1.9E+02	imp:n=1.9E+02
739	6	-7.940	+701	-702	+672	-810	imp:p=1.9E+02	imp:n=1.9E+02
c								
741	0		+753	-601	+810	-811	imp:p=1.4E+01	imp:n=1.4E+01
742	8	-.125	+751	-753	+810	-811	imp:p=1.4E+01	imp:n=1.4E+01
744	9	-.387	+715	-751	+810	-811	imp:p=1.1E+01	imp:n=1.1E+01
748	9	-.387	+711	-715	+810	-811	imp:p=1.3E+01	imp:n=1.3E+01
752	9	-.387	+707	-711	+810	-811	imp:p=2.4E+01	imp:n=2.4E+01
756	9	-.387	+761	-707	+810	-811	imp:p=8.0E+01	imp:n=8.0E+01
758	8	-.125	+702	-761	+810	-811	imp:p=5.4E+02	imp:n=5.4E+02
759	6	-7.940	+701	-702	+810	-811	imp:p=5.4E+02	imp:n=5.4E+02
c								
760	0		(864	867	875	-876 320 -878 879 -601):& (864 -867 875 -876 320 +877 879 -601)	imp:p=1.0E+00	imp:n=1.0E+00
c								
c tally cells								
900	0		+601	-622	+672	-899 +861	imp:p=4.0E+00	imp:n=4.0E+00
901	0		+601	-622	+899	-810 +861	imp:p=4.0E+00	imp:n=4.0E+00
902	0		+601	-622	+810	-811	imp:p=1.2E+01	imp:n=1.2E+01
903	11	-1.225E-3	+701	-736	+811	-812	imp:p=1.2E+02	imp:n=1.2E+02 \$
comment these out for importance optimization								
904	11	-1.225E-3	(+701	-736	+812	-814):& (+736 -815 -814):(+816 -701 -814)	imp:p=6.2E+02	imp:n=6.2E+02
905	11	-1.225E-3	(+816	-815	+814	-813):& (+815 -817 -813):(+818 -816 -813)	imp:p=6.2E+02	imp:n=6.2E+02
906	11	-1.225E-3	(+11	-12	-13) (813:+817:-818) & (+818:-11:810) (-817:12:810)	imp:p=6.2E+02	imp:n=6.2E+02	
907	11	-1.225E-3	+851	-818	-810		imp:p=6.2E+02	imp:n=6.2E+02 \$
far cells at end of rail car								
908	11	-1.225E-3	+850	-851	-810		imp:p=6.2E+02	imp:n=6.2E+02
909	11	-1.225E-3	+11	-850	-810		imp:p=6.2E+02	imp:n=6.2E+02
910	11	-1.225E-3	+817	-852	-810		imp:p=6.2E+02	imp:n=6.2E+02
911	11	-1.225E-3	+852	-853	-810		imp:p=6.2E+02	imp:n=6.2E+02
912	11	-1.225E-3	+853	-12	-810		imp:p=6.2E+02	imp:n=6.2E+02

```

c
c upper trunnions
801 5 -7.821 (-867 +320 +870 -861):&
      (+867 +320 -871 -861)          imp:p=1.0E+00 imp:n=1.0E+00
802 5 -7.821 (+869 -870 +863 -861):&
      (+871 -872 +863 -861)          imp:p=1.0E+00 imp:n=1.0E+00
803 5 -7.821 (+868 -869 +863 -862):&
      (+872 -873 +863 -862)          imp:p=1.0E+00 imp:n=1.0E+00
804 7 -1.690 (+868 -870 -863):&
      (+871 -873 -863)              imp:p=1.0E+00 imp:n=1.0E+00
805 0        (-869 -810 -861 (+862:-868)):&
      (+872 -810 -861 (+862:+873))    imp:p=1.0E+00 imp:n=1.0E+00
c
c lower trunnions
811 5 -7.821 (-867 +320 +870 -864):&
      (+867 +320 -871 -864)          imp:p=4.0E+00 imp:n=4.0E+00
812 5 -7.821 (+869 -870 +866 -864):&
      (+871 -872 +866 -864)          imp:p=2.5E+00 imp:n=2.5E+00
813 5 -7.821 (+868 -869 +866 -865):&
      (+872 -873 +866 -865)          imp:p=5.0E+00 imp:n=5.0E+00
814 0        (+868 -870 -866):&
      (+871 -873 -866)              imp:p=5.4E+00 imp:n=5.4E+00
815 0        (+877 -869 +865 -864):&
      (+872 -878 +865 -864)          imp:p=5.0E+00 imp:n=5.0E+00
816 0        (+877 -868 -865):&
      (+873 -878 -865)              imp:p=5.4E+00 imp:n=5.4E+00

c =====
c =
c =                               SURFACE CARDS
c =
c =
c =====
c
c model boundaries
c initial model had rail car at 41' 8" long
c rail cars typically are 40 to 60 feet
c PacTec typical transport car (for OCRWM) 49' 6"
c set outer bounds at 60 feet
c assume cask CG is middle of active fuel (within 6 inches of actual)
11 pz -914.4          $ end of rail car
12 pz 914.4           $ end of rail car
13 cz 652.4           $ 5 meter from (vertical planes) side of rail car
c
c fuel/basket region
201 pz -190.70        $ bottom of lower end fitting (bottom cavity)
205 pz -190.7032      $ top of lower end fitting (3.08")
208 pz -182.88        $ bottom of active fuel (144")
211 px -88.7034       $ steel liner inner (8.05 inch typ. square)
212 px -68.20565      $ steel liner modeled as 13 ga. 0.09" thick not 0.10"
213 py -10.2494       $
214 py 10.2494        $
250 pz 182.88         $ top of active fuel
255 pz 201.02068      $ top of plenum (7.142")
260 pz 209.91         $ top of upper end fitting (3.5")
261 pz 223.32         $ top of cavity (void)
271 px -88.93175      $ steel liner outer (8.05 + .2 inch square)
272 px -67.97675      $
273 py -10.4775       $
274 py 10.4775        $
275 px -89.56675      $ boral gap (8.05 + .7 inch square)

```

```

276 px -67.34175      $
277 py -11.1125      $
278 py 11.1125       $
282 cz 91.44         $ inner radius of cavity (72 inch diameter)
291 px -89.662       $ basket lattice unit cell (8.05+.775 inch square)
292 px -67.2465      $ origin (center of assy) @ x=-78.45425 y=0
293 py -11.20775     $
294 py 11.20775      $
295 px -88.31326     $ fuel envelope 7.763 x 7.763 inch
296 px -68.59524     $
297 py -9.85901      $
298 py 9.85901       $
299 cz 90.932        $ assumes .2" instead of 3/8" outer basket ("rails")
to conserve mass
2990 cz 90.867       $ assumes 0.026" for steel inserts on periphery
2991 py -79.4385     $ rail cutting surfaces
2992 py -55.0545     $
2993 py -12.192      $
2994 py 12.192       $
2995 py 55.0545      $
2996 py 79.4385      $
c
c wall gamma shield
311 cz 93.853        $ split primary gamma shield into 10 layers
312 cz 96.266        $ layer thickness = 2.413 cm or 0.95 inch
313 cz 98.679        $ also applies to bottom and top (diff. thickness)
314 cz 101.092       $
315 cz 103.505       $
316 cz 105.918       $
317 cz 108.331       $
318 cz 110.744       $
319 cz 113.157       $
320 cz 115.57        $ outside cask body
c
c bottom gamma shield
410 pz -216.73       $ cask bottom
411 pz -214.127      $ layer thickness = 2.603 cm or 1.025 inch
412 pz -211.524      $
413 pz -208.921      $
414 pz -206.318      $
415 pz -203.715      $
416 pz -201.112      $
417 pz -198.509      $
418 pz -195.906      $
419 pz -193.303      $
c
c top gamma shield
511 pz 225.987       $ layer thickness = 2.667 cm or 1.05 inch
512 pz 228.654       $
513 pz 231.321       $
514 pz 233.988       $
515 pz 236.655       $
516 pz 238.56        $ top of cask walls
517 pz 241.989       $
518 pz 244.656       $
519 pz 247.323       $
520 pz 249.99        $
521 cz 105.09        $ outer radius of top part of lid
522 pz 252.022       $ assume 0.8" thick to account for tolerances and bolt
holes

```

c

c neutron shields

c 601 pz -186.25

601 pz -185.615

c 602 pz -184.34

602 pz -183.705

621 pz 203.00

622 pz 204.91

650 cz 116.1542

651 cz 121.285

670 cz 126.4158

671 cz 127.0

672 cz 128.27

c

c impact limiters

701 pz -311.98

702 pz -311.345

703 pz -299.05

704 pz -293.17

705 pz -287.29

706 pz -281.41

707 pz -275.53

708 pz -269.65

709 pz -263.77

710 pz -257.89

711 pz -252.01

712 pz -246.13

713 pz -240.25

714 pz -234.37

715 pz -228.49

716 pz -222.61

c

721 pz 255.87

722 pz 261.75

723 pz 267.63

724 pz 273.51

725 pz 279.39

726 pz 285.27

727 pz 291.15

728 pz 297.03

729 pz 302.91

730 pz 308.79

731 pz 314.67

732 pz 320.55

733 pz 326.43

734 pz 332.31

735 pz 338.255

736 pz 345.24

c

750 pz 220.78

751 pz -195.14

752 pz 228.4

753 pz -187.52

761 pz -304.995

762 pz 344.605

c

c miscellaneous surfaces

801 kz 122.2547369 0.8185941 +1 \$ upper splitting mating plane

802 kz -92.06 0.8593425329 -1 \$ lower splitting mating plane

899 cz 128.271 \$ void cell outside cask

\$ bottom edge of side resin lower housing

\$ bottom edge of side resin lower housing

\$ top edge of side resin lower housing

\$ top edge of side resin lower housing

\$ bottom edge of side resin upper housing

\$ top edge of side resin upper housing

\$ homogenized inner aluminum box

\$ splitting shell for neutron shielding

\$ homogenized outer aluminum box

\$ outer radius of resin shield on side

\$ outer radius of resin housing on side

\$ bottom of top impact limiter

\$ balsa/redwood boundary

\$ balsa/redwood boundary

\$ balsa/redwood boundary

\$ balsa/redwood boundary

\$ balsa/redwood boundary

```

810 cz 152.4          $ vertical planes on side (10' wide rail car)
811 cz 182.88         $ top/bottom @ 12' diameter impact limiters
812 cz 198.12         $ top/bottom @ 13' diameter impact limiters (not used)
813 cz 352.4          $ 2 meter from vertical planes on side
814 cz 215.57         $ 1 meter from cask body (HAC)
815 pz 349.99         $ 1 meter from cask top lid (HAC)
816 pz -316.73        $ 1 meter from cask bottom (HAC)
817 pz 545.24         $ 2 meter from top impact limiter
818 pz -511.98        $ 2 meter from bottom impact limiter
824 pz -190           $ axial tally segments
825 pz -170           $ 20 cm wide
826 pz -150           $ centered on fuel midplane
827 pz -130
828 pz -110
829 pz -90
830 pz -70
831 pz -50
832 pz -30
833 pz -10
834 pz 10
835 pz 30
836 pz 50
837 pz 70
838 pz 90
839 pz 110
840 pz 130
841 pz 150
842 pz 170
843 pz 190
844 pz 210
845 pz 230
846 pz 250
c occupied position surfaces
850 pz -762.0         $ 40 foot rail car
851 pz -609.6         $ 50 foot rail car
852 pz 609.6
853 pz 762.0
882 cz 30             $ radial segmentation
883 cz 55
885 cz 140.57
886 cz 165.57
887 cz 232.88
888 cz 282.88
861 c/y 0 177.6 15.254 $ top trunnion base radius
862 c/y 0 177.6 14.2875 $ top trunnion
863 c/y 0 177.6 6.35   $ top trunnion resin radius
864 c/y 0 -197.685 12.0624 $ bottom trunnion base (9.498" dia.)
865 c/y 0 -197.685 11.2776 $ bottom trunnion
866 c/y 0 -197.685 5.715 $ bottom trunnion hole radius
867 py 0              $ trunnion ambiguous surface
868 py -136.2202
869 py -128.27
870 py -127
871 py 127
872 py 128.27
873 py 136.2202
c
c lower trunnion "channel" in impact limiter
875 px -12.6974       $ these surfs form a box around lower trunnions
876 px 12.6974        $ 1/4" gap is assumed

```

877 py -136.8552 \$
 878 py 136.8552 \$
 879 pz -210.3824 \$

C =====
 C =
 C = DATA CARDS
 C =
 C =====

C
 C materials

C
 C *****
 C In-Core Region
 C Density = 3.949 g/cm³; Composition by weight fraction
 C 3.0 w/o enrichment
 C 410 kg U
 C Chemical composition from SCALE Standard Comp. Library
 C *****

C
 m1 92234 -0.000195 \$ U-234
 92235 -0.021902 \$ U-235
 92236 -0.000101 \$ U-236
 92238 -0.707883 \$ U-238
 8016 -0.098148 \$ O
 6012 -0.000011 \$ C
 14000 -0.000377 \$ Si
 15031 -0.000006 \$ P
 24000 -0.004200 \$ Cr
 22000 -0.000239 \$ Ti
 25055 -0.000276 \$ Mn
 26000 -0.010400 \$ Fe
 28000 -0.008289 \$ Ni
 40000 -0.145805 \$ Zr
 50000 -0.002152 \$ Sn
 72000 -0.000015 \$ Hf
 1001 0.000000 \$ H

C
 C *****
 C Plenum
 C Density = 1.543 g/cm³; Composition by weight fraction
 C Chemical composition from SCALE Standard Comp. Library
 C *****

C
 m2 6012 -0.00045 \$ C
 14000 -0.00714 \$ Si
 15031 -0.00025 \$ P
 24000 -0.11569 \$ Cr
 22000 -0.00156 \$ Ti
 25055 -0.01115 \$ Mn
 26000 -0.38641 \$ Fe
 28000 -0.09859 \$ Ni
 40000 -0.37321 \$ Zr
 50000 -0.00551 \$ Sn
 72000 -0.00004 \$ Hf
 c 8016 0.00000 \$ O
 c 1001 0.00000 \$ H
 C

```

c *****
c Top Region
c Density = 1.970 g/cm^3; Composition by weight fraction
c Chemical composition from SCALE Standard Comp. Library
c *****
c
m3 6012 -0.00074 $ C
    14000 -0.01112 $ Si
    15031 -0.00042 $ P
    24000 -0.18702 $ Cr
    22000 -0.00187 $ Ti
    25055 -0.01851 $ Mn
    26000 -0.63795 $ Fe
    28000 -0.14238 $ Ni
c 40000 0.00000 $ Zr
c 50000 0.00000 $ Sn
c 72000 0.00000 $ Hf
c 8016 0.00000 $ O
c 1001 0.00000 $ H
c
c *****
c Bottom Region
c Density = 2.595 g/cm^3; Composition by weight fraction
c Chemical composition from SCALE Standard Comp. Library
c *****
c
m4 6012 -0.00080 $ C
    14000 -0.01000 $ Si
    15031 -0.00045 $ P
    24000 -0.19000 $ Cr
c 22000 0.00000 $ Ti
    25055 -0.02000 $ Mn
    26000 -0.68375 $ Fe
    28000 -0.09500 $ Ni
c 40000 0.00000 $ Zr
c 50000 0.00000 $ Sn
c 72000 0.00000 $ Hf
c 8016 0.00000 $ O
c 1001 0.00000 $ H
c
c *****
c Carbon Steel
c Density = 7.8212 g/cm^3 SCALE Standard Comp. Library
c *****
c
m5 6012 -0.0100 $ C
    26000 -0.9900 $ Fe
c
c *****
c Stainless Steel 304
c Density = 7.94 g/cm^3 SCALE Standard Comp. Library
c *****
c
m6 26000 -0.68375 $ Fe
    24000 -0.19000 $ Cr
    28000 -0.09500 $ Ni
    25055 -0.02000 $ Mn
    14000 -0.01000 $ Si
    6012 -0.00080 $ C
    15031 -0.00045 $ P

```

```

C
C *****
C Homogenized Neutron Resin/Aluminum Shield
C Reference: Page 6, TN Calc. 1042-08, Rev. 0
C Based on TN-24 Resin
C Density = 1.69 g/cm^3
C B-10 and B-11 based on natural abundance
C Note Al is in resin and the aluminum boxes
C *****
C
C
m7 1001 -0.0426 $ H-1
    5010 -0.0018 $ B-10
    5011 -0.0071 $ B-11
    6000 -0.2953 $ C
    8016 -0.3503 $ O
    13027 -0.2851 $ Al
    30000 -0.0178 $ Zn
C
C *****
C Balsa Wood
C TN-68 SAR
C Density = 0.125 g/cm^3
C *****
C
m8 6012 0.2857 $ C
    8016 0.2381 $ O
    1001 0.4762 $ H
C
C *****
C Redwood
C Assume same composition as Balsa
C TN-68 SAR
C Density = 0.387 g/cm^3
C *****
C
m9 6012 0.2857 $ C
    8016 0.2381 $ O
    1001 0.4762 $ H
C
C *****
C Pure Aluminum
C Density = 2.702 g/cm^3 SCALE Standard Comp. Library
C *****
C
m10 13027 -1.0 $ Al
C
C *****
C AIR: ANSI/ANS-6.6.1 Dry air
C Density = 0.001225 g/cm^3
C Composition by weight fraction
C *****
C
m11 6012 -0.00014 $ C
    7014 -0.75519 $ N
    8016 -0.23179 $ O
    18000 -0.01288 $ Ar
C
C *****
C BORAL: TN40 STORAGE CRITICALITY SPECIFICATION
C Density = 2.45 g/cm^3 (770 lbs of boral, about 95.8% theo.)

```

```

c      Composition by weight fraction
c      Based on Calculation 1042-6 (TN40 Storage Crit)
c      0.01 gm/cm^2 B-10 areal density
c      core thickness of 0.025"
c      panel thickness of 0.075"
c      redistribution of wt. frac. to simulate 75% B4C
c      *****
c      actual wt. frac
ml2  6012    -0.066  $      0.088
      13027   -0.695  $      0.594
      5010    -0.044  $      0.058
      5011    -0.195  $      0.060
c source
c
sdef   cel=d1 x=d2 y=d3 z=fcel=d4 erg=d5 par=1
c
c 22 inner assemblies (0.55)
c 18 outer assemblies (0.45)
c
c      inner  outer
sil s   11    12    $ use distribution numbers to separate zones
spl     0.550 0.450 $ sample based on source strength or num assy if uniform
c
c      INNER ASSYS      OUTER ASSYS
#      si11             sp11      si12             sp12
      1                 d         1                 d         $
      23:299:2071      1         23:299:2072      1         $ fuel zone
c
c sample source/fuel cell
c sample volume uniformly
c use lattice element (0,0)
c
c      X DIMENSIONS      Y DIMENSIONS
#      si2             sp2      si3             sp3
      -88.31326         0        -9.85901         0
      -68.59524         1         9.85901         1
c
c zone dependent axial distributions
c burnup is taken from Prairie site specific calculation
c cask center
c
ds4 s  41 42 $ distribution numbers
c
c      INNER ASSYS      OUTER ASSYS
#      si41             sp41      si42             sp42
      -182.88 0          -182.88 0
      -152.4  0.0146     -152.4  0.0146
      -121.92 0.0686     -121.92 0.0686
      -91.44  0.0959     -91.44  0.0959
      -60.96  0.1104     -60.96  0.1104
      -30.48  0.1104     -30.48  0.1104
      0        0.1104     0        0.1104
      30.48   0.1096     30.48   0.1096
      60.96   0.1066     60.96   0.1066
      91.44   0.1044     91.44   0.1044
      121.92  0.0959     121.92  0.0959
      152.4   0.0586     152.4   0.0586
      182.88  0.0146     182.88  0.0146
c
c generic Cm-244 fission spectrum

```

```

c
sp5      -3 0.906 3.848
c
c surface tallies
c
c
fc2      NEUTRON TALLY ON TRUNNION SURFACE
f2:n     868 873
fs2      -862 NT
sd2      641 1E-10 641 1E-10
de2 LOG   2.5-8   1.0-7   1.0-6   1.0-5   1.0-4   1.0-3   1.0-2   1.0-1
          5.0-1   1.0     2.5     5.0     7.0     10.0    14.0    20.0
df2 LOG   3.67-6  3.67-6  4.46-6  4.54-6  4.18-6  3.76-6  3.56-6  2.17-5
          9.26-5  1.32-4  1.25-4  1.56-4  1.47-4  1.47-4  2.08-4  2.27-4
c
c
fc4      NEUTRON VOLUME TALLIES AROUND THE TRUNNION
f4:n     601 602 632 662 805
sd4      4j 2.4E4
de4 LOG   2.5-8   1.0-7   1.0-6   1.0-5   1.0-4   1.0-3   1.0-2   1.0-1
          5.0-1   1.0     2.5     5.0     7.0     10.0    14.0    20.0
df4 LOG   3.67-6  3.67-6  4.46-6  4.54-6  4.18-6  3.76-6  3.56-6  2.17-5
          9.26-5  1.32-4  1.25-4  1.56-4  1.47-4  1.47-4  2.08-4  2.27-4
c
c
fc12     GAMMA TALLY ON TRUNNION SURFACE
f12:p    868 873
fs12     -862 NT
sd12     641 1E-10 641 1E-10
de12     LOG 0.01   0.03   0.05   0.07   0.1    0.15   0.2    0.25
          0.3    0.35   0.4    0.45   0.5    0.55   0.6    0.65
          0.7    0.8    1      1.4    1.8    2.2    2.6    2.8
          3.25   3.75   4.25   4.75   5.0    5.25   5.75   6.25
          6.75   7.5    9      11.0   13.0   15.0
df12     LOG 3.96-6  5.82-7  2.90-7  2.58-7  2.83-7  3.79-7  5.01-7  6.31-7
          7.59-7  8.78-7  9.85-7  1.08-6  1.17-6  1.27-6  1.36-6  1.44-6
          1.52-6  1.68-6  1.98-6  2.51-6  2.99-6  3.42-6  3.82-6  4.01-6
          4.41-6  4.83-6  5.23-6  5.60-6  5.80-6  6.01-6  6.37-6  6.74-6
          7.11-6  7.66-6  8.77-6  1.03-5  1.18-5  1.33-5
c
c
fc14     GAMMA VOLUME TALLIES AROUND THE TRUNNION
f14:p    601 602 632 662 805
sd14     4j 2.4E4
de14     LOG 0.01   0.03   0.05   0.07   0.1    0.15   0.2    0.25
          0.3    0.35   0.4    0.45   0.5    0.55   0.6    0.65
          0.7    0.8    1      1.4    1.8    2.2    2.6    2.8
          3.25   3.75   4.25   4.75   5.0    5.25   5.75   6.25
          6.75   7.5    9      11.0   13.0   15.0
df14     LOG 3.96-6  5.82-7  2.90-7  2.58-7  2.83-7  3.79-7  5.01-7  6.31-7
          7.59-7  8.78-7  9.85-7  1.08-6  1.17-6  1.27-6  1.36-6  1.44-6
          1.52-6  1.68-6  1.98-6  2.51-6  2.99-6  3.42-6  3.82-6  4.01-6
          4.41-6  4.83-6  5.23-6  5.60-6  5.80-6  6.01-6  6.37-6  6.74-6
          7.11-6  7.66-6  8.77-6  1.03-5  1.18-5  1.33-5
c
c
fc102    NEUTRON TALLY: SIDE, TOP/BOTTOM D=12', TOP/BOTTOM D=13.5', 5M
f102:n   672 810 811 812 813 13 NT
fs102    -824 -825 -826 -827 -828 -829 -830 -831 -832
          -833 -834 $ midplane segment number 11

```

```

      -835 -836 -837 -838 -839 -840 -841 -842 -843 -844 -845 -846 T
sd102  94215  16119  17R    15883 14983 16123      16199 72664 520209 125J
del102 LOG    2.5-8    1.0-7    1.0-6    1.0-5    1.0-4    1.0-3    1.0-2    1.0-1
          5.0-1    1.0      2.5      5.0      7.0      10.0     14.0     20.0
df102 LOG    3.67-6  3.67-6  4.46-6  4.54-6  4.18-6  3.76-6  3.56-6  2.17-5
          9.26-5  1.32-4  1.25-4  1.56-4  1.47-4  1.47-4  2.08-4  2.27-4

```

c

c

fc112 NEUTRON TALLY: CONTACT AND 2 METERS FROM IMPACT LIMITERS

f112:n 818 701 736 817 NT

fs112 -882 -883 -282 -320 -885 -886 -811 T

```

del112 LOG    2.5-8    1.0-7    1.0-6    1.0-5    1.0-4    1.0-3    1.0-2    1.0-1
          5.0-1    1.0      2.5      5.0      7.0      10.0     14.0     20.0
df112 LOG    3.67-6  3.67-6  4.46-6  4.54-6  4.18-6  3.76-6  3.56-6  2.17-5
          9.26-5  1.32-4  1.25-4  1.56-4  1.47-4  1.47-4  2.08-4  2.27-4

```

		0.3	0.35	0.4	0.45	0.5	0.55	0.6	0.65
		0.7	0.8	1	1.4	1.8	2.2	2.6	2.8
		3.25	3.75	4.25	4.75	5.0	5.25	5.75	6.25
		6.75	7.5	9	11.0	13.0	15.0		
df202	LOG	3.96-6	5.82-7	2.90-7	2.58-7	2.83-7	3.79-7	5.01-7	6.31-7
		7.59-7	8.78-7	9.85-7	1.08-6	1.17-6	1.27-6	1.36-6	1.44-6
		1.52-6	1.68-6	1.98-6	2.51-6	2.99-6	3.42-6	3.82-6	4.01-6
		4.41-6	4.83-6	5.23-6	5.60-6	5.80-6	6.01-6	6.37-6	6.74-6
		7.11-6	7.66-6	8.77-6	1.03-5	1.18-5	1.33-5		

c

c

fc212 GAMMA TALLY: CONTACT AND 2 METERS FROM IMPACT LIMITERS

f212:p 818 701 736 817 NT

fs212 -882 -883 -282 -320 -885 -886 -811 T

de212	LOG	0.01	0.03	0.05	0.07	0.1	0.15	0.2	0.25
		0.3	0.35	0.4	0.45	0.5	0.55	0.6	0.65
		0.7	0.8	1	1.4	1.8	2.2	2.6	2.8
		3.25	3.75	4.25	4.75	5.0	5.25	5.75	6.25
		6.75	7.5	9	11.0	13.0	15.0		
df212	LOG	3.96-6	5.82-7	2.90-7	2.58-7	2.83-7	3.79-7	5.01-7	6.31-7
		7.59-7	8.78-7	9.85-7	1.08-6	1.17-6	1.27-6	1.36-6	1.44-6
		1.52-6	1.68-6	1.98-6	2.51-6	2.99-6	3.42-6	3.82-6	4.01-6
		4.41-6	4.83-6	5.23-6	5.60-6	5.80-6	6.01-6	6.37-6	6.74-6
		7.11-6	7.66-6	8.77-6	1.03-5	1.18-5	1.33-5		

c

c

fc222 GAMMA TALLY: 1 METER SIDE ACCIDENT

f222:p 814

fs222 -824 -825 -826 -827 -828 -829 -830 -831 -832

-833 -834 \$ midplane segment number 11

-835 -836 -837 -838 -839 -840 -841 -842 -843 -844 -845 -846 T

de222	LOG	0.01	0.03	0.05	0.07	0.1	0.15	0.2	0.25
		0.3	0.35	0.4	0.45	0.5	0.55	0.6	0.65
		0.7	0.8	1	1.4	1.8	2.2	2.6	2.8
		3.25	3.75	4.25	4.75	5.0	5.25	5.75	6.25
		6.75	7.5	9	11.0	13.0	15.0		
df222	LOG	3.96-6	5.82-7	2.90-7	2.58-7	2.83-7	3.79-7	5.01-7	6.31-7
		7.59-7	8.78-7	9.85-7	1.08-6	1.17-6	1.27-6	1.36-6	1.44-6
		1.52-6	1.68-6	1.98-6	2.51-6	2.99-6	3.42-6	3.82-6	4.01-6
		4.41-6	4.83-6	5.23-6	5.60-6	5.80-6	6.01-6	6.37-6	6.74-6
		7.11-6	7.66-6	8.77-6	1.03-5	1.18-5	1.33-5		

c

c

fc232 GAMMA TALLY: 1 METER END ACCIDENT, BOTTOM, TOP

f232:p 816 815 NT

fs232 -882 -883 -282 -320 -885 -886 -811 T

de232	LOG	0.01	0.03	0.05	0.07	0.1	0.15	0.2	0.25
		0.3	0.35	0.4	0.45	0.5	0.55	0.6	0.65
		0.7	0.8	1	1.4	1.8	2.2	2.6	2.8
		3.25	3.75	4.25	4.75	5.0	5.25	5.75	6.25
		6.75	7.5	9	11.0	13.0	15.0		
df232	LOG	3.96-6	5.82-7	2.90-7	2.58-7	2.83-7	3.79-7	5.01-7	6.31-7
		7.59-7	8.78-7	9.85-7	1.08-6	1.17-6	1.27-6	1.36-6	1.44-6
		1.52-6	1.68-6	1.98-6	2.51-6	2.99-6	3.42-6	3.82-6	4.01-6
		4.41-6	4.83-6	5.23-6	5.60-6	5.80-6	6.01-6	6.37-6	6.74-6
		7.11-6	7.66-6	8.77-6	1.03-5	1.18-5	1.33-5		

c

c

fc242 GAMMA TALLY: TOP RAIL CAR EDGE AS A FUNCTION OF DISTANCE

f242:p 852 853 12 \$ 40', 50', 60' rail car

```

de242  LOG  0.01  0.03  0.05  0.07  0.1  0.15  0.2  0.25
           0.3  0.35  0.4  0.45  0.5  0.55  0.6  0.65
           0.7  0.8  1  1.4  1.8  2.2  2.6  2.8
           3.25 3.75 4.25 4.75 5.0 5.25 5.75 6.25
           6.75 7.5 9 11.0 13.0 15.0
df242  LOG  3.96-6 5.82-7 2.90-7 2.58-7 2.83-7 3.79-7 5.01-7 6.31-7
           7.59-7 8.78-7 9.85-7 1.08-6 1.17-6 1.27-6 1.36-6 1.44-6
           1.52-6 1.68-6 1.98-6 2.51-6 2.99-6 3.42-6 3.82-6 4.01-6
           4.41-6 4.83-6 5.23-6 5.60-6 5.80-6 6.01-6 6.37-6 6.74-6
           7.11-6 7.66-6 8.77-6 1.03-5 1.18-5 1.33-5

```

c

c

fc252 GAMMA TALLY: BOTTOM RAIL CAR EDGE AS A FUNCTION OF DISTANCE

f252:p 851 850 11 \$ 40', 50', 60' rail car

```

de252  LOG  0.01  0.03  0.05  0.07  0.1  0.15  0.2  0.25
           0.3  0.35  0.4  0.45  0.5  0.55  0.6  0.65
           0.7  0.8  1  1.4  1.8  2.2  2.6  2.8
           3.25 3.75 4.25 4.75 5.0 5.25 5.75 6.25
           6.75 7.5 9 11.0 13.0 15.0
df252  LOG  3.96-6 5.82-7 2.90-7 2.58-7 2.83-7 3.79-7 5.01-7 6.31-7
           7.59-7 8.78-7 9.85-7 1.08-6 1.17-6 1.27-6 1.36-6 1.44-6
           1.52-6 1.68-6 1.98-6 2.51-6 2.99-6 3.42-6 3.82-6 4.01-6
           4.41-6 4.83-6 5.23-6 5.60-6 5.80-6 6.01-6 6.37-6 6.74-6
           7.11-6 7.66-6 8.77-6 1.03-5 1.18-5 1.33-5

```

c

c

f24:p 906

fc24 FARTHEST TALLY FOR WWG

c

c control cards

c

c nonu

\$ turn off subcritical fission

mode p n

\$ coupled neutron, gamma mode

nps 2.0E7

\$ cut nps at ~ ? hours

prdump j j 1 2 j

\$ print once, dump every 15 min, MCTAL, keep last 2 dumps

cut:p j 0.01 3j

\$ cut photons < 0.01 MeV bottom ANSI/ANS-6.1.1-1977

cut:n j 2.5E-8 3j

\$ cut neutron < 2.5E-8 MeV bottom ANSI/ANS-6.1.1-1977

phys:p 10 1 1

\$ no bremsstrahlung, no coherent scattering for n, gammas

print

10

\$

Source coefficients and distribution

-20

\$

Weight window information

30

\$

Tally description

-35

\$

Coincident detectors

40

\$

Material composition

50

\$

Cell volumes and masses, surface areas

60

\$

basic

Cell importances

62

\$

basic

Forced collision and exponential transform

-70

\$

Surface coefficients

-72

\$

basic

Cell temperatures

-85

\$

Electron range and straggling tables multigroup: flux values

for biasing adjoint calcs

-86

\$

Electron bremsstrahlung and secondary production

-90

\$

KCODE source data

-98

\$

Physical constants and compile options

100

\$

basic

Cross section tables

-102

\$

Assignment of S(a,b) data to nuclides

-110

\$

First 50 starting histories

120

\$

Analysis of the quality of your importance function

126

\$

basic

Particle activity in each cell

-128

\$

Universe map

-130

\$

Neutron/photon/electron weight balance

```

-140 $      Neutron/photon nuclide activity
-150 $      DXTRAN diagnostics
  160 $ default TFC bin tally analysis
  161 $ default f(x) tally density plot
  162 $ default Cumulative f(x) and tally density plot
-170 $      Source distribution frequency tables, surface source
-175 $ shorten Estimated keff results by cycle
-178 $      Estimated keff results by batch size
-180 $      Weight window generator bookkeeping summary controlled by
WWG(7), not print card
-190 $ basic Weight window generator summary
-198 $      Weight windows from multigroup fluxes
-200 $ basic Weight window generated windows

c
c below is the weight window
c uncomment the following to generate the weight windows
c wwgc 24 2072 0 4J 0

```

5.6.3 MCNP Primary Gamma Input File

```

TN-40 TRAN GAMMA UNIFORM 42GWD/2.35%/24.4Y NORMAL PRODUCTION RUN 10/12/05
c
c      10      20      30      40      50      60      70
c      |      |      |      |      |      |      |
c 345678901234567890123456789012345678901234567890123456789012345678
c
c ** This model changes the DBF per Prairie Island comments **
c ** This model extends TPA decay from 9 years (DB) to 13 years **
c ** This model changes axial profile to assumed Prairie Island shape **
c
c The following general design parameters are applied throughout this model:
c
c 1. Uniform loading (modeled as two zones)
c 2. Homogenized fuel; discrete steel box and basket aluminum
c 3. Trunnions and impact limiters included
c 4. Assumed burnup profile based on PI plant data
c 5. Gamma source from DB Fuel (includes TPAs distributed in 2 groups)
c 6. 10CFR71 acceptance criteria for dose locations
c 7. Approximated periphery basket (including rails and outer SST inserts)
c 8. Fuel enrichment 3.0 wt. % assumed
c 9. Resin boxes modeled as homogenized Al box & resin mix
c 10. Conservative Boral credit modeled as aluminum around fuel tubes
c
c
c =====
c =
c =
c =
c =
c =====
c
c 1      0      -11:+12:+13      $ imp:p=0.0E+00
c
c fuel lattice
c
c center fuel assys
2011 10 -2.45 (-275:+276:-277:+278)      u=11 $ imp:p=1.0E+00      $
boral gap
2021 0      (-295:+296:-297:+298) &

```

	+211 -212 +213 -214	u=11 \$ imp:p=1.0E+00	\$
void around fuel			
2031 6 -7.940	(-211:+212:-213:+214) &		
	+271 -272 +273 -274	u=11 \$ imp:p=1.0E+00	\$
steel liner			
2041 10 -2.702	(-271:+272:-273:+274) &		
	+275 -276 +277 -278	u=11 \$ imp:p=1.0E+00	\$
aluminum sandwich			
2061 0	+295 -296 +297 -298	-205 u=11 \$ imp:p=1.0E+00	\$
void gap			
2051 4 -2.595	+295 -296 +297 -298 +205 -208	u=11 \$ imp:p=1.0E+00	\$
bottom end fitting			
2071 1 -3.949	+295 -296 +297 -298 +208 -250	u=11 \$ imp:p=1.0E+00	\$
fuel			
2081 2 -1.543	+295 -296 +297 -298 +250 -255	u=11 \$ imp:p=1.0E+00	\$
plenum			
2091 3 -1.970	+295 -296 +297 -298 +255 -260	u=11 \$ imp:p=1.0E+00	\$
top end fitting			
2101 0	+295 -296 +297 -298 +260	u=11 \$ imp:p=1.0E+00	\$
void gap			
c			
c periphery fuel assys			
2012 10 -2.45	(-275:+276:-277:+278)	u=12 \$ imp:p=1.0E+00	\$
boral gap			
2022 0	(-295:+296:-297:+298) &		
	+211 -212 +213 -214	u=12 \$ imp:p=1.0E+00	\$
void around fuel			
2032 6 -7.940	(-211:+212:-213:+214) &		
	+271 -272 +273 -274	u=12 \$ imp:p=1.0E+00	\$
steel liner			
2042 10 -2.702	(-271:+272:-273:+274) &		
	+275 -276 +277 -278	u=12 \$ imp:p=1.0E+00	\$
aluminum sandwich			
2062 0	+295 -296 +297 -298	-205 u=12 \$ imp:p=1.0E+00	\$
void gap			
2052 4 -2.595	+295 -296 +297 -298 +205 -208	u=12 \$ imp:p=1.0E+00	\$
bottom end fitting			
2072 1 -3.949	+295 -296 +297 -298 +208 -250	u=12 \$ imp:p=1.0E+00	\$
fuel			
2082 2 -1.543	+295 -296 +297 -298 +250 -255	u=12 \$ imp:p=1.0E+00	\$
plenum			
2092 3 -1.970	+295 -296 +297 -298 +255 -260	u=12 \$ imp:p=1.0E+00	\$
top end fitting			
2102 0	+295 -296 +297 -298 +260	u=12 \$ imp:p=1.0E+00	\$
void gap			
c			
c			
c empty compartment and periphery basket			
2013 10 -2.702	(-275:+276:-277:+278)	u=2 \$ imp:p=1.0E+00	\$
boral gap			
2043 10 -2.702	(-271:+272:-273:+274) &		
	+275 -276 +277 -278	u=2 \$ imp:p=1.0E+00	\$
aluminum sandwich			
2073 0	+271 -272 +273 -274	u=2 \$ imp:p=1.0E+00	\$
empty basket			
241 10 -2.702	+272:-273	u=5 \$ imp:p=1.0E+00	\$
solid aluminum			
245 0	-272 +273	u=5 \$ imp:p=1.0E+00	\$
empty assy			

```

251 10 -2.702      -271:-273      u=6 $ imp:p=1.0E+00      $
basket
255 0      +271      +273      u=6 $ imp:p=1.0E+00      $
empty assy
261 10 -2.702      -271:+274      u=7 $ imp:p=1.0E+00      $
basket
265 0      +271      -274      u=7 $ imp:p=1.0E+00      $
empty assy
271 10 -2.702      +272:+274      u=8 $ imp:p=1.0E+00      $
basket
275 0      -272      -274      u=8 $ imp:p=1.0E+00      $
empty assy
299 0      -292 +291 -294 +293      u=9 $ imp:p=1.0E+00      &
lat=1 fill=-1:8 -5:5 0:0

```

c

c x coords

```

c      -1      0      1      2      3      4      5      6      7      8
c
      9      9      9      9      9      9      9      9      9      9 $ -5
      9      9      9      2      2      2      2      9      9      9 $ -4
      9      7      8      12     12     12     12      7      8      9 $ -3
      9      2     12     11     11     11     11     12      2      9 $ -2
      9      2     12     11     11     11     11     12      2      9 $ -1
      9     12     11     11     11     11     11     11     12      9 $ 0
      9      2     12     11     11     11     11     12      2      9 $ 1
      9      2     12     11     11     11     11     12      2      9 $ 2
      9      6      5     12     12     12     12      6      5      9 $ 3
      9      9      9      2      2      2      2      9      9      9 $ 4
      9      9      9      9      9      9      9      9      9      9 $ 5

```

c

c cavity cells

```

23 0      +201 -261 -2990      fill=9      $ imp:p=1.0E+00
24 6 -7.940 +201 -261 +2990 -299      $ imp:p=1.0E+00 $ outer SST
inserts
2771 10 -2.702 +201 -261 +299 -282 -2991      $ imp:p=1.0E+00
2772 10 -2.702 +201 -261 +299 -282 +2991 -2992      $ imp:p=1.0E+00
2773 10 -2.702 +201 -261 +299 -282 +2992 -2993      $ imp:p=1.0E+00
2774 10 -2.702 +201 -261 +299 -282 +2993 -2994      $ imp:p=1.0E+00
2775 10 -2.702 +201 -261 +299 -282 +2994 -2995      $ imp:p=1.0E+00
2776 10 -2.702 +201 -261 +299 -282 +2995 -2996      $ imp:p=1.0E+00
2778 10 -2.702 +201 -261 +299 -282 +2996      $ imp:p=1.0E+00

```

c

c main shield shell cells

```

301 5 -7.821 (261 -511 -801):&
      (802 801 282 -311):(419 -201 -802) $ imp:p=1.0E+00
302 5 -7.821 (511 -512 -801):&
      (802 801 311 -312):(418 -419 -802) $ imp:p=3.0E+00
303 5 -7.821 (512 -513 -801):&
      (802 801 312 -313):(417 -418 -802) $ imp:p=9.1E+00
304 5 -7.821 (513 -514 -801):&
      (802 801 313 -314):(416 -417 -802) $ imp:p=2.8E+01
305 5 -7.821 (514 -515 -801):&
      (802 801 314 -315):(415 -416 -802) $ imp:p=8.7E+01
306 5 -7.821 (515 -516 -801):&
      (802 -516 315 -316):(414 -415 -802) $ imp:p=2.7E+02
307 5 -7.821 (802 -516 316 -317):(413 -414 -802) $ imp:p=7.8E+02
308 5 -7.821 (802 -516 317 -318):(412 -413 -802) $ imp:p=2.3E+03
309 5 -7.821 (802 -516 318 -319):(411 -412 -802) $ imp:p=6.3E+03
310 5 -7.821 (802 -516 319 -320):(410 -411 -802) $ imp:p=1.7E+04

```

c

```

c top of lid
501 5 -7.821 +516 -517 -521 $ imp:p=1.2E+03
502 5 -7.821 +517 -518 -521 $ imp:p=5.4E+03
503 5 -7.821 +518 -519 -521 $ imp:p=1.8E+04
504 5 -7.821 +519 -520 -521 $ imp:p=4.0E+04
505 10 -2.702 +520 -522 -320 $ imp:p=4.0E+04 $ A1 impact
limiter spacer on top
c
c top impact limiters
601 0 (+622 -750 +320 -651) $ imp:p=1.7E+05
602 0 (+622 -750 +651 -672) $ imp:p=1.4E+06
603 8 -.125 (+750 -752 +320 -651) $ imp:p=2.6E+05
604 8 -.125 (+750 -752 +651 -672) $ imp:p=3.3E+05
605 10 -2.702 (+516 -518 +521 -318) $ imp:p=1.8E+03
606 10 -2.702 (+518 -520 +521 -318):&
      (+516 -520 +318 -320) $ imp:p=1.3E+05
607 9 -.387 (+522 -721 -651):&
      (+752 -522 +320 -651) $ imp:p=1.3E+05
608 9 -.387 (+752 -721 +651 -672):&
      (+721 -722 -672) $ imp:p=1.4E+05
609 9 -.387 +722 -723 -672 $ imp:p=1.7E+05
610 9 -.387 +723 -724 -672 $ imp:p=1.6E+05
611 9 -.387 +724 -725 -672 $ imp:p=1.6E+05
612 9 -.387 +725 -726 -672 $ imp:p=1.7E+05
613 9 -.387 +726 -727 -672 $ imp:p=1.7E+05
614 9 -.387 +727 -728 -672 $ imp:p=1.8E+05
615 9 -.387 +728 -729 -672 $ imp:p=1.9E+05
616 9 -.387 +729 -730 -672 $ imp:p=2.1E+05
617 9 -.387 +730 -731 -672 $ imp:p=2.4E+05
618 9 -.387 +731 -732 -672 $ imp:p=2.7E+05
619 9 -.387 +732 -733 -672 $ imp:p=2.8E+05
620 9 -.387 +733 -734 -672 $ imp:p=3.3E+05
621 9 -.387 +734 -735 -672 $ imp:p=3.8E+05
622 8 -.125 +735 -762 -672 $ imp:p=3.8E+05
623 6 -7.940 +762 -736 -672 $ imp:p=3.8E+05
c
632 0 +622 -750 +651 +672 -810 $ imp:p=2.9E+06
634 8 -.125 +750 -752 +651 +672 -810 $ imp:p=4.2E+05
638 9 -.387 +752 -723 +651 +672 -810 $ imp:p=1.7E+05
640 9 -.387 +723 -725 +672 -810 $ imp:p=3.2E+05
642 9 -.387 +725 -727 +672 -810 $ imp:p=3.1E+05
644 9 -.387 +727 -729 +672 -810 $ imp:p=3.4E+05
646 9 -.387 +729 -731 +672 -810 $ imp:p=3.0E+05
648 9 -.387 +731 -733 +672 -810 $ imp:p=3.0E+05
650 9 -.387 +733 -735 +672 -810 $ imp:p=3.5E+05
652 8 -.125 +735 -762 +672 -810 $ imp:p=5.2E+05
653 6 -7.940 +762 -736 +672 -810 $ imp:p=5.2E+05
c
662 0 +622 -750 +651 +810 -811 $ imp:p=4.5E+06
664 8 -.125 +750 -752 +651 +810 -811 $ imp:p=5.1E+05
668 9 -.387 +752 -723 +651 +810 -811 $ imp:p=2.4E+05
672 9 -.387 +723 -727 +810 -811 $ imp:p=2.5E+05
676 9 -.387 +727 -731 +810 -811 $ imp:p=5.8E+05
680 9 -.387 +731 -735 +810 -811 $ imp:p=7.9E+05
682 8 -.125 +735 -762 +810 -811 $ imp:p=1.2E+06
683 6 -7.940 +762 -736 +810 -811 $ imp:p=1.2E+06
c
c side neutron shield
851 7 -1.690 +602 -621 +650 -651 +861 $ imp:p=4.6E+04
852 7 -1.690 +602 -621 +651 -670 +861 $ imp:p=6.7E+04

```

853	5	-7.821	+621	-622	+320	-671		\$ imp:p=1.4E+05
854	5	-7.821	+601	-602	+320	-671		\$ imp:p=1.2E+05
855	5	-7.821	+601	-622	+671	-672	+861	\$ imp:p=1.0E+05
856	7	-1.690	+602	-621	+320	-650	+861	\$ imp:p=4.6E+04
857	7	-1.690	+602	-621	+670	-671	+861	\$ imp:p=6.7E+04
c								
c bottom impact limiters								
c								
701	8	-.125	(+751	-601	+320	-651	-875):&	
			(+751	-601	+320	-651	876)	\$ imp:p=4.5E+05
702	8	-.125	(+751	-601	+651	-672	-875):&	
			(+751	-601	+651	-672	876)	\$ imp:p=4.3E+05
7031	9	-.387	(+410	-751	+320	-651) &	
			(-875:876:-879)					\$ imp:p=6.0E+04
7032	9	-.387	(+716	-410	-651)			\$ imp:p=6.0E+04
7041	9	-.387	(+716	-751	+651	-672)	&	
			(-875:876:-879)					\$ imp:p=6.6E+04
7042	9	-.387	(+715	-716	-672)			\$ imp:p=6.6E+04
705	9	-.387	+714	-715	-672			\$ imp:p=6.4E+04
706	9	-.387	+713	-714	-672			\$ imp:p=6.6E+04
707	9	-.387	+712	-713	-672			\$ imp:p=6.8E+04
708	9	-.387	+711	-712	-672			\$ imp:p=7.1E+04
709	9	-.387	+710	-711	-672			\$ imp:p=7.3E+04
710	9	-.387	+709	-710	-672			\$ imp:p=7.6E+04
711	9	-.387	+708	-709	-672			\$ imp:p=8.1E+04
712	9	-.387	+707	-708	-672			\$ imp:p=8.1E+04
713	9	-.387	+706	-707	-672			\$ imp:p=8.0E+04
714	9	-.387	+705	-706	-672			\$ imp:p=9.0E+04
715	9	-.387	+704	-705	-672			\$ imp:p=9.8E+04
716	9	-.387	+703	-704	-672			\$ imp:p=1.0E+05
717	9	-.387	+761	-703	-672			\$ imp:p=1.0E+05
718	8	-.125	+702	-761	-672			\$ imp:p=1.2E+05
719	6	-7.940	+701	-702	-672			\$ imp:p=1.2E+05
c								
721	0		+753	-601	+672	-810	&	
			(-875:876:-877:878)					\$ imp:p=2.9E+05
722	8	-.125	+751	-753	+672	-810	&	
			(-875:876:-877:878)					\$ imp:p=2.9E+05
724	9	-.387	+715	-751	+672	-810	&	
			(-875:876:-877:878:-879)					\$ imp:p=3.3E+05
726	9	-.387	+713	-715	+672	-810		\$ imp:p=2.9E+05
728	9	-.387	+711	-713	+672	-810		\$ imp:p=3.7E+05
730	9	-.387	+709	-711	+672	-810		\$ imp:p=3.5E+05
732	9	-.387	+707	-709	+672	-810		\$ imp:p=4.1E+05
734	9	-.387	+705	-707	+672	-810		\$ imp:p=3.7E+05
736	9	-.387	+761	-705	+672	-810		\$ imp:p=3.2E+05
738	8	-.125	+702	-761	+672	-810		\$ imp:p=3.1E+05
739	6	-7.940	+701	-702	+672	-810		\$ imp:p=3.1E+05
c								
741	0		+753	-601	+810	-811		\$ imp:p=2.0E+05
742	8	-.125	+751	-753	+810	-811		\$ imp:p=2.0E+05
744	9	-.387	+715	-751	+810	-811		\$ imp:p=3.6E+05
748	9	-.387	+711	-715	+810	-811		\$ imp:p=4.7E+05
752	9	-.387	+707	-711	+810	-811		\$ imp:p=6.8E+05
756	9	-.387	+761	-707	+810	-811		\$ imp:p=8.7E+05
758	8	-.125	+702	-761	+810	-811		\$ imp:p=1.7E+06
759	6	-7.940	+701	-702	+810	-811		\$ imp:p=1.7E+06
c								
760	0		(864	867	875	-876	320	-878
			(864	-867	875	-876	320	+877
			879	-601):&				\$ imp:p=2.4E+05

```

c
c tally cells
900 0          +601 -622 +672 -899 +861          $ imp:p=6.9E+05
901 0          +601 -622 +899 -810 +861          $ imp:p=1.9E+05
902 0          +601 -622 +810 -811              $ imp:p=8.2E+04
903 11 -1.225E-3 +701 -736 +811 -812          $ imp:p=5.0E+06      $
comment these out for importance optimization
904 11 -1.225E-3 (+701 -736 +812 -814):&
              (+736 -815 -814):(+816 -701 -814) $ imp:p=5.0E+06
905 11 -1.225E-3 (+816 -815 +814 -813):&
              (+815 -817 -813):(+818 -816 -813) $ imp:p=5.0E+06
906 11 -1.225E-3 (+11 -12 -13) (813:+817:-818) &
              (+818:-11:810) (-817:12:810)      $ imp:p=5.0E+06
907 11 -1.225E-3 +851 -818 -810              $ imp:p=5.0E+06      $ far
cells at end of rail car
908 11 -1.225E-3 +850 -851 -810              $ imp:p=5.0E+06
909 11 -1.225E-3 +11 -850 -810              $ imp:p=5.0E+06
910 11 -1.225E-3 +817 -852 -810              $ imp:p=5.0E+06
911 11 -1.225E-3 +852 -853 -810              $ imp:p=5.0E+06
912 11 -1.225E-3 +853 -12 -810              $ imp:p=5.0E+06
c
c upper trunnions
801 5 -7.821 (-867 +320 +870 -861):&
              (+867 +320 -871 -861)          $ imp:p=1.0E+05
802 5 -7.821 (+869 -870 +863 -861):&
              (+871 -872 +863 -861)          $ imp:p=1.0E+05
803 5 -7.821 (+868 -869 +863 -862):&
              (+872 -873 +863 -862)          $ imp:p=1.8E+05
804 7 -1.690 (+868 -870 -863):&
              (+871 -873 -863)              $ imp:p=3.6E+05
805 0        (-869 -810 -861 (+862:-868)):&
              (+872 -810 -861 (+862:+873))    $ imp:p=3.6E+05
c
c lower trunnions
811 5 -7.821 (-867 +320 +870 -864):&
              (+867 +320 -871 -864)          $ imp:p=2.1E+05
812 5 -7.821 (+869 -870 +866 -864):&
              (+871 -872 +866 -864)          $ imp:p=2.1E+05
813 5 -7.821 (+868 -869 +866 -865):&
              (+872 -873 +866 -865)          $ imp:p=1.7E+05
814 0        (+868 -870 -866):&
              (+871 -873 -866)              $ imp:p=2.5E+05
815 0        (+877 -869 +865 -864):&
              (+872 -878 +865 -864)          $ imp:p=1.7E+05
816 0        (+877 -868 -865):&
              (+873 -878 -865)              $ imp:p=2.7E+05

c =====
c =
c = SURFACE CARDS
c =
c =====
c
c model boundaries
c initial model had rail car at 41' 8" long
c rail cars typically are 40 to 60 feet
c PacTec typical transport car (for OCRWM) 49' 6"
c set outer bounds at 60 feet
c assume cask CG is middle of active fuel (within 6 inches of actual)
11 pz -914.4          $ end of rail car

```

12 pz 914.4	\$ end of rail car
13 cz 652.4	\$ 5 meter from (vertical planes) side of rail car
c	
c fuel/basket region	
201 pz -190.70	\$ bottom of lower end fitting (bottom cavity)
205 pz -190.7032	\$ top of lower end fitting (3.08")
208 pz -182.88	\$ bottom of active fuel (144")
211 px -88.7034	\$ steel liner inner (8.05 inch typ. square)
212 px -68.20565	\$ steel liner modeled as 13 ga. 0.09" thick not 0.10"
213 py -10.2494	\$
214 py 10.2494	\$
250 pz 182.88	\$ top of active fuel
255 pz 201.02068	\$ top of plenum (7.142")
260 pz 209.91	\$ top of upper end fitting (3.5")
261 pz 223.32	\$ top of cavity (void)
271 px -88.93175	\$ steel liner outer (8.05 + .2 inch square)
272 px -67.97675	\$
273 py -10.4775	\$
274 py 10.4775	\$
275 px -89.56675	\$ boron gap (8.05 + .7 inch square)
276 px -67.34175	\$
277 py -11.1125	\$
278 py 11.1125	\$
282 cz 91.44	\$ inner radius of cavity (72 inch diameter)
291 px -89.662	\$ basket lattice unit cell (8.05+.775 inch square)
292 px -67.2465	\$ origin (center of assy) @ x=-78.45425 y=0
293 py -11.20775	\$
294 py 11.20775	\$
295 px -88.31326	\$ fuel envelope 7.763 x 7.763 inch
296 px -68.59524	\$
297 py -9.85901	\$
298 py 9.85901	\$
299 cz 90.932	\$ assumes .2" instead of 3/8" outer basket ("rails")
to conserve mass	
2990 cz 90.867	\$ assumes 0.026" for steel inserts on periphery
2991 py -79.4385	\$ rail cutting surfaces
2992 py -55.0545	\$
2993 py -12.192	\$
2994 py 12.192	\$
2995 py 55.0545	\$
2996 py 79.4385	\$
c	
c wall gamma shield	
311 cz 93.853	\$ split primary gamma shield into 10 layers
312 cz 96.266	\$ layer thickness = 2.413 cm or 0.95 inch
313 cz 98.679	\$ also applies to bottom and top (diff. thickness)
314 cz 101.092	\$
315 cz 103.505	\$
316 cz 105.918	\$
317 cz 108.331	\$
318 cz 110.744	\$
319 cz 113.157	\$
320 cz 115.57	\$ outside cask body
c	
c bottom gamma shield	
410 pz -216.73	\$ cask bottom
411 pz -214.127	\$ layer thickness = 2.603 cm or 1.025 inch
412 pz -211.524	\$
413 pz -208.921	\$
414 pz -206.318	\$

415 pz	-203.715	\$
416 pz	-201.112	\$
417 pz	-198.509	\$
418 pz	-195.906	\$
419 pz	-193.303	\$
c		
c top gamma shield		
511 pz	225.987	\$ layer thickness = 2.667 cm or 1.05 inch
512 pz	228.654	\$
513 pz	231.321	\$
514 pz	233.988	\$
515 pz	236.655	\$
516 pz	238.56	\$ top of cask walls
517 pz	241.989	\$
518 pz	244.656	\$
519 pz	247.323	\$
520 pz	249.99	\$
521 cz	105.09	\$ outer radius of top part of lid
522 pz	252.022	\$ assume 0.8" thick to account for tolerances and bolt holes
c		
c neutron shields		
c 601 pz	-186.25	\$ bottom edge of side resin lower housing
601 pz	-185.615	\$ bottom edge of side resin lower housing
c 602 pz	-184.34	\$ top edge of side resin lower housing
602 pz	-183.705	\$ top edge of side resin lower housing
621 pz	203.00	\$ bottom edge of side resin upper housing
622 pz	204.91	\$ top edge of side resin upper housing
650 cz	116.1542	\$ homogenized inner aluminum box
651 cz	121.285	\$ splitting shell for neutron shielding
670 cz	126.4158	\$ homogenized outer aluminum box
671 cz	127.0	\$ outer radius of resin shield on side
672 cz	128.27	\$ outer radius of resin housing on side
c		
c impact limiters		
701 pz	-311.98	
702 pz	-311.345	
703 pz	-299.05	
704 pz	-293.17	
705 pz	-287.29	
706 pz	-281.41	
707 pz	-275.53	
708 pz	-269.65	
709 pz	-263.77	
710 pz	-257.89	
711 pz	-252.01	
712 pz	-246.13	
713 pz	-240.25	
714 pz	-234.37	
715 pz	-228.49	
716 pz	-222.61	
c		
721 pz	255.87	
722 pz	261.75	
723 pz	267.63	
724 pz	273.51	
725 pz	279.39	
726 pz	285.27	
727 pz	291.15	
728 pz	297.03	

```

729 pz 302.91
730 pz 308.79
731 pz 314.67
732 pz 320.55
733 pz 326.43
734 pz 332.31
735 pz 338.255
736 pz 345.24
c
750 pz 220.78          $ bottom of top impact limiter
751 pz -195.14         $ balsa/redwood boundary
752 pz 228.4           $ balsa/redwood boundary
753 pz -187.52         $ balsa/redwood boundary
761 pz -304.995        $ balsa/redwood boundary
762 pz 344.605         $ balsa/redwood boundary
c
c miscellaneous surfaces
801 kz 122.2547369 0.8185941 +1    $ upper splitting mating plane
802 kz -92.06 0.8593425329 -1    $ lower splitting mating plane
899 cz 128.271         $ void cell outside cask
810 cz 152.4           $ vertical planes on side (10' wide rail car)
811 cz 182.88          $ top/bottom @ 12' diameter impact limiters
812 cz 198.12          $ top/bottom @ 13' diameter impact limiters (not used)
813 cz 352.4           $ 2 meter from vertical planes on side
814 cz 215.57          $ 1 meter from cask body (HAC)
815 pz 349.99          $ 1 meter from cask top lid (HAC)
816 pz -316.73         $ 1 meter from cask bottom (HAC)
817 pz 545.24          $ 2 meter from top impact limiter
818 pz -511.98         $ 2 meter from bottom impact limiter
824 pz -190            $ axial tally segments
825 pz -170            $ 20 cm wide
826 pz -150            $ centered on fuel midplane
827 pz -130
828 pz -110
829 pz -90
830 pz -70
831 pz -50
832 pz -30
833 pz -10
834 pz 10
835 pz 30
836 pz 50
837 pz 70
838 pz 90
839 pz 110
840 pz 130
841 pz 150
842 pz 170
843 pz 190
844 pz 210
845 pz 230
846 pz 250
c occupied position surfaces
850 pz -762.0          $ 40 foot rail car
851 pz -609.6          $ 50 foot rail car
852 pz 609.6
853 pz 762.0
882 cz 30              $ radial segmentation
883 cz 55
885 cz 140.57

```

```

886 cz 165.57
887 cz 232.88
888 cz 282.88
861 c/y 0 177.6 15.254 $ top trunnion base radius
862 c/y 0 177.6 14.2875 $ top trunnion
863 c/y 0 177.6 6.35 $ top trunnion resin radius
864 c/y 0 -197.685 12.0624 $ bottom trunnion base (9.498" dia.)
865 c/y 0 -197.685 11.2776 $ bottom trunnion
866 c/y 0 -197.685 5.715 $ bottom trunnion hole radius
867 py 0 $ trunnion ambiguous surface
868 py -136.2202
869 py -128.27
870 py -127
871 py 127
872 py 128.27
873 py 136.2202
c
c lower trunnion "channel" in impact limiter
875 px -12.6974 $ these surfs form a box around lower trunnions
876 px 12.6974 $ 1/4" gap is assumed
877 py -136.8552 $
878 py 136.8552 $
879 pz -210.3824 $

```

```

c =====
c =
c = DATA CARDS
c =
c =====

```

c materials

```

c
c *****
c In-Core Region
c Density = 3.949 g/cm^3; Composition by weight fraction
c 3.0 w/o enrichment
c 410 kg U
c Chemical composition from SCALE Standard Comp. Library
c *****
c
ml 92234 -0.000195 $ U-234
    92235 -0.021902 $ U-235
    92236 -0.000101 $ U-236
    92238 -0.707883 $ U-238
    8016 -0.098148 $ O
    6012 -0.000011 $ C
    14000 -0.000377 $ Si
    15031 -0.000006 $ P
    24000 -0.004200 $ Cr
    22000 -0.000239 $ Ti
    25055 -0.000276 $ Mn
    26000 -0.010400 $ Fe
    28000 -0.008289 $ Ni
    40000 -0.145805 $ Zr
    50000 -0.002152 $ Sn
    72000 -0.000015 $ Hf
c 1001 0.000000 $ H
c
c *****
c Plenum

```

```
c      Density = 1.543 g/cm^3;  Composition by weight fraction
c      Chemical composition from SCALE Standard Comp. Library
c      *****
c
m2      6012      -0.00045      $ C
        14000     -0.00714      $ Si
        15031     -0.00025      $ P
        24000     -0.11569      $ Cr
        22000     -0.00156      $ Ti
        25055     -0.01115      $ Mn
        26000     -0.38641      $ Fe
        28000     -0.09859      $ Ni
        40000     -0.37321      $ Zr
        50000     -0.00551      $ Sn
        72000     -0.00004      $ Hf
c      8016      0.00000      $ O
c      1001      0.00000      $ H
c
c      *****
c      Top Region
c      Density = 1.970 g/cm^3;  Composition by weight fraction
c      Chemical composition from SCALE Standard Comp. Library
c      *****
c
m3      6012      -0.00074      $ C
        14000     -0.01112      $ Si
        15031     -0.00042      $ P
        24000     -0.18702      $ Cr
        22000     -0.00187      $ Ti
        25055     -0.01851      $ Mn
        26000     -0.63795      $ Fe
        28000     -0.14238      $ Ni
c      40000     0.00000      $ Zr
c      50000     0.00000      $ Sn
c      72000     0.00000      $ Hf
c      8016      0.00000      $ O
c      1001      0.00000      $ H
c
c      *****
c      Bottom Region
c      Density = 2.595 g/cm^3;  Composition by weight fraction
c      Chemical composition from SCALE Standard Comp. Library
c      *****
c
m4      6012      -0.00080      $ C
        14000     -0.01000      $ Si
        15031     -0.00045      $ P
        24000     -0.19000      $ Cr
c      22000     0.00000      $ Ti
        25055     -0.02000      $ Mn
        26000     -0.68375      $ Fe
        28000     -0.09500      $ Ni
c      40000     0.00000      $ Zr
c      50000     0.00000      $ Sn
c      72000     0.00000      $ Hf
c      8016      0.00000      $ O
c      1001      0.00000      $ H
c
c      *****
c      Carbon Steel
```

```

c      Density = 7.8212 g/cm^3 SCALE Standard Comp. Library
c      *****
c
c
m5      6012      -0.0100      $ C
        26000     -0.9900      $ Fe
c
c      *****
c      Stainless Steel 304
c      Density = 7.94 g/cm^3 SCALE Standard Comp. Library
c      *****
c
c
m6      26000     -0.68375     $ Fe
        24000     -0.19000     $ Cr
        28000     -0.09500     $ Ni
        25055     -0.02000     $ Mn
        14000     -0.01000     $ Si
        6012      -0.00080     $ C
        15031     -0.00045     $ P
c
c      *****
c      Homogenized Neutron Resin/Aluminum Shield
c      Reference: Page 6, TN Calc. 1042-08, Rev. 0
c      Based on TN-24 Resin
c      Density = 1.69 g/cm^3
c      B-10 and B-11 based on natural abundance
c      Note Al is in resin and the aluminum boxes
c      *****
c
c
m7      1001      -0.0426      $ H-1
        5010      -0.0018      $ B-10
        5011      -0.0071      $ B-11
        6000      -0.2953      $ C
        8016      -0.3503      $ O
        13027     -0.2851      $ Al
        30000     -0.0178      $ Zn
c
c      *****
c      Balsa Wood
c      TN-68 SAR
c      Density = 0.125 g/cm^3
c      *****
c
c
m8      6012      0.2857      $ C
        8016      0.2381      $ O
        1001      0.4762      $ H
c
c      *****
c      Redwood
c      Assume same composition as Balsa
c      TN-68 SAR
c      Density = 0.387 g/cm^3
c      *****
c
c
m9      6012      0.2857      $ C
        8016      0.2381      $ O
        1001      0.4762      $ H
c
c      *****
c      Pure Aluminum
c      Density = 2.702 g/cm^3 SCALE Standard Comp. Library

```

```

c *****
c
m10 13027 -1.0 $ Al
c
c *****
c AIR: ANSI/ANS-6.6.1 Dry air
c Density = 0.001225 g/cm^3
c Composition by weight fraction
c *****
c
m11 6012 -0.00014 $ C
    7014 -0.75519 $ N
    8016 -0.23179 $ O
    18000 -0.01288 $ Ar
c
c *****
c BORAL: TN40 STORAGE CRITICALITY SPECIFICATION
c Density = 2.45 g/cm^3 (770 lbs of boral, about 95.8% theo.)
c Composition by weight fraction
c Based on Calculation 1042-6 (TN40 Storage Crit)
c 0.01 gm/cm^2 B-10 areal density
c core thickness of 0.025"
c panel thickness of 0.075"
c redistribution of wt. frac. to simulate 75% B4C
c *****
c actual wt. frac
m12 6012 -0.066 $ 0.088
    13027 -0.695 $ 0.594
    5010 -0.044 $ 0.058
    5011 -0.195 $ 0.060
c
c source
c
sdef cel=d1 x=d2 y=d3 z=fcel=d4 erg=fcel=d5
c
c sample cells according to strength
c there are 22 inner and 18 outer
# sil spl
c
    39GWD 39GWD
    1 d $ 17.5yr 16 year
    23:299:2051 1.83E+13 $ 3.99E+13 4.86E+13 inner assys lower end fitting
    23:299:2071 3.92E+16 $ 4.49E+16 4.72E+16 inner assys fuel
    23:299:2081 6.16E+13 $ 8.94E+13 1.27E+14 inner assys plenum
    23:299:2091 3.65E+13 $ 4.92E+13 7.22E+13 inner assys upper end fitting
    23:299:2052 1.50E+13 $ 3.27E+13 3.98E+13 outer assys lower end fitting
    23:299:2072 3.21E+16 $ 3.67E+16 3.86E+16 outer assys fuel
    23:299:2082 5.04E+13 $ 7.31E+13 1.04E+14 outer assys plenum
    23:299:2092 2.99E+13 $ 4.03E+13 5.90E+13 outer assys upper end fitting
c
c sample source/fuel cell
c sample volume uniformly
c use lattice element (0,0)
c
c X DIMENSIONS Y DIMENSIONS
# si2 sp2 si3 sp3
    -88.31326 0 -9.85901 0
    -68.59524 1 9.85901 1
c
c zone dependent axial distirubtions
c burnup is taken from Prairie site specific calculation

```

c cask center

c

ds4 s 41 44 42 43 \$ 41-43 are end fittings/plenum
41 45 42 43 \$ 44 and 45 are fuel zones

c

	lower end fit		plenum		upper end fit	
#	si41	sp41	si42	sp42	si43	sp43
	-190.7032	0	182.88	0	201.02068	0
	-182.88	1	201.02068	1	223.32	1

c

	INNER ASSYS		OUTER ASSYS	
#	si44	sp44	si45	sp45
	-182.88	0	-182.88	0
	-152.40	0.0556	-152.40	0.0556
	-121.92	0.0818	-121.92	0.0818
	-91.44	0.0889	-91.44	0.0889
	-60.96	0.0921	-60.96	0.0921
	-30.48	0.0921	-30.48	0.0921
	0.00	0.0921	0.00	0.0921
	30.48	0.0920	30.48	0.0920
	60.96	0.0913	60.96	0.0913
	91.44	0.0909	91.44	0.0909
	121.92	0.0889	121.92	0.0889
	152.40	0.0786	152.40	0.0786
	182.88	0.0556	182.88	0.0556

c

c zone dependent energy distributions

c

ds5 s 51 52 53 54 \$ each cell has independent energy distribution
55 56 57 58 \$

c

c INNER ASSYS GAMMA SPECTRA

c

	lower end		fuel		plenum		upper end	
#	si51	sp51	si52	sp52	si53	sp53	si54	sp54
	0.01	0.00E+00	0.01	0.00E+00	0.01	0.00E+00	0.01	0.00E+00
	0.05	1.15E+10	0.05	4.82E+14	0.05	1.58E+10	0.05	7.03E+09
	0.1	2.19E+09	0.1	1.41E+14	0.1	2.81E+09	0.1	1.29E+09
	0.2	5.27E+08	0.2	8.83E+13	0.2	7.15E+08	0.2	3.11E+08
	0.3	2.62E+07	0.3	2.70E+13	0.3	3.61E+07	0.3	1.55E+07
	0.4	3.43E+07	0.4	1.81E+13	0.4	5.27E+07	0.4	2.02E+07
	0.6	2.17E+06	0.6	1.47E+13	0.6	1.94E+08	0.6	1.28E+06
	0.8	7.54E+05	0.8	9.70E+14	0.8	8.56E+08	0.8	2.83E+08
	1	2.84E+07	1	8.23E+12	1	7.65E+08	1	2.89E+08
	1.33	6.38E+11	1.33	2.75E+13	1.33	2.17E+12	1.33	1.29E+12
	1.66	1.80E+11	1.66	5.38E+12	1.66	6.11E+11	1.66	3.63E+11
	2	1.64E-06	2	4.63E+10	2	1.47E+01	2	1.10E-03
	2.5	4.27E+06	2.5	2.48E+09	2.5	5.48E+06	2.5	2.51E+06
	3	6.63E+03	3	1.73E+08	3	8.50E+03	3	3.90E+03
	4	6.28E-15	4	2.68E+07	4	1.52E-11	4	5.62E-12
	5	0.00E+00	5	9.04E+06	5	0.00E+00	5	0.00E+00
	6.5	0.00E+00	6.5	3.63E+06	6.5	0.00E+00	6.5	0.00E+00
	8	0.00E+00	8	7.12E+05	8	0.00E+00	8	0.00E+00
	10	0.00E+00	10	1.51E+05	10	0.00E+00	10	0.00E+00

c

c OUTER ASSYS GAMMA SPECTRA

c

	lower end		fuel		plenum		upper end	
#	si55	sp55	si56	sp56	si57	sp57	si58	sp58
	0.01	0.00E+00	0.01	0.00E+00	0.01	0.00E+00	0.01	0.00E+00

```

0.05 1.15E+10 0.05 4.82E+14 0.05 1.58E+10 0.05 7.03E+09
0.1 2.19E+09 0.1 1.41E+14 0.1 2.81E+09 0.1 1.29E+09
0.2 5.27E+08 0.2 8.83E+13 0.2 7.15E+08 0.2 3.11E+08
0.3 2.62E+07 0.3 2.70E+13 0.3 3.61E+07 0.3 1.55E+07
0.4 3.43E+07 0.4 1.81E+13 0.4 5.27E+07 0.4 2.02E+07
0.6 2.17E+06 0.6 1.47E+13 0.6 1.94E+08 0.6 1.28E+06
0.8 7.54E+05 0.8 9.70E+14 0.8 8.56E+08 0.8 2.83E+08
1 2.84E+07 1 8.23E+12 1 7.65E+08 1 2.89E+08
1.33 6.38E+11 1.33 2.75E+13 1.33 2.17E+12 1.33 1.29E+12
1.66 1.80E+11 1.66 5.38E+12 1.66 6.11E+11 1.66 3.63E+11
2 1.64E-06 2 4.63E+10 2 1.47E+01 2 1.10E-03
2.5 4.27E+06 2.5 2.48E+09 2.5 5.48E+06 2.5 2.51E+06
3 6.63E+03 3 1.73E+08 3 8.50E+03 3 3.90E+03
4 6.28E-15 4 2.68E+07 4 1.52E-11 4 5.62E-12
5 0.00E+00 5 9.04E+06 5 0.00E+00 5 0.00E+00
6.5 0.00E+00 6.5 3.63E+06 6.5 0.00E+00 6.5 0.00E+00
8 0.00E+00 8 7.12E+05 8 0.00E+00 8 0.00E+00
10 0.00E+00 10 1.51E+05 10 0.00E+00 10 0.00E+00

c
c surface tallies
c
c
fc12 GAMMA TALLY ON TRUNNION SURFACE
f12:p 868 873
fs12 -862 NT
sd12 641 1E-10 641 1E-10
de12 LOG 0.01 0.03 0.05 0.07 0.1 0.15 0.2 0.25
      0.3 0.35 0.4 0.45 0.5 0.55 0.6 0.65
      0.7 0.8 1 1.4 1.8 2.2 2.6 2.8
      3.25 3.75 4.25 4.75 5.0 5.25 5.75 6.25
      6.75 7.5 9 11.0 13.0 15.0
df12 LOG 3.96-6 5.82-7 2.90-7 2.58-7 2.83-7 3.79-7 5.01-7 6.31-7
      7.59-7 8.78-7 9.85-7 1.08-6 1.17-6 1.27-6 1.36-6 1.44-6
      1.52-6 1.68-6 1.98-6 2.51-6 2.99-6 3.42-6 3.82-6 4.01-6
      4.41-6 4.83-6 5.23-6 5.60-6 5.80-6 6.01-6 6.37-6 6.74-6
      7.11-6 7.66-6 8.77-6 1.03-5 1.18-5 1.33-5

c
c
fc14 GAMMA VOLUME TALLIES AROUND THE TRUNNION
f14:p 601 602 632 662 805
sd14 4j 2.4E4
de14 LOG 0.01 0.03 0.05 0.07 0.1 0.15 0.2 0.25
      0.3 0.35 0.4 0.45 0.5 0.55 0.6 0.65
      0.7 0.8 1 1.4 1.8 2.2 2.6 2.8
      3.25 3.75 4.25 4.75 5.0 5.25 5.75 6.25
      6.75 7.5 9 11.0 13.0 15.0
df14 LOG 3.96-6 5.82-7 2.90-7 2.58-7 2.83-7 3.79-7 5.01-7 6.31-7
      7.59-7 8.78-7 9.85-7 1.08-6 1.17-6 1.27-6 1.36-6 1.44-6
      1.52-6 1.68-6 1.98-6 2.51-6 2.99-6 3.42-6 3.82-6 4.01-6
      4.41-6 4.83-6 5.23-6 5.60-6 5.80-6 6.01-6 6.37-6 6.74-6
      7.11-6 7.66-6 8.77-6 1.03-5 1.18-5 1.33-5

c
c
fc202 GAMMA TALLY: SIDE, TOP/BOTTOM D=12', TOP/BOTTOM D=13.5', 5M
f202:p 672 810 811 812 813 13 NT
fs202 -824 -825 -826 -827 -828 -829 -830 -831 -832
      -833 -834 $ midplane segment number 11
      -835 -836 -837 -838 -839 -840 -841 -842 -843 -844 -845 -846 T
sd202 94215 16119 17R 15883 14983 16123 16199 72664 520209 125J
de202 LOG 0.01 0.03 0.05 0.07 0.1 0.15 0.2 0.25

```

		0.3	0.35	0.4	0.45	0.5	0.55	0.6	0.65
		0.7	0.8	1	1.4	1.8	2.2	2.6	2.8
		3.25	3.75	4.25	4.75	5.0	5.25	5.75	6.25
		6.75	7.5	9	11.0	13.0	15.0		
df202	LOG	3.96-6	5.82-7	2.90-7	2.58-7	2.83-7	3.79-7	5.01-7	6.31-7
		7.59-7	8.78-7	9.85-7	1.08-6	1.17-6	1.27-6	1.36-6	1.44-6
		1.52-6	1.68-6	1.98-6	2.51-6	2.99-6	3.42-6	3.82-6	4.01-6
		4.41-6	4.83-6	5.23-6	5.60-6	5.80-6	6.01-6	6.37-6	6.74-6
		7.11-6	7.66-6	8.77-6	1.03-5	1.18-5	1.33-5		

c

c

fc212 GAMMA TALLY: CONTACT AND 2 METERS FROM IMPACT LIMITERS

f212:p 818 701 736 817 NT

fs212 -882 -883 -282 -320 -885 -886 -811 T

de212	LOG	0.01	0.03	0.05	0.07	0.1	0.15	0.2	0.25
		0.3	0.35	0.4	0.45	0.5	0.55	0.6	0.65
		0.7	0.8	1	1.4	1.8	2.2	2.6	2.8
		3.25	3.75	4.25	4.75	5.0	5.25	5.75	6.25
		6.75	7.5	9	11.0	13.0	15.0		
df212	LOG	3.96-6	5.82-7	2.90-7	2.58-7	2.83-7	3.79-7	5.01-7	6.31-7
		7.59-7	8.78-7	9.85-7	1.08-6	1.17-6	1.27-6	1.36-6	1.44-6
		1.52-6	1.68-6	1.98-6	2.51-6	2.99-6	3.42-6	3.82-6	4.01-6
		4.41-6	4.83-6	5.23-6	5.60-6	5.80-6	6.01-6	6.37-6	6.74-6
		7.11-6	7.66-6	8.77-6	1.03-5	1.18-5	1.33-5		

c

c

fc222 GAMMA TALLY: 1 METER SIDE ACCIDENT

f222:p 814

fs222 -824 -825 -826 -827 -828 -829 -830 -831 -832

-833 -834 \$ midplane segment number 11

-835 -836 -837 -838 -839 -840 -841 -842 -843 -844 -845 -846 T

de222	LOG	0.01	0.03	0.05	0.07	0.1	0.15	0.2	0.25
		0.3	0.35	0.4	0.45	0.5	0.55	0.6	0.65
		0.7	0.8	1	1.4	1.8	2.2	2.6	2.8
		3.25	3.75	4.25	4.75	5.0	5.25	5.75	6.25
		6.75	7.5	9	11.0	13.0	15.0		
df222	LOG	3.96-6	5.82-7	2.90-7	2.58-7	2.83-7	3.79-7	5.01-7	6.31-7
		7.59-7	8.78-7	9.85-7	1.08-6	1.17-6	1.27-6	1.36-6	1.44-6
		1.52-6	1.68-6	1.98-6	2.51-6	2.99-6	3.42-6	3.82-6	4.01-6
		4.41-6	4.83-6	5.23-6	5.60-6	5.80-6	6.01-6	6.37-6	6.74-6
		7.11-6	7.66-6	8.77-6	1.03-5	1.18-5	1.33-5		

c

c

fc232 GAMMA TALLY: 1 METER END ACCIDENT, BOTTOM, TOP

f232:p 816 815 NT

fs232 -882 -883 -282 -320 -885 -886 -811 T

de232	LOG	0.01	0.03	0.05	0.07	0.1	0.15	0.2	0.25
		0.3	0.35	0.4	0.45	0.5	0.55	0.6	0.65
		0.7	0.8	1	1.4	1.8	2.2	2.6	2.8
		3.25	3.75	4.25	4.75	5.0	5.25	5.75	6.25
		6.75	7.5	9	11.0	13.0	15.0		
df232	LOG	3.96-6	5.82-7	2.90-7	2.58-7	2.83-7	3.79-7	5.01-7	6.31-7
		7.59-7	8.78-7	9.85-7	1.08-6	1.17-6	1.27-6	1.36-6	1.44-6
		1.52-6	1.68-6	1.98-6	2.51-6	2.99-6	3.42-6	3.82-6	4.01-6
		4.41-6	4.83-6	5.23-6	5.60-6	5.80-6	6.01-6	6.37-6	6.74-6
		7.11-6	7.66-6	8.77-6	1.03-5	1.18-5	1.33-5		

c

c

fc242 GAMMA TALLY: TOP RAIL CAR EDGE AS A FUNCTION OF DISTANCE

f242:p 852 853 12 \$ 40', 50', 60' rail car

```

de242  LOG  0.01  0.03  0.05  0.07  0.1  0.15  0.2  0.25
           0.3  0.35  0.4  0.45  0.5  0.55  0.6  0.65
           0.7  0.8  1  1.4  1.8  2.2  2.6  2.8
           3.25  3.75  4.25  4.75  5.0  5.25  5.75  6.25
           6.75  7.5  9  11.0  13.0  15.0
df242  LOG  3.96-6  5.82-7  2.90-7  2.58-7  2.83-7  3.79-7  5.01-7  6.31-7
           7.59-7  8.78-7  9.85-7  1.08-6  1.17-6  1.27-6  1.36-6  1.44-6
           1.52-6  1.68-6  1.98-6  2.51-6  2.99-6  3.42-6  3.82-6  4.01-6
           4.41-6  4.83-6  5.23-6  5.60-6  5.80-6  6.01-6  6.37-6  6.74-6
           7.11-6  7.66-6  8.77-6  1.03-5  1.18-5  1.33-5

```

c

c

fc252 GAMMA TALLY: BOTTOM RAIL CAR EDGE AS A FUNCTION OF DISTANCE

f252:p 851 850 11 \$ 40', 50', 60' rail car

```

de252  LOG  0.01  0.03  0.05  0.07  0.1  0.15  0.2  0.25
           0.3  0.35  0.4  0.45  0.5  0.55  0.6  0.65
           0.7  0.8  1  1.4  1.8  2.2  2.6  2.8
           3.25  3.75  4.25  4.75  5.0  5.25  5.75  6.25
           6.75  7.5  9  11.0  13.0  15.0
df252  LOG  3.96-6  5.82-7  2.90-7  2.58-7  2.83-7  3.79-7  5.01-7  6.31-7
           7.59-7  8.78-7  9.85-7  1.08-6  1.17-6  1.27-6  1.36-6  1.44-6
           1.52-6  1.68-6  1.98-6  2.51-6  2.99-6  3.42-6  3.82-6  4.01-6
           4.41-6  4.83-6  5.23-6  5.60-6  5.80-6  6.01-6  6.37-6  6.74-6
           7.11-6  7.66-6  8.77-6  1.03-5  1.18-5  1.33-5

```

c

c

f24:p 906

fc24 FARTHEST TALLY FOR WWG

c

c control cards

```

mode p          $ gamma mode
nps  1.5E9      $ cut nps at ~ 8 hours
prtmp j j 1 2 j $ pring end, dump every 15 min, MCTAL, keep last 2 dumps
cut:p j 0.01 3j $ cut photons < 0.01 MeV bottom ANSI/ANS-6.1.1-1977
print 10 $      Source coefficients and distribution
      20 $      Weight window information
      30 $      Tally description
     -35 $      Coincident detectors
      40 $      Material composition
      50 $      Cell volumes and masses, surface areas
     -60 $ basic Cell importances
      62 $ basic Forced collision and exponential transform
     -70 $      Surface coefficients
     -72 $ basic Cell temperatures
     -85 $      Electron range and straggling tables multigroup: flux values
for biasing adjoint calcs
     -86 $      Electron bremsstrahlung and secondary production
     -90 $      KCODE source data
     -98 $      Physical constants and compile options
    100 $ basic Cross section tables
    -102 $      Assignment of S(a,b) data to nuclides
    -110 $      First 50 starting histories
    120 $      Analysis of the quality of your importance function
    126 $ basic Particle activity in each cell
    -128 $      Universe map
    -130 $      Neutron/photon/electron weight balance
    -140 $      Neutron/photon nuclide activity
    -150 $      DXTRAN diagnostics
    160 $ default TFC bin tally analysis
    161 $ default f(x) tally density plot

```

```

162 $ default Cumulative f(x) and tally density plot
-170 $ Source distribution frequency tables, surface source
-175 $ shorten Estimated keff results by cycle
-178 $ Estimated keff results by batch size
-180 $ Weight window generator bookkeeping summary controlled by
WWG(7), not print card
-190 $ basic Weight window generator summary
-198 $ Weight windows from multigroup fluxes
-200 $ basic Weight window generated windows

c
c below is the weight window
c uncomment the following to generate the weight windows
c ww g 24 2072 0 4J 0
c ww g: p 8.00E-01 1.00E+00 1.50E+00 2.50E+00 $ generate WW for few key energies
w w p: p 5 3 5 0 0 0
w w e: p 8.0000E-01 1.0000E+00 1.5000E+00 2.5000E+00
w w n1: p -1.0000E+00 4.7924E+02 5.3779E+02 5.5192E+02 5.0853E+02
0.0000E+00 1.3095E+02 5.0106E+03 3.1242E+02 2.4707E+02
8.3549E+01 1.8219E+01 2.0308E+01 2.0873E+01 1.9308E+01
0.0000E+00 3.9571E+01 1.8266E+02 4.6364E+01 4.5550E+01
1.9954E+01 6.3705E+00 6.3062E+00 5.8077E+00 7.9413E+00
7.1619E+00 7.9466E+00 7.2564E+00 7.6111E+00 6.7117E+00
7.8450E+00 7.0578E+00 4.6968E+00 0.0000E+00 4.9156E+00
4.2571E+00 5.1346E+00 5.3390E+00 4.2994E+00 5.0028E+00
5.2506E+00 4.4225E+00 4.8702E+00 1.4938E+00 4.5296E-01
1.3429E-01 3.8862E-02 1.1053E-02 3.0498E-03 8.7198E-04
2.4883E-04 7.1395E-05 1.1514E-02 2.5644E-03 6.7592E-04
1.7137E-04 4.5318E-05 5.1783E-06 4.5035E-06 5.6127E-06
5.1557E-06 4.1718E-05 2.1959E-05 2.1323E-05 1.8147E-05
2.9077E-05 2.7676E-05 2.6245E-05 2.4810E-05 2.3277E-05
2.1535E-05 1.9821E-05 1.8027E-05 1.6234E-05 1.4448E-05
1.2829E-05 1.1307E-05 9.8993E-06 8.7074E-06 8.0667E-06
3.8559E-06 4.3843E-06 5.8738E-06 1.1034E-05 1.2165E-05
1.2850E-05 1.2904E-05 1.2225E-05 1.0658E-05 8.8027E-06
8.1865E-06 3.5002E-06 3.6376E-06 4.3142E-06 5.5804E-06 $ go 20
lines down
6.1267E-06 6.4124E-06 6.8110E-06 7.4812E-06 2.5103E-05 $ index 100
(cell 851)
1.5414E-05 2.3034E-05 3.0355E-05 8.8634E-06 $ first cell
852
2.5103E-05 1.5414E-05
7.1215E-06
5.6559E-06 8.9884E-06 3.4899E-05 7.6275E-06 3.0673E-05
2.8070E-05 2.6039E-05 2.4335E-05 2.2723E-05 2.1213E-05
1.9606E-05 1.7988E-05 1.6350E-05 1.4718E-05 1.3132E-05
1.1621E-05 1.0226E-05 8.9371E-06 7.8589E-06 7.2944E-06
4.0325E-06 4.3934E-06 6.1579E-06 1.1024E-05 1.2454E-05
1.3056E-05 1.3197E-05 1.2509E-05 1.0693E-05 8.4180E-06
7.7788E-06 3.3673E-06 3.5672E-06 4.3165E-06 5.6553E-06
6.3306E-06 6.5654E-06 6.8204E-06 7.5660E-06 1.3241E-05
3.4861E-06 3.4627E-06 3.3930E-06 3.3872E-06 3.3793E-06
3.3755E-06 3.3494E-06 4.6824E-06 7.8162E-06 2.6969E-05
5.3477E-06 7.6486E-06 2.5721E-05 2.5658E-04 1.8583E-05
1.4697E-05 1.1209E-05 4.2679E-06 7.4331E-05 2.4992E-05
2.0928E-05 1.4992E-04 1.1982E-05 9.0481E-06
w w n2: p -1.0000E+00 2.6416E+01 3.8797E+01 3.7877E+01 3.1018E+01
0.0000E+00 1.2621E+01 3.6118E+02 2.1168E+01 9.9732E+00
2.5670E+00 2.0627E+00 2.7281E+00 2.7907E+00 2.3884E+00
0.0000E+00 3.5325E+00 1.5020E+01 3.5559E+00 1.6348E+00
7.1000E-01 7.1775E-01 7.0300E-01 5.8619E-01 8.6405E-01

```

7.0085E-01	9.2517E-01	7.1738E-01	7.6031E-01	6.0840E-01
7.7271E-01	5.9664E-01	5.0045E-01	0.0000E+00	4.7201E-01
4.4404E-01	4.4563E-01	4.4498E-01	4.4820E-01	5.0074E-01
5.0072E-01	4.3173E-01	4.5728E-01	1.2745E-01	3.8197E-02
1.1817E-02	3.8262E-03	1.2746E-03	4.0751E-04	1.4571E-04
5.4138E-05	2.1296E-05	1.6465E-03	4.0549E-04	1.3140E-04
4.5056E-05	1.7332E-05	4.1175E-06	3.9497E-06	4.4253E-06
4.2298E-06	1.7141E-05	1.0075E-05	1.1089E-05	9.9781E-06
1.1887E-05	1.0936E-05	1.0015E-05	9.2021E-06	8.4453E-06
7.7606E-06	7.1606E-06	6.6202E-06	6.1256E-06	5.7118E-06
5.3139E-06	4.9852E-06	4.7158E-06	4.5076E-06	4.4078E-06
3.8325E-06	3.9727E-06	4.3122E-06	4.8212E-06	4.8904E-06
4.8052E-06	4.5252E-06	4.1552E-06	3.7382E-06	3.3452E-06
3.2759E-06	3.7920E-06	3.7454E-06	3.7475E-06	3.5633E-06
3.5230E-06	3.4854E-06	3.1516E-06	3.1170E-06	1.0246E-05
6.6142E-06	9.7516E-06	1.1673E-05	4.5474E-06	
1.0246E-05	6.6142E-06			
				4.7554E-06
4.3276E-06	5.1422E-06	1.4238E-05	4.7855E-06	1.2774E-05
1.1622E-05	1.0557E-05	9.5956E-06	8.7578E-06	7.9689E-06
7.2828E-06	6.6793E-06	6.1455E-06	5.6668E-06	5.2609E-06
4.8909E-06	4.5505E-06	4.2734E-06	4.0542E-06	3.9728E-06
3.8031E-06	3.9959E-06	4.3156E-06	4.4527E-06	4.6597E-06
4.7678E-06	4.4195E-06	4.1549E-06	3.6316E-06	3.0454E-06
2.9702E-06	3.5527E-06	3.6378E-06	3.7397E-06	3.5493E-06
3.6009E-06	3.5652E-06	3.2133E-06	3.1647E-06	7.0835E-06
3.6583E-06	3.6610E-06	3.6630E-06	3.6694E-06	3.6775E-06
3.6769E-06	3.6611E-06	5.8741E-06	1.0121E-05	3.8117E-05
6.7098E-06	9.6910E-06	3.5156E-05	7.0642E-05	1.0956E-05
8.9196E-06	1.6047E-05	4.1713E-06	4.4477E-05	2.5318E-05
6.8572E-06	3.9162E-06	5.6294E-06	4.4523E-06	
wnn3:p -1.0000E+00	3.7412E+00	4.4051E+00	4.5375E+00	4.1216E+00
0.0000E+00	1.9031E+00	3.8071E+01	3.9090E+00	1.5734E+00
5.7994E-01	3.7082E-01	4.4512E-01	4.5354E-01	4.0996E-01
0.0000E+00	7.1811E-01	2.1849E+00	7.1860E-01	4.1150E-01
2.0096E-01	1.2953E-01	1.2678E-01	1.1017E-01	1.4740E-01
1.2322E-01	1.4709E-01	1.2445E-01	1.5023E-01	1.2623E-01
1.4799E-01	1.2372E-01	8.9336E-02	0.0000E+00	8.9329E-02
8.1925E-02	9.0412E-02	8.8926E-02	8.5167E-02	8.7213E-02
8.8982E-02	8.2431E-02	1.0734E-01	3.1554E-02	1.0512E-02
3.7185E-03	1.3736E-03	5.2603E-04	1.9555E-04	8.1317E-05
3.5173E-05	1.6101E-05	6.8938E-04	1.9817E-04	7.6316E-05
3.1109E-05	1.3693E-05	3.9609E-06	3.9028E-06	4.2673E-06
4.1051E-06	1.3515E-05	8.5848E-06	9.4557E-06	8.6183E-06
9.9399E-06	9.3299E-06	8.7134E-06	8.1674E-06	7.6481E-06
7.1464E-06	6.7080E-06	6.3102E-06	5.9766E-06	5.6563E-06
5.4267E-06	5.2062E-06	5.0347E-06	4.9479E-06	4.9588E-06
3.8518E-06	3.9072E-06	4.1569E-06	4.3849E-06	4.3098E-06
4.2963E-06	4.0815E-06	3.7999E-06	3.4336E-06	3.1335E-06
3.0967E-06	3.8454E-06	3.7717E-06	3.7471E-06	3.4974E-06
3.3627E-06	3.2514E-06	2.9471E-06	2.9861E-06	8.4317E-06
5.9163E-06	9.2380E-06	1.0535E-05	4.4103E-06	
8.4317E-06	5.9163E-06			
				4.4073E-06
4.1476E-06	4.6954E-06	1.1214E-05	4.4535E-06	1.0293E-05
9.5178E-06	8.7972E-06	8.1605E-06	7.5961E-06	7.0904E-06
6.6341E-06	6.1913E-06	5.8101E-06	5.4882E-06	5.1925E-06
4.9219E-06	4.7084E-06	4.5250E-06	4.3982E-06	4.3778E-06
3.8378E-06	3.9422E-06	4.1544E-06	4.1276E-06	4.3770E-06
4.4493E-06	4.2162E-06	3.8786E-06	3.3747E-06	2.8683E-06

	2.8162E-06	3.6744E-06	3.7568E-06	3.7754E-06	3.5147E-06
	3.3655E-06	3.3647E-06	2.9433E-06	2.9010E-06	5.4682E-06
	3.7632E-06	3.7647E-06	3.7666E-06	3.7680E-06	3.8004E-06
	3.8010E-06	3.7612E-06	6.5034E-06	1.0981E-05	4.0803E-05
	7.8400E-06	1.1113E-05	4.3453E-05	7.0180E-05	1.0642E-05
	7.8058E-06	6.5446E-06	4.1026E-06	3.1959E-05	1.4227E-05
	8.9483E-06	0.0000E+00	4.7515E-06	4.3386E-06	
wnn4:p	-1.0000E+00	1.1128E+00	1.2719E+00	1.3126E+00	1.2030E+00
	0.0000E+00	4.6928E-01	7.6998E+00	7.1310E-01	3.4324E-01
	1.2987E-01	1.0612E-01	1.2452E-01	1.2690E-01	1.1606E-01
	0.0000E+00	1.8632E-01	5.0000E-01	1.6127E-01	9.7304E-02
	5.0868E-02	3.7377E-02	3.6663E-02	3.2286E-02	4.3562E-02
	3.7005E-02	4.3381E-02	3.7706E-02	4.2230E-02	3.6518E-02
	4.2808E-02	3.7119E-02	2.6831E-02	0.0000E+00	2.6548E-02
	2.3994E-02	2.6521E-02	2.7063E-02	2.5741E-02	2.6688E-02
	2.6943E-02	2.3856E-02	3.0825E-02	9.9530E-03	3.6923E-03
	1.4656E-03	6.0753E-04	2.6090E-04	1.1172E-04	5.1763E-05
	2.4938E-05	1.2726E-05	3.0081E-04	1.0147E-04	4.6041E-05
	2.2013E-05	1.1000E-05	3.8639E-06	3.8445E-06	4.0534E-06
	3.9424E-06	9.8329E-06	7.2038E-06	8.1545E-06	7.6196E-06
	8.5680E-06	8.1971E-06	7.8889E-06	7.5370E-06	7.1450E-06
	6.7558E-06	6.4702E-06	6.2040E-06	5.9969E-06	5.7971E-06
	5.6377E-06	5.5396E-06	5.4782E-06	5.5281E-06	5.5828E-06
	3.8331E-06	3.8206E-06	3.9923E-06	4.1548E-06	4.0861E-06
	3.7829E-06	3.5133E-06	3.3025E-06	3.1857E-06	3.0618E-06
	3.1082E-06	3.8541E-06	3.7349E-06	3.6721E-06	3.4335E-06
	3.3773E-06	3.1450E-06	2.9953E-06	3.0143E-06	7.1726E-06
	5.3780E-06	7.8604E-06	9.9838E-06	4.2522E-06	
	7.1726E-06	5.3780E-06			
					4.1443E-06
	4.0177E-06	4.3654E-06	9.2171E-06	4.2447E-06	8.6710E-06
	8.0942E-06	7.5382E-06	7.1205E-06	6.7122E-06	6.3400E-06
	6.0123E-06	5.7331E-06	5.4615E-06	5.2318E-06	5.0211E-06
	4.8093E-06	4.6441E-06	4.5070E-06	4.4702E-06	4.5198E-06
	3.8563E-06	3.9131E-06	4.0408E-06	3.7396E-06	3.7333E-06
	3.7239E-06	3.9499E-06	3.6815E-06	3.2540E-06	2.7409E-06
	2.7449E-06	3.7520E-06	3.7808E-06	3.7851E-06	3.4067E-06
	3.2798E-06	3.1959E-06	2.7225E-06	2.7188E-06	4.6654E-06
	3.8159E-06	3.8167E-06	3.8182E-06	3.8137E-06	3.8586E-06
	3.8595E-06	3.8123E-06	7.0550E-06	1.1635E-05	4.7361E-05
	9.5474E-06	1.4248E-05	5.3783E-05	1.1840E-04	1.0324E-05
	1.8482E-05	0.0000E+00	3.9363E-06	2.7006E-05	4.7021E-06
	1.0683E-05	0.0000E+00	4.4044E-06	4.0063E-06	

Table 5-1
TN-40 Cask Shield Materials

<u>Component</u>	<u>Material</u>	<u>Density (g/cm³)</u>	<u>Thickness (inches)</u>
Cask Body Wall	Carbon Steel	7.82	9.50
Lid	Carbon Steel	7.82	10.50
Bottom	Carbon Steel	7.82	10.25
Resin ^a	Polyester Resin	1.58	4.50
	Styrene		
	Aluminum Hydrate		
	Zinc Borate		
Aluminum Box	Aluminum	2.7	0.12
Outer Shell	Carbon Steel	7.82	0.50
Basket/	Stainless Steel (fuel compartment)	7.94	0.09
	Aluminum	2.7	0.25 x 2
	Neutron Poison Material ^b	2.45	0.075
Impact Limiter	Stainless Steel	7.94	0.25
	Redwood	0.387	35.0 ^c
	Balsa Wood	0.125	2.5 ^c

Notes:

- ^a The neutron shielding is borated polyester resin compound with a density of 1.58 g/cc. The four major constituents are listed in the table.
- ^b This is modeled as aluminum for shielding purposes with a reduced density.
- ^c Thickness of wood is variable.

Table 5-2
Summary Of TN-40 Dose Rates
 (Exclusive Use)

Normal Conditions Of Transport	Package Surface mSv/h (mrem/h)			Vehicle Edge mSv/h (mrem/h)			2 Meter from Vehicle mSv/h (mrem/h)			
	Radiation	Top	Side	Bottom	Top	Side	Bottom	Top	Side	Bottom
Gamma	0.12 (6.3)	0.76 (76)	0.088 (5.2)	0.14 (14)	0.27 (27)	0.14 (14)	-	0.043 (4.3)	-	
Neutron	0.0003 (0.03)	1.63 (163)	0.0008 (0.08)	0.16 (16)	0.31 (31)	0.16 (16)	-	0.047 (4.7)	-	
Total	0.063 (6.3)	2.39 (239)	0.053 (5.3)	0.29 (29)	0.58 (58)	0.29 (29)	-	0.090 (9.1)	-	
Limit	10 (1000)	10 (1000)	10 (1000)	2 (200)	2 (200)	2 (200)		0.1 (10)		

Hypothetical Accident Conditions ⁽¹⁾	1 Meter from Package Surface mSv/h (mrem/h)		
	Radiation	Top	Side
Gamma	0.43 (43)	0.32 (32)	0.28 (28)
Neutron	0.68 (68)	5.34 (534)	1.45 (145)
Total	1.11 (111)	5.66 (566)	1.73 (173)
Limit	10 (1000)	10 (1000)	10 (1000)

⁽¹⁾ The neutron shield and the impact limiters are removed

Table 5-3
PWR Fuel Assembly Design Characteristics

Parameter	Westinghouse Standard (14x14)
Max Length (in)	161.1
Max Width (in)	7.763
Rod Pitch (in)	0.556
No of Fueled Rods	179
Fuel Rod Length (in)	152
Maximum Active Fuel Length (in)	144.0
Fuel Rod OD (in)	0.4220
Clad Thickness (in)	0.0243
Fuel Pellet OD (in)	0.3659
Clad Material	Zr-4
Guide Tube OD (in)	0.539
Guide Tube Wall Thickness (in)	0.017
Guide Tube #	16
Instrument Tube #	1
Instr. Tube OD (in)	0.422
Instr. Tube Wall Thickness (in)	0.0243
Maximum MTU/assembly	0.410

Table 5-4
Westinghouse 14 X 14 STD Fuel Assembly Hardware Characteristics

Item	Material	Average Mass (kg/assembly)
<u>Fuel Zone</u>		
Cladding	Zircaloy	83.4
Spacers	Inconel	5.37
Guide & Instrument Tubes	Stainless Steel	7.74
<u>Fuel-Gas Plenum Zone</u>		
Cladding	Zircaloy	4.13
Springs	Stainless Steel	5.68
Guide & Instrument Tubes	Stainless Steel	0.38
Spacer	Inconel	0.68
<u>Top End Fitting Zone</u>		
Top Nozzle	Stainless Steel	6.30
Hold Down Springs	Inconel	0.51
<u>Bottom End Fitting Zone</u>		
Bottom Nozzle	Stainless Steel	7.89
Total		122.0

Table 5-5
Material Compositions For Fuel Assembly Hardware Materials

Element	Atomic Number	Material Composition, grams per kg of material				
		Zircaloy-4	Inconel-718	Inconel X-750	Stainless Steel 304	UO ₂ Fuel (per kg U)
H	1	1.30E-02	-	-	-	-
Li	3	-	-	-	-	1.00E-03
B	5	3.30E-04	-	-	-	1.00E-03
C	6	1.20E-01	4.00E-01	3.99E-01	8.00E-01	8.94E-02
N	7	8.00E-02	1.30E+00	1.30E+00	1.30E+00	2.50E-02
O	8	9.50E-01	-	-	-	1.34E+02
F	9	-	-	-	-	1.07E-02
Na	11	-	-	-	-	1.50E-02
Mg	12	-	-	-	-	2.00E-03
Al	13	2.40E-02	5.99E+00	7.98E+00	-	1.67E-02
Si	14	-	2.00E+00	2.99E+00	1.00E+01	1.21E-02
P	15	-	-	-	4.50E-01	3.50E-02
S	16	3.50E-02	7.00E-02	7.00E-02	3.00E-01	-
Cl	17	-	-	-	-	5.30E-03
Ca	20	-	-	-	-	2.00E-03
Ti	22	2.00E-02	7.99E+00	2.49E+01	-	1.00E-03
V	23	2.00E-02	-	-	-	3.00E-03
Cr	24	1.25E+00	1.90E+02	1.50E+02	1.90E+02	4.00E-03
Mn	25	2.00E-02	2.00E+00	6.98E+00	2.00E+01	1.70E-03
Fe	26	2.25E+00	1.80E+02	6.78E+01	6.88E+02	1.80E-02
Co	27	1.00E-02	4.69E+00	6.49E+00	8.00E-01	1.00E-03
Ni	28	2.00E-02	5.20E+02	7.22E+02	8.92E+01	2.40E-02
Cu	29	2.00E-02	9.99E-01	4.99E-01	-	1.00E-03
Zn	30	-	-	-	-	4.03E-02
Zr	40	9.79E+02	-	-	-	-
Nb	41	-	5.55E+01	8.98E+00	-	-
Mo	42	-	3.00E+01	-	-	1.00E-02
Ag	47	-	-	-	-	1.00E-04
Cd	48	2.50E-04	-	-	-	2.50E-02
In	49	-	-	-	-	2.00E-03
Sn	50	1.60E+01	-	-	-	4.00E-03
Gd	64	-	-	-	-	2.50E-03
Hf	72	7.80E-02	-	-	-	-
W	74	2.00E-02	-	-	-	2.00E-03
Pb	82	-	-	-	-	1.00E-03
U	92	2.00E-04	-	-	-	1.00E+03

Table 5-6
Source Distribution

E_{lower} (MeV)	E_{upper} (MeV)	Source ^[1] (particles/sec/assembly)				
		Bottom Fitting Gamma	Active Fuel Gamma	Plenum Gamma	Top Fitting Gamma	Combined Gamma
0.01	0.05	1.15E+10	4.82E+14	1.58E+10	7.03E+09	4.82E+14
0.05	0.10	2.19E+09	1.41E+14	2.81E+09	1.29E+09	1.41E+14
0.10	0.20	5.27E+08	8.83E+13	7.15E+08	3.11E+08	8.83E+13
0.20	0.30	2.62E+07	2.70E+13	3.61E+07	1.55E+07	2.70E+13
0.30	0.40	3.43E+07	1.81E+13	5.27E+07	2.02E+07	1.81E+13
0.40	0.60	2.17E+06	1.47E+13	1.94E+08	1.28E+06	1.47E+13
0.60	0.80	7.54E+05	9.70E+14	8.56E+08	2.83E+08	9.70E+14
0.80	1.00	2.84E+07	8.23E+12	7.65E+08	2.89E+08	8.23E+12
1.00	1.33	6.38E+11	2.75E+13	2.17E+12 ^[2]	1.29E+12 ^[2]	3.16E+13 ^[2]
1.33	1.66	1.80E+11	5.38E+12	6.11E+11 ^[2]	3.63E+11 ^[2]	6.54E+12 ^[2]
1.66	2.00	1.64E-06	4.63E+10	1.47E+01	1.10E-03	4.63E+10
2.00	2.50	4.27E+06	2.48E+09	5.48E+06	2.51E+06	2.50E+09
2.50	3.00	6.63E+03	1.73E+08	8.50E+03	3.90E+03	1.73E+08
3.00	4.00	6.28E-15	2.68E+07	1.52E-11	5.62E-12	2.68E+07
4.00	5.00	0.00E+00	9.04E+06	0.00E+00	0.00E+00	9.04E+06
5.00	6.50	0.00E+00	3.63E+06	0.00E+00	0.00E+00	3.63E+06
6.50	8.00	0.00E+00	7.12E+05	0.00E+00	0.00E+00	7.12E+05
8.00	10.00	0.00E+00	1.51E+05	0.00E+00	0.00E+00	1.51E+05
Total Gamma		8.32E+11	1.78E+15	2.80E+12	1.66E+12	1.79E+15
Total Neutron ^[3]		2.63E+08				

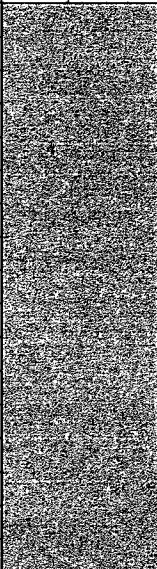

1. The design basis gamma source term correspond to the Westinghouse 14x14 Standard fuel assembly with 2.35 wt.% U-235 enrichment , 42,000 MWD/MTU burnup, 24.4 year cooling time and TPA insert source term.
2. Total gamma source from the fuel assembly and the TPA source shown in Table 5-7.
3. The neutron source spectrum is modeled as Cm-244 using the built-in MCNP distribution.

Table 5-7
TPA Gamma Source

Gamma Source from TPA (gammas/sec per assembly)				
Plenum		Top End Fitting		Total
1 – 1.33 MeV	1.33 - 1.66 MeV	1 – 1.33 MeV	1.33 - 1.66 MeV	
1.35E+12	3.81E+11	9.13E+11	2.57E+11	2.90E+12

Table 5-8
Fuel Qualification Table

MINIMUM COOLING TIMES (YEARS)

Maximum Assembly Average Burnup (GWD/MTU)	Assembly Average Enrichment (wt. % U235)								
	2	2.25	2.35	2.75	3	3.25	3.4	3.6	3.85
17	15	15	15	15	15	15	15	15	15
18	15	15	15	15	15	15	15	15	15
19	15	15	15	15	15	15	15	15	15
20	15	15	15	15	15	15	15	15	15
21	15	15	15	15	15	15	15	15	15
22	15	15	15	15	15	15	15	15	15
23	15	15	15	15	15	15	15	15	15
24	15	15	15	15	15	15	15	15	15
25	15	15	15	15	15	15	15	15	15
26	15	15	15	15	15	15	15	15	15
27	15	15	15	15	15	15	15	15	15
28	15	15	15	15	15	15	15	15	15
29			15	15	15	15	15	15	15
30			15	15	15	15	15	15	15
31			15	15	15	15	15	15	15
32			15	15	15	15	15	15	15
33			16	15	15	15	15	15	15
34			17	15	15	15	15	15	15
35			17	16	15	15	15	15	15
36			18	16	15	15	15	15	15
37			19	17	16	15	15	15	15
38			20	18	17	16	16	15	15
39			21	19	18	17	16	16	15
40			23	20	19	18	17	16	16
41			24	21	20	19	18	17	17
42			25	22	21	19	19	18	18
43					22	20	20	20	19
44						21	21	21	21
45						23	22	22	22

Notes:

1. For fuel characteristics that fall between the assembly average enrichment values in the table, use the next lower enrichment, and next higher burnup to determine minimal cooling time.
2. Enrichment and burnup are also required to meet criticality requirements as defined in Figure 6-1.

Table 5-9
Minimum Cooling (Years) Required
To Meet Radiation and Decay Heat Limits

Maximum Assembly Average Burnup (GWD/MTU)	Assembly Average Initial Enrichment (Wt. % U235)									
	2	2.25	2.35	2.75	3	3.25	3.4	3.6	3.85	
17	7.4	7.0								
18	7.8	7.4								
19	8.3	7.8								
20	8.7	8.2								
21	9.2	8.7								
22	9.7	9.2								
23	10.3	9.7								
24	10.9	10.2								
25	10.9	10.2								
26	11.5	10.8	10.5							
27	12.1	11.4	11.1							
28	12.8	12.0	11.7	10.6	10.1	9.6				
29			12.3	11.2	10.6	10.1				9.8
30			13.0	11.7	11.1	10.6	10.3			
31			13.6	12.3	11.7	11.1	10.8			
32			14.4	13.0	12.3	11.6	11.3			
33			15.2	13.7	12.9	12.2	11.8	11.4		
34			16.0	14.4	13.5	12.8	12.4	11.9	11.5	
35			16.8	15.1	14.2	13.4	13.0	12.5	12.0	
36			17.8	15.9	14.9	14.1	13.6	13.1	12.6	
37			18.7	16.7	15.7	14.8	14.3	13.7	13.2	
38			19.8	17.6	16.5	15.5	15.0	14.4	13.8	
39			20.9	18.5	17.3	16.3	15.7	15.0	14.4	
40			22.0	19.5	18.2	17.1	16.5	15.7	15.1	
41			23.2	20.5	19.2	18.0	17.3	16.5	16.3	
42			24.4	21.7	20.2	18.9	18.2	17.8	17.5	
43					21.2	19.8	19.2	19.0	18.9	
44							20.8	20.6	20.4	20.2
45							22.1	21.9	21.7	21.6

Table 5-10
Estimated 2 Meter Side Dose Rates (MREM/HR)

	Assembly Average Initial Enrichment (Wt. % U235)										
Maximum Assembly Average Burnup (GWD/MTU)	2	2.25	2.35	2.75	3	3.25	3.4	3.6	3.85		
17	10	10									
18	10	10									
19	10	10									
20	10	10									
21	10	10									
22	10	10									
23	10	10									
24	10	10									
25	10	10									
26	10	10	10								
27	10	10	10							10	10
28	10	10	10							10	10
29			10	10	10	10	10				
30			10	10	10	10	10				
31			10	10	10	10	10				
32			10	10	10	10	10				
33			10	10	10	10	10	10	10		
34			10	10	10	10	10	10	10		
35			10	10	10	10	10	10	10		
36			10	10	10	10	10	10	10		
37			10	10	10	10	10	10	10		
38			10	10	10	10	10	10	10		
39			10	10	10	10	10	10	10		
40			10	10	10	10	10	10	10		
41			10	10	10	10	10	10	10	9.4	
42			10	10	10	10	10	10	9.4	9.1	
43					10	10	9.6	9.2	8.7		
44							10	9.4	8.9	8.5	
45							9.6	9.2	8.7	8.2	

Table 5-11
Decay Heat Output (kW PER CASK)

Maximum Assembly Average Burnup (GWD/MTU)	Assembly Average Initial Enrichment (Wt. % U235)								
	2	2.25	2.35	2.75	3	3.25	3.4	3.6	3.85
17	11.4	11.8							
18	11.8	12.1							
19	12.1	12.4							
20	12.4	12.8							
21	12.8	13.1							
22	13.1	13.4							
23	13.4	13.7							
24	13.8	14.1							
25	14.1	14.4							
26	14.4	14.7	14.9						
27	14.8	15.1	15.2						
28	15.1	15.4	15.5	16.0	16.3	16.6			
29			15.8	16.3	16.6	16.9			
30			16.1	16.7	16.9	17.2	17.4		
31			16.5	17.0	17.3	17.6	17.7		
32			16.7	17.3	17.6	17.9	18.0		
33			17.0	17.6	17.9	18.2	18.4	18.6	
34			17.3	17.8	18.2	18.5	18.7	18.9	19.1
35			17.6	18.2	18.5	18.8	19.0	19.2	19.5
36			17.8	18.5	18.8	19.1	19.3	19.6	19.8
37			18.0	18.7	19.1	19.4	19.6	19.8	20.1
38			18.2	18.9	19.3	19.7	19.9	20.1	20.4
39			18.4	19.2	19.6	19.9	20.2	20.4	20.7
40			18.5	19.4	19.8	20.2	20.4	20.7	20.9
41			18.6	19.5	20.0	20.4	20.6	21.0	21.0
42			18.7	19.6	20.1	20.6	20.8	20.9	21.0
43					20.3	20.8	21.0	21.0	21.0
44					21.0	21.0	21.0	21.0	
45					21.0	21.0	21.0	21.0	

Table 5-12
Axial Source Term Peaking Summary

Fractional Core Height			Gamma Profile	Neutron Profile
0	to	0.083	0.700	0.240
0.083	to	0.167	1.030	1.126
0.167	to	0.250	1.120	1.574
0.250	to	0.333	1.160	1.811
0.333	to	0.417	1.160	1.811
0.417	to	0.500	1.160	1.811
0.500	to	0.583	1.158	1.798
0.583	to	0.667	1.150	1.749
0.667	to	0.750	1.144	1.713
0.750	to	0.833	1.120	1.574
0.833	to	0.917	0.990	0.961
0.917	to	1.000	0.700	0.240
Average:			1.049	1.367

Table 5-13
Fuel Assembly Materials Input For MCNP

Lower End Fitting Zone

Element/Isotope	Mass Density (g/cc)	Weight Fraction	Number Density (atom/barn-cm)	Atom Fraction
C	2.08E-03	0.080%	1.04E-04	0.364%
Si	2.59E-02	1.000%	5.56E-04	1.944%
P	1.17E-03	0.045%	2.27E-05	0.079%
Cr	4.93E-01	19.000%	5.71E-03	19.949%
Ti	0.00E+00	0.000%	0.00E+00	0.000%
Mn	5.19E-02	2.000%	5.69E-04	1.987%
Fe	1.77E+00	68.375%	1.91E-02	66.841%
Ni	2.47E-01	9.500%	2.53E-03	8.836%
Zr	0.00E+00	0.000%	0.00E+00	0.000%
Sn	0.00E+00	0.000%	0.00E+00	0.000%
Hf	0.00E+00	0.000%	0.00E+00	0.000%
O	0.00E+00	0.000%	0.00E+00	0.000%
H	0.00E+00	0.000%	0.00E+00	0.000%
TOTAL	2.595	100.0%	0.02863	100.0%

In-Core Zone

Element/Isotope	Mass Density (g/cc)	Weight Fraction	Number Density (atom/barn-cm)	Atom Fraction
U-234	7.70E-04	0.019%	1.98E-06	0.007%
U-235	8.65E-02	2.190%	2.22E-04	0.828%
U-236	3.98E-04	0.010%	1.02E-06	0.004%
U-238	2.80E+00	70.788%	7.07E-03	26.424%
O	3.88E-01	9.815%	1.46E-02	54.526%
C	4.35E-05	0.0011%	2.18E-06	0.008%
Si	1.49E-03	0.038%	3.19E-05	0.119%
P	2.45E-05	0.0006%	4.76E-07	0.0018%
Cr	1.66E-02	0.420%	1.92E-04	0.718%
Ti	9.44E-04	0.024%	1.19E-05	0.044%
Mn	1.09E-03	0.028%	1.19E-05	0.045%
Fe	4.11E-02	1.040%	4.43E-04	1.655%
Ni	3.27E-02	0.829%	3.36E-04	1.255%
Zr	5.76E-01	14.581%	3.80E-03	14.203%
Sn	8.50E-03	0.215%	4.31E-05	0.161%
Hf	5.86E-05	0.001%	1.98E-07	0.001%
H	0.00E+00	0.000%	0.00E+00	0.000%
TOTAL	3.949	100.0%	0.02676	100.0%

Table 5-13
Fuel Assembly Materials Input for MCNP – Cont'd

Plenum Zone

Element/Isotope	Mass Density (g/cc)	Weight Fraction	Number Density (atom/ barn-cm)	Atom Fraction
C	6.88E-04	0.045%	3.45E-05	0.240%
Si	1.10E-02	0.714%	2.36E-04	1.640%
P	3.87E-04	0.025%	7.53E-06	0.052%
Cr	1.78E-01	11.569%	2.07E-03	14.358%
Ti	2.41E-03	0.156%	3.03E-05	0.211%
Mn	1.72E-02	1.115%	1.89E-04	1.310%
Fe	5.96E-01	38.641%	6.43E-03	44.650%
Ni	1.52E-01	9.859%	1.56E-03	10.839%
Zr	5.76E-01	37.321%	3.80E-03	26.400%
Sn	8.50E-03	0.551%	4.31E-05	0.299%
Hf	5.86E-05	0.004%	1.98E-07	0.001%
O	0.00E+00	0.000%	0.00E+00	0.000%
H	0.00E+00	0.000%	0.00E+00	0.000%
TOTAL	1.543	100.0%	0.01440	100.0%

Upper End Fitting Zone

Element/Isotope	Mass Density (g/cc)	Weight Fraction	Number Density (atom/barn-cm)	Atom Fraction
C	1.46E-03	0.074%	7.31E-05	0.337%
Si	2.19E-02	1.112%	4.70E-04	2.164%
P	8.20E-04	0.042%	1.59E-05	0.073%
Cr	3.68E-01	18.702%	4.27E-03	19.662%
Ti	3.67E-03	0.187%	4.62E-05	0.213%
Mn	3.65E-02	1.851%	4.00E-04	1.842%
Fe	1.26E+00	63.795%	1.36E-02	62.448%
Ni	2.80E-01	14.238%	2.88E-03	13.261%
Zr	0.00E+00	0.000%	0.00E+00	0.000%
Sn	0.00E+00	0.000%	0.00E+00	0.000%
Hf	0.00E+00	0.000%	0.00E+00	0.000%
O	0.00E+00	0.000%	0.00E+00	0.000%
H	0.00E+00	0.000%	0.00E+00	0.000%
TOTAL	1.970	100.0%	0.02170	100.0%

Table 5-14
Package Materials Input for MCNP

<u>Zone</u>	<u>Material</u>	<u>Density (g/cc)</u>	<u>Element/ Nuclide</u>	<u>Library Identifier</u>	<u>Weight Fraction (atm fraction)</u>
Basket Plates & Impact Limiter Skin	SS304	7.94	Cr	24000	0.1900
			Mn	25000	0.0200
			Fe	26000	0.68375
			Ni	28000	0.0950
			Si	14000	0.0100
			P	15031	0.00045
			C	6012	0.00080
Basket Plates & Rails	Aluminum	2.702	Al	13027	1.0000
Cask Body	Carbon Steel	7.8212	Fe	26000	0.9900
			C	6012	0.0100
Resin/Aluminum	Resin (1.58 g/cc) & Al (2.702 g/cc)	1.687	O	8016	0.3503
			Al	13027	0.2851
			C	6012	0.2953
			H	1001	0.04260
			B-10	5010	0.0018
			B-11	5011	0.0071
			Zn	30000	0.0178
Impact Limiter	Balsa Wood	0.125	C	6012	(0.2857)
			O	8016	(0.2381)
			H	1001	(0.4762)
Impact Limiter	Redwood	0.387	C	6012	(0.2857)
			O	8016	(0.2381)
			H	1001	(0.4762)

Table 5-15
Flux-to-Dose Rate Conversion Factors For Gamma

Photon Energy (MeV)	Conversion Factor (rem/hr) / ($\gamma/\text{cm}^2\text{-s}$)
0.01	3.96E-06
0.03	5.82E-07
0.05	2.90E-07
0.07	2.58E-07
0.1	2.83E-07
0.15	3.79E-07
0.2	5.01E-07
0.25	6.31E-07
0.3	7.59E-07
0.35	8.78E-07
0.4	9.85E-07
0.45	1.08E-06
0.5	1.17E-06
0.55	1.27E-06
0.6	1.36E-06
0.65	1.44E-06
0.7	1.52E-06
0.8	1.68E-06
1	1.98E-06
1.4	2.51E-06
1.8	2.99E-06
2.2	3.42E-06
2.6	3.82E-06
2.8	4.01E-06
3.25	4.41E-06
3.75	4.83E-06
4.25	5.23E-06
4.75	5.60E-06
5	5.80E-06
5.25	6.01E-06
5.75	6.37E-06
6.25	6.74E-06
6.75	7.11E-06
7.5	7.66E-06
9	8.77E-06
11	1.03E-05
13	1.18E-05
15	1.33E-05

Table 5-16
Flux-Dose-Rate Conversion Factors For Neutron

Neutron Energy (MeV)	Conversion Factor (rem/hr) / (n/cm²-s)
2.50E-08	3.67E-06
1.0E -07	3.67E-06
1.00E-06	4.46E-06
1.00E-05	4.54E-06
1.00E-04	4.18E-06
1.00E-03	3.76E-06
1.00E-02	3.56E-06
1.00E-01	2.17E-05
5.00E-01	9.26E-05
1	1.32E-04
2.5	1.25E-04
5	1.56E-04
7	1.47E-04
10	1.47E-04
14	2.08E-04
20	2.27E-04

Table 5-17
Average End Dose Rates As A Function Of Railcar Length

Rail Car Length (feet)	Average Dose Rates as a Function of Railcar Length (mrem/hr)								Limit
	Neutron		N, Gamma		Gamma		Total		
	Top	Bottom	Top	Bottom	Top	Bottom	Top	Bottom	
40	0.0394	0.0410	0.0453	0.0769	0.686	0.425	0.770	0.543	2
50	0.0329	0.0325	0.0246	0.0433	0.408	0.252	0.466	0.328	
60	0.0607	0.0540	0.0202	0.0266	0.107	0.078	0.188	0.159	

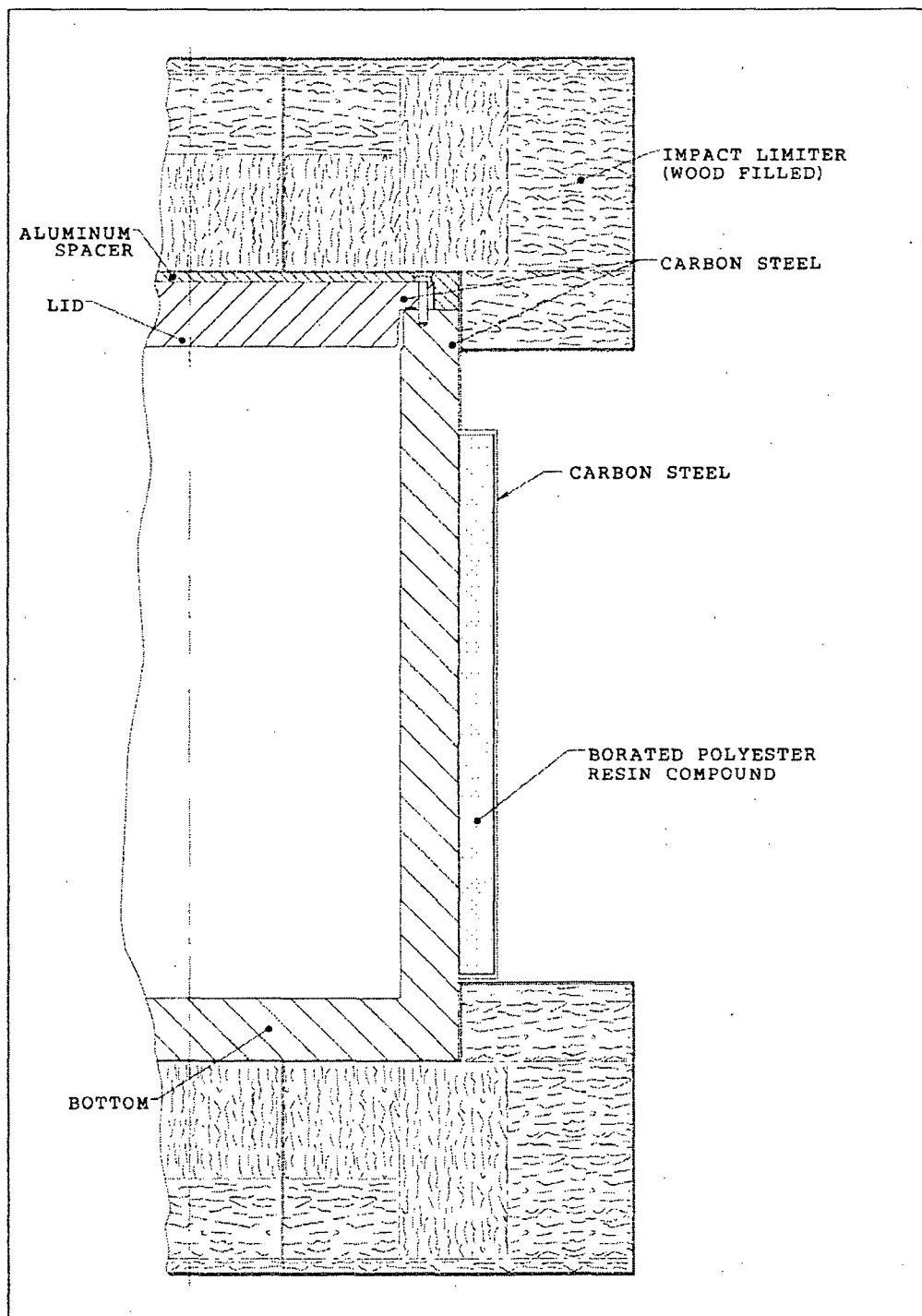


Figure 5-1
Cask Shielding Configuration

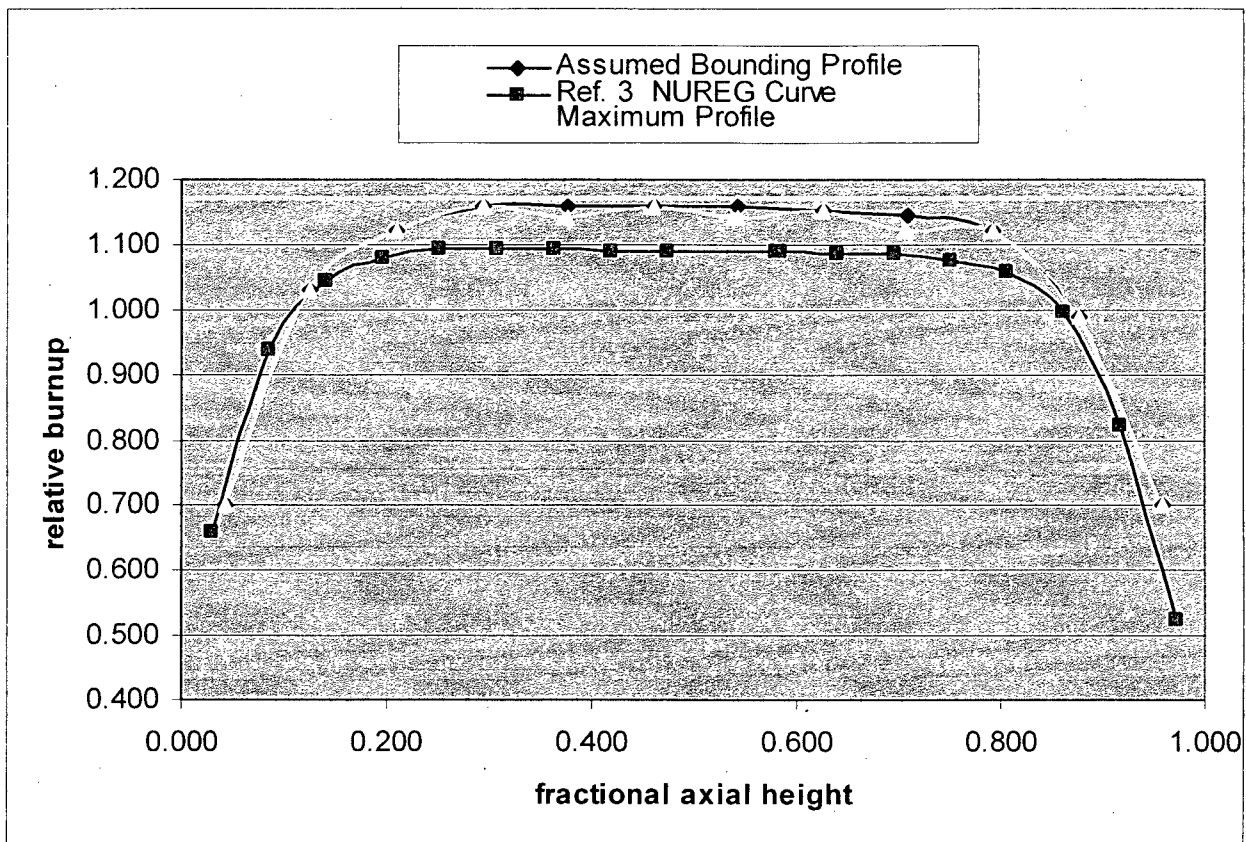


Figure 5-2
Axial Burnup Profile For Design Basis Fuel

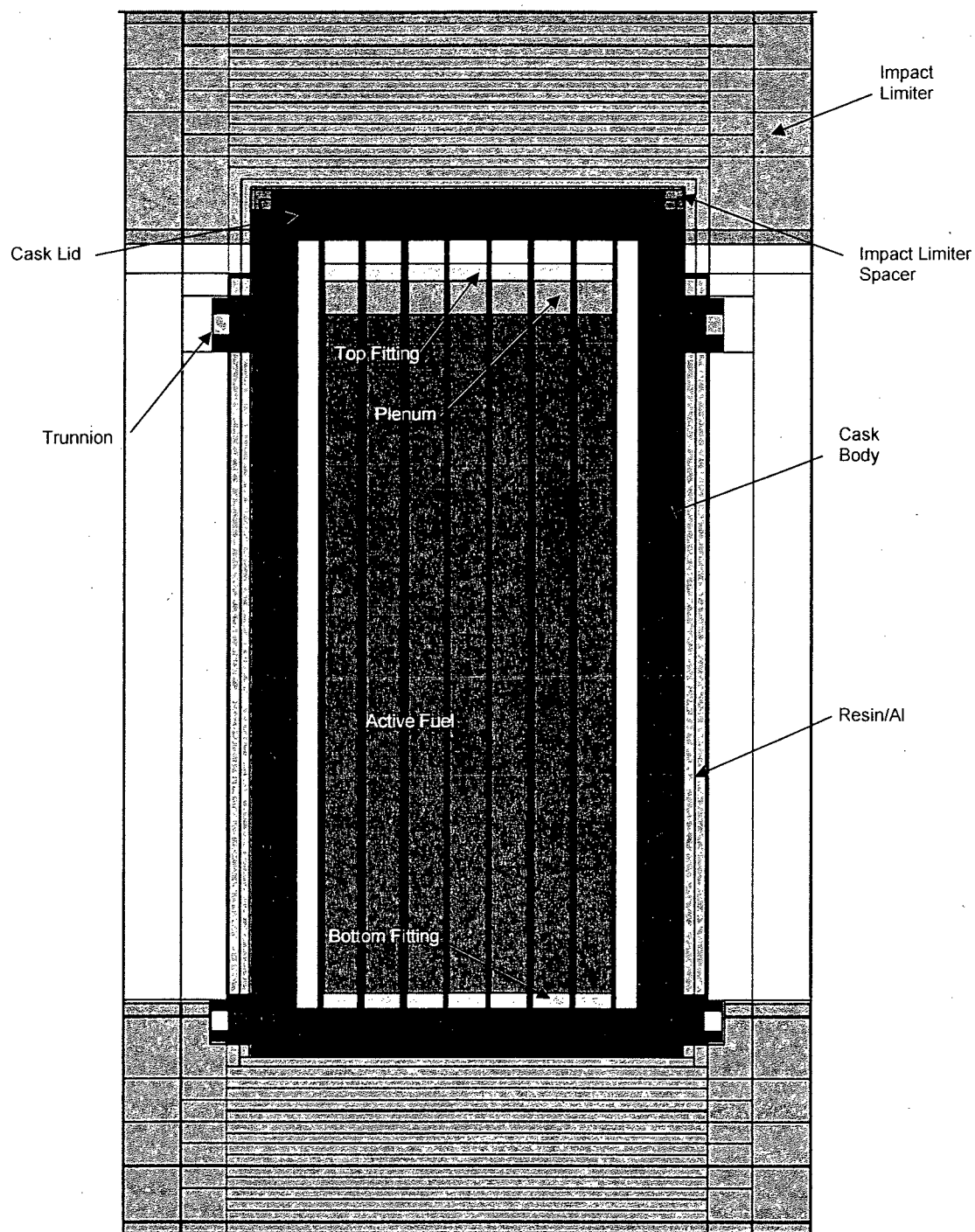
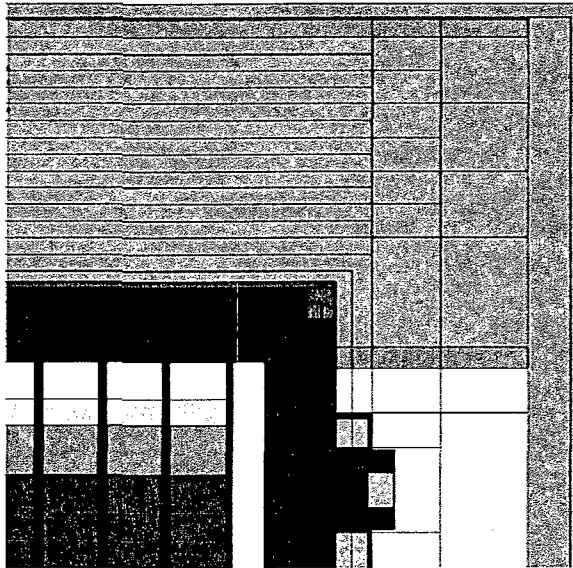
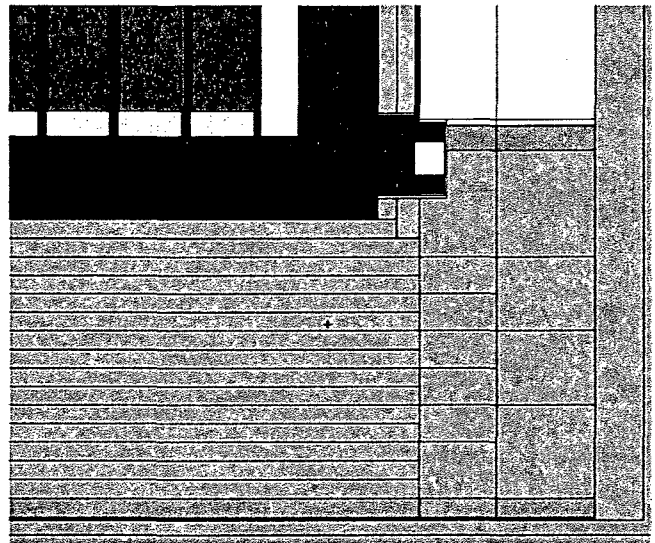


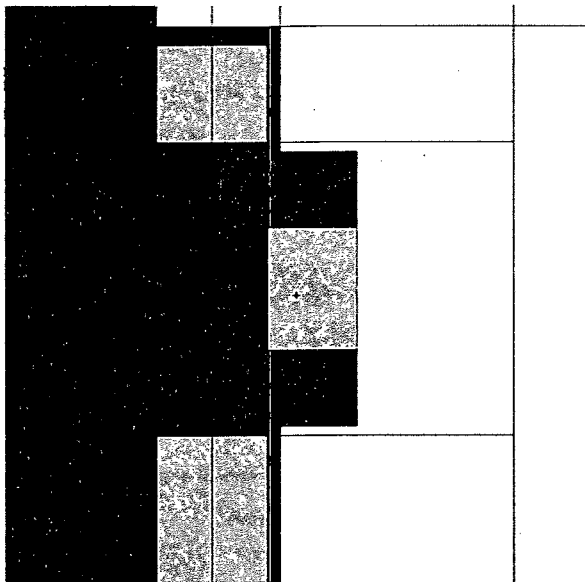
Figure 5-3
Side View Of TN-40 Transport MCNP Model



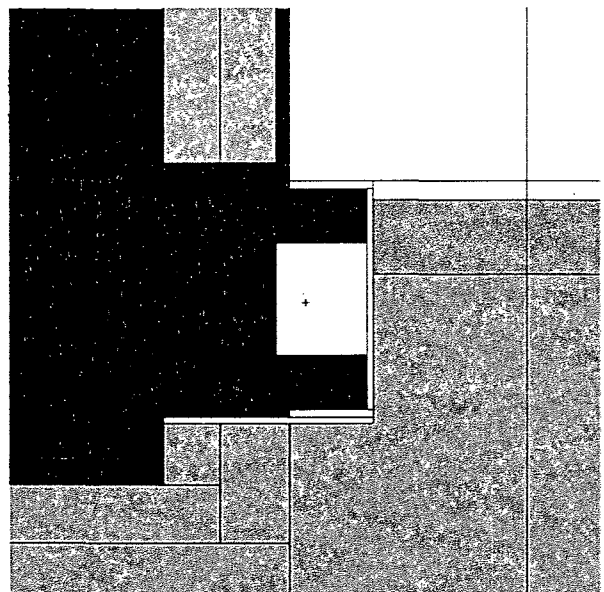
a) top view



b) bottom view

Enlarged Side View of TN-40 Transport MCNP Model

a) top trunnion



b) bottom trunnion

Enlarged View of Trunnion Area**Figure 5-4**
Detail Views Of TN-40 Transport MCNP Model

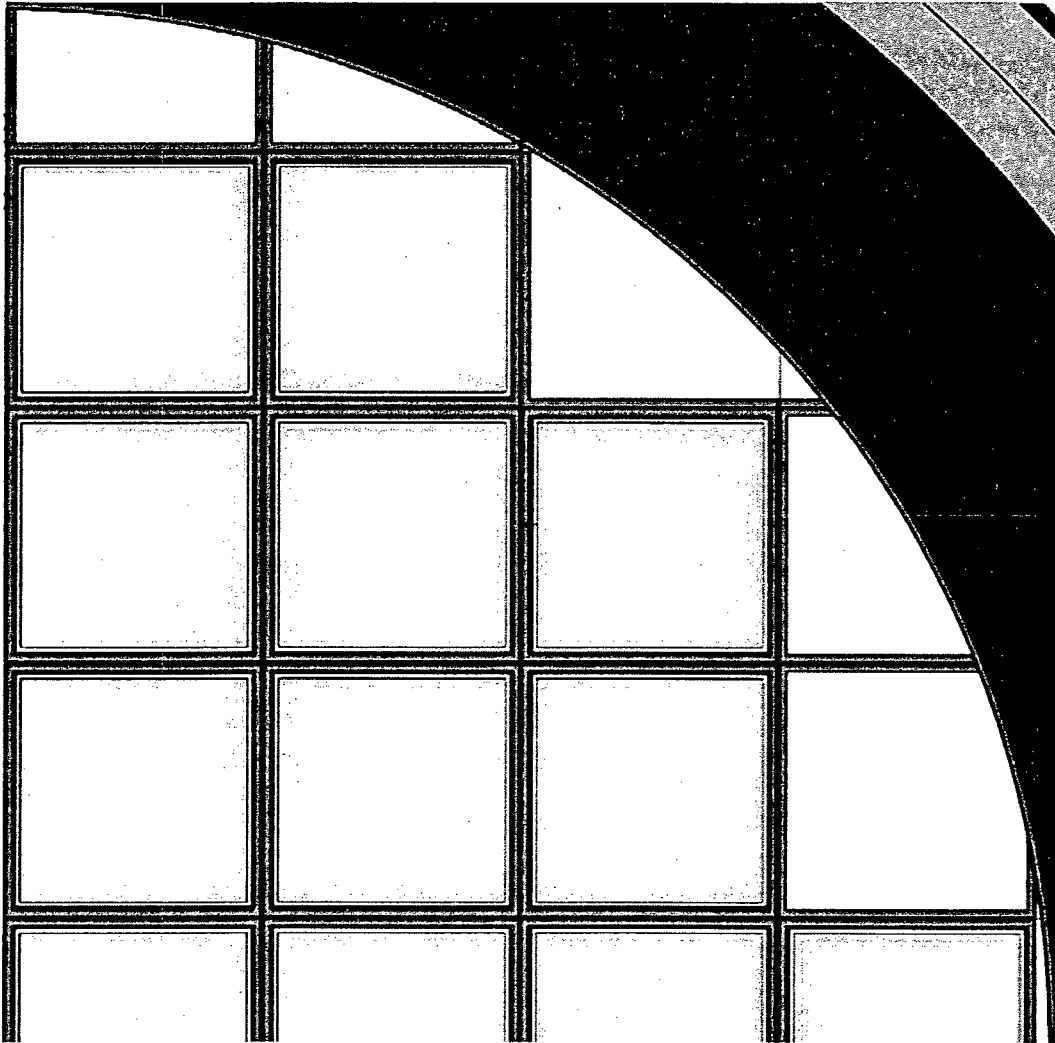


Figure 5-5
Plan View Of TN-40 Transport MCNP Model Basket Structure

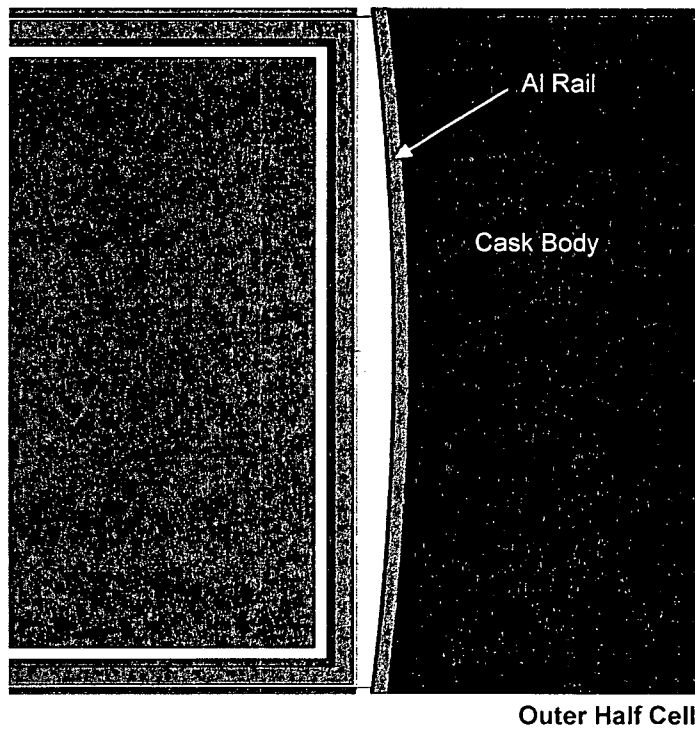
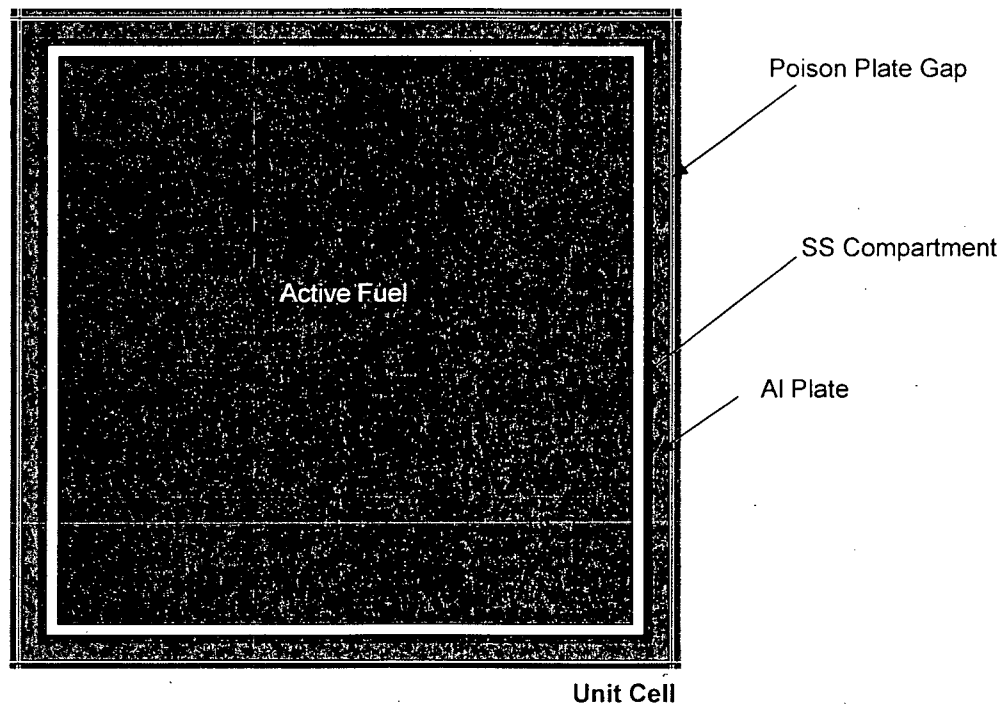


Figure 5-6
Details Of Lattice Unit Cell And Rails/Outer SST

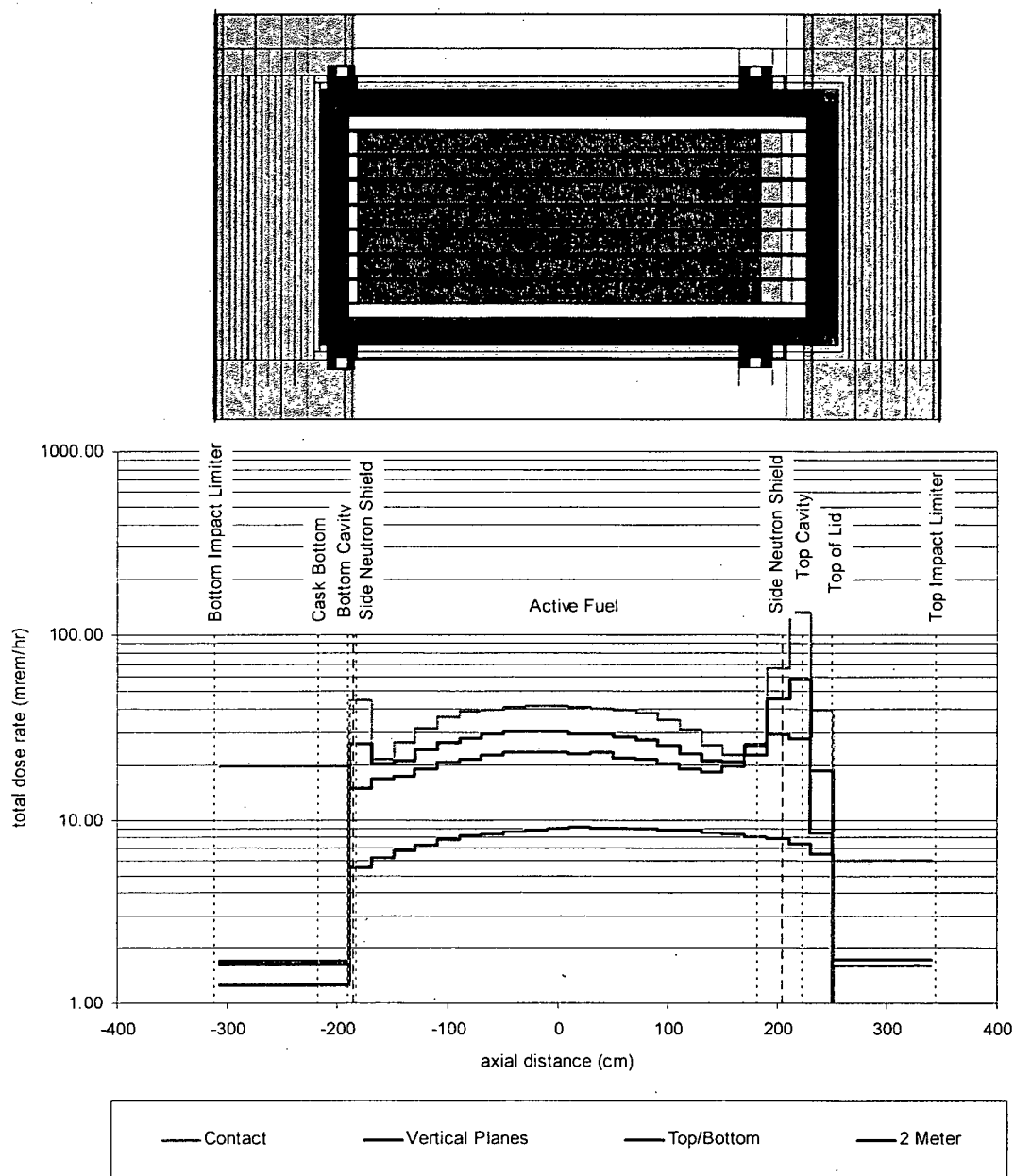


Figure 5-7
Summary of TN-40 Side NCT Dose Rates

CHAPTER 6

CRITICALITY EVALUATION

TABLE OF CONTENTS

	<u>PAGE</u>
6.0 Criticality Evaluation	6-1
6.1 Discussion and Results	6-1
6.2 Package Fuel Loading	6-2
6.3 Model Specification	6-3
6.4 Criticality Calculations	6-3
6.4.1 Calculational Method	6-3
6.4.2 Fuel Loading Optimization	6-3
6.4.3 Criticality Results	6-3
6.5 Critical Benchmark Experiments	6-4
6.5.1 Benchmark Experiments and Applicability	6-4
6.5.2 Results of the Benchmark Calculations	6-5
6.6 References	6-6
6.7 Input File Listing	6-8
6.7.1 SAS2H Input Deck for Design Basis Fuel Assembly – Zone 8	6-8
6.7.2 CSAS25 Input Deck for Design Basis Criticality Case	6-8

LIST OF TABLES

Table 6-1	Minimum Burnup as a Function of Enrichment	6-9
Table 6-2	Parameters For PWR Assemblies For Shipment	6-10
Table 6-3	Required Assembly and Reactor Parameters for SAS2H Models	6-10
Table 6-4	Axial Burnup Profiles from Reference [10]	6-10
Table 6-5	Modified Axial Burnup Profiles Used for SAS2H Depletion Analysis	6-11
Table 6-6	BPRA Design Parameters for SAS2H Models	6-11
Table 6-7	Burnup Dependent Horizontal Burnup Gradients	6-11

Table 6-8	Basket and Cask Design Dimensions for the CSAS25 Models.....	6-11
Table 6-9	Description of the KENO Model.....	6-12
Table 6-10	Best-Estimate Correction Factors for SAS2H Isotopic Content	6-12
Table 6-11	Burned Fuel Isotopic Composition	6-12
Table 6-12	Material Property Data	6-12
Table 6-13	Material ID IN KENO	6-13
Table 6-14	Most Reactive Configuration – Fresh Fuel Assumption	6-13
Table 6-15	Most Reactive Configuration – Burned Fuel	6-13
Table 6-16	Results of Burnup Credit Calculations	6-13
Table 6-17	Moderator Density Variations.....	6-14
Table 6-18	Results of the Additional Reactivity Margin Calculations	6-15
Table 6-19	Dancoff Factor Calculation for Density Variations.....	6-15
Table 6-20	CSAS25 Results	6-16
Table 6-21	USL-1 Results.....	6-20
Table 6-22	USL Determination for Criticality Analysis.....	6-21

LIST OF FIGURES

Figure 6-1	TN-40 Loading Curve.....	6-22
Figure 6-2	Example SAS2H Model.....	6-23
Figure 6-3	Fuel Assembly Positions within the Basket	6-23
Figure 6-4	Radial Cross Section of the Basket with Centered Fuel Assemblies.....	6-23
Figure 6-5	Radial Cross Section of the Basket with Stainless Steel.....	6-23
Figure 6-6	Axial Cross Section of the Basket with Cuboid Plugs.....	6-24
Figure 6-7	Radial Cross Section of the Basket with Inward Fuel Assemblies	6-24
Figure 6-8	TN-40 KENO Model for Horizontal Burnup Gradient.....	6-24
Figure 6-9	TN-40 KENO Model with Internal Moderator between Poison Plates ...	6-24
Figure 6-10	TN-40 KENO Model for Cask A Loading Configuration.....	6-25
Figure 6-11	TN-40 KENO Model for Cask B Loading Configuration.....	6-25
Figure 6-12	TN-40 KENO Model for Cask C Loading Configuration	6-25

6.0 CRITICALITY EVALUATION

The TN-40 cask, as transported, will provide criticality control to meet the criticality performance requirements specified in Sections 71.55 and 71.59 of 10 CFR Part 71 [2]. The criticality control design ensures that the effective multiplication factor (k_{eff}) of the contained fuel is no greater than an Upper Subcritical Limit (USL) for the most reactive configuration. The USL includes a confidence band with an administrative safety margin of 0.05. The design has a Criticality Safety Index (CSI, given in 10 CFR 71.59(b) as $CSI = 50/"N"$) of 0 because "N" is infinity (∞). The number "N" is based on all of the following conditions being satisfied, assuming packages are stacked together in any arrangement and with close full reflection on all sides of the stack by water:

1. Five times "N" undamaged packages with nothing between the packages are subcritical;
2. Two times "N" damaged packages, if each package is subjected to the tests specified in 10 CFR Part 71.73 (HAC) is subcritical with optimum interspersed hydrogenous moderation; and
3. The value of "N" cannot be less than 0.5.

6.1 Discussion and Results

The TN-40 basket uses fixed neutron poison plates (or poison plates) for criticality control. The stainless steel basket consists of tubular fuel compartments held together via discrete axial welds forming a 40-compartment basket. The assembly of fuel compartments is connected to aluminum plates at the basket periphery. The aluminum plates provide the circular perimeter geometry that fits the basket inside the cask inner shell and provide for efficient heat transfer from the basket to the cask body. The poison plates are confined between the tubular fuel compartments and the grouped compartments as shown in the various figures in Chapter 1.

The TN-40 cask is shown to be subcritical for an infinite array of flooded undamaged casks and for an infinite array of damaged casks after being subjected to Hypothetical Accident Conditions (HAC) events. The design has a CSI of 0 as "N" is equal to ∞ . A CSI of 0 (less than 50) ensures that, per 10 CFR Part 71.59 (c)(1), the package may be shipped by a carrier in a nonexclusive conveyance, from a criticality requirements point of view.

The calculations performed to confirm the subcriticality requirements listed above utilize a credit for the fuel assembly burnup or "burnup credit." Taking burnup credit requires a different analytical approach for criticality analysis than is used in traditional analysis with a fresh fuel assumption. For fresh fuel, the only key fuel parameters to be taken into account in the analyses are the initial enrichment and the most reactive fuel configuration. The analysis of burned fuel must include consideration of the most reactive assembly as a function of burnup, end effects (underburned fuel at the ends), reactor operating history, fuel composition, initial enrichment and cooling time. Therefore, additional calculations and codes are required for burned fuel to determine

the isotopic composition of the burned fuel as a function of fuel design, initial enrichment, burnup, and cooling time using an assumed bounding reactor operating history. In addition, the benchmarking method to determine code biases is different. For the criticality code, additional benchmarks are required to account for the burned fuel composition. An additional bias (correction factors) for the depletion code, which determines the isotopic composition of the burned fuel, must also be addressed in the evaluation.

The depletion calculations determine the isotopic composition of the burned fuel with the SAS2H control module of SCALE-4.4 [1] while the criticality calculations determine k_{eff} with the CSAS25 control module of SCALE-4.4. The bias due to the isotopic composition of the fuel is accounted for by adjusting the calculated isotopic content based on comparison with available measure isotopic data of burned fuel from a variety of reactors and operating histories. The correction factors are based on the SAS2H benchmarks of measured data. The bias due to the criticality code with the additional benchmark data to account for the composition of the burned fuel is not required and is based on the reactor critical benchmark results summarized in reference [3].

This burnup credit criticality analysis determines the most reactive configuration for the basket and assembly location. The burnup credit analysis evaluates all of the eligible fuel assembly designs allowed for transport in the TN-40 package. The criticality calculations utilize the Westinghouse 14x14 Standard fuel assembly because it is the most reactive fuel assembly authorized for transport. The calculations determine k_{eff} with the CSAS25 control module of SCALE-4.4 [1] for bounding configurations of initial enrichment, assembly average burnup, and a minimum cooling time of 15 years, including all uncertainties to assure criticality safety under all credible conditions. The initial enrichment as a function of minimum assembly average burnup required to ensure subcriticality is shown in Table 6-1. A third order polynomial is utilized to fit this data so that the required assembly burnup for all assembly average enrichments that lie in between the minimum and maximum can be calculated. A burnup curve based on the third order polynomial is shown in Figure 6-1. The "acceptable" region in the curve pertains to those fuel assemblies with a burnup-enrichment combination AND a minimum cooling time greater than 15 years, that are eligible for transportation in the TN-40 cask.

The results of the evaluation demonstrate that the maximum k_{eff} , including statistical uncertainty, is less than the USL determined from a statistical analysis of benchmark criticality experiments. The statistical analysis procedure includes a confidence band with an administrative safety margin of 0.05.

6.2 Package Fuel Loading

The TN-40 Cask is capable of transporting 40 intact Westinghouse 14x14 (WE 14) class of PWR fuel assemblies with or without Non Fuel Assembly Hardware (NFAH). Burnplate Poison Rod Assemblies (BPRAs) are the only NFAH that are discussed in this evaluation since they bound all other NFAH. Each BPRA typically consists of 4, 8, 12, or 16 burnable poison (BP or discrete BP) rods. The fuel assemblies considered as authorized contents include those listed in Table 6-2.

Table 6-2 also lists the fuel parameters for the PWR fuel assemblies. Equivalent reload fuel assemblies that are bounded by the parameters listed in Table 6-2 are also considered as authorized contents. The design basis fuel assembly for the TN-40 cask criticality analysis was determined to be the WE 14x14 Standard fuel assembly.

6.3 Model Specification

PROPRIETARY INFORMATION WITHHELD UNDER 10CFR2.390

6.4 Criticality Calculations

PROPRIETARY INFORMATION WITHHELD UNDER 10CFR2.390

As mentioned in Section 6.1 the TN-40 is evaluated to demonstrate that the package remains subcritical for all assembly configurations and initial enrichments authorized for storage and shipment in the cask with burnup credit.

6.4.1 Calculational Method

PROPRIETARY INFORMATION WITHHELD UNDER 10CFR2.390

6.4.2 Fuel Loading Optimization

PROPRIETARY INFORMATION WITHHELD UNDER 10CFR2.390

6.4.3 Criticality Results

Table 6-17 lists the bounding results for the burnup credit analysis. The highest calculated k_{eff} , including 2σ uncertainty, and all applicable biases, is 0.9386. The polynomial function that determines the maximum allowable burnup as a function of initial enrichment is listed in Table 6-1. The configurations allowed in Table 6-2 are bounded by the analysis presented herein for all conditions of transport.

These criticality calculations are performed with CSAS25 of SCALE-4.4. For each case, the result includes (1) the KENO-calculated k_{KENO} ; (2) the one sigma uncertainty σ_{KENO} ; and (3) the final k_{eff} , which is equal to $k_{\text{KENO}} + 2\sigma_{\text{KENO}}$.

The criterion for subcriticality is that

$$k_{\text{KENO}} + 2\sigma_{\text{KENO}} + \text{horizontal bias} \leq \text{USL},$$

where USL is the upper subcritical limit established by an analysis of benchmark criticality experiments. From Section 6.5, the minimum USL over the parameter range (in this case, assembly separation, pin pitch) is 0.9415. Using the most reactive case from Table 6-18:

$$k_{\text{KENO}} + 2\sigma_{\text{KENO}} = 0.9354 + 2(0.0008) + 0.0016 = 0.9386 \leq 0.9415.$$

Typical input files for the design basis SAS2H case and the CSAS25 cases are shown in Section 6.7.1 and Section 6.7.2.

6.5 Critical Benchmark Experiments

The criticality safety analysis of the TN-40 cask used the CSAS25 module of the SCALE system of codes. The CSAS25 control module allows simplified data input to the functional modules BONAMI-S, NITAWL-II, and KENO V.a. These modules process the required cross-section data and calculate the k_{eff} of the system. BONAMI-S performs resonance self-shielding calculations for nuclides that have Bondarenko data associated with their cross sections. NITAWL-II applies a Nordheim resonance self-shielding correction to nuclides having resonance parameters. Finally, KENO V.a calculates the effective neutron multiplication (k_{eff}) of a 3-D system.

Criticality codes are verified by comparing benchmark calculations to actual critical benchmark experiments. The difference between the calculated reactivity and the experimental reactivity is referred to as calculational bias. This bias may be a function of system parameters such as fuel lattice separation, fuel enrichment, neutron absorber properties, reflector properties, or fuel/moderator volume ratio, or there may be no specific correlation with system parameters. The purpose of this computer code verification is to statistically determine the magnitude of the calculational bias and whether any such dependencies exist so that they may be properly accounted for in licensing criticality analyses.

The benchmark problems used to perform this verification are representative of benchmark arrays of commercial light water reactor (LWR) fuels with the following characteristics:

1. water moderation
2. boron neutron absorbers
3. close reflection
4. uranium oxide and mixed oxide (MOX) fuels.

The 142 uranium oxide and MOX experiments were chosen to model a wide range of uranium enrichments, fuel pin pitches, assembly separation, and fixed neutron absorbers in order to test the ability of the code to accurately calculate k_{eff} . The benchmark calculations performed for this evaluation were selected from Reference [4].

6.5.1 Benchmark Experiments and Applicability

A summary of all of the pertinent parameters for each experiment is included in Table 6-20 along with the results of each run. The best correlation is observed for fuel assembly separation distance with a correlation of 0.64. All other parameters show much lower correlation ratios indicating no real correlation. All parameters were evaluated for trends and to determine the most conservative USL.

The USL is calculated in accordance with NUREG/CR-6361, [4]. USL Method 1 (USL-1) applies a statistical calculation of the bias and its uncertainty plus an safety margin (0.05) to the linear fit of results of the experimental benchmark data. The basis for the administrative margin is from Reference [5]. Results from the USL evaluation are presented in Table 6-21.

The minimum enrichment of U-235, 1.60 wt.%, that credited in this calculation lies beyond the range of applicability of the benchmark experiments since the minimum is 2.35 wt. % U-235. Guidance for extrapolating the USL-1 values beyond the range of applicability is provided in NUREG/CR-6361 [4]. Extrapolation is permitted if the data is shown to exhibit no trending with enrichment. As shown in Table 6-20, the correlation coefficient for U-235 enrichment with and without soluble boron experiments is 0.31 indicating that there is no trending of k_{eff} with enrichment. Therefore, the USL-1 value for U-235 enrichment can be extrapolated based on the formula shown in Table 6-21.

The criticality evaluation used the same cross section set, fuel materials and similar material/geometry options that were used in the 142 benchmark calculations. The modeling techniques and the applicable parameters listed in Table 6-22 for the actual criticality evaluations fall within the range of those addressed by the benchmarks.

6.5.2 Results of the Benchmark Calculations

The results from the comparisons of physical parameters of each of the fuel assembly types to the applicable USL value are presented in Table 6-22. The minimum value of the USL was determined to be 0.9415 based on comparisons to the limiting assembly parameters as shown in Table 6-22.

6.6 References

1. Oak Ridge National Laboratory, RSIC Computer Code Collection, "SCALE: A Modular Code System for Performing Standardized Computer Analysis for Licensing Evaluations for Workstations and Personal Computers," NUREG/CR-0200, Revision 6, ORNL/NUREG/CSD-2/V2/R6.
2. 10 CFR 71, Packaging and Transportation of Radioactive Materials.
3. M. D. DeHart "SCALE-4 Analysis of Pressurized Water Reactor Critical Configurations: Volume 1 – Summary," Oak Ridge National Laboratory, March 1995, ORNL/TM-12294/V1.
4. U.S. Nuclear Regulatory Commission, "Criticality Benchmark Guide for Light-Water-Reactor fuel in Transportation and Storage Packages," NUREG/CR-6361, Published March 1997, ORNL/TM-13211.
5. U.S. Nuclear Regulatory Commission, "Recommendations for Preparing the Criticality Safety Evaluation of Transportation Packages," NUREG/CR-5661, Published April 1997, ORNL/TM-11936.
6. Oak Ridge National Laboratory, "An Extension of the Validation of SCALE (SAS2H) Isotopic Predictions for PWR Spent Fuel," ORNL/TM-13317, Published September 1996.
7. U.S. Nuclear Regulatory Commission, "Parametric Study of the Effect of Control Rods for PWR Burnup Credit," NUREG/CR-6759, Published February 2002, ORNL/TM-2001/69.
8. U.S. Nuclear Regulatory Commission, "Study of the Effect of Integral Burnable Absorbers for PWR Burnup Credit," NUREG/CR-6760, Published March 2002, ORNL/TM-2000-329.
9. U.S. Nuclear Regulatory Commission, "Parametric Study of the Effect of Burnable Poison Rods for PWR Burnup Credit," NUREG/CR-6761, Published March 2002, ORNL/TM-2000/373.
10. U.S. Nuclear Regulatory Commission, "Recommendations for Addressing Axial Burnup in PWR Burnup Credit Analyses," NUREG/CR-6801, Published March 2003, ORNL/TM-2001/273.
11. "Topical Report on Actinide-Only Burnup Credit for PWR Spent Nuclear Fuel Packages," DOE/RW-0472, Revision 2.

12. U.S. Nuclear Regulatory Commission, "Assessment of Reactivity Margins and Loading Curves for PWR Burnup-Credit Cask Designs," NUREG/CR-6800, Published March 2003, ORNL/TM-2002/6.
13. U.S. Nuclear Regulatory Commission, "Strategies for Application of Isoptic Uncertainties in Burnup-Credit," NUREG/CR-6811, Published June 2003, ORNL/TM-2001/257.

6.7 Input File Listing

6.7.1 SAS2H Input Deck for Design Basis Fuel Assembly – Zone 8

PROPRIETARY INFORMATION WITHHELD UNDER 10CFR2.390

6.7.2 CSAS25 Input Deck for Design Basis Criticality Case

PROPRIETARY INFORMATION WITHHELD UNDER 10CFR2.390

Table 6-1
Minimum Burnup as a Function of Enrichment

Maximum Assembly Average Initial Enrichment (wt. % U-235)	Minimum Assembly Average Burnup (GWD/MTU)
1.60	0
2.30	16
2.85	22
3.30	26
3.85	31

A minimum cooling time of 15 years is required for loading fuel assemblies prior to transport with burnup. The mathematical formula to determine the minimum burnup as a function of initial enrichment is shown below:

$$B = 3.1808 \cdot E^3 - 30.379 \cdot E^2 + 104.46 \cdot E - 102.38$$

where,

B = Minimum Assembly Average Burnup in GWD/MTU, and
E = Maximum Assembly Average Enrichment in wt. % U-235

Table 6-2
Parameters For PWR Assemblies For Shipment

Manufacturer (1)	Array	Version	Active Fuel Length (in)	Number of Fuel Rods per Assembly	Fuel Rod Pitch (in.)	Fuel Pellet OD (in)
Exxon/ANF	14x14	Standard	144	179	0.556	0.3565
Exxon / ANF	14x14	High BU	144	179	0.556	0.3565
Exxon/ANF	14x14	Top Rod	144	179	0.556	0.3505
WE	14x14	Standard	144	179	0.556	0.3659
WE	14x14	OFA	144	179	0.556	0.3444

Manufacturer (1)	Array	Version	Clad Thickness (in)	Clad OD (in)	Guide/ Instrument Tube OD (in)	Guide/ Instrument Tube ID (in)
Exxon/ANF	14x14	Standard	0.0300	0.424	16@0.541 1@0.424	16@0.507 1@0.374
Exxon/ANF	14x14	High BU	0.0310	0.426	16@0.541 1@0.424	16@0.507 1@0.374
Exxon/ANF	14x14	Top Rod	0.02950	0.417	16@0.541 1@0.424	16@0.507 1@0.374
WE	14x14	Standard	0.0243	0.422	16@0.539 1@0.422	16@0.505 1@0.3734
WE	14x14	OFA	0.0243	0.400	16@0.528 1@0.4015	16@0.490 1@0.3499

(1) Equivalent reload assemblies from the manufacturers are also acceptable.

Table 6-3
Required Assembly and Reactor Parameters for SAS2H Models

PROPRIETARY INFORMATION WITHHELD UNDER 10CFR2.390

Table 6-4
Axial Burnup Profiles from Reference [10]

PROPRIETARY INFORMATION WITHHELD UNDER 10CFR2.390

Table 6-5
Modified Axial Burnup Profiles Used for SAS2H Depletion Analysis

PROPRIETARY INFORMATION WITHHELD UNDER 10CFR2.390

Table 6-6
BPRA Design Parameters for SAS2H Models

PROPRIETARY INFORMATION WITHHELD UNDER 10CFR2.390

Table 6-7
Burnup Dependent Horizontal Burnup Gradients

PROPRIETARY INFORMATION WITHHELD UNDER 10CFR2.390

Table 6-8
Basket and Cask Design Dimensions for the CSAS25 Models

PROPRIETARY INFORMATION WITHHELD UNDER 10CFR2.390

Table 6-9
Description of the KENO Model

PROPRIETARY INFORMATION WITHHELD UNDER 10CFR2.390

Table 6-10
Best-Estimate Correction Factors for SAS2H Isotopic Content

PROPRIETARY INFORMATION WITHHELD UNDER 10CFR2.390

Table 6-11
Burned Fuel Isotopic Composition

PROPRIETARY INFORMATION WITHHELD UNDER 10CFR2.390

Table 6-12
Material Property Data

PROPRIETARY INFORMATION WITHHELD UNDER 10CFR2.390

Table 6-13
Material ID IN KENO

PROPRIETARY INFORMATION WITHHELD UNDER 10CFR2.390

Table 6-14
Most Reactive Configuration – Fresh Fuel Assumption

PROPRIETARY INFORMATION WITHHELD UNDER 10CFR2.390

Table 6-15
Most Reactive Configuration – Burned Fuel

PROPRIETARY INFORMATION WITHHELD UNDER 10CFR2.390

Table 6-16
Results of Burnup Credit Calculations

PROPRIETARY INFORMATION WITHHELD UNDER 10CFR2.390

Table 6-17
Moderator Density Variations

Model Description	k_{KENO}	1σ	k_{eff}
Internal Moderator Density (IMD) Variation for 3.85 wt. % U-235, 31 GWD/MTU, 15 Years Cooling, 25 Isotopes			
IMD=01%	0.4463	0.0004	0.4471
IMD=10%	0.5278	0.0005	0.5288
IMD=30%	0.6660	0.0006	0.6672
IMD=50%	0.7744	0.0007	0.7758
IMD=70%	0.8531	0.0008	0.8547
IMD=90%	0.9115	0.0007	0.9129
External Moderator Density (EMD) Variation for 3.85 wt. % U-235, 31 GWD/MTU, 15 Years Cooling, 25 Isotopes			
EMD=01%	0.9336	0.0010	0.9356
EMD=10%	0.9340	0.0007	0.9354
EMD=30%	0.9345	0.0007	0.9359
EMD=50%	0.9339	0.0007	0.9353
EMD=70%	0.9323	0.0008	0.9339
EMD=90%	0.9354	0.0008	0.9370

Table 6-18
Results of the Additional Reactivity Margin Calculations

PROPRIETARY INFORMATION WITHHELD UNDER 10CFR2.390

Table 6-19
Dancoff Factor Calculation for Density Variations

Density	Dancoff Factor
100% Density	2.4848178E-01
090% Density	2.7464780E-01
070% Density	3.4011218E-01
050% Density	4.3231434E-01
030% Density	5.7273322E-01
010% Density	8.0957848E-01
001% Density	9.7393459E-01

Table 6-20
CSAS25 Results

Run ID	U Enrich. wt. %	Pu Enrich. Wt. %	Pitch (cm)	H ₂ O/fuel volume	Separation of assemblies (cm)	AEG	k _{eff}	1 σ
B1645SO1	2.46		1.41	1.015	1.78	32.8118	0.9965	0.0008
B1645SO2	2.46		1.41	1.015	1.78	32.7528	1.0006	0.0008
BW1231B1	4.02		1.511	1.139		31.1429	0.9966	0.0009
BW1231B2	4.02		1.511	1.139		29.8872	0.9990	0.0007
BW1273M	2.46		1.511	1.376		32.2213	0.9961	0.0007
BW1484A1	2.46		1.636	1.841	1.636	34.5373	0.9975	0.0008
BW1484A2	2.46		1.636	1.841	4.908	35.1630	0.9934	0.0008
BW1484B1	2.46		1.636	1.841		33.9415	0.9984	0.0008
BW1484B2	2.46		1.636	1.841	1.636	34.5780	0.9961	0.0009
BW1484B3	2.46		1.636	1.841	4.908	35.2638	0.9978	0.0008
BW1484C1	2.46		1.636	1.841	1.636	34.6547	0.9936	0.0009
BW1484C2	2.46		1.636	1.841	1.636	35.2469	0.9944	0.0010
BW1484S1	2.46		1.636	1.841	1.636	34.5159	1.0002	0.0008
BW1484S2	2.46		1.636	1.841	1.636	34.5530	0.9990	0.0008
BW1484SL	2.46		1.636	1.841	6.544	35.4203	0.9944	0.0009
BW1645S1	2.46		1.209	0.383	1.778	30.1060	0.9987	0.0008
BW1645S2	2.46		1.209	0.383	1.778	29.9920	1.0049	0.0008
BW1810A	2.46		1.636	1.841		33.9524	0.9987	0.0006
BW1810B	2.46		1.636	1.841		33.9711	0.9995	0.0006
BW1810cr	2.46		1.636	1.841		33.1556	0.9995	0.0008
BW1810D	2.46		1.636	1.841		33.0876	0.9981	0.0010
BW1810E	2.46		1.636	1.841		33.1520	0.9991	0.0007
BW1810F	2.46		1.636	1.841		33.9581	1.0029	0.0007
BW1810gr	2.46		1.636	1.841		32.9478	0.9986	0.0007
BW1810H	2.46		1.636	1.841		32.9370	0.9981	0.0008
BW1810I	2.46		1.636	1.841		33.9613	1.0028	0.0007
BW1810J	2.46		1.636	1.841		33.1379	0.9995	0.0008
DSN399-1	4.74		1.6	3.807	1.8	33.9611	1.0047	0.0010
DSN399-2	4.74		1.6	3.807	5.8	34.4255	0.9988	0.0011
DSN399-3	4.74		1.6	3.807		35.3180	1.0035	0.0010
DSN399-4	4.74		1.6	3.807		35.3816	0.9985	0.0010
EPRU65	2.35		1.562	1.196		33.9138	0.9959	0.0008
EPRU65B	2.35		1.562	1.196		33.4073	1.0000	0.0009
EPRU75	2.35		1.905	2.408		35.8676	0.9968	0.0009
EPRU75B	2.35		1.905	2.408		35.3074	1.0002	0.0008
EPRU87	2.35		2.21	3.687		36.6120	1.0011	0.0009
EPRU87B	2.35		2.21	3.687		36.3460	1.0003	0.0008
NSE71SQ	4.74		1.26	1.823		33.7627	0.9978	0.0009
NSE71W1	4.74		1.26	1.823		34.0088	0.9981	0.0010
NSE71W2	4.74		1.26	1.823		34.3856	0.9995	0.0010

Table 6-20
CSAS25 Results Cont'd

Run ID	U Enrich. wt. %	Pu Enrich. Wt. %	Pitch (cm)	H ₂ O/fuel volume	Separation of assemblies (cm)	AEG	k _{eff}	1 σ
P2438BA	2.35		2.032	2.918	5.05	36.2244	0.9973	0.0009
P2438SLG	2.35		2.032	2.918	8.39	36.2906	0.9985	0.0009
P2438SS	2.35		2.032	2.918	6.88	36.2690	0.9979	0.0009
P2438ZR	2.35		2.032	2.918	8.79	36.2891	0.9976	0.0009
P2615BA	4.31		2.54	3.883	6.72	35.7276	1.0005	0.0011
P2615SS	4.31		2.54	3.883	8.58	35.7456	0.9959	0.0011
P2615ZR	4.31		2.54	3.883	10.92	35.7709	0.9980	0.0010
P2827L1	2.35		2.032	2.918	13.72	36.2491	1.0051	0.0008
P2827L2	2.35		2.032	2.918	11.25	36.2939	1.0005	0.0010
P2827L3	4.31		2.54	3.883	20.78	35.6740	1.0095	0.0009
P2827L4	4.31		2.54	3.883	19.04	35.7173	1.0066	0.0010
P2827SLG	2.35		2.032	2.918	8.31	36.3010	0.9957	0.0008
P3314BA	4.31		1.892	1.6	2.83	33.1874	1.0000	0.0009
P3314BC	4.31		1.892	1.6	2.83	33.2334	0.9992	0.0009
P3314BF1	4.31		1.892	1.6	2.83	33.2422	1.0024	0.0009
P3314BF2	4.31		1.892	1.6	2.83	33.2121	1.0001	0.0010
P3314BS1	2.35		1.684	1.6	3.86	34.8545	0.9957	0.0010
P3314BS2	2.35		1.684	1.6	3.46	34.8324	0.9940	0.0008
P3314BS3	4.31		1.892	1.6	7.23	33.4328	0.9996	0.0009
P3314BS4	4.31		1.892	1.6	6.63	33.4152	1.0000	0.0008
P3314SLG	4.31		1.892	1.6	2.83	34.0109	0.9971	0.0010
P3314SS1	4.31		1.892	1.6	2.83	33.9613	0.9984	0.0010
P3314SS2	4.31		1.892	1.6	2.83	33.7719	1.0014	0.0009
P3314SS3	4.31		1.892	1.6	2.83	33.8956	0.9995	0.0010
P3314SS4	4.31		1.892	1.6	2.83	33.7604	0.9962	0.0009
P3314SS5	2.35		1.684	1.6	7.8	34.9476	0.9947	0.0010
P3314SS6	4.31		1.892	1.6	10.52	33.5406	1.0010	0.0008
P3314W1	4.31		1.892	1.6		34.3962	1.0009	0.0010
P3314W2	2.35		1.684	1.6		35.2153	0.9972	0.0008
P3314ZR	4.31		1.892	1.6	2.83	33.9897	0.9977	0.0010
P3602BB	4.31		1.892	1.6	8.3	33.3198	1.0031	0.0010
P3602BS1	2.35		1.684	1.6	4.8	34.7746	1.0034	0.0009
P3602BS2	4.31		1.892	1.6	9.83	33.3649	1.0047	0.0010
P3602N11	2.35		1.684	1.6	8.98	34.7410	1.0025	0.0008
P3602N12	2.35		1.684	1.6	9.58	34.8378	1.0048	0.0009
P3602N13	2.35		1.684	1.6	9.66	34.9334	1.0006	0.0009
P3602N14	2.35		1.684	1.6	8.54	35.0287	0.9969	0.0010
P3602N21	2.35		2.032	2.918	10.36	36.2787	0.9999	0.0009
P3602N22	2.35		2.032	2.918	11.20	36.1963	1.0014	0.0008
P3602N31	4.31		1.892	1.6	14.87	33.2015	1.0063	0.0010

Table 6-20
CSAS25 Results Cont'd

Run ID	U Enrich. wt. %	Pu Enrich. Wt. %	Pitch (cm)	H ₂ O/fuel volume	Separation of assemblies (cm)	AEG	k _{eff}	1 σ
P3602N32	4.31		1.892	1.6	15.74	33.3085	1.0072	0.0010
P3602N33	4.31		1.892	1.6	15.87	33.4168	1.0084	0.0010
P3602N34	4.31		1.892	1.6	15.84	33.4653	1.0028	0.0010
P3602N35	4.31		1.892	1.6	15.45	33.5169	1.0030	0.0009
P3602N36	4.31		1.892	1.6	13.82	33.5832	1.0003	0.0010
P3602N41	4.31		2.54	3.883	12.89	35.5269	1.0127	0.0010
P3602N42	4.31		2.54	3.883	14.12	35.6711	1.0068	0.0009
P3602N43	4.31		2.54	3.883	12.44	35.7505	1.0049	0.0009
P3602SS1	2.35		1.684	1.6	8.28	34.8708	1.0007	0.0009
P3602SS2	4.31		1.892	1.6	13.75	33.4133	1.0026	0.0010
P3926L1	2.35		1.684	1.6	10.06	34.8569	1.0003	0.0009
P3926L2	2.35		1.684	1.6	10.11	34.9374	1.0020	0.0008
P3926L3	2.35		1.684	1.6	8.5	35.0657	0.9967	0.0010
P3926L4	4.31		1.892	1.6	17.74	33.3262	1.0066	0.0009
P3926L5	4.31		1.892	1.6	18.18	33.4035	1.0054	0.0010
P3926L6	4.31		1.892	1.6	17.43	33.5141	1.0038	0.0009
P3926SL1	2.35		1.684	1.6	6.59	35.0674	0.9950	0.0009
P3926SL2	4.31		1.892	1.6	12.79	33.5810	0.9998	0.0009
P4267B1	4.31		1.890	1.59		31.7989	0.9992	0.0008
P4267B2	4.31		1.890	1.59		31.5288	1.0027	0.0007
P4267B3	4.31		1.715	1.09		30.9907	1.0057	0.0009
P4267B4	4.31		1.715	1.09		30.5098	0.9993	0.0008
P4267B5	4.31		1.715	1.09		30.1008	1.0009	0.0008
P4267SL1	4.31		1.89	1.59		33.4692	0.9987	0.0011
P4267SL2	4.31		1.715	1.09		31.9346	0.9995	0.0011
P62FT231	4.31		1.891	1.6	5.67	32.9228	1.0020	0.0009
P71F14F3	4.31		1.891	1.6	5.19	32.8227	1.0009	0.0010
P71F14V3	4.31		1.891	1.6	5.19	32.8587	0.9977	0.0010
P71F14V5	4.31		1.891	1.6	5.19	32.8662	0.9980	0.0010
P71F214R	4.31		1.891	1.6	5.19	32.8669	0.9976	0.0009
PAT80L1	4.74		1.6	3.807	2.0	35.0276	1.0014	0.0009
PAT80L2	4.74		1.6	3.807	2.0	35.1079	0.9986	0.0011
PAT80SS1	4.74		1.6	3.807	2.0	35.0125	0.9998	0.0009
PAT80SS2	4.74		1.6	3.807	2.0	35.1128	0.9967	0.0010
W3269A	5.7		1.422	1.93		33.1383	0.9976	0.0009
W3269B1	3.7		1.105	1.432		32.4010	0.9962	0.0008
W3269B2	3.7		1.105	1.432		32.3940	0.9965	0.0008
W3269B3	3.7		1.105	1.432		32.2464	0.9945	0.0008
W3269C	2.72		1.524	1.494		33.7731	0.9979	0.0009

Table 6-20
CSAS25 Results
(Concluded)

Run ID	U Enrich. wt. %	Pu Enrich. Wt. %	Pitch (cm)	H ₂ O/fuel volume	Separation of assemblies (cm)	AEG	k _{eff}	1 σ
W3269SL1	2.72		1.524	1.494		33.3854	0.9973	0.0010
W3269SL2	5.7		1.422	1.93		33.1006	1.0024	0.0010
W3269W1	2.72		1.524	1.494		33.5160	0.9972	0.0012
W3269W2	5.7		1.422	1.93		33.1786	1.0015	0.0010
W3385SL1	5.74		1.422	1.932		33.2320	1.0004	0.0009
W3385SL2	5.74		2.012	5.067		35.8876	1.0014	0.0010
BAW1484A	2.46		1.636	1.84	1.636	34.6521	0.9942	0.0008
E196U6N	2.35		1.5621	1.2		33.9138	0.9959	0.0008
E196U87C	2.35		2.2098	3.69		36.6120	1.0011	0.0009
P2438X24	2.35		2.032	2.92	8.67	36.2930	0.9969	0.0008
SAXU56	5.74		1.4224	1.93		33.2826	0.9966	0.0011
SAXU792	5.74		2.0117	5.07		35.9058	0.9985	0.0010
EPRI70UN	0.71	2	1.778	1.2		31.6715	0.9983	0.0010
EPRI70B	0.71	2	1.778	1.2		30.9080	0.9999	0.0010
EPRI87B	0.71	2	2.2098	1.53		33.3225	1.0077	0.0009
EPRI99UN	0.71	2	2.5146	3.64		35.1831	1.0066	0.0009
EPRI99B	0.71	2	2.5146	3.64		34.4193	1.0099	0.0009
SAXTON52	0.71	6.6	1.3208	1.68		30.2872	1.0011	0.0010
SAXTON56	0.71	6.6	1.4224	2.16		31.4804	1.0004	0.0012
SAXTN56B	0.71	6.6	1.4224	2.16		31.0115	0.9997	0.0009
SAXTN735	0.71	6.6	1.8669	4.7		34.1857	1.0019	0.0011
SAXTN792	0.71	6.6	2.01168	5.67		34.6577	1.0026	0.0010
SAXTN104	0.71	6.6	2.6416	10.75		35.8301	1.0051	0.0009
Correlation	0.31	-0.37	0.46	0.25	0.63	-0.01	N/A	N/A
Correlation (without Soluble Boron)	0.31	-0.37	0.49	0.27	0.66	0.00	N/A	N/A

Table 6-21
USL-1 Results

Parameter	Range of Applicability	Formula for USL-1 (5% Margin)
U Enrichment (wt% U-235) (all experiments)	2.35 – 5.74	$0.9406 + (9.7267\text{E-}04) * X$ ($X < 3.7186$) 0.9442 ($X \geq 3.7186$)
U Enrichment (wt% U-235) (excluding soluble boron)	2.35 – 5.74	$0.9398 + (1.0481\text{E-}03) * X$ ($X < 3.7865$) 0.9437 ($X \geq 3.7865$)
Pu Enrichment (wt% Pu)	2.0 – 6.6	0.9424
Fuel Rod Pitch (cm) (all experiments)	1.10– 2.64	$0.9351 + (5.2323\text{E-}03) * X$ ($X < 1.7753$) 0.9443 ($X \geq 1.7753$)
Fuel Rod Pitch (cm) (excluding soluble boron)	1.10– 2.64	$0.9339 + (5.6645\text{E-}03) * X$ ($X < 1.7861$) 0.9440 ($X \geq 1.7861$)
Water/Fuel Volume Ratio	0.38- 10.8	$0.9415 + (7.3797\text{E-}04) * X$ ($X < 2.1094$) 0.9431 ($X \geq 2.1094$)
Assembly Separation (cm) (all experiments)	1.64 – 20.8	$0.9410 + (4.9375\text{E-}04) * X$ ($X < 6.9867$) 0.9444 ($X \geq 6.9867$)
Assembly Separation (cm) (excluding soluble boron)	1.64 – 20.8	$0.9405 + (5.3296\text{E-}04) * X$ ($X < 7.4071$) 0.9444 ($X \geq 7.4071$)
Average Energy Group Causing Fission (AEG)	29.9 – 36.6	$0.9449 + (-3.2943\text{E-}05) * X$ ($X > 35.689$) 0.9437 ($X \leq 35.689$)

Table 6-22
USL Determination for Criticality Analysis

Parameter	Value from Limiting WE 14x14 Analysis	Bounding USL
Enrichment (wt. % U-235) (all experiments)	1.60 (minimum) ⁽¹⁾	0.9421
Enrichment (wt. % U-235) (excluding soluble boron)	1.60 (minimum) ⁽¹⁾	0.9415
Enrichment (wt. % Pu) (all experiments)	Not relevant since there is no variation in the USL	0.9424
Pin Pitch (cm) (all experiments)	1.412	0.9425
Pin Pitch (cm) (excluding soluble boron)	1.412	0.9419
Water to Fuel Volume Ratio	1.610 ⁽²⁾	0.9427
Assembly Separation (cm) (all experiments)	1.92 ⁽³⁾	0.9419
Assembly Separation (cm) (excluding soluble boron)	1.92 ⁽³⁾	0.9415
Average Energy Group Causing Fission (AEG)	< 34 ⁽⁴⁾	0.9437

- 1) Extrapolation of the USL-1 formula is performed at this enrichment to determine the minimum USL since the k_{eff} data showed no trending with enrichment.
- 2) The water to fuel volume ratio is calculated using 179 rods.
- 3) Separation Distance = $2*(0.09") + 2*(0.250) + 0.075" = 0.755" \sim 1.92$ cm, calculated with nominal dimensions for the stainless steel in the fuel compartment, nominal boron and aluminum plate width and inward fuel assembly positioning.
- 4) Examination of the results shows that the value is between 32 and 34 and hence a conservative value that produces the minimum USL was chosen.

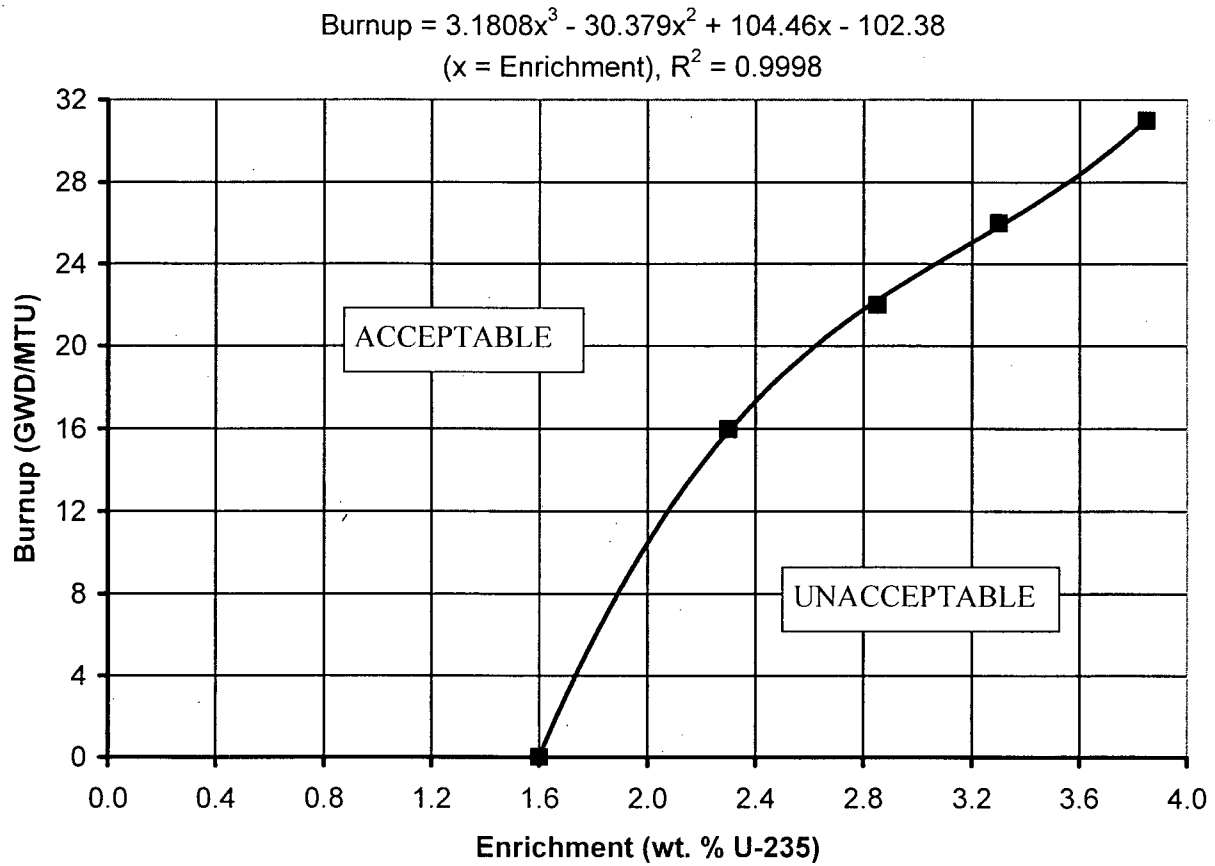


Figure 6-1
TN-40 Loading Curve

Figure 6-2
Example SAS2H Model

PROPRIETARY INFORMATION WITHHELD UNDER 10CFR2.390

Figure 6-3
Fuel Assembly Positions within the Basket

PROPRIETARY INFORMATION WITHHELD UNDER 10CFR2.390

Figure 6-4
Radial Cross Section of the Basket with Centered Fuel Assemblies

PROPRIETARY INFORMATION WITHHELD UNDER 10CFR2.390

Figure 6-5
Radial Cross Section of the Basket with Stainless Steel

PROPRIETARY INFORMATION WITHHELD UNDER 10CFR2.390

Figure 6-6
Axial Cross Section of the Basket with Cuboid Plugs

PROPRIETARY INFORMATION WITHHELD UNDER 10CFR2.390

Figure 6-7
Radial Cross Section of the Basket with Inward Fuel Assemblies

PROPRIETARY INFORMATION WITHHELD UNDER 10CFR2.390

Figure 6-8
TN-40 KENO Model for Horizontal Burnup Gradient

PROPRIETARY INFORMATION WITHHELD UNDER 10CFR2.390

Figure 6-9
TN-40 KENO Model with Internal Moderator between Poison Plates

PROPRIETARY INFORMATION WITHHELD UNDER 10CFR2.390

Figure 6-10
TN-40 KENO Model for Cask A Loading Configuration

PROPRIETARY INFORMATION WITHHELD UNDER 10CFR2.390

Figure 6-11
TN-40 KENO Model for Cask B Loading Configuration

PROPRIETARY INFORMATION WITHHELD UNDER 10CFR2.390

Figure 6-12
TN-40 KENO Model for Cask C Loading Configuration

PROPRIETARY INFORMATION WITHHELD UNDER 10CFR2.390

CHAPTER 7

OPERATING PROCEDURES

TABLE OF CONTENTS

	<u>PAGE</u>
7.0 OPERATING PROCEDURES	7-1
7.1 Package Loading	7-1
7.1.1 Preparation for Loading	7-1
7.1.2 Loading.....	7-2
7.1.3 Preparation for Transport	7-3
7.2 Package Unloading.....	7-5
7.2.1 Receipt of Package from Carrier	7-5
7.2.2 Preparation for Unloading.....	7-6
7.2.3 Contents Removal.....	7-7
7.3 Preparation Of Empty Package For Transport.....	7-8
7.4 Other Procedures	7-10
7.4.1 Preparation of Cask Used in Storage for Transport.....	7-10
7.5 References	7-13

LIST OF FIGURES

Figure 7-1	Torquing Patterns	7-14
Figure 7-2	Typical Setup for Filling Cask with Water.....	7-15

7.0 OPERATING PROCEDURES

This chapter contains TN-40 transport package loading and unloading procedures that are intended to show the general approach to cask operational activities. A separate Operations Manual (OM) will be prepared for the TN-40 transport package to describe the operational steps in greater detail. The OM, along with the information in this chapter, will be used to prepare the site-specific procedures that will address the particular operational considerations related to the TN-40 cask. The operations required to convert the TN-40 cask from its storage configuration to its transport configuration are also described here.

7.1 Package Loading

For the TN-40 casks that have been loaded and used for storage under 10CFR72 requirements, use procedures for preparation of casks for transport described in Section 7.4.

7.1.1 Preparation for Loading

7.1.1.1 Upon arrival of the empty packaging, on its transport vehicle (rail or heavy haul trailer) and shipping frame, perform a receipt inspection to check for any damages or irregularities. Verify that the records for the packaging are complete and accurate.

7.1.1.2 Remove the personnel barrier (if used), security device, the impact limiter attachment bolts, tie-rods, and the associated hardware, as necessary.

7.1.1.3 If they are mounted on the cask, remove the front and the rear impact limiters, as well as the top impact limiter spacer.

7.1.1.4 Remove the tie-down straps.

7.1.1.5 Clean the external surfaces of the cask, if necessary, to get rid of the road dirt.

7.1.1.6 Using a spreader bar and lifting straps, lift the cask from the transport frame and lower it onto the upending/downending frame.

7.1.1.7 Attach the lift beam to the cask handling crane hook, and engage the lift beam to the two upper (top) trunnions.

7.1.1.8 Rotate the cask slowly from the horizontal to the vertical position.

7.1.1.9 Lift the cask from the transport/shipping frame and place it in the cask preparation area.

- 7.1.1.10 Disengage the lift beam from the cask.
- 7.1.1.11 Replace the neutron shield pressure relief valve with a plug.
- 7.1.1.12 Remove the lid bolts and the lid.
- 7.1.1.13 Remove the lid seal, vent and drain port cover seals and overpressure (OP) port seals and inspect the sealing surfaces. Install new seals in the vent and drain port covers and the lid. This step may be performed at any time prior to closing the loaded cask.
- 7.1.1.14 Visually inspect the bolts and the bolt hole threads for the lid, vent, drain, and OP ports.
- 7.1.1.15 Verify that the basket is installed in the cask. Verify that there is no foreign material in the cask.
- 7.1.1.16 Move the cask to the cask loading area using the lift beam attached to the top trunnions.

7.1.2 Loading

Note: The term 'cask loading pool' is used to describe the area where the cask is to be loaded.

- 7.1.2.1 Lower the cask into the cask loading pool and fill the interior with water.
- 7.1.2.2 Disengage the lift beam and move it aside.
- 7.1.2.3 Load the pre-selected spent fuel assemblies into the basket compartments. Procedures shall be developed to ensure that the fuel loaded into the cask meets the fuel specifications in Section 1.2.3 of the SAR.
- 7.1.2.4 Verify the identity of the fuel assemblies loaded into the cask, and document the location of each fuel assembly on the cask loading report.
- 7.1.2.5 Configure the lid prior to installation so that water may be drained through the drain port and that helium can be used to fill the cask as the water is drained. Using the lift beam and the lid lifting slings, lower the lid onto the cask shell flange over the two alignment pins.
- 7.1.2.6 Engage the lift beam on the upper (top) trunnions, and lift the cask so that the top of the cask is above the pool water surface, and install some of the lid bolts. The lid bolts should be hand tight.

Note: Throughout this procedure, all bolt threads are to be coated with Nuclear Grade Neolube, Loctite N-5000, or equivalent.

7.1.2.7 Using the drain port in the lid, drain water from the cask and fill the resulting void space with helium. This may be done either before or after lifting the cask out of the pool depending on the maximum lift capacity. If the pool contains borated water, the effects of adding this non-borated water to the pool must be considered. While lifting the cask out of the pool, the exterior of the cask may be rinsed with clean demineralized water to facilitate decontamination.

7.1.2.8 Move the cask to the decontamination area and disengage the lift beam.

7.1.3 Preparation for Transport

Caution: The maximum potential for worker exposure exists during the decontamination of the cask and other operations near the lid, after the water is pumped out of the cask. Worker exposure can be minimized by use of temporary shielding (lead "bean bags," plastic neutron shielding, etc.), and by minimizing the exposure time and maximizing the distance, as well as using any measures to facilitate decontamination.

7.1.3.1 Decontaminate the cask until acceptable surface contamination levels are obtained.

7.1.3.2 Install the remaining lid bolts and torque them to 1125 ± 25 ft-lb. Follow the torquing sequence shown in Figure 7-1. A circular pattern of torquing may be used after the final pass to eliminate further bolt movement.

7.1.3.3 Remove the plug from the neutron shield vent, and reinstall the pressure relief valve, making sure that it is operable and set.

7.1.3.4 Evacuate the cask cavity using the Vacuum Drying System (VDS) to remove the remaining moisture, and verify the dryness as follows:

Remove any excess water from the seal areas through the passageways at the overpressure drain and vent ports.

If it is installed, remove the quick disconnect from the drain port, and install the drain port cover. Torque the bolts to 40 - 44 ft-lbs using the sequence shown in Figure 7-1.

With the vent port quick disconnect removed to improve evacuation, connect the VDS to a flanged vacuum connector installed over the vent port. Purge or evacuate the helium supply lines and evacuate the cask to 4 millibar (4 x

10^{-4} MPa) or less. Make provisions to prevent or correct any icing of the evacuation lines, if necessary.

Close the valve at the cask and shut off or disconnect the vacuum pump. If, in a period of 30 minutes, the pressure does not exceed 4 millibar (4×10^{-4} MPa), the cask is adequately dried. Otherwise, repeat the vacuum pumping until this criterion is met within 36 hours.

Backfill the evacuated cask cavity with helium (minimum 99.99% purity), to slightly above atmospheric pressure. Then, remove the vacuum connector and immediately install the quick disconnect fitting.

Attach the vacuum/backfill manifold to the vent port fitting, purge or evacuate the helium supply lines, and re-evacuate the cask to below 100 mbar.

- 7.1.3.5 Isolate the vacuum pump, and backfill the cask cavity to approximately 1.5 atm abs (7.4 psig) with helium (minimum 99.99% purity). Note: Equilibrium cavity pressure shall be 2.0 atm abs, maximum)
- 7.1.3.6 Install the vent port cover. For ports containing quick-disconnects, purge the cavity below the cover with helium. Install the port cover. (A partial pressure of 50% helium under the cover may be assumed for leak test calculations.) Torque the coverbolts to 40 - 44 ft-lb following the torquing sequence shown in Figure 7-1 prior to leak testing. This may be followed by torquing in a circular pattern to verify no motion.
- 7.1.3.7 Leak test the inner lid, inner vent and drain port cover seals. The maximum acceptable cask seal leak rate is 1×10^{-4} ref cm^3/sec . The leak test shall be performed in accordance with ANSI N14.5 [1].
- 7.1.3.8 If the cask does not pass the leak test, determine and correct the source of the leak. Repeat the leak test.
- 7.1.3.9 If the cask still does not pass the leak test, evaluate the test method or return the cask to the pool and replace the lid seals.
- 7.1.3.10 Re-engage the lift beam to the upper (top) trunnions of the cask.
- 7.1.3.11 Move the transport vehicle with transport frame in place into the loading position and prepare the upending/downending frame.
- 7.1.3.12 Lift the cask off the decontamination pad, and place the rear trunnions on the rear trunnion supports of the upending/downending frame.
- 7.1.3.13 Rotate the cask from the vertical to the horizontal position.
- 7.1.3.14 Using a spreader bar and lifting straps, lift the cask from the upending/downending frame and lower it onto the transport frame.

- 7.1.3.15 Install the tie-down straps.
- 7.1.3.16 Check if the surface dose rates and the surface contamination levels are within the regulatory limits.
- 7.1.3.17 Prior to installing the impact limiters, inspect them visually for damage. The impact limiters may not be used without repair if any wood has been exposed. Damage due to handling other than small dings and scratches must be evaluated for their effect on the performance during the hypothetical drop and puncture accidents.
- 7.1.3.18 Install the top impact limiter spacer on the front end (lid end) of the cask then remove the spacer lifting eye bolts.
- 7.1.3.19 Install the front (top) and the rear (bottom) impact limiters onto the cask. Lubricate the attachment bolts with Loctite N-5000 or an equivalent and torque to 60 - 80 ft-lb.
- 7.1.3.20 Install thirteen impact limiter attachment tie-rods between the front and the rear impact limiters.
- 7.1.3.21 Render the impact limiter lifting lugs inoperable by covering the lifting holes or installing a bolt inside the holes to prevent their inadvertent use.
- 7.1.3.22 Install security seal on one tie-rod and lock sleeve.
- 7.1.3.23 Install the personnel barrier.
- 7.1.3.24 Check the temperature on all accessible surfaces to make sure that it is <185°F.
- 7.1.3.25 Perform a final radiation and contamination survey to satisfy the shield test requirements and to assure compliance with 10 CFR 71.47 and 71.87.
- 7.1.3.26 Apply appropriate DOT labels and placards in accordance with 49 CFR 172. Prepare the final shipping documentation.
- 7.1.3.27 Release the loaded cask for shipment.

7.2 Package Unloading

7.2.1 Receipt of Package from Carrier

- 7.2.1.1 Upon arrival of the loaded cask, perform a receipt inspection of the cask to check for any damage or irregularities. Verify that the security seal is intact, and perform a radiation survey.

- 7.2.1.2 Verify that the records for the packaging are complete and accurate.
- 7.2.1.3 Remove the personnel barrier, the security seal, tie-rods, and the associated hardware. Remove the impact limiter attachment bolts.
- 7.2.1.4 Render the impact limiter lifting lugs operable by removing the covering on the lifting holes or the bolt inside the lifting holes, that prevented their inadvertent use.
- 7.2.1.5 Remove the front and rear impact limiters as well as the top impact limiter spacer, using a suitable crane and a two-legged sling or an equivalent.
- 7.2.1.6 Remove the tie down straps.
- 7.2.1.7 Place an upending/downending frame near the transport vehicle.
- 7.2.1.8 Using a spreader bar and lift slings, lift the cask from the transport vehicle and place it on the upending/downending frame.
- 7.2.1.9 Attach the lift beam to the cask handling crane hook, and then engage the lift beam to the two upper (top) trunnions.
- 7.2.1.10 Rotate the cask slowly from the horizontal to the vertical position.
- 7.2.1.11 Lift the cask from the upending/downending frame, and place it in the designated work area.
- 7.2.1.12 Disengage the lift beam from the cask, and move the crane as well as the lift beam from the area.
- 7.2.1.13 Clean the external surfaces of the cask, if necessary, to get rid of the road dirt.
- 7.2.1.14 Remove the neutron shield pressure relief valve, and install the plug in the neutron shield vent hole.
- 7.2.2 Preparation for Unloading
 - 7.2.2.1 Remove the vent cover.
 - 7.2.2.2 Collect a cavity gas sample through the vent port quick-disconnect coupling.
 - 7.2.2.3 Analyze the gas sample for radioactive material, and add necessary precautions based on the cavity gas sample results.

Note: If degraded fuel is suspected, additional measures, appropriate for the specific conditions, are to be planned, reviewed, and approved by the appropriate site personnel, as well as implemented to minimize worker exposures and radiological releases to the environment. These additional measures may include provision of filters, as well as respiratory protection and other methods to control releases and exposures to ALARA.

- 7.2.2.4 In accordance with the site requirements, vent the cavity gas through the vent port until atmospheric pressure is reached.

Note: The following procedure is for wet unloading. Alternate dry (hot cell) unloading procedures are acceptable.

- 7.2.2.5 Remove the vent port quick-disconnect and the drain port cover. Attach the vent port adapter and the drain port quick-disconnect, if utilized.

- 7.2.2.6 Loosen the lid bolts and remove all but six lid bolts, approximately equally spaced.

- 7.2.2.7 Attach the cask to the crane using a lift beam. Attach the lid lifting equipment.

- 7.2.2.8 Attach the fill and drain lines to the drain port and the vent port.

- 7.2.2.9 Ensure that appropriate measures are in place for proper handling of steam. Both fill and drain lines should be designed for a minimum of 100 psig steam, to prevent steam burns and radiation exposures due to a possible line failure.

- 7.2.2.10 Lower the cask into the spent fuel pool cask pit. Lower the cask until the top surface is just above the water level.

Note: If the maximum lift weight is not exceeded, the cask may be filled with pool water before lowering the cask into the pool or while the cask is partially submerged in the spent fuel pool.

7.2.3 Contents Removal

- 7.2.3.1 Begin pumping pool or demineralized water into the cask through the drain port, at a rate of 1 gpm, while continuously monitoring the exit-pressure (see Figure 7-2). Continue pumping the water at a rate of 1 gpm for at least 80 minutes. By this time, the water level in the cask will have reached the active fuel length. If the pool contains borated water, the effects of adding non-borated water to the pool must be considered.

- 7.2.3.2 The flow rate can then be gradually increased, while monitoring the pressure at the outlet. If the pressure gage reading exceeds 55.3 psig, close the inlet valve until the pressure falls below 50 psig. Re-flooding may then be resumed.
- 7.2.3.3 When the cask is full of water, remove the hoses from the drain and vent ports. Remove the remaining six lid bolts.
- 7.2.3.4 Lower the cask and place it in the cask loading area of the pool.
- 7.2.3.5 Raise the lift beam from the cask, removing the cask lid.
- 7.2.3.6 Unload the spent fuel assemblies in accordance with the site procedures.
- 7.2.3.7 At least one lid penetration must be completely open (both port cover and quick-disconnect fitting removed) prior to installation of the lid. Using the lift beam and lid lifting slings, lower the lid placing it on the cask shell flange, over the two alignment pins.
- 7.2.3.8 Engage the lift beam on the upper (top) trunnions, and lift the cask out of the pool.
- 7.2.3.9 Using the drain port in the lid, drain the water from the cask in accordance with the procedures. This may be done either before or after lifting the cask out of the pool. While lifting the cask out of the pool, the exterior of the cask may be rinsed with clean demineralized water to facilitate decontamination. If the pool contains borated water, the effects of adding non-borated water to the pool must be considered.
- 7.2.3.10 Disconnect the drain line.
- 7.2.3.11 Move the cask to the decontamination area, and disengage the lift beam.

7.3 Preparation Of Empty Package For Transport

- 7.3.1 Decontaminate the cask until acceptable surface contamination levels are obtained.
- 7.3.2 Lubricate and install the lid bolts and torque them to 400 ft-lb. Follow the torquing sequence shown in Figure 7-1. A circular pattern of torquing may be used afterwards to eliminate further bolt movement.
- 7.3.3 Remove the plug from the neutron shield vent, and reinstall the pressure relief valve, making sure that it is operable and set.

- 7.3.4 If required by user or shipper, evacuate the cask cavity using the Vacuum Drying System (VDS) to remove the remaining moisture.
- 7.3.5 Isolate the vacuum pump, and backfill the cask cavity with nitrogen.
- 7.3.6 Install the vent and drain port covers.
- 7.3.7 Re-engage the lift beam to the upper (top) trunnions of the cask.
- 7.3.8 Move the transport vehicle with transport frame installed into the loading position and place the upending/downending frame near the transport vehicle.
- 7.3.9 Lift the cask off the decontamination pad, and place the rear trunnions on the rear trunnion supports of the upending/downending frame.
- 7.3.10 Rotate the cask from the vertical to the horizontal position.
- 7.3.11 Using a spreader bar and lift slings, lift the cask from the upending/downending frame and place it on the transport frame.
- 7.3.12 Install the tie-down straps.
- 7.3.13 Check if the surface dose rates and the surface contamination levels are within the regulatory limits for an empty cask.

Note: If the impact limiters are going to be shipped separately, skip the next 4 steps.
- 7.3.14 Install the top impact limiter spacer on the front end of the cask. Then remove the spacer lifting eye bolts.
- 7.3.15 Install the front and the rear impact limiters onto the cask. Lubricate the attachment bolts with Loctite N-5000 or an equivalent, and torque to 60 - 80 ft-lb.
- 7.3.16 Install thirteen impact limiter attachment tie-rods between the front and the rear impact limiters.
- 7.3.17 Render the impact limiter lifting lugs inoperable, by covering the lifting holes or installing a bolt inside the holes to prevent their inadvertent use.
- 7.3.18 Perform a final radiation and contamination survey to satisfy the shield test requirements and to assure compliance with 10 CFR 71.47 and 71.87.
- 7.3.19 Install the personnel barrier.

7.3.20 Apply appropriate DOT labels and placards in accordance with 49 CFR 172, and prepare the final shipping documentation.

7.3.21 Release the empty cask for shipment.

7.4 Other Procedures

7.4.1 Preparation of Cask Used in Storage for Transport

The TN-40 cask is designed for storage as well as transport. The following steps are required to convert the TN-40 from its storage configuration to the transport configuration. In some cases, the casks which have been used for storage may not have the transport regulatory plate or nameplate installed on them. These plates must be installed prior to transport. In addition, some casks that have been used for storage may not have the impact limiter bracket mounts installed. As required, the mounts must be welded to the outer shell for transport.

7.4.1.1 Review the loading records and ensure that the fuel within the storage cask meets the fuel qualification requirements for the transport.

Note: The following steps may be performed at the ISFSI site. However, space and equipment requirements may require all operations to be performed at the plant loading area. The following steps permit either option.

A. Storage Area

7.4.1.2 Disconnect the overpressure system from the monitoring panel. Depressurize the overpressure tank and disconnect the tubing at the protective cover.

Note: The following 4 steps may not be necessary if preparation is done on the storage pad

7.4.1.3 Position the cask transporter over the cask.

7.4.1.4 Engage the lifting arms and lift the cask to the designated lift height.

7.4.1.5 Move the cask to the loading area.

7.4.1.6 Lower the cask down onto the floor, disconnect the cask transporter and remove the transporter from the loading area.

B. Loading Area

- 7.4.1.7 Remove the protective cover.
- 7.4.1.8 Tighten the transport lid bolts to 1125 ± 25 ft-lb following the torquing sequence shown in Figure 7-1.
- 7.4.1.9 Remove the overpressure tank assembly and the top neutron shield.
- 7.4.1.10 Remove the vent port cover and utilizing the quick connect valve, adjust the cavity pressure to 14.7 psig maximum.
- 7.4.1.11 Reinstall the vent port cover.
- 7.4.1.12 For ports containing quick-disconnects, purge the cavity below the cover with helium. Install the port cover. (A partial pressure of 50% helium under the cover may be assumed for leak test calculations.) Torque the coverbolts to 40 - 44 ft-lb following the torquing sequence shown in Figure 7-1 prior to leak testing. This may be followed by torquing in a circular pattern to verify no motion.
- 7.4.1.13 Leak test the inner lid, inner vent and drain port cover seals. The maximum acceptable cask seal leak rate is 1×10^{-4} ref cm³/sec. The leak test shall be performed in accordance with ANSI N14.5 [1].
- 7.4.1.14 If the cask does not pass the leak test, determine and correct the source of the leak. Repeat the leak test.
- 7.4.1.15 If the cask still does not pass the leak test, evaluate the test method or return the cask to the pool and replace the lid seals.
- 7.4.1.16 Re-engage the lift beam to the upper (top) trunnions of the cask.
- 7.4.1.17 Move the transport vehicle with transport frame in place into the loading position and prepare the upending/downending frame.
- 7.4.1.18 Lift the cask, and place the rear trunnions on the rear trunnion supports of the upending/downending frame.
- 7.4.1.19 Rotate the cask from the vertical to the horizontal position.
- 7.4.1.20 Using a spreader bar and lifting straps, lift the cask from the upending/downending frame and lower it onto the transport frame.
- 7.4.1.21 Install the tie-down straps.

- 7.4.1.22 Check if the surface dose rates and the surface contamination levels are within the regulatory limits.
- 7.4.1.23 Prior to installing the impact limiters, inspect them visually for damage. The impact limiters may not be used without repair if any wood has been exposed. Damage due to handling other than small dings and scratches must be evaluated for their effect on the performance during the hypothetical drop and puncture accidents.
- 7.4.1.24 Install the top impact limiter spacer on the front end (lid end) of the cask and then remove the spacer lifting eye bolts.
- 7.4.1.25 Install the front (top) and the rear (bottom) impact limiters onto the cask. Lubricate the attachment bolts with Loctite N-5000 or an equivalent and torque to 60 - 80 ft-lb in the final pass.
- 7.4.1.26 Install thirteen impact limiter attachment tie-rods between the front and the rear impact limiters.
- 7.4.1.27 Render the impact limiter lifting lugs inoperable by covering the lifting holes or installing a bolt inside the holes to prevent their inadvertent use.
- 7.4.1.28 Install security seal on one tie-rod and lock sleeve.
- 7.4.1.29 Install the personnel barrier.
- 7.4.1.30 Check the temperature on all accessible surfaces to make sure that it is <185°F.
- 7.4.1.31 Perform a final radiation and contamination survey to satisfy the shield test requirements and to assure compliance with 10 CFR 71.47 and 71.87.
- 7.4.1.32 Apply appropriate DOT labels and placards in accordance with 49 CFR 172. Prepare the final shipping documentation.
- 7.4.1.33 Release the loaded cask for shipment.

7.5 References

1. ANSI N14.5-1997, "Leakage Tests on Packages for Shipment of Radioactive Materials."

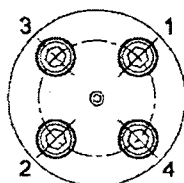
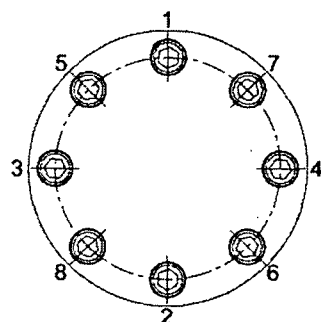
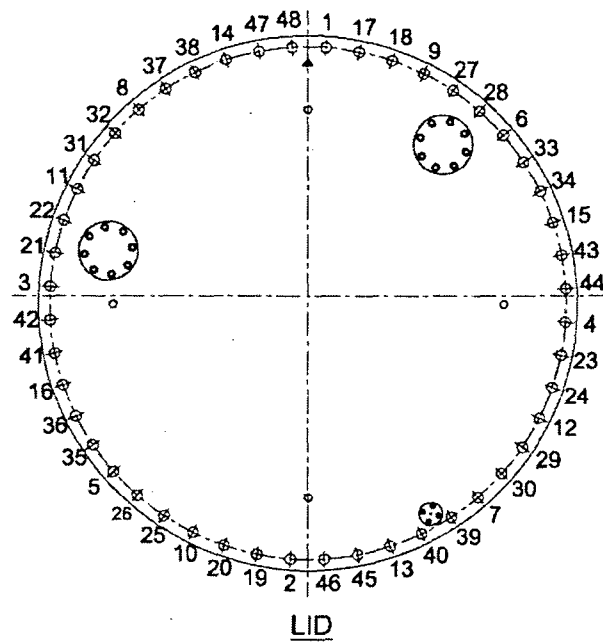


Figure 7-1
Torquing Patterns

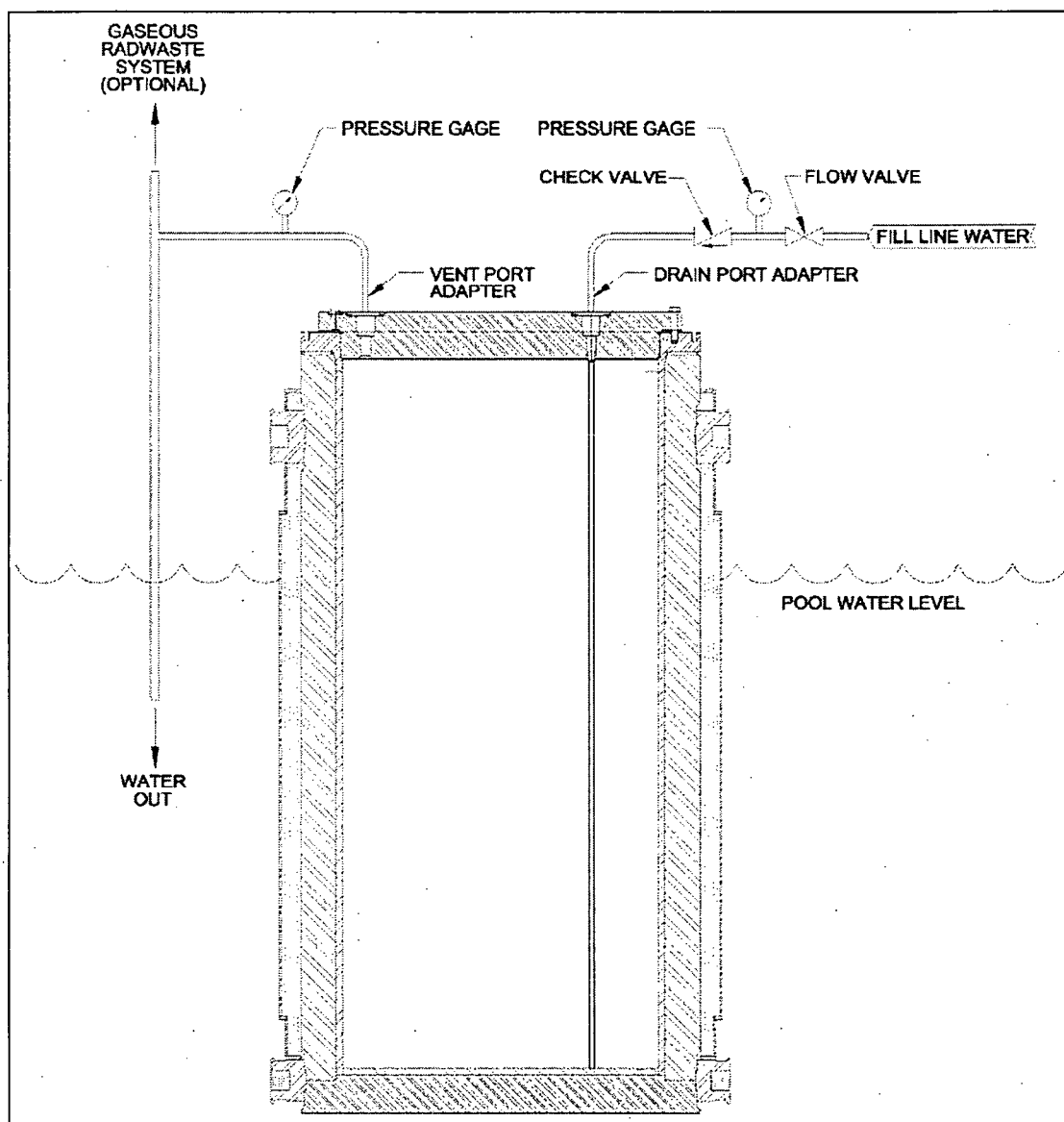


Figure 7-2
Typical Setup for Filling Cask with Water

CHAPTER 8 ACCEPTANCE TESTS AND MAINTENANCE PROGRAM

TABLE OF CONTENTS

	<u>PAGE</u>
8.0 ACCEPTANCE TESTS AND MAINTENANCE PROGRAM	8-1
8.1 Acceptance Tests	8-1
8.1.1 Visual Inspection	8-1
8.1.2 Structural and Pressure Tests	8-1
8.1.3 Containment Boundary Leak Tests	8-2
8.1.4 Component Tests	8-3
8.1.5 Shielding Tests	8-4
8.1.6 Neutron Absorber Tests	8-5
8.1.7 Thermal Acceptance Tests	8-5
8.2 Maintenance Program	8-5
8.2.1 Structural and Pressure Tests	8-5
8.2.2 Leak Tests	8-5
8.2.3 Subsystem Maintenance	8-6
8.2.4 Shielding	8-7
8.2.5 Thermal	8-7
8.3 References	8-8

8.0 ACCEPTANCE TESTS AND MAINTENANCE PROGRAM

8.1 Acceptance Tests

The following reviews, inspections, and tests shall be performed on the TN-40 packaging prior to initial transport. Many of these tests will be performed at the fabricator's facility prior to delivery of the cask to the utility for use. Tests will be performed in accordance with written procedures approved by Transnuclear, Inc. For the TN-40 casks that have been fabricated, loaded and used for storage under 10CFR72 requirements, use of acceptance tests performed during their fabrication are also acceptable.

8.1.1 Visual Inspection

Visual inspections are performed at the fabricator's facility to ensure that the packaging conforms to the drawings and specifications. The visual inspection includes verifying that all specified coatings are applied and the packaging is clean and free of cracks, pinholes, uncontrolled voids or other defects that could significantly reduce its effectiveness. To the maximum extent practical, weld inspection is performed in accordance with the applicable ASME code sections [1]. Dimensions and tolerances shown on the drawings provided in Chapter 1 are confirmed by measurements. Prior to shipping, the packaging will be inspected to ensure that it is in good physical condition. This inspection shall include verification that all accessible cask surfaces are free of grease, oil or other contaminants, and that all cask components are in an acceptable condition for use. The sealing surfaces on the flange, lid and covers are inspected to ensure that there are no gouges, cracks or scratches that could result in an unacceptable leakage.

8.1.2 Structural and Pressure Tests

The structural analyses performed on the packaging are presented in Chapter 2. To ensure that the packaging can perform its design function, the structural materials are chemically and physically tested to confirm that the required properties are met. To the maximum extent practical, welding is performed using qualified processes and qualified personnel, according to the ASME Boiler and the Pressure Vessel Code [1]. Base materials and welds are examined in accordance with the ASME Boiler and Pressure Vessel code requirements. NDE requirements for welds are specified on the drawings provided in Chapter 1. All NDE is performed in accordance with written and approved procedures. The inspection personnel are qualified in accordance with SNT-TC-1A [2].

The containment welds are designed, fabricated, tested and inspected in accordance with ASME B&PV Code Subsection NB. Alternatives to the code taken regarding the containment vessel are described in Chapter 2, Section 2.11. The basket is designed, fabricated, and inspected in accordance with the ASME B&PV Code Subsection NB. Alternatives to the code taken regarding the basket are described in Section 2.11 Welds

of the noncontainment structure are inspected per the NDE acceptance criteria of ASME B&PV Code, Subsection NF.

The impact limiter attachment bolt material is tested to show the Charpy fracture toughness is at least 20 ft-lb at -20°F. The tie rod material is tested to show the Charpy impact test energy is at least 35 ft-lb at -20°F.

Pressure Tests

A pressure test is performed on the cask assembly at a pressure of 25 psig. This is slightly higher than 1.5 times the maximum normal operating pressure of 15.7 psig. The test pressure is held for a minimum of 10 minutes. The test is performed in accordance with ASME B&PV Code, Section III, Subsection NB, Paragraph NB-6200 or NB-6300. All visible joints/surfaces are examined for possible leakage after application of the pressure. Temporary gaskets and seals may be used in place of the metallic seals during the test.

In addition, a bubble leak test is performed at a pressure of 3 - 5 psig on the neutron shield enclosure (outer shell, outer shell top and bottom rings). The purpose of this test is to identify any potential leak passages in the enclosure welds. The bubble leak test pressure is greater than the relief valve set pressure.

Load Tests

The lifting trunnions are designed to exceed 10CFR71 lifting requirements. A load test of 1.5 times the design lift load is applied to the trunnions for a period of ten minutes, to ensure that the trunnions can perform satisfactorily. Acceptance criteria are described in Section 2.11.

A force equal to 1.5 times the impact limiter weight will be applied to the lifting lugs of each limiter for a period of ten minutes. At the conclusion of the test, the impact limiter lifting lugs (including welds) will be:

- a. Visually examined for defects and permanent deformations.
- b. Examined by the liquid penetrant method for defects. Acceptance Standards will be in accordance with Article NF-5350 of Section III of the ASME Boiler and Pressure Vessel Code.

8.1.3 Containment Boundary Leak Tests

Leakage tests are performed on the containment seals at the fabricator's facility. These tests are usually performed using the helium mass spectrometer method. Alternative methods are acceptable, provided that the required sensitivity is achieved. The leak test is performed in accordance with ANSI N14.5 [3]. The acceptance criterion is 1 x

10^{-5} ref cm^3/s He. The personnel performing the leakage test are qualified in accordance with SNT-TC-1A [2].

8.1.4 Component Tests

8.1.4.1 Valves, Rupture Discs, and Fluid Transport Devices

There are no valves in the packaging performing a safety related function. The TN-40 design incorporates quick-disconnect couplings for ease of draining and venting. However, these couplings do not form part of the containment boundary. They are covered by bolted closures with metallic seals. There is no required acceptance test for these components.

8.1.4.2 Gaskets

The lid and all the other containment penetrations are sealed using double metallic seals. The inner seal forms part of the containment boundary. Metallic seals are not temperature sensitive, and are therefore tested at room temperature. Metallic seals of the same type as those to be used for transport are installed for the fabrication leak test, described in Section 8.1.3. The tested seals are replaced before loading the packaging for storage or for transport. Seals are leak-tested at the time of storage closure and/or prior to transport as described in Chapter 7.

8.1.4.3 Impact Limiter Leakage Test

The following test will be performed, after all the seal welds are completed on the impact limiter, to verify that the impact limiter wood will be protected from any moisture exchange with the environment.

Pressurize each impact limiter container to a pressure between 2 and 3 psig using helium. Test all the weld seams for leakage using a soap bubble test.

8.1.4.4 Functional Tests

The following functional tests will be performed prior to first use of the cask. Generally these tests will be performed at the fabrication facility.

- a. Installation and removal of the lid, penetration covers, and other fittings will be observed. Each component will be checked for difficulties in installation and removal. After removal, each component will be visually examined for indications of deformation, galling, improper functioning, etc. Any defects will be corrected prior to acceptance of the cask.
- b. After installation of the basket, each basket compartment will be checked by gage to demonstrate that the fuel assemblies will fit in the basket.

8.1.5 Shielding Tests

The analyses performed to ensure the shielding integrity are presented in Chapter 5. The radial neutron shield is protected from damage or loss by the aluminum and steel enclosure. The neutron shield material is a proprietary, borated, reinforced polymer.

The primary function of the resin is to provide neutron shielding, which is performed primarily by the hydrogen content of the resin. The resin also provides some gamma shielding, which is a function of the overall resin density, and is not sensitive to composition.

The shielding performance of the resin can be verified adequately by chemical analysis and verification of density. Uniformity is assured by installation process control.

The following are acceptance values for density and chemical composition for the resin. The values used in the shielding calculations of Chapter 5 are included for comparison.

Chapter 5 values		Acceptance Testing Values		
Element	nominal wt %	Element	wt %	acceptance range (%)
H	5.05	H	5.05	-10 / +20
B	1.05	B	1.05	± 20

The minimum resin density in acceptance testing is 1.547 g/cm³. Resin composition or density test results which fall outside of this range will be evaluated to ensure that the shielding regulatory dose limits are not exceeded.

Density testing will be performed on every mixed batch of resin. Chemical analysis will be made on the first batch mixed with a given set of components, and thereafter whenever a new lot of one of the major components is introduced. Major components are aluminum oxide, zinc borate and the polyester resin, which combined make up 92% of the resin by weight.

Qualification tests of the personnel and procedure used for mixing and pouring the polyester resin used for radial neutron shielding are performed. Qualification testing includes verification that the chemical composition and density are achieved, and the process is performed in such a manner as to prevent voids.

Tests are performed at loading to ensure that the radiation dose limits are not exceeded for each cask.

8.1.6 Neutron Absorber Tests

Boral[®] is the neutron absorber used for criticality control in the TN-40 basket. The neutron absorber plates may be monolithic, or they may consist of paired plates, one containing boron in the specified areal density, and the other composed of aluminum or aluminum alloy to make up the balance of the specified thickness and thermal conductance.

The TN-40 safety analyses do not rely upon the tensile strength of these materials. The radiation and temperature environment in the cask is not sufficiently severe to damage these materials.

The Boral[®] neutron absorber material consists of a core of aluminum and boron carbide powders between two outer layers of aluminum. The criticality calculations take credit for 75% of the minimum specified B10 areal density of Boral[®].

8.1.7 Thermal Acceptance Tests

The thermal evaluation presented in Chapter 3 is based on design configurations and thermal properties taken from industry recognized standards for the specified materials. Therefore thermal acceptance tests of the TN-40 cask are not required.

8.2 Maintenance Program

8.2.1 Structural and Pressure Tests

Within 14 months prior to any lift of a TN-40 transport package, the lifting (top) trunnions shall be subject to either of the following:

A test load equal to 150% of the maximum service load. After sustaining the test load for a period of not less than 10 minutes, critical major load-bearing area, shall be subjected to visual inspection for defects, and all components shall be inspected for permanent deformation.

or

Dimensional testing, visual inspection and nondestructive examination of accessible critical areas of the trunnions including the bearing surfaces.

8.2.2 Leak Tests

After lid or port cover removal, the affected metallic containment seals shall be replaced and leak tested prior to spent fuel shipment to show a leak rate less than 1×10^{-4} ref cm^3/sec per ANSI N14.5 [3]. These tests are usually performed using the helium mass spectrometer method. Alternative methods are acceptable, provided that the required sensitivity is achieved. Because the seals are used only once, the preshipment leak

tests may be used to fulfill the ANSI N14.5 requirements for maintenance and periodic testing.

No leak tests are required prior to shipment of an empty TN-40 packaging.

8.2.3 Subsystem Maintenance

8.2.3.1 Fasteners

The lid bolts, vent, drain and overpressure transport cover bolts shall be inspected after each use for deformed or stripped threads. Damaged parts shall be evaluated for continued use and replaced as required. At a minimum, the lid bolts, vent, drain and overpressure transport cover bolts shall be replaced at least once per fifty (50) shipments (round trip). If the cask is used in a storage mode, the fasteners need not be inspected or replaced until after the first shipment.

8.2.3.2 Impact Limiters

A visual examination of the impact limiters before each shipment will be performed to ensure that the impact limiters have not been degraded between shipment. If there is no evidence of weld cracking or other damage which could result in water in-leakage, the wood will not be degraded. If there is visual damage, the impact limiter will be removed from service, repaired, if possible, and inspected for degradation of the wood. Impact limiters will be leak tested once every five years to ensure that water has not entered the impact limiters. If the leak test indicates that the impact limiters have a leak, a humidity test will be performed to verify that there is no free water in the impact limiters. An impact limiter that has a leak will be removed from service and repaired.

8.2.3.3 Valves, Rupture Discs, and Gaskets on Containment Vessel

If a port cover or the lid is removed, the seals are replaced prior to spent fuel transport. At the time the TN-40 is first converted from storage to transport use, it is most likely that the fuel that has been in storage will remain in the TN-40 for transport, and therefore, the lid will not be removed. In this case, the lid seal and seals of penetrations which have not been opened will not be replaced. The seals will be leak tested after retorquing the bolts in accordance with Section 7.4.

The metallic seals may be reused for transport of an empty TN-40 packaging.

The leak test port (the overpressure port in the storage configuration) is closed by the overpressure transport cover with a single metallic seal. This flange and seal are not part of the containment boundary. The quick connect couplings in the vent and drain ports are not part of the containment boundary.

There are no valves or rupture discs on the TN-40 packaging containment.

8.2.4 Shielding

There are no periodic tests or inspections required for the TN-40 shielding. Radiation surveys will be performed of the package exterior to ensure that the limits specified in 10 CFR 71.47 are met prior to each shipment.

8.2.5 Thermal

There are no periodic tests or inspections required for the TN-40 heat transfer components.

8.3 References

1. ASME Boiler and Pressure Vessel Code, Section III, 1989.
2. SNT-TC-1A, "American Society for Nondestructive Testing, Personnel Qualification and Certification in Nondestructive Testing," 1987.
3. ANSI N14.5-1997, "Leakage Tests on Packages for Shipment of Radioactive Materials."